Synthesis of novel heterocyclic systems as potential inhibitors of HIV-1 enzymes

THESIS

Submitted in fulfillment of the requirements for the degree of

DOCTOR OF PHILOSOPHY

of

Rhodes University

by

Khethobole Cassius Sekgota

APRIL 2019

Department of Chemistry

Rhodes University

Makhanda

Abstract

This study has focussed on the application of Baylis-Hillman methodology in the development of efficient synthetic pathways to libraries of novel 3-[(*N*-cycloalkylbenzamido)methyl]-2-quinolones and indolizine-2-carboxamides and on an exploration of their medicinal potential. The approach to 3-[(*N*-cycloalkylbenzamido)methyl]-2(1*H*)-quinolones involved a six-step pathway comprising: Baylis-Hillman reaction of 2-nitrobenzaldehyde derivatives and methyl acrylate to afford nitro-Baylis-Hillman adducts; thermal cyclisation of the adducts to give a range of 3-(acetoxymethyl)-2(1*H*)-quinolones in good to excellent yields; hydrolysis of the acetates; conversion of the resulting alcohols to the 3-chloromethyl analogues; amination; and, finally, acylation to afford the target amides. Variable temperature NMR methods were used to facilitate analysis of the ^{1}H and ^{13}C NMR spectra which were complicated by internal rotation and cycloalkyl ring-flipping effects.

On the other hand, the indolizine-2-carboxamides were obtained in several steps commencing with the Baylis-Hillman reaction of pyridine-2-carboxaldehyde and methyl acrylate. Thermal cyclisation of the Baylis-Hillman adduct afforded indolizine esters, hydrolysis of which gave the corresponding acids which served as precursors to the target indolizine-2-carboxamides. The final amidation step, however, proved to be particularly challenging. Various coupling strategies were explored to access indolizine-2-carboxamides. These included the use of 2,2,2-trifluoroethyl borate which showed limited promise, but propylphosphonic acid anhydride (T3P) proved to be the most effective coupling agent, permitting the formation of 24 novel indolizine-2-carboxamides from hydrazines, aliphatic amines and a range of heterocyclic amines.

A high-field NMR-based kinetic study of the mechanism of the Baylis-Hillman reaction of pyridine-4-carboxaldehyde and methyl acrylate in the presence of 3-hydroxyquinuclidine in deuterated chloroform was initiated, reaction progress being followed by the automated collection of ^{1}H and DEPT 135 NMR spectra over *ca.* 24 hours using a high-field (600 MHz) NMR instrument. The results have provided critical new insights into the mechanism. NMR analysis has also been used to elucidate the multiplicity of signals associated with rotameric equilibria observed at ambient probe temperature. Variable temperature 1D- and 2D-NMR spectra were used to facilitate the unambiguous characterisation of the 2-quinolone benzamides and some of the indolizine-2-carboxamides.

The 3-[(*N*-cycloalkylbenzamido)methyl]-2(1*H*)-quinolones, together with selected precursors, and a number of the indolizine-2-carboxamides have been screened *in vitro* as potential HIV-

1 enzyme inhibitors. A survey of the activity of the 2-quinolones against HIV-1 integrase, protease and reverse transcriptase revealed selective inhibition of HIV-1 integrase with the most active IN inhibitor, 3-[(cyclopentylamino)methyl-6-methoxy-2(1*H*)-quinolone **115e**, producing residual enzyme activity of 40% at a concentration of 20 µM. Many of the 2-quinolones exhibited no significant cytotoxicity against HEK 293 cells at 20 µM concentrations. 3-[(*N*-Cyclohexylamino)methyl]-6-methoxy-2(1*H*)-quinolone **114e** was the only compound to exhibit ant-plasmodial activity (55% *pf*LDH activity). The survey of indolizine-2-carboxamides also revealed encouraging inhibition against HIV-1 integrase. None of these compounds exhibited cytotoxicity at 20 µM against HEK 293 cells, while a number of them exhibited some activity against *Plasmodium falciparum* (3D7 strain) and *Trypanosoma brucei*. Selected indolizine-2-carboxamides exhibited significant anti-tubercular activity in the 7H9 CAS GLU Tx and 7H9 ADC GLU Tw media.

In view of the inherent fluorescent character and biological potential of the synthesised indolizine-2-carboxamides, their photophysical properties were explored to establish their possible dual use as bio-imaging and therapeutic agents. The major absorption and corresponding emission bands, and the associated molar absorption coefficients (Ɛ) expressed in the form of log Ɛ were determined. Their high extinction coefficients, large Stokes shift and red-shifted emissions in the visible region indicate their potential for use as fluorophores.

Acknowledgements

Firstly, I would like to express my sincere gratitude to my supervisor, Dr. Setshaba David Khanye, for his support, encouragement and availing of resources without which the project would not have been a success.

To my co-supervisor, Prof. Emeritus Perry T. Kaye, I am eternally grateful for his advises and deliberations which proved most helpful, informative and gifted this project moments of considerable success. The splendour of his effortless-patience, care, enthusiasm and commitment has been a source of inspiration. I would also like to extend my heartfelt appreciation to Prof. Kevin Lobb for his invaluable assistance with variable temperature NMR, kinetic and mechanistic studies.

I am grateful to all the current and former students in our lab for their constructive inputs and collegiality. It was a great pleasure and privilege mentoring am impeccable student as Kamogelo Mafokwana (MSc to PhD upgrade) whose ethics and commitment made this experience a memorable one.

I would also like to thank my friends for their support. To each one of you, either in Makhanda or elsewhere, your support can never go unnoticed. May I take the liberty to give special thanks to all members of staff, not to mention the technicians, in the Department of Chemistry and post-graduate students in our lab for support and encouragement.

To my relatives, your support is always a pillar of strength. I am especially thankful for selfless support I benefited from my sister, Mabatho Marutha. No amount of words can express my appreciation for the endless support and guidance from my brother, Maropeng Ngobeni. To my in-laws, the Kubheka family, thank you for being so thoughtful and supportive in this endeavour.

I thank my siblings: my brothers, Mantshitla and Masilo and, my sister, Matate for their moral support and love throughout the journey.

To my little lad, Kheropole Tlhankga Mvuyelwa Sekgota, at your infancy I invested in a dream, a dream I would spread for you to walk on. To my niece, Mosibudi Poelano Sekgota, had I been there you too would have enjoyed my presence, tread on this dream.

I am grateful to NRF and MRC for financial support without which this project would not have been possible.

This research project has been a knowledge-generation endeavour which in order grasp and understand underlying abstract principles, many times, my mind hurled into an intellectual and creative realm from which it was at dissonance with my body and the local environment. Ideas that nourished and refreshed the mind were established, praxes of which continuously required the ability to transform despair into hope; failure into challenge; and sustained optimism. When fatigue had set in, almost convinced that the course was beyond my capacity and the reward of doubtful value, there was always a team that cherished and encouraged me throughout the course and, believed in me more than myself. Whenever they casually recited a family praise which ushered in morale, "*Ke Sekgota sa mmabodingwana a tau, Sekgota sa mafolosa nkwe thabeng mabala a kganya le tlase. A kganya le mmadithaga modubatse. Ke motho yo a tšwago bolepse, tlhaku di a lewa, tša sita ra ribega ka morifi.*"; I knew for truth that I represent their aspirations and upon completion, the reward is momentous and of invaluable value. There exists no token of thanks to appreciate your support nor vocabulary to express my gratitude.

I would like to dedicate this thesis to my parents, Modjadji Nancy and Mohlatlego Paulus Sekgota and my beautiful wife, Gugu Kubheka.

"Morena boloka setshaba sa heso"

Table of Contents

Abstract i

Acknowledgements iii

1. Introduction 1

1.1. Fundamentals and evolution of drug discovery 1

1.2. Ro5 and bRo5 drugs 6

1.3. Receptors of Ro5 and bRo5 drugs 12

1.3.1. Pharmacokinetics of anti-HIV drugs 13

1.3.2. Potential HIV-1 vaccination 15

1.3.3. Anti-retroviral therapy 16

1.3.3.1. New generation anti-retroviral regimens *18*

1.4. Quinolones in Medicinal Chemistry 20

1.4.1. Properties of 3-substituted 2-quinolones 23

1.4.1.1. Fluorescence properties of 2-quinolones *24*

1.4.2. Synthesis and reactivity of 3-substituted 2-quinolones. 26

1.4.3. Syntheisis of benzannulated beterocyclic compounds using Baylis-Hillman methodology. 28

1.4.3.1. The Baylis-Hillman approach to 2-quinolone derivatives. *29*

1.5. Review of Indolizine chemistry 32

1.5.1. Biological activity and synthesis of indolizines 33

1.5.2. Baylis-Hillman approach to indolizines 38

1.5.3. Physical properties of indolizines 38

1.5.3.1. Modulation of indolizine optical properties *40*

1.5.3.2. Molar absorptivity of indolizines. *42*

1.6. Research context and objectives of the current investigation 44

2. Results and Discussion 46

2.1. Preparation of Baylis-Hillman adducts. 46

2.1.1. Amination of the 3-(chloromethyl)-2(1*H*)-quinolone derivatives (**113**) 49

2.1.2. Approaches to amide bond formation. 53

2.1.3. Synthesis of 3-[(cycloalkylbenzamido)methyl]-2(1*H*)-quinolones **117-119**. 57

*2.1.3.1. Structural elucidation of the benzamides (**117-119**).* *60*

2.2. Preparation of indolizine derivatives *via* aza-Baylis-Hillman intermediates 70

2.2.1. Thermal cyclisation of 2-pyridinyl derivatives. 74

2.2.2. Saponification of methyl indolizine-2-carboxylate. 79
2.2.3. Saponification of methyl 3-acetylindolizine-2-carboxylate **132** 82
2.2.4. Exploratory studies of the synthesis of indolizine-2-carboxamides 85
2.2.4.1. Boron-catalysed amide bond formation 86
2.2.4.2. Direct catalytic amidation of indolizine-2-carboxylic acid with diisocyanates. 87
2.2.4.3. Thermal cyclisation of amido-Baylis-Hillman adducts. 89
2.2.4.4. Approaches to Baylis-Hillman-derived carboxamides from Baylis-Hillman-derived carboxylic acids. 93
2.2.5. T3P-catalysed synthesis of amides. 95
2.2.6. Preparation of secondary amides. 95
*2.2.6.1. Synthesis of N-(pyrazinecarboxanoyl)indolizine-2-carboxamide **179** 99*
*2.2.6.2. N-[N-(Indolizin-2-ylcarbonyl)isoxazolin-3-on-4-yl]indolizine-2-carboxamide **180** 102*
2.2.7. Extension of T3P-mediated indolizine-2-carboxamide syntheses. 107
*2.2.7.1. T3P-mediated reactions of acid (**138** and **139**) with 4-imidazolidinedione **146** and -methylimidazolidine-2,4-dione **147**. 107*
2.2.7.2. T3P-mediated Coupling of indolizine-2-carboxylic acids with further heteroaromatic amine. 114
2.2.7.3. Synthesis of isoniazid analogues. 125
*2.2.7.4. Coupling of indolizine-2-carboxylic acid **134** with heteroaryl alkylamines 131*
2.3. Biological evaluation of 2-quinolone derivatives 141
2.4. Biological assay of indolizine derivatives 144
2.4.1. HIV-1 IN and PR assays 144
2.4.2. TB assays 145
2.4.3. Preliminary Malaria, trypanosome and cytotoxicity assays. 148
2.5. Photophysical properties of indolizine-2-carboxamides 151
2.6. Further chemical kinetic and mechanistic studies of the Baylis-Hillman reaction 156
2.7. Conclusions 170

3. Experimental 173

3.1. General details 173
3.2. Part I 174
3.2.1. Synthesis of Baylis-Hillman adducts 174
3.2.2. Cyclisation of Baylis-Hillman adducts. 178
3.2.3. Hydrolysis of 3-(Acetoxymethyl)-2(1*H*)-quinolone derivatives. 181

3.2.4. Chlorination of 3-(hydroxymethyl)-2(1*H*)-quinolones. 184
3.2.5. Synthesis of 3-[(cycloalkylamino)methyl]-2(1*H*)-quinolone. 187
3.2.6. Synthesis of 3-(benzamidomethyl)-(1*H*)-2-quinolones 193
3.3. Part II 199
3.3.1. Synthesis of aza-Baylis-Hillman adducts 199
3.3.2. Preparation of indolizine esters and acids 205
3.3.3. Synthesis of *N*-(heteroarylalkyl)indolizine-2-carboxamides 208
3.3.4. Synthesis of tertiary indolizine-2-carboxamides 211
3.3.5. Further synthesis of acetylated and non-acetylated *N*-heteroarylindolizine-2-carboxamides 214
3.3.6. Synthesis of indolizine-2-carbohydrazides **197-199** 221
3.4. Bioassay protocols 223
3.4.1. HIV-1 Integrase Assay 223
3.4.2. HIV-1 Protease assay 223
3.4.3. HIV-1 RT assay 224
3.4.4. Plasmodium falciparum (pLDH) assay 224
3.4.5. Trypanosome assay 225
3.4.6. Cytotoxicity assay 225
3.5. Mechanistic studies 226

4. References 230

1. Introduction

1.1. Fundamentals and evolution of drug discovery

Drug discovery is an interdisciplinary endeavour that primarily involves a combination of appropriate expertise from chemistry, pharmacology and biochemistry to effect product transfer from fundamental research to the pharmaceutical industry. The advent of genomics and bioinformatics has greatly enhanced the drug discovery process and diversified treatment options by exposing the genetic basis of multifactorial diseases and identifying targets for therapeutic intervention.[1] Since 1865, when August Kekulé's pioneering theory on the structure of aromatic organic molecules led to successful research on dyes and the realisation that dyes have selective affinity for biological tissues, chemistry has had a driving influence in drug research.[2] This led to scientists postulating the existence of chemoreceptors in parasites and microorganisms and that cancer cells could be differentiated from analogous structures in host tissues.[3]

Natural products from terrestrial and marine plants, microorganisms, vertebrates and invertebrates have been used for treating and preventing human diseases since the dawn of medicine. They continue to play an inspirational role in the discovery of new compounds thereby increasing structural diversity and providing novel lead compounds. In fact, the majority of the world's population (up to 80%) relies on natural product-based medicines for primary health care which also inspire drug development in developed countries.[4,5, 6] In the period of thirty-four years, from 1981 to 2006, Newman and Cragg published four major reviews covering sources of new and approved drugs for the treatment of human diseases.[5, 7-9]

The development of high-throughput screening based on molecular targets has led to a constant demand for the generation of large libraries of compounds. High-throughput screening typically focuses on a limited collection of compounds that contain structural features of natural products. Up to the present time, combinatorial chemistry has led to the *de novo* development of two new compounds approved for medicinal use, *viz*, sorafenib (Nexavar) **1** and atalurin (Translarna) **2**. Sorafenib was developed as an antitumor agent by Bayer, and the United States Food and Drug Administration (U.S. FDA) approved its use in the treatment of renal cell carcinoma and hepatocellular carcinoma in 2005 and 2007, respectively. By mid-2014 sorafenib had been approved in more than 100 countries for the treatment of these conditions and, following further approval, for the treatment of thyroid cancer. Atalurin was approved by the EU in 2014 for the treatment of patients with genetic disorders resulting from mutations.[7]

Chemists have long been involved in the isolation of the active principles in medicinal plants.[10] For example, Sertürner isolated morphine **3** from opium extract in 1815; papaverine **4** was isolated in 1845 and discovered to be an antispasmodic in 1917.[11] As more active principles were isolated, the pharmaceutical industries addressed the problem of providing standardised preparations of isolated active ingredients.[12] Nine years after Alexander Fleming's discovery of penicillin **5** in 1929, a metabolite from a penicillium mould, Howard Florey, Ernest Chain and co-workers successfully isolated penicillin from penicillium mould thereby opening a new era of antibiotics.[13, 14] Before the discovery of penicillin, infections such as pneumonia, rheumatic fever or gonorrhoea were life-threatening. The serendipitous discovery and subsequent development of penicillin represents one of the most important developments in medicinal chemistry.[15, 16] Interestingly, however, the Egyptians had already used mould as an antibiotic by applying poultices of mouldy bread to infected wounds. Such antibiotics are produced by bacteria and fungi and are capable of inhibiting the growth of or destroying microbial species.[15]

Inspired by the high potency and apparent lack of toxicity of penicillin, a search for more antibiotics ensued requiring the establishment of well-equipped departments of microbiology and biochemistry to augment chemistry in the search for agents that exert other biological activities.[17] Over the years, numerous new drugs have been discovered including: Ivermectin **6** as an anti-parasitic;[18] Iovastatin **7** as a HMGA-CoA (3-hydroxy-ω-methylglutaryl-CoA) reductase inhibitor to lower the level of cholesterol in the blood;[19] and Cyclosporin **8** and Tacrolimus **9** (FK 506) as immunosuppressants.[1]

The emergence of new, complex, and hard-to-treat diseases has rendered traditional drug discovery methodologies inadequate, and new technologies, such as large-scale genomics and proteomics, automated organic synthesis, and advanced biological screening have been developed to identify and target eccentric and difficult drug targets.[20, 21] Information derived from the identification of drug targets informs the design of the molecular structure of potential drugs – a key technique in enhancing drug discovery by enabling the rational design of small molecules to bind at such targets.[22] Despite these advances, average research and development costs per new molecular entity have increased dramatically in recent years. In addition, regulatory agencies are less tolerant to risk in new drugs for diseases for which safe drugs already exist. This has the effect of channelling research and development towards complex and hard-to-treat diseases. This translates to more costly and lengthier clinical trials and the need to deliver high-quality, safe and efficient treatments for complex diseases.[23]

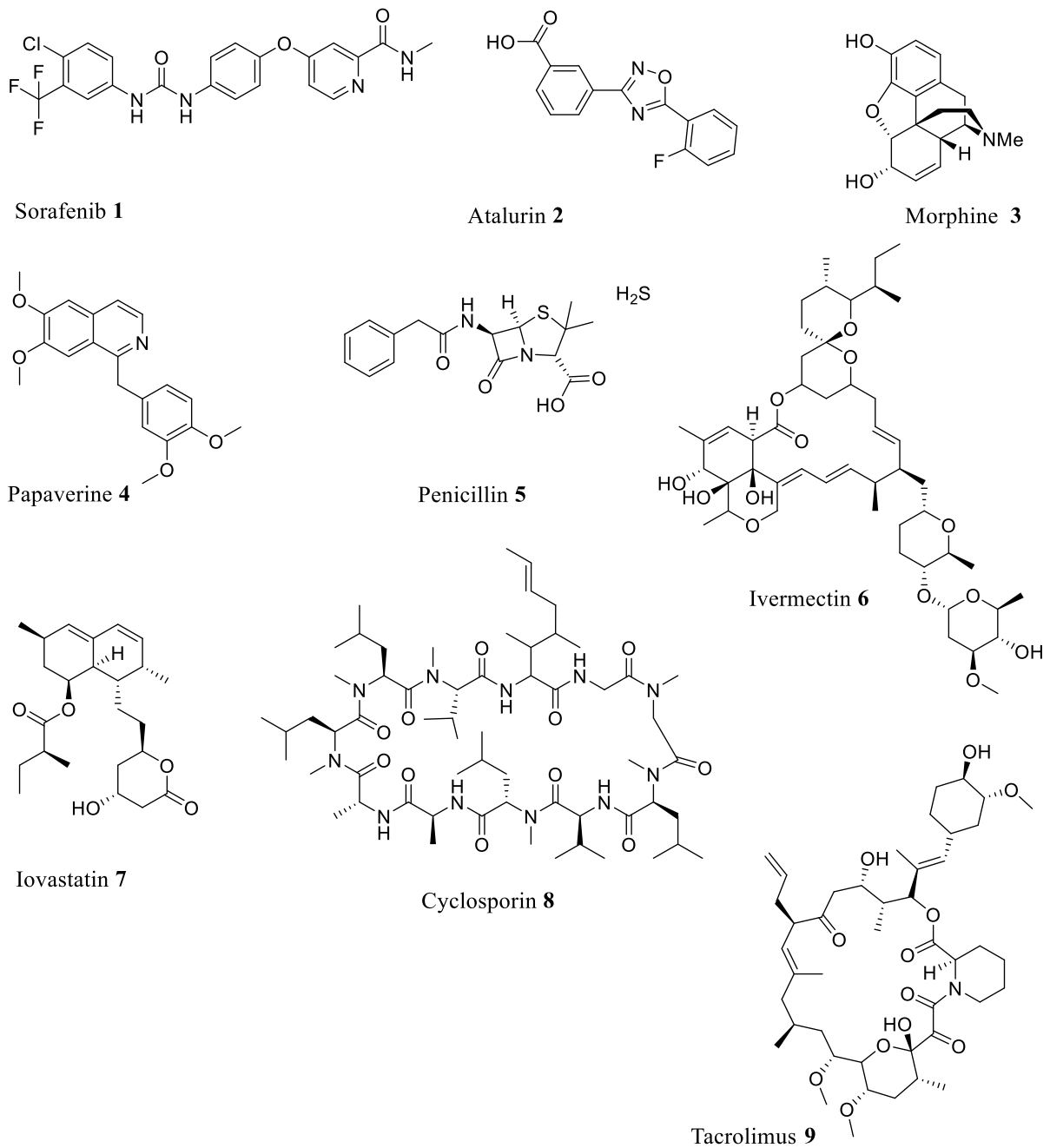

Figure 1. Examples of compounds established for the treatment of human disease.

While the quality of drug target selection remains to be improved, compound attrition due to poor bioavailability and pharmacokinetics in phase II and III clinical evaluations has decreased significantly. This improvement is attributed to the critical attention being given to oral bioavailability, the re-purposing of known drugs and clinical candidates as well as the introduction of *in vitro* permeability assays using human colorectal carcinoma cells (caco-2), Mardin-Darby canine kidney (MCDK) cells and parallel artificial membrane permeability assays (PAMPA). These developments led to use of the Lipinski rule of five (Ro5) which

reduced the halting rate of drugs in clinical studies from 39% in the year 1991 to 8% in 2000. However, attrition due to toxicity increased and the lack of efficacy remained constant.[21-23]

Lipinski's rule of five (Ro5) which was proposed in 1997 stated that 90% of drugs that fulfil three out of four of the following properties are more likely to be orally absorbed: molecular weight ≤ 500 Da, calculated logP (cLogP) ≤ 5 and ≥ 0, hydrogen-bond donors (HBD) ≤ 5 and hydrogen-bond acceptors (HBA) ≤ 10 (**Table 1**).[24]

Table 1. Fundamental amenable factors of the Ro5 compliant drugs.[20, 22, 23]

Ro5 properties	**Property Change**	**Impact**
Molecular weight	Increase	• Decrease solubility • Decrease permeability • Increase transporter-mediated efflux toxicity • Increase toxicity linked with human ether-a-go-go-related gene (hERG)
cLogP	Increase	• Increase lipophilicity • Improve permeability • Decrease solubility • Increase drug promiscuity and toxicity • Increase accumulation in membranes and adipose tissues
HBD and HBA	Increase	• Poor permeability

Additional guidelines such as polar surface area (PSA ≤ 140 $Å^2$), number of rotatable bonds (NRotB ≤ 10), and different ligand efficiency metrics, in terms of which a compound's affinity is compared to its size and/or lipophilicity, have since been introduced, thereby expanding the correlations with absorption, distribution, metabolism, excretion and toxicity (ADMET) parameters. The simplicity of the Lipinski's Ro5 has facilitated the rapid development of drugs, but its direct implementation (including additional guidelines) has often led to misuse and misinterpretation. Consequently, weighted or combination methods, 3D properties, quantitative estimates of drug likeliness (QED), Egan's egg, the golden triangle, radius of

gyration, dissolution of energies, *etc.*, have been introduced to mitigate the shortcomings of the Ro5. [21, 23]

In comparison to intravenous drug delivery methods, such as buccal, nasal and transdermal, oral delivery has many advantages when systemic exposure of a drug is desired. Advantages associated with solid oral drugs include increased reliability of exposure, ability to deliver large variations in dosage and relatively greater stability under storage compared with liquids and suspensions.[25] Intravenous drug delivery, an invasive drug delivery method, also requires cell permeability. It is, however, prone to infections and local side reactions and is undesirable for many patients, especially children. Oral drug delivery is preferred by far over other methods. For instance, research shows that 54-89% of oncology patients preferred oral delivery, and that quality of life for chronic patients improved compared to intravenous therapy. Because of its convenience, oral delivery remains the preferred method of drug delivery for the vast majority of drug therapies and, consequently, oral bioavailability represents a major challenge in drug development.[21, 22]

Despite the advances in target identification through proteomics,[26] less than a quarter of recently approved drugs are active against novel targets which are usually G protein-coupled receptors (GPCRs), transporters or enzymes. Adversely, approximately 3000 of the genes in the human genome are related to disease with 600-1500 considered to be susceptible to manipulation using drugs that comply with the rule of five guidelines. Although a significant number of established classes of drug targets, such as ligand-gated ion channels, G-protein-coupled receptors (GPCRs) and nuclear receptors remain unexplored, exploration of the large number of targets which have poor or no response towards Ro5 compliant drugs could provide innovative drug discovery opportunities.[21, 24, 27] The latter targets generally have binding sites that are large, highly lipophilic or polar, flexible, flat or featureless. Ongoing advances in genomics and proteomics facilitate the discovery of small molecules that reside outside Ro5 guidelines and such molecules are termed “beyond Ro5” (bR05). Recent analyses of bRo5 drugs and clinical candidates have revealed significant possibilities for the discovery of orally bioavailable and cell-permeable compounds, supporting a view that strict implementation of Lipinski’s Ro5 may have derailed drug research and development from seizing opportunities involving novel but more difficult targets.[21]

1.2. Ro5 and bRo5 drugs

The Ro5, in addition to considerations of drug toxicity and promiscuity, primarily focuses on two factors, *viz.*; the permeability and absorption of orally dosed drugs. Intestinal and plasma dissolution, permeability across the intestinal wall, and hepatic first-pass metabolism are vital aspects addressed in Ro5 compliant drugs. These aspects may be affected by a number of physiological and physiochemical factors that include varying intestinal pH, chemical and metabolic stability of the drug in the gastrointestinal system and the plasma, transporter-mediated efflux and the digestive and metabolic status of the patient.[22]

Absorption of orally dosed drugs can be categorised into *paracellular*, *transcellular* and *active transport*.[28] *Paracellular absorption* involves transfer of a substance across an enterocyte by passing through the intracellular space between cells and is limited to small hydrophilic compounds with molecular weight (MW) ≤ 350 Da and low lipophilicity.[28, 29] *Transcellular transport* is the most common drug absorption process that requires passive diffusion through the apical membrane, facing the gastrointestinal tract, into the enterocyte, followed by diffusion across the cell and through the basolateral membrane into the blood.[30, 31] In passive diffusion, compounds partition into the cell membrane following desolvation from the polar aqueous gastrointestinal tract. The compound is then resolvated upon entry into the aqueous plasma (blood). Efflux transporters, such as P-glycoprotein (Pgp), actively transport compounds from the blood into the enterocyte and/or from the enterocyte into the gastrointestinal tract.[23, 32] Lastly, *active transport* (uptake) requires recognition by native, efflux transporter proteins and is limited to small analogues of peptides, amino acids, lipids and sugars.[23] Figure 2 shows schematic representation of transcellular and paracellular absorption.

Enzymes in the gastrointestinal tract, blood, enterocytes and lymph may metabolise the drug to a less active and highly soluble species. For a drug to reach the systemic circulatory system it must first be absorbed, amid potentially adverse metabolism, into the blood where it may travel *via* the portal vein to the liver and undergo hepatic metabolism. Systemic circulation ensues after hepatic metabolism, and oral bioavailability refers to the fraction of the oral dose that achieves systemic circulation after absorption and first-pass metabolism (overall metabolism during absorption and hepatic metabolism).[23]

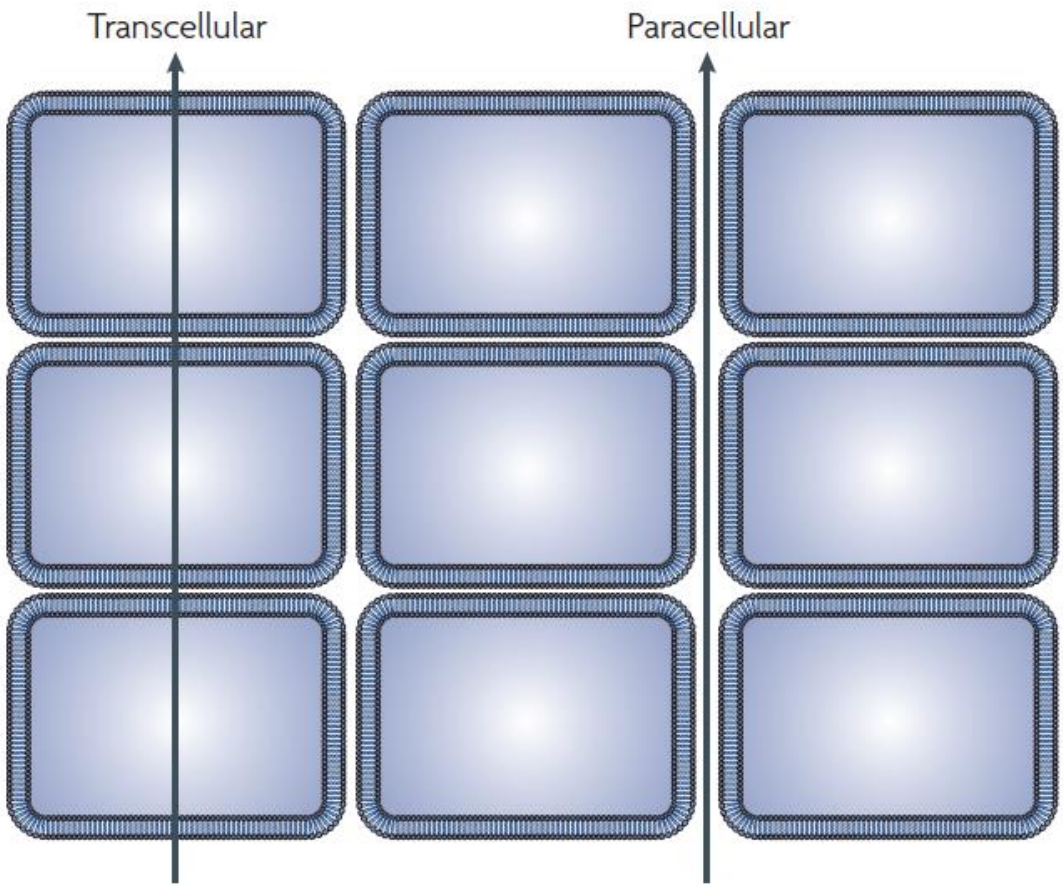

Figure 2. A schematic diagram illustrating two modalities of the transfer of molecules across the tissue: paracellular (diffusion) and transcellular (crossing of phospholipid layers.[33] (Reproduced with permission.)

Secondary metabolites of microbes and plants have provided reliable leads for the discovery of drugs the majority of which fall in the class "beyond rule of 5" (bRo5) molecules. The first four rules of the Lipinski's Ro5 are effectively not applicable to natural products or any molecule that is recognised by the active transport system.[7] Natural products are unique, highly diverse systems that are biased to bind in protein folds. Their binding selectivity may be improvable through structural modification, and their larger structures may be suited for targeting "undruggable" target spaces while maintaining bioavailability. Natural product drugs, through their capability to target unexplored potential drug targets, cover a wide range of diseases – parasitic, bacterial and fungal infections, allergies, cardiovascular and metabolic diseases, cancer, organ transplantation and multiple sclerosis.[34]

Figure 3 shows an inclusive classification by Newman[7] of drugs discovered from 1981 to 2014. A total of 1562 new molecular entities of natural products or related structures that include

biological macromolecules, unaltered natural products, botanical drugs (or defined mixtures thereof) and natural product derivatives account for 50.1% of the drugs in Newman's analysis; these exclude synthetic natural product mimics which account for a further 10%.[7]

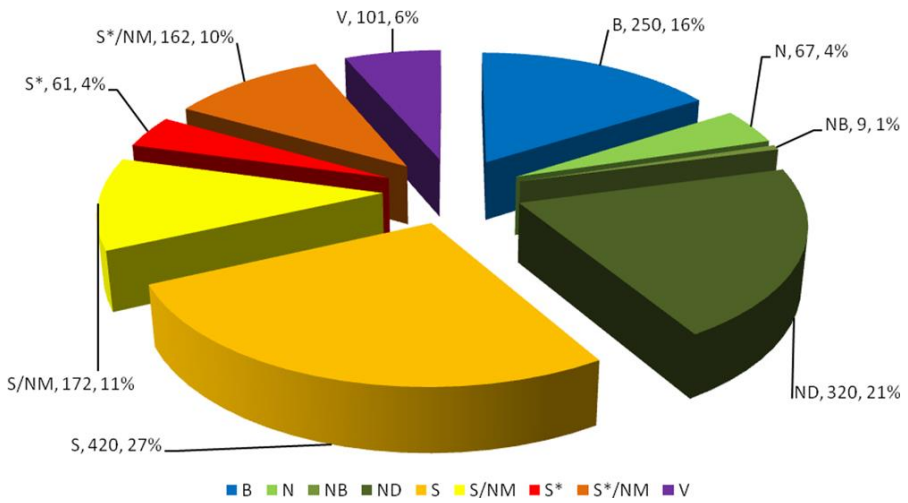

Figure 3. Newman's analysis of all new approved drugs from 1981 to 2014. Notations: B – Biological macromolecule, N – Unaltered natural product, NB – Botanical drug (defined mixture), ND – Natural product derivative, S – Synthetic drug, S* – Synthetic drug (NP pharmacophore), V –Vaccine, NM – Mimic of natural product.[7, 8] (Reproduced with permission.)

The development costs inevitably affect willingness to invest in innovative research that can generate new drugs. Table 2 summarises inflation-adjusted changes in drug development costs. The average cost of developing a prescription drug was reported to be $2.6 billion in 2017, representing a sharp increase of 145% from $1.2 billion in 2005. The drug development costs include an initial budget of $1.4 billion, an estimate of $1.2 billion provided by the investors during the ten or more years of research and development, and a further $312 million spent on post-approval development.[6, 35]

Table 2. Inflation-adjusted analyses of drug development costs in the period 2003-2012.[36]

Study period	**Clinical success rate (%)**	**Cost estimate ($)**
First-in-humans, 1983-1994	21.5	802 million
First-in-humans, 1989-2002	24.0	868 million
Company R&D expenditures, 1985-2001	24.0	1.2 billion
First-in-humans, 1990-2003 (large molecule)	30.2	1.2 billion
2000-2002 (launch)	8.0	1.7 billion
2009 (launch)	N/A	2.2 billion
2007	11.7	1.8 billion
In clinical development, 1997-1999	10.7	1.5 billion

The steady rise in costs comes despite efforts in recent years to improve efficiency in pharmaceutical research and development. This increase is attributed to scrutiny in clinical trials, a greater focus on chronic and complex diseases as well as tests for insurers seeking comparative drug effectiveness data.[35] A study conducted by DiMasi *et al.*,[36] which involved the observation of 1442 self-originated compounds of top 50 pharmaceutical firms revealed the average clinical success rate to be 11.83%.

However, despite rising costs and improved drug development procedures and associated assays, clinical success rates have been declining in recent years.[37] Moreover, declining innovation has become dominant issue in the pharmaceutical industry due to the poor oral bioavailability of new lead compounds and the lengthy duration, usually ten years or more, between the initial discovery of a potential therapeutic agent and its subsequent launch as a new molecular entity on the market. Drugs reaching the market today are typically products of research programmes initiated at least ten years ago.[27, 38] Normalised drug output has remained constant. Consequently, the industry has placed each aspect of the drug discovery process under scrutiny and has begun to apply ADMET analysis to lead compounds.[39]

Clinical phase transition rates reflect where drug development fails most and thus informs the need for appropriate interventions to effectively control drug development costs. Of the 1738 new chemical entries that were developed during the sub-periods 1993-1998 and 1999-2004,

the phase transition rates were *ca.* 65% for phase I to phase II clinical studies, *ca.* 40% for phase II to phase III, and *ca.* 65% for phase III to regulatory review (Figure 3). Success rates of 90 - 100% for regulatory review to final approval were obtained. The overall clinical succession rate was 16% for both sub-periods 1993-1998 and 1999-2000, but the *ca.* 65% entry into phase II clinical testing and the subsequent *ca.* 40% phase II to III transition demonstrate that attrition occurs mainly in the early stages of discovery (Phase I and II) for drugs initiated into clinical trials.[36, 40]

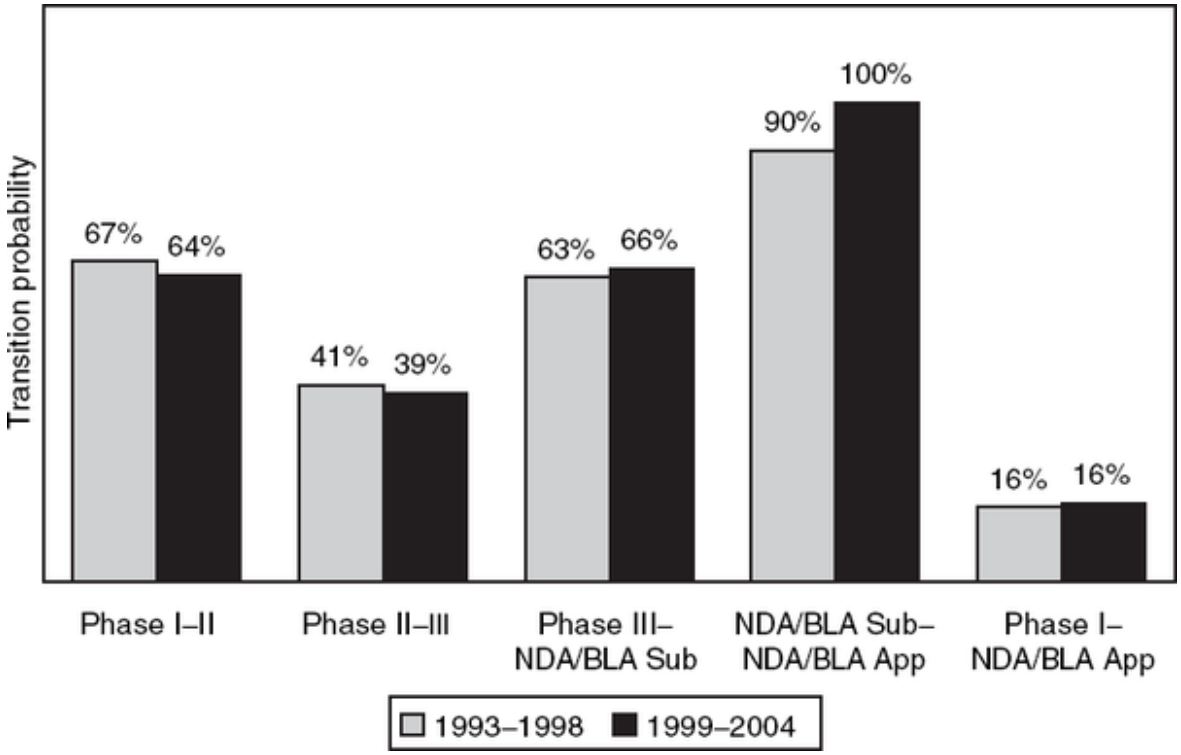

Figure 4. Phase transition and overall clinical succession rates for new molecular entities during the sub-periods 1993-1998 and 1999-2004.[40] BLA, biologics license application; NDA, new drug application. (Reproduced with permission.)

Various factors have collectively contributed to a decline in the discovery of new drugs from natural products. These include: the introduction of high-throughput screening (HTS) against defined molecular targets; the development of combinatorial chemistry; advances in molecular biology, cellular biology and genomics; a focus on therapy development for complex and chronic diseases and the preservation of biological species as per the Rio Convention on Biological Diversity. Consequently, rather than following traditional resource intensive natural product programmes that are premised on extract-library screening, bioassay-guided isolation,

structure elucidation and follow-on upscaling, modern drug discovery now involves rapid screening, hit identification and hit-to-lead development. [34]

Although ongoing research has elicited renewed interest in natural products as a source of chemical diversity and lead generation, modern drug discovery protocols tend to utilize defined synthetic chemical libraries.[34] However, characteristics, such as chemical diversity, significant numbers of chiral centres, high steric complexity, significantly low ratios of aromatic rings to heavy atoms, higher numbers of hydrogen-bond donors and acceptors, diversity of ring systems, greater molecular rigidity and biochemical specificity, often make natural product molecules ideal lead structures for drug discovery despite their exceptions to the Ro5 guidelines.[34, 41] Modern drug discovery programmes have occasionally developed beyond Ro5 drugs to afford drugs, that are not natural products, with important medicinal activities. For example, the orally active anti-cancer drug, Navitoclax **9**, opens the scope for drug discovery potential beyond the limitations of the Ro5. [24] Cyclosporin **8** is another "beyond Ro5", natural product prototype with multiple intramolecular hydrogen bonding possibilities and solvent-dependent conformational mobility.[42] With appropriate formulation, cyclosporin is orally bioavailable and adopts various intramolecular hydrogen-bonding patterns depending on whether the solvent medium is aqueous polar or non-aqueous polar.[43] Navitoclax is a "beyond Ro5", oncology drug currently in Phase III clinical studies; its therapeutic target is a protein-protein-interaction that was discovered using fragment screening. The discovery of Navitoclax illustrates that oral activity for "beyond Ro5" synthetic compounds is possible and also that elegance and resources, and serendipity are crucial for the discovery of "bRo5" drugs.[24]

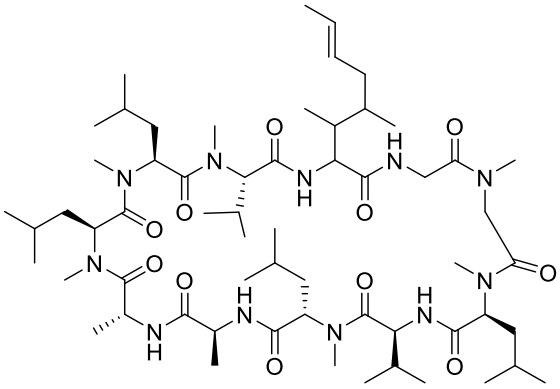

Cyclosporin **8**

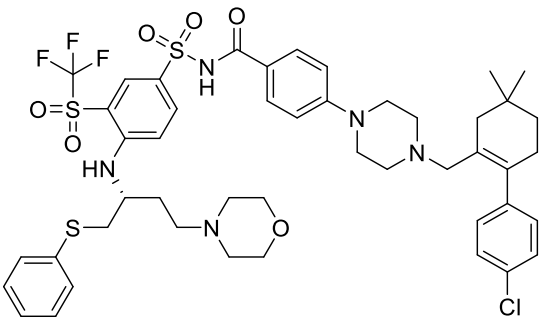

Navitoclax **9**

Figure 5. Representatives of "beyond Ro5" drugs: the natural product cyclosporin **8** and the synthetic molecule Navitoclax **9.**[24]

Because the interfaces involved in protein-protein-interactions (PPIs) are usually flat and large (1000 – 2000 A^2) compared to the deep clefts and cavities (300 – 500 A^2) required to bind smaller Ro5 compliant drugs, PPIs pose a special challenge for drugs that conform to the Ro5 limits. Inhibitors of PPIs therefore require physiochemical properties outside the Ro5 guidelines. It is the exclusion of Ro5 non-compliant drugs in most HTS screening libraries that has led to their failure in the discovery of PPI inhibitor leads. Furthermore, the PPIs depend on multiple, small energetic interactions across a broad area rather than the smaller, 3-dimensional cavities characteristic of monomeric protein drug targets. Albeit with considerable effort, the PPIs have in recent times, moved from "undruggable" to "druggable" targets largely due to advances in screening and genomics. [24]

1.3. Receptors of Ro5 and bRo5 drugs

The oral administration of a drug is usually feasible when it has been established to be orally bioavailable and thus able to diffuse through the lipid bilayer membrane of the gastrointestinal tract. While the Lipinski Ro5 guidelines have been crucial in the development of orally bioavailable drugs, it has become apparent that there are orally bioavailable drugs that violate the Ro5 guidelines – especially metabolites of natural products. The latter class of drugs generally have structural features that allow them to act as substrates for naturally occurring transporters. Biophysical forces, such as hydrophobic and hydrogen-bonding interactions, which are involved in oral absorption, are similar to those involved in carrier-mediated drug absorption through interaction of the drug with proteins. [33, 44]

Carrier-mediated cellular uptake is likely to be far more widespread than is currently understood. This view is supported by:[33]

i) many discoveries of specific cases in which drugs are known to be transported into cells through defined carriers,
ii) the postulation that carriers exist to enable certain lipophilic cations to cross membranes through diffusion,
iii) the fact that drugs accumulate greatly in certain tissues and
iv) cellular uptake can be enhanced by a prodrug approach using moieties that are known to be substrates for carriers

The diffusion of drugs into membranes from the aqueous media involves the making and breaking of hydrogen-bonds and, depends on the lipophilicity or hydrophobicity which tend to increase with molecular mass. The diffusion therefore relies on the number of hydrogen-

bond acceptor and donor atoms, polarity and, to some extent, the mass of the molecule. These factors are crucial in estimating the absorption, distribution, metabolism and excretion (ADME) of a drug regardless of its bioavailability being *via* diffusion- or carrier-mediated processes.[33]

Because poor bioavailability can result in variable exposure to an active drug, which may lead to side-effects, sufficient understanding of the molecular properties in relation to oral bioavailability is an essential consideration in the development of bioactive molecules as therapeutic agents. *Molecular flexibility* has also been identified as a requirement for membrane permeation whereas *water complexation* by the conformational constraints associated with amides and high polar surface areas negatively affect bioavailability. Transcellular diffusion can also be limited by enzymatic clearance factors that include energy-driven export from the blood to the gut by transporter enzymes of intestinal or liver cells (e.g. P-glycoroteins), or by first-pass metabolism involving oxidation by cytochrome p-450, sulfonation, glucuronidation, glycosylation, *etc*. [44] A drug may be chemically modified by attaching soluble macromolecules, such as proteins, polysaccharides, monoclonal antibodies or synthetic polymers, through degradable linkages, thus selectively altering its biodistribution, pharmacokinetics, solubility or antigenicity. For example, considerable efforts have been made to design active transport mechanisms involving proteins of the ATP-binding cassettes to enable permeability into the normally impermeable blood brain barrier, which contains tight endothelial cell junctions which prevent molecules from entering the central nervous system.[45, 46]

1.3.1. Pharmacokinetics of anti-HIV drugs

The human immunodeficiency virus is a retrovirus that can be transmitted *via* sexual contact, sharing needles, blood transfusions, and from mother to child in infected individuals during pregnancy and breast feeding. It is the causative agent of the human immunodeficiency virus/acquired immunodeficiency syndrome (HIV/AIDS), a disease that continues to instill fear, revulsion, despair and utter helplessness among many communities, especially in under-developed societies. Researchers in various fields of study, government departments, non-governmental organisations and many other societal fraternities each have grievous tales about HIV/AIDS, with statisticians forecasting 40 million deaths from the disease in the twenty-first century.[47]

Since the discovery of the human immunodeficiency virus (HIV) in 1981, a cascade of anti-HIV drugs targeting the virus enzymes has been developed. Human immunodeficiency virus

is a member of the lentivirus genus *retroviridae* and exists in two, closely related strains, HIV-1 and HIV-2. HIV-2 has 40% genetic identity with HIV-1 and is less virulent than HIV-1.[48, 49] HIV is an RNA virus that contains the enzyme, reverse transcriptase (RT), which transcribes the viral genomic RNA into a DNA copy that is eventually integrated into the host cell genome by the enzyme integrase (IN). Entry of the RNA virion is mediated by interaction of the extracellular domain of HIV-1 gp120 and cellular chemokine co-receptors, CCR5 and CXCR4, as well as CD4 cells. Following binding to the co-receptors the virion enters the host cell, and retro-transcription of the viral RNA to a double-stranded DNA is effected by the viral reverse transcriptase.[47] Virion maturation is effected by the enzyme, protease (PR). The life-cycle of the virus is illustrated in Figure 6 and explicitly covered elsewhere.[50,51, 52]

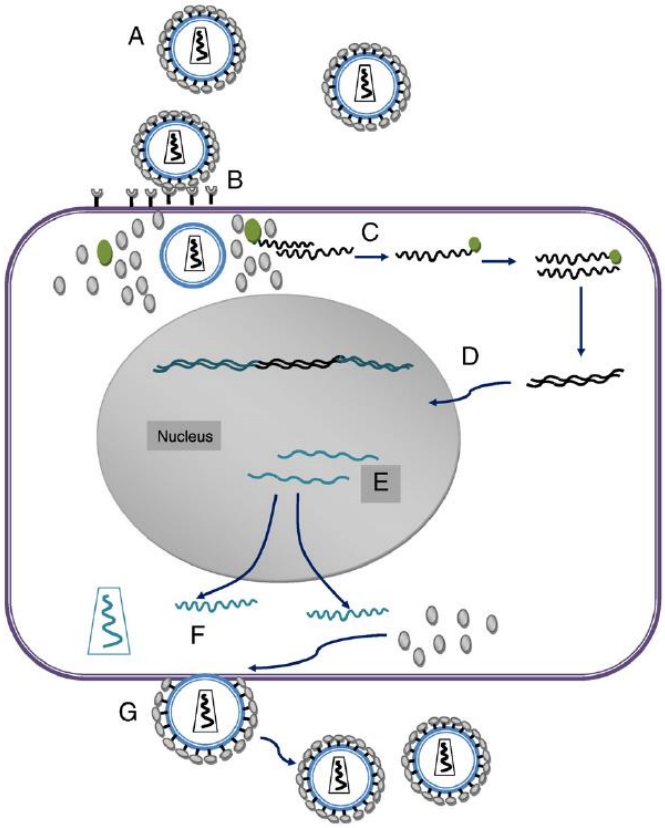

Figure 6. HIV life cycle: A. HIV virion; B. fusion and entry into the host cell; C. reverse transcription; D. integration involving integrase; F and G. virion maturation involving protease and release.[47] (Reproduced with permission.)

Complete eradication of the HIV infection by anti-retroviral therapy is impeded by the existence of intracellular and anatomical reservoirs. *Cellular reservoirs* include: (i) quiescent $CD4^+$ lymphocytes; (ii) follicular dendritic cells; and (iii) macrophage and dendritic cells, while *anatomical reservoirs* include the central nervous system (CNS) and the male genital tract. In addition, the intestinal tract can act as an infection reservoir.[46, 53]

1.3.2. Potential HIV-1 vaccination

According to the World Health Organisation (WHO), a vaccine is a biological preparation that imparts immunity against a particular disease. Vaccines generally contain a harmonised agent, usually microbial, that resembles a disease-causing microorganism.[54] They provide long-term protection against infection in the recipients. Despite the enormous genetic complexity of the HIV-1 virus and the inherent differences in its envelope proteins, there has been significant progress in the quest for an HIV-1 vaccine. A vaccine that induces strong T-cell-mediated immune response in the absence of broadly neutralising antibodies may prove beneficial. Such vaccination may prevent the early and massive destruction of CD4 T cells and thus reduce secondary transmission through viral replication. [55]

Since HIV-1 infection can occur through the intact mucosal surfaces, vaccination targeted at mucosal sites will be crucial for the initial control of infection in individuals exposed to the virus. Candidate HIV vaccines that are designed to induce a mucosal immune response have thus far focused on HIV-induced B (IgA) and helper T cells or on cytotoxic T lymphocytes (CTL) in the spleen.[56]

The HIV-1 virus has a multiplicity of highly effective defence mechanisms to protect it from antibodies binding with its glycoproteins gp120 and gp41 that are used for fusion. Its antibody recognition mechanism has evolved over time, and has few vulnerabilities.[57] It has been discovered, however, that some broadly reactive human monoclonal antibodies (mAbs), such as b12, 2G12, 2F5 and 4E10, can neutralise various isolated genetic HIV-1 subtypes and a few rare sera from HIV-1 infected individuals exhibit broad neutralising activity. By identifying critical vulnerabilities, broadly neutralising mAbs present promising possibilities for vaccine development.[57] Various sites for such interaction with the viral envelope have been established (Figure 7).

Although anti-retroviral drugs and prophylaxis have significantly reduced the AIDS epidemic, vaccine development is imperative to address HIV infection.[58, 59] The HVTN 702 vaccine trials currently under clinical evaluation in South Africa are estimated to cost $130 million, excluding the cost of the combination vaccine. However, this vaccination does not involve broadly neutralising antibodies, an aspect that many researchers criticize.[59] On the other hand, in 2017, Johnson & Johnson announced a successful development of a well-tolerated vaccine that elicits HIV-1 antibody response in 100% of healthy volunteers in phase 1/2a.[60]

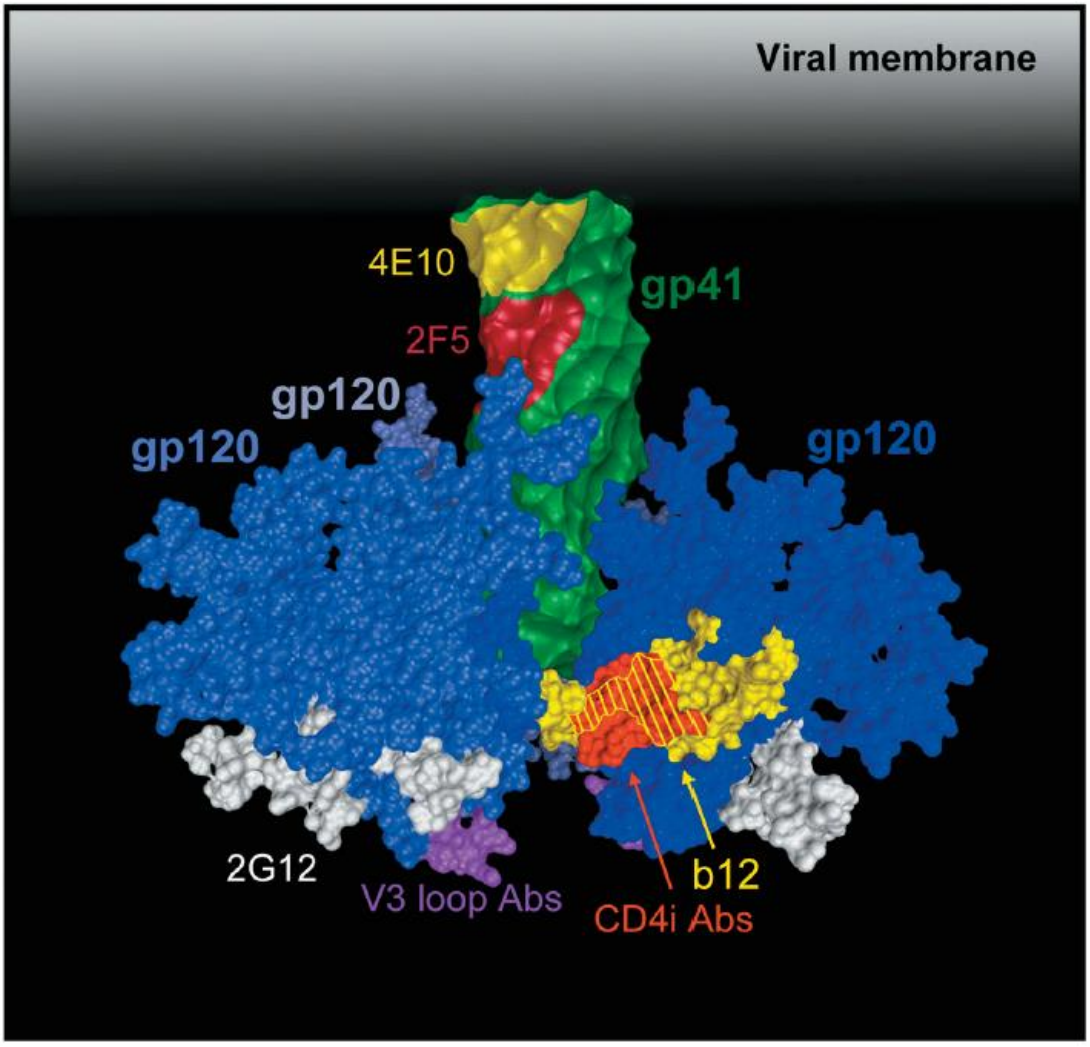

Figure 7. An *in silico* homology model depicting locations of the HIV-1 envelope (gp's 41 and 120) spike where broadly neutralising mAbs interact.[57] (Reproduced with permission.)

1.3.3. Anti-retroviral therapy

Approved anti-HIV drugs can be divided into seven groups depending on the target within the replicative cycle of the HIV: (i) nucleoside reverse transcriptase inhibitors (NRTIs); (ii) nucleotide reverse transcriptase inhibitors (NtRTIs); (iii) non-nucleoside reverse transcriptase inhibitors (NNRTIs); (iv) protease inhibitors (PIs); (v) fusion inhibitors (FIs); (vi) co-receptor inhibitors (CRIs) and (vii) integrase (IN) inhibitors.[61]

More than 78 million people around the world have become infected with HIV and 39 million people had died of AIDS related illnesses by the end of 2016.[62] However, the average rate of new infections has dramatically declined from 2.6 million in 2015 to 1.8 million in 2016. New infections among young children have declined by 58% from an average of 580 000 in 1997 to

240 00 in 2001.[63] Out of the global 35 million people infected with HIV, Sub-Saharan Africa had 24.7 million people living with the virus, 1.5 million new annual infections accounting for 70% new global infections and over 1 million annual deaths. In the sub-period 2005 to 2013, Sub-Saharan Africa had a 39% decline in mortality rate, a decline in new infections by 33%, a dramatic 47% decline in new HIV infections among children, and increased treatment coverage to 37% of people living with HIV.[60, 64, 65]

In view of the urgent need to preserve the health and well-being of HIV infected individuals, various therapeutic strategies have been devised. These include the rational design of drugs that target specific viral enzymes. Enzyme targets that have been identified as crucial for sustaining the life-cycle of HIV are: reverse transcriptase (RT) which is responsible for transcription of the viral single-stranded RNA genome to double-stranded proviral DNA; integrase (IN) which facilitates integration of viral DNA into host DNA; and protease (PR) which cleaves the precursor viral polyproteins into smaller mature viral proteins.

The need for continuous development of anti-retroviral (ARV) drugs is largely influenced by the development of resistance to current drugs due to mutations during viral replication and patient non-compliance, which lead to treatment failure.[66] The introduction of highly active anti-retroviral therapy (HAART) has improved disease prognosis and contained opportunistic diseases. HAART typically involves the use of two nucleoside reverse transcriptase inhibitors (NRTIs) plus either a protease inhibitor (PI) or a non-nucleoside reverse transcriptase inhibitor (NNRTI). HAART thus targets intracellular steps in the viral life-cycle orchestrated by viral RT and PR. Health complications associated with HAART have prompted the development of novel and potent anti-retroviral agents that inhibit entry of HIV into the host cell by preventing binding of the HIV envelope gp120 to the host cell CD4 receptor, by blocking the chemokine receptors, and/or by inhibiting fusion into the cell, which is facilitated by gp41.

However, the benefits of anti-retroviral therapy like HAART can still be compromised by the development of drug resistance associated with mutations of proteins targeted by the anti-retroviral agents. Transmission of drug resistant HIV-1 strains is also a growing concern as such strains generally express resistance to at least one class of the available anti-retroviral agents. Resistance complicates ongoing efforts to control the viral replication.[66] There are now more anti-retroviral drugs approved for HIV than for all other viral infections combined.[67] In fact, by 2008 there were twenty-five anti-retroviral drugs approved for the treatment of HIV.[48, 61, 67] These drugs have transformed the prognosis of HIV patients from high morbidity and mortality to a chronic, manageable but still complex disease. The advent of anti-retroviral

therapy on the prevention of mother to child transmission as well as the development of anti-retroviral prophylaxis - Pre-exposure prophylaxis (PrEP) and Post-exposure prophylaxis (PEP), are remarkable achievements.

According to Auerbach and Hoppe,[68] PrEP and PEP flag important socio-psychological aspects that must be addressed in order to effect behavioural change among people at risk of HIV infection. Thus, taking into account the reality of one's circumstances, the nature of one's sexual and drug practice, prophylaxis provides a wide range of choices one can take about how best to prevent HIV infection. PrEP in particular, may change the common notion of protected and/or unprotected sex and (un)safe drug use. In spite of the availability of these therapies, people are responsible for taking care of their own lives. PrEP and PEP confers agency on sexual partners who depend on the willingness of partners to use condoms because they are as available as a once-daily pill. [68, 69]

There is a rising demand for anti-retroviral drugs for people for whom first-line therapy has failed. These include: people with tuberculosis (TB) and other opportunistic diseases; children; and pregnant and lactating women. Global funding for HIV in 2013 was *ca*. $10 billion with a greater portion of the funds going toward service provision than to research on ARVs. The provision of service for established patients averaged $177 per patient per year (ppy) for first-line ARV combination therapy whilst generic versions averaged $122 ppy. There is therefore a need to develop easy to administer, patient-friendly and potent ARVs that are less expensive. Affordable anti-retroviral therapy (ART) would bring much needed relief in global health funding, especially in resource-constrained countries where funds are desperately needed to address other pressing needs.[64]

1.3.3.1. New generation anti-retroviral regimens

The efficiency of HAART has been hindered by drug resistance, toxicity, tolerability problems and monitoring requirements. In HAART, at least three ARVs are required to promote efficiency and to forestall the development of drug resistance. Its principles inspired the advent of optimal combinations of ARVs of varying classes in a single daily tablet with improved patient compliance and normalised life expectancy.[70] While the new regimen offers great advantages over previous regimens, it remains sub-optimal in regard to the development of resistance, the potential for renal toxicity, neuropsychiatric side-effects, possible interaction with contraceptive implants and cost. The World Health Organisation (WHO) preferred first-line ART regimen is comprised of efavirenz **10**, tenofovir disoproxil **11**, used as the fumarate

(TDF), and either lamivudine **12** or emtiricitabine **13**. The second-line regimens cost more because they involve use of compounds, which are difficult to manufacture, and complex protease inhibitors. Their generic regimens cost over $300 ppy.[64]

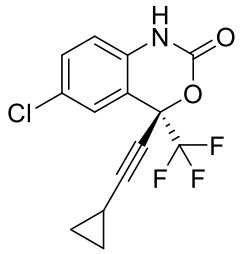

Efavirenz **10**

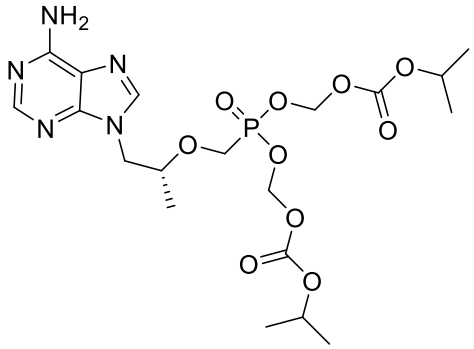

Tenofovir diisoproxil **11**

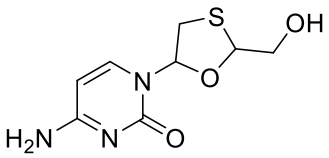

Lamivudine **12**

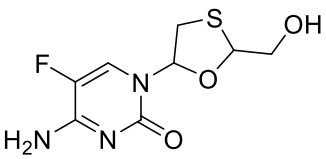

Emtiricitabine **13**

Figure 8. Anti-retrovirals in WHO's approved first-line one-tablet regimen. [64]

The development of resistance to the first-line regimens is associated with viral mutations due, mainly, to the absence of routine virological monitoring, and is often encountered in resource-limited settings. On one hand, decentralisation of service delivery, standardised treatment regimens and simplified treatment monitoring in resource-limited settings saves costs in the much needed expansion of ARV therapy, but exacerbates the rate of resistance development on the other.[71] Options for second-line treatments are very limited and require a delay in changing from the first-line to the second-line treatment.[72, 73] The South African national treatment guidelines recommend a routine two months delay in the initiation of second-line treatment for patients encountering resistance. Although the delay period is long, it is required for laboratory confirmation of virologic failure – a period which is lengthier for patients living in under-resourced areas.[73] The determination of second-line and subsequent regimens is influenced by their affordability.

An underlying principle in synthetic medicinal research is, where possible, to develop simple and efficient methods to access structurally complex and diverse molecules from readily available and inexpensive starting materials. In the present study, we employ Baylis-Hillman

methodology to generate highly functionalized adducts which serve as convenient scaffolds to access 2-quinolones or indolizines with the potential for further synthetic elaboration.

1.4. Quinolones in Medicinal Chemistry

The advent of synthetic quinolones as competitive medicinal agents dates back to the discovery of the 4-quinolone antibiotic, Nalidixic acid **14**, in the early 1960s.[74] Subsequently, a succession of quinolone derivatives containing a fluorine substituent were introduced, adding to the arsenal of quinolone-based antibiotics. The fluoroquinolones were employed in the treatment of sexually transmitted diseases and infections of the urinary tract, respiratory tract, gastrointestinal tract, bones and joints.[75] Apart from the well-known, medicinally active quinolines,[75] 2- and 4-quinolones and the isosteric coumarins and chromones exhibit a wide range of biological activities, including antimicrobial, antimalarial, anti-inflamatory, antitumor, anti-parasitic and anti-HIV. Ciproflaxin **15** represents a class of established, synthetic 4-quinolones that possess significant biological activities. Among the twenty-five anti-HIV compounds approved by 2009 were the quinoline and 4-quinolone based drugs saquinavir **16** and elvitegravir **17**, respectively.[61, 76]

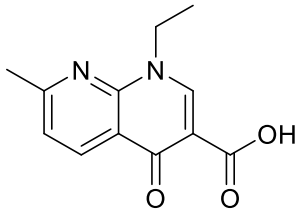

Nalidixic acid **14**

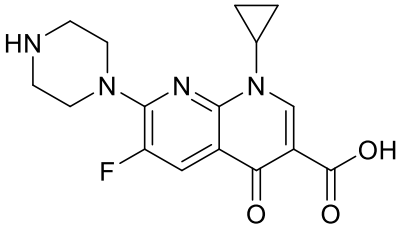

Ciproflaxin **15**

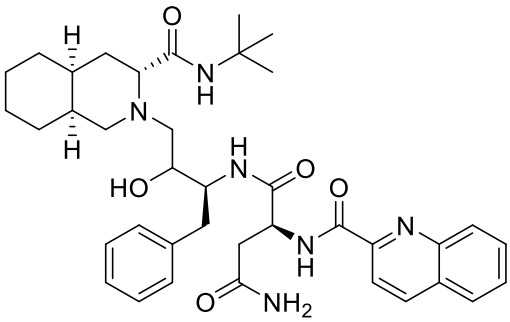

Saquinavir **16**

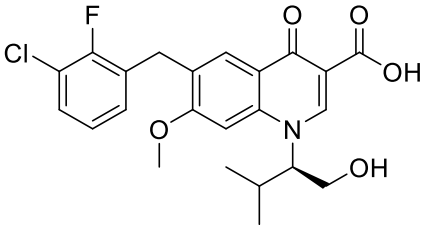

Elvitegravir **17**

Figure 9. Representatives of quinoline and 4-quinolone derivatives with important medicinal activities.

Many compounds containing the 2-quinolone core are present in various alkaloids, especially in the *Rutacae* family, and have been found to possess interesting biological activities. There has been considerable interest in developing facile synthetic methods to access 2-quinolones (also called carbostyrils or 1-aza coumarins) as anticancer, antibacterial, antihypersensive, cardiotonic, anti-inflamatory and antiviral agents and, in our case, as potential anti-HIV agents. It has been established that 4-substituted 3-phenyl-2-quinolones exhibit high binding affinity to the glycine site of the *N*-methyl-D-aspartate (NMDA) receptor, an important target for candidates developed for the treatment of several neurological and neurodegenerative disorders.[74] In addition, amides of 3-hydroxy-2-quinolone-4-carboxylic acid exhibit affinity for the 5-HT_3 serotonin receptor.[77, 78]

Using an *in silico* screening approach, the hydrophobic cavity of the C-terminal domain of the HIV-1 capsid protein has been targeted to explore its ability to accommodate small synthetic molecules and the 2-(1H)-quinolone-based compound **18** has shown promising activity, with an IC_{50} value of 1.06 µM, while the heterocyclic compound **19**, which contains the pyridine-2-one moiety, exhibited an IC_{50} value of 1.78 µM. The 2-quinolone derivatives were therefore recognised as lead anti-HIV compounds. In addition, the 2-(1*H)*-quinolone ring was found to form a hydrogen bond with an NH moeiety in the hydrophobic cavity.[79] The 2-quinolone isosteres, coumarins, isolated from the roots of *Clausena harmandiana*, a plant that has shown therapeutic activities against stomach-ache, headache and as a health promoting herb, showed cytotoxicity against human small lung cancer, oral human epidermal carcinoma and Vero cell lines thereby reflecting their anticancer activities.[80]

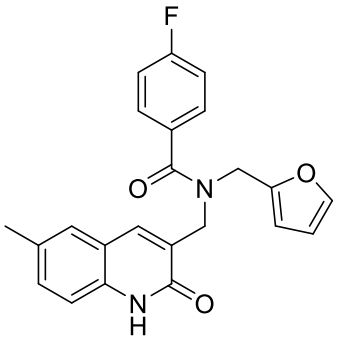

18

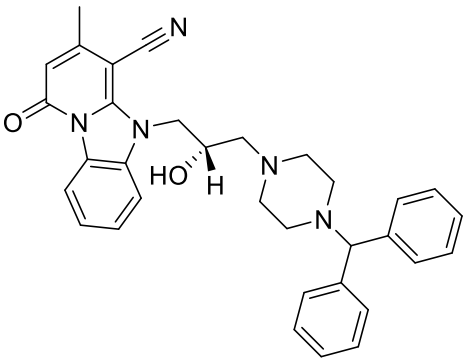

19

Figure 10. Chemical structures of active anti-HIV molecules: 3-[(*N*-benzamido-*N*-furfuryl)methyl]-2-quinolone **18** and the azacarbazole derivative **19**, identified through molecular docking studies.[79]

Although less prevalent than 4-quinolones, a myriad 2-quinolones, that exhibit profound medicinal properties and serve as lead structures for the synthesis of useful drugs, have been isolated from animal and bacterial species.[75, 81] The diverse biological significance of the 2-(1*H*)-quinolone derivatives is remarkably demonstrated in their complementarity to the established antimicrobial quinolines such as quinine, chloroquine and amodiaquine.

O'Donnnell *et al.*[75] reported twenty-six 2-quinolone derivatives that exhibit antimicrobial activities against *Methicillin*-resistant *Staphylococcus aureus*, *Staphylococcus aureus*, *Micrococcus luteus*, *Bacillus subtillis*, *Escherichia coli* and *Salmonella typhimurium.* The 2-(1*H*)-quinolones, namely, rebamipide **20**, repirinast **21** and casimoroine **22** exhibit anticancer, antihistamine and antimutagenic properties, respectively. Various *N*-alkylated 4-quinolones are also known to exhibit antimicrobial properties.[81] Al Amiery *et al.*[82] reported the direct synthesis of *N*-amino-2-quinolone **23**, by refluxing the isosteric coumarin and excess hydrazine in absolute ethanol, and found that the corresponding imine derivatives **24** and **25** exhibited anticancer, antioxidant and antimicrobial activities.

Traditional anti-cancer chemotherapeutic agents act by controlling DNA replication and, consequently, cell proliferation.[83] Most anti-cancer drugs, including doxorubicin and etoposide, for example, effect cell death of tumour cells by targeting topoisomerase which plays a crucial role in DNA duplication.[84] Anti-cancer drugs used in standard treatment are, however, inherently toxic thereby limiting their dosage to patients. Nonetheless, flavonols, such as quercetin **26**, which are also toxic, exhibit anti-cancer activity by scavenging free radicals and inhibiting proliferation of the human breast cancer cell line. Their structural similarity to 3-aryl-2-quinolone has inspired consideration of compounds containing the non-toxic 2-quinolone moiety to extend the arsenal of anticancer drugs.[85]

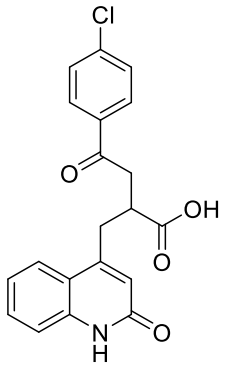

Rebamipide **20**

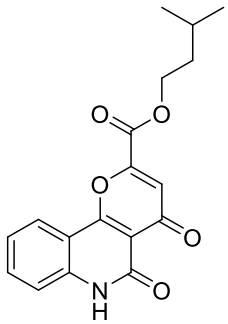

Repirinast **21**

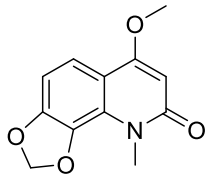

Casimiroine **22**

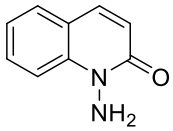

N-Amino-2-quinolone **23**

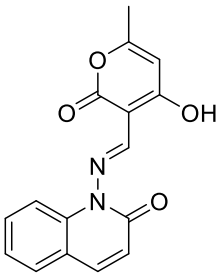

N-Imino-2-quinolone derivative **24**

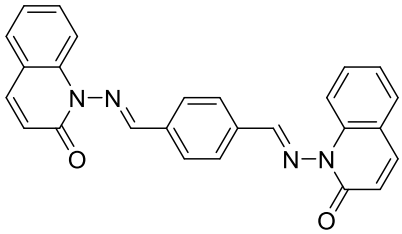

N-Imino-2-quinolone derivative **25**

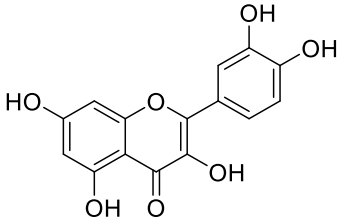

Quercetin **26**

Figure 11. Examples of 2-(1*H*)-quinolone and chromone derivatives with significant medicinal activities. [81, 75]

1.4.1. Properties of 3-substituted 2-quinolones

The ubiquitous, naturally occurring, 3-substituted 2-quinolones exhibit a broad range of pharmacological activities and physiochemical properties.[86] Their strong fluorescent properties and high stability enables them to be employed in laser dyes and optical probes and as donor chromophores in fluorescence resonance energy transfer (FRET) systems.[87] A series of synthetic protocols that include conventional methods, such as Vilsmeier-Haack, Knorr, Friedlander, Larock and various metal-catalysed transformations, have been developed to access 3-substituted 2-quinolones. These methods often involve the use of costly substrates, and 4-substituted 2-quinolones are usually obtained.[88] The 2-quinolones are valuable synthetic intermediates for accessing 2,3-disubstituted quinolines since they can undergo chlorination under Vilsmeier-Haack conditions to afford 2-chloroquinolines which are susceptible to nucleophilic substitution.[77]

1.4.1.1.Fluorescence properties of 2-quinolones

Since protein kinases play a central role in virtually all cell physiology and are therefore involved in the life cycles of antigens, they are ideal targets for therapeutic agents.[89] Several costly methods to screen kinase inhibitors have been reported and include scintillation proximity assay (SPA), which requires radioisotope (RI)-labelled adenosine triphosphate (ATP), and time-resolved fluorescence resonance energy transfer (TR-FRET) demanding luminescent lanthanide complex-labelled antibodies.[90, 91] A non-RI, low cost, convenient and homogeneous method that involves use of fluorescence correlation spectroscopy (FCS) for high-throughput screening of kinase inhibitors has also been developed.[92] Fluorescence correlation spectrometry (Figure 12) is an important and powerful sensing method owing to its high selectivity and ease of operation.[93] It is a single molecule detection technique using a fluorescent probe that sensitively measures fluctuation of the fluorescence intensity emitted from only a few fluorescent molecules that diffuse in and out of a small molecule receptor at the sub-femtolitre level in solution.[92] In addition to screening of kinase inhibitors, FCS has been extensively used in a wide range of applications that include the detection of fluoride ions and mercury and for medical diagnosis.[93, 94]

The fluorescence correlation spectroscopy (FCS) assay is based on competitive binding between a standard fluorescent probe and an inhibitor candidate; if the candidate has low affinity for the kinase or is absent, the probe binds with the target enzyme resulting in fluorescence change.[92, 95] However, if the probe is released from the enzyme to make way for the candidate, and initial fluorescence is restored. FCS is applicable to both active and inactive kinases.[92]

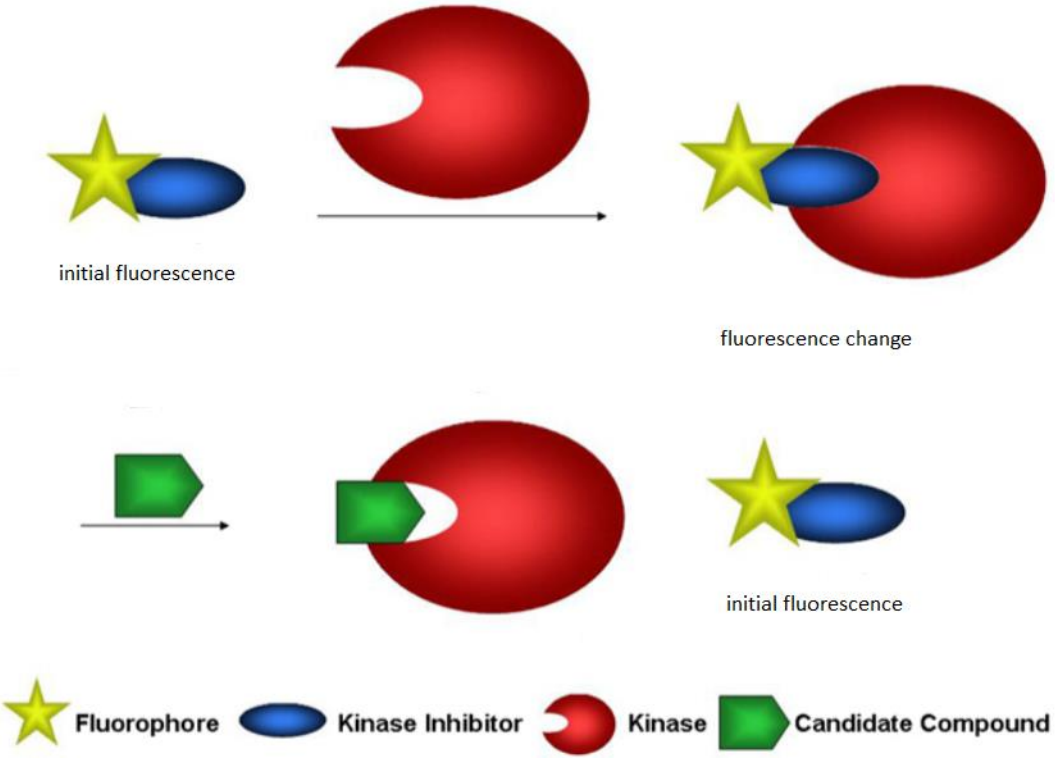

Figure 12. A schematic representation of the fundamentals of the fluorescence spectrometry assay.[92] (Reproduced with permission.)

In 1980, Knierzinger and Wolfbeis[96] demonstrated the fluorescence of a series of 3-substituted 2-quinolone derivatives. Electron-withdrawing groups in the 3-position enhance fluorescence; compound **27**, for example, showed strong fluorescence whereas the unsubstituted 2-quinolone showed suppressed fluorescence. In 2008, Wall *et al.*,[97] using the FCS screening technique, revealed the inhibitory activity of ethyl 4-phenyl-2-(1*H*)-quinolone-3-carboxylate **28** against the macrophage colony-stimulating factor-1 (CSF-1) receptor responsible for controlling growth and differentiation of macrophage lineage. Boron difluoride complexes of 3-cinnamoyl-4-hydroxy-1-methyl-2-quinolone derivatives, such as compound **29**, were recently evaluated as probes for the detection of native proteins using bovine serum albumin (BSA).[98]

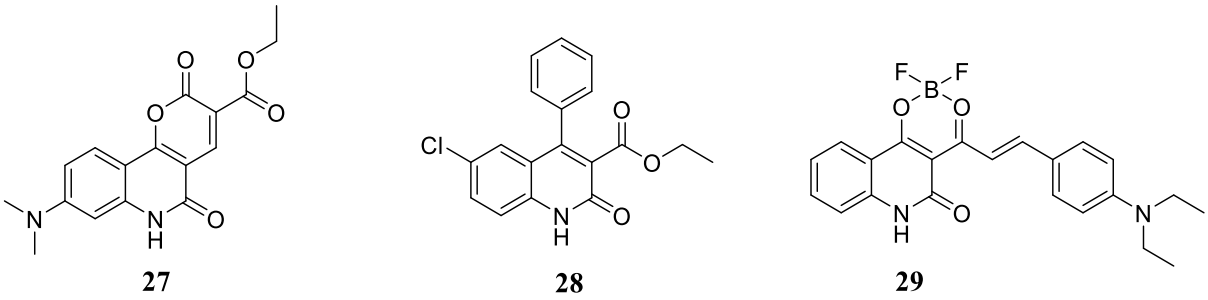

Figure 13. Examples of 2-quinolone-based fluorophores.[96-98]

1.4.2. Synthesis and reactivity of 3-substituted 2-quinolones.

The development of metal-catalysed chemical transformations has significantly expanded the methodology arsenal for synthetic organic chemistry, permitting the formation of various carbon-carbon and carbon-heteroatom bonds and providing one-step access to complex molecular structures from simple reagents. For instance, palladium complexes are employed as catalysts in the annulation of unsaturated molecules such as 1,3-dienes, allenes and alkynes with *o*-halogenoanilines or vinylic halides.[99, 100] Introduction of carbon monoxide expands the utility of the procedure. Inspired by successful carbonylative annulation of *o*-iodophenol with an internal alkyne, annulation involving an aniline **30** and an internal alkyne **31** in the presence of carbon monoxide afforded a 3,4-disubstituted-2-quinolone **32** (Scheme 1). The method, however, requires use of a protecting agent because primary anilines yield unwanted by-products due their nucleophilicity.[77,101]

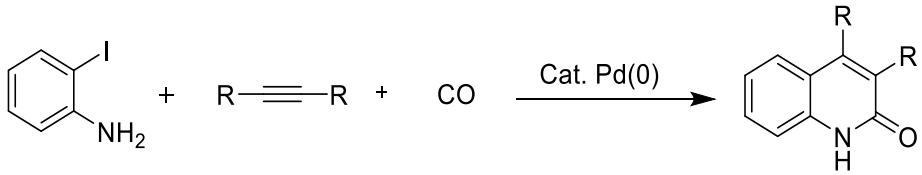

30 **31** **32**

Scheme 1.

In 2015, Zhang *et al.*[100] reported a serendipitous palladium(II)-catalysed synthesis of 3-acetyl-2(1*H*)-quinolone **33** from *N*-(2-formylphenyl)but-2-ynamide **34** in the presence of 2,2'-bipyridine (bpy) in a mixture of acetic acid (AcOH) and 1,2-dichloroethane (Scheme 2). The minor product **35** can, under basic conditions, undergo an intra-molecular aldol condensation to yield a 2(1*H*)-quinolone core. In 2014, Mai *et al.*[102] reported a silver-catalysed, radical, tandem cyclisation to synthesise 3,4-disubstituted dihydro-2(1*H*)-quinolones **36** using alkyl or keto acids **37** as the source of the radicals. Dihydro-2(1*H*)-quinolones have been shown to act as HIV-1 integrase inhibitors, anticancer and antihypertensive agents. In 2013, Ishida *et al.*[99] successfully explored use of silver salts, such as $AgNO_3$, $AgBF_4$, $AgOC(O)CF_3$ and AgOAc, for the synthesis of medicinally important 4-hydroxy-3-phenyl-2(1*H*)-quinolone **40** *via* oxidative cyclocarbonylation of acetylenic anilines **41** with carbon dioxide (CO_2) in the presence of 1,8-diazabicyclo(5.4.0)undec-7-ene (DBU). See **Scheme *2***.

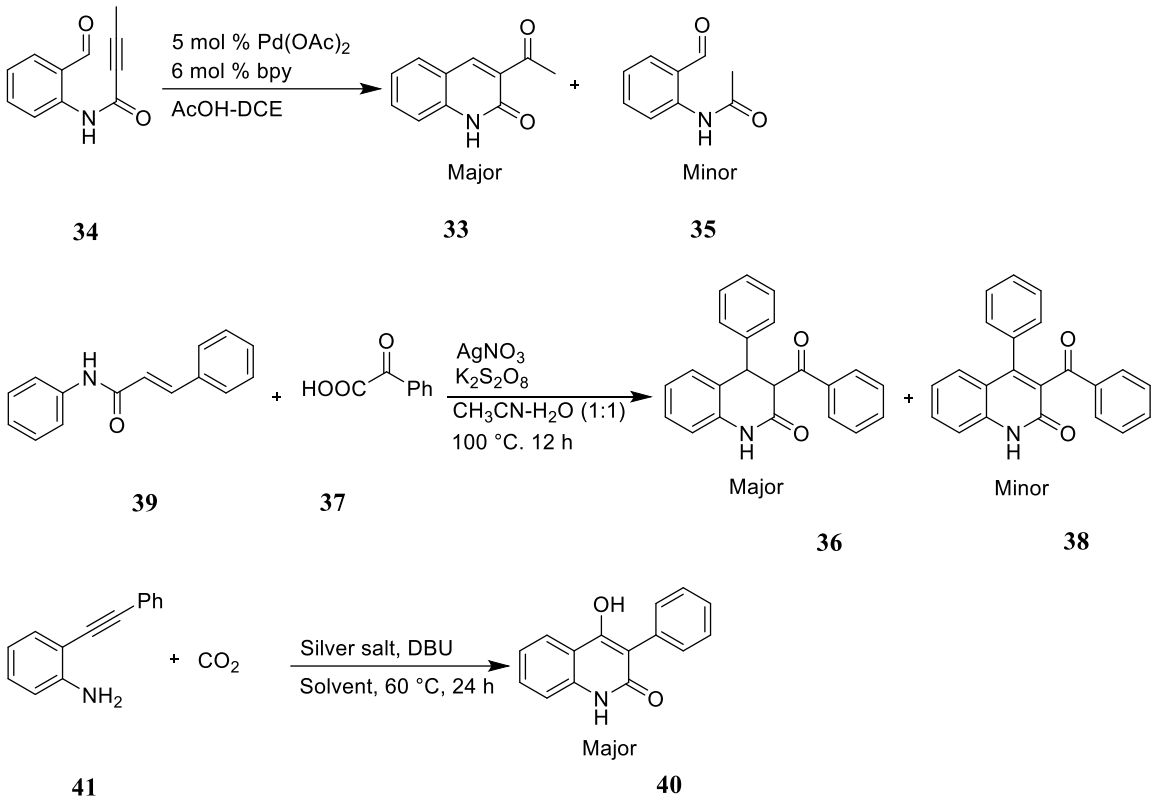

Scheme 2. Recent metal-catalysed syntheses of 2(1*H*)-quinolones

It is synthetically challenging to prepare 3-substituted 2(1*H*)-quinolones since substitution on the quinolone core is favoured at the 6-position. Because of their diverse biological activities, developing routes to access 3-substituted 2(1*H*)-quinolones is of particular interest.[103] The transformation of 4-hydroxyquinolone **42** into the corresponding 3-substituted quinolone **43** has been achieved using the reaction pathway outlined in **Scheme *3***, the final step involving regioselective lithiation of 4-methoxy-2(1*H*)-quinolone **44**.[103]

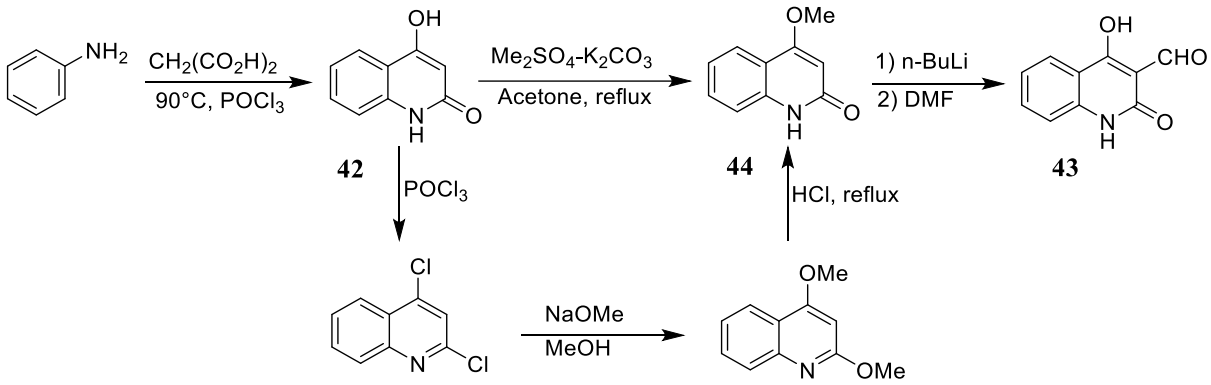

Scheme 3. Pathways to 3-formyl-4-hydroxy-2(1*H*)-quinolone.[103]

Various metal-free chemical transformations to access such 2(1*H*)-quinolones have been developed and include the use of readily available 2-substituted indoles and β-nitroalkenes in the presence of polyphosphoric acid (PPA), a process which proceeds through an unprecedented transannulation pathway (Scheme 4).[88, 82, 85] In addition, reaction of 3-substituted coumarins with amines or 2-substituted indoles may also be used to access 3-substituted 2-quinolones as illustrated in **Scheme 4**. [82, 88]

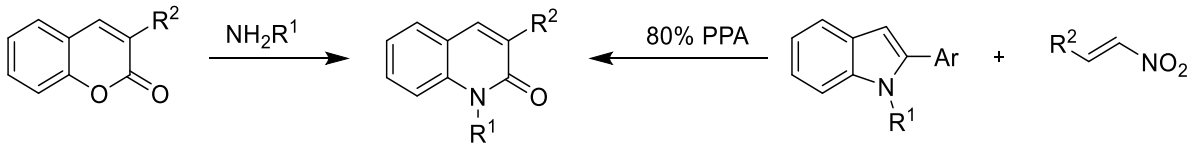

Scheme 4. Synthesis of 2-quinolones from aromatic heterocycles.

1.4.3. Syntheisis of benzannulated beterocyclic compounds using Baylis-Hillman methodology.

The tertiary amine, 1,4-diazabicylo[2,2,2]octane (DABCO)-catalysed coupling of aldehydes and acrylate esters or methyl vinyl ketone, first reported by Hillman and Baylis,[104] provides access to a wide range of aromatic heterocycles that include quinolones, quinolines, coumarins, chromenes and indolizines. These reactions have been extensively explored in our research group.[50, 105-108] The structural versatility of the Baylis-Hillman adducts has prompted the need to develop synthetic methodologies which accelerate their generally slow formation.[109, 110] Factors considered include the nature of the solvent, aldehyde and the catalyst.[111] Use of aldehydes bearing an electron-withdrawing group have shown improvement in yields and reduction in the duration of the reaction, as has the use of methanol-water solvent mixtures.[112] Reactions that involve use of heterocyclic aldehydes such as 2-pyridinecarbaldehyde have been shown to progress to completion in a period of minutes or hours.[113, 114] Optimisation of the conditions for Baylis-Hillman reactions, also known as Morita-Baylis-Hillman reactions, requires knowledge of the physicochemical properties of the aldehyde. The synthesis of a wide range of Baylis-Hillman adducts through nuanced methodologies has been widely reported elsewhere.[107, 109, 112] Herein, we focus initially on accessing quinolone derivatives using Baylis-Hillman methodology.

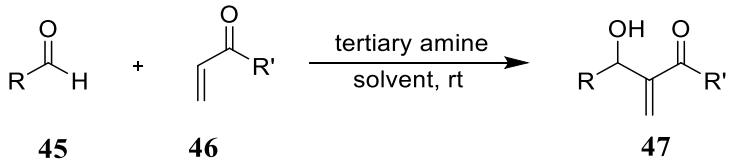

Scheme 5. General representation of the Baylis-Hillman reaction.

Serendipity exposed a veritable cascade of transformations involving the construction of benzannulated heterocyclic products *via* cyclisation of Baylis-Hillman adducts.[105] Subsequently, controlled regioselective cyclisation, using appropriate adducts (**48**, **49)**, permitted access to coumarin, 2-thiochromenone and 2-quinolone derivatives **50**; 2H-chromene, and 2*H*-thiochromenes and 2*H*-quinoline derivatives **51** to quinoline derivatives **52** and to indolizines **53** (**Scheme 5**).[107, 108] The relative unavailability of 2-aminobenzaldehydes prompted the use of the corresponding nitrobenzaldehydes as precursors for nitrogen heterocyclic analogues. The nitro group is reduced to an amino group following the Baylis-Hillman reaction thus permiting intramolecular cyclisation. The chemoselectivity is influenced by the catalyst used, reaction conditions and the nature of acrylate moiety (**Scheme 6**).[107, 111, 115]

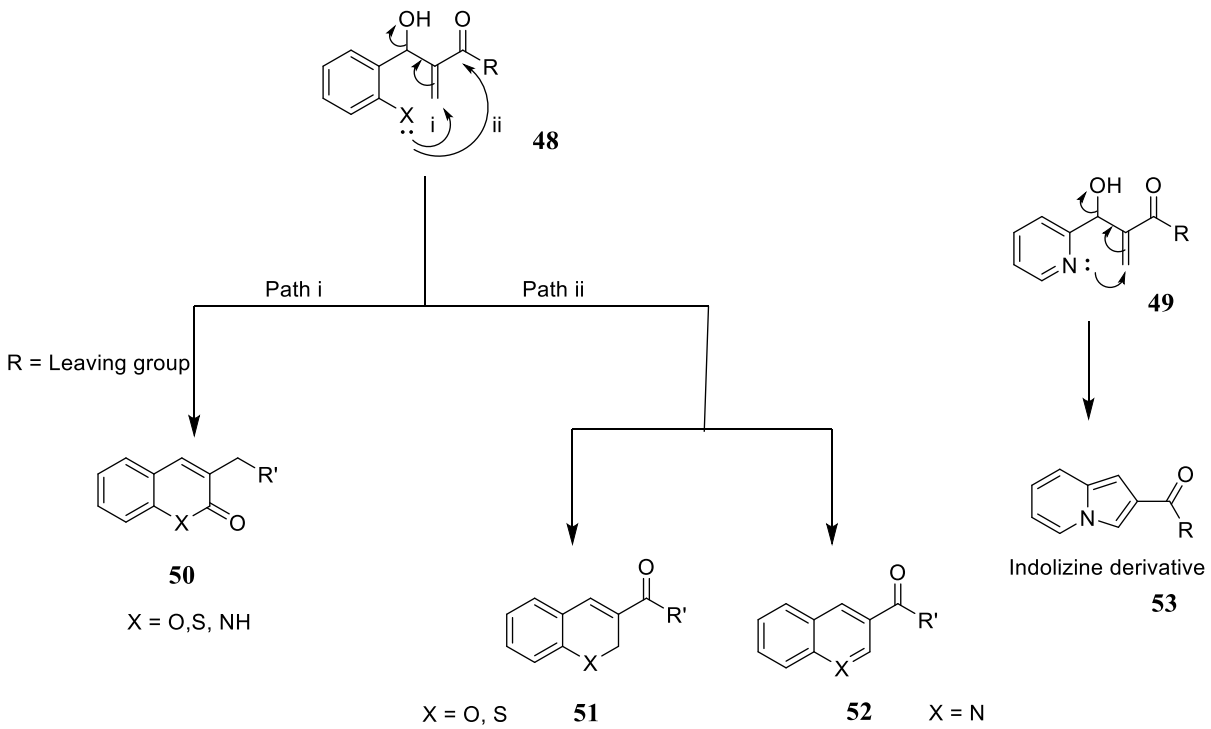

Scheme 6. Regioselective cyclisation of Baylis-Hillman adducts **48** and **49** to: indolizine derivatives **53**; quinoline, chromene and thiochromene derivatives **51** and **52** (Path ii); and 2-quinolone, coumarin and 2-thiochromenone derivatives **50** (Path i).

1.4.3.1.The Baylis-Hillman approach to 2-quinolone derivatives.

2-Quinolones, while less prominent than the isomeric 4-quinolones, nevertheless feature in various compounds which exhibit medicinal properties. Notable amongst these are the 4-aryl-6-chloro-2-quinolinone **54** prepared by Cheng *et al*.[116] as an *in vitro* anti-hepatitis B viral agent;

the 3-indolyl-2(1*H*)-quinolone **55** prepared by Kuethe *et al.*[117] as a KDR kinase inhibitor; the 3-anilino-2(1*H*)-quinolone **56** reported by O'Brien *et al.*[118] as a 3-phohsphoinositide-dependent kinase 1 (PDK1) enzyme inhibitor and, more recently, the 4-hydroxy-2-quinolone-3-carboxamide **57** developed by Mugnaini *et al.*[119] as a cannaboid receptor 2 (CB2R) ligand (**Figure 14**).

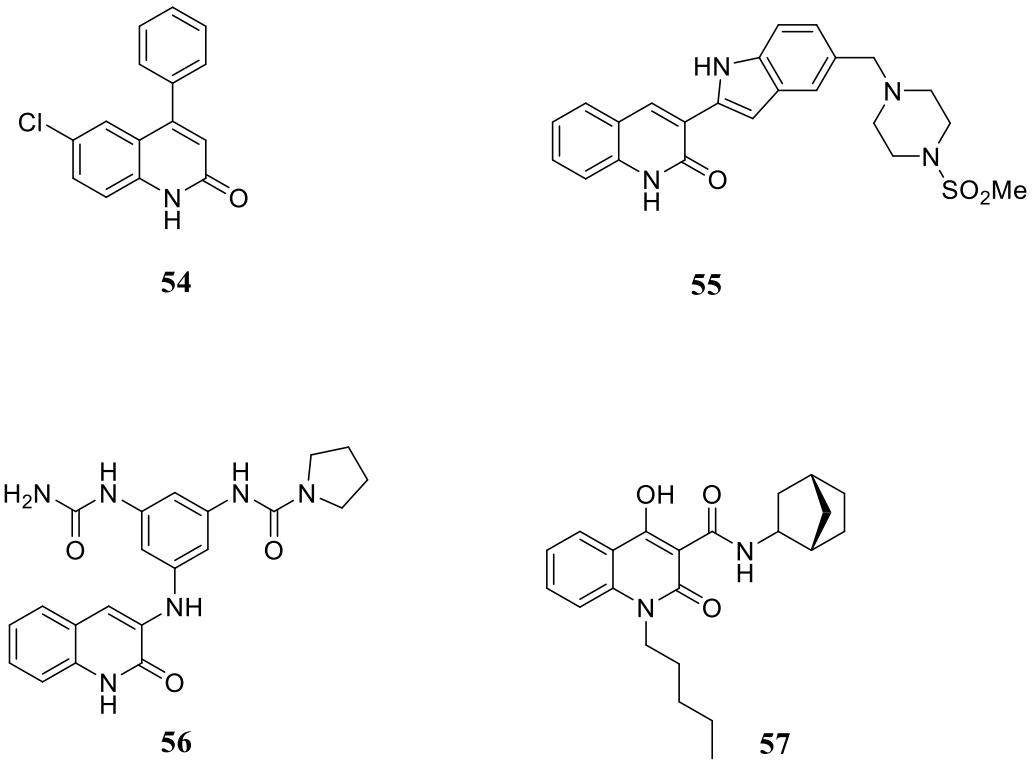

Figure 14. 2-Quinolone derivatives that exhibit a range of biological activities.

Catalytic hydrogenation of the nitro group, using 10% palladium-on-carbon in ethanol, of the MVK-derived Baylis-Hillman adduct **58a** yielded the quinoline-*N*-oxide **60** whilst similar reduction of the methyl acrylate derived-Baylis-Hillman adduct **58b** gave 3,4-dihydro-3-methyl-2-quinolone **61** and 3-methyl-2(1*H*)-quinolone **64** *via* 3,4-dihydro-4-hydroxy-3-methyl-2(1*H*)-quinolone intermediate **63** (**Scheme 7**).[36, 47] Nucleophilic conjugate addition to the Baylis-Hillman adduct **58b** followed by catalytic hydrogenation afforded the 3-substituted 2(1*H*)-quinolones **65**.[51]

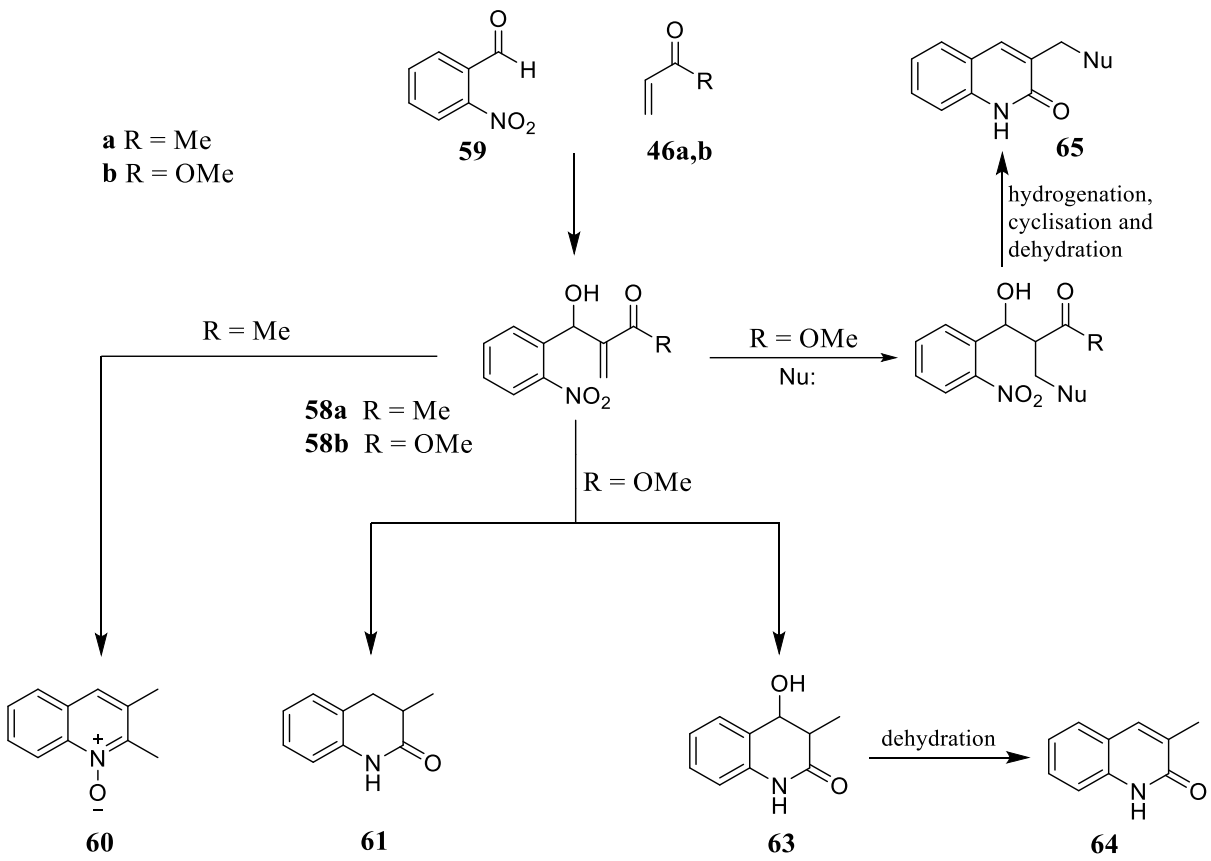

Scheme 7. Catalytic hydrogenation pathways to benzanullated N-heterocycles, using a palladium-on-carbon catalyst, from 2-nitrophenyl Baylis-Hillman adducts.[105, 106]

The chemoselective reduction of the nitro group in the Baylis-Hillman adducts **58a** and **58b**, was first demonstrated by our group in 1998.[105] The concomitant regioselective cyclisation has inspired the development of alternative reduction protocols.[120] Thus, $SnCl_2$ was successfully employed in the synthesis of 3-substituted 2-quinolones **66** as potential antimalarials.[109, 120] Development of new and efficient methodologies for the preparation of these important 2-quinolone moieties continues to be an attractive and interesting area of research. New and efficient reduction methodologies involve use of iron or zinc in acetic acid;[121, 122] use of trifluoracetic acid results in the formation of quinoline-*N*-oxide **67**, [123, 124] whereas use of zinc and a catalytic amount of trifluoroacetic acid results in the formation of 3-substituted 2(1*H*)-quinolone **68**.[125]

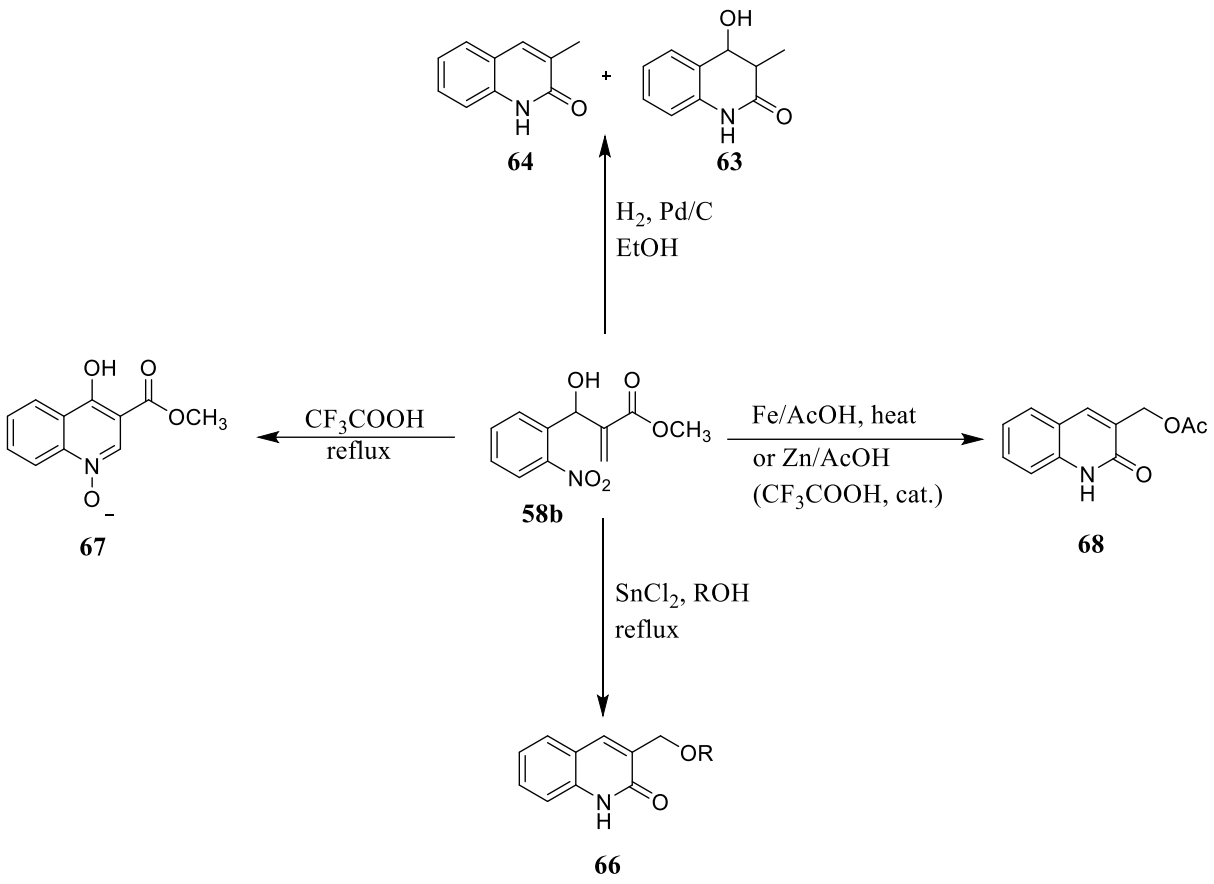

Scheme 8. Reductive cyclisation of Baylis-Hillman ester adducts to afford 2-quinolone derivatives.

The Baylis-Hillman adduct has the potential for further synthetic elaboration and is an ideal scaffold for the synthesis of densely functionalised quinolone moieties. The application of the Baylis-Hillman methodology in the synthesis of quinolines and 2-quinolones followed the discovery of the formation of indolizines from pyridine-2-carboxaldehyde-derived Baylis-Hillman adducts (see section 1.5.2).[105, 111, 126]

1.5. Review of Indolizine chemistry

Indolizine **69** is an interesting heterocyclic system and is present in molecules with diverse biological activities, including anti-cancer, anti-microbial and anti-tubercular.[127, 128] Indolizine is an isomer of indole **70** and is also known as pyrrolo[1,2-*a*]pyridine. It contains 5- and 6-membered fused rings which share a common nitrogen atom and has a planar 10π conjugated electronic structure.[129, 130] Despite the discovery of the anti-cancer activities first displayed by camptothecin **71** in 1966,[131] the biological potential of indolizine derivatives is still largely unexplored, but has been recently affirmed by the discovery of irinotecan **72** and topotecan **73**

as anti-cancer agents,[132] and a series of 1-substituted indolizines as anti-microbial and anti-tubercular agents.[133] Because of their interesting and promising biological properties, indolizines have increasingly found application in biological and pharmaceutical research. Owing to their presence in medicinally important alkaloids, several methods of synthesising indolizine derivatives have been developed. [133, 134]

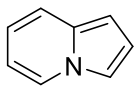

Indolizine **69**

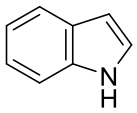

Indole **70**

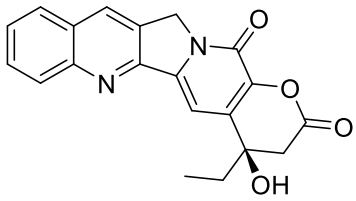

Camptothecin **71**

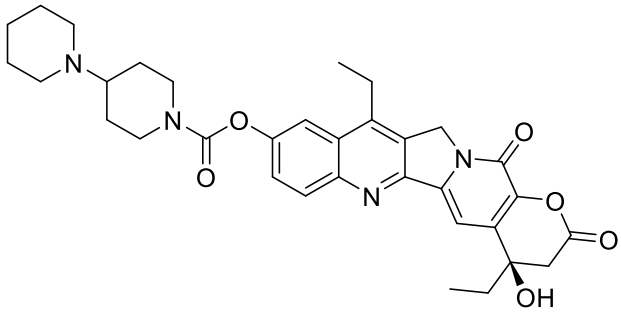

Irinotecan **72**

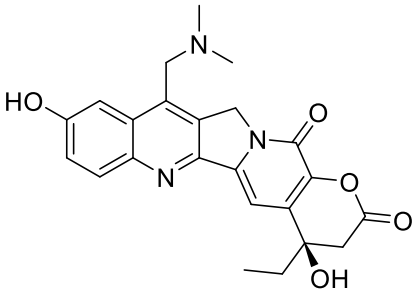

Topotecan **73**

Figure 15.

1.5.1. Biological activity and synthesis of indolizines

Thirty-three years after the first report on the synthesis of thiophene, the Italian chemist Angeli [135] envisaged the possibility of a pyrrolopyridine structure **69** being obtained from an imine-anhydride **74** of pyrrolpyruvic acid which he had prepared. He called the envisaged molecule pyrindole. Twenty-two years later, the first synthesis of pyrindole was reported in 1912 by Scholtz.[135] Scholtz's synthesis of pyrindole, now commonly known as indolizine, involved treatment of 2-methylpyridine with acetic anhydride at 200 – 220 ºC to form a picolide intermediate followed by acid hydrolysis of the intermediate to obtain the indolizine. The indolizine was obtained as a colourless crystalline solid which had weak basicity, reaction characteristics of pyrroles and indoles, and was structurally and chemically isomeric with indole and isoindole. The product was validated by Diels and Alder who established the presence of four double bonds by catalytic reduction of indolizine to a fully saturated molecule, 1-azabicyclo[4.3.0]nonane **75**.[136, 137] The isomeric relationship between indoles and indolizine

suggested that indolizine analogues and certain biologically active indoles might have similar or better physiological activities.[128, 129]

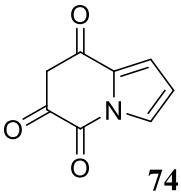

74

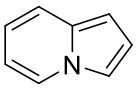

69

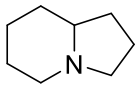

75

Figure 16.

In response to the problematic development of multidrug resistance (MDR) as a result of prolonged cancer chemotherapy treatment, natural products containing indole moieties, such as epothilones, discodermolide and modified taxanes have been found which exhibit activity against MDR-resistant cancer cell lines. In addition, the screening of small synthetic indoles has revealed that the indole-imidazole derivative **76** and indole-glyoxylamides, such as indibulin **77**, showed appreciable cytotoxicity against MDR cell lines.[138] The introduction of the indolizine nucleus in chemotherapy presented a significant development in modern drug development.[129] Compounds, such as **79** and **80** (Figure 17) which contain the indolizine nucleus, also exhibit anti-cancer activity. Moreover, the indolizine derivatives show a variety of biological activities, including CNS depressant **78**, anti-tubercular/anti-microbial (**81** and **82**), and anti-inflamatory characteristics (**83** and **84**).

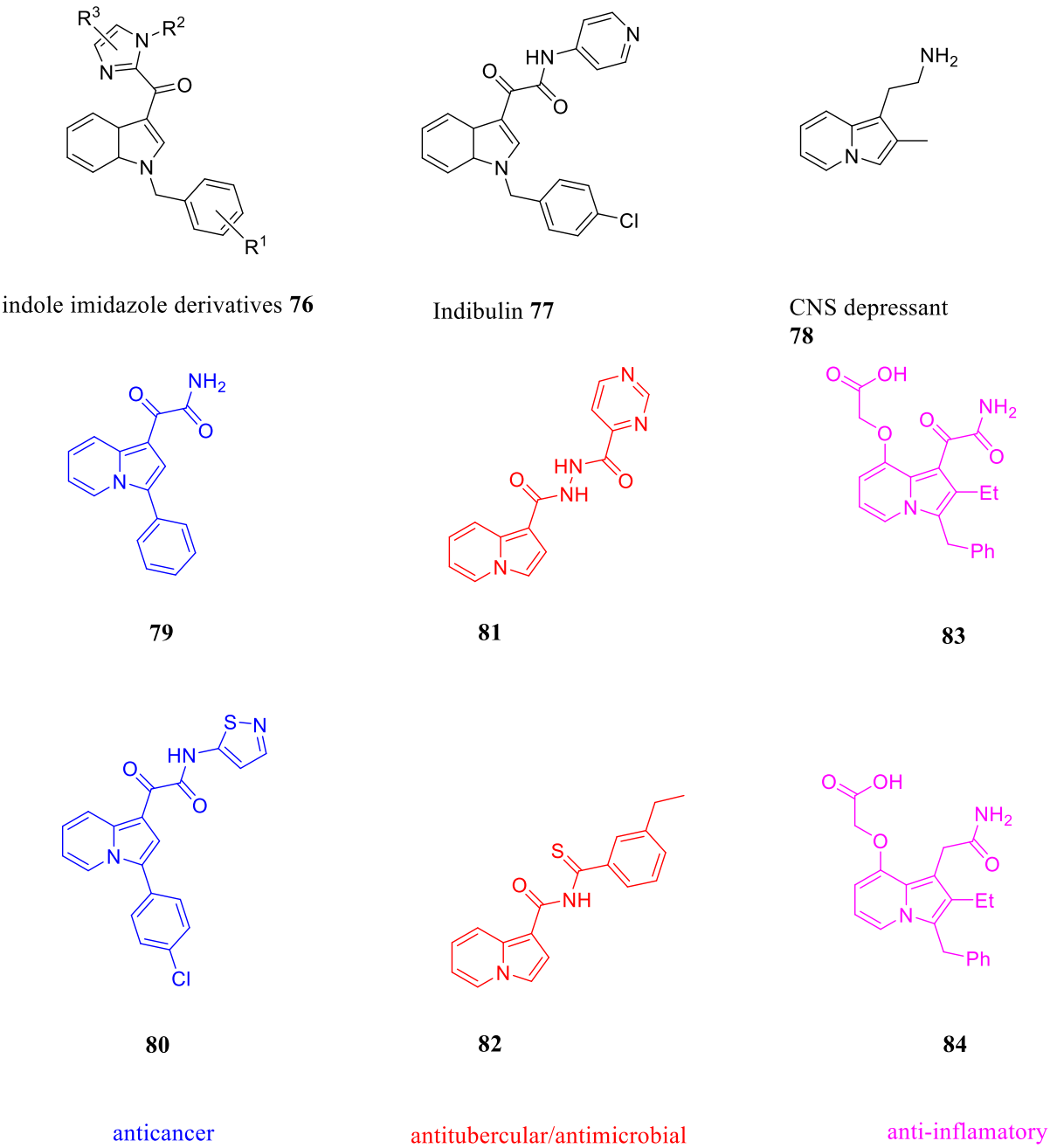

Figure 17. Examples of indole- and indolizine-based molecules with biological activity.

The photophysical properties of indolizines have rendered them suitable for employment as dyes in dye-sensitized solar cells (DSSC) and in organic light-emitting devices (OLEDS).[139] As a result of increasing demand for indolizine derivatives, various synthetic approaches have been explored. These include the transition metal-catalysed cycloisomerisation of readily available non-conjugated 2-propargylpyridines. Thus, Zhang *et al.*, [140] have developed a rhodium-catalysed methodology which proceeds *via* a rhodium-carbene intermediate and, in a mechanistic study, have demonstrated the ruthenium-assisted formation of the indolizine salt

85 (**Scheme 9**) which proceeds *via* a thermally stable but reactive ruthenium-carbene intermediate. The process involves a three-component cross-coupling of the propargylpyridine **86**, an alkyne **87** and a ruthenium complex in the presence of HBF_4.

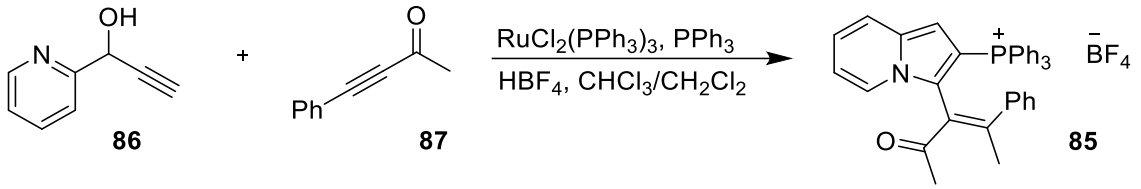

Scheme 9. Ru-catalysed synthesis of 1-substituted indolizine salts.

The significant ring strain present in cyclopropenes, in addition to facilitating a variety of cycloaddition reactions involving 2-cyclopropenylpyridine (**Scheme 10**), has been exploited in the synthesis of indolizines in the presence of $RhCl(PPh_3)_3$ or CuI.[141]

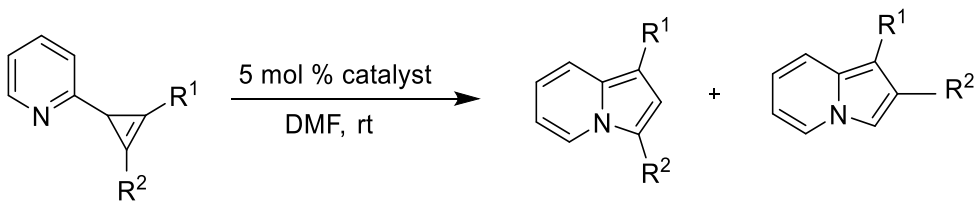

Scheme 10. Synthesis of indolizines using 2-cyclopropenylpyridides.

Cyclization of propargylic pyridines to indolizines can also be effected in the presence of iodine, Pd or metals that include Pt, Ag, In, Au, Cu in a polar protic solvent as illustrated in **Scheme 11**.[142, 143] Metal-catalysed oxidative carbonylation of propargylic pyridines has also been explored in the synthesis of indolizines under mild conditions;[143] the highly functionalised indolizines obtained from oxidative carbonylation, coupled with the relatively mild reaction conditions, makes this a particularly useful method. Equally mild and convenient, but providing far less functionalisation, is the employment of ubiquitous and cheap copper-catalysed methodology.[139]

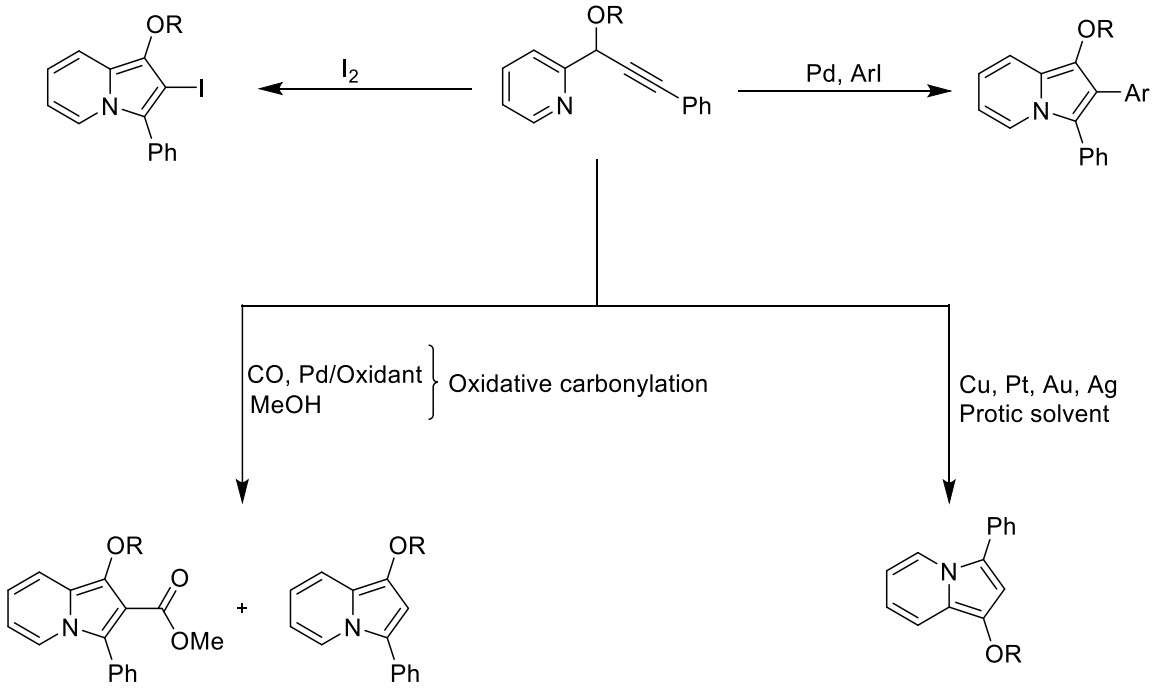

Scheme 11. Metal-catalysed synthesis of indolizines.[142, 143]

The Chichibabin indolizine synthesis, involving a base-mediated cyclisation of a 1-(2-oxoalkyl)-2-methylpyridinium or 1-(alkoxycarbonyl)methyl-2-methylpyridinium salts, is very useful for the synthesis of 2-substituted indolizines or 2,3-dihydro-2-indolizinones, respectively (**Scheme 12**).[144] Base treatment of the pyridinium salt results in the formation of an ylide which undergoes cyclisation, dehydration and aromatization to afford the indolizine.[144, 145]

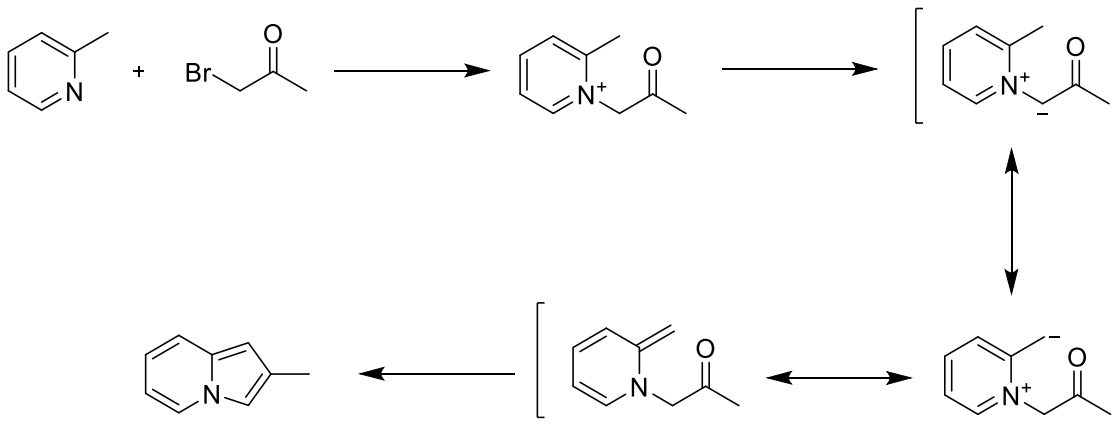

Scheme 12. Chichibabin reaction involving a 1-(2-oxoalkyl)-2-methylpyridinium salt.[64]

1.5.2. Baylis-Hillman approach to indolizines.

The synthesis of indolizines using a Baylis-Hillman adduct was first reported by Bode and Kaye in 1990.[126] Attempted distillation of the liquid adduct, 3-hydroxy-2-methylene-3-(2-pyridyl)propanoate **86** afforded a crystalline material which was identified as methyl indolizine-2-carboxylate **90**.[113, 126] The optimal condition for synthesis of indolizine carboxylate ester was found to be reflux of the hydroxy ester in acetic anhydride.[126, 146]

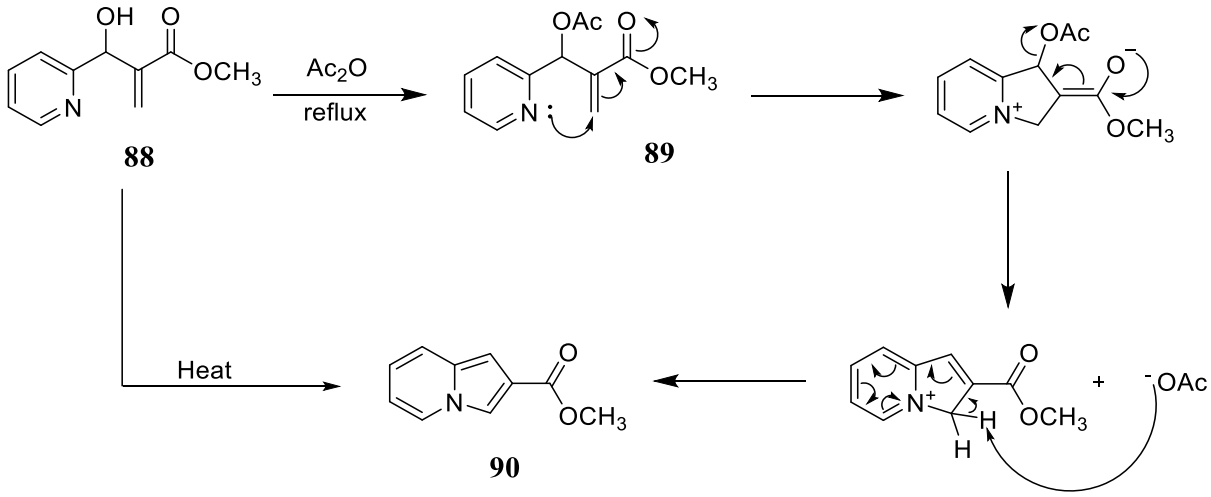

Scheme 13. Thermal cyclisation of the Baylis-Hillman hydroxy ester or the acetylated derivative to the indolizine ester.[110, 126, 145]

Initial attempts to synthesise the corresponding indolizine-2-carboxamides using various procedures were not successful.[114] These included the following.

i) Attempted generation of the acid chloride from the indolizine-2-carboxylic acid and subsequent addition of an amine.

ii) Heating a mixture of methyl indolizine-2-carboxylate and a primary amine in a sealed tube at high temperature. This method provided a low yield but was unsuccessful when secondary and sterically hindered amines were used.

iii) Finally, use of the coupling agent 1,1´-carbonyldiinidazole (CDI) permitted access to a series of amides from indolizine-2-carboxylic acid.[145, 147]

1.5.3. Physical properties of indolizines

Indolizines exhibit a plethora of pharmacological and physicochemical properties, and the indolizine system is isoelectronic with the indole nucleus and resembles the purine structure.[148, 149] Indolizine is a weak base with a pKa value of 3.49; it is a colourless crystalline solid with

certain reaction characteristics similar to that of pyrrole and indole. [135] The weak basicity of indolizine relative to pyridine and quinoline (with pKa values of 5.19 and 4.90, respectively), reflects the delocalisation of the nitrogen lone pair into the aromatic π-cloud in indolizine.[150] In fact, protonation may occur at C-1 and C-3 rather than at N – an observation consistent with the contribution of the canonical forms of **91** and **92** to the resonance hybrid structure (**Scheme 14**).[135, 150] Various NMR studies have confirmed protonation on these carbons.[151-153] It is a relatively unstable molecule with a partition coefficient value (log P) of 2.45. [150] The resonance energy of indolizines is significantly larger than that of pyrrole and therefore indolizine is best viewed as a 10π-electron aromatic system to which the three canonical forms in **Scheme 14** contribute.[135] The pyridine ring, which is a component of the indolizine, is generally stable and can permit various chemical transformations provided its aromaticity is maintained.[139] Nuclear Magnetic Resonance (NMR) has established delocalisation throughout both rings. [135]

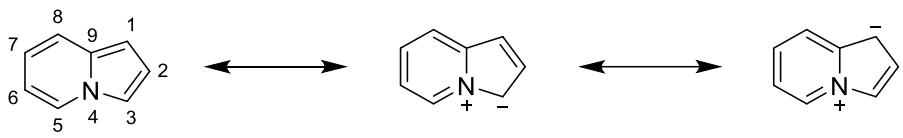

69 **91** **92**

Scheme 14. Canonical forms contribution to the resonance hybrid of indolizine. [135]

The ultraviolet spectrum of indolizine reveals an intense band at *ca.* 230 nm, a medium intensity band at *ca.* 290 nm and a broad, medium intensity band at *ca.* 345 nm.[154, 155] Interestingly, the spectrum of the indolizinium cation is significantly different from the indolizine spectrum, whereas small shifts are generally observed when heteroatomic compounds are protonated. This change is consistent with the interruption of delocalisation and loss of aromaticity on protonation at C-1 or C-3.[154] Wiench *et al*.[156], using theoretical *ab initio* molecular orbital (MO) calculations, confirmed formation of a nitrogen cation upon protonation of indolizine derivatives.

The chemical reactivity of indolizines resemble that of pyrroles, indoles and isoindoles. Thus, they readily undergo electrophilic substitution preferentially at the C-3 position and then at the C-1 position but seldom at both position simultaneously.[135, 157] The hydrogen at C-5 of the indolizine has been identified as the most acidic and this permits electrophilic substitution *via* Negeshi cross-coupling on a 5-lithiated analogue (**Scheme 15**).[122] A computational study conducted by Park *et al.*[158] confirmed that the pyrrole ring has an extended highest occupied

molecular orbital (HOMO), whereas the lowest unoccupied molecular orbital is mostly located in the pyrridine ring favoring electophilic substitution in the pyrrole ring.

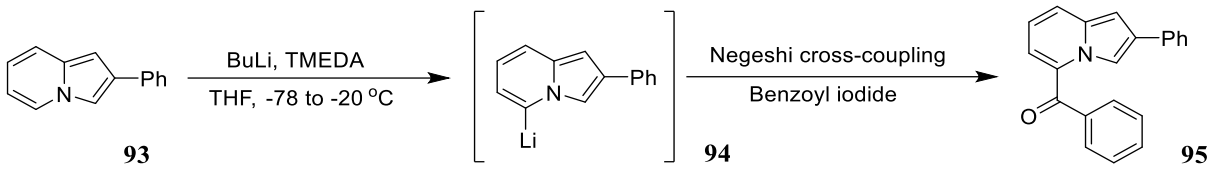

Scheme 15. Structural modification of the indolizine fluorophore, exploiting the most acidic proton of the indolizine.[159]

1.5.3.1.Modulation of indolizine optical properties

To uncover the full potential of indolizine derivatives, significant research efforts have addressed their stability,[150, 154] inherent (and manipulated) optical,[130, 159, 160] and medicinal properties.[128, 161] The use of organic π-conjugated molecules as fluorescent probes and sensors is founded on the photoluminescence character of these molecules. Small, fluorescent molecules are particularly valuable for their ability to detect conditions in solutions, on surfaces or within biological systems, and their fluorescence is modulated by factors, such as pH or binding of specific analytes.[152]

Indolizines exhibit high fluorescence and have been used as luminescent materials, such as opto-electronic devices, dyes, sensors and probes.[162, 163] Polycyclic indolizine derivatives have been identified as potential opto-electronic materials due to their ability to provide high-efficiency, long-wavelength fluorescence quantum yields.[161]

Typical fluorescence-based indicators exhibit a red-shift in emission upon protonation but, in indolizines, the emission is blue-shifted to a lower wavelength for systems susceptible to C-protonation that interupts conjugation in the molecule. The photophysical studies of a series of 6-amino-8-cyanobenzo[1,2-*b*]indolizines **96** by Outlaw *et al.*,[152] showed blue-shifting upon titration with trifluoroacetic acid, and NMR analysis indicated that protonation occurred on the pyridine ring of the indolizine to give compound **97** with concomitant loss of aromaticity. The change in π-conjugation was thus responsible for the observed change in optical properties. In a different study, Zhang *et al.*,[164] using NMR analysis, demonstrated that halochromism of 3,4-dicyanobenzo-5-imino-1,1-dimethyl[1,2-*b*]indolizine **98** was based on the protonation of the imine group to afford the corresponding indolizinium amine **99** (**Scheme 16**).

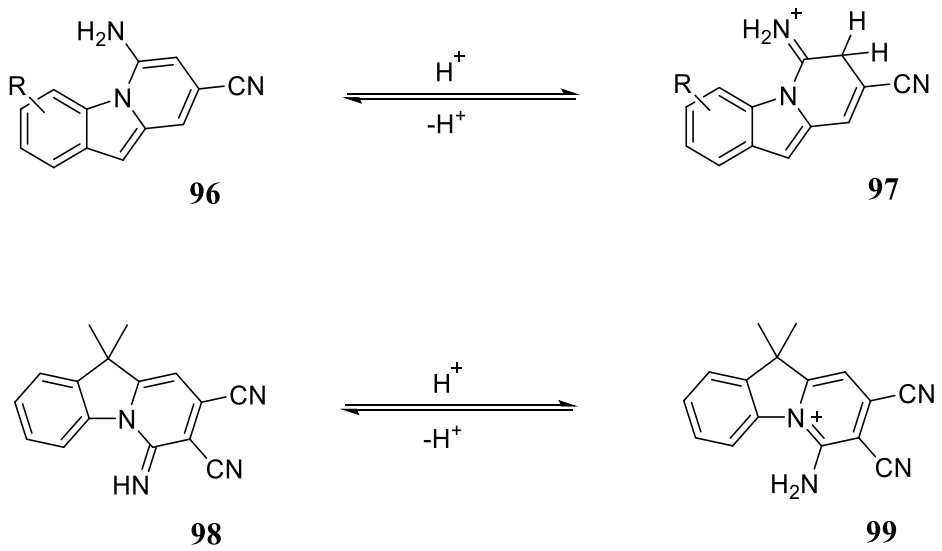

Scheme 16. Reversible protonation of amino-indolizine derivatives. [152, 164]

The increasing applications of fluorescent probes has prompted ongoing research for dyes with diverse spectral and physicochemical properties, such as stable and biocompatible molecules possessing high fluorescent quantum yields, large Stokes shifts and significant molar absorption coefficients.[160, 165] Kim *et al.*[166] recently developed a novel indolizine-based fluorescent molecular framework, 9-aryldihydropyrrolo[3,4-*b*]indolizine-3-one, named Seoul-Fluor **100**, which can be rationally modified to furnish a wide variety of photophysical properties. It has three different sites for synthetic modification or elaboration with substituents (R^1 and R^2) on the phenyl and pyridine rings used for electronic perturbation resulting in change in absorption (λ_{abs}) and emission (λ_{em}) wavelengths and *N*-substituents (R^3) as functional handles for bioconjugation.

Structure photophysical properties relationship (SPPR) studies demonstrated that the Seoul-Fluor system **100** has: a manipulable emission spectrum covering the visible-colour range; controllable quantum yields; and environment sensitive fluorescent properties that can be altered through intramolecular charge transfer processes.[167,168] Using 2-(2-nitrophenyl)indolizines and aryl aldehydes, Park *et al.*[169] successfully employed the oxidative Pictet-Spengler methodology to afford a series of indolizino[3,2-*c*]quinolines **101** which exhibited fluorescent properties that are ideal for cell imaging, such as high intensity in water, large Stokes shifts, which prevent self-quenching, and good solubility which minimises aggregation with proteins.

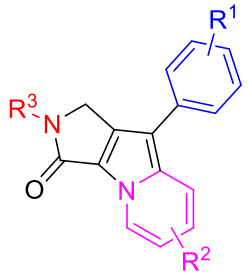

Seoul-Fluor **100**

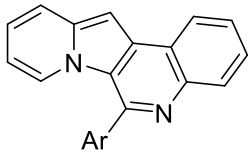

indolizino[3,2-c]quinoline **101**

Figure 18. Fluorescent indolizines with potential biological applications.[166]

1.5.3.2. Molar absorptivity of indolizines.

The molar absorption coefficient (Ɛ) is an intrinsic property of a chemical entity that defines the absorptivity of light by a chemical entity at any given wavelength.[170] Chemical entities with high molar absorption coefficients (also known as extinction coefficients) are sought for a range of applications in chemistry and medicine.[171]

The attainment of molecular entities with high molar absorption coefficients has presented significant challenges because extension of the necessary π-conjugated systems has not always guaranteed appreciable increases in molar absorptivity.[170] Owing to their innate brightness which, in turn, is associated with excellent molar absorptivity, a limited number of fluorophores such as cyanine **102**,[172] borondipyrromethene (BODIPY) **103** and aza-BODIPY **104**,[173, 174] fluorescein **105** [175] and rhodamine **106**,[176] have been extensively used as fluorescence organic dyes.

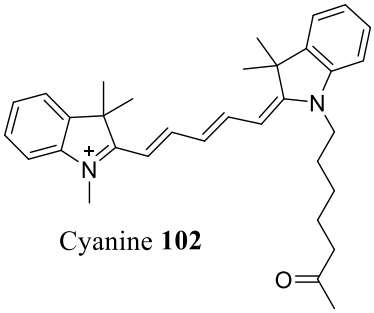

Cyanine **102**

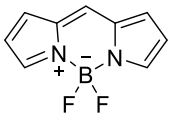

BODIPY **103**

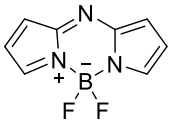

aza-BODIPY **104**

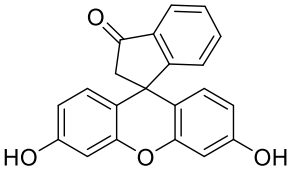

Fluorescein **105**

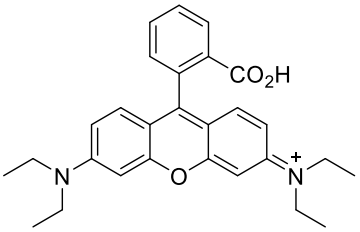

Rhodamine **106**

Figure 19. Chemical entities with high molecular extinction coefficients that are widely used as dyes.

In addition to their occurrence in living organisms, such as species of the genus *dendrobates* (poison dart frogs), *monomorium* (ants), *dendrobium* (orchids), *tylophora* and the *leguminosae* family (plants)[135, 177] and their wide range of biological activities,[133, 139, 178] indolizines have come to the fore as promising compounds with interesting scientific potential.[179] They emit intense fluorescence and their ultraviolet-visible absorption properties are very sensitive to the influence of substituents thereby opening a wide range of possible applications.[179, 180] For example, indolizines have been employed as a fluorescent moiety in modified β-cyclodextrins.[181]

1.6. Research context and objectives of the current investigation.

The core principles in the advancement of medicinal chemistry over the past decades have been premised on the mechanism of action of drugs and the variation of chemical structures to establish bioactive compounds. In fact, progress in drug research has been due to the understanding of the chemistry of drugs including detailed knowledge of the physicochemical properties of the drug.[182]

Rational drug design which involves the target-orientated synthesis of compounds possessing particular predetermined physicochemical properties has resulted in the development of potent and selective inhibitors.[183] The first step in the development of enzyme inhibition-based drug design requires an understanding of the enzyme receptor and the mechanistic details concerning the enzymatic pathways.[182, 184] Alternatively, *in silico* screening, a less preferred and empirical drug discovery technique, which often incorporates rational drug design concepts in identifying the receptor, involves *in silico* screening large numbers of structurally distinct molecules against a pharmacological target in the hope of finding a lead compound.[185] This technique, however, may yield unsatisfactory lead compounds which typically possess poor physicochemical properties.[186]

In the quest to prevent and eradicate diseases that continuously threaten human life, libraries of unique, highly potent, small molecules need to be created to identify lead compounds and thus accelerate the rate of new drug discovery.[186] Rational drug design requires a multidisciplinary approach to develop small molecules with desirable structures and physicochemical properties for targeting specific biomolecules that are essential for the life-cycle of particular antigens.[187] The structural features and cellular functions of the target may be unknown prompting their prior elucidation in order to facilitate drug design and greater adherence to the Lipinski rule of 5 guidelines.[187,188, 189]

A convenient starting point is to identify relevant pharmacologically significant motifs which can be incorporated or elaborated to produce novel molecules with improved activity,[20, 190, 190] and in our study, we report the rational design of series of compounds containing medicinally privileged nuclei, 2-quinolone and indolizine, as potential HIV-1 enzyme inhibitors. These series of compounds will also be evaluated for potential anti-malarial, anti-tuberculosis and trypanocidal activity. More specifically, we have worked towards achieving the following objectives.

1. The application of the Morita-Baylis-Hillman methodology in synthesising series of novel 2-quinolones (Part I) and indolizine derivatives (Part II) – as illustrated in **Scheme 17**.
2. *In vitro* biological evaluation of the new compounds against HIV-1 enzymes, *p. falciparum*, *mycobacteria tuberculosis* and trypanosome enzyme T. brucei.
3. A photophysical study of indolizine derivates
4. Kinetic study of the Baylis-Hillman reaction of pyridine-4-carboxaldehyde and methyl acrylate in the presence of 3-hydroxyquinuclidine.

Over the past years, using the Baylis-Hillman approach pioneered in our group,[126] a series of indolizine-2-carboxamides with a peptido-mimetic moiety have been prepared as potential inhibitors of the essential HIV-1 enzymes, namely, reverse transcriptase (RT), integrase (IN) and protease (PR).[147] This project was aimed at addressing the demand for medicinally important heterocyclic molecules using the Baylis-Hillman methodology. Appropriate substrates were to be employed to access methyl indolizine-2-carboxylate **90** and of 3-acetoxymethyl-2(1*H*)-quinolones **111** as critical synthons in the construction of complex *N*-heterocyclic derivatives.

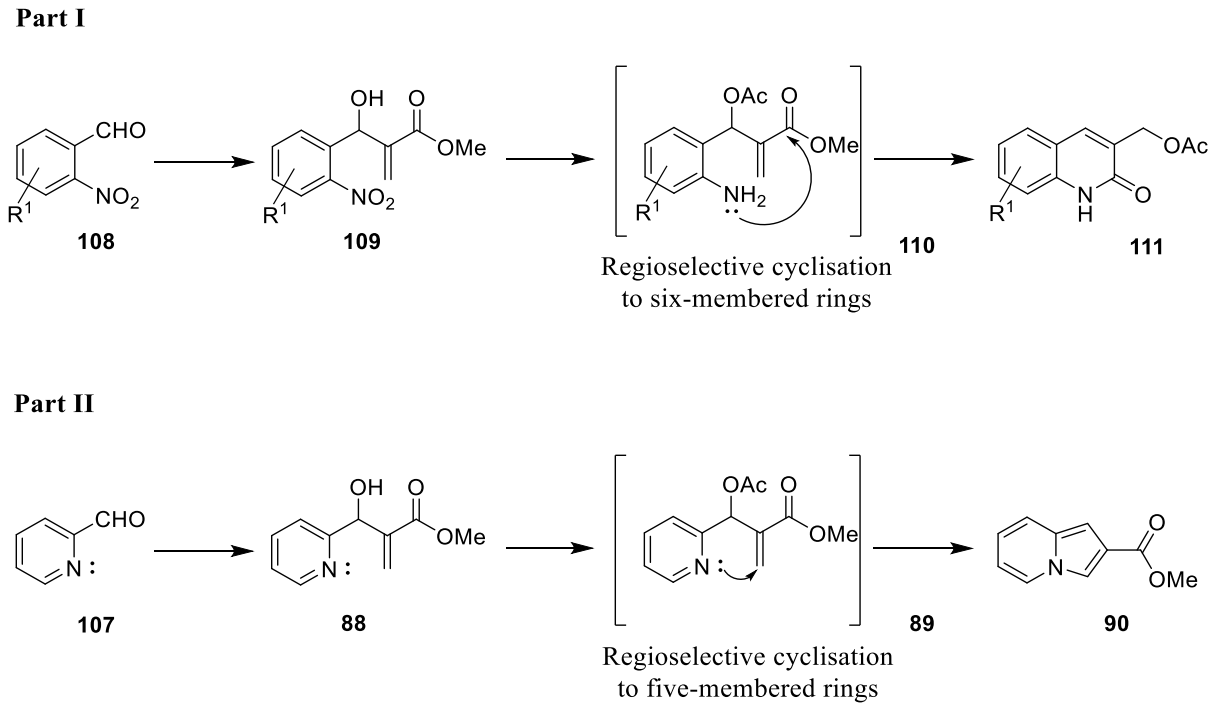

Scheme 17. Baylis-Hillman approach to nitrogen heterocyclic synthons.

2. Results and Discussion

In the following sections attention will be given to: the application of the Baylis-Hillman (BH) methodology in the construction and bioassay of 2-quinolone (**2.1**) and indolizine derivatives (**2.2**); photophysical studies of the indolizine derivatives (**2.5**); and an NMR-based kinetic study of the B-H reaction (**2.6**).

2.1. Preparation of Baylis-Hillman adducts.

The Baylis-Hillman reaction allows direct synthesis of highly versatile α-methylene-β-hydroxycarbonyl adducts, from the base-catalysed reactions of α,β-unsaturated carbonyl compounds with aldehydes (**Scheme *5***).[191] In this project: 1,4-diazabicyclo[2.2.2]octane (DABCO) was used as the catalyst in the synthesis of methyl 3-hydroxyl-3-(2-nitrophenyl)-2-methylenepropanoate derivatives **109a-f**, whilst 3-hydroxyquinuclidine (3-HQ) was used to catalyse the synthesis of 3-hydroxyl-3-(2-pyridinyl)-2-methylenepropanoate **88** from 2-pyridinecarboxaldehyde and methyl acrylate. These functionally diverse Baylis-Hillman adducts permitted facile access to cyclic molecules – specifically 3-actoxymethyl-2(1*H*)-quinolone derivatives **111** (Part I) and methyl indolizine-2-carboxylate **90** (Part II), respectively. See Scheme 17.

In Part I of this project, which is a continuation and extension of an MSc project,[115] 2-nitrobenzaldehydes **108a-f** were reacted with methyl acrylate, in the presence of DABCO afford the functionally diverse BH adducts **109a-f** in up to 86% yield (**Table 3**).

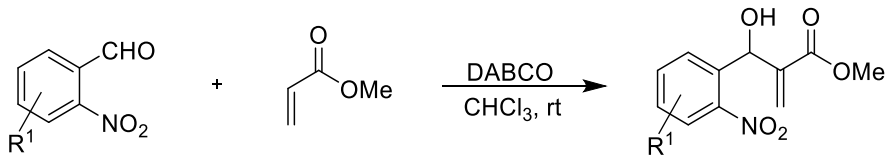

	R^1
a	H
b	4,5-CH_2O-
c	5-Cl
d	4-Cl
e	5-OMe
f	3-OMe

Scheme 18. Synthesis of 2-nitrophenyl BH adducts.

Table 3. Yields of the Baylis-Hillman synthons **109**.

Baylis-Hillman adducts 109		R^1	% Yield
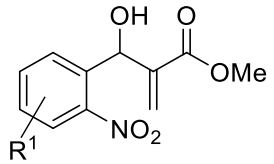	**a**	H	65
	b	4,5-OCH_2O-	37
	c	5-Cl	47
	d	4-Cl	86
	e	5-OMe	52
	f	3-OMe	45

With the Baylis-Hillman adducts **109a-f** in hand, various chemical transformations became possible, including nucleophilic conjugate addition, nucleophilic allylic substitution, acetylation of the alcohol group and intramolecular cyclisation of the Baylis-Hillman adduct.[110, 115, 192] In recent years, the Baylis-Hillman adduct has been widely utilised in the synthesis of cyclic frameworks, usually oxygen and nitrogen heterocycles.[109]

In the earlier studies,[115] we had developed a convenient protocol to access the 3-chloromethyl-2(1*H*)-quinolones **113a-f** and, in the present study, we have developed and completed the six-step route to the desired *N*-substituted amides **117a-i** as outlined in **Scheme 19**. The acetates **111a-f** were readily obtained in good to excellent yield (62-99%), by reductive cyclisation of the corresponding BH adducts **109a-f** using iron powder in refluxing acetic acid. In a slight modification of Basavaiah's method,[121] hydrolysis of the acetate esters was effected using K_2CO_3 in methanol-water (1:1) to afford the alcohols **112a-f** in yields of up to 87%. The 3-(chloromethyl)-2(1*H*)-quinolones **113a-f** were reported in yields of up to 91% by reacting each of the corresponding alcohols **112a-f** with excess thionyl chloride (*Caution: reaction is exothermic and initial cooling may be necessary)* for 30 minutes – a significant improvement, in terms of yield and convenience, on an initial method of conducting the reaction in refluxing benzene for 12 hours.

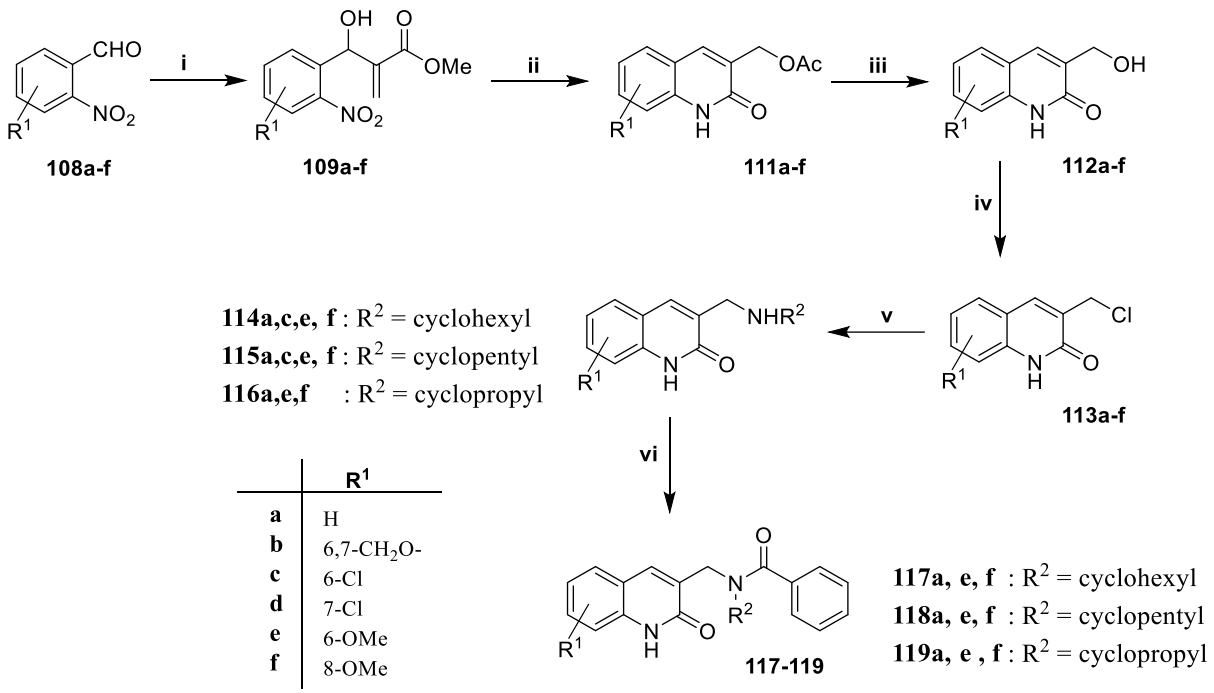

Scheme 19. Six-step route to target products **117**. Reaction conditions: (i) $CH_2{=}CHCO_2Me$, DABCO, $CHCl_3$; (ii) Fe powder, AcOH, reflux; (iii) K_2CO_3, MeOH-H_2O; (iv) $SOCl_2$, DCM; (v) cyclopropylamine, cyclopentylamine or cyclohexylamine, CH_2Cl_2; (vi) Triethylamine (TEA), PhCOCl.

The DEPT 135 stacked spectra (Figure 20) reveal successive changes beginning with the BH adduct **109a** at the top and ending with 3-(chloromethyl)-2(1*H*)-quinolone **113a** at the bottom. The DEPT 135 spectrum of the BH adduct **108a** shows four aromatic, hydrogen-bearing carbons and a vinylic methylene signal in the region, 120-150 ppm, as well as the expected methine and O-methyl signals at *ca.* 70 and 50 ppm, respectively. The methine and methylene signals are prominent characteristics of the BH adduct spectrum and, together with the O-methyl signal, can be used to confirm successful chemical transformation of the adduct. Reductive cyclisation of the adduct resulted in the disappearance of the O-methyl, methine, and methylene signals and the emergence of a new methylene signal at *ca.* 60 ppm and the acetyl methyl signal at *ca* 20 ppm, in addition to five signals in the aromatic region. Hydrolysis of the acetate **111a** to the alcohol **112a** was confirmed by the disappearance of the acetyl methyl signal, and a slight upfield shift of the methylene signal. On chlorination of the alcohol **112a**, the methylene signal is shifted significantly upfield from *ca.* 60 ppm to *ca.* 40 ppm.

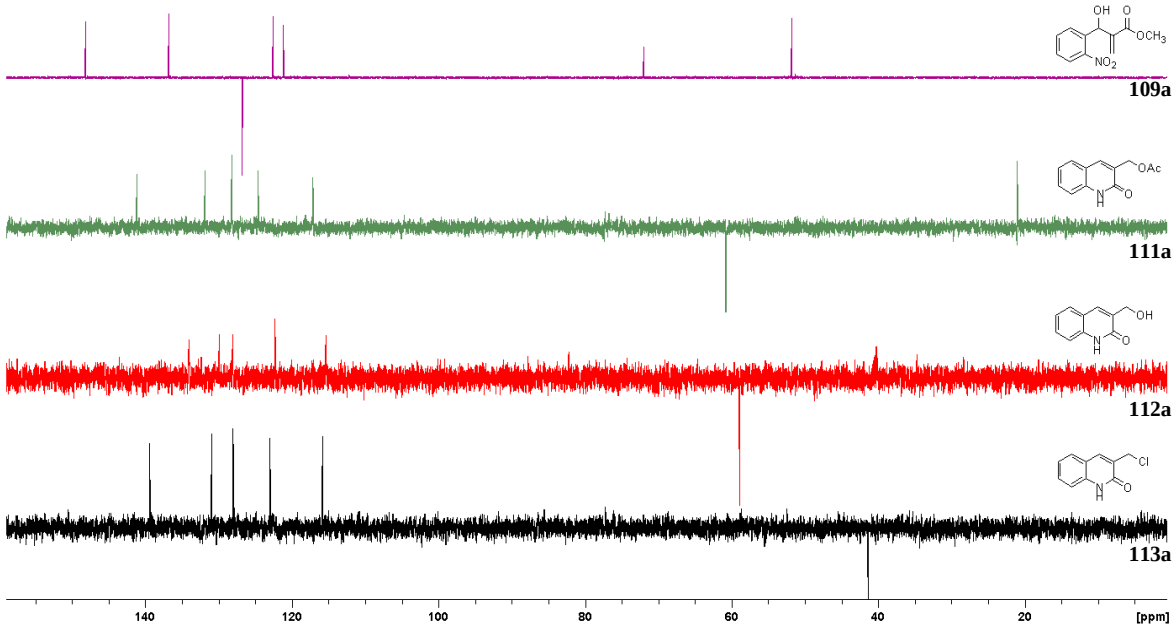

Figure 20. Stacked DEPT 135 NMR spectra of successive compounds **109a**, **111a**, **112a**, and **113a** in $CDCl_3$**.**

Transformation of the alcohols to corresponding allyl chlorides provided substrates with a good leaving group which are susceptible to nucleophilic substitution. Chlorination was achieved using thionyl chloride and the desired products were obtained in excellent yields without by-product(s). *Caution must, however, be exercised when working with thionyl chloride as it is corrosive and reacts rapidly with moisture in the atmosphere.* A plausible mechanism for the chlorination has been provided elsewhere.[115]

2.1.1. Amination of the 3-(chloromethyl)-2(1*H*)-quinolone derivatives (113)

Following the approach outlined in Scheme 19, amination was conveniently achieved by stirring each of the selected allyl chlorides (**113)** with an excess of each of the primary cycloalkylamines (cyclopropropylamine, cyclopentylamine and cyclohexylamine) in a stoppered flask at room temperature. The progress of the reactions were monitored by thin layer chromatography (TLC) and, after completion, the reaction mixtures were concentrated *in vacuo* and the crude products purified by preparative layer chromatography (PLC) to afford the corresponding 3-[(cycloalkylamino)methyl]-2(1*H*)-quinolones (**114**), (**115**) and (**116**) in yields ranging from 60 to 93% (Table 4).

Table 4. Yields obtained for the series of 3-[(cycloalkylamino)methyl]-2(1*H*)-quinolone derivatives.

3-[(cycloalkylamino)methyl]-2(1*H*)-quinolones		**R^1**	**R^2**	**% Yield**
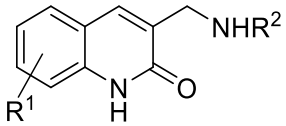	**114a**	H	cyclohexyl	75
	114c	6-Cl		89
	114e	6-OMe		65
	114f	8-OMe		76
	115a	H	cyclopentyl	60
	115c	6-Cl		93
	115e	6-OMe		81
	115f	8-OMe		88
	116a	H	cyclopropyl	93
	116e	6-OMe		73
	116f	8-OMe		81

The 3-[(cyclohexylaminmo)methyl]-2(1*H*)-quinolones were fully characterised using 1D- and 2D-NMR, high-resolution mass and IR spectrometric analysis. In the ^{1}H-NMR spectrum (**Figure 21**) of compond **114a**, for example, all five quinolone proton signals are clearly evident in the aromatic region; the methylene singlet shifted from 4.70 ppm (in the precursor allylic chloride **113a**) to 3.82 ppm, indicating that amination had been successfully achieved. Signals in the high-field region correspond to the cyclohexylamine protons. The complexity of cyclohexylamine signals is attributed to multiple couplings between diastereotopic ring protons.[193] The multiplet at 3.17 ppm corresponds to the methine proton of the cyclohexylamine.

The corresponding ^{13}C-NMR spectrum (**Figure 22**) shows the signal for the eight quinolone carbons in the aromatic region and the carbonyl carbon signal at 164.0 ppm. The *N*-methylene signal appears at 46.4 ppm, the *N*-methine carbon signal appears at 56.0 ppm, while the cyclohexylamine methylene carbons resonate at higher field. As expected, the IR spectrum (**Figure 23**) shows the crucial NH band at 3290 cm^{-1} and the 2-quinolone carbonyl (C=O) band at 1648 cm^{-1} confirming the formation of the desired product.

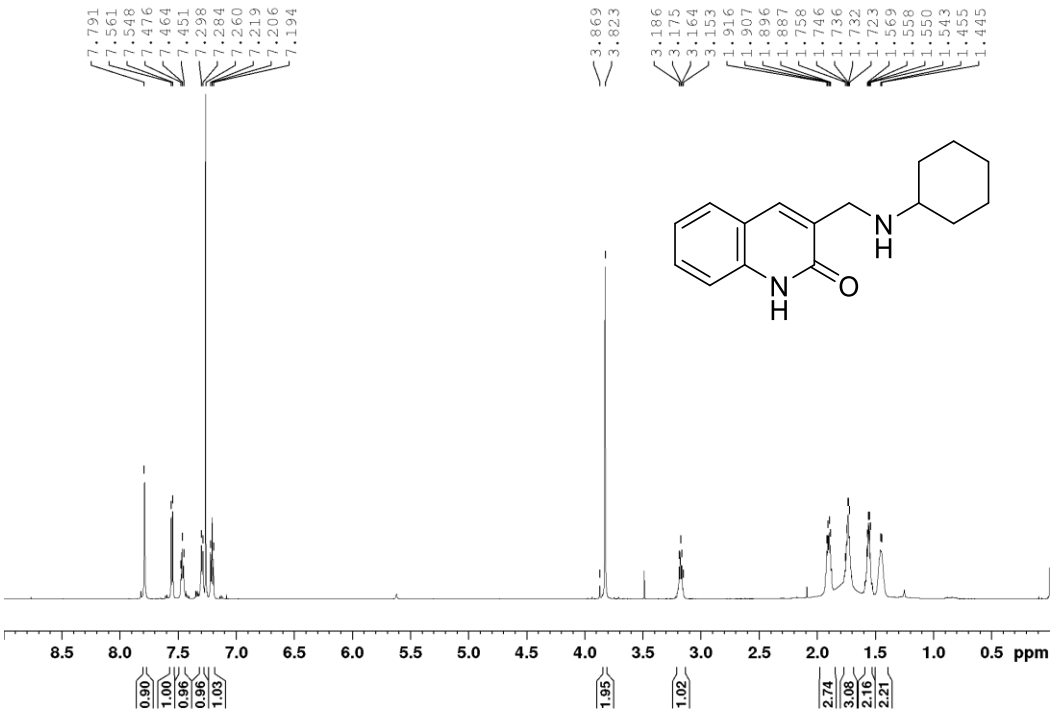

Figure 21. 600 MHz ^{1}H-NMR spectrum of **114a** in $CDCl_3$.

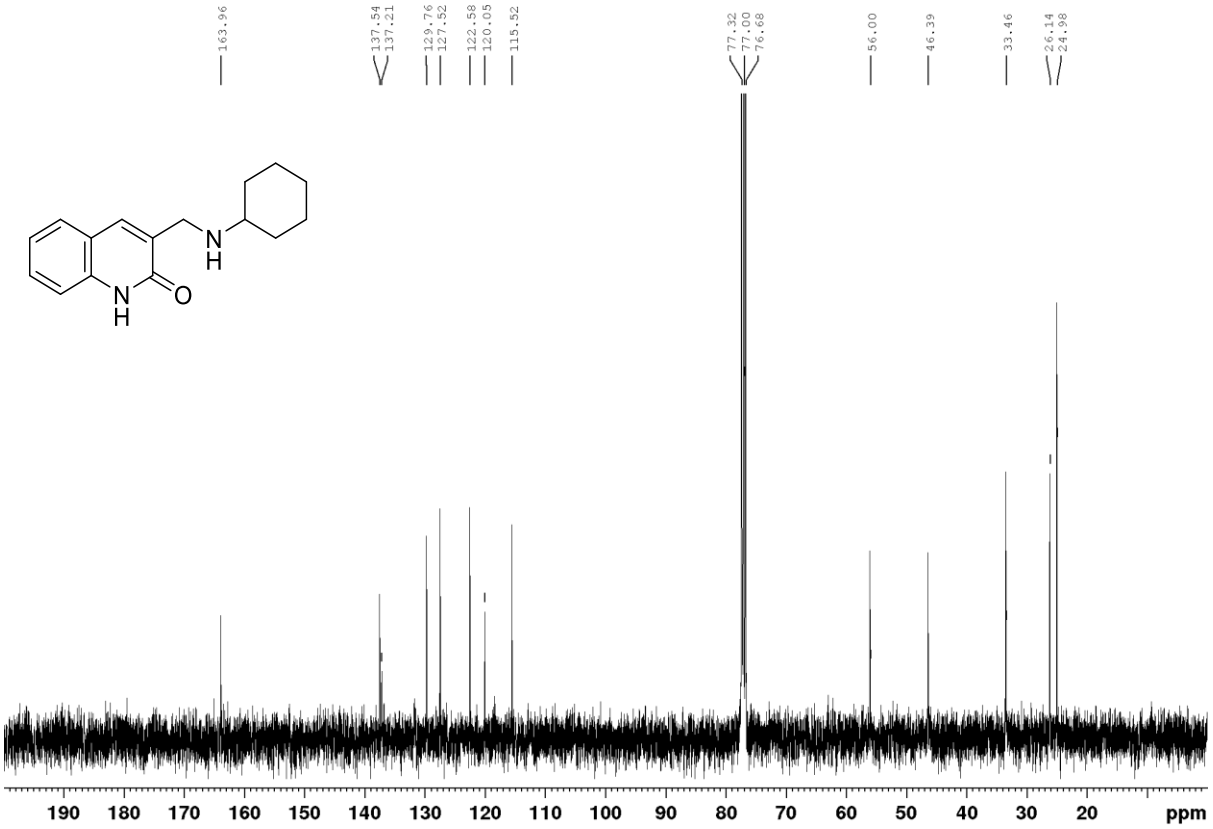

Figure 22. 150 MHz ^{13}C-NMR spectrum of **114a** in $CDCl_3$.

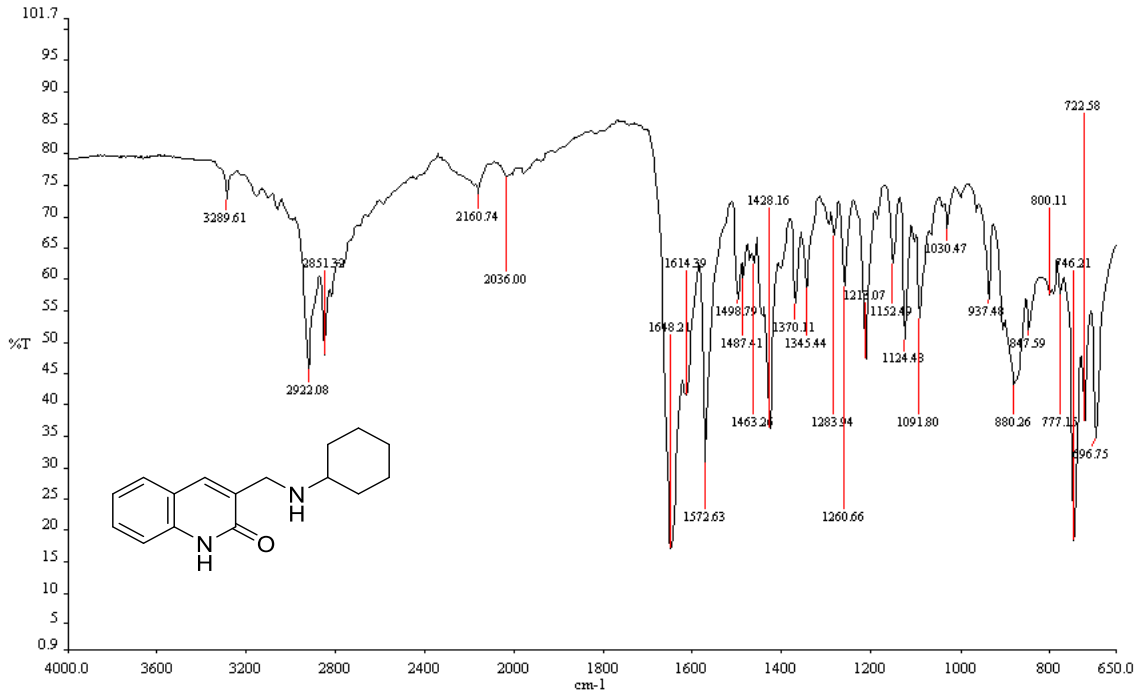

Figure 23. IR spectrum of **114a**.

The ESI mass spectrum of compound **116f** shows a peak at *m/z* = 245.1301 corresponding to the pseudo-molecular ion. The peak at *m/z* = 188.0715 (**Figure 24**) corresponds to the resonance stabilised cation arising from the cleavage of the C-N bond.

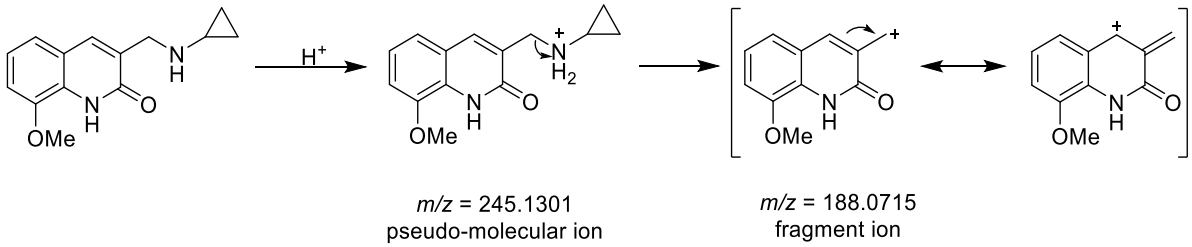

Scheme 20.

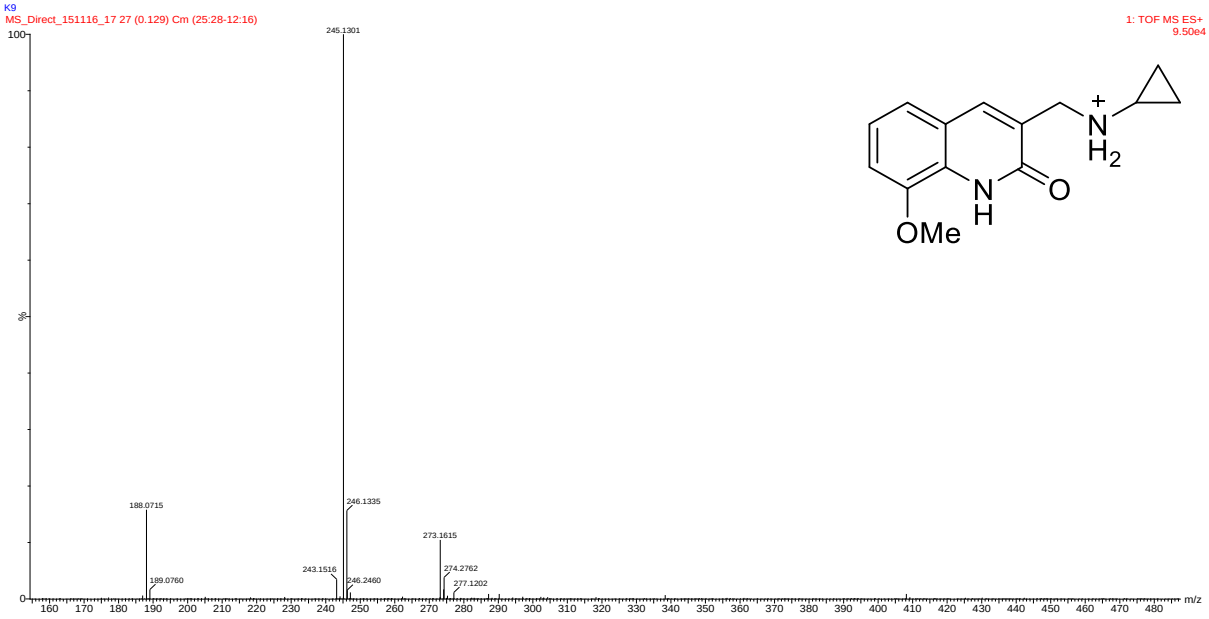

Figure 24. ESI mass spectrum of compound **116f**.

2.1.2. Approaches to amide bond formation.

The amide functional group is a ubiquitous, neutral, stable, hydrogen-bond donating and accepting functionality that is prevalent in small, complex synthetic or natural molecules including proteins.[20, 194] Consequently, the amide bond plays a key role in synthetic medicinal chemistry and a detailed analysis of the Comprehensive Medicinal Chemistry database revealed that more than 25% of known drugs contain an amide functionality.[20] It is not surprising that amide bond formation had been considered to account for 16% of the reactions carried out in medicinal chemistry laboratories.[195] Amidation was potentially important in the present study which focussed on the preparation of quinolone and indolizine carboxamide derivatives.

In principle, amide synthesis is a simple chemical transformation that may be achieved by thermal condensation of an acid and an amine *via* a stable salt intermediate (**Scheme 21**). In practice, activating agents or activated reagents are generally used for amide bond formation. In the absence of an activating agent this reaction favours the starting material, hence it is usually driven forward through heating and removal of water generated by condensation.[196 197]

Unactivated process

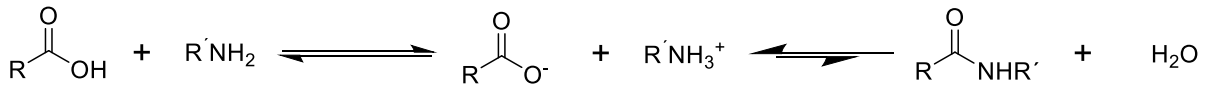

Activated process

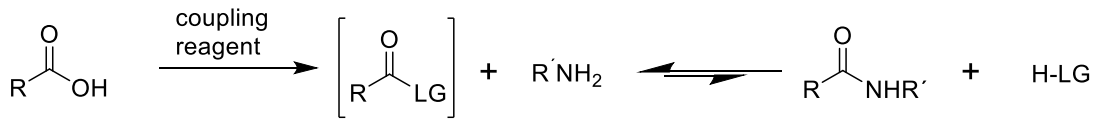

Acyl halide

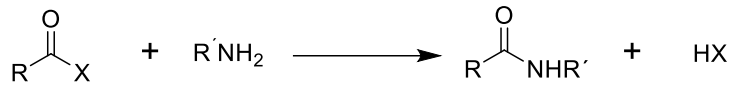

Scheme 21. Typical approaches to amide bond formation.

Direct condensation can be achieved under extreme conditions that include conducting the reaction at high temperature, in a sealed vessel and, in some cases, under high pressure which frequently makes this approach incompatible with the complexity of modern drug candidates.[195] Activation of the acid by introducing a good leaving group in place of the hydroxyl group of the carboxylic acid facilitates attack by the amine, and a plethora of methodologies involving activation, also known as coupling reactions, have been developed. The choice of a suitable method is influenced by the nature and reactivity of the substrates, availability and cost of the activating agent, and ease of purification.[194, 195, 198] Conversion of carboxylic acids to amides is also regularly achieved by generating highly active acyl halides which are generally isolable.

Carboxylic acids can also be activated by conversion to activated esters and acyl azides, which the use of coupling agents activate the acid *in situ* - generating, for example, acyl imidazoles, cardodiimides, cyanuric acetate, *etc* as intermediates.[197, 199, 200] In essence, amide coupling may be summarised as follows:[20, 196, 198]

i) Synthesis and isolation of an active acylating agent, *e.g.* an acyl halide, as a reagent, or

ii) *in situ* generation of an activated acyl derivatives, using, for example, carbonyldiimidazole (CDI), either in the presence of or followed by addition of an amine.

In this project, benzoyl chloride was used as the acylating agent in the synthesis of the 3-[(cycloalkylbenzamido)methyl]-2(1*H*)-quinolones **117-119**; whilst isocyanates, boric acid and tris(2,2,2-trifluoroethyl) borate were explored as coupling agents in the synthesis of indolizine-2-carboxamides (**Section 2.2.4**). Eventually, however, propylphosphonic acid anhydride (T3P) **120** emerged as the most successful coupling agent (**Section 2.2.5**).

Although moderately costly, T3P is a non-toxic phosphorus-based cyclic anhydride, easy to handle and has been found to be effective coupling reagent in large-scale syntheses of amides. It can also be used as a catalyst in other condensation reactions such as esterification, and as a mild reagent in alcohol oxidation.[201] Its inherent water scavenging properties make it ideal for effecting coupling.[200] As a result of its selectivity, propylphosphonic anhydride (T3P) **120** has been widely used in the synthesis of drug candidates, especially peptides since it has demonstrated suppression of epimerization.[199, 202] The water-soluble by-products can be readily extracted by use of an aqueous work-up. Its counterpart, ethylmethylphosphonic anhydride (EMPA) **121** is considerably more toxic and, as a result, its use is limited.[199]

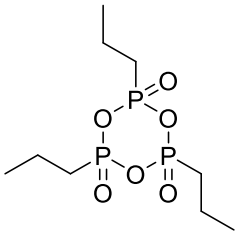

120

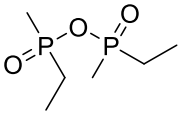

121

Figure 25. Phosphorus-based amide coupling reagents.

The electrophilic nature of the anhydride phosphorus atoms facilitates nucleophilic attack by a wide range of nucleophiles, including *in situ* generated carboxylate, resulting in a mixed anhydride intermediate **122**. This acyclic intermediate, which is in essence an activated carboxylic acid is subsequently attacked by a nucleophilic reagent, an amine in our case, resulting in the formation of an amide and a water-soluble by-product (**Scheme 22**).[200, 201]

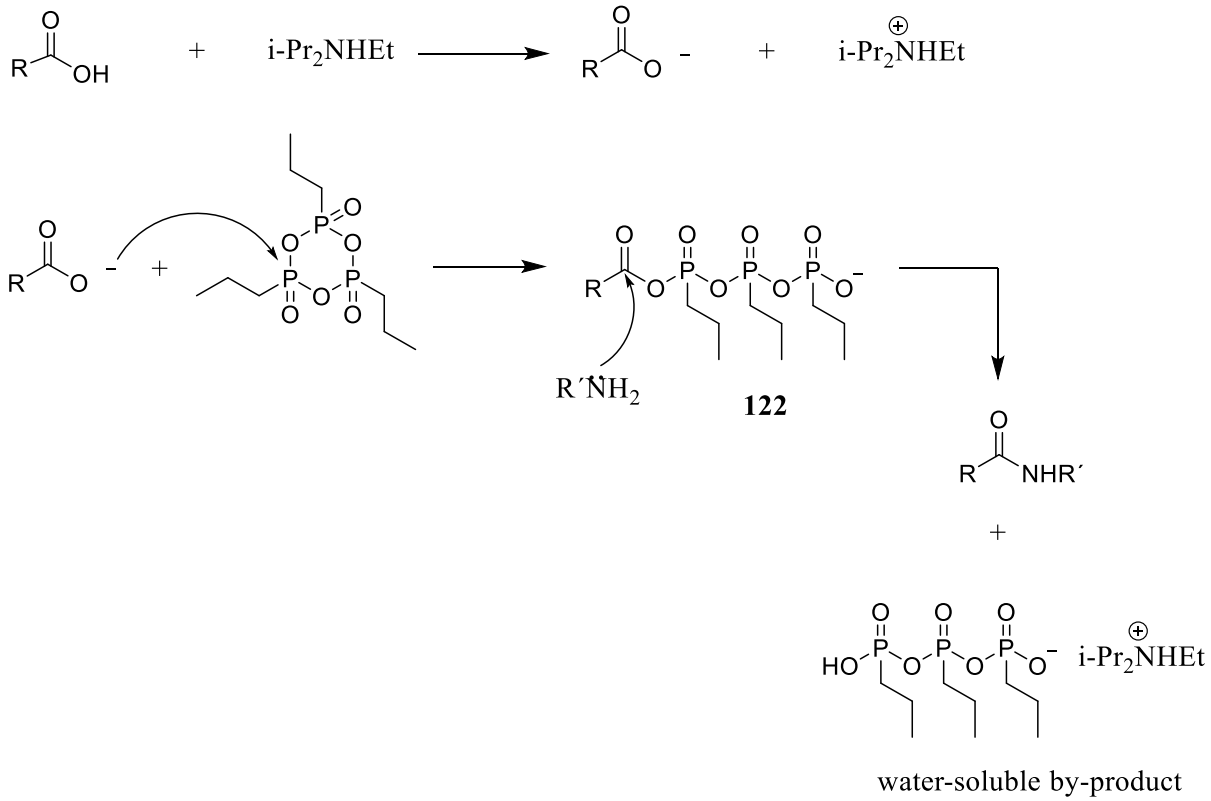

Scheme 22. Mechanism of amide coupling using phosphonic acid anhydride.

For the synthesis of indolizine-2-carboxamides (see Part II), the rationale in exploring the use of boric acid, trimethyl borate, tris(2,2,2-trifluoroethyl) borate and isocyanates was suggested by their common use in amide synthesis and inspired by the following conditions.

i) A catalytic amount of boric acid (or trimethyl borate) has been shown to mediate direct amide synthesis under azeotropic conditions in high boiling point solvents.[203]

ii) Use of tris(2,2,2-trifluoroethyl)borate [$B(OCH_2CF_3)_3$] has shown a significant improvement over other boronic acid-based coupling agents. In addition, the latter has been shown to facilitate trans-amidation thereby providing a convenient method for attaining secondary amides from appropriate primary and different secondary amides. [203] Furthermore, $B(OCH_2CF_3)_3$ has been reported as an efficient coupling agent in the direct synthesis of a wide range of amino acid amides from unprotected amino acids, a process which may otherwise require protection of the free amine moeity, coupling and deprotection, successively.[204]

iii) Lastly, isocyanates are known to be highly reactive and readily undergo direct condensation with carboxylic acids in the presence of a base to form amides and carbon dioxide as a by-product.[198] The acid-isocyanate condensation pathway proceeds *via* an anhydride intermediate,[198] whereas, boron-mediated activation of

the carboxylic acid occurs *via in situ* generation of a four coordinate-boron species.[203]

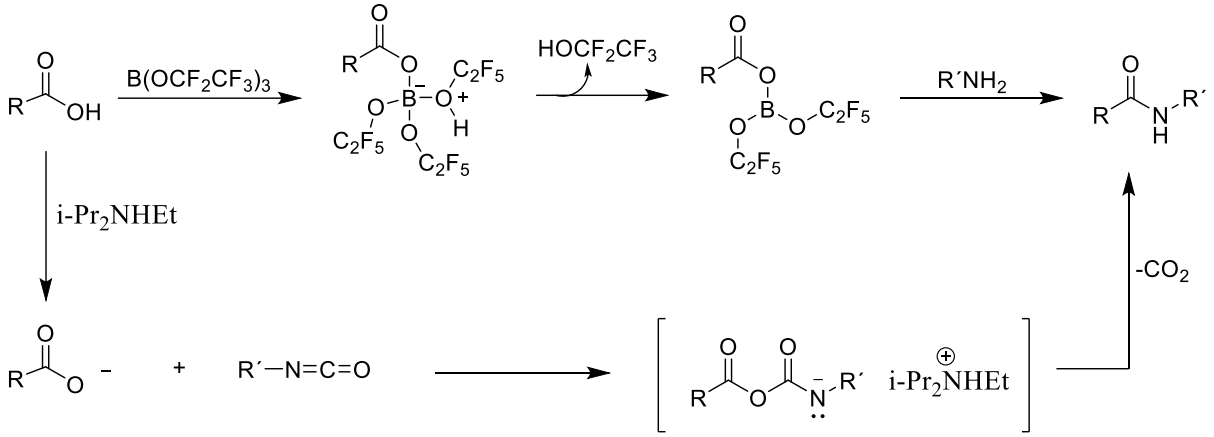

Scheme 23. Illustration of acid-isocyanate condensation versus boron-mediated coupling.[198, 203]

These reactions require anhydrous conditions and, in some cases, an excess of either the carboxylic acid or the amine to obtain a good yield. In addition to their aqueous-sensitivity, they are also sensitive to alcohols (including those formed as by-products), the presence of which may drastically hinder conversion or completely quench the reaction. Water or alcohol by-products are often removed by use of a Dean-Stark trap or, alternatively, by drying agents in cases where water is a by-product. Both the above boron-mediated and condensation approaches are particularly effective for unsaturated carboxylic acids.[198, 203, 204]

2.1.3. Synthesis of 3-[(cycloalkylbenzamido)methyl]-2(1*H*)-quinolones 117-119.

With a series of nucleophilic active, secondary amines in hand (**Table 4**), amide bond formation with benzoic acid or an activated derivative was sought. Since coupling of an amine and an acyl chloride is one of the easiest and most efficient methods for amide synthesis, coupling was effected using benzoyl chloride as the activated acyl derivative. This method produces hydrochloric acid (HCl) as a by-product, which was effectively mopped up with triethylamine.

The final acylation step (**Scheme 19**) thus involved reaction of selected 3-[(cycloalkylamino)methyl]-2(1*H*)-quinolones (**114**–**116)** with excess benzoyl chloride to access the targeted tertiary benzamides, 3-[(*N*-cycloalkybenzamido)methyl]-2(1*H*)-quinolones **117-119**, at room temperature. The reaction progress was monitored by TLC and, after

completion, the HCl generated was neutralised with triethylamine (TEA) and the desired product purified by column chromatography to afford the benzamides **117-119**.

Table **5** summarises the yields obtained for a series of nine benzamides synthesised from selected amines. All benzamides were characterised using NMR, IR and HRMS methods. Analysis of the NMR spectra of many of these compounds was complicated due to signal broadening and in some cases, a multiplicity of signals – phenomena attributed to the rotameric equilibria regularly encountered with carboxamides (**Scheme 25**), and variable temperature 1D- and 2D-NMR studies were undertaken to elucidate the products.

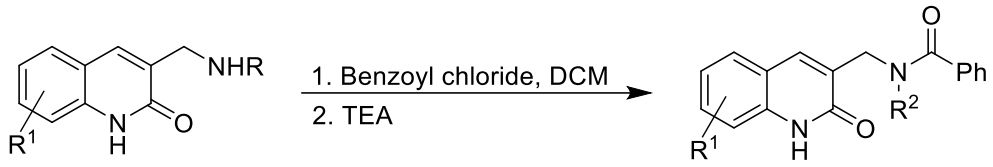

114a, e, f : R^2 = cyclohexyl
115a, e, f : R^2 = cyclopentyl
116a, e, f : R^2 = cyclopropyl

117a, e, f : R^2 = cyclohexyl
118a, e, f : R^2 = cyclopentyl
119a, e , f : R^2 = cyclopropyl

Scheme 24. Synthesis of tertiary benzamides (**117-119**).

Table 5. Yields of tertiary benzamides synthesised as potential anti-HIV agents.

Benzamides		R^1	R^2	% Yield
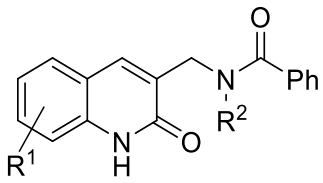	**117a**	H	cyclohexyl	60
	117e	6-OMe		86
	117f	8-OMe		32
	118a	H	cyclopentyl	17
	118e	6-OMe		60
	118f	8-OMe		57
	119a	H	cyclopropyl	36
	119e	6-OMe		53
	119f	8-OMe		39

Dynamic NMR methods have been widely used in the study of conformational changes. It helps evaluate the torsional barrier to rotation in amides by measuring changes in NMR line shapes as a function of temperature.[205] In the benzamides (**117-119**), the existence of rotamers

resulting from hindered rotation about the N-(CO) bond of the amide moiety was explored using dynamic NMR analysis.[206, 207] The inherent torsion about the N-(CO) bond arises from delocalisation which stabilises the planar rotamer (**Scheme 25**).

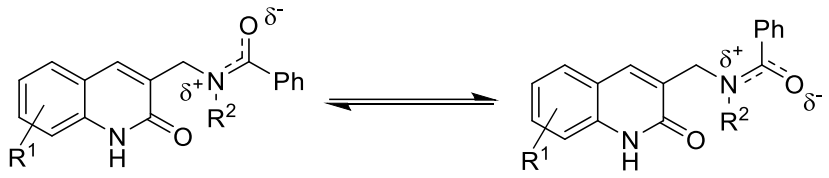

Scheme 25. Illustration of rotameric options for the benzamide derivatives (**117-119)**.

Since the rotamers exist due to exchange through an intramolecular process (**Scheme 25**), their NMR spectra reflect the differences in the resonance frequencies of their nuclei and the rate of exchange. The rate of exchange (rotation) is generally low at lower temperatures often resulting broad signals for particular nuclei. At high temperature, the exchange is fast and, assuming a singlet, a single sharp peak corresponding to the average NMR frequencies of the nuclei under study is observed. At intermediate and coalescence temperatures, the signals broaden and merge to give a broad signal. In ^{13}C NMR spectra, the broadening may be sufficient to result in the apparent disappearance of the signal(s).

Above the coalescence temperature, the rate of exchange of rotamers to the point where their magnetic environments are time-averaged resulting in the detection of one set of spins with a life-time determined by spin-lattice and spin-spin relaxation mechanism. These studies are usually conducted using ^{1}H NMR because of its sensitivity. Moreover, carbon signals tend to broaden intensely thereby disappearing into the noise.[208] **Figure 26** below shows dynamic ^{1}H NMR studies of *N*,*N*-dimethylacetamide reported elsewhere,[205, 206] focusing on the resonance frequencies of the *N*-methyl groups which become apparently chemically equivalent on rapid internal rotation at higher temperatures.

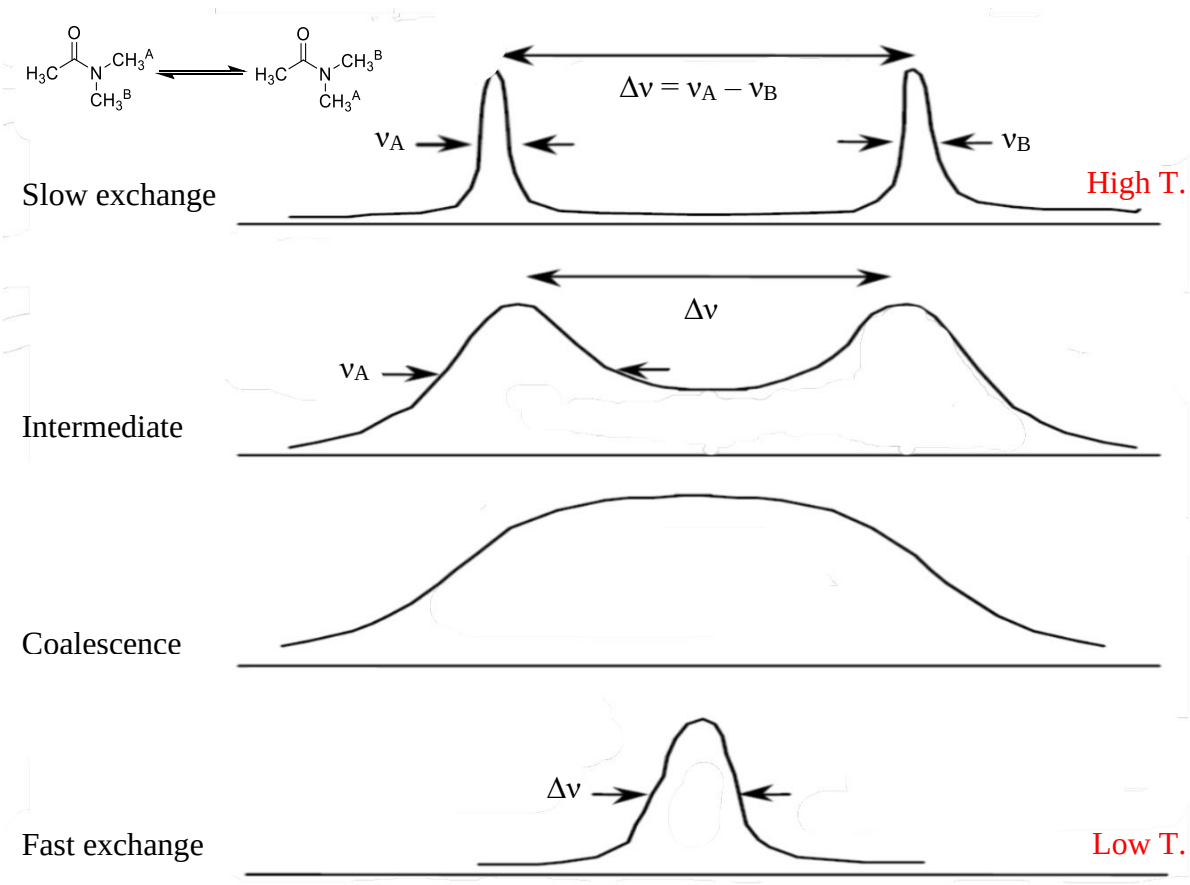

Figure 26. Intramolecular exchange of chemically equivalent on NMR line shapes.[205]

2.1.3.1.Structural elucidation of the benzamides (117-119).

Interpretation of the NMR spectra and the assignment of signals was facilitated by running spectra of the benzamides (**117-119**) in DMSO-d_6 at different temperatures between 298 and 373 K. The rate of rotation around the N-(CO) bond at various temperatures was not determined as this study was mainly concerned with establishing a synthetic route to the target benzamides and their unambiguous characterisation. For example, **Figure 27** shows the variable temperature ^{1}H NMR spectra of 3-[(*N*-cyclohexylbenzamido)methyl)]-6-methoxy-(1*H*)-2-quinolone **117e** from 313 to 373K to demonstrate facilitation of interpretation resulting from raising the temperature.

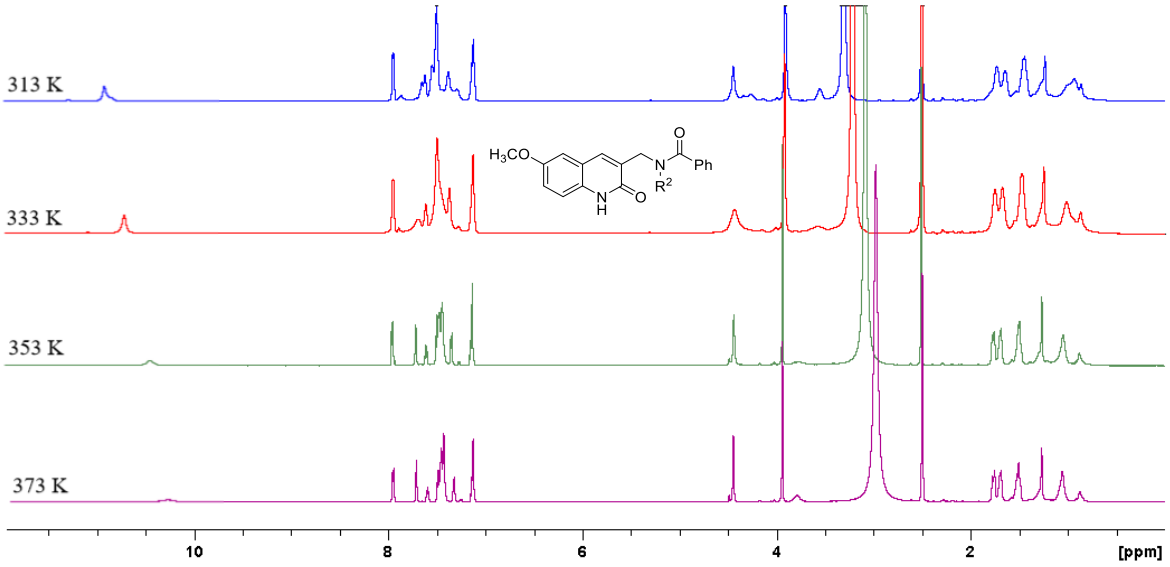

Figure 27. Variable temperature ^{1}H NMR spectra of compound **117e**.

On comparing the spectra of compound **117e** at different temperatures, it is apparent that the spectrum becomes more clearly resolved as the temperature is increased. Varying the temperature provided particular details which, when combined with the use of 2-D spectra permitted detailed structural elucidation of the benzamides (**117-119**). The apparent absence of the expected ^{1}H- and/or ^{13}C NMR *N*-methylene and/or *N*-methine signals in certain spectra is attributed to site-exchange line-broadening effects. The presence of these nuclei in such cases is, however, supported by the HRMS and, in the case of 3-[(*N*-cyclohexylbenzamido)methyl)]-(1*H*)-2-quinolone **117a**, an HSQC experiment (**Figure 28**), conducted at 298 K, revealed a peak correlating to an *N*-methylene ^{13}C signal with the observed ^{1}H signal overlapping with the DMSO-d_6 signal. The cross peak (circled in blue) corresponding to the *N*-methylene of the minor rotamer does confirm correlation to an apparently absent *N*-methylene ^{13}C signal.

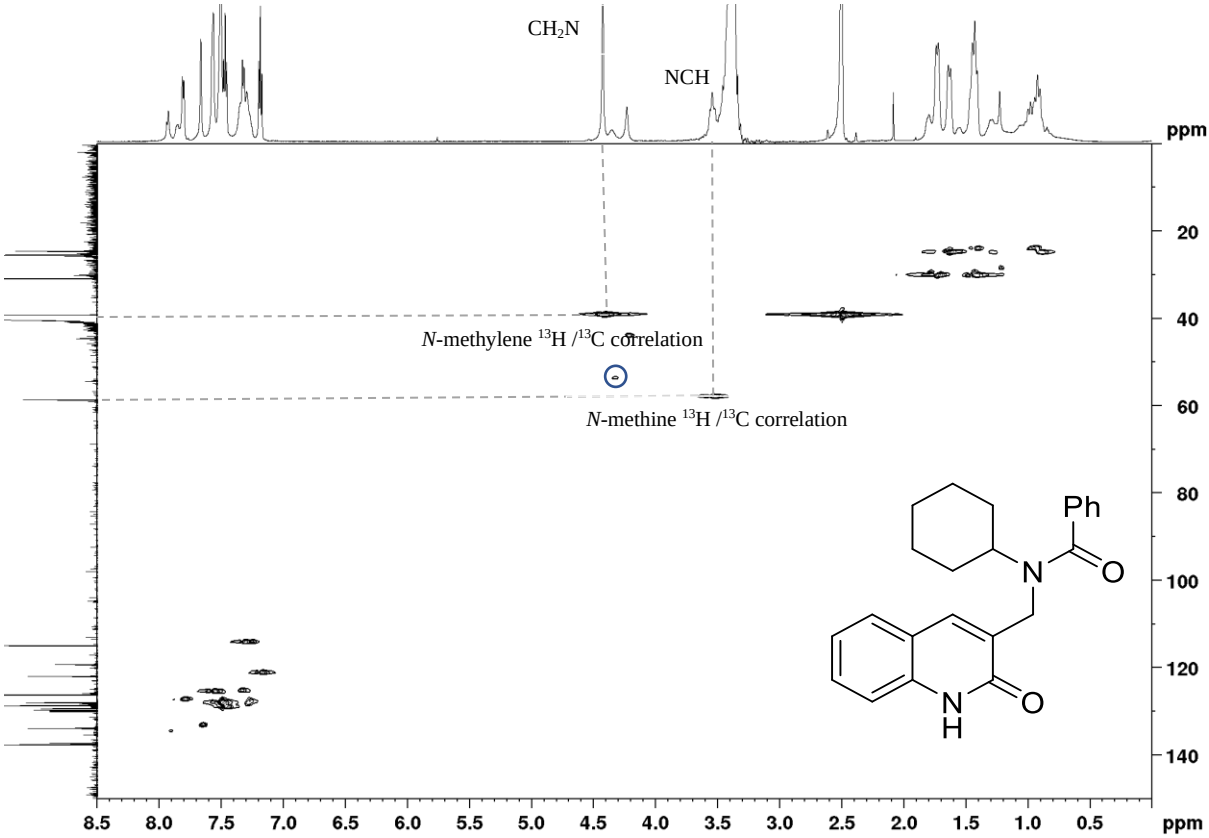

Figure 28. HSQC spectrum of **117a** in DMSO-d_6 at 298 K.

Even with a better resolved ^{1}H NMR spectrum that shows the limited effect of signal-broadening of the methylene and the methine signals, the HSQC spectrum of **117a** at 373 K reveals the apparent absence of the methylene, methine and cyclohexyl carbon signals but shows correlation of cyclohexyl carbons with corresponding proton signals (**Figure 29**). This analysis exemplifies the usefulness of NMR experiments obtained at different temperatures for satisfactory structural elucidation – as evidenced by the observation that at 373 K a clearer ^{1}H NMR spectrum was obtained whilst at 298 K, a better ^{13}C NMR was obtained.

The effect of site-exchange in the NMR analysis of compound **117a** is evidenced in the HSQC spectrum at 373 K (**Figure 29**) by the absence of the *N*-methine carbon as well as the cross peaks due to signal broadening of the corresponding *N*-methine proton, and the absence of cyclohexyl methylene carbons. However, at 298 K, the DEPT-135 spectrum (**Figure 30**) showed both the methine and the methylene signals at 58.2 and 39.2 ppm, respectively as well as the three cyclohexyl methylene carbons at 24.1, 25.0 and 30.4 ppm.

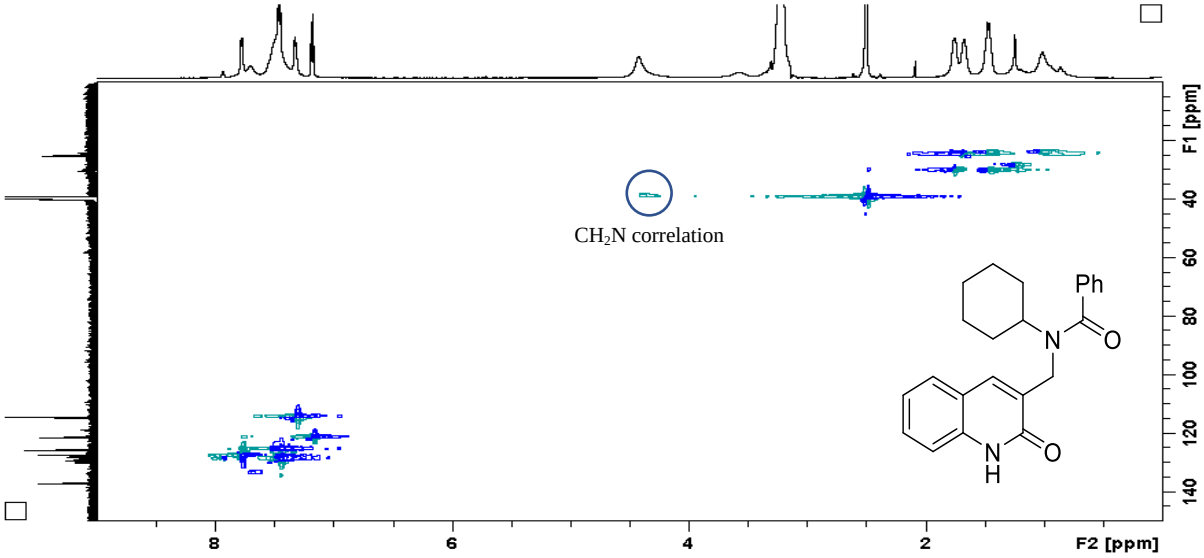

Figure 29. HSQC spectrum of **117a** at 373 K in DMSO-d_6.

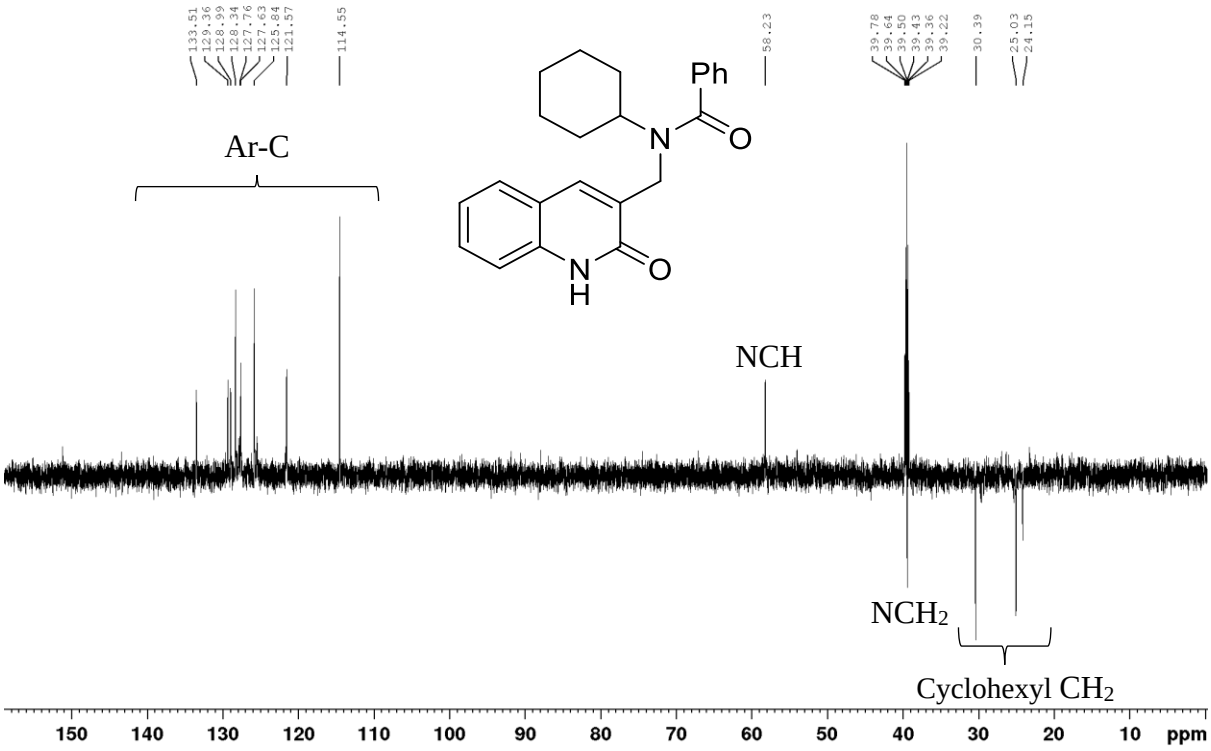

Figure 30. DEPT-135 NMR spectrum of **117a** at 298 K in DMSO-d_6.

In addition to the use of IR and HRMS analysis, the inherent intramolecular exchange required the use of variable temperature 1D- and 2D-NMR analyses in the characterisation of all nine benzamides (**117-119**) synthesised. The ^{1}H NMR spectrum of **117a** at normal probe temperature, 298 K, (**Figure 31**) demonstrates the complexity associated with hindered rotation in the aromatic region and reduced ring flipping in the aliphatic cyclohexyl ring. In the

corresponding ^{13}C NMR spectrum, a clear spectrum was obtained at 298 K as shown in the HSQC spectrum (**Figure 28**). The singlet at 4.42 ppm corresponds to the N-methylene protons (CH_2N) whilst the signal at 3.54 ppm corresponds to the methine proton (NCH). In contrast, at 373 K, the spectrum (**Figure 32**) is comprised of relatively sharp, time-averaged signals resulting from fast rotation and ring flipping.

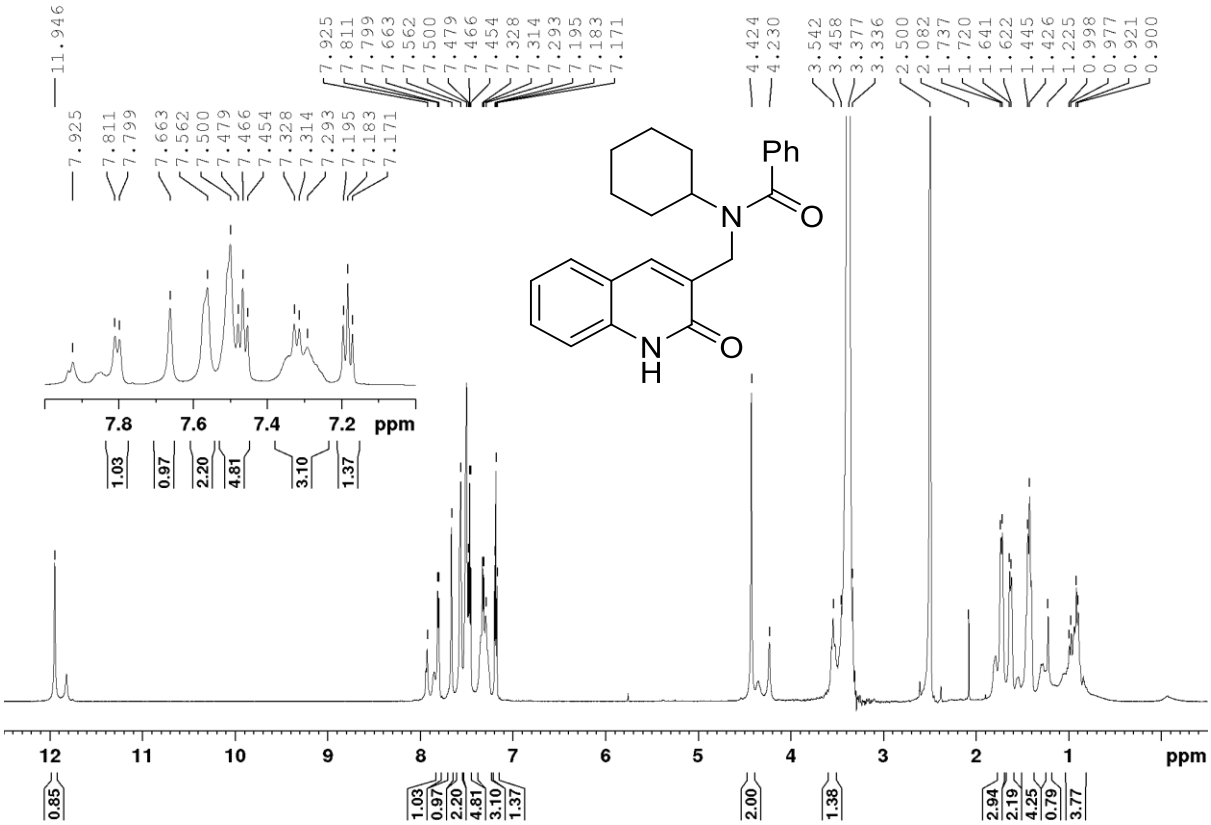

Figure 31. The ^{1}H NMR spectrum of **117a** at 298 K in DMSO-d_6.

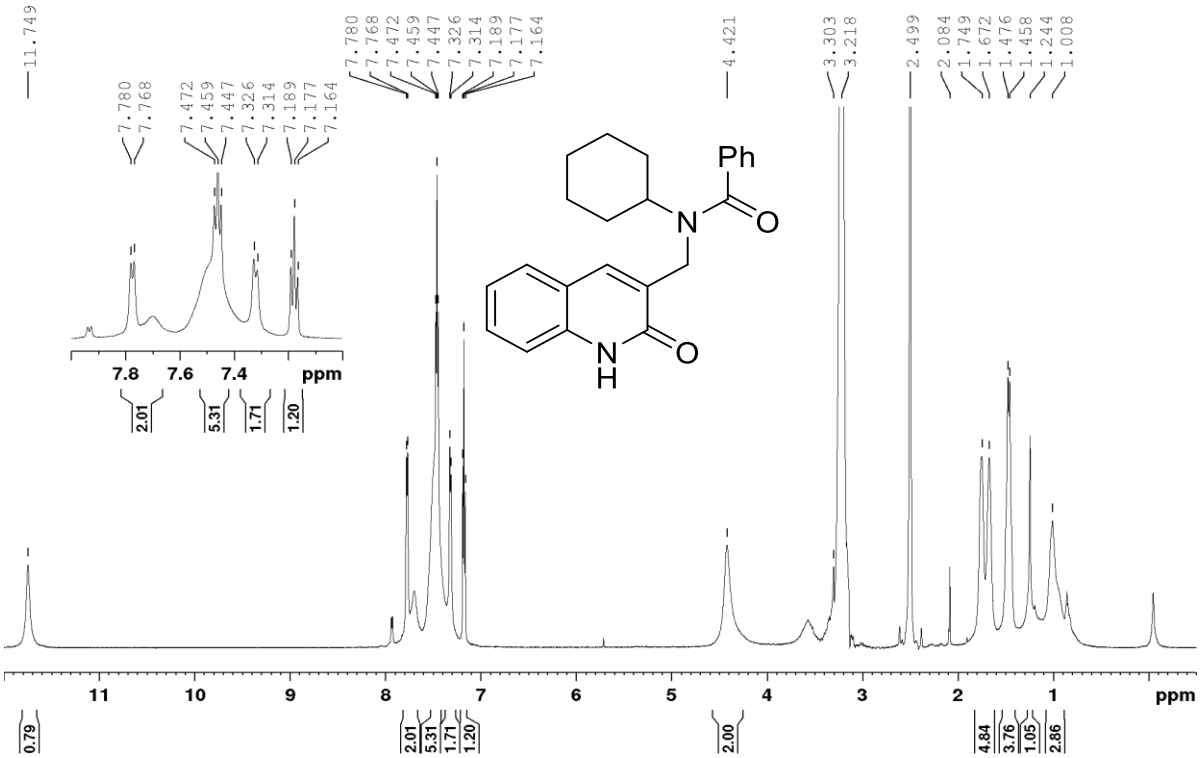

Figure 32. The ^{1}H NMR spectrum of **117a** at 373 K in DMSO-d_6.

Figure 33 shows the ^{1}H NMR spectrum of 3-[(*N*-cyclopentylbenzamido)methyl)]-6-methoxy-2(1*H*)-quinolone **118e** obtained at 313 K reflecting an intermediate site-exchange process. Unlike the ^{1}H NMR spectrum of **117a** in **Figure 32**, and instead of a singlet representing the two *N*-methylene (CH_2) protons, the spectrum obtained at 313 K showed a number of signals corresponding to the geminal methylene protons (CH_2N) and, the methine proton (NCH) that resonate as broad signals at *ca.* 3.55, 4.44 and 5.26 ppm due to the intermediate exchange process. Notable, in **Figure 33** are the multiple signals between 10.0 and 12.0 ppm corresponding to the quinolone NH proton, but this cannot be employed as a reliable indication of the presence of rotamers as they are isotopically exchangeable with H_2O in DMSO-d_6. The methoxy protons resonated at 3.79 and 3.92 ppm instead of a singlet and this was seldom encountered.

These observations signify slow intramolecular site-exchange and hence the presence of rotamers at 313 K. Although the aromatic and cyclohexyl proton signals were resolved as the temperature was raised to 333 K and 353 K, negligible improvements in the corresponding ^{13}C NMR spectra were observed. A significant transition to fast site-exchange, beyond coalescence, for this molecule, occurs somewhere between 353 and 373 K. Such transitions

could be clearly observed when the temperature was increased in small increments; in our case, the temperature was raised at 20 K increments.

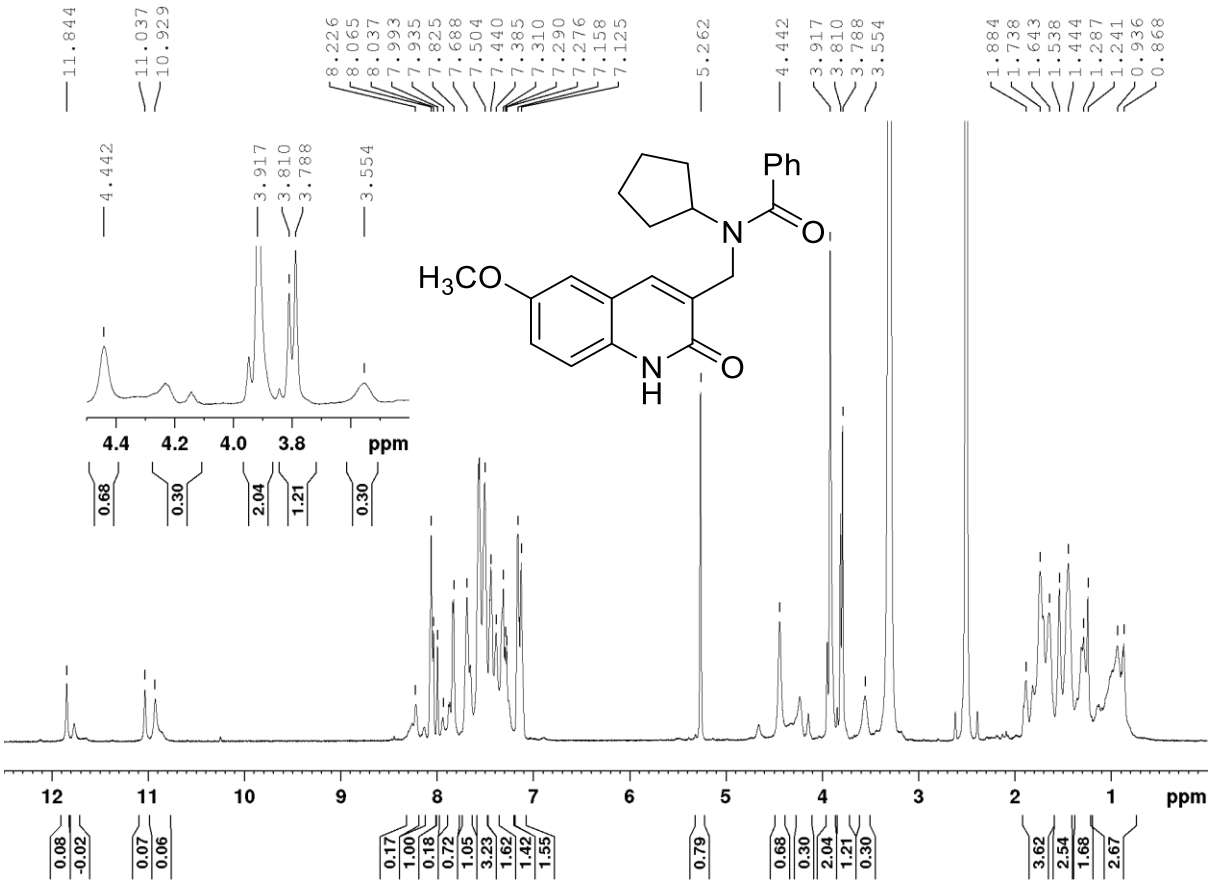

Figure 33. ^{1}H NMR spectrum of **118e** in DMSO-d_6 at 313 K.

Figure 34 shows a stack-plot of the ^{13}C NMR spectra of **118a** which reveals the presence of methine and methylene carbon signals at 313 K which subsequently broaden and disappear into the noise as the temperature is increased from 333 K to 373 K. In the carbonyl region, the appearance of three carbonyl signals instead of two is associated with hindered rotation. The effect of hindered rotation is also evident in the resolution of aromatic carbon signals as the temperature is increased in 20 K increments. The two signals corresponding to the cyclopentyl methylene carbons were, however, not affected signifying that their chemical environment is essentially constant regardless of apparent cyclopentyl ring flipping, mainly between the envelope and the half-chair conformation.[209] The IR spectrum, as expected, exhibits absorption bands at 1656 and 1621 cm^{-1} corresponding to the two carbonyl groups whilst the ESI mass spectrum of compound **118a** reveals the pseudo-molecular ion peak at m/z = 347.1764.

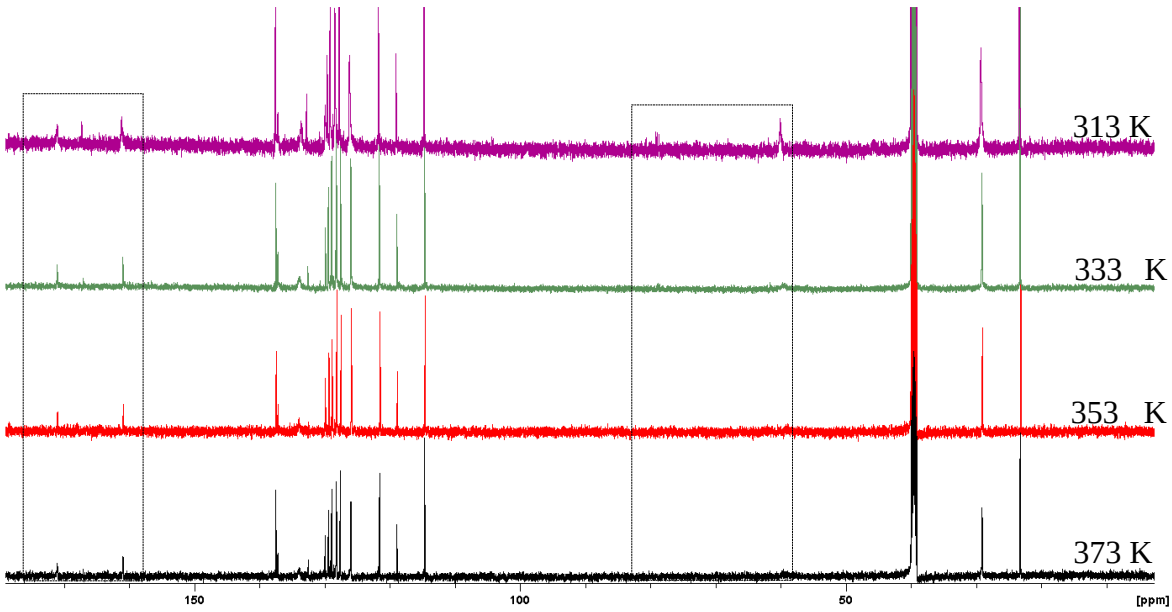

Figure 34. A stack-plot of ^{13}C NMR spectra of **118a** at different temperatures.

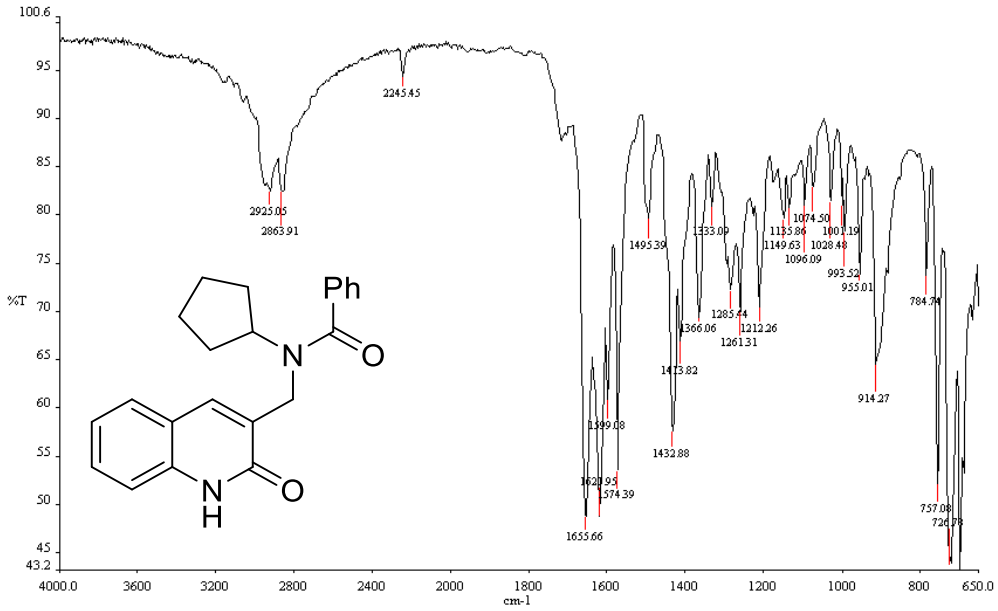

Figure 35. IR spectrum of **118a**.

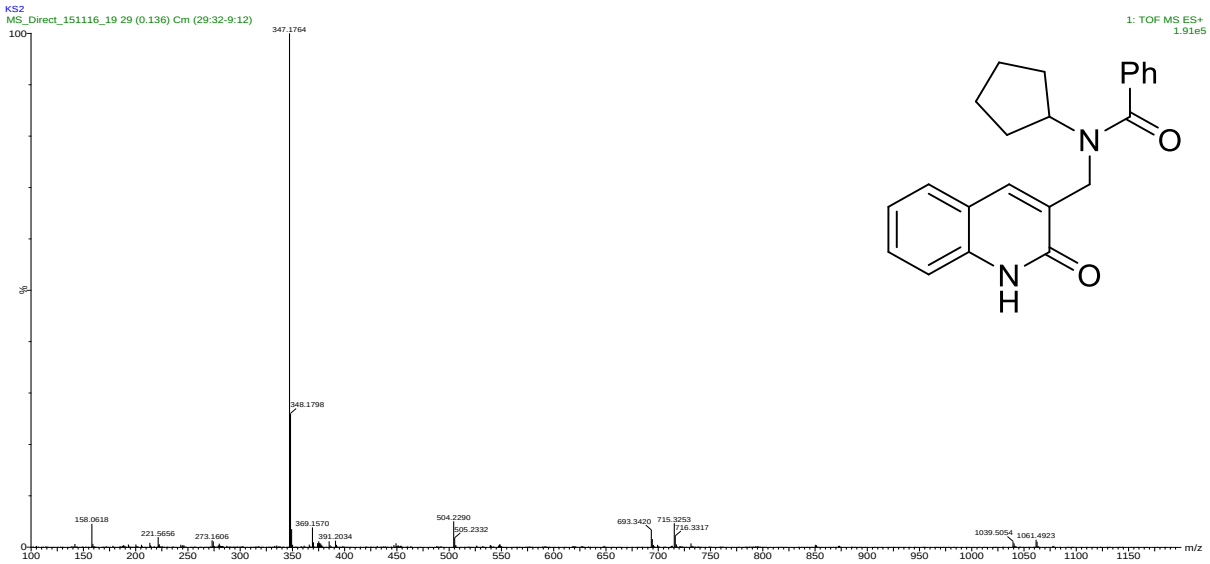

Figure 36. ESI mass spectrum of **118a**.

In light of the NMR site-exchange effects discussed above and the realisation that changing the temperature brings about significant changes in the spectrum, we reported NMR data for each of the benzamides (**117-119**) at a temperature at which the best NMR spectrum was obtained. For example, the ^{1}H NMR spectrum of **119a** obtained at 333 K shows the expected ten aromatic protons. The signal at 5.27 ppm corresponds to the methylene protons, the signal at *ca.* 1.2 ppm the cyclopropyl methylene protons, and the signal at 11.846 ppm to the quinolone NH proton.

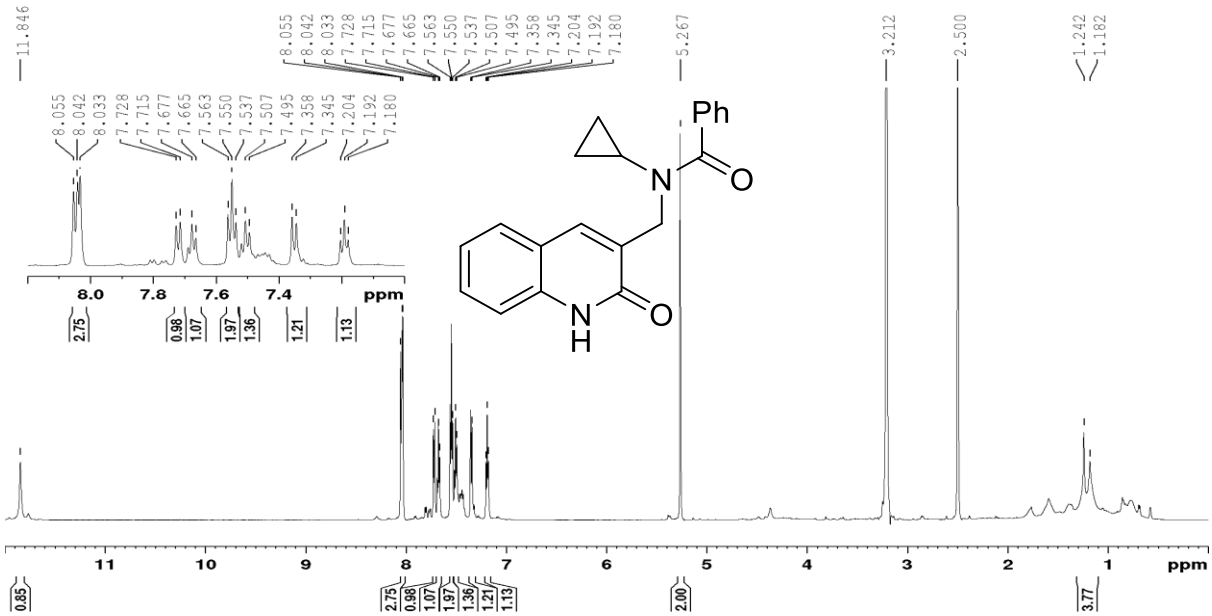

Figure 37. ^{1}H NMR spectrum of **119a** at 333K in DMSO-d_6..

The corresponding ^{13}C NMR spectrum (**Figure 38**) in conjunction with the HSQC spectrum (**Figure 39**), reveals the presence of four aromatic quaternary carbons at 118.6, 127.5, 129.5 and 138.3 ppm. And the signals at 160.7 and 165.4 ppm correspond to the carbonyl carbons. The cyclopropyl methine (NCH) methylene carbons resonate at 61.6 and 23.2 ppm, respectively.

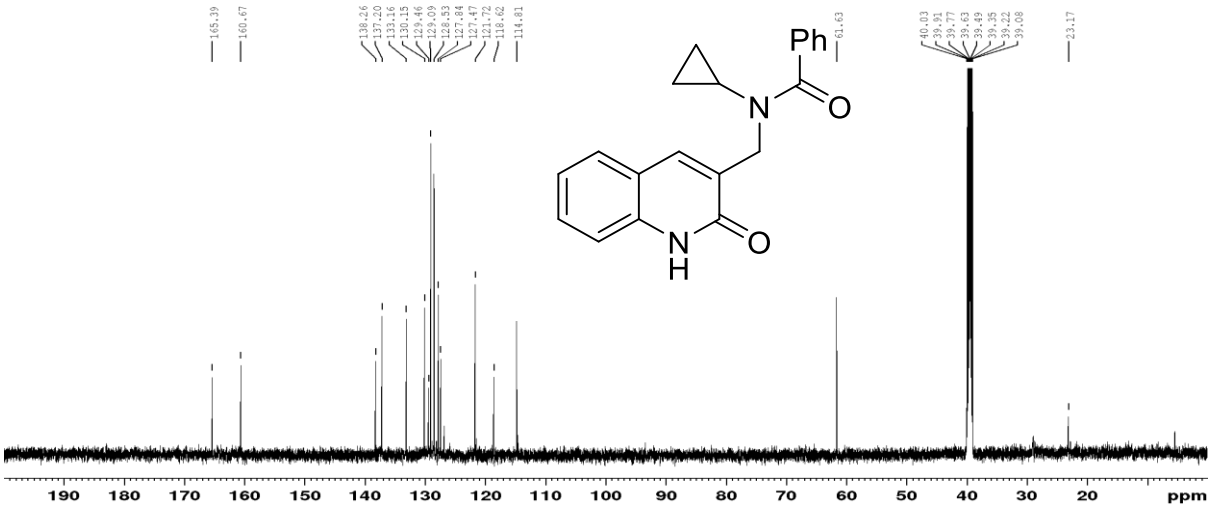

Figure 38. ^{13}C NMR spectrum of **119a** at 333K in DMSO-d_6.

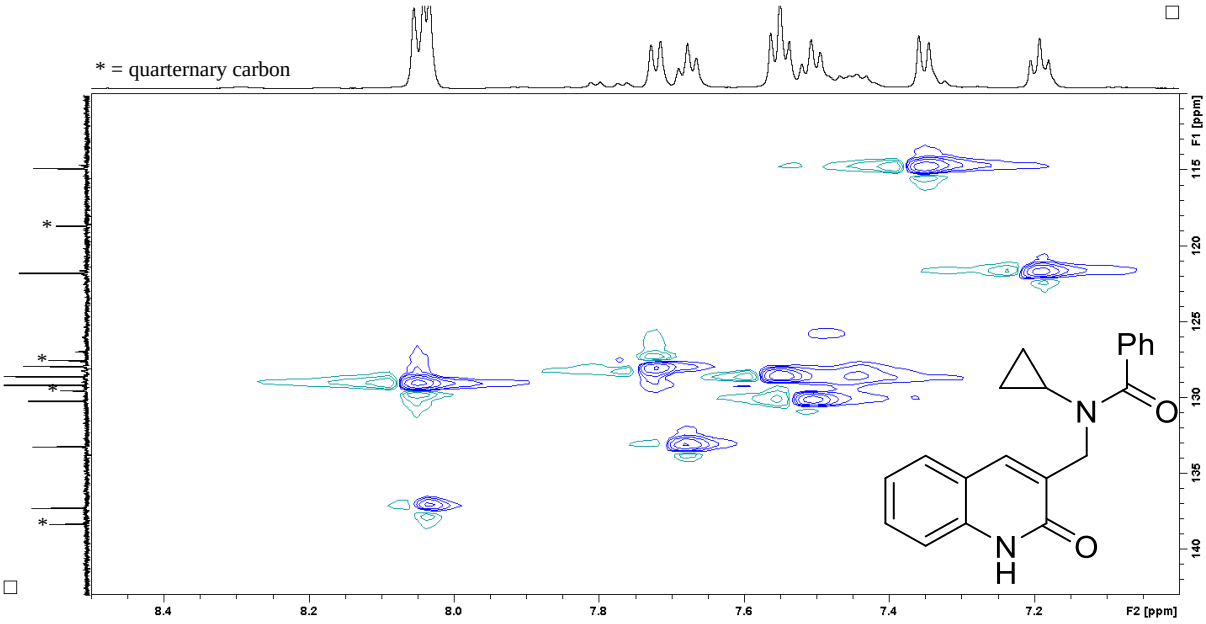

Figure 39. HSQC spectrum of **119a** at 333 K in DMSO-d_6.

2.2. Preparation of indolizine derivatives *via* aza-Baylis-Hillman intermediates

In this section, attention is focussed on the application of Baylis-Hillman methodology in the construction of indolizine derivatives. This approach involves two steps: i) a Baylis-Hillman reaction to obtain a suitable *N*-heterocyclic adduct; and ii) intramolecular cyclisation to afford the indolizine. The Baylis-Hillman reaction involved the use of appropriate heterocyclic aldehydes with methyl acrylate **46b** as the activated alkene in chloroform in the presence of the tertiary amine catalyst, 3-hydroxyquinuclidine (3-HQ) **123** (**Table 6**). All the reactions were conducted in a stoppered flask at room temperature under atmospheric pressure. The duration of the reaction ranged from two to twenty-one days with the reaction progress being monitored by TLC.

The Baylis-Hillman adducts were prepared using a range of heterocyclic reagents, comprising pyridine-2-carboxaldehyde **124**, 2,6-pyridinedicarboxaldehyde **125**, indole-2-carboxaldehyde **126**, quinoline-2-carboxaldehyde **127**, 1*H*-imidzole-2-carboxldehyde **128** and 4-methyl-1-phenylpyrazol-3-carboxaldehyde **129**. The pyridine derivative **88** was obtained in an excellent yield of 95%. Other pyridine (**130a** and **130b**) and quinoline (**132**) derivatives were obtained in yields of 57% and 45% yield, respectively. The indole (**131**) and pyrazole (**134**) adducts were obtained in disappointing yields (22% and 29%. respectively), but the imidazole-5-carboxaldehyde **128** failed to give any of the corresponding Baylis-Hillman adduct. These results indicate that the azino-2-carboxaldehydes (**124**, **125** and **127**) are the most reactive. In fact, compounds **88**, **130a** and **130b** were isolated after two days, whereas *N*-phenylpyrazole-5-aldehyde **129** yielded the desired product in 19% after 21 days. All of the Baylis-Hillman adducts were fully characterised by NMR, IR and high-resolution mass spectrometric analysis.

Figure 40 illustrates the assignment of significant signals in the ^{1}H NMR spectrum of compound **88**. The spectrum reveals a singlet at 3.67 ppm corresponding to the methoxy group (OCH_3), and three signals characteristic of Baylis-Hillman products at 5.59, 5.94 and 6.32 ppm corresponding to the methine proton on the stereogenic centre C-3 and the diastereotopic vinylic methylene protons, respectively. The pyridine protons resonate, as expected, in the aromatic region, with the two triplets at 7.16 and 7.63 ppm corresponding to the 4´- and 5´-protons, while the doublets at 7.38 and 8.47 ppm are due to the 6´- and 3´-protons, respectively.

Table 6. Reactants, Baylis-Hillman products and yields.

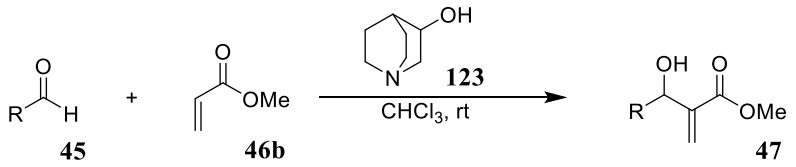

Entry	Heterocyclic aldehyde	Product; Yield (%)
1	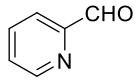 **124**	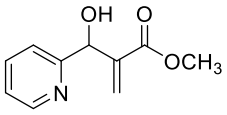 **88**; 95%
2	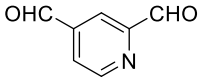 **125**	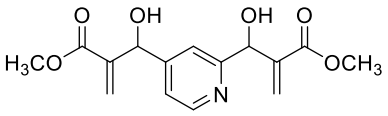 **130a**; 22% + 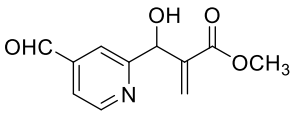 **130b**; 35%
3	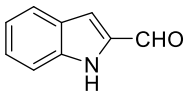 **126**	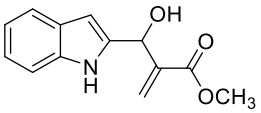 **131**; 22%
4	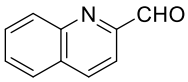 **127**	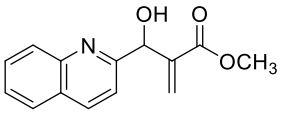 **132**; 45%
5	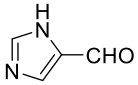 **128**	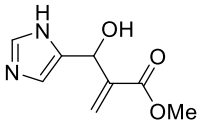 **133**; 0%
6	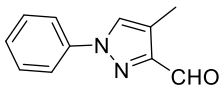 **129**	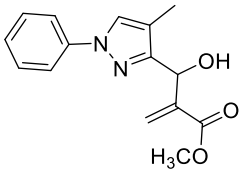 **134**; 19%

The corresponding ^{13}C NMR spectrum of product **88** exhibits the expected ten carbon signals. The methoxy carbon resonates at 51.8 ppm and the stereogenic centre C-3 resonates at 72.0 ppm. In conjunction with the DEPT-135 NMR spectrum, it can be shown that the methylene carbon resonates at 126.8 ppm and the four proton-bearing aromatic carbons in the range of 121 to 149 ppm. The quaternary carbons C-2 and C-2´ resonate at 141.5 and 159.4 ppm,

respectively, and the carbonyl carbon resonates at 166.4 ppm. Infra-red spectroscopy (**Figure 43**) revealed the broad hydroxyl (OH) and the carbonyl (C=O) stretching bands at 3225 and 1700 cm^{-1}, respectively; the breadth of the hydroxyl band may be attributed to a combination of intramolecular, and in the neat sample used, intermolecular hydrogen-bonding.

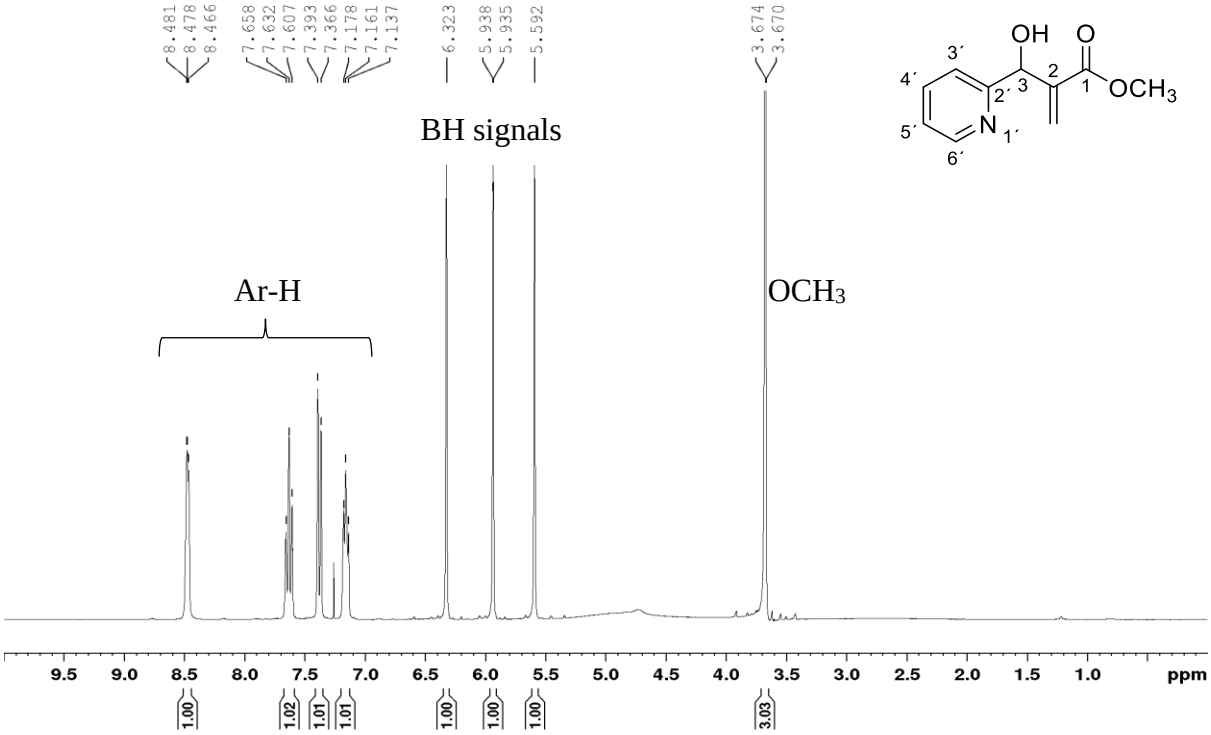

Figure 40. 600 MHz ^{1}H NMR spectrum of compound **88** in $CDCl_3$.

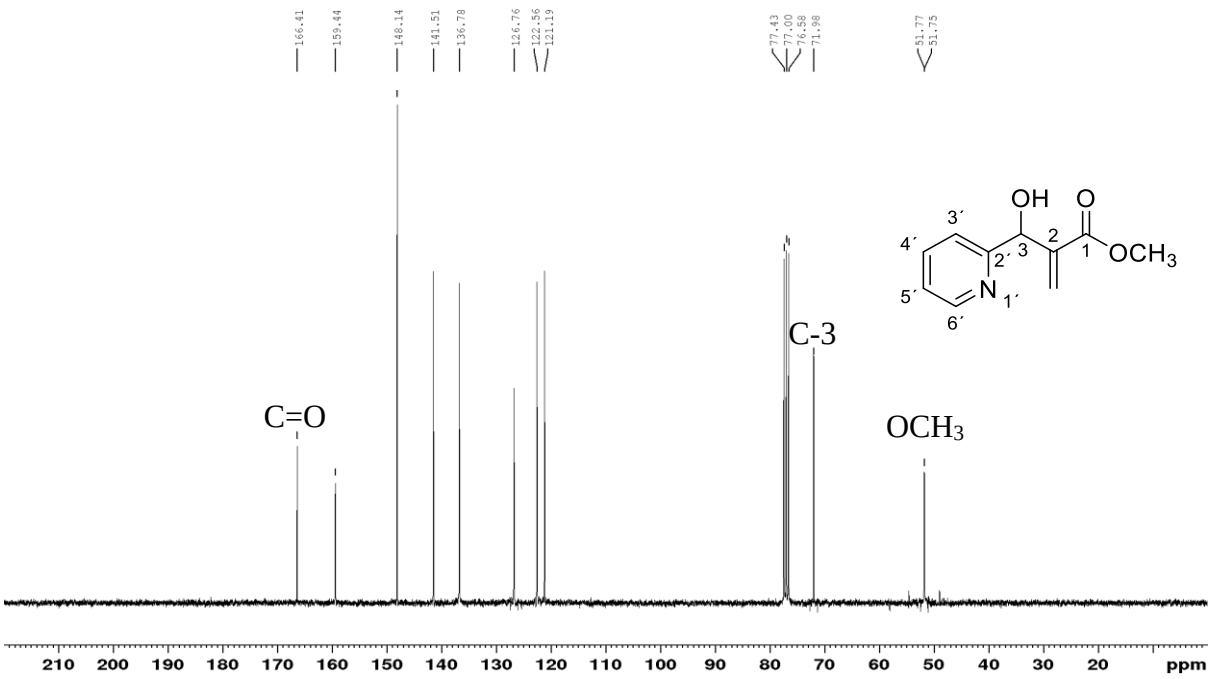

Figure 41. 150 MHz ^{13}C NMR spectrum of compound **88** in $CDCl_3$.

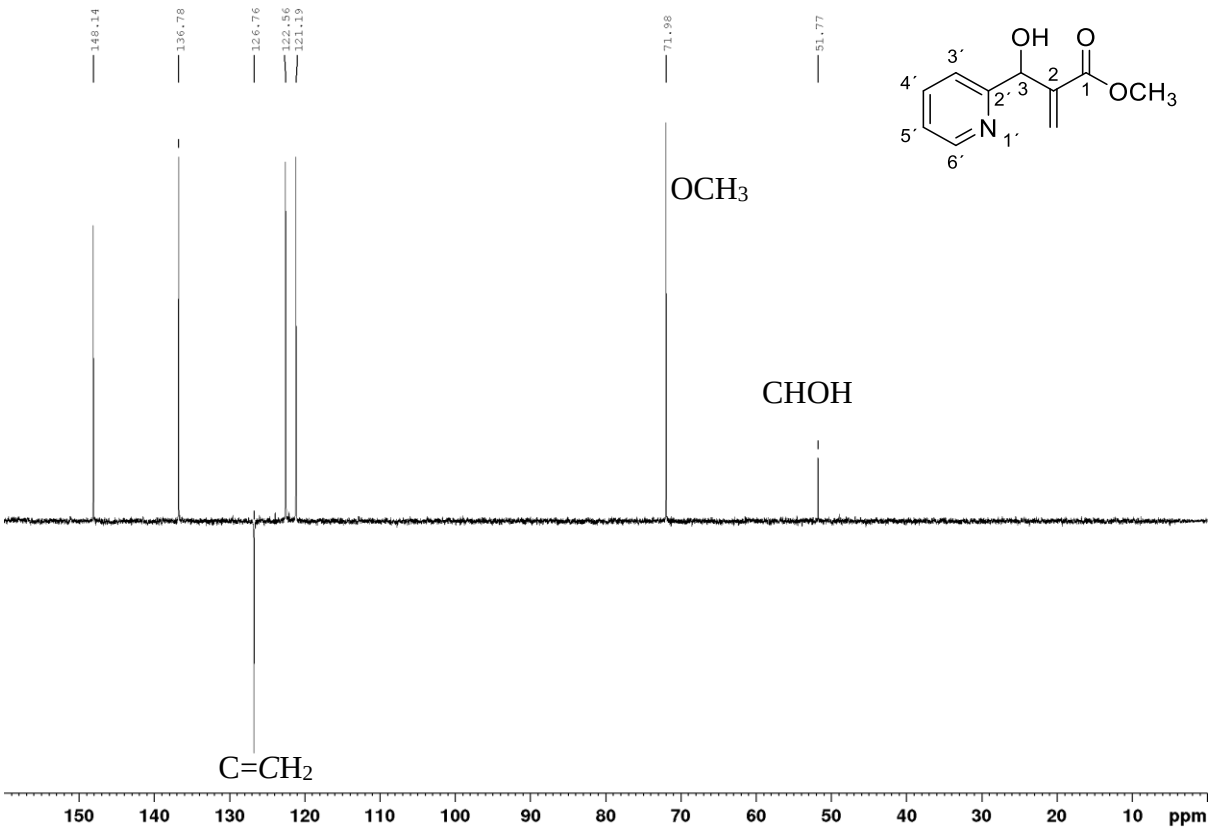

Figure 42. DEPT-135 spectrum of compound **88** in $CDCl_3$.

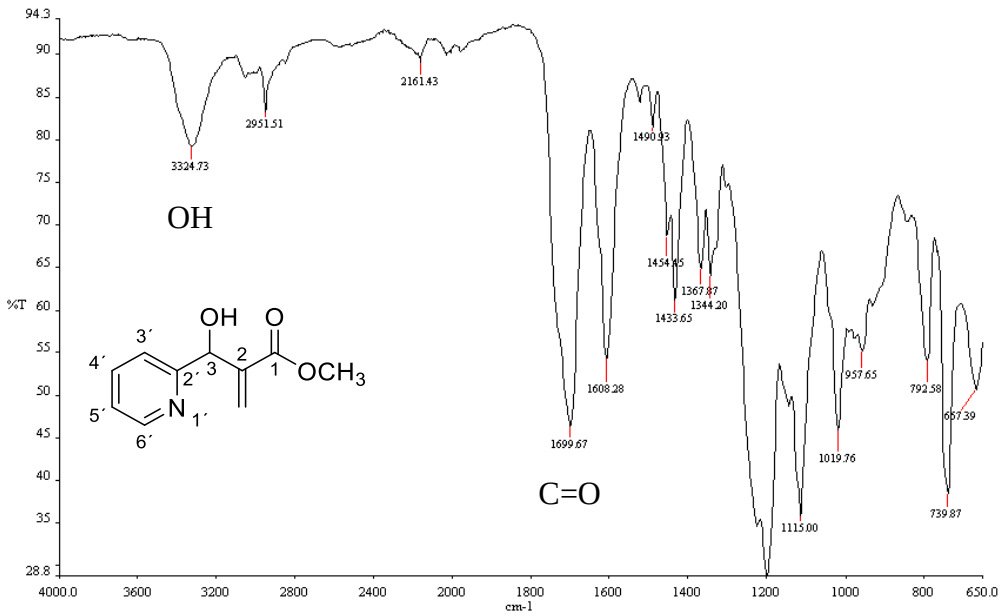

Figure 43. IR spectrum of compound **88**.

In addition to the Diels-Alder reaction, ring closing metathesis, the Ugi reaction and the Passerini reaction, the Baylis-Hillman reaction has emerged as an efficient complexity-

generating reaction.[109] Appreciation of the synthetic utility of the Baylis-Hillman reaction in organic chemistry is evidenced by a number of reviews including textbook chapters that specifically cover the application of this reaction in great detail.[210-213] Baylis-Hillman methodology has been widely used to access a variety of medicinally useful compounds, especially cyclic compounds.[214]

The capacity of the Baylis-Hillman methodology to access indolizines, such as methyl 2-indolizinecarboxylate **90**, was discovered serendipitously in our group.[126] The convenience of this methodology spurred the synthesis of a series of indolizine-2-carboxamides. Failure to convert the indolizine-2-carbonyl acid to the acid chloride prevented facile access to secondary and tertiary amide derivatives. In the quest to develop an effective coupling methodology, various established methods for converting carboxylic acids to amides were explored. These included heating the methyl indolizine-2-carboxylate **90** in a sealed tube with primary amines and treating the ester **90** with ethanolic dimethylamine at room temperature for three days – a method which afforded the corresponding tertiary amide in minute yield. The 1,1´-carbonyldiimidazole (CDI)-mediated coupling of indolizine-2-carboxylic acid with aliphatic secondary amines finally provided access to tertiary amides in good yields.[114]

In an extension of these earlier studies, we herein report a comprehensive coupling methodology which proved to be effective even for amines that would have been considered sterically bulky and relatively unreactive towards amidation.

2.2.1. Thermal cyclisation of 2-pyridinyl derivatives.

The synthesis of the Baylis-Hillman adduct **88** was followed by direct thermal cyclisation of the adduct which was effected by refluxing the adduct in excess acetic anhydride for 2 days to afford the indolizine ester **90** in 93% yield. Refluxing the mixture for 7 days provided the 3-acetylated product **136** in a good yield of 83%. In each case, the excess acetic anhydride was removed *in vacuo* and the crude products were purified by column chromatography to afford light green and light brown crystals, respectively. Previously, in our group, cyclisation to the indolizine ester has been effected by refluxing the acetylated Baylis-Hillman adduct **89** in excess acetic anhydride,[126, 145] or by reacting acetyl chloride with the alcohol **88** in CH_2Cl_2 in the presence of pyridine.[215] In the present study, refluxing the Baylis-Hillman alcohol **88** for prolonged periods afforded the indolizine ester **90** or the 3-acetylated indolizine ester **136**.

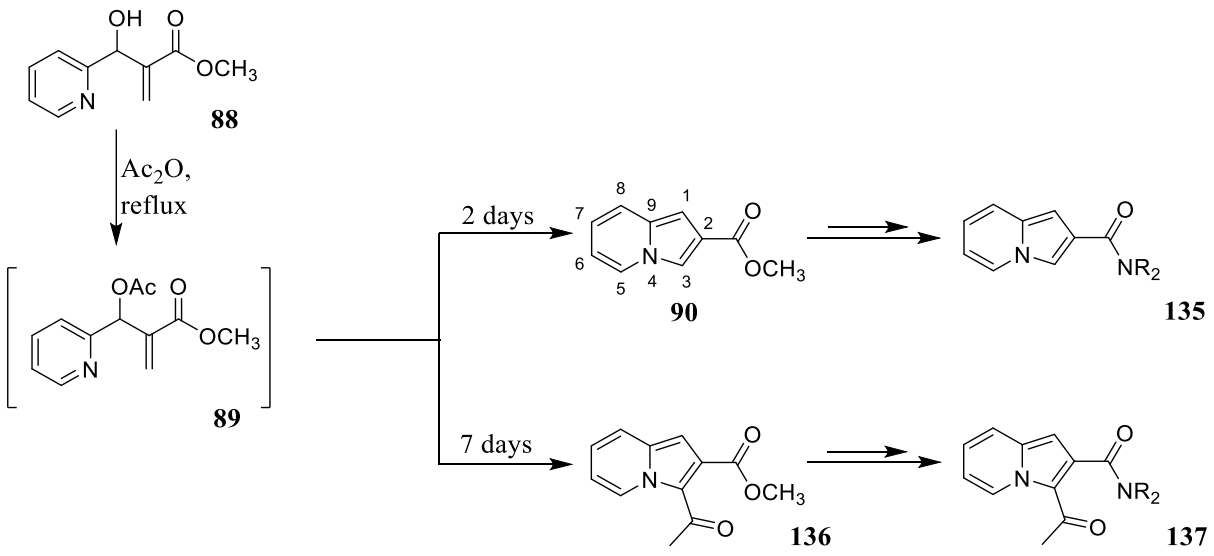

Scheme 26. Synthetic pathway to indolizine-2-carboxamides.

The successful, one-step intramolecular cyclisation of the alcohol **88** results in aromatisation and the loss of the chirality at C-3 and the diastereotopic vinylic methylene protons. Thus, a successful transformation is evidenced by the disappearance of the Baylis-Hillman characteristic signals in the ^{1}H NMR spectrum (**Figure 44**), and the absence of the signal for the methylene carbon in the DEPT-135 spectrum. In fact, six proton-bearing aromatic carbon signals are evident in the DEPT 135 spectrum of compound **90**.

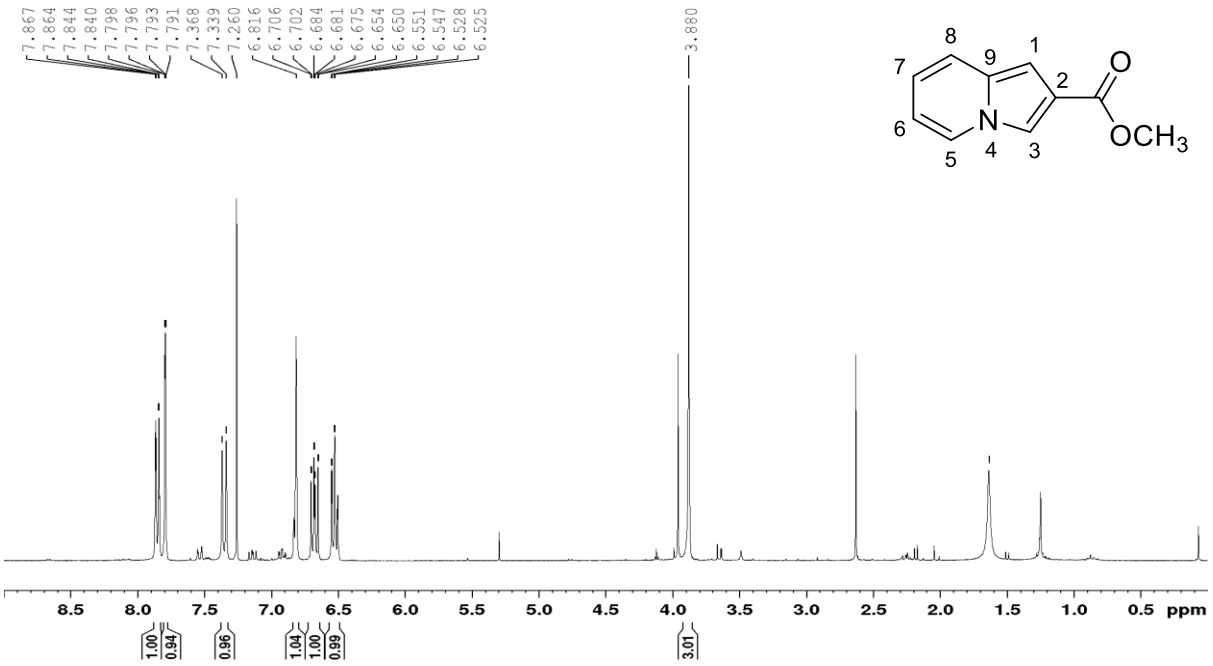

Figure 44. 300 MHz ^{1}H NMR of compound **90** in $CDCl_3$.

As expected, the ^{1}H NMR spectrum of compound **90** (**Figure 44**) reveals a singlet at 3.88 ppm corresponding to the methoxy group, a significant shift from 3.67 ppm in the ^{1}H NMR spectrum of the precursor. The indolizine protons resonate in the aromatic region, with a triplet of doublets at 6.53 ppm and the multiplet at 6.68 ppm corresponding to the 7- and 6-protons, while the doublet at 7.35 ppm, the doublet of doublets at 7.79 ppm and 7.85 ppm are due to the 5-, 3- and 8-protons. The signals at 6.82 and 7.79 ppm correspond to the 1- and 3-protons, respectively. The appearance of the 3-methine signal at 7.79 ppm as a doublet instead of a singlet is due to long range ^{1}H-^{1}H coupling, a distinct feature of the ^{1}H NMR spectra of indolizines. The expanded ^{1}H NMR spectrum (**Figure 45**) reveals traces of signals in the aromatic region and, **Figure 44** shows traces of the acetyl and methoxy proton signals at *ca.* 2.6 and 3.9 ppm.

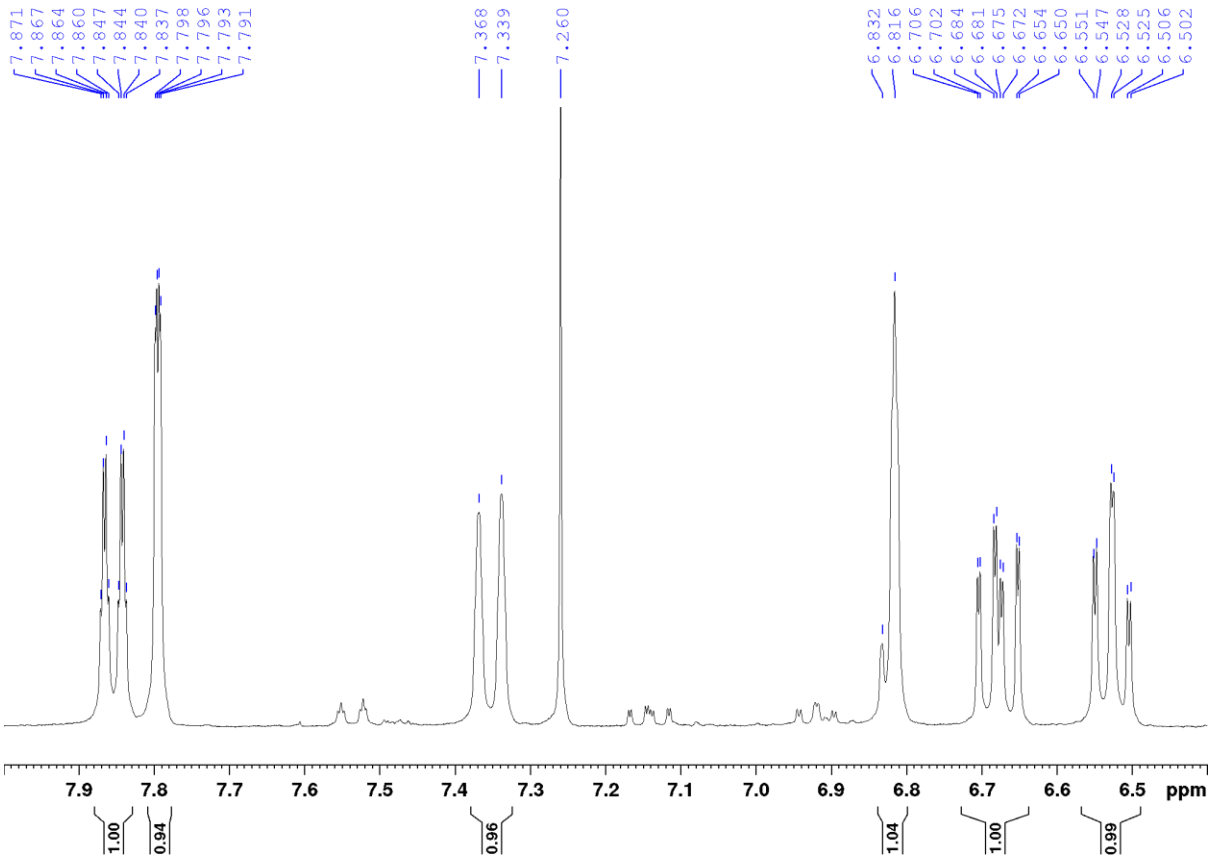

Figure 45. Expanded 300 MHz ^{1}H-NMR spectrum of compound **90** in $CDCl_3$.

On the other hand, the appearance of two methyl singlets in the ^{1}H NMR spectrum of compound **136** (**Figure 46**) confirms acetylation of the indolizine; the singlet at 2.63 ppm corresponds to the acetyl protons while that at 3.96 ppm corresponds to the methoxy proton (the methoxy protons in the ^{1}H NMR spectrum of compound **90** (**Figure 44**) resonates at 3.88 ppm), the aromatic protons of the acetylated indolizine **136** are shifted downfield (compared

to those of compound **90**) due to the deshielding effect of the acetyl group. The presence of the acetyl group appears to significantly reduce the degree of long range ^{1}H-^{1}H coupling as the 5- and 6-H proton signals appear as doublets at 7.53 and 9.80 ppm, respectively, while the 7-H and 6-H proton signals resonating at 6.83 and 6.91ppm, respectively, retain the multiplicity evident in the spectrum of compound **90**.

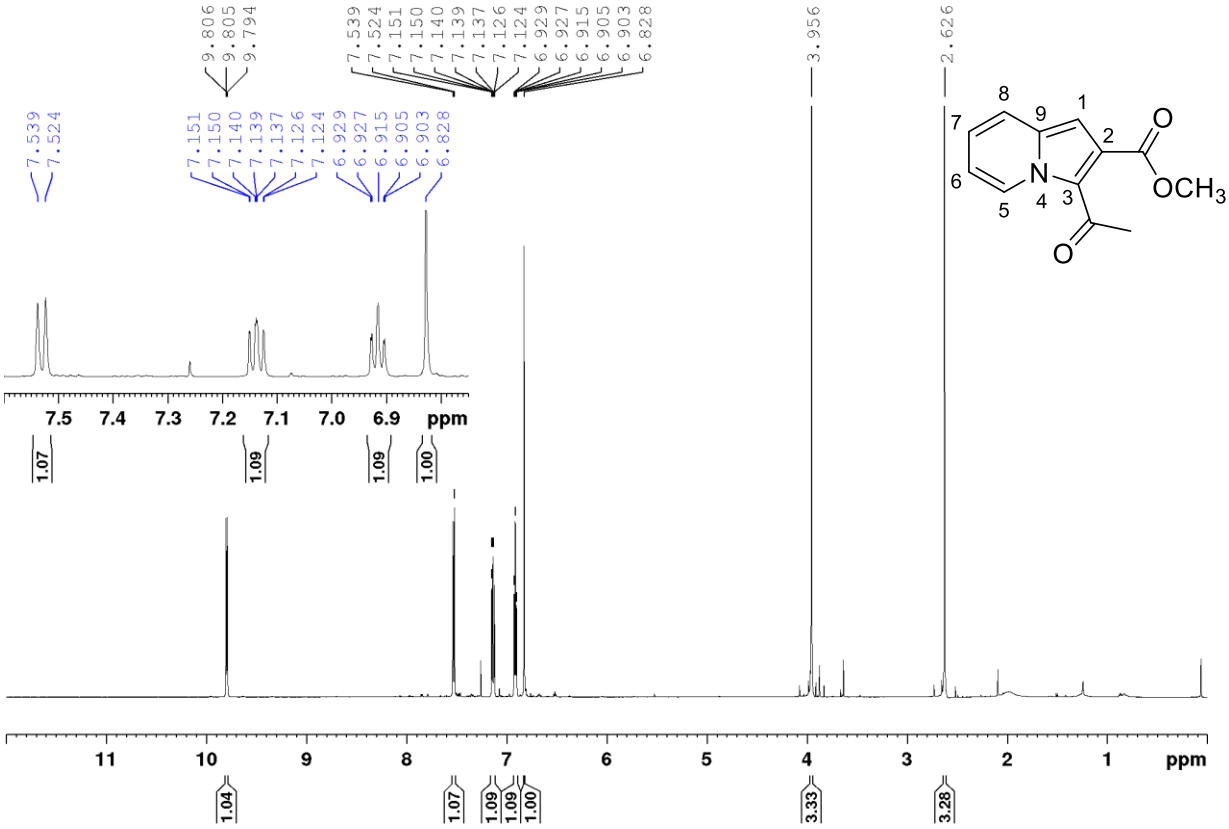

Figure 46. 600 MHz ^{1}H NMR spectrum of compound **136** in $CDCl_3$.

The corresponding ^{13}C NMR spectrum for compound **136** (**Figure 47**) exhibits twelve carbon signals as expected. The signals at 30.1 and 52.5 ppm correspond to the acetyl and methoxy carbons, respectively. The five signals with lower intensity correspond to the quaternary and carbonyl carbons while the other five higher-intensity signals between 104 and 129 ppm are due to the proton-bearing aromatic carbons. The acetyl and ester carbonyl carbons resonate at 166.2 and 189.0 ppm, respectively. The signals for the quaternary carbons, C-9 and C-3, are interspersed between the aromatic methine carbons at 121.1 and 126.8 ppm, and the C-2 nucleus resonates at 135.8 ppm.

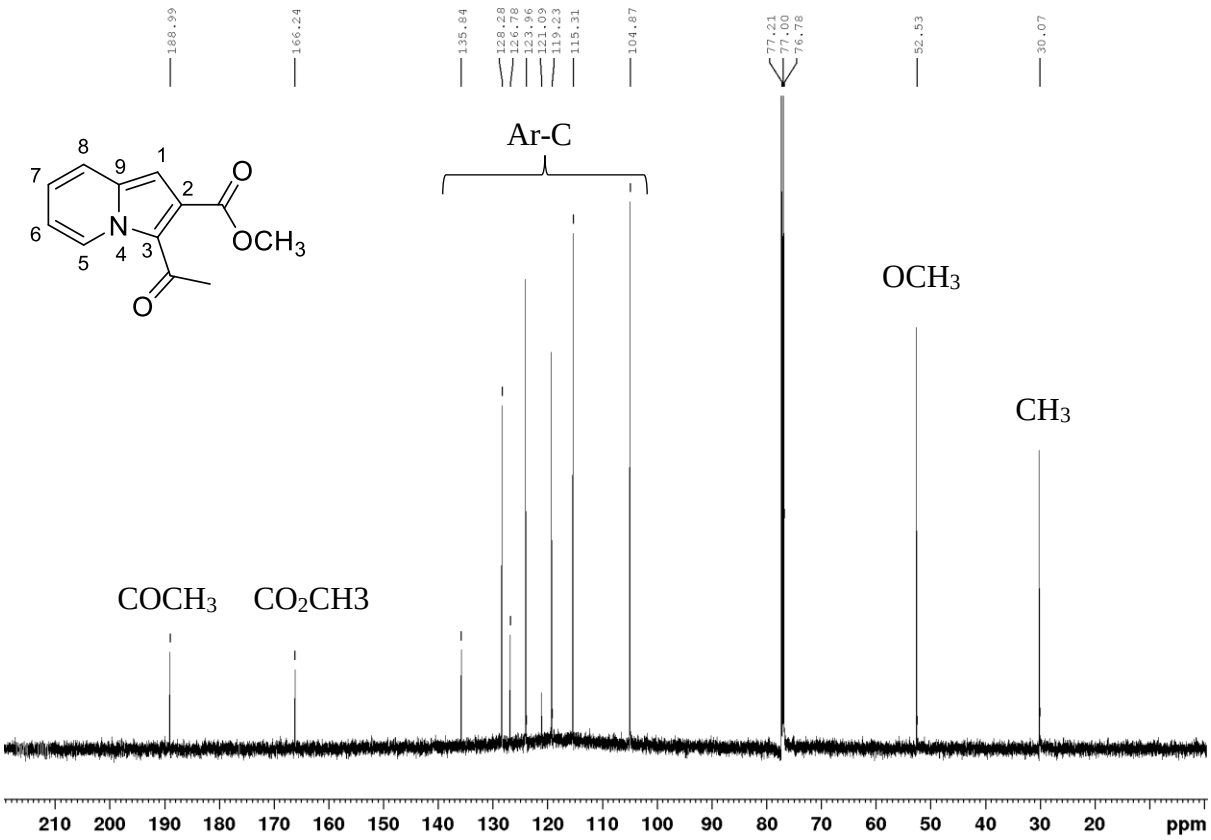

Figure 47. 150 MHz ^{13}C NMR spectrum of compound **136** in $CDCl_3$.

Comparison of the DEPT-135 NMR spectra of methyl indolizine-2-carboxylate **90** and methyl 3-acetylindolizine-2-carboxylate **136** reveals the absence of one aromatic methine carbon due to acetylation at the C-3 carbon in compound **136** – a confirmation that acetylation occurred at this position. Electron delocalisation considerations (see **Scheme 14**) suggest the likelihood of electrophilic substitution at C-1 and/or C-3. However, a protonation study by Fraser *et al.*[151] revealed preference for substitution at C-3 over C-1. In addition, Galasso *et al.*[216] conducted a theoretical study to determine the physical properties of various indolizines including an unsubstituted indolizine which revealed the electron density is second highest at the C-3 position after the bridgehead nitrogen. Because of this, electrophilic substitution readily occurs at the C-3 position.

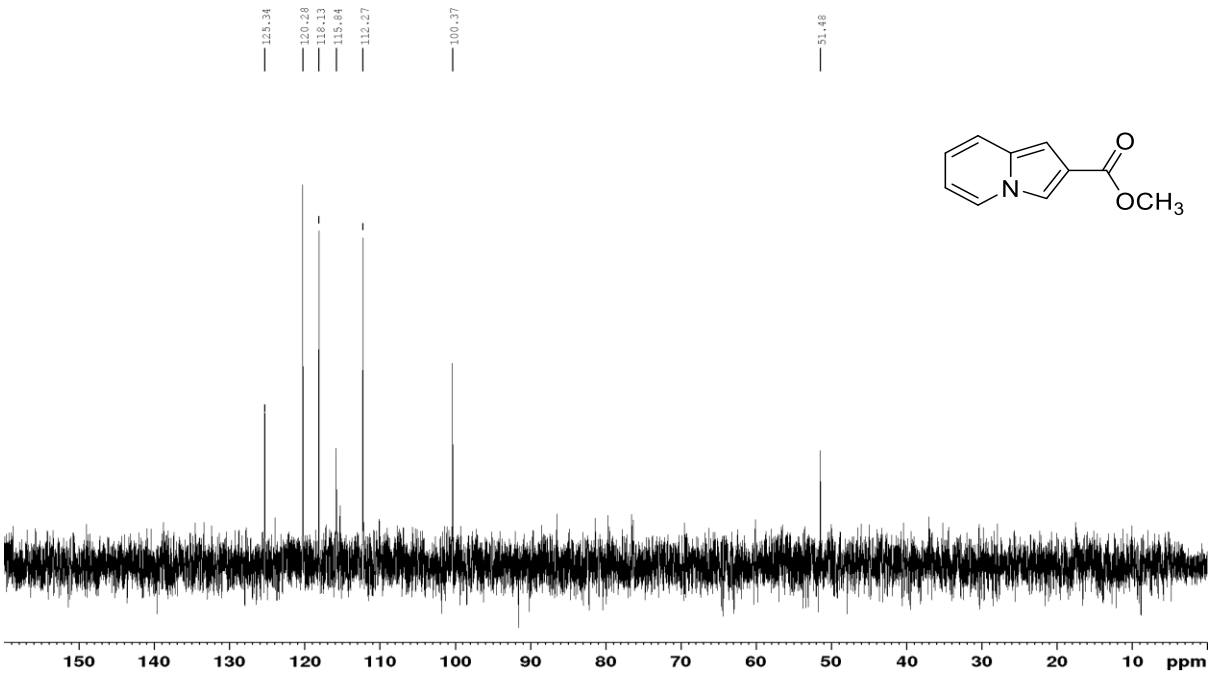

Figure 48. DEPT-135 NMR spectrum of compound **90** in $CDCl_3$.

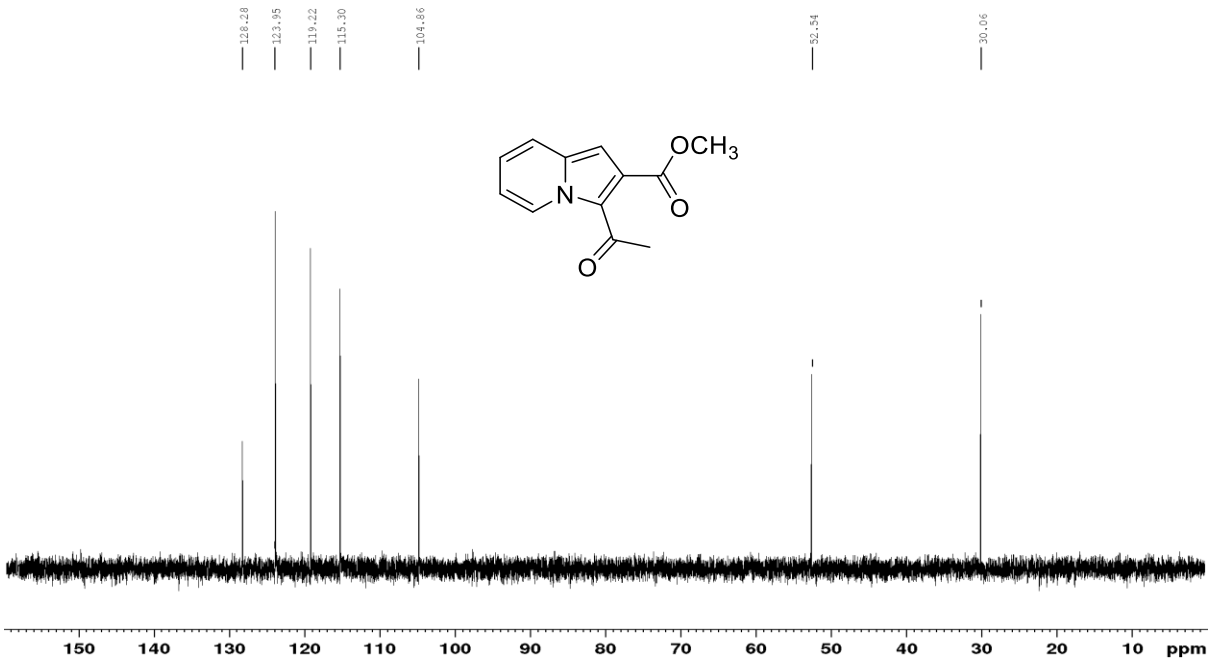

Figure 49. DEPT-135 NMR spectrum of compound **136** in $CDCl_3$.

2.2.2. Saponification of methyl indolizine-2-carboxylate.

The saponification of esters to the corresponding carboxylic acids is a very common functional group interconversion extensively used in organic chemistry.[217] This transformation is imperative as carboxylic acids can be activated to more reactive acyl derivatives. Although the

preparation of indolizine-2-carboxamides from the corresponding esters would appear to provide easy access, this process has been reported to require extreme conditions in return for disappointing yields and is limited to coupling with aliphatic amines.[218-220]

Therefore, hydrolysis of the esters generated by thermal cyclisation of the Baylis-Hillman adducts is crucial in the sequence toward the target molecules and is, therefore, an important step in our synthetic strategy. Although a myriad hydrolysis procedures exist, a mild, easy to handle and environmentally benign procedure is desired.[221, 222] Saponification of methyl indolizine-2-carboxylate **90** to indolizine-2-carboxylic acid **138** was effected by stirring a mixture of the ester and sodium hydroxide in a 1:1 mixture of H_2O and MeOH in a stoppered flask at room temperature. Finally, water was added to dissolve the solid material present and the pH adjusted to *ca.* 2-3 using dilute hydrochloric acid. Work-up afforded indolizine-2-carboxylic acid **138** as yellow crystals in an excellent yield of 86%. With the acid in hand, various coupling procedures to attain the target amides could be explored.

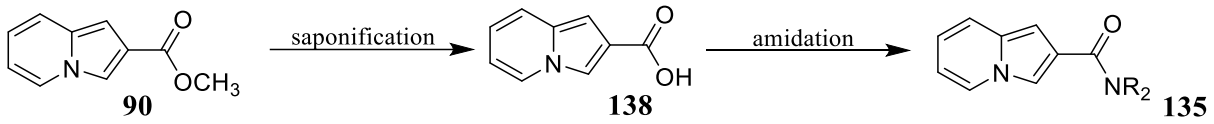

Scheme 27. Chemical transformation of ester **90** to an acid **138** intermediate for subsequent coupling with amines.

Successful saponification of the esters was confirmed by NMR and infra-red spectroscopic analysis of the product which revealed the absence of the methoxy proton signal (**Figure 50**) and the presence of a broad IR hydroxyl stretching band characteristic of a carboxylic acid (*ca.* 3500-2500 cm^{-1}; **Figure 51)**. This conversion of the ester to an acid resulted in significant down-field shift of the aromatic protons – an observation attributed to resonance/delocalisation as shown in **Scheme 28** and, the enhancement of long-range ^1H-^1H coupling in the indolizine nucleus. In the ^1H NMR spectrum (**Figure 50**) of the indolizine-2-carboxylic acid **138** the 1- and 3-methine protons appear as doublets instead of singlets and couple strongly with each other. The absence of the methoxy signal confirms successful saponification.

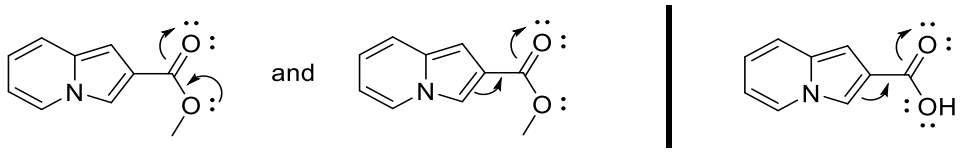

Scheme 28. Deshielding effect in the acid relative to the corresponding ester associated with electron donating index.

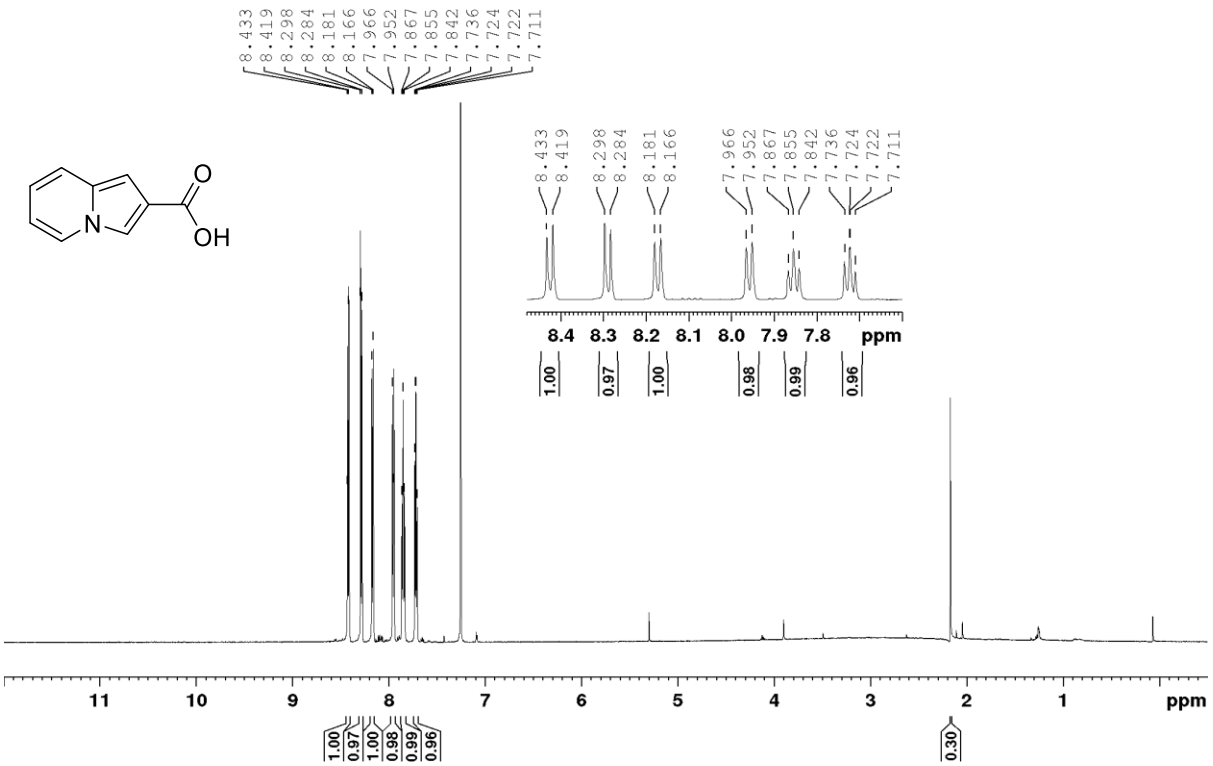

Figure 50. 600 MHz ^{1}H NMR spectrum of indolizine-2-carboxylic acid **138** in $CDCl_3$.

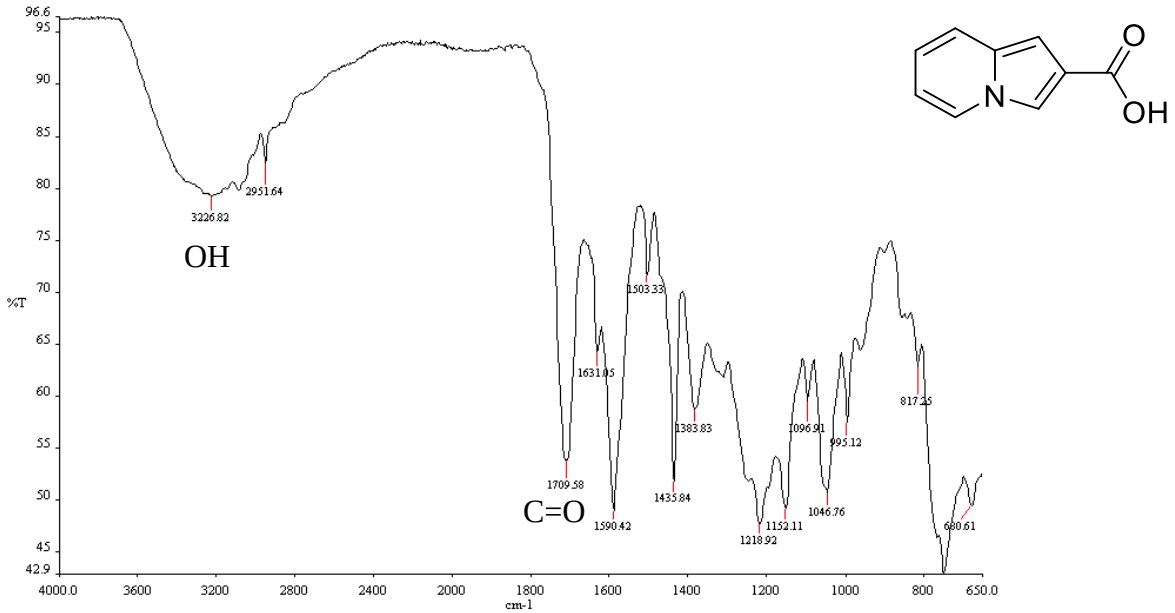

Figure 51. IR spectrum of indolizine-2-carboxylic acid **138**.

2.2.3. Saponification of methyl 3-acetylindolizine-2-carboxylate 132

Challenges frequently encountered in the hydrolysis of multi-functionalised molecules include selectivity, sensitivity of the substrate, cost of the hydrolysing agent, epimerization in the case of esters with an α-stereogenic centre and elimination reactions induced by basic conditions.[222] Saponification of ester **136** to afford the corresponding acid **139** was conducted following the procedure used in the formation of acid **138**. The product **139** was obtained in 93% yield and, in some cases, as a mixture with the deacetylated product **138**.

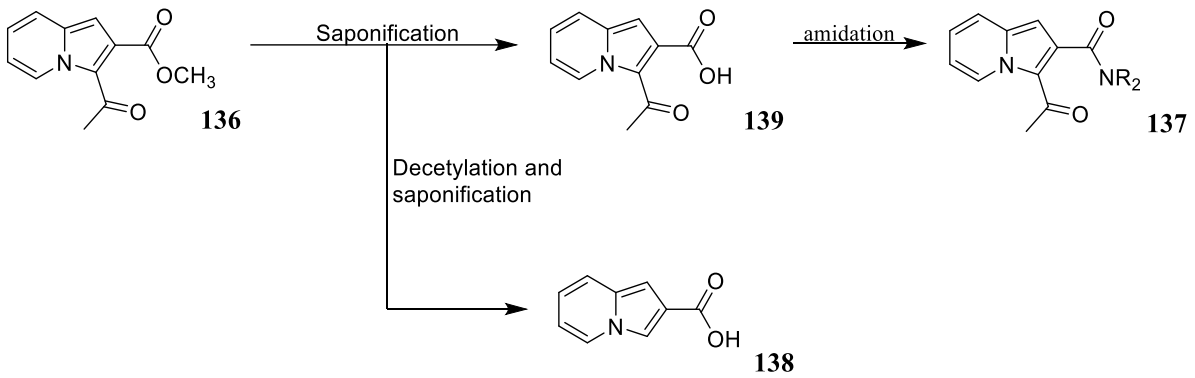

Scheme 29. Pathway for the conversion of the ester **136** to the acid **139** as a substrate for subsequent amidation.

NMR analysis of the acid **139** indicated the expected absence of the methoxy group while the ^{13}C NMR spectrum (**Figure 52**) confirmed the absence of the methoxy carbon that resonated at 52.5 ppm in the ^{13}C NMR spectrum of the precursor ester **136**. The ^{13}C NMR signal at 29.6 ppm corresponds to the methyl carbon of the acetyl group. The aromatic quaternary carbons C-9, C-3 and C-2 resonate at 120.0, 28.6 and 135.5 ppm, while the carbonyl carbons of the acid and the acetyl groups resonate at 167.1 and 186.14 ppm, respectively. The five aromatic methine carbon nuclei resonate with high signal intensity between 140 and 129 ppm.

Scheme 30 demonstrates plausible mechanisms for both saponification and deacetylation (blue) to afford compounds **139** and **138**. The basic conditions intended for saponification also enabled C-3 deacetylation resulting in the formation of deacetylated indolizine acid **138**. Deacetylation is widely used in protein synthesis[223] and in the deprotection of amines[224] – a process termed *N*-deacetylation. The process of deacetylation often requires the use of a strong base or acid at a high temperature.[224] In an attempt to improve the rate of deacetylation of *chitin*, No *et al.*[225] reported a modified methodology involving elevated pressure and temperature of 15 psi and 121 °C in the presence of 50% NaOH.

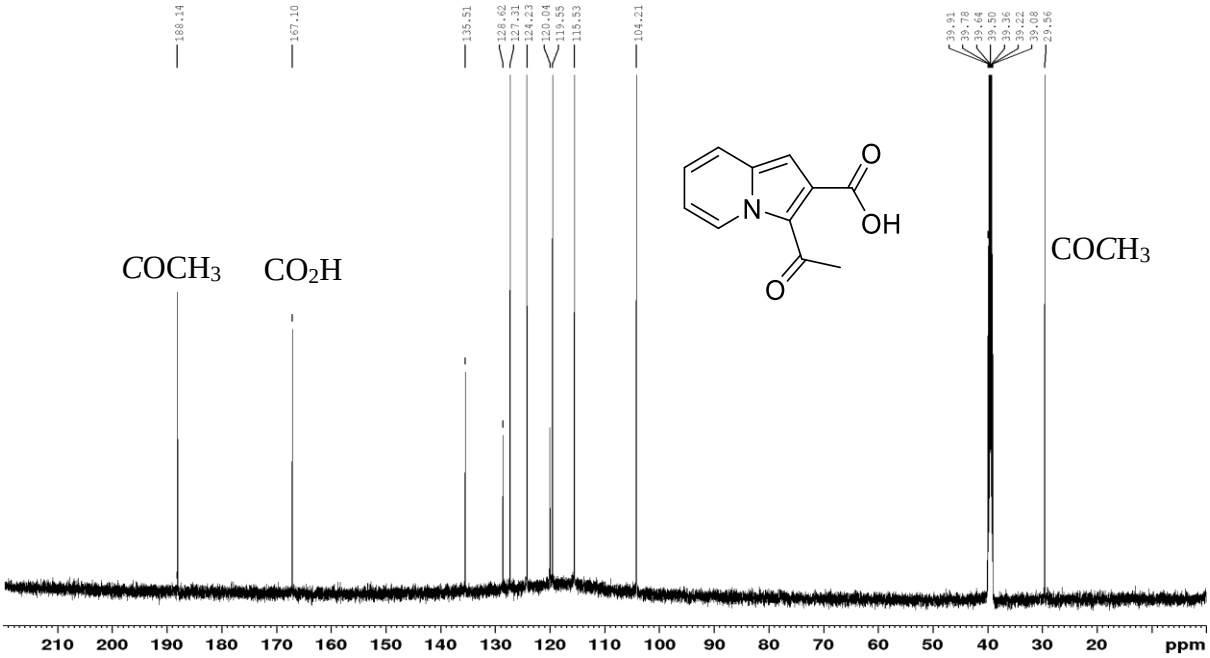

Figure 52. 150 MHz ^{13}C NMR spectrum of the acid **139** in DMSO-d_6.

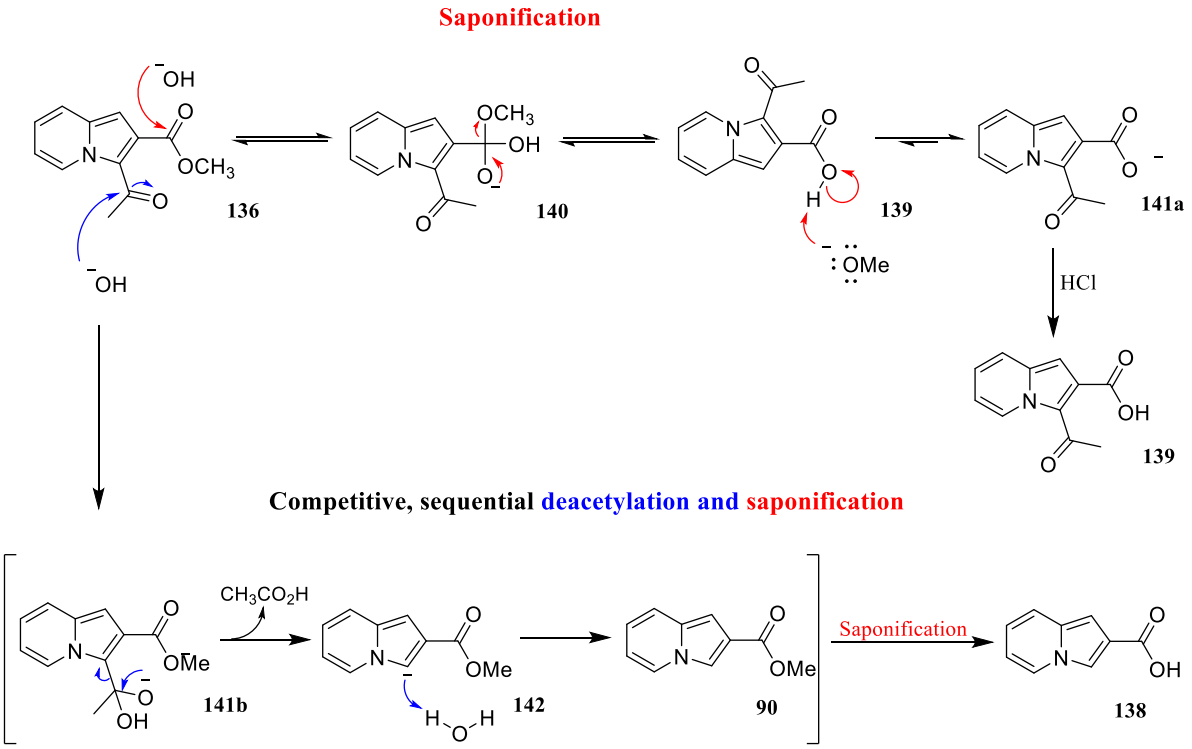

Scheme 30. Plausible mechanisms for the observed saponification and deacetylation steps in the formation of the carboxylic acid **138** from the 3-acetylated ester **136**.

Following the nucleophilic attack on the ketone carbonyl carbon by the hydroxide ($^{-}$OH), a tetrahedral intermediate **141b** is formed, and elimination of acetic acid results in the formation

of a carbanion **142** which subsequently abstracts a proton from a water molecule to yield the deacetylated methyl indolizine-2-carboxylate **90**. Alternatively, intramolecular proton abstraction may lead to loss of acetate, *via* the intermediate **141c**, and formation of the ester **90** (**Scheme 31.**).

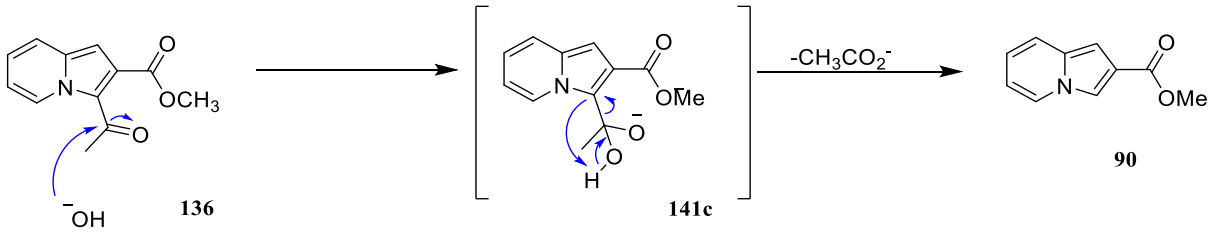

Scheme 31. Intramolecular deacetylation to indolizine ester **90**.

The reaction conditions drive the resulting deacetylated ester **90** to saponification which results in the formation of the indolizine-2-carboxylic acid **138**. In cases where both deacetylation and saponification occurred, the proposed mechanism suggests that the hydroxide-promoted C-3 deacetylation occurs first followed by saponification.

The chemoselective cleavage of a C-C bond in the absence of catalytic acid or a transition-metal catalyst is a desirable achievement.[226] The β-diketones have been widely used as substrates for C-C cleavage for the construction α-functionalised ketones. In this regard, Lei *et al.*[227] pioneered the Cu-catalysed deacetylation of β-diketones and arylation for the synthesis of α-aryl ketones. Other C-C bond cleavage transformations include Pd-catalysed deacetylative allylation for the preparation of α-allyl ketones,[228] the Cu-catalysed synthesis of α-thioaryl ketones[229] and, the deacetylation catalysed by triflic acid (CF_3SO_3H) in the synthesis of 3-acylindoles.[230]

It has been reported elsewhere[226] that when heating a reaction mixture of α-acetylacetophenone **143** and sodium benzenesulphinate **144** in the presence of a catalytic amount of sodium sulphite (Na_2SO_3) and iodine (I_2) at 60 °C, the acetyl group was replaced by a benzenesulfonyl group to yield compound **145** (**Scheme 32**). A mechanism which is similar to our proposed mechanism in **Scheme 30** but using a sulfite mediated process rather than one mediated by NaOH was reported (**Scheme 34**).

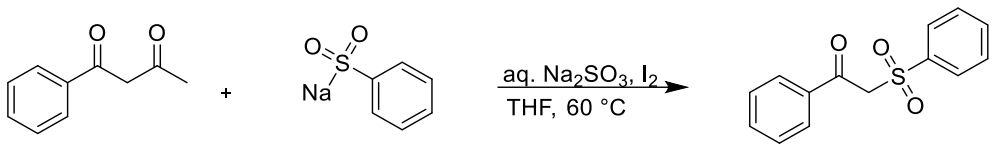

143 **144** **145**

Scheme 33. One pot synthesis of β-keto sulphone.

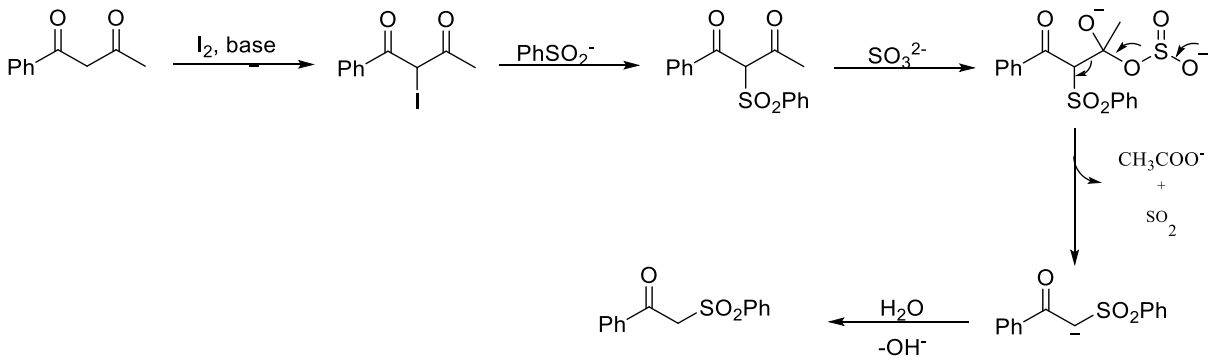

Scheme 34. Proposed mechanism for the synthesis of compound **145**. [226]

Among the pool of available saponification reagents,[231] trimethyltin hydroxide (Me_3SnOH) has been reported to be a high yielding, mild and selective agent for the hydrolysis of esters under extremely mild conditions in a few hours.[222, 232]

2.2.4. Exploratory studies of the synthesis of indolizine-2-carboxamides

Despite the medicinal significance of amides and their ubiquity in drugs, the development of an effective and comprehensive amide synthetic method remains a challenge. Most of the established methods are relatively inefficient, with adverse environmental impacts and difficulties in purification of the product.[233] Amides can be prepared *via* a wide range of different reaction pathways using a variety of appropriate precursors. A direct and simple method of preparing amides involves the condensation of a carboxylic acid and an amine. However, this method usually requires high temperature reaction conditions in order to achieve conversion of the initially formed ammonium carboxylate salts to the desired amide; such conditions are not compatible with the use of sensitive reagents.[234] Consequently, amides are generally formed through activation of the acid by a stoichiometric coupling reagent. The ongoing search for effective catalysts for direct amidation has led to an arsenal of coupling agents with some offering considerably increased efficiency, albeit with limited substrate scope.[233] Moreover, due to complications regarding toxicity of some coupling agents, purification and, in some cases, sensitivity and tedious work-up, the pharmaceutical

significance of the amide bond inspired the chemists to invest in developing benign and inexpensive amide formation reactions.[235, 236] Herein, we report the attempted atom-economical, boron-catalysed synthesis of the indolizine-2-carboxamides from indolizine-2-carboxylic acid and the non-catalyzed amide formation using the acid **132** and amine or an amine surrogate such as isocyanate.

2.2.4.1. Boron-catalysed amide bond formation

The stoichiometric application of organoboron derivatives as effective Lewis acid catalysts in the formation of amides has been known since 1965.[237] In their review, de Figuiredo *et al.*[234] listed twenty-three organoboron-derived catalysts that are frequently employed in amide synthesis. The inexpensive, commercially available and environmentally friendly boric acid, $B(OH)_3$, has been extensively employed as an effective catalyst for direct amidation.[238]

Consequently, our expectation was that refluxing the carboxylic acid and the amine in a high-boiling solvent with concomitant water removal, would afford the desired amides. Using a Dean-Stark apparatus, mixtures of indolizine-2-carboxylic acid **138** (1 eq.) and each of the amines, 2,4-imidazolidinedione **147**, 1-methylimidazolidine-2,4-dione **148** and picolylamine **151** (1.2 eq.) and 20 mol% $B(OH)_3$ were subjected to 6 hours of vigorous reflux in toluene. However, TLC analysis revealed that none of the expected products were formed. The catalyst was gradually increased to one equivalent but even after refluxing for 12 hours TLC analysis revealed the absence of any product. The catalyst was changed to trimethyl borate and to phenyl boronic acid but, following the same procedure, the reactions still failed to afford any product. Changing the solvent to acetonitrile and, thereafter, to methanol also proved unsuccessful.

The expensive borate ester, tris(2,2,2-trifluoroethyl)borate, which is known to exhibit good functional group tolerance and is insensitive to moisture was found to facilitate direct amidation of the indolizine-2-carboxylic acid **138**. Thus, a mixture of the borate ester (2 eq.), indolizine-2-carboxylic acid **138** and 2-aminothiazole **153** in acetonitrile was refluxed for 24 hours, after which TLC analysis showed the formation of a product. The solvent was removed *in vacuo* and the crude product purified by column chromatography [elution with hexane:EtOAc (1:5)] to afford, as yellow crystals, the *N*-(2-thiazolyl)indolizine-2-carboxamide **154** in an extremely low yield of 2%. While the tris(2,2,2-trifluoroethyl)borate-catalysed reaction presented some amidation potential, its efficacy under varying conditions was not explored. Furthermore, it was expected that amidation involving secondary or sterically hindered amines was unlikely to succeed. Considerable efforts were made to develop an effective, boron-catalysed coupling

methodology as shown in **Scheme 35** which summarises attempted amidation reactions with the boron catalysts such as, boric acid, borate esters and, tris(2,2,2-trifluoroethyl)borate.

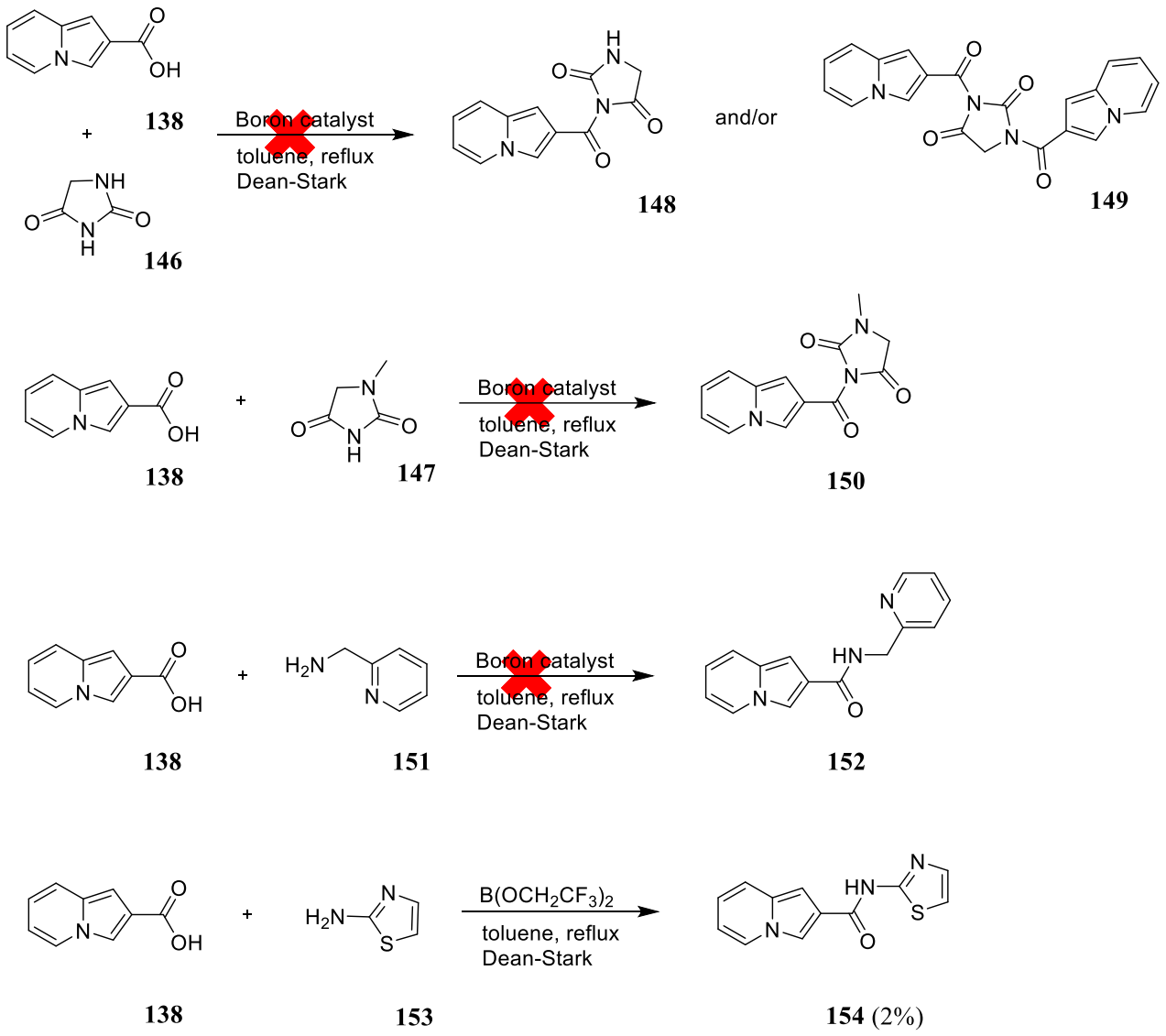

Scheme 35. Attempted boron-catalysed amidation reactions.

2.2.4.2. Direct catalytic amidation of indolizine-2-carboxylic acid with diisocyanates. In order to avoid high temperatures and/or the use of coupling reagents for activating the acid, attention has recently been devoted to alternative methods which involve the coupling of carboxylic acids with readily available amine surrogates, such as azides and isocyanates. This approach is considered atom economic and has been employed in the high-yield condensation of carboxylic acids with various aryl and electron-deficient isocyanates. In this reaction, carbon dioxide is a by-product and the scavenging of water is unnecessary.[198]

The pathway shown in **Scheme 36** depicts this synthetic approach which circumvents initial amide bond formation. The ammonium carboxylate salt **155** serves as the substrate which is typically heated to produce the amide with loss of CO_2.

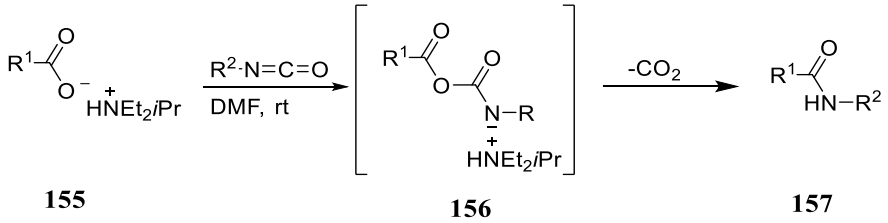

Scheme 36. Amide synthesis using a carboxylic acid salt and isocyanate.

We therefore attempted the condensation of indolizine-2-carboxylic acid **138** with tolylene-2,4-diisocyanate **158** and isophoronediisocyanate **159** under ambient reaction conditions (**Scheme 37**). To a stirred solution of acid **138** (2 eq.) and *N*,*N*-diisopropylethylamine (DIPEA; 0.5 eq.) in *N*,*N*-dimethylformamide (15 mL) was added the diisocyanate (2 eq.). The reaction mixture was stirred in a stoppered flask for 7 days after which TLC analysis revealed that no reaction had occurred.

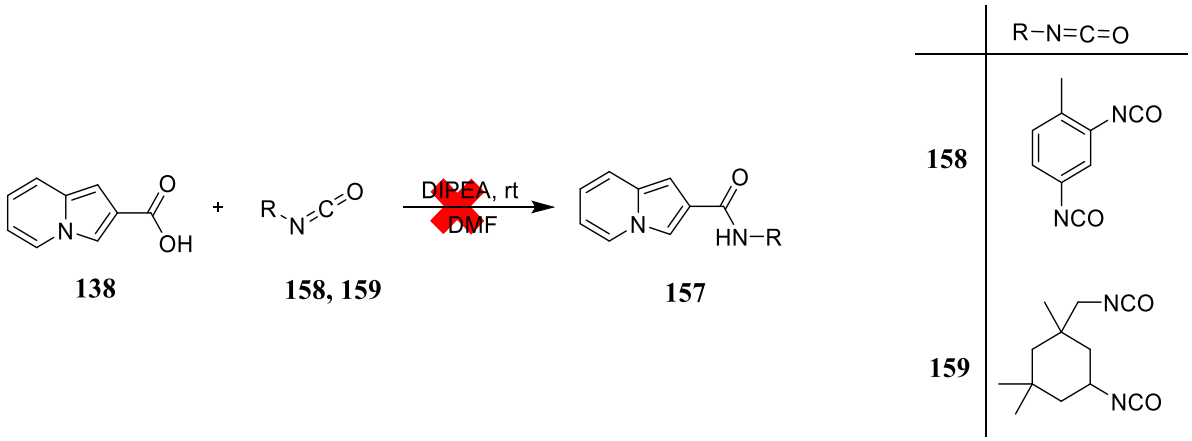

Scheme 37. Attempted amide synthesis using isocyanate.

This approach would, in any event, have presented the challenges of synthesising a series of amine surrogates and, due to limitations in the synthesis of secondary amine surrogates, it was considered unlikely that tertiary amides could be obtained using this procedure.

2.2.4.3.Thermal cyclisation of amido-Baylis-Hillman adducts.

Having attempted various foregoing approaches to indolizine-2-carboxamides, we resorted to a two-step procedure to access the desired amides *via* Baylis-Hillman methodology. We envisaged that amido-Baylis-Hillman adducts **162**, obtainable from the reaction of pyridine-2-carboxaldehyde **107** and acrylamide derivatives **161**, would undergo thermal cyclisation to afford the target indolizine-2-carboxamides **163**.

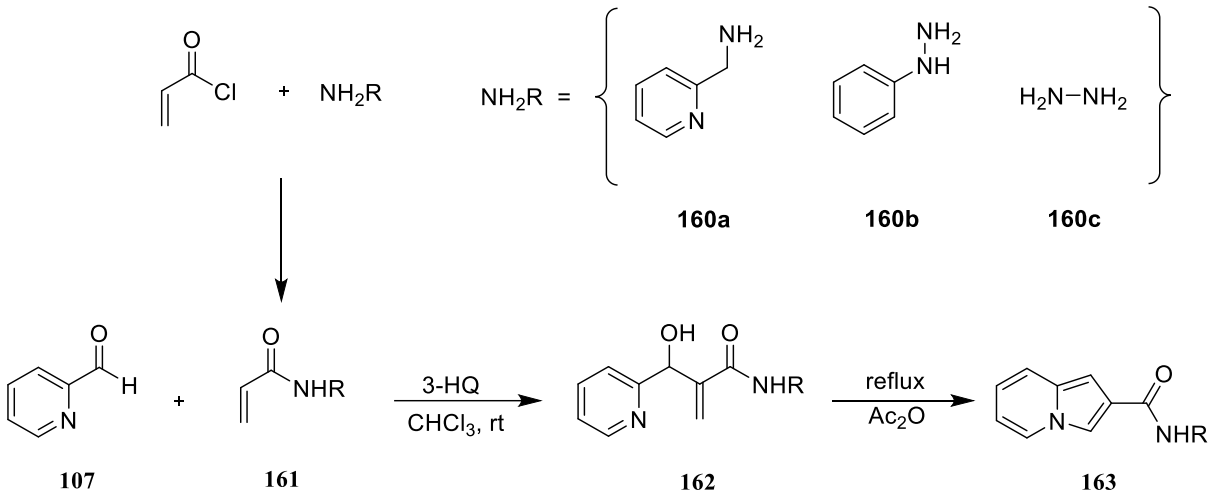

Scheme 38. A two-step methodology towards indolizine-2-carboxamides *via* amido-Baylis-Hillman adducts.

The initial step in the synthesis of indolizine-2-carboxamides through this procedure was to prepare the acrylamide derivatives **161**. Thus, 2-picolylamine **160a** was added dropwise into a stirred solution of acryolyl chloride in DCM in an ice bath. Triethylamine was subsequently added to mop up the hydrochloric acid produced as a by-product. (*Caution must be exercised when adding 2-picolylamine to the acryloyl chloride as the reaction is highly exothermic.*) After 2 hours, completion of the reaction was signified by the homogeneous solution turning into a gel, TLC analysis of which confirmed formation of the product. Extraction with CH_2Cl_2, washing with water, and drying of the organic phase over magnesium sulphate afforded, following *in vacuo* concentration, a light-yellow gel comprising *N*-picolylacrylamide **161a** in 45% yield.

Examination of the ^{13}C NMR spectrum of this compound (**Figure 53**) showed the presence of nine carbon signals including the expected seven sp^2 carbons. The carbonyl carbon resonates at 165.6 ppm whilst the quaternary carbon C-7 resonates at 156.2 ppm. The corresponding DEPT 135 NMR spectrum (**Figure 54**) confirmed the presence of the vinylic methylene carbon

resonating at 126.5 ppm, while the signal at 44.4 ppm corresponds to the *N*-methylene carbon. The IR spectrum (**Figure 55**) shows the NH and C=O bands at 3269 and 1658 cm^{-1}, respectively. Interestingly, attempts to prepare N^2-(phenyl)acryloylhydrazine **161b** and *N*-acryolylhydraazine **161c** from phenylhydrazine **160b** and hydrazine **160c**, respectively, were not successful.

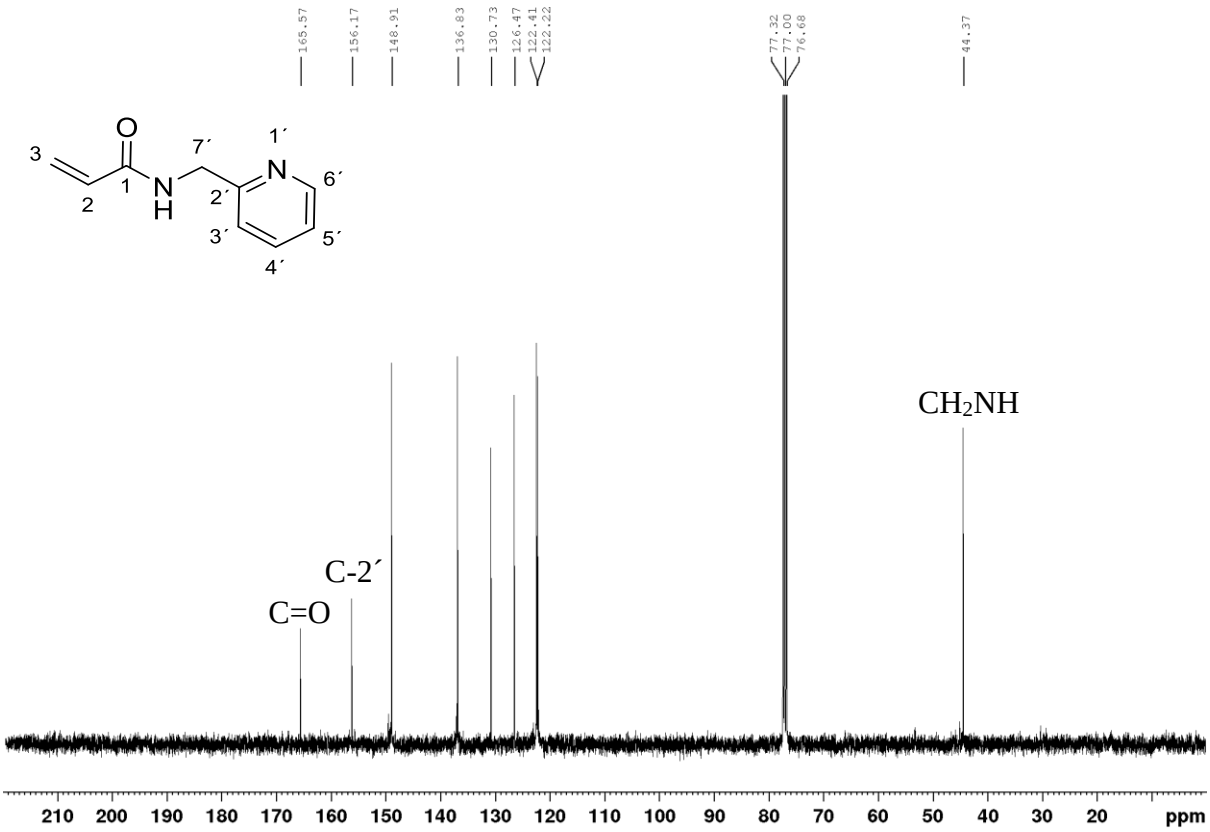

Figure 53. 600 MHz ^{13}C NMR spectrum of *N*-picolylacrylamide **161a**.

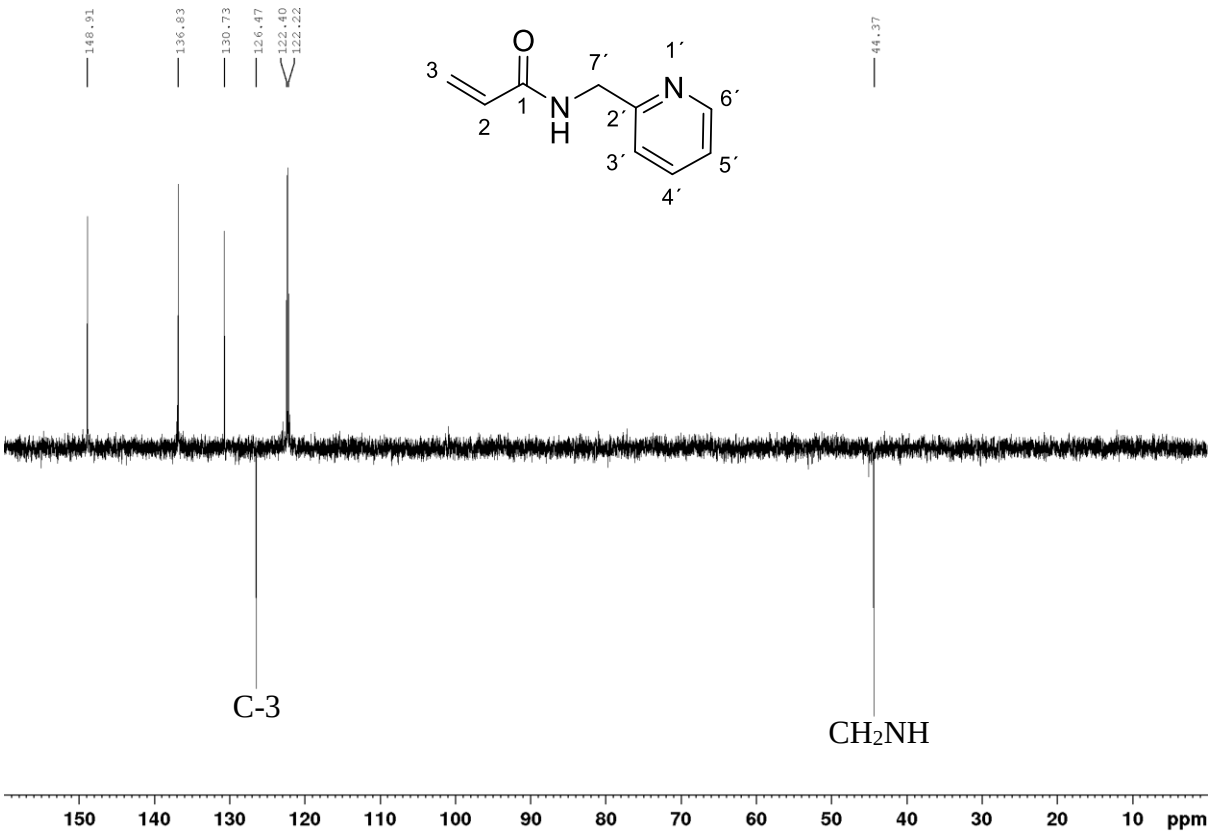

Figure 54. 600 MHz DEPT-135 NMR spectrum of *N*-(picolyl)acrylamide **161a**.

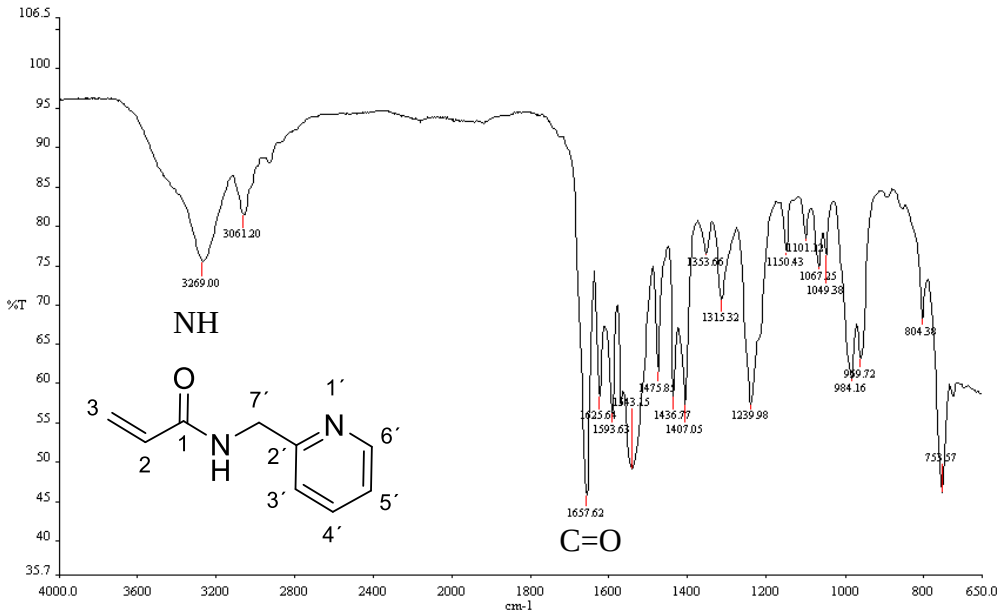

Figure 55. IR spectrum of *N*-(picolyl)acrylamide **161a**.

Reactions of the prepared *N*-(picolyl)acrylamide **161a** or commercially available acrylamide under the influence of 3-hydroxyquinuclidine (3-HQ), were expected to lead to the generation of the Baylis-Hillman carboxamides, such as *N*-picolyl-[3-hydroxy-2-methylene-3-(2-

pyridinyl)]propanamide **162a** and 3-hydroxy-2-methylene-3-(2-pyridinyl)propanamide **164**, as precursors for the target indolizine-2-carboxamides **163**.

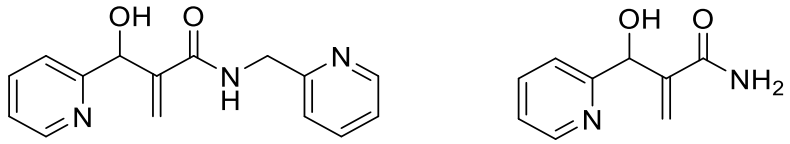

162a **164**

Figure 56. Baylis-Hillman carboxamide adducts synthesised as substrates for thermal cyclisation.

The functional group diversity in the Baylis-Hillman adducts provides opportunities for atom economic and selective construction of a range of intriguing chemical systems.[215, 239] The strategic positioning of these functional groups often permits participation in an array of synthetic transformations leading to the useful products. The intramolecular cyclisation process often involves the construction of a C-N bond.[240] The generality of selective cyclisation of the Baylis-Hillman adduct in the construction of benzannulated heterocyclic products could permit a convenient synthesis of a range of heterocyclic frameworks including the *N*-(picolyl)indolizine-2-carboxamide **152** and indolizine-2-carboxamide **165** *via* distillation of the Baylis-Hillman carboxamides **162a** and **164**, respectively. **Scheme 13** (page 38) shows a plausible mechanism for the chemoselective cyclisation of the Baylis-Hillman ester adducts upon distillation in acetic anhydride. Accordingly, distillation of compound **164** was expected to furnish compound **165** (**Scheme 39**). Thermal cyclisation of 3-hydroxy-2-methylene-3-(2-pyridinyl)propamide **164** for a duration of 24 hours indeed afforded indolizine-2-carboxamide **165** and its *N*-acetylated derivative **166**.

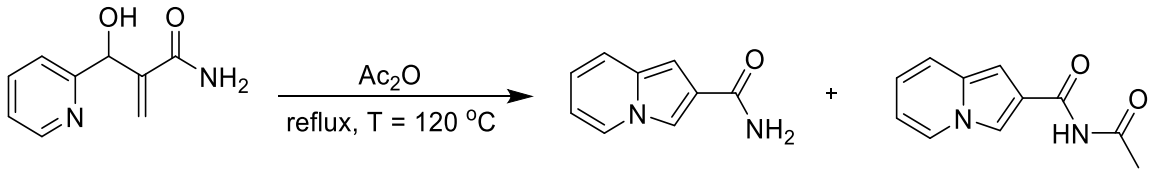

164 **165** **166**

Scheme 39. Intramolecular cyclisation of compound **164**.

However, this process is particularly laborious when a series of indolizine-2-carboxamides is required since commercially available acrylamides are limited and a specific acrylamide derivative must be prepared for each of the subsequent Baylis-Hillman and thermal cyclisation reactions. Finally, we reverted to the indolizine-2-carboxylic acid substrate and engaged

propanephosphonic acid anhydride (T3P) **118** catalysis for amide coupling to access the desired range of amides.

2.2.4.4.Approaches to Baylis-Hillman-derived carboxamides from Baylis-Hillman-derived carboxylic acids.

Although it has been shown that thermal condensation of carboxylic acids and amines can form a significant amount of the amide product, usually with azeotropic removal of water, the reaction is dependent on the substrate and on the temperature, substrate concentration, solvent and thermodynamic and kinetic parameters.[235] At lower temperatures, thermal condensation ceases to effect amide formation and the use of appropriate catalysts become relevant.[241] This has encouraged the development of efficient, broad-scope catalytic methods for amide bond formation the majority of which rely on activation of the carboxylic acid using a coupling reagent and subsequent coupling of the activated species with an amine (**Scheme 43**).[242] It has also been suggested alternative approach include the use of metal catalysts and as a result, there has been increased attention to the development of metal-based catalysts for amide formation.[243]

Metal catalysis raises the possibility of amide synthesis from substrates other than carboxylic acids, thereby unveiling previously unavailable synthetic routes to target molecules.[242] For instance, a series of metals or metal complexes of zinc, tin, lanthanum, iron, aluminium and nickel have been reported to facilitate *N*-formylation of amines in good to excellent yields using formic acid under solvent-free conditions at 70 °C (**Scheme 40**).[244, 245]

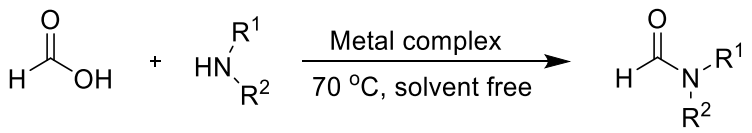

Scheme 40. Metal complex-catalysed synthesis of amides from formic acid.

Although limited in substrate scope and to the synthesis of secondary amides (the procedure is incompatible with secondary amines), metal catalysis, using indium triiodide, zinc powder or group (IV) metal alkoxide complexes, such as tetrakis-(*tert*-butoxide)zirconium (IV) in conjunction with 1-hydroxy-7-azabenzotriazole as an activator (Scheme 41), have also been successfully demonstrated.[246, 247]

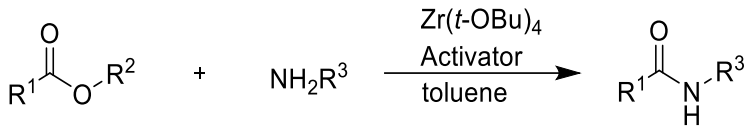

Scheme 41. Metal-catalysed synthesis of amides from an ester substrates.

Utilisation of aldehydes as substrates for amide synthesis has also attracted considerable attention. This, oxidant-catalysed process (**Scheme 42**), involves the formation of a hemiaminal intermediate and its subsequent oxidation to the amide product.[248] To avoid the potential formation of an imine due to hydration, and subsequent dehydrogenation of the imine to an amine, secondary amines may be used for this transformation.

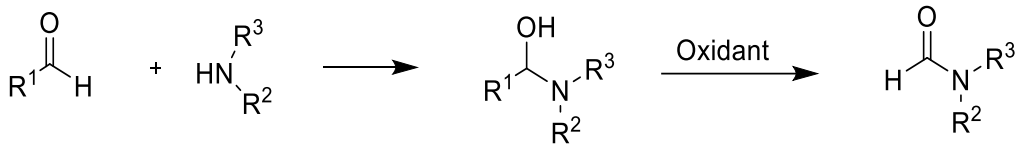

Scheme 42. General approach for amide formation from aldehydes and amines.

Although coupling agents suffer the inherent drawback of producing a stoichiometric amount of by-product along with the desired product,[234, 235, 242] a number of these agents have proved to be very efficient in facilitating amide formation *via* activated intermediates (**Scheme 43**).

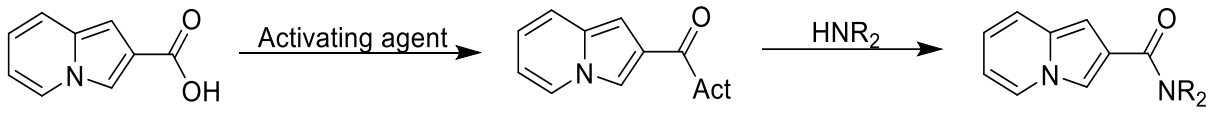

Scheme 43. Representation of activation-based synthesis of desired targets.

A new range of catalytic strategies that involve the use of propyl phosphonic anhydride (T3P) have been developed to provide efficient, practicable and reproducible approaches to amide synthesis under mild conditions and with broad substrate scope. The functional group tolerance and potency of the T3P-catalysed approach is a “trademark” feature and, consequently, attention was turned to the use of this coupling agents.

2.2.5. T3P-catalysed synthesis of amides.

Using T3P as a catalyst, we were successful in synthesising a series of amides from indolizine-2-carboxylic acid and commercially available primary, secondary or sterically hindered aromatic and aliphatic amines. The catalytic efficacy of T3P was examined by initially coupling indolizine-2-carboxylic acid with 2,4-imidazolidinedione **148** (commonly known as hydantoin) and its *N*-methylated derivative under various reaction conditions (**Scheme 49**, p108). Firstly, the coupling of indolizine-2-carboxylic acid and 2,4-imidazolidinedione **148** in a mixture of anhydrous ethyl acetate and pyridine (1:2) did not furnish the desired product. Replacement of ethyl acetate with anhydrous chloroform, however, led to the formation of two products according to TLC analysis. Refluxing the reaction mixture to accelerate the reaction rate resulted in an intractable product. Lastly, replacement of pyridine with the easy to handle and relatively benign diisopropylethylamine (DIPEA) drastically improved the reaction. The latter condition was applied in all subsequent reactions, including reactions involving relatively non-nucleophilic amines and, where necessary, under reflux. The desired products were obtained in moderate yields. As indicated in the following pages, the reaction was executed with a wide range of amines and either indolizine-2-carboxylic acid or 3-acetylindolizine-2-carboxylic acid.

2.2.6. Preparation of secondary amides.

Several procedures for attaining indolizine ester intermediates have been examined over the past years in our group, including (i) conversion of BH alcohols to corresponding acetoxy derivatives and subsequent thermal cyclisation of the acetylated BH adduct and (ii) direct distillation of the alcohol.[145, 215, 218] The seminal discovery that thermal conversion of methyl 3-hydroxy-2-methylene-3-(2-pyridinyl)propanoate **88** into the crystalline methyl indolizine-2-carboxanoate **90** was found to occur at *ca.* 140 °C with a maximum of 22% yield. Thermal cyclisation was presumed to follow the intramolecular addition-elimination sequence and, clearly, conversion of the alcohol **88** to a corresponding acetate **89** drastically improved the process. Acetylation of the product has been achieved either by refluxing the alcohol in acetic anhydride for 30 minutes or by reaction of the alcohol **88** with acyl chloride in the presence of pyridine at room temperature.[218]

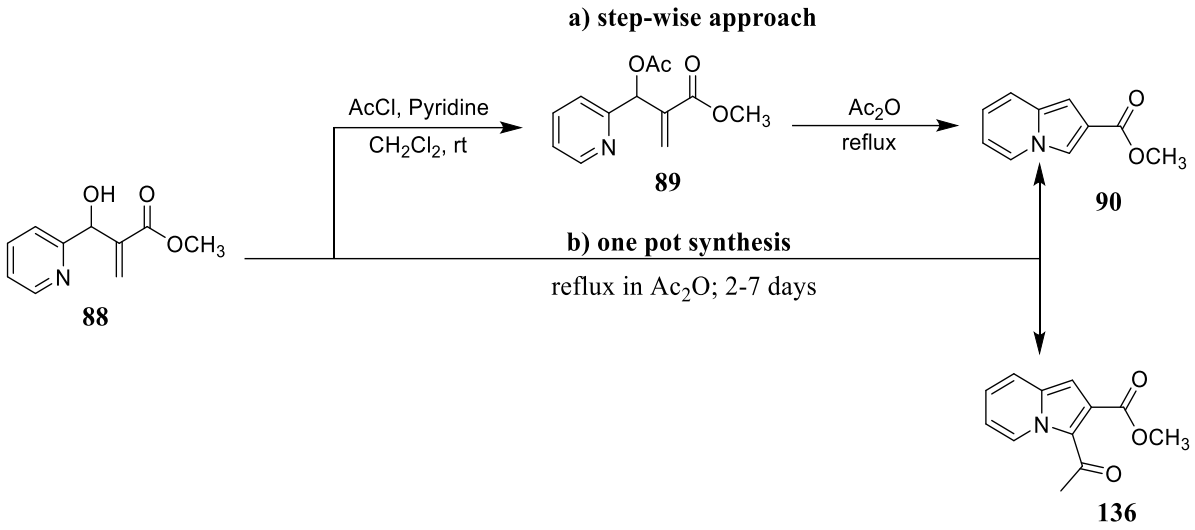

Scheme 44. Brief demonstration for the preparation of synthetic substrate.

In this research, indolizine esters were obtained from the BH alcohol, *i.e.* without isolating the acetylated intermediate. The alcohol was refluxed in acetic anhydride for two to seven days to obtain methyl indolizine-2-carboxylate or 3-acetylindolzine-2-caboxylate in excellent yield. Subsequent hydrolysis of the esters (see section **2.2.2** and **2.2.3**) provided the carboxylic acids required for the synthesis of the target amides.

Particular attention was given to the selection of the amines required in exploring the potential synergy of coupling the indolizine moiety to a medicinally significant amine moiety. According to Ortona and Antinori,[249] the standard six-month TB therapy usually includes administration of a cocktail of isoniazid **168**, rifampicin **169** and pyrazinamide **171** in the first two months, with the addition of ethambutol **167** in case resistance is encountered, followed by completion of the course with isoniazid **168** and rifampicin **169**. Prolonged therapy has frequently led to patient non-compliance and, in turn, contributed to the emergence of multi-drug resistant TB (MDR-TB) which is difficult and expensive to treat. The hard-to-treat MDR-TB strains are being found increasingly, thus emphasising the need for the ongoing development of new and potent drugs including the possibility of incorporating the well-known anti-TB drugs ethambutol **167**, isoniazid **168** and rifampicin **169** (**Figure 57.**).[250]

The FDA approved anti-tuberculosis amines, such as pyrazinamide **171**, cycloserine **170**, and ethambutol **167** and its truncates, such as 2-(2-aminoethoxy)ethanol **172**, 2-amino-1-butanol **173** and 4-amino-1-butanol **174** (**Figure 58**), were thus considered for coupling with the carboxylic acids.

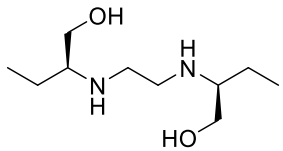

Ethambutol **167**

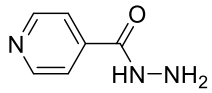

Isoniazid **168**

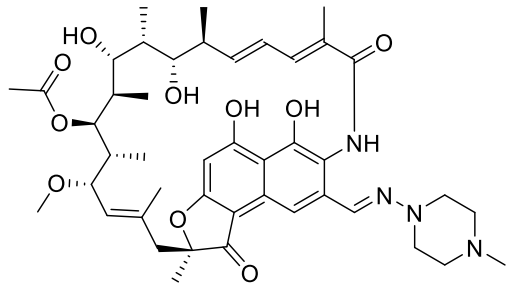

Rifampicin **169**

Figure 57. FDA approved anti-TB drugs.

The target mycobacteria in TB therapy have a unique cell wall in which mycolic acid confers resistance to chemical attack and dehydration, and inhibits the permeability of hydrophobic antibiotics. The design of new anti-mycobacterials therefore requires molecules with high lipophilicity to facilitate permeability through the cell wall of the mycobacteria. Also, to be taken into consideration is the development of affordable drugs that can suppress or eradicate the extensive drug-resistant TB (XDR-TB) strain. XDR-TB is an MDR-TB with additional resistance to fluoroquinolone and any of the second-line regimen drugs.[251] After treatment initiation, MDR-TB therapy, coupled with close monitoring for adverse drug reactions, spans at least 20 months, and the global success rate was reported to average *ca.* 48% in 2011.[252] In 2012, an assessment of 107 XDR-TB patients treated in South Africa revealed a very dismal success rate with a mortality rate of *ca*. 78%.[253] Drug-resistant TB is a particular risk to individuals with HIV and this often leads to rapid transmission of the disease and heightened mortality rate among sufferers.[254] The physiological adversities associated with drug-drug interactions (DDIs) between anti-TB drugs and antiretroviral therapy (ART) renders the development of multitherapy drugs imperative.[252] This, in turn, addresses the complexities of managing HIV-TB co-infections, including other simultaneous infections such as malaria.

Unfortunately, the attempted preparation (**Scheme 45**) of amides containing the ethambutol truncates **172-174** (**Figure 58**) produced insoluble white solids, TLC analysis of which revealed the presence of starting materials. Also, attempted coupling of the indolizine-2-carboxylic acid **138** with each of the nucleotide nitrogenous bases adenine **175**, guanosine **176**, thymidine **177** and adenosine **178** was not successful. Encouraged by the observation that T3P-catalysed synthesis of *N*-(2-thiazolyl)indolizine-2-carboxamide **154** improved the yield thirteen folds (**Scheme 51**) compared to the tris(2,2,2-trifluoroethyl)borate-catalysed reaction (**Scheme 35**), we proceeded to explore the T3P-mediated coupling of indolizine-2-carboxylic

acid with pyrazinamide **171** (**Section 2.2.6.1)** and cycloserine **170** (**Section 2.2.6.2**), respectively.

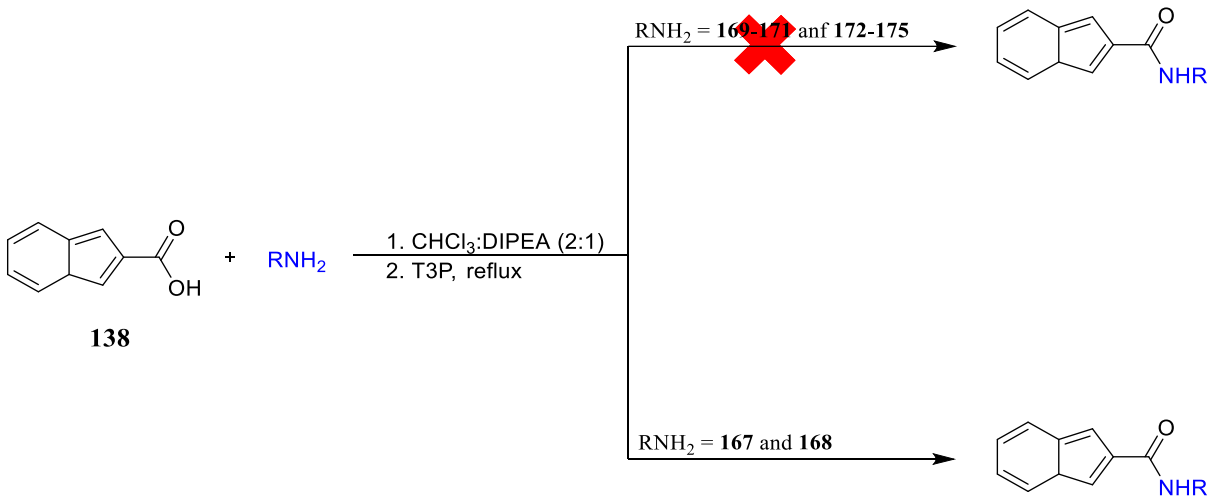

Scheme 45. Schematic representation for attempted coupling of indolizine-2-carboxylic acid **134** with ethambutol truncates **172-174**, nitrogenous bases **175-178** and, successful coupling with the FDA approved anti-TB amines **170** and **171** (see blue compounds in **Figure 58**).

Given the set of available amines in **Figure 58** (blue), the intention has been to prepare amides bearing multiple pharmacophores with the potential to act simultaneously as anti-HIV and anti-tubercular agents, or even antimalarial agents. To this end, coupling to the indolizine moiety was explored with the anti-tuberculosis agents, cycloserine **170** and pyrazinamide **171**.

Anti-TB amines

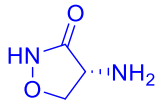

cycloserine **170**

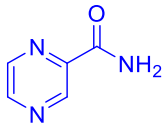

pyrazinamide **171**

Ethambutol truncates

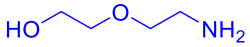

2-(2-aminoethoxy)ethanol **172**

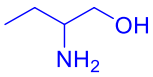

2-amino-1-butanol **173**

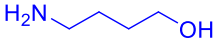

4-amino-1-butanol **174**

Nitrogenous bases

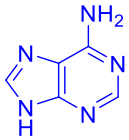

adenine **175**

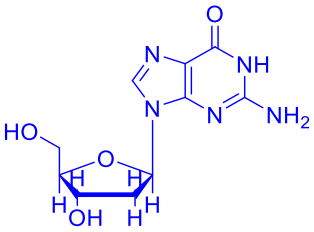

guanosine **176**

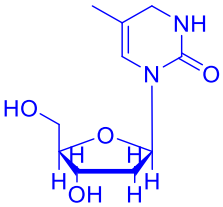

thymidine **177**

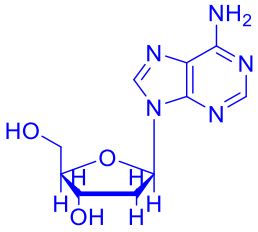

adenosine **178**

Figure 58. List of molecules with inherent medicinal significance: anti-TB drugs, truncated ethambutol molecules and nitrogenous bases.

2.2.6.1. Synthesis of N-*(pyrazinecarboxanoyl)indolizine-2-carboxamide* 179

The prominent anti-TB agent, pyrazinamide **171**, was therefore coupled with indolizine-2-carboxylic acid **138** using T3P (**Scheme 46**). The coupling of indolizine-2-carboxylic acid **138** (1 eq.) and pyrazinamide **171** (1.2 eq.) was conducted in a mixture of $CHCl_3$:DIPEA (2:1; 12 mL) cooled to between -20 °C and -10 °C in a stoppered flask prior to the slow addition of T3P (3 eq.) to maintain the temperature below 0 °C. The reaction mixture was then stirred in a stoppered flask and allowed to warm to room temperature, followed by reflux at 80 °C for 2 days. The reaction progress was monitored by TLC analysis. The reaction mixture was filtered and the filtrate concentrated *in vacuo*. However, after the subsequent solvent extraction, only starting materials were obtained. The synthesis was then repeated but, following concentration

in vacuo the crude product was purified using preparative plate chromatography on silica gel to give a trace amount (<1%) of the *N*-(pyrazinecarbanoyl)indolizine-2-carboxamide **179** as a yellow gel.

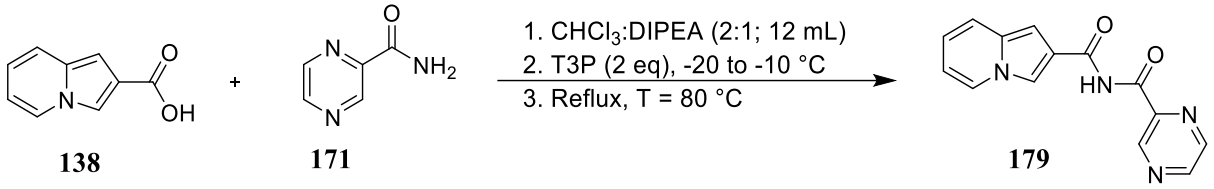

Scheme 46. Syntheis of *N*-(pyrazinecarboxanoyl)indolizine-2-carboxamide **179**.

Although secondary acylation on the nitrogen of the amide may be inhibited by the relative electron deficiency of the amide nitrogen caused by electron delocalisation, the very low yield is attributed to the apparent sensitivity of the product to water. In earlier reaction trials (not reported) this product decomposed when exposed to atmospheric moisture. The yield would be improved by conducting the reaction under azeotropic conditions or by adding molecular sieves to absorb the water generated during coupling. Because of the limited amount eventually obtained, the *N*-(pyrazinecarbanoyl)indolizine-2-carboxamide **179** was characterised using ^{1}H NMR and COSY spectra. Analysis of the COSY spectrum **(Figure 61)** permitted unambiguous characterisation of the amide. The ^{1}H NMR spectrum (**Figure 59**) exhibits nine proton signals, including two singlets, in the aromatic region. The triplet of doublets at 6.56 ppm and the multiplet at 6.69 ppm correspond to the 7-H and 6-H protons, whereas the doublet at 7.37 ppm and the doublet of doublets at 8.08 ppm correspond to 5-H and 8-H, respectively. The triplet at 8.68 ppm corresponds to the 5´-H proton whilst the doublets at 8.77 and 9.24 ppm correspond to the pyrazine 6´-H and 3´-H protons, respectively (see **Figure 60**). The COSY spectrum (**Figure 61**) reflects the long-range coupling between 5´- and 3´-H signals, and hence 5´-H appears as a triplet.

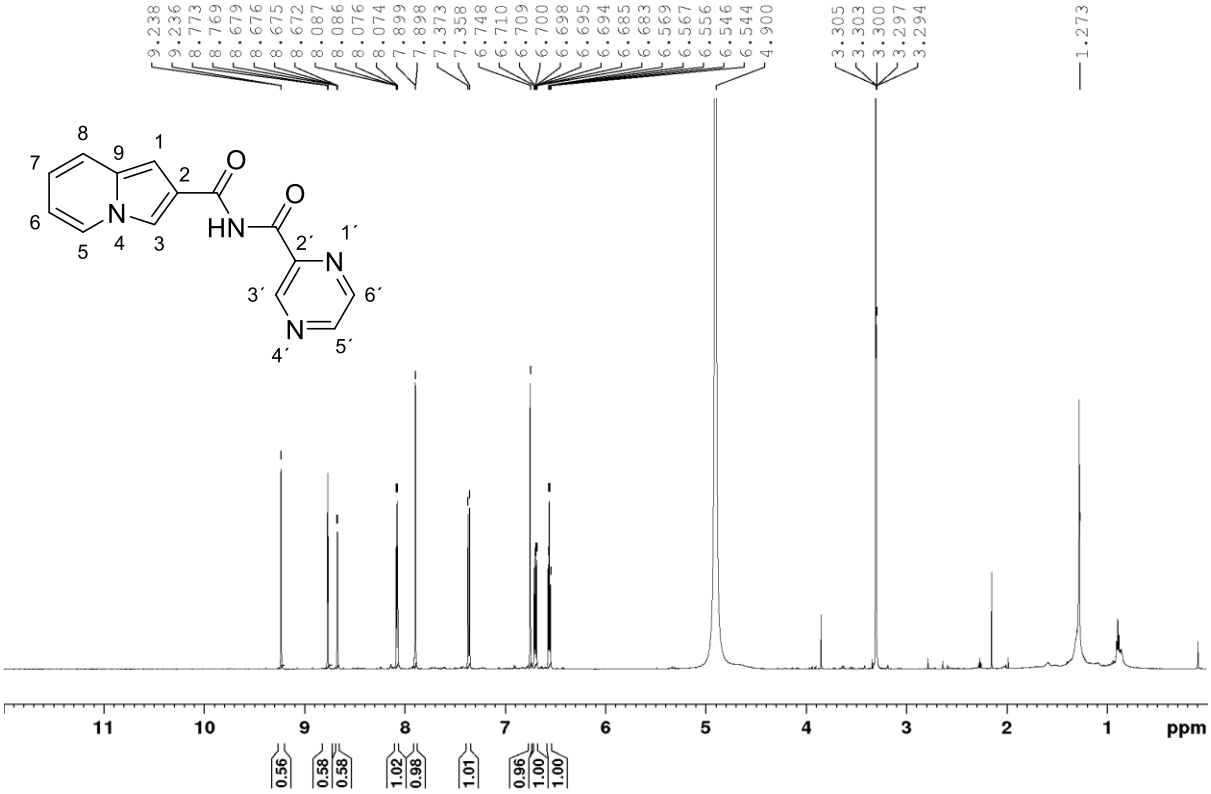

Figure 59. 600 MHz ^{1}H NMR spectrum of compound **179** in methanol-d_4.

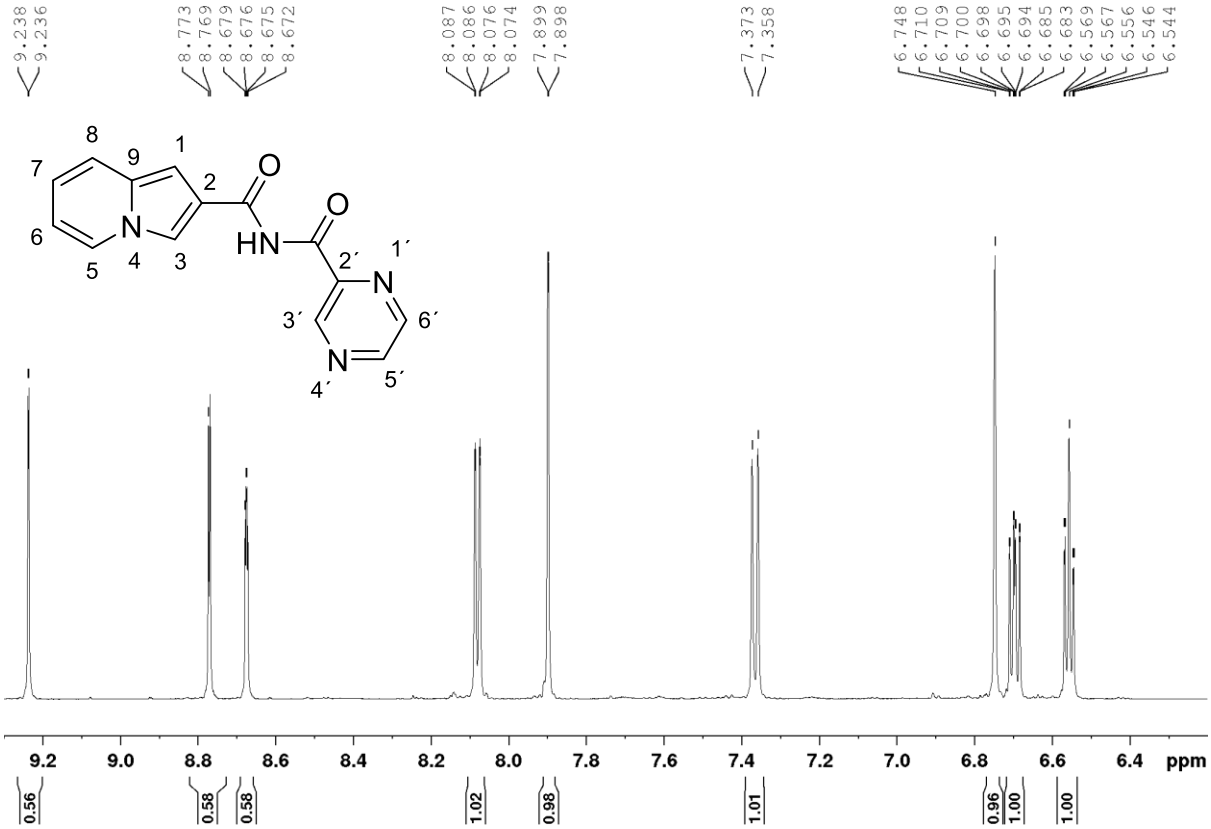

Figure 60. Zoomed ^{1}H NMR spectrum of compound **179** (focusing on the aromatic region).

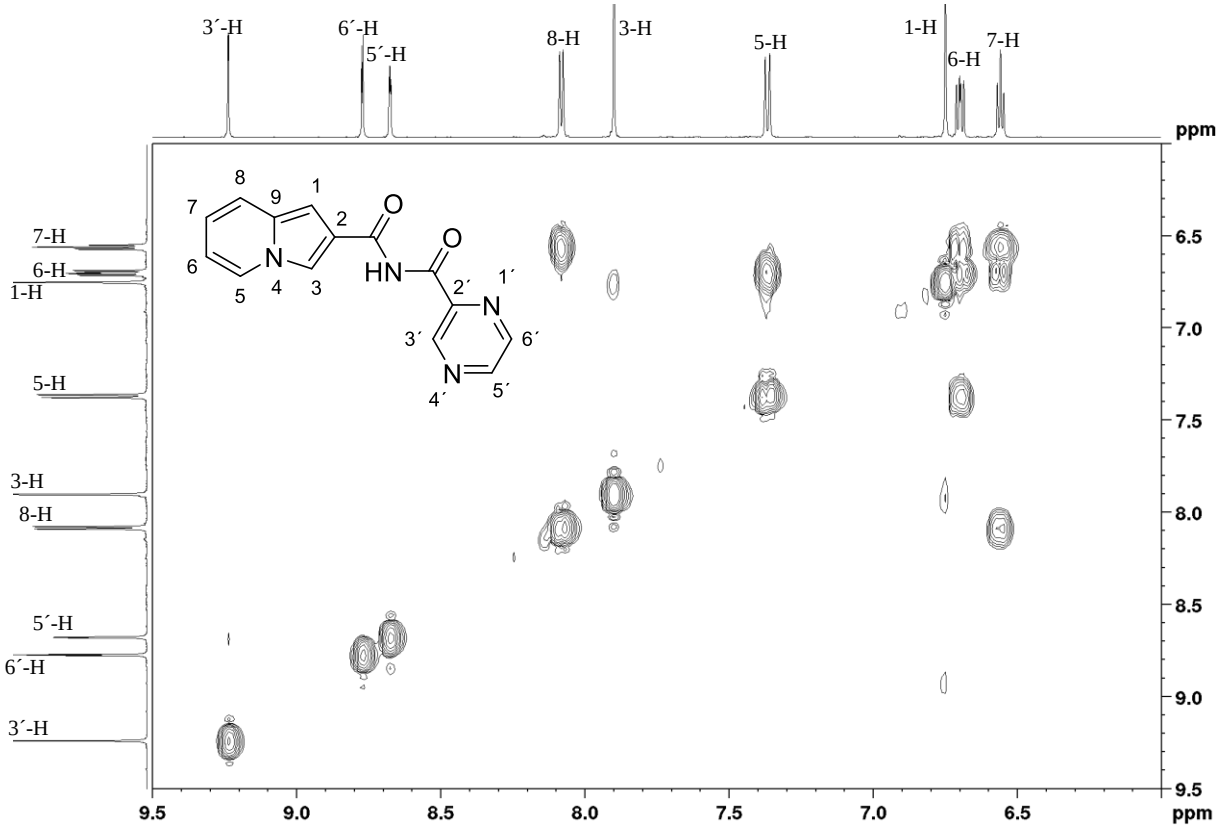

Figure 61.COSY spectrum of compound **179** in methanol-d_4.

2.2.6.2. N-*[*N-*(Indolizin-2-ylcarbonyl)isoxazolin-3-on-4-yl]indolizine-2-carboxamide* 180

For coupling of the antibiotic (*R*)-4-amino-3-isoxazolidone, also known as cycloserine **170**, the procedure described for the synthesis of *N*-(pyrazinecarbanoyl)indolizine-2-carboxamide **179** was used. Following reaction, the mixture was cooled to room temperature, diluted with $CHCl_3$ and filtered. The residue was washed with chilled methanol to afford, as brick-red crystals, *N*-[*N*-(indolizin-2-ylcarbonyl)isoxazolin-3-on-4-yl]indolizine-2-carboxamide **180**, but in only 2% yield (**Scheme 47**). At this stage in the investigation, it was essential to isolate sufficient material for preliminary bioactivity. The optimisation of reaction yield of biologically active compounds would be the subject of future studies.

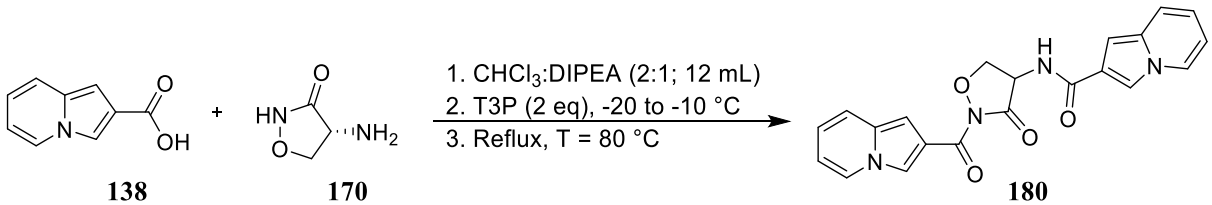

Scheme 47. Synthesis of diamide **180**.

Our expectation was that we would obtain both mono- and disubstituted products. However, only the disubstituted product **180** was isolated and this indicates that both the exo- and endo-cyclic cycloserine nitrogens react with indolizine-2-carboxylic acid **138**. This observation confirms the coupling capacity of the T3P in amide synthesis, albeit in low yield. The low yield clearly warrants optimisation studies in the future. The spectroscopic data provide interesting insights into the structure of this compound. The identity of the brick-red crystals was established using 1- and 2-D NMR as well as IR spectroscopy. At first, ^{1}H NMR analysis of the cycloserine conjugate **180** at room temperature produced a complex spectrum (**Figure 62**).

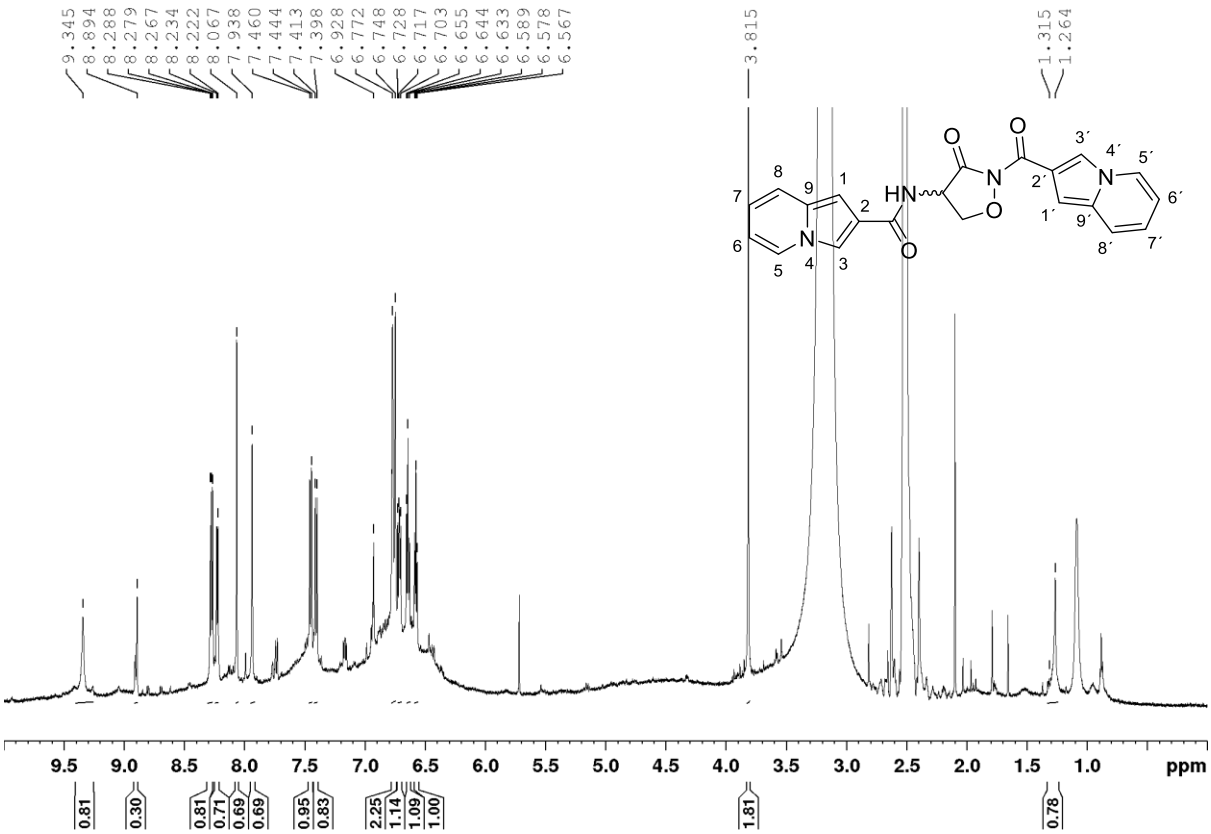

Figure 62. ^{1}H NMR spectrum of compound **180** in DMSO-d_6 at 298 K.

However, the apparent complexity of the ^{1}H NMR spectrum at room temperature arises from the phenomena of hindered internal rotation of the carboxamide groups due to lone-pair delocalisation (shown for one of the amide moieties in **Scheme 48**) and the possibility of keto-enol tautomerism.

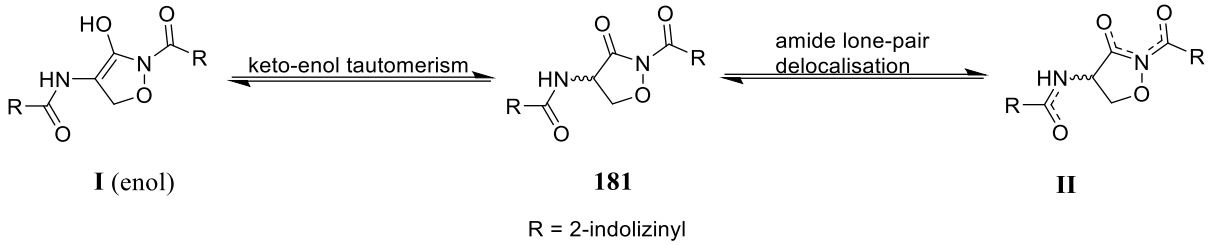

Scheme 48. Possible electron delocalisation and tautomerism phenomena in compound **180**.

The delocalisation results in the partial double-bond character of the N-CO bonds that gives rise to slow rotation resulting in the detection of rotamers in NMR spectra at low or even normal probe temperature. The resulting complexity can be overcome by analysing the spectrum at high temperature. Thus, in **Figure 63** which depicts the ^{1}H NMR spectrum of compound **180** at elevated temperature (353 K), the twelve indolizine protons are accounted for in the aromatic region.

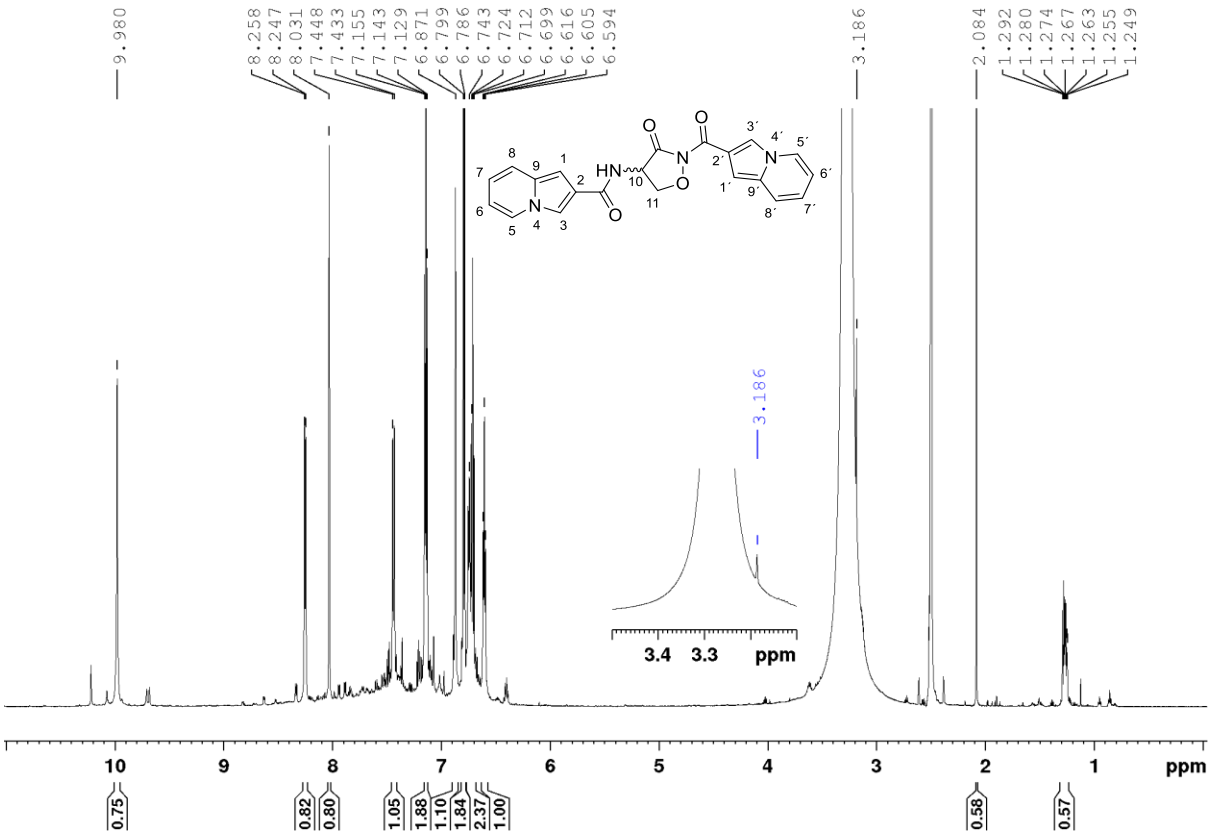

Figure 63. ^{1}H NMR spectrum of compound **180** in DMSO-d_6 at 353 K.

At 298 K, the isoxazoline methylene protons (CH_2O) resonate as a singlet at 3.82 ppm (**Figure 62**), indicating dominance of the enol tautomer in which their diastereotopicity is removed. At 353 K (**Figure 63**), however, this signal is almost invisible and analysis of the COSY spectrum at 353 K (**Figure 64**) shows the correlation of the methine proton (10-H) with:- a cross peak

largely masked by the water signal from the DMSO-d_6 solvent and corresponding to the diastereotopic methylene protons – a situation consistent with dominance of the keto form of the isoxazolin-3-one moiety at 353 K; and a cross peak at *ca.* 3.8 ppm corresponds to the almost invisible methylene signal for the enol (now minor) tautomer.

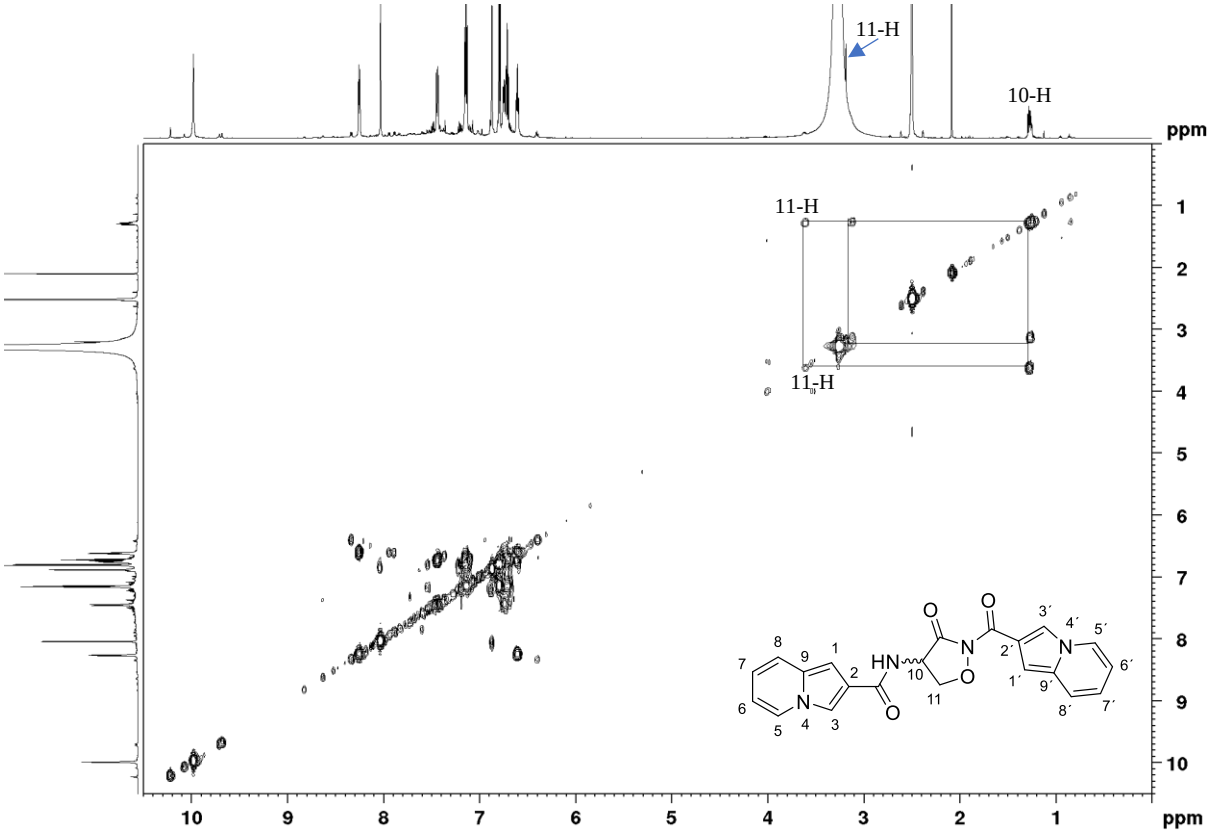

Figure 64. COSY spectrum of compound **180** in DMSO-d_6 at 353 K.

It is worth noting that the ^{13}C NMR spectrum obtained at 353 K (**Figure 65)** shows the presence of fifteen carbon signals, six carbons less than expected (due to signal broadening and coalescence associated with lone-pair electron delocalisation, tautomerism and hindered internal rotation of carboxamides), with the signals at 40.0 and 30.4 ppm corresponding to the C-11 and C-10 carbons, respectively. The corresponding DEPT-135 shows eleven rather than thirteen carbon signals including nine aromatic carbon signals instead of twelve signals. The appearance of fewer carbons than expected is a result of chemical shift equivalence of some carbon nuclei, especially the pyridine carbons in the indolizine moiety. Analysis of the ^{13}C NMR spectrum (**Figure 65**) in conjunction with the DEPT-135 spectrum (**Figure 66**) revealed the presence of two aromatic quaternary carbon signals at 121.70 and 131.87 ppm as well as the carbonyl signals at 149.6 and 163.6 ppm in the ^{13}C NMR spectrum. As expected, the IR

spectrum (**Figure 67**) reveals the NH band at 3220 cm^{-1} and the amide C=O band at *ca.* 1644 cm^{-1}.

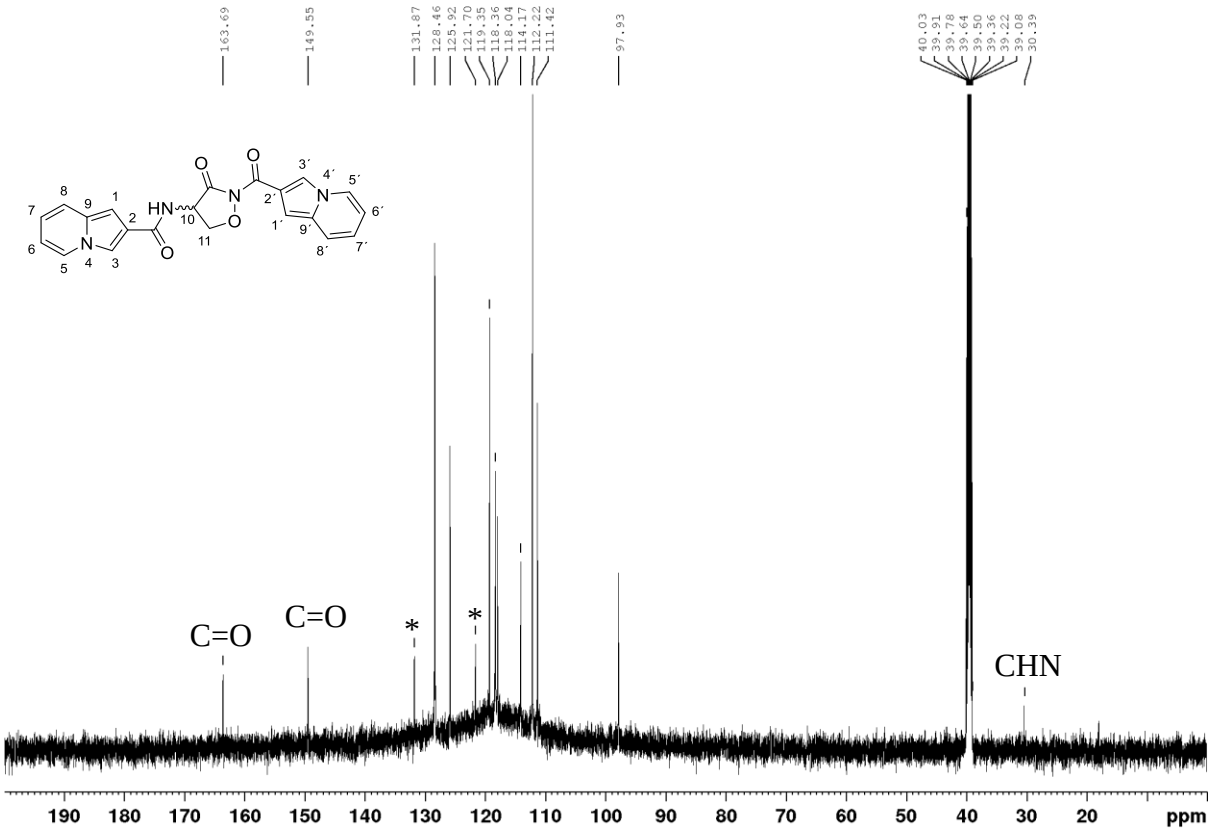

Figure 65. 150 MHz ^{13}C NMR spectrum of compound **180** at 353 K in DMSO-d_6.

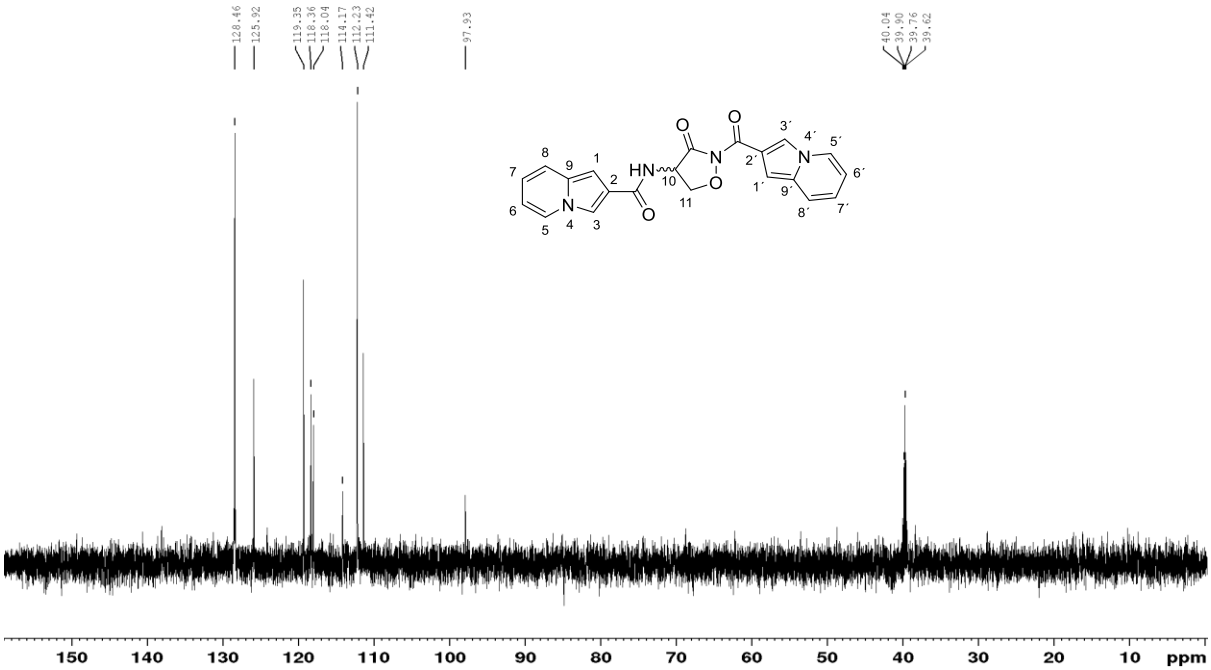

Figure 66. 150 MHz DEPT-135 spectrum of compound **180** at 353 K in DMSO-d_6.

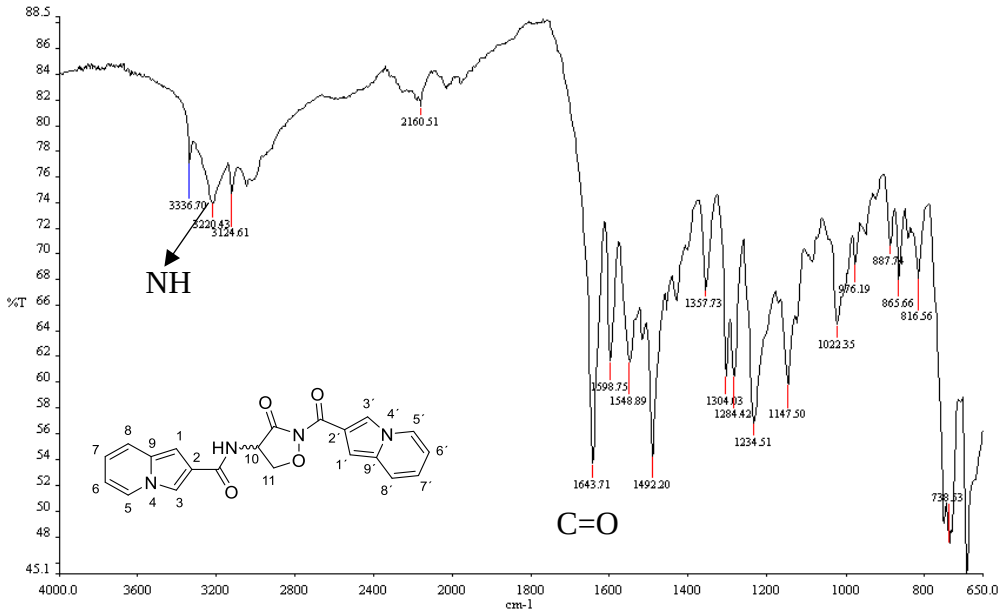

Figure 67. IR spectrum of compound **180**.

2.2.7. Extension of T3P-mediated indolizine-2-carboxamide syntheses.

Although the yield in the initial T3P-mediated reactions were very low, it was decided to persevere with the approach for coupling of 2,4-imidazolidinedione **146** and 1-methylimidazolidine-2,4-dione **147** with indolizine-2-carboxylic acid **138** and afterwards, with 3-acetylindolizine-2-carboxylic acid **139**.

*2.2.7.1. T3P-mediated reactions of acid (***138** *and* **139***) with 4-imidazolidinedione* **146** *and -methylimidazolidine-2,4-dione* **147**.

The coupling reactions were conducted with T3P in a stoppered flask for a period of two to three days after which concentration *in vacuo* and subsequent purification afforded the desired products. Coupling of the indolizine-2-carboxylic acid **138** with 2,4-imidazolidinedione **146** (**Scheme 49**) provided two products — the mono-substituted 3-(indolizine-2-carbonyl)-2,4-imidazolidinedione **148** in a much more encouraging 48% yield, and the disubstituted 1,3-bis(indolizine-2-carbonyl)-2,4-imidazolidinedione **149** in 9% yield. As expected, having one available nitrogen, 1-methylimidazolidine-2,4-dione **147** afforded the mono-substituted derivative **150**, but in a lower yield of 16% (**Scheme 49**).

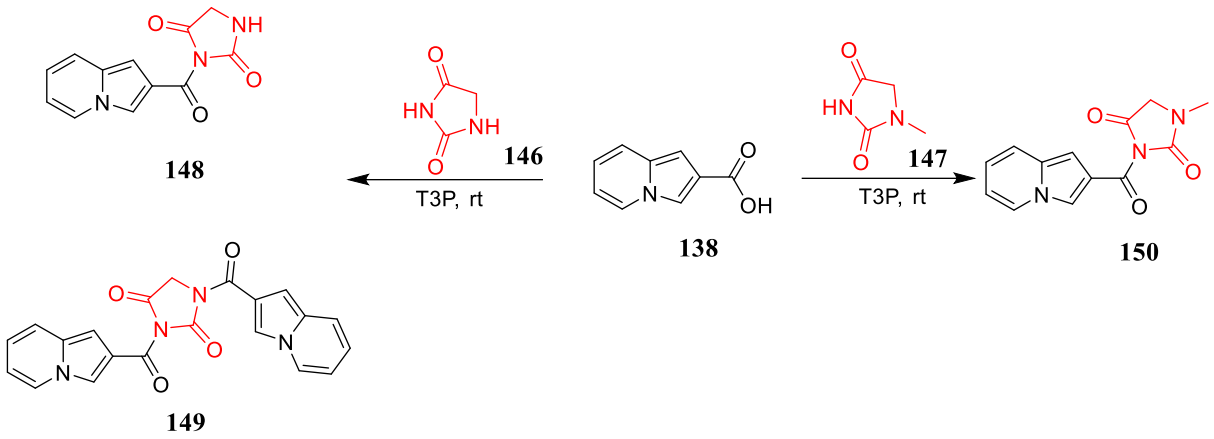

Scheme 49. T3P-mediated synthesis of amide derivatives from indolizine-2-carboxylic acid **138** and heterocyclic amines **146** and **147**.

As illustrated in **Scheme 50**, coupling reactions of 3-acetylindolizine-2-carboxylic acid **139** under similar conditions afforded deacetylated indolizine-2-carboxamide derivatives. For instance, the coupling of the 3-acetylated acid **139** with 2,4-imidazolidinedione **146** gave the deacetylated amide **148** in 23% yield, presumably *via* the anticipated product **183** as an intermediate, and the monoacetylated diamide **185** in 10% yield, presumably *via* compound **184**. The imido proton, being more acidic than the amido proton in the 2,4-imidazolidinedione **146** is expected to be removed first by the base, DIPEA, thus favouring attack *via* the imido nitrogen. This expectation was confirmed by the ^{3}J NMR coupling between the methylene and amido protons evident in the COSY spectrum. However, prior deacetylation of intermediate **183**, under the reaction conditions followed by reaction with the 3-acetylindolizine-2-carboxylic acid **139** cannot be precluded. Similarly, coupling of the 3-acetylindolizine-2-carboxylic acid **139** with amine **147** afforded amide **150** presumably *via* the acetylated intermediate **182**.

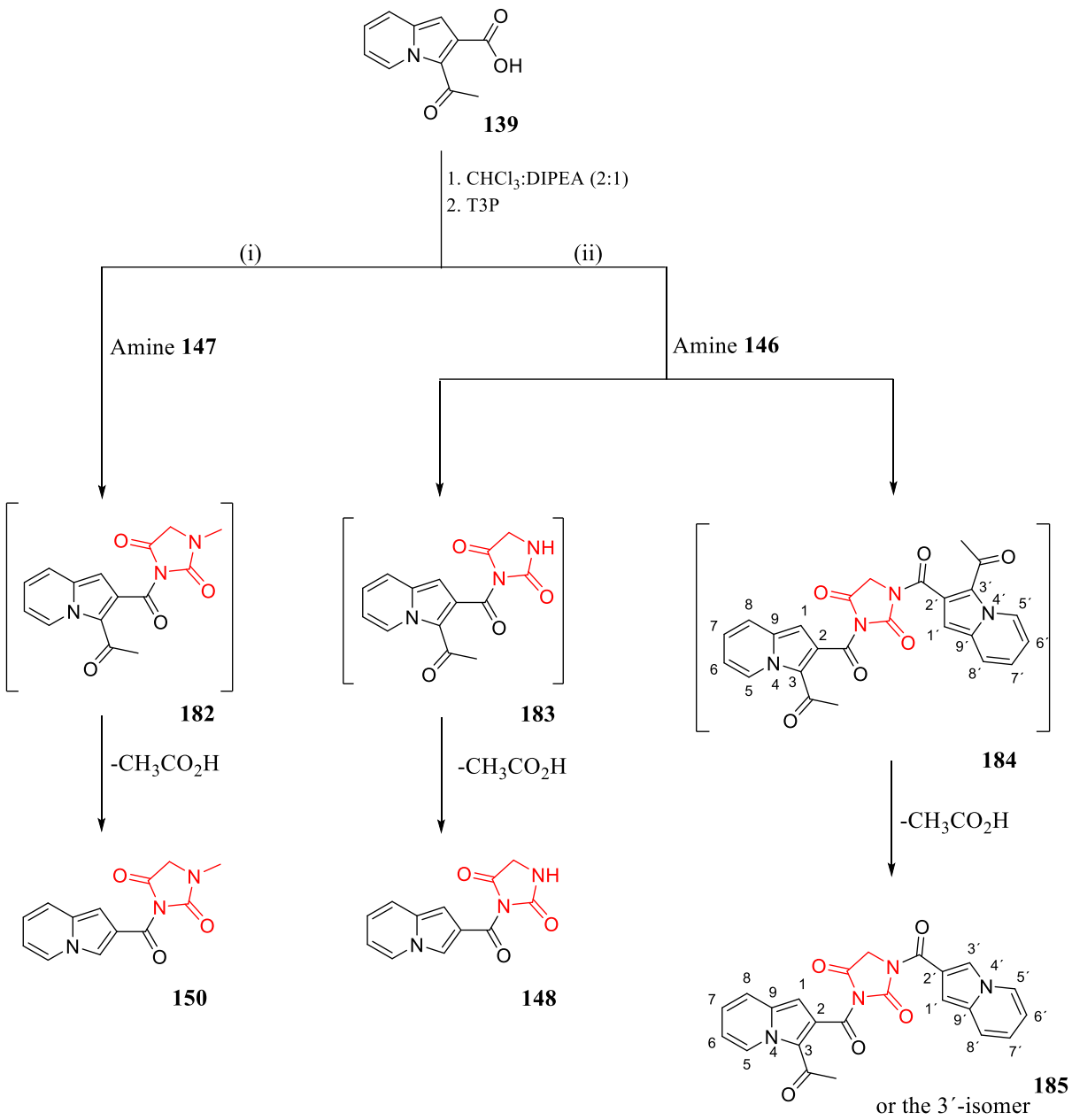

Scheme 50. T3P catalysed amide synthesis from acetylated acid and heterocyclic amines. Reagents: (i) 1-methylimidazolidine-2,4-dione **147**; (ii) 2,4-imidazolidinedione **146**.

This series of amides was extensively characterised using 1D- and 2D-NMR spectroscopy as well as HRMS and IR spectroscopy. The ^{1}H NMR spectrum of amide **150** showed the methylene (CH_2N) singlet at 3.95 ppm and the methyl (NCH_3) singlet at 2.90 ppm, whilst the methylene (CH_2N) signal of the related amide **148** appeared upfield as a doublet (J = 6.48 Hz) at 1.36 ppm. Their IR spectra clearly showed carbonyl bands at 1713 and 1723 cm^{-1}, respectively. Analysis of the ^{1}H NMR spectrum (**Figure 68**) of the disubstituted 2,4-imidazolidinedione **185** shows the methylene (CH_2N) signal shifted downfield, compared to amide **148**, to 2.63 ppm

The observation of eleven aromatic protons, three aromatic singlets at 6.75, 6.89 and 7.90 that respectively correspond to the 1-, 1´ and 3´-methine protons of the pyrrole rings and the presence of three methyl protons (CH_3) resonating at 3.34 ppm as a singlet confirm the presence of two indolizine moieties and an acetyl group on one of them. Indeed, analysis of the corresponding COSY spectrum shows correlation of the four pyridine protons for each indolizine moiety – a triplet for the 7-H and the 7´-H nuclei correlating with upfield doublets of doublets for the 6-H and 6´-H nuclei which correlate, in turn, to the relatively downfield doublets corresponding to 5-H and 5´-H. The ^{13}C NMR spectrum (**Figure 70** and **Figure 71**) exhibits twenty carbon signals whilst the DEPT-135 NMR spectrum (**Figure 72**) shows eleven proton-bearing aromatic carbon signals and two signals upfield corresponding to the N-methylene and acetyl carbons. Analysis of the ^{13}C NMR spectrum in conjunction with the corresponding DEPT-135 NMR spectrum (**Figure 72**) revealed the presence of eight quaternary carbon signals, including carbonyl carbons, of which the aromatic C-9/9´ appear at 120.9 and 121.7 ppm whereas C-3, C-2´ and C-2 appear at 131.1, 134.3 and 138.0 ppm, respectively. The signals at 169.0 and 169.6 correspond to the carbonyl carbons of the amide moieties whilst the signal at 190.5 correspond to the carbonyl carbon of the acetyl group. The assignment of carbon signals was facilitated by inspection of the HSQC spectrum (**Figure 73**) and the pyrrole protons were found to correlate with carbon signals at 101.3, 106.0 and 117.6 while C-8 and C-8´ resonated at 127.0 and 129.2 ppm, respectively. Moreover, the acetyl ($CO\mathit{C}H_3$) and the methylene (CH_2N) carbons were found to resonate at 29.9 and 49.9 ppm, respectively. The IR spectrum (**Figure 74**) shows three carbonyl (C=O) bands at 1713 cm^{-1}, corresponding to the acetyl carbonyl group, and at 1666 and 1582 cm^{-1} corresponding to the amide carbonyl groups.

These results, along with successful achievement of the synthesis of amides **179** and **180** (Section **2.2.6.1** to **2.2.6.2**), which involved use of weakly nucleophilic and seemingly unreactive amines, encouraged further exploration with weakly nucleophilic but medicinally important heteroaromatic amines (**Section 2.2.7.2** to **2.2.7.3**) and the nucleophilic heteroaryl alkylamines (**Section 2.2.7.4**).

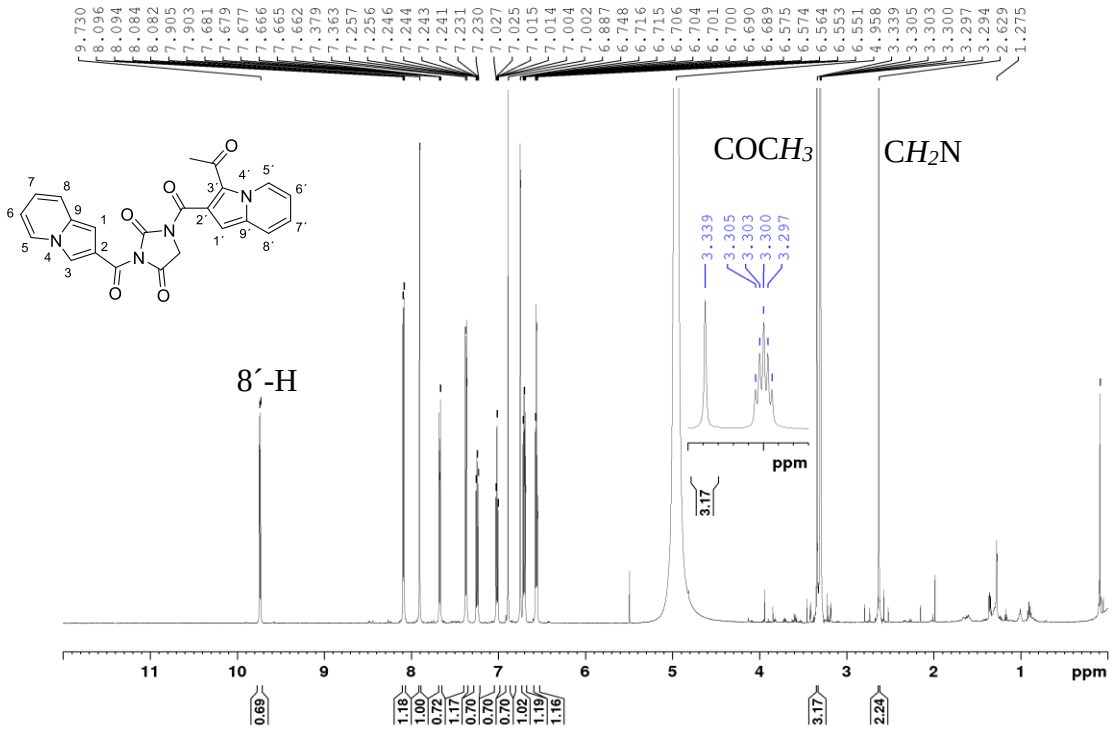

Figure 68. 600 MHz NMR spectrum of the mono-acetylated diamide **185** in methanol-d_4.

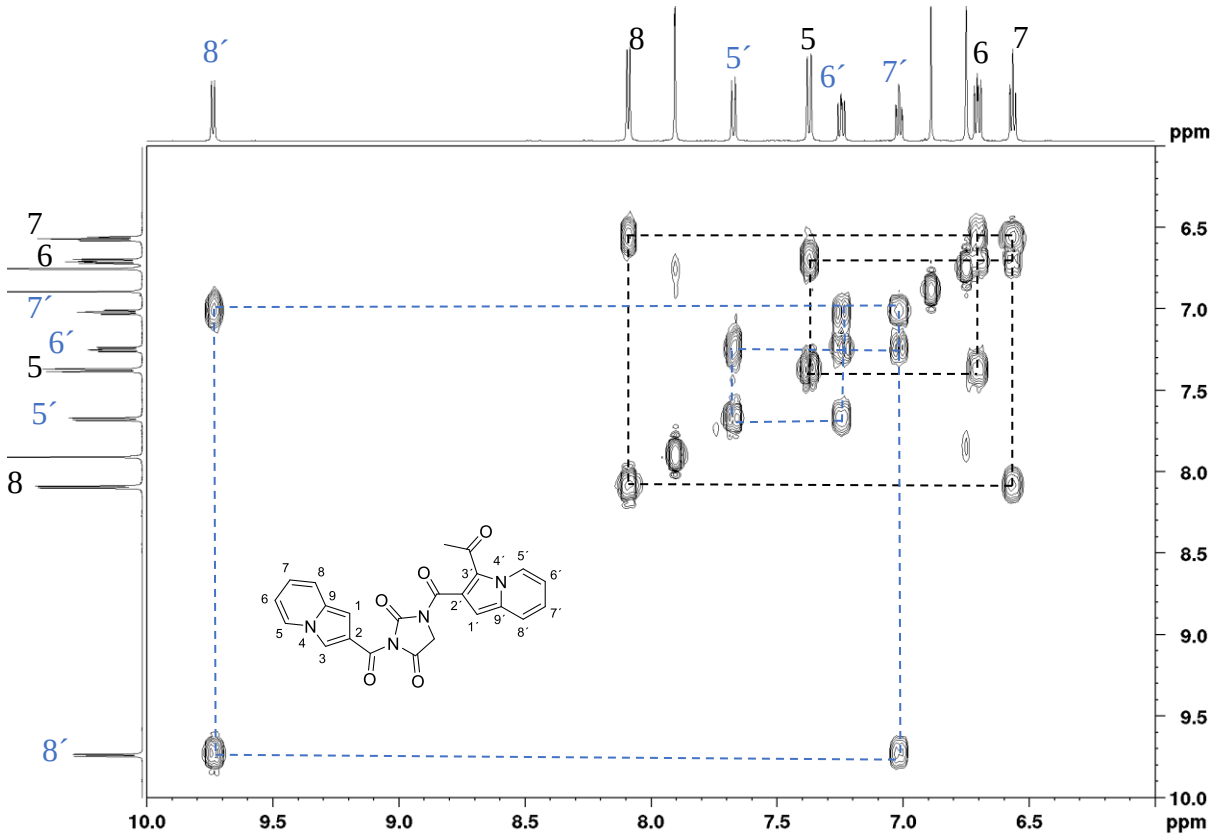

Figure 69. COSY spectrum of the mono-acetylated diamide **185** in methanol-d_4.

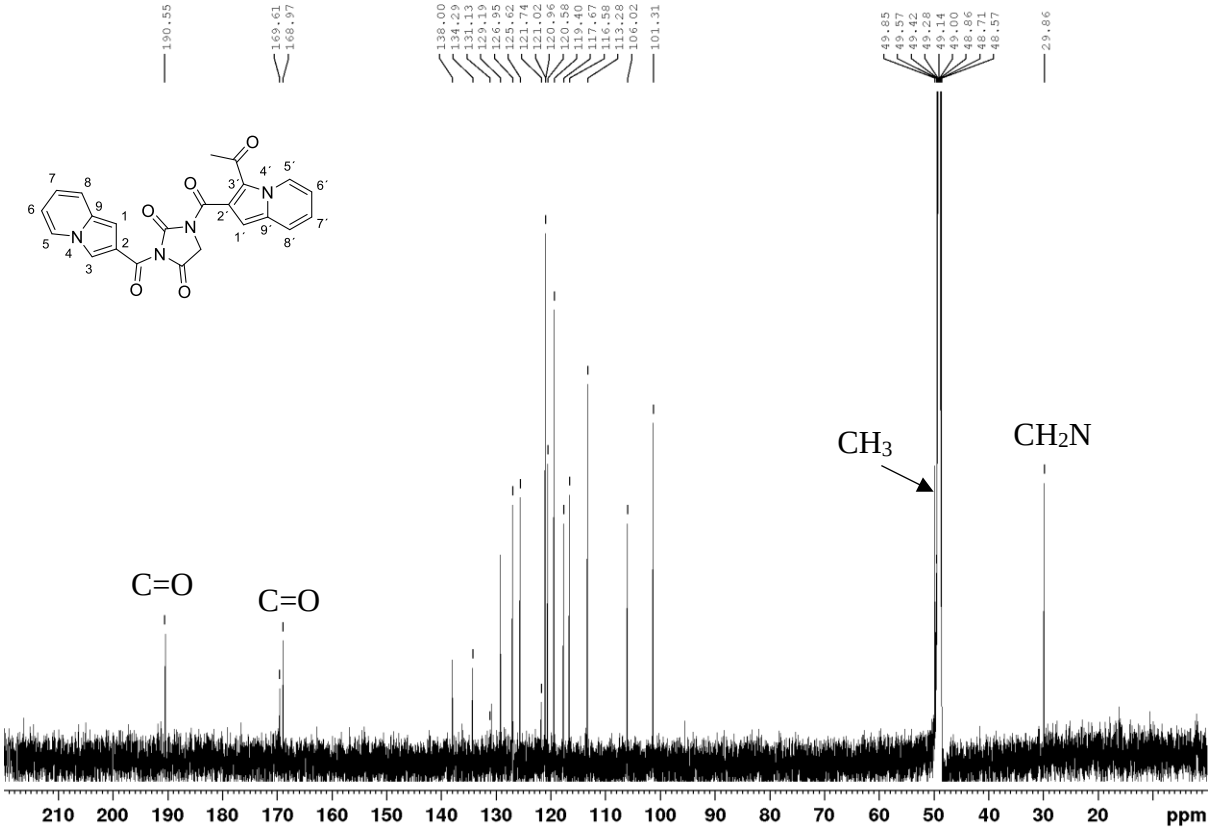

Figure 70. 150 MHz ^{13}C NMR spectrum of amide **185** in methanol-d_4.

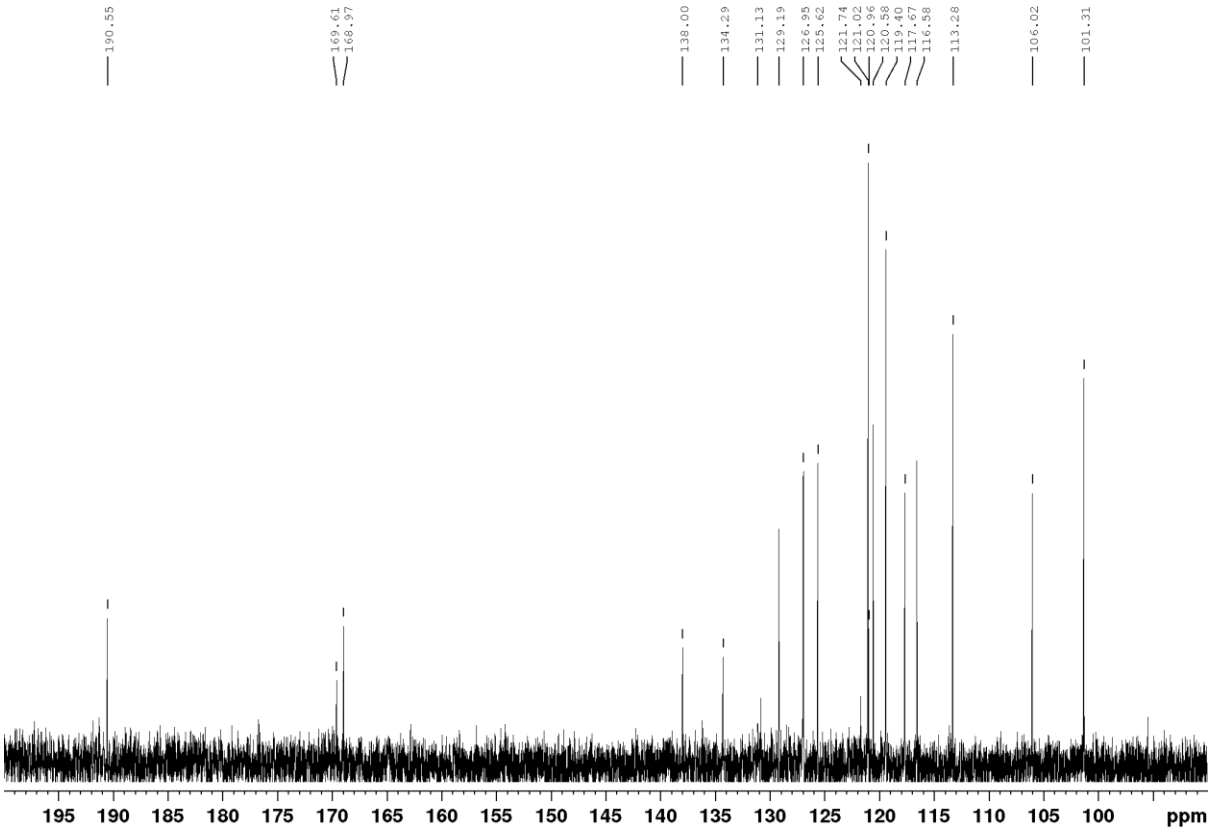

Figure 71. Zoomed partial 150 MHz ^{13}C NMR spectrum of amide **185** in methanol-d_4.

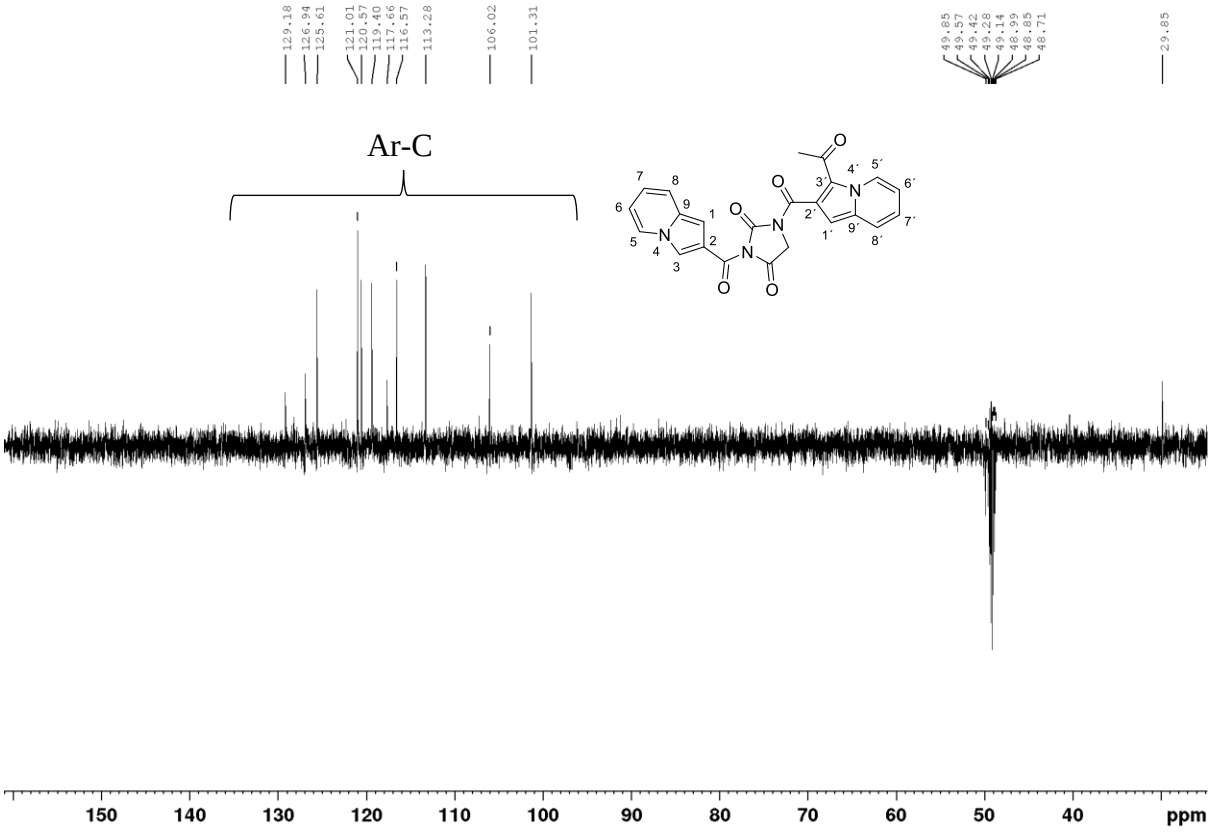

Figure 72. DEPT-135 NMR spectrum of amide **185** in methanol-d_4.

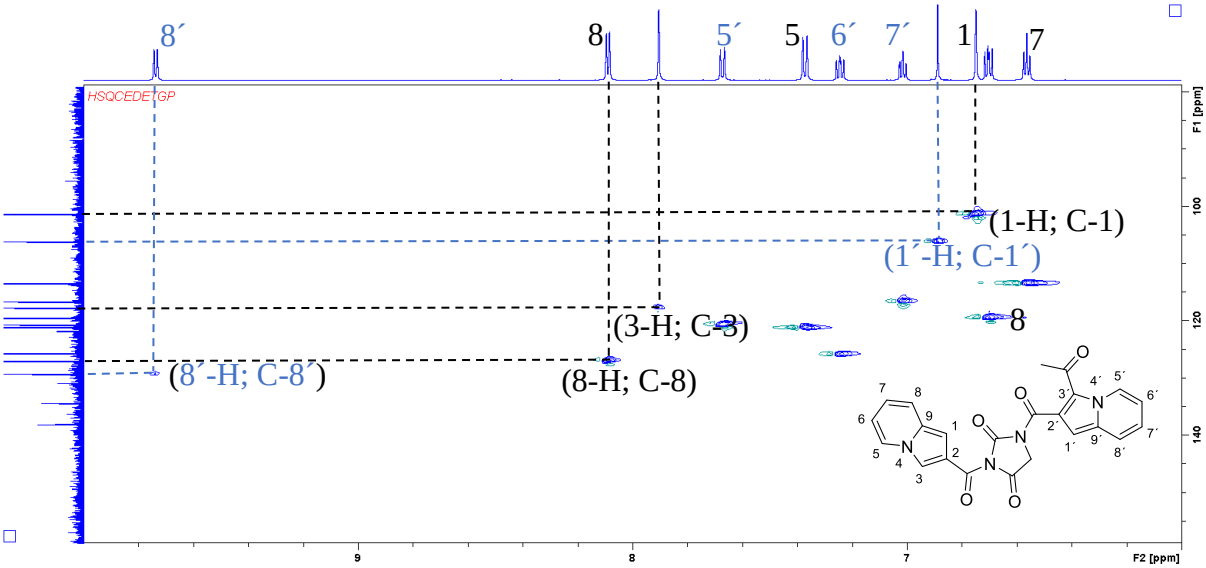

Figure 73. 600 HSQC spectrum of amide **185** in methanol-d_4.

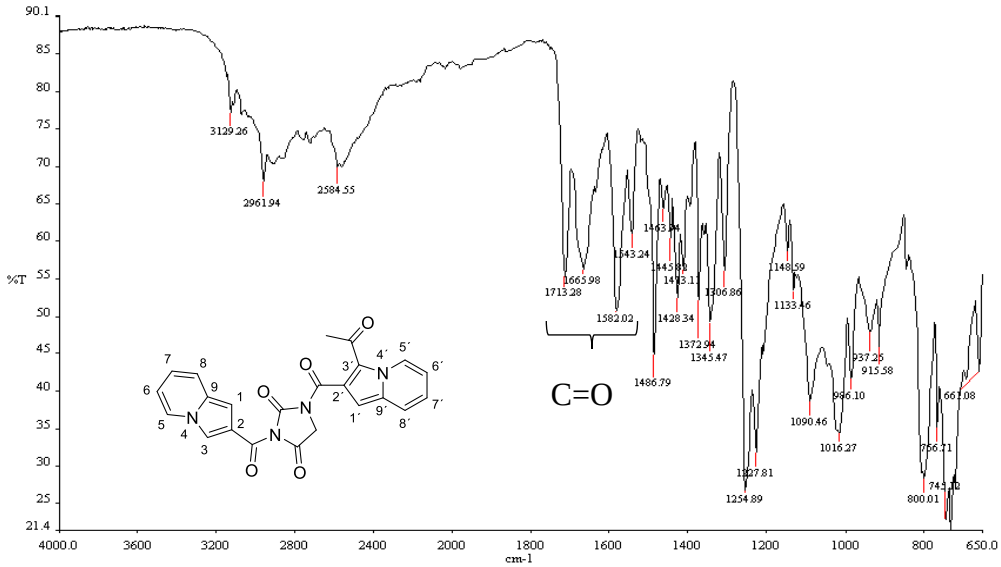

Figure 74. IR spectrum of amide **185**.

2.2.7.2. T3P-mediated coupling of indolizine-2-carboxylic acids with further heteroaromatic amine.

Following the procedure used for coupling with the heterocyclic amines **146-147** to give indolizine-2-carboxamides **148**, **150** and **185**, the indolizine-carboxylic acid **138** and **139** were reacted with a further series of heteroaromatic amines. The objective was to introduce biologically significant heteroaromatic amines to the indolizine moiety through the amide bond. As depicted in **Scheme 51**, amines that were reacted with indolizine-2-carboxylic acid **138** included 3,5-diamino-1,2,4-triazole **186**, 2-aminothiazole **153** and 2-aminopyridine **189** to afford the corresponding amides, *viz.*, 3-acetyl-*N*-(5-amino-1,2,4-triazol-3-yl)indolizine-2-carboxamide **187** (32%) and 3,5-bis-(indolizine-2-carboxamido)-1,3,4-triazole **188** (14%); *N*-(2-thiazolyl)indolizine-2-carboxamide **154** **(**26%); and *N*-(2-pyridinyl)indolizinee-2-carboxamide **190**. However, *N*-(2-pyridinyl)indolizine-2-carboxamide **190** proved difficult to isolate from the crude mixture and the small amount obtained decomposed; formation of the expected product was supported by HRMS and IR data, the latter showed the NH and the amide C=O bands at 3337 and 1672 cm^{-1}, respectively.

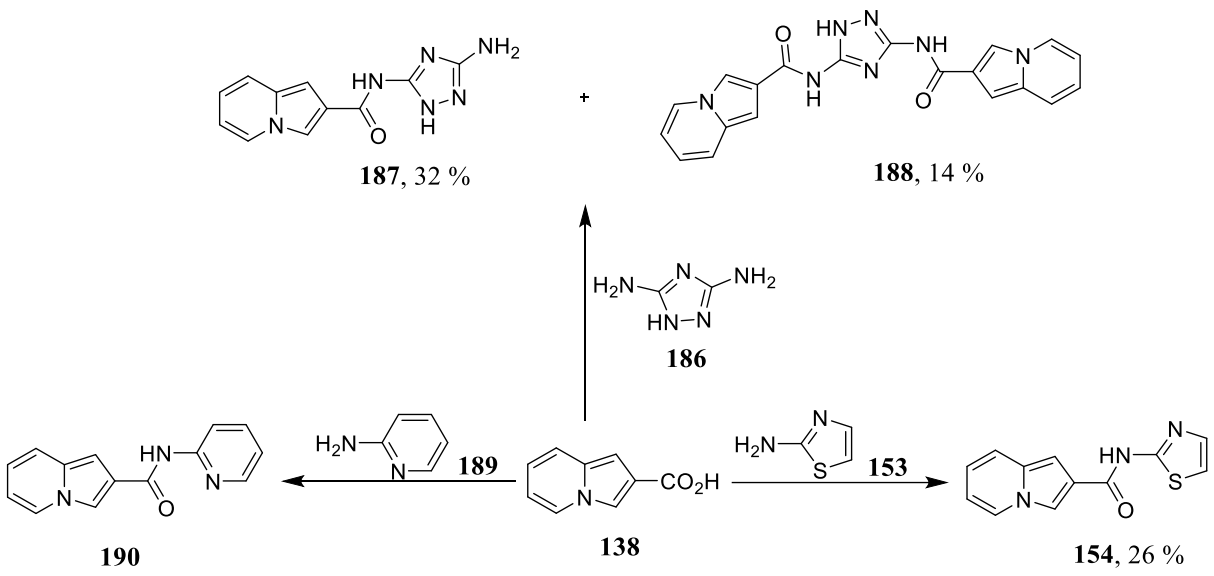

Scheme 51. Synthesis of *N*-heteroarylindolizine-2-carboxamides.

For the synthesis of amides **187** and **188** from the reaction of indolizine-2-carboxylic acid **138** and amine **186**, filtration of the resulting mixture and subsequent washing of the residue with chilled chloroform afforded amide **187** as yellow crystals in modest yield of 32%. Concentration of the filtrate and chromatographic purification of the concentrate using column chromatography afforded a diamide **188**, also as yellow crystals, in 14% yield.

The ^{1}H NMR spectrum of amide **187** (**Figure 75** and **Figure 76**) indicate the presence of six aromatic protons and signals for the amide NH and NH_2 protons. Analysis of the expanded COSY NMR spectrum (**Figure 77**) reveals that the NH_2 protons resonate as doublets at 7.24 and 7.53 ppm each with *J*-coupling of 3.5 Hz as a result of delocalisation of NH_2 lone pair into triazole ring leading to hindered rotation about sp^2 C-NH_2 bond and, hence, diastereotopicity of the amino group protons (see inset in **Figure 77**). The ^{1}H NMR spectrum (**Figure 75**) revealed that the amide NH resonates at 12.4 ppm as expected. The triplet of doublets at 6.64 ppm and the multiplet at 6.77 ppm correspond to the 7-H and 6-H protons, respectively, whilst the singlet at 7.10 ppm and the doublet at 7.48 ppm correspond to the 1-H and 5-H protons, respectively. The 3- and 8-H protons, which were expected to appear as a singlet and doublet, respectively, overlap at 8.29 ppm as doublet and doublet of doublet, respectively.

The ^{13}C NMR spectrum of the diamide **188** (**Figure 78**) exhibited seventeen carbon signals including the two characteristic signals of the carbonyl carbons at 162.1 and 168.9 ppm, whilst the corresponding DEPT 135 NMR spectrum (**Figure 79**) exhibited nine carbon signals corresponding to the methine carbons of the indolizine moieties. The below expected number of carbon signals results from the overlap of the chemically equivalent carbons. However,

deductive analysis of the carbon spectra reveals the presence of eight quaternary carbons including the carbonyl carbons of the dimeric amide **188**.

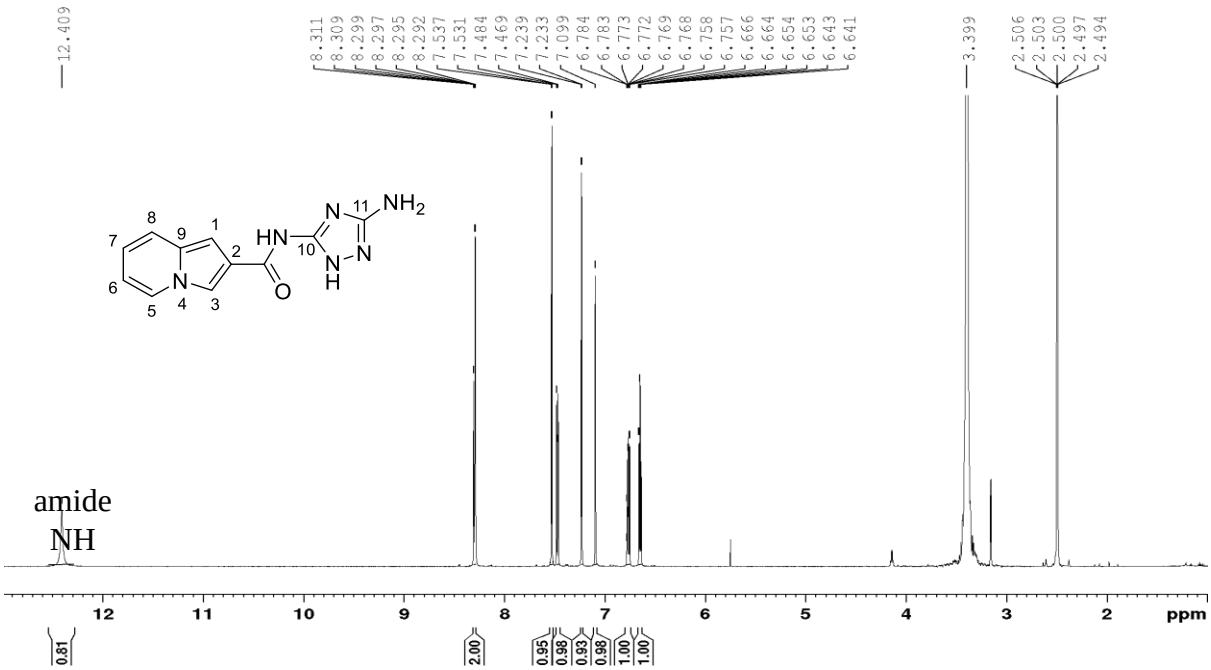

Figure 75. 600 MHz ^{1}H NMR spectrum of amide **187** in DMSO-d_6.

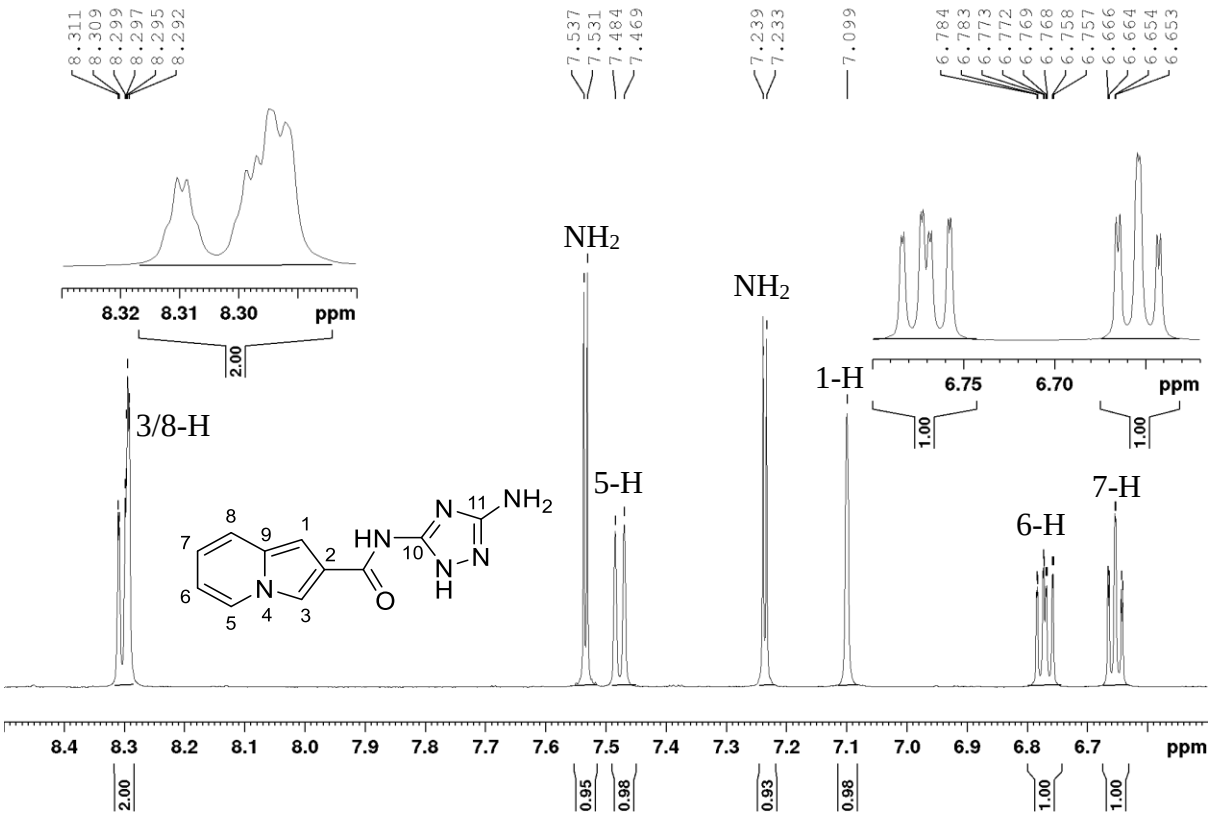

Figure 76. Zoomed, partial ^{1}H NMR spectrum of amide **187** focusing on the aromatic region.

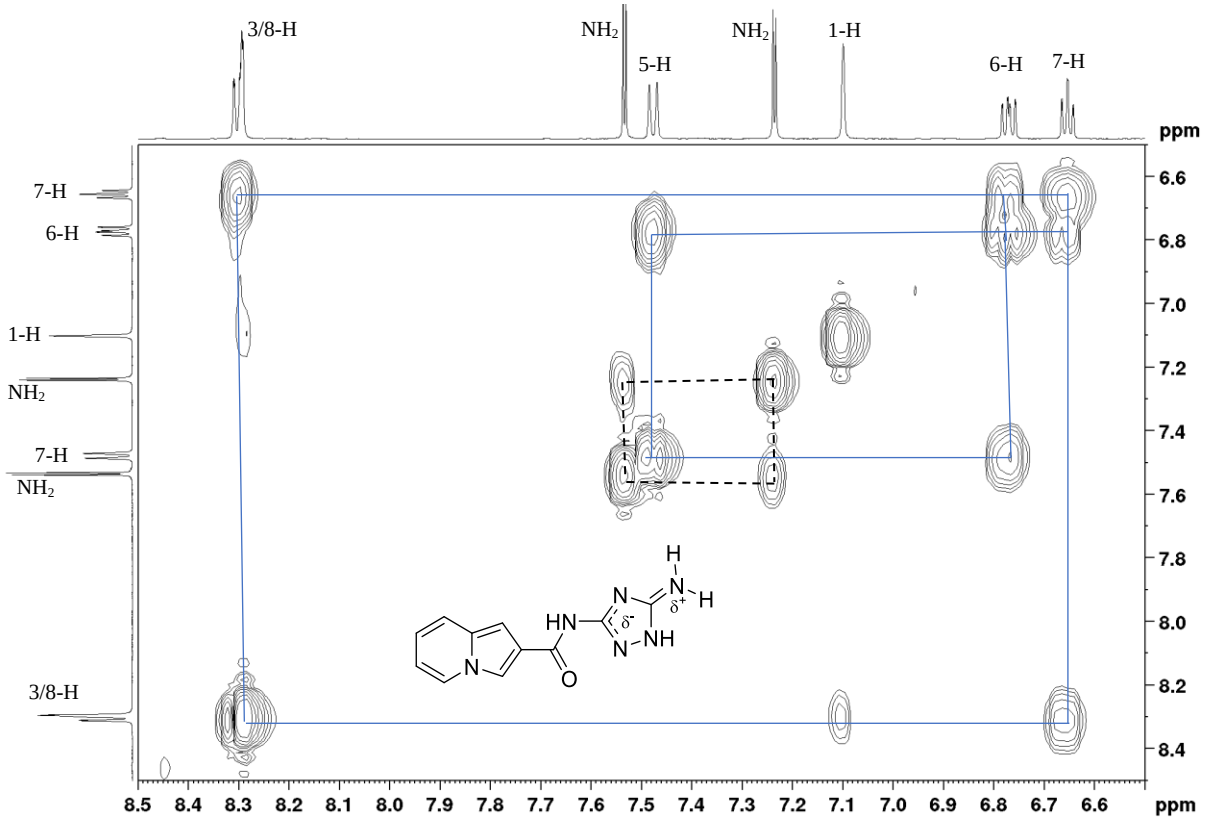

Figure 77. COSY spectrum of amide **187**, showing the partial double bond responsible for diastereotopicity of the amino protons.

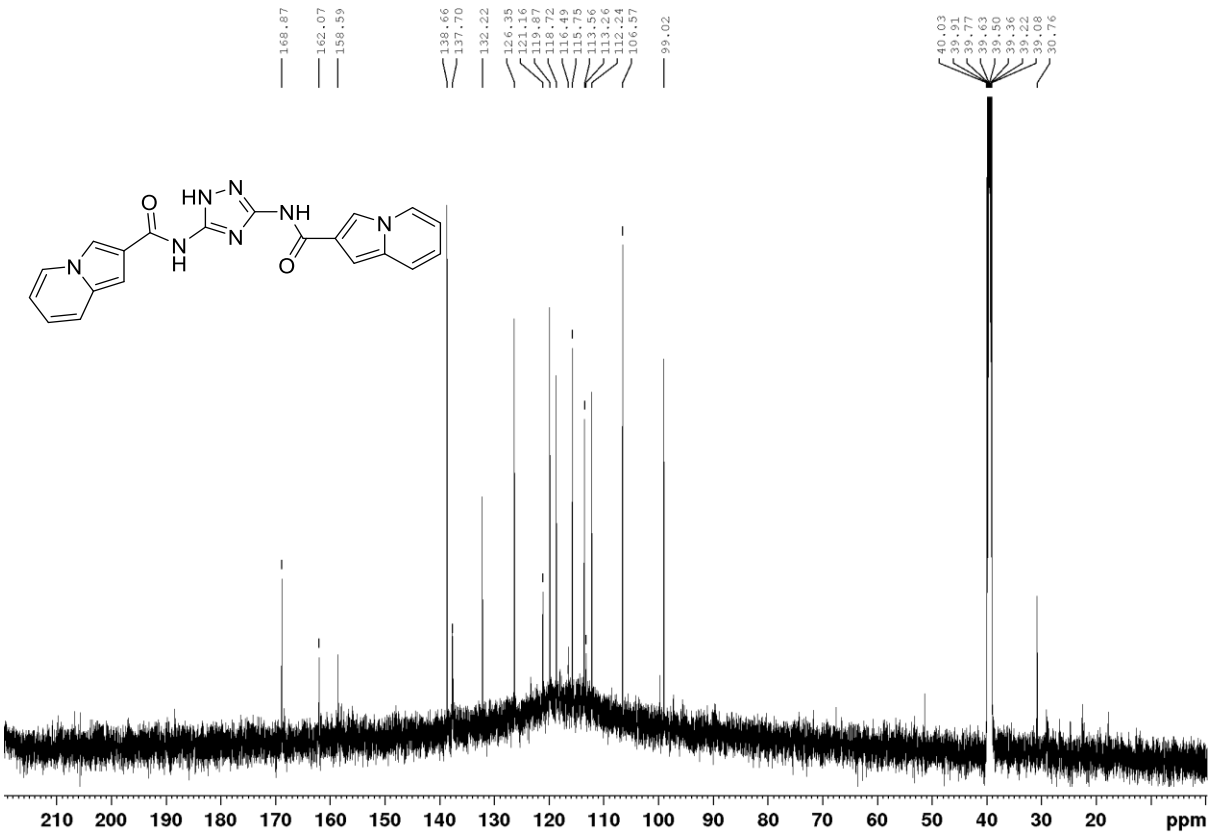

Figure 78. 150 MHz ^{13}C NMR spectrum of diamide **188** in DMSO-d_6.

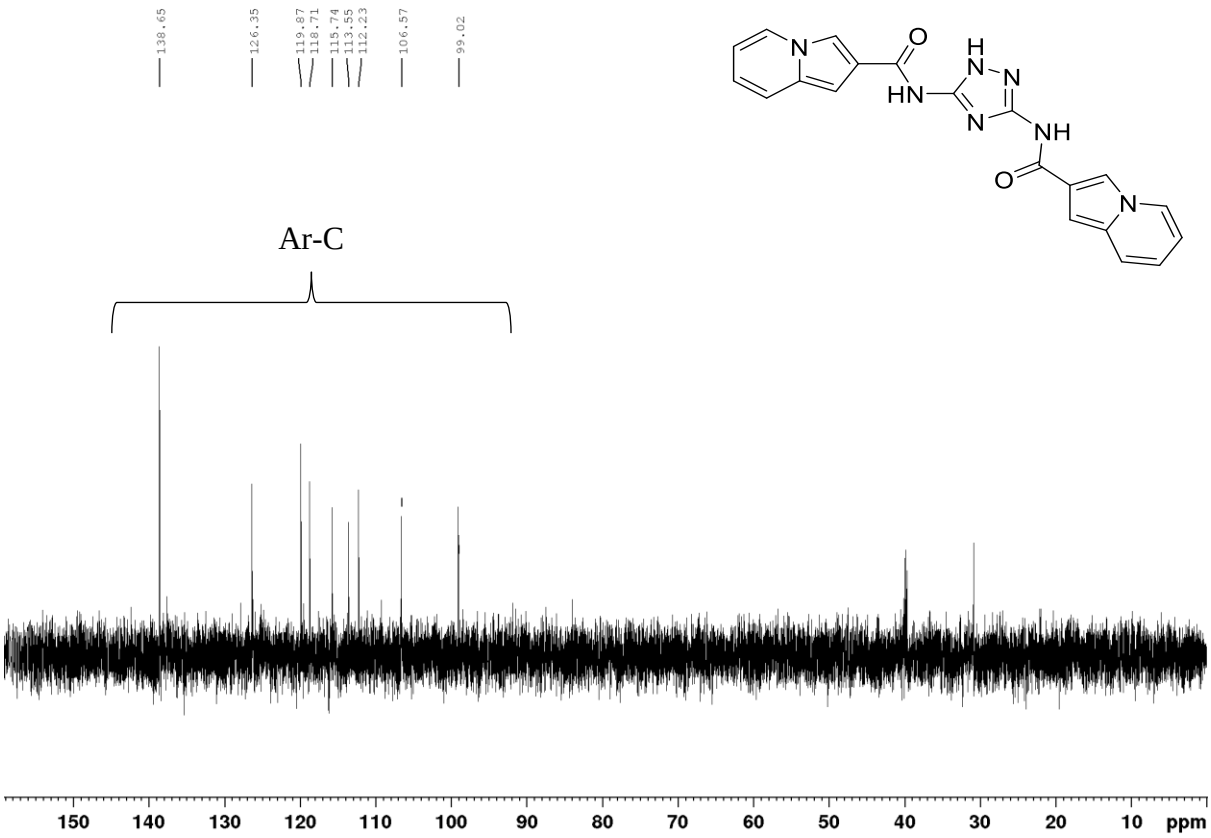

Figure 79. DEPT-135 spectrum of the diamide **188** in DMSO-d_6.

At first, the *N*-(2-thiazolyl)indolizine-2-carboxamide **154** was synthesised in exploratory studies involving the use of 2,2,2-trifluoroethyl borate as a catalyst (**see Section 2.2.4.1**). The subsequent application of the T3P-facilitated methodology drastically improved the yield thirteen-fold from 2 to 26%.

Scheme 52 shows an overview of further amidation reactions with 3-acetylindolizine-2-carboxylic acid **139** and the amines 3,5-diamino-1,2,4-triazole **186**, 2-aminothiazole **153**, 3-amino-1,2,4-triazole **191** and 2-aminopyridine **189** to furnish: 3-acetyl-*N*-(5-aminotriazol-3-yl)indolizine-2-carboxamide **192** and 3-(3-acetylindolizine-2-carboxamido)-5-(indolizine-2-carboxamido)-1,2,4-triazole **193**; 3-acetyl-*N*-(thiazol-2-yl)indolizine-2-carboxamide **194**; 3-acetyl-*N*-(triazol-3-yl)indolizine-2-carboxamide **195**; and 3-acetyl-*N*-(2-pyridinyl)indolizine-2-carboxamide **196**, respectively. As expected, IR analysis of the amide **196** showed the NH band at 3241 cm^{-1} and the acetyl and amide C=O stretches at 1682 and 1603 cm^{-1}; IR analysis of the crude deacetylated derivative **190** (**Scheme 51**) showed the NH and C=O bands at 3337 and 1672 cm^{-1}, respectively.

Despite the encouraging observation that amide **196** prepared from the reaction of 3-acetylindolizine-2-carboxylic acid **139** and 2-aminopyridine **189** was isolable and did not readily decompose (unlike the non-acetylated analogue **190** in **Scheme 51**), there is no

conclusive trend in relative reactivity of the 3-acetylated and the non-acetylated acids. A better yield of 32% for the monomer **187** was obtained when the non-acetylated acid **138** was reacted with 3,5-diamino-1,2,4-triazole **186** (**Scheme 51**) whereas the yield for the 3-acetylated analogue **192** (**Scheme 52**) was only 3%. Coupling of the acids **139** and **138** with 2-aminothiazole **153** provided the desired amides in similar yields (**154** and **194**, 23% each). Coupling of the 3-acetylated acid **139** with 3-amino-1,2,4-triazole **191** gave the corresponding amide in 9% yield, compared to 32% for the non-acetylated analogue **187**.

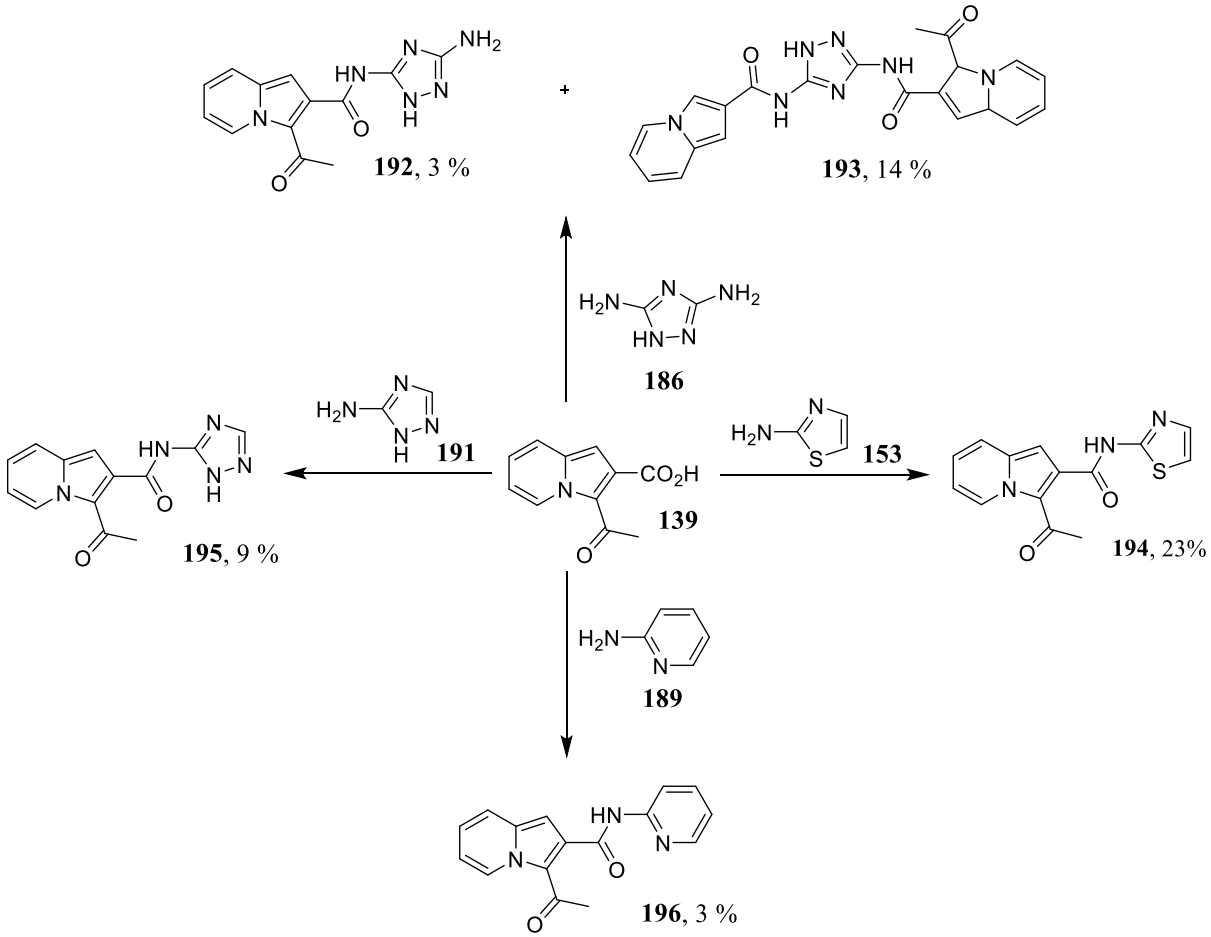

Scheme 52. Synthesis of amides from 3-acetylindlizine-2-carboxylic acid **139** and heteroaromatic amines.

It is perhaps needless to deliberate about amide **192** and **193** since their deacetylated derivatives have been discussed in the preceding **Section 2.2.7.2** and because their spectroscopy is nuanced. However, the ^{1}H NMR spectra for the 3-acetylated carboxamides exhibit a singlet for the three acetyl protons at *ca.* 2.5 ppm, and one aromatic proton less compared to their non-acetylated counterparts, as illustrated in the spectrum for the thiazole derivative **194** in **Figure 80**. The signal at 12.9 ppm corresponds to the amide proton while the acetyl protons resonate at *ca.* 2.4 ppm. The seven aromatic protons resonate between 6.95 and 9.76 ppm. The

corresponding ^{13}C NMR spectra exhibit the acetyl carbonyl signal at *ca.* 187 ppm, the amide carbonyl between 160 and 167 ppm and the aceetyl methyl carbon at *ca.* 29 ppm. The appearance of the NH absorption band at 3115 cm^{-1} and the acetyl and amide carbonyl (C=O) bands at 1669 and 1615 cm^{-1}, respectively, in the IR spectrum (**Figure 82**) confirms successful formation of the amide **194**.

The presence of the pseudo-molecular ion (MH^+) peak in the ESI MS spectrum of compound **194** is clearly evident as the base peak at *m/z* 286.0344 (**Figure 81**). The ESI MS spectrum of amide **196** showed the base peak corresponding to the pseudo-molecular ion (MH^+) peak at *m/z* 280.077 whilst that of amide **195** showed the pseudo-molecular ion peak at *m/z* 270.0724.

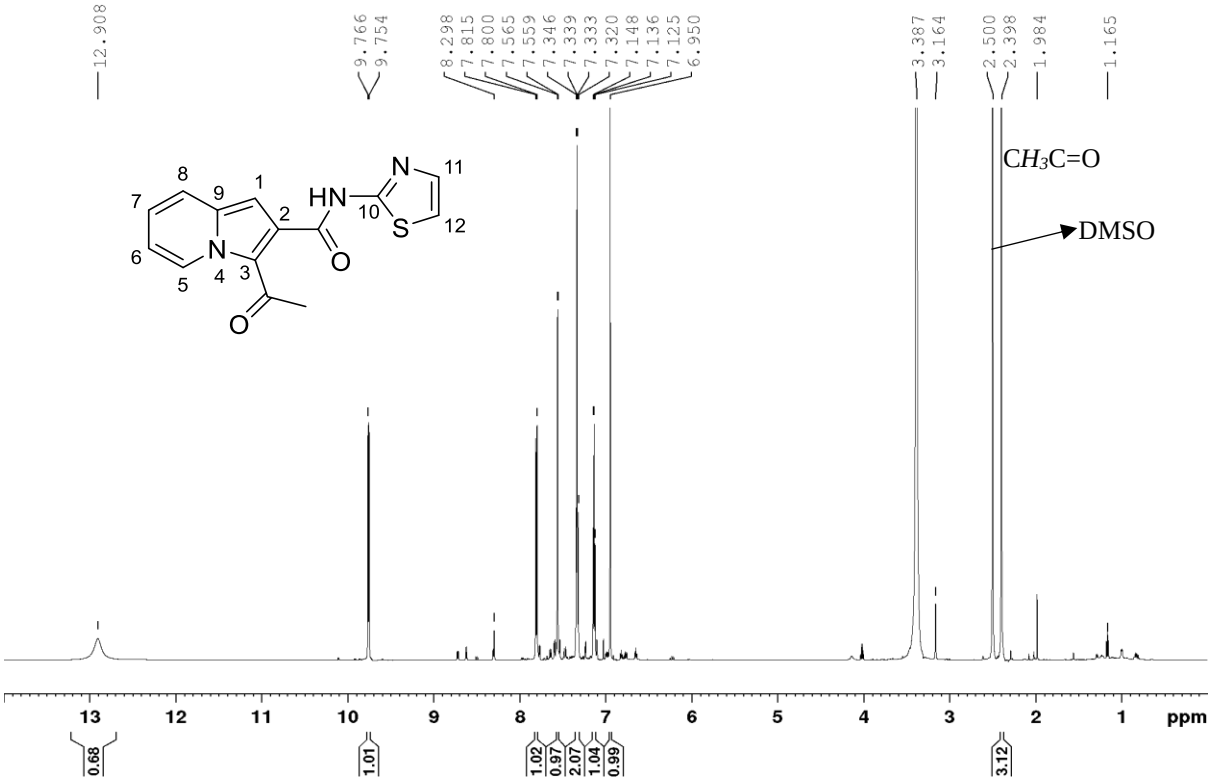

Figure 80. 600 MHz ^1H NMR spectrum of amide **194** in DMSO-d_6.

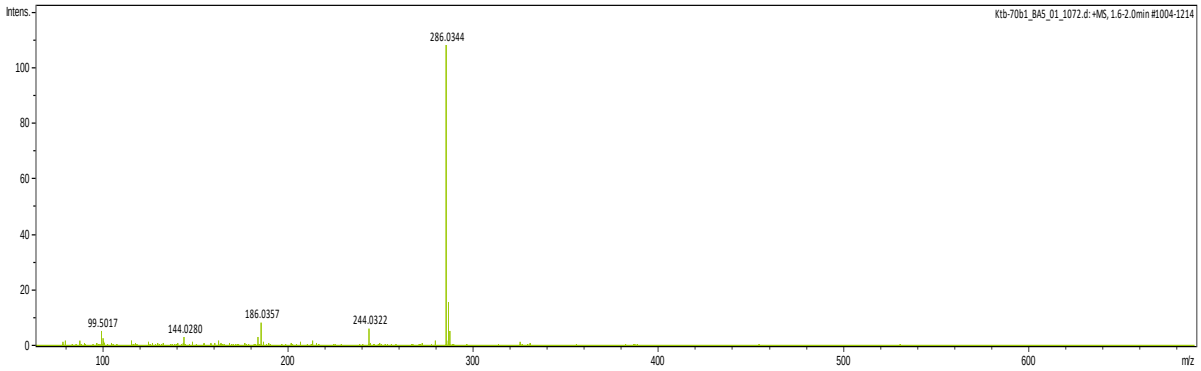

Figure 81. HRMS spectrum of amide **194** using electrospray ionisation.

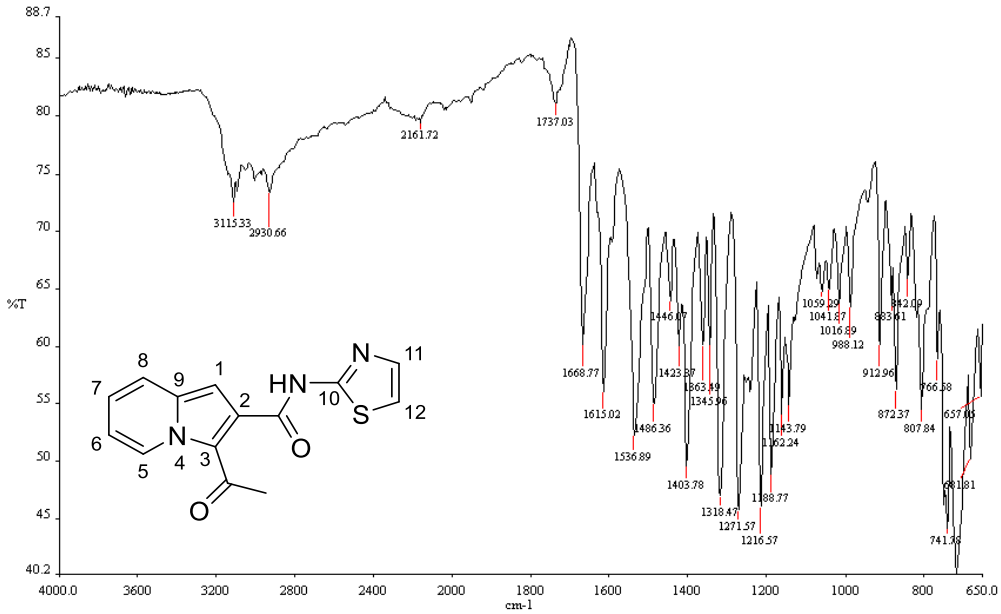

Figure 82. IR spectrum of amide **194**.

The relatively stable, orange, crystalline 3-acetyl-*N*-(2-pyridinyl)indolizine-2-carboxamide **196** was obtained in low yield from the reaction of 2-aminopyridine and acid **139**; purification was achieved using column chromatography. Subsequent characterisation using 1- and 2-D NMR, infrared and mass spectroscopy permitted unambiguous identification of the molecule. Thus, the ^{1}H NMR spectrum (**Figure 83**) exhibits signals for nine protons in the aromatic region with the NH proton resonating at 10.0 ppm, and a signal at 2.54 ppm corresponding to the acetyl methyl protons. Analysis of the correlation spectroscopy data (**Figure 84**) revealed that the signals at 7.07, 7.29, 7.74 and 9.85 ppm correspond to the protons of the pyridine moiety, whilst the signal at 6.90 ppm corresponds to the 1-H proton of the pyrrole component of the indolizine moiety and the four remaining protons of the pyridyl component resonate at 7.14, 7.86, 8.28 and 8.37 ppm. The ^{13}C NMR spectrum (**Figure 85**) exhibits fourteen signals whilst the corresponding DEPT 135 NMR spectrum (**Figure 86**) exhibits nine aromatic signals with the signal at 29.2 ppm corresponding to the acetyl methyl carbon. Juxtaposition of the ^{13}C NMR and DEPT 135 spectra confirmed the presence of three quaternary carbon signals, indicating that two quaternary carbons are overlapping, with signals at 166.2 and 187.8 ppm corresponding to the amide and acetyl carbonyl carbons, respectively. The NH and carbonyl functional groups were also evident in the IR spectrum with the NH absorbing at 3241 cm^{-1} and the bands at 1682 and 1601 cm^{-1} representing the acetyl and carbonyl groups, respectively. The high-resolution ESI mass spectrum (**Figure 87**) of 3-acetyl-*N*-(2-pyridinyl)indolizine-2-carboxamide **196** reveals a base peak at *m*/*z* 280.0773 corresponding to the pseudo-molecular

ion (MH^+) while the fragment peak at *m*/*z* 186.0345 corresponds to the acylium cation resulting from the amide fragmentation as shown in **Scheme 53** .

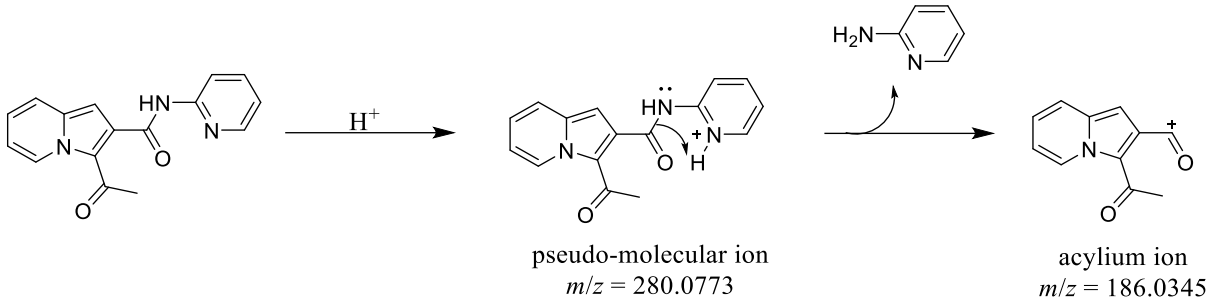

Scheme 53. Representation of possible fragmentation of amide **196**.

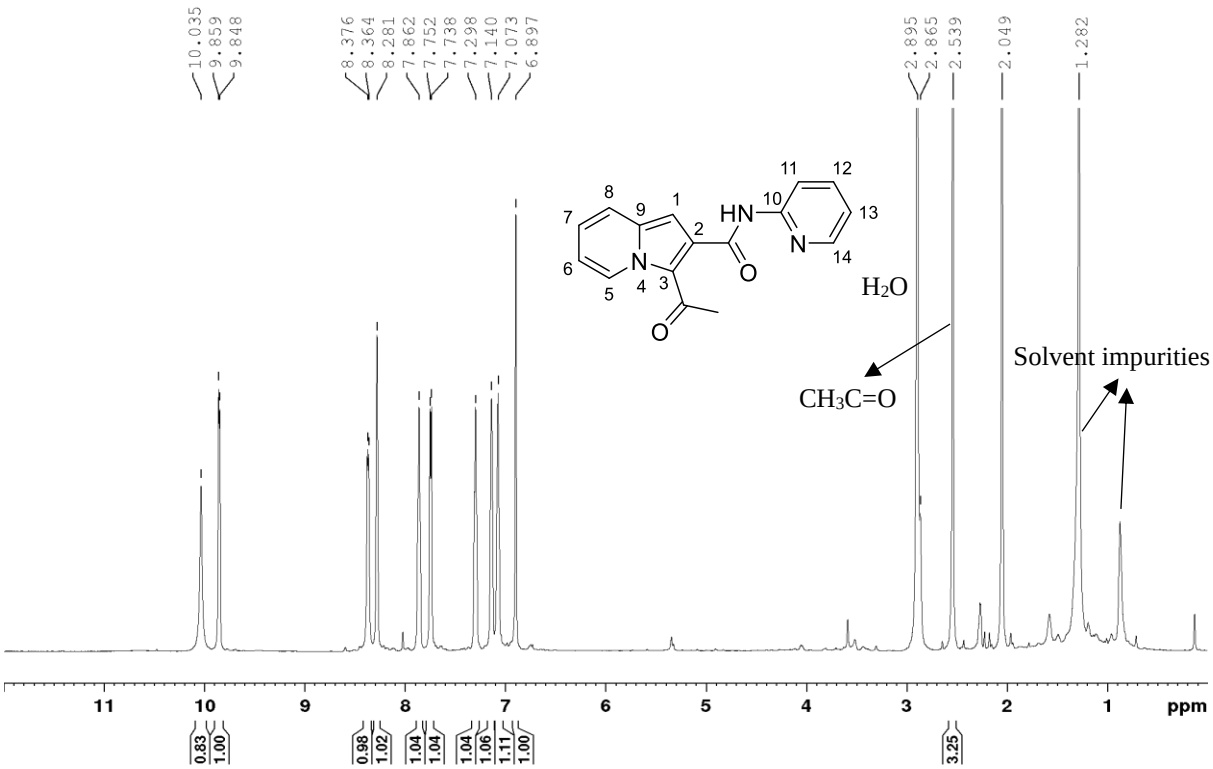

Figure 83. 600 MHz ^{1}H NMR spectrum of 3-acetyl-*N*-(2-pyridinyl)indolizine-2-carboxamide **196** in acetone-d_6.

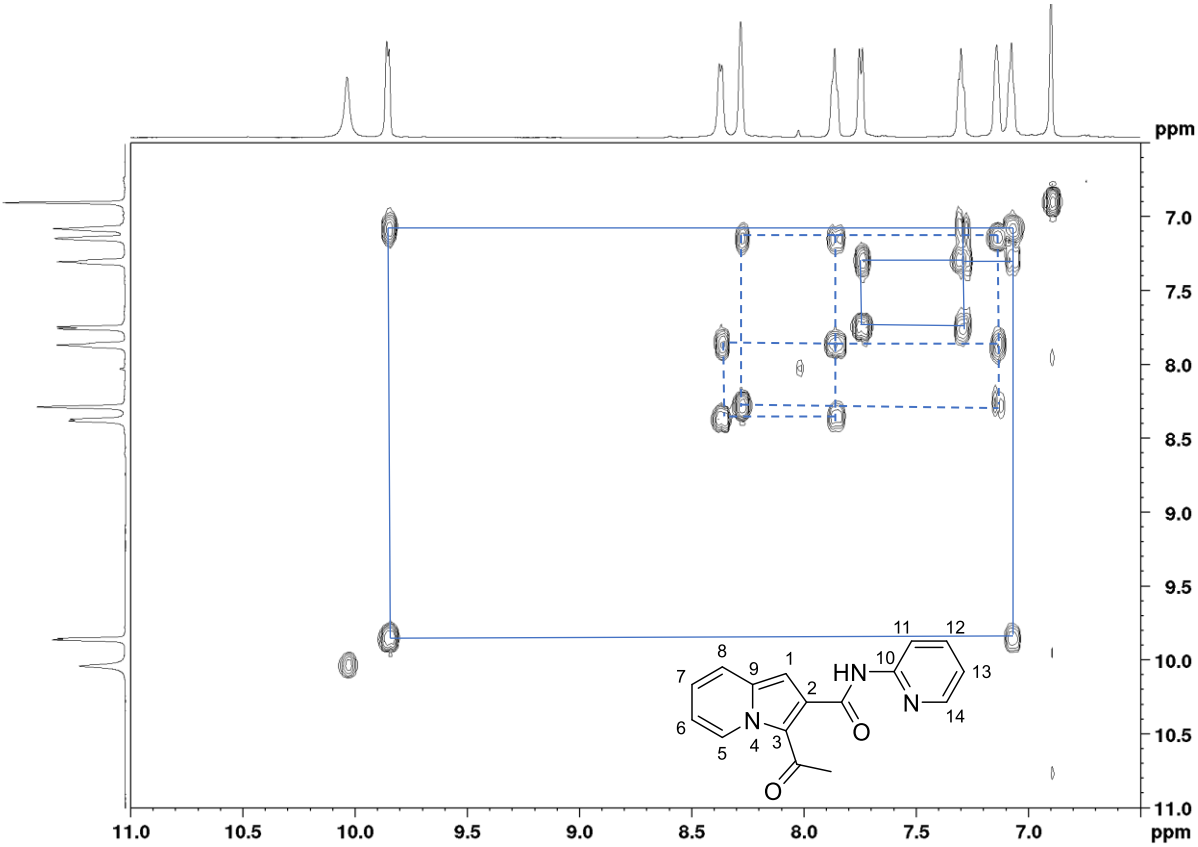

Figure 84. COSY spectrum of 3-acetyl-*N*-(2-pyridinyl)indolizine-2-carboxamide **196** in acetone-d_6. Solid lines indicate pyridine proton correlation, broken lines those for the indolizine system.

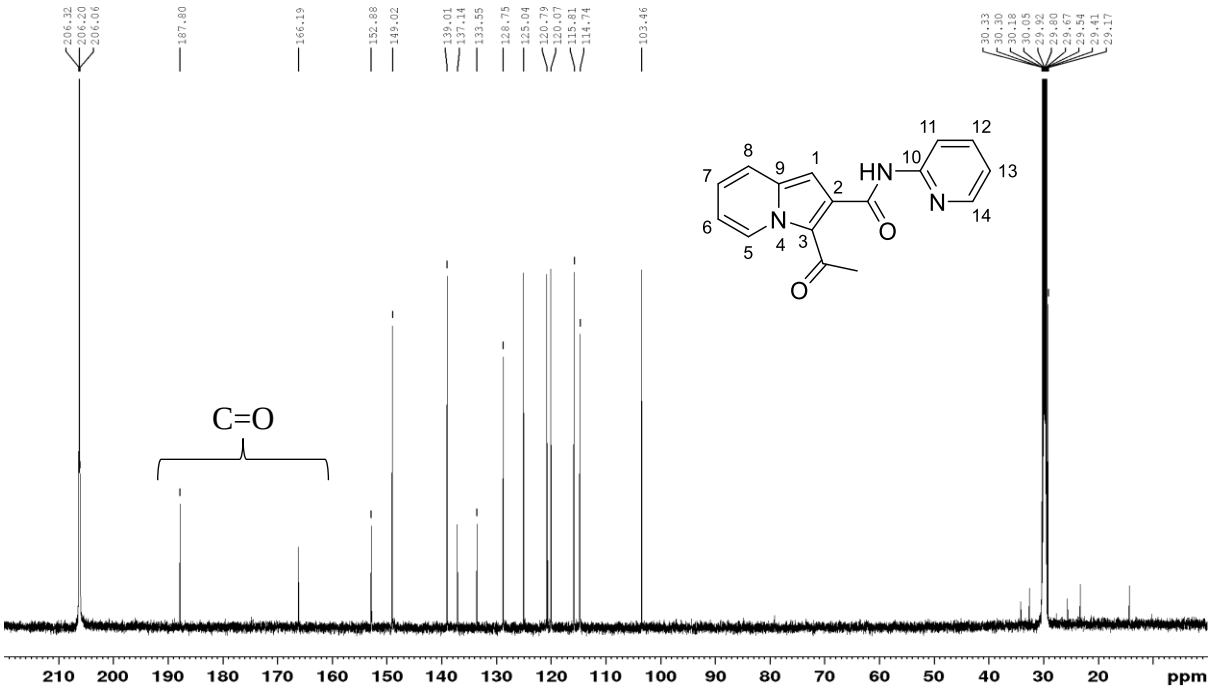

Figure 85. 150 MHz ^{1}H NMR spectrum of 3-acetyl-*N*-(2-pyridinyl)indolizine-2-carboxamide **196** in acetone-d_6.

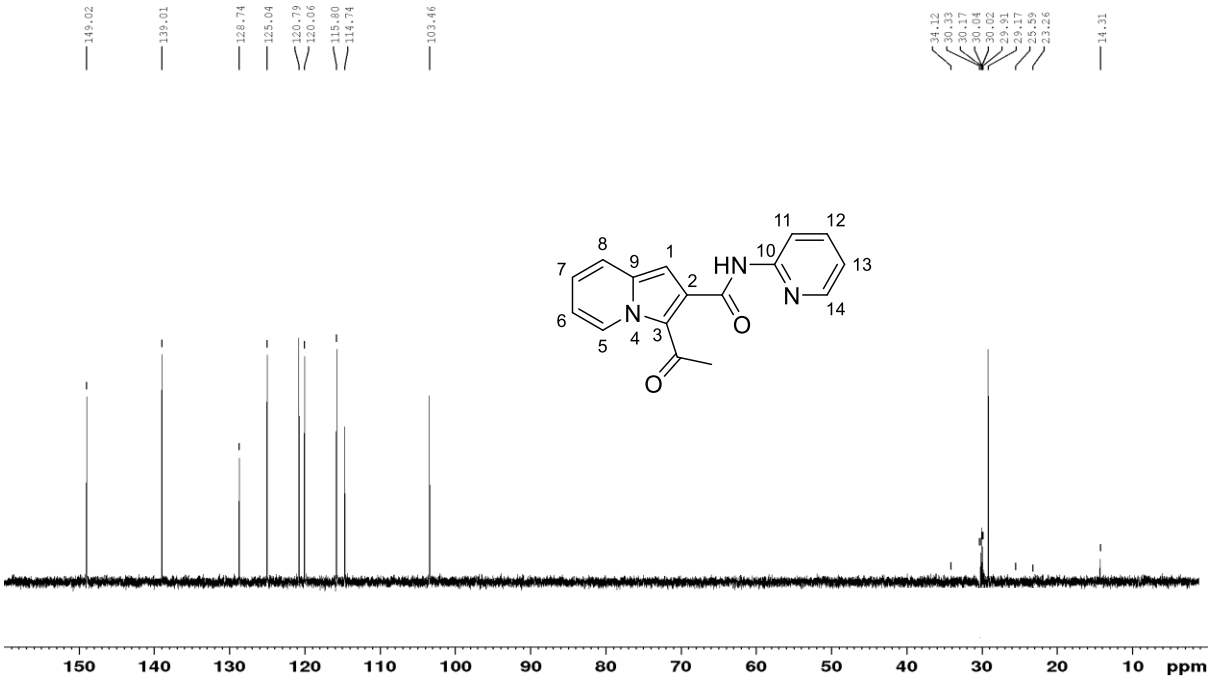

Figure 86. DEPT 135 NMR spectrum of 3-acetyl-*N*-(2-pyridinyl)indolizine-2-carboxamide **196** in acetone-d_6.

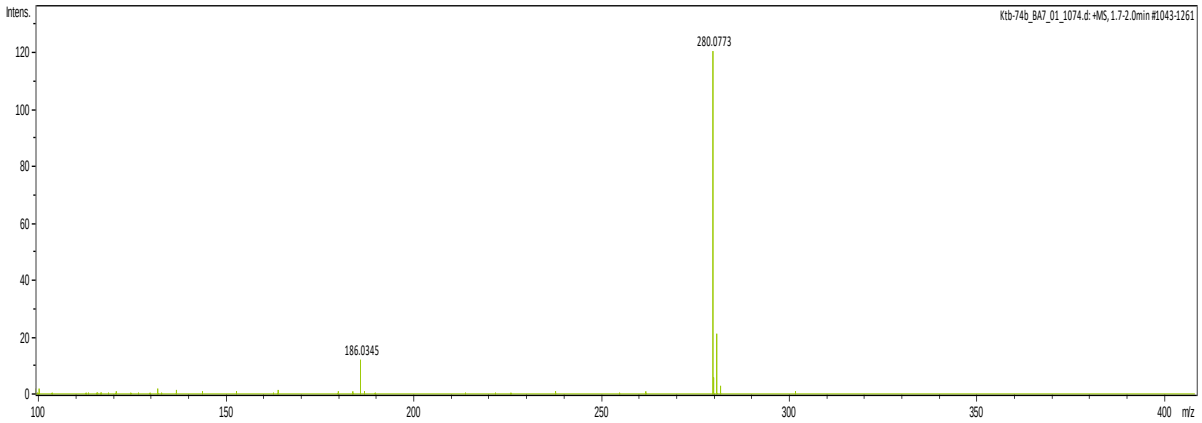

Figure 87. High-resolution ESI mass spectrum of 3-acetyl-*N*-(2-pyridinyl)indolizine-2-carboxamide **196**.

These amides (**192-196**) would be evaluated, mainly, against the essential HIV-1 enzymes and mycobacteria TB, malaria (*Pf*LDH) and Trypanosoma. In addition to the desired physiological synergy, these heteroaromatic amines provide variations in aromaticity, electrostatic, and hydrogen-bonding properties. Despite the apparent aqueous sensitivity of these amides (evidenced by their decomposition during aqueous work-up, inclusive of all amides presented so far), a characteristic that presents challenges to their potential to effect the intended

medicinal activities *in vivo*, their synthesis has affirmed the efficiency of the coupling reagent (T3P) employed under specified thermodynamic reaction conditions for a range of amines. Amides **187** and **192** were obtained as residues and washed with chilled chloroform, whilst the remaining amides were obtained by concentrating the corresponding filtrates *in vacuo* followed by chromatographic purification.

2.2.7.3.Synthesis of isoniazid analogues.

It has been established that isoniazid **168** can be taken for chemoprophylaxis of tuberculosis and that it delays the development of symptomatic HIV and AIDS in symptom-free patients who are seropositive for HIV.[255, 256] The increased frequency and accelerated fatality from MDR-TB among individuals infected with HIV have raised concerns that the development of novel and potent dual-target tuberculosis prophylactic and anti-HIV therapeutic drugs are imperative.[257] The majority of drug resistance cases,[258] specifically in HIV-TB co-infected individuals, has been reported to be against isoniazid – a crucial component in the chemotherapy regimen. We therefore undertook to explore the development of indolizine-based isoniazid analogues as potential dual-target HIV-TB drugs.

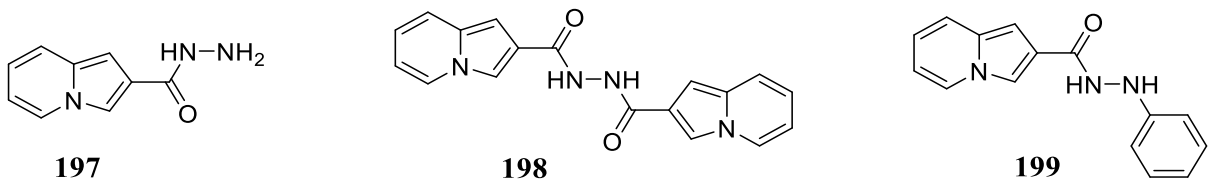

Figure 88. Representation of isoniazid analogues synthesised.

Generation of the isoniazid analogues **197** and **198** involved refluxing the indolizine-2-carboxylic acid **138** and hydrazine monohydrate in the presence of propylphosphonic anhydride (T3P). Indolizine-2-carbohydrazide **197** was obtained as a light brown amorphous solid (7%), which was filtered off and washed with chilled chloroform, while *N,N´*-bis-(indolizine-2-carbonyl)hydrazine **198** was obtained as a yellow gel (4%) from work-up of the filtrate. Indolizine-2-carboxylic acid was then refluxed with phenyl hydrazine in the presence of propylphosphonic anhydride. The resulting homogeneous brick-red reaction mixture was concentrated *in vacuo* and purified by preparatory plate chromatography on silica gel to afford, N^2-phenylindolizine-2-carbohydrazide **199** (17%). The presence of water introduced by the hydrazine monohydrate reagent in the synthesis of analogues **197** and **198** appears to be responsible for the low yields encountered. Initially, it seemed the coupling of indolizine-2-

carboxylic acid with hydrazine (in the form of hydrazine monohydrate) and with phenylhydrazine could be achieved under the ambient conditions used for the reaction with the heteroaryl alkmylamines. Instead, due to poor solubility, rather drastic conditions were required for progression of the reaction. Consequently, in the synthesis of indolizine-2-carbohydrazide **197** and *N,N´*-bis-(indolizine-2-carbonyl)hydrazine **198**, and N^2-phenylindolizine-2-carbohydrazide **199** the reaction mixtures were heated to 80 °C to effect solubility. The reaction mixtures were then stirred for two days at 80 °C after which filtration and appropriate work-up afforded the desired products.

All of these analogues were unambiguously characterised using NMR, HRMS and infrared spectroscopy. The IR spectrum for analogue **197** revealed the presence of an NH absorption band at 3325 cm^{-1}, an NH_2 band at 3127 cm^{-1} and an amide C=O band at 1666 cm^{-1}, whilst the corresponding disubstituted hydrazine analogue **198** showed prominent coupled NH bands at 3339 and 3223 cm^{-1} and coupled amide C=O bands at 1643 and 1582 cm^{-1} due to vibrational couplings. The IR amide C=O band for analogue **199** was observed at 1643 cm^{-1}.

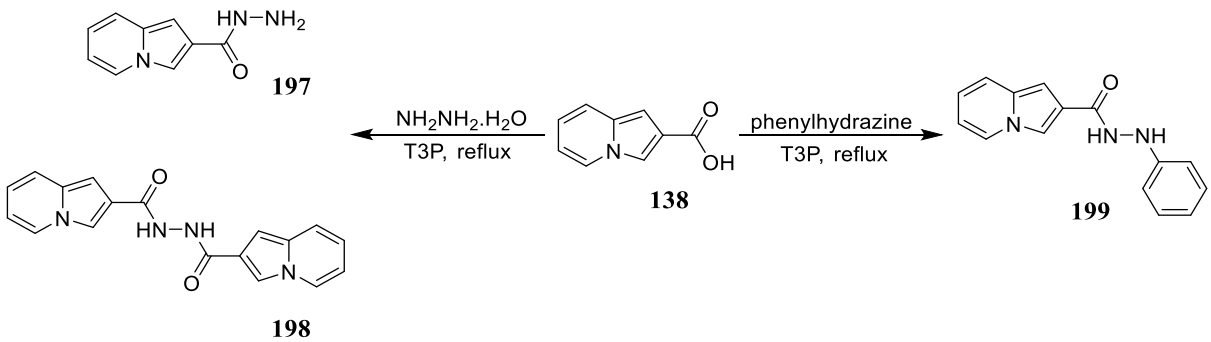

Scheme 54. T3P-mediated synthesis of isoniazid analogues.

The ^{1}H NMR spectrum of compound **197** depicted in **Figure 89** reveals, as expected, the presence of six signals corresponding to the aromatic indolizine protons, a singlet at 9.50 ppm corresponding to the "amido" NH and a broad signal at 4.48 ppm corresponding to the NH_2 protons, thus confirming the successful synthesis of compound **197**. The ^{1}H NMR spectrum of the symmetrically disubstituted analogue **198** (**Figure 90**) also exhibits six aromatic protons that include a triplet of doublets at 6.54 ppm and a multiplet at 6.69 ppm corresponding to the 7- and 6-H protons respectively, doublets at 7.34 and 7.82 ppm corresponding to the 4- and 1-H protons, and a doublet at 8.06 ppm corresponding to 8-H. The singlet at 6.72 ppm corresponds to 3-H proton whilst those at 7.05 and 7.92 ppm correspond to the hydrazine protons. The presence of six aromatic protons is consistent with the symmetric structure of the

N,N´-disubstituted hydrazine derivative **198**. The presence of two singlets at 7.05 and 7.92 ppm are attributed to the hydrazine NH and the tautomeric imidic acid (see **Scheme 55**). The amide-imidic acid tautomerism of compound **198** results from intramolecular proton transfer of one of the hydrazine hydogens between the adjacent carbonyl oxygen and nitrogen. The exchange rate for amide-imidic acid tautomerism[259] is apparently rapid at the probe temperature such that resonance frequencies of the indolizine protons is averaged out resulting in the corresponding ^{1}H NMR spectrum exhibiting six aromatic proton signals representing indolizine protons in both the amide (**I**) and imidic acid (**II**) form. On careful spectroscopic examination, such tautomerism can be observed and interpreted to provide useful details.[260] The almost 1:1 ratio in the integration of the amide-imidic acid proton pair denotes that the **I**:**II** tautomeric populations are almost equal.

Amide (**I**) Imidic acid (**II**)

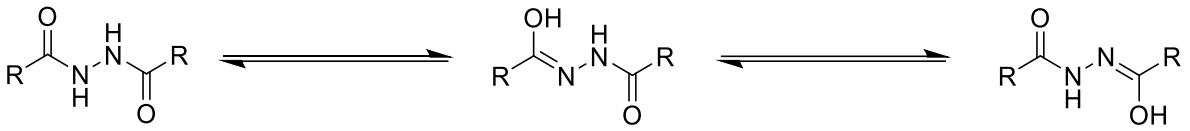

R = 2-indolizinyl

Scheme 55. Representation of amide-imidic acid tautomerism.

The ^{1}H NMR spectrum of N^{2}-phenylindolizine-2-carbohydrazide **199** (**Figure 91**) confirms the presence of twelve protons in the region between 6.7 and 10.1 ppm corresponding to the eleven aromatic proton and one of the hydrazide protons; the hydrazide proton resonate at 10.1 ppm. Analysis of the corresponding ^{13}C NMR spectrum (**Figure 92**) in conjunction with the DEPT 135 NMR spectrum (**Figure 93**) showed the presence of nine different proton-bearing carbons, three quaternary carbons, marked with an asterisk, and a carbonyl carbon confirming the successful synthesis of the analogue **199**. The COSY spectrum (**Figure 94**) was employed to identify the signals corresponding to the protons of the hydrazide group at 7.85 and 10.1 ppm, which clearly correlate with each other but with no other protons.

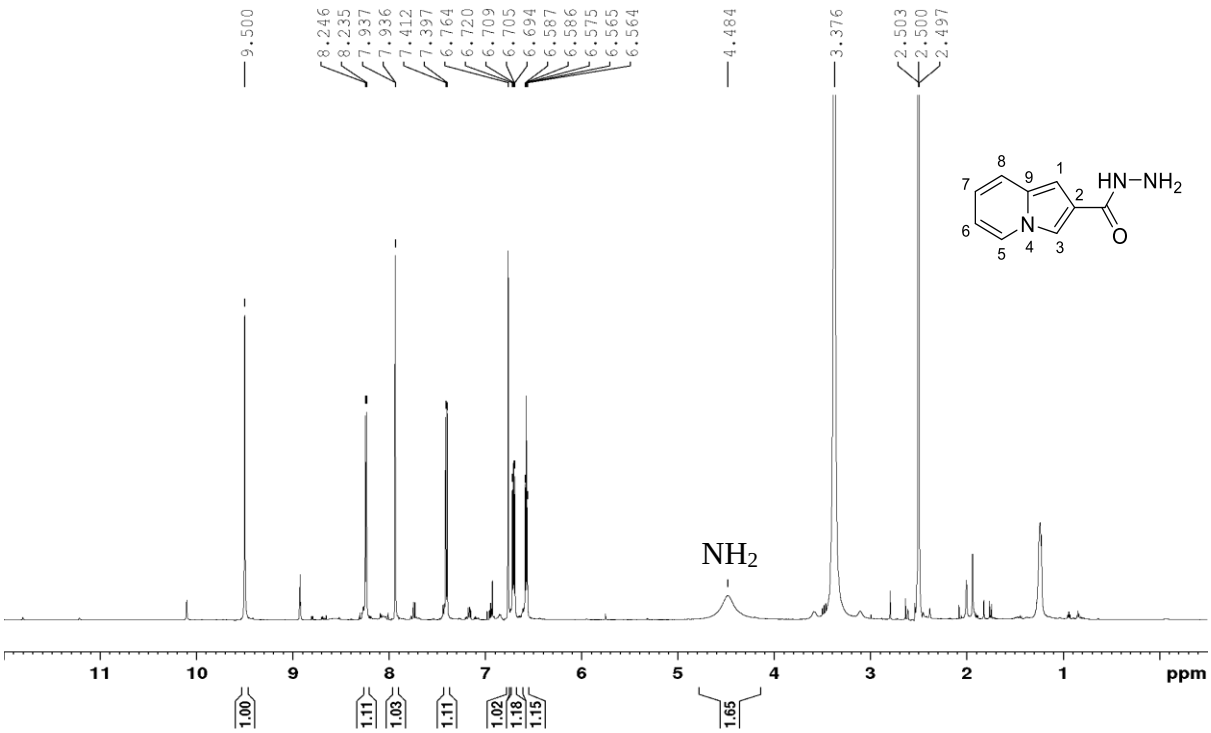

Figure 89. 600 MHz ^{1}H NMR spectrum of indolizine-2-carbohydrazide **197** in DMSO-d_6.

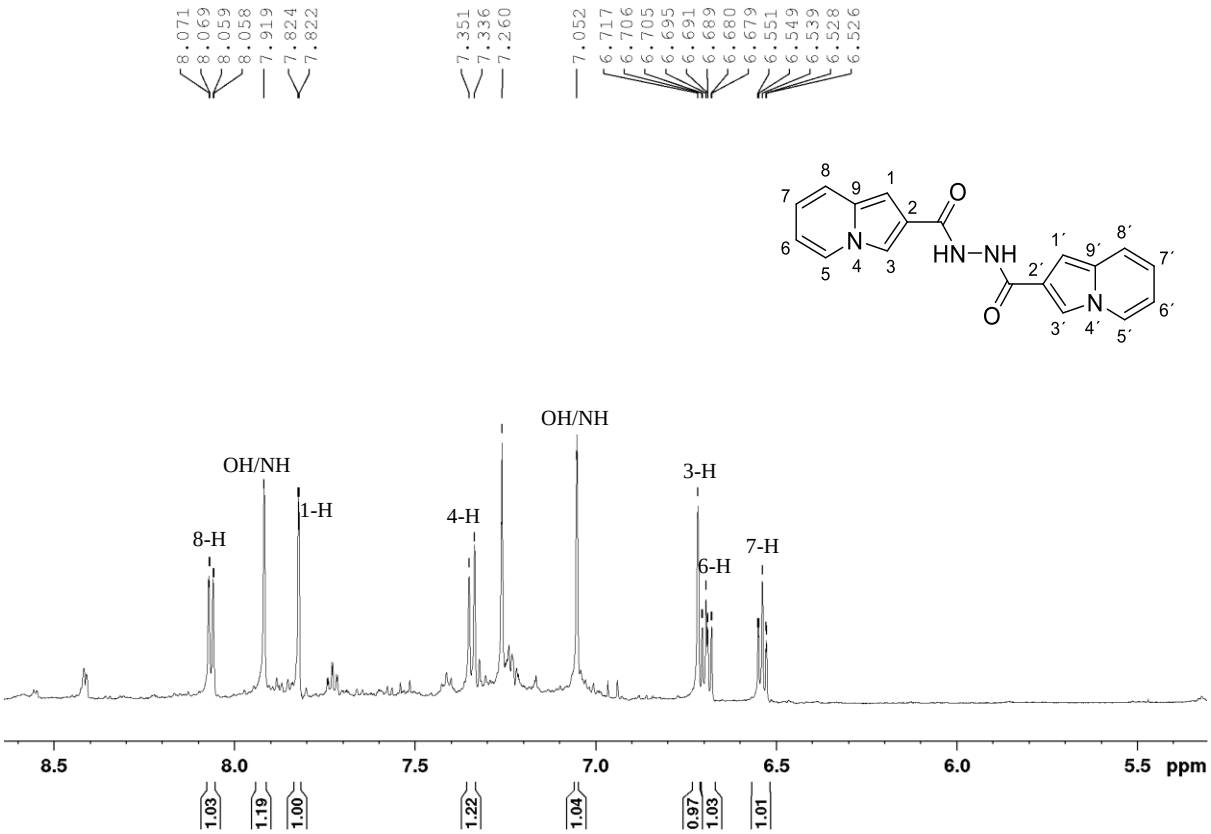

Figure 90. 600 MHz ^{1}H NMR spectrum of compound **198** in $CDCl_3$.

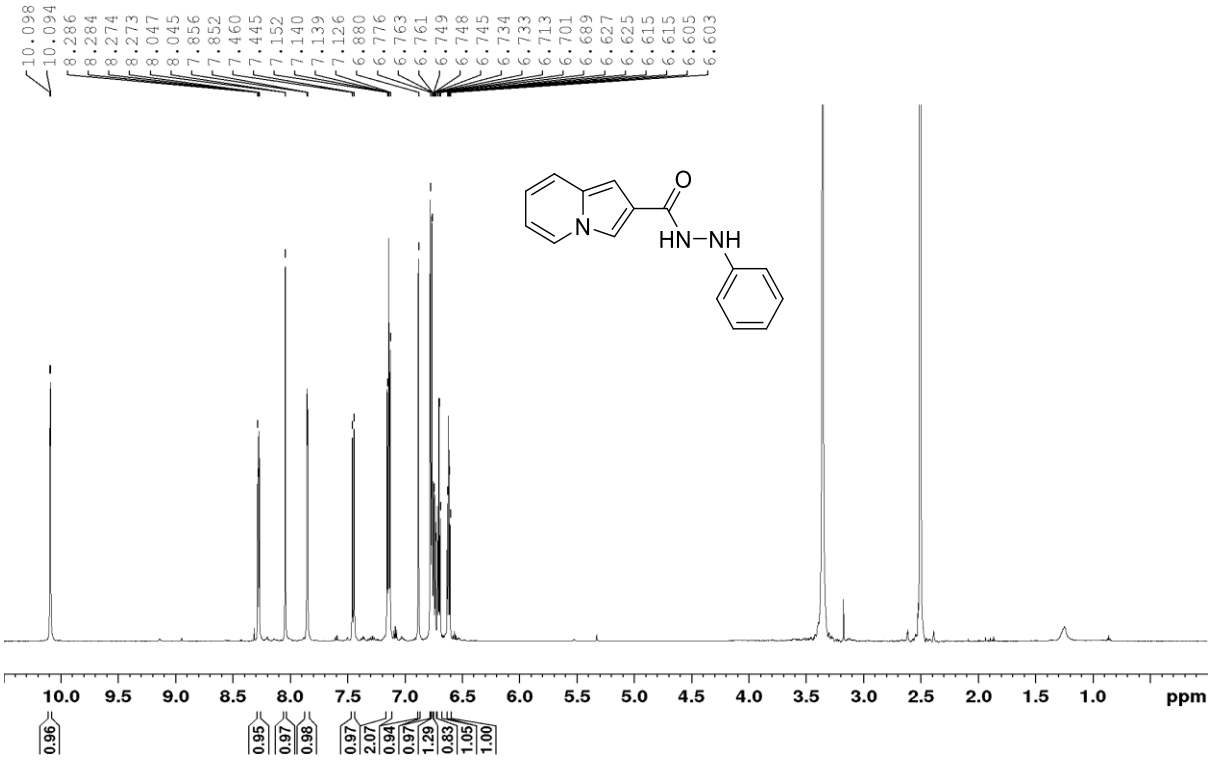

Figure 91. 600 MHz ^{1}H NMR spectrum of compound **199** in DMSO-d_6.

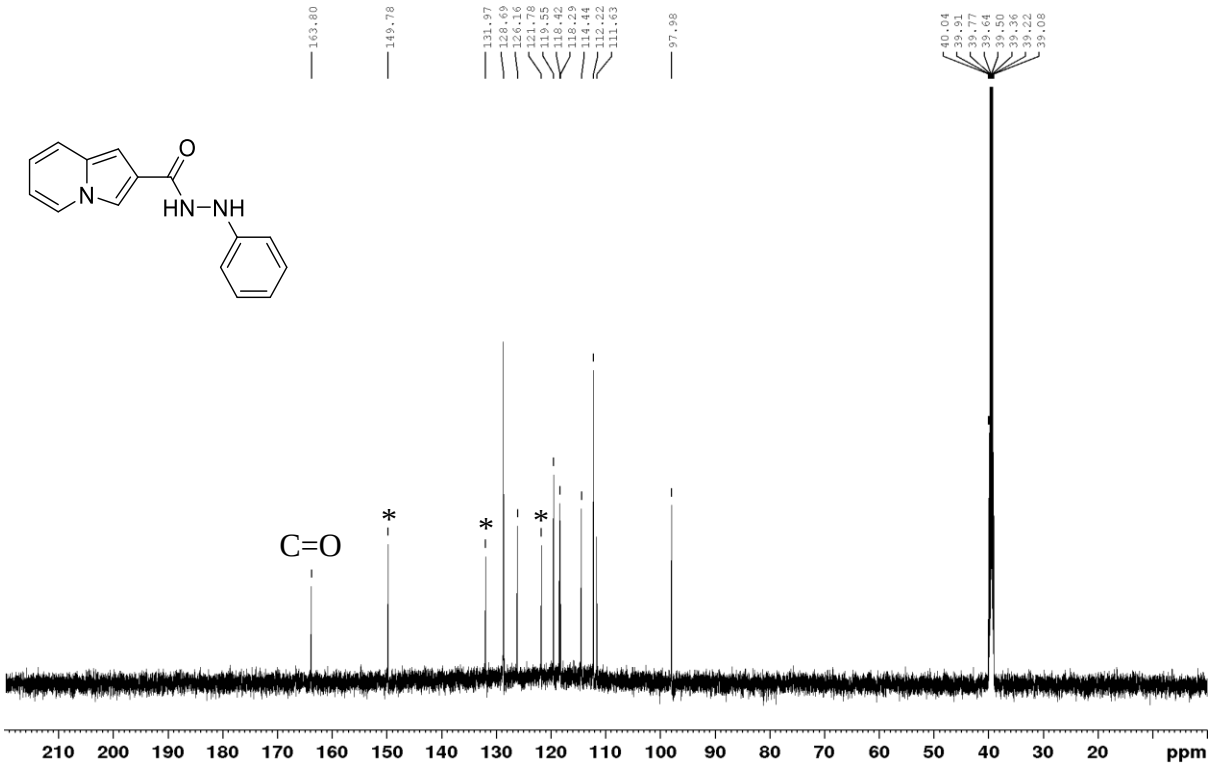

Figure 92. 150 MHz ^{1}H NMR spectrum of compound **199** in DMSO-d_6. * indicates quaternary carbons.

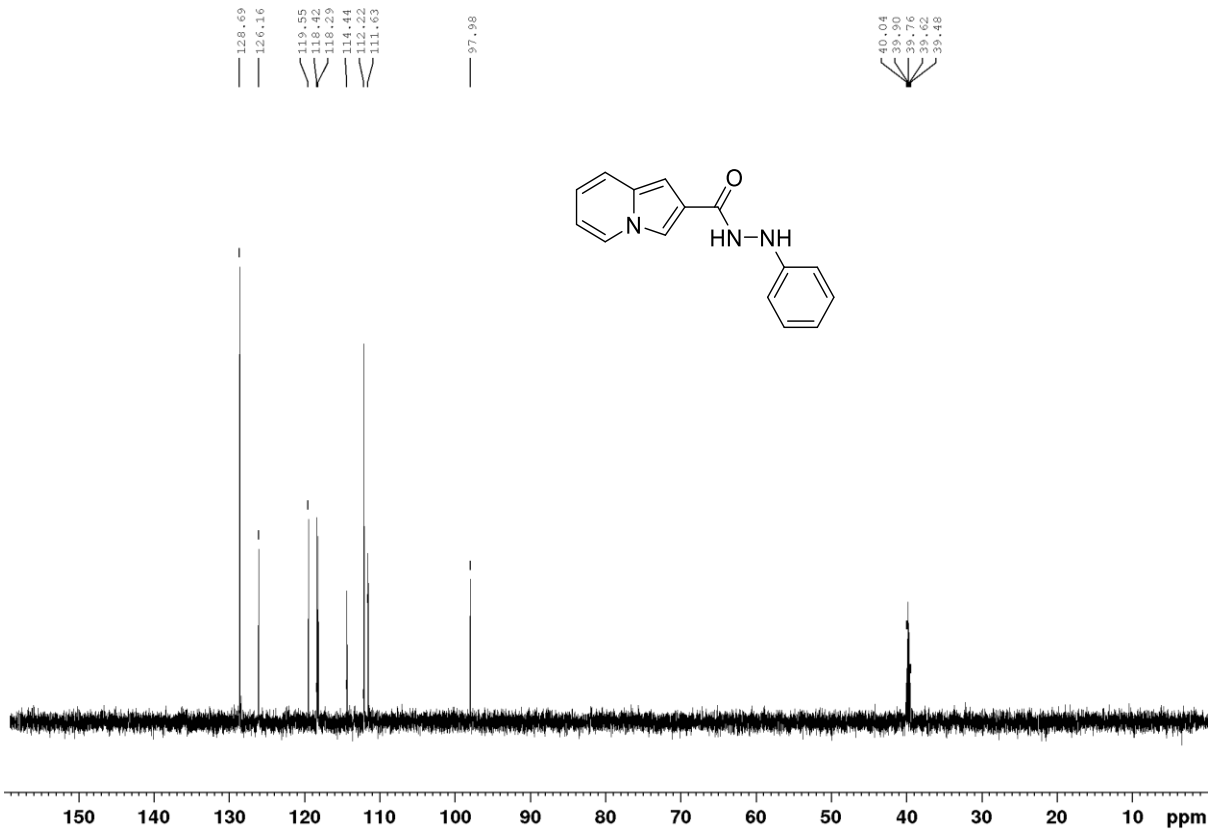

Figure 93. DEPT 135 NMR spectrum of compound **199** in DMSO-d_6.

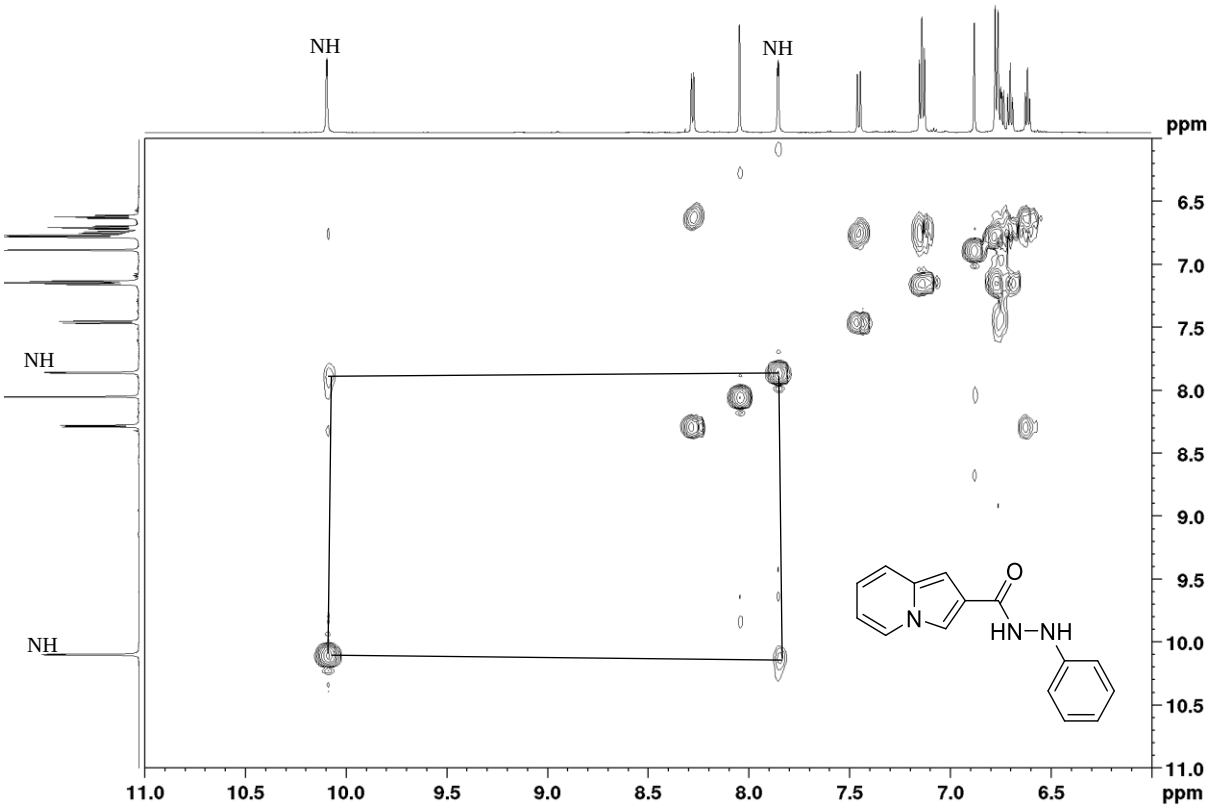

Figure 94. COSY spectrum of compound **199** in DMSO-d_6.

2.2.7.4. Coupling of indolizine-2-carboxylic acid **134** *with heteroaryl alkylamines*

We sought to extend the scope of the study to include lipophilic amides in which the intrinsic lipophilicity was to be jointly imparted by linked moieties and the aliphatic linker bonded to the indolizine-2-carboxamide. Over the past few years, a new approach has been adopted in the design and development of new anti-TB drugs with activity against the MDR and XDR-TB strains as well as the emerging, totally drug-resistant tuberculosis (TDR-TB) strain.[261-263] Lipophilicity has been identified as the essential physicochemical property for anti-tuberculosis drug candidates.[264] In addition to its impact on the pharmacokinetics and toxicity, the effect of lipophilicity on solubility, permeability and bioavailability of compounds is well understood and can therefore be adjusted to achieve the desired properties.[265] Betaquiline **200**, a highly lipophilic molecule with cLogP of 7.3 is being used in emergency MDR-TB therapy. However, low lipophilicity does not preclude therapeutic activity since a number of molecules with low lipophilicity have been used as prominent anti-TB drugs, these include ethambutol **167**, isoniazid **168**, cycloserine **170** and pyrazinamide **171**.[264]

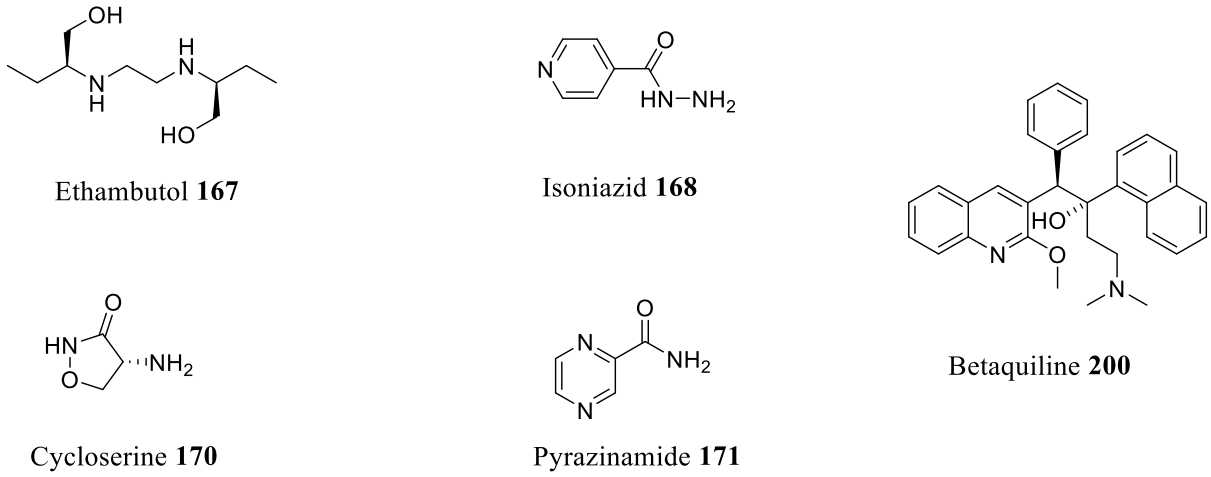

Figure 95. Representative anti-TB drugs

Crucial to containing and defeating the tuberculosis epidemic, especially in countries with a concomitant HIV epidemic, is the development of new, affordable, shorter and safe treatment regimens. Such new drugs should exhibit physiochemical properties that enable potency against MDR-TB, and also address the HIV co-infection.[266 267] In addition to HIV and TB, malaria, a disease caused by protozoan parasites of the genus *Plasmodium*, is a leading cause of illness and death in the world.[261] The high incidence of malaria annually is a result of deteriorating health systems, the development of drug and insecticide resistance and climate change.[268, 269] The (overlapping) geographical prevalence of each or a number of these diseases

presents greater possibilities of co-infections, resulting in devastating health effects and increased demands for appropriate medication. Such co-infections usually interact bilaterally and synergistically.[269]

Moreover, human immune response to HIV, TB and malaria infections may each influence the clinical course of the others, and co-infections are usually associated with compromised immune systems. These are challenges which have begun to be addressed by developing compounds that are innovative, contain multiple functionalities and target multiple infections (HIV, TB or malaria). The current therapy used to address co-infections is drug combination therapy that involves co-formulation of at least two agents into a single tablet termed – a "multicomponent drug" – as opposed to the traditional cocktail therapy. Advantages of considering multifunctional hybrid compounds over multicomponent drugs include expense and lower risk of drug-drug interactions.[270] We envisage the development of multitarget therapies using single agents with the advantages of synergistic multi-target inhibitory activity, simplified dosing, tolerable toxicity and improved patient compliance.

The diverse medicinal potential of the indolizine moiety is already well explored and can be exploited in the development of novel compounds that effectively control, inhibit or manage co-infections, including trypanosomiasis. Trypanosomiasis, also called sleeping sickness, is a disease caused by the extracellular eukaryotic flagellate parasite, *Trypanosoma brucei*. At present, there is limited treatment for this disease, which can be fatal if untreated, and drugs for the late-stage treatment are highly toxic.[271] Although the disease has been known for centuries, the attention paid to the development of trypanosomiasis chemotherapy has lagged behind compared to other tropical diseases.[272] Three of the four drugs approved for its treatment were developed over 50 years ago and are not considered to be ideal.[273]

Herein, we report the synthesis of a series of *N*-(heteroarylalkyl)indolizine-2-carboxamides from the coupling of a range of heteroarylalkylamines with either indolizine-2-carbobylic acid **138** or 3-acetylindolizine-2-carboxylic acid **139** (**Scheme 56**). Unlike the classes of carboxamides discussed earlier, as expected, these compounds are not sensitive to moisture and, thus, their synthesis permitted conventional work-up, such as solvent extraction. To a regulated (0 °C to -10 °C), cooled mixture of the acid (**138** or **139**) and the heteroarylalkylamine in a mixture of DIPEA:CH_2Cl_2 (2:1) was added propylphosphonic anhydride (T3P). Stirring was continued allowing the mixture to warm to room temperature, and the reaction progress

was monitored by TLC. The reaction reached completion after varying periods of at least 6 hours, depending on the heteroarylalkylamine reactant. After completion, the reaction was diluted with H_2O and the pH adjusted to 2-3 using concentrated HCl and then extracted with $CHCl_3$. The organic layer was sequentially washed with aqueous 1M-$NaHCO_3$, dried over $MgSO_4$ and concentrated *in vacuo*. Purification of the resulting crude mixtures afforded the desired amides in yields ranging from 25 to 37%.

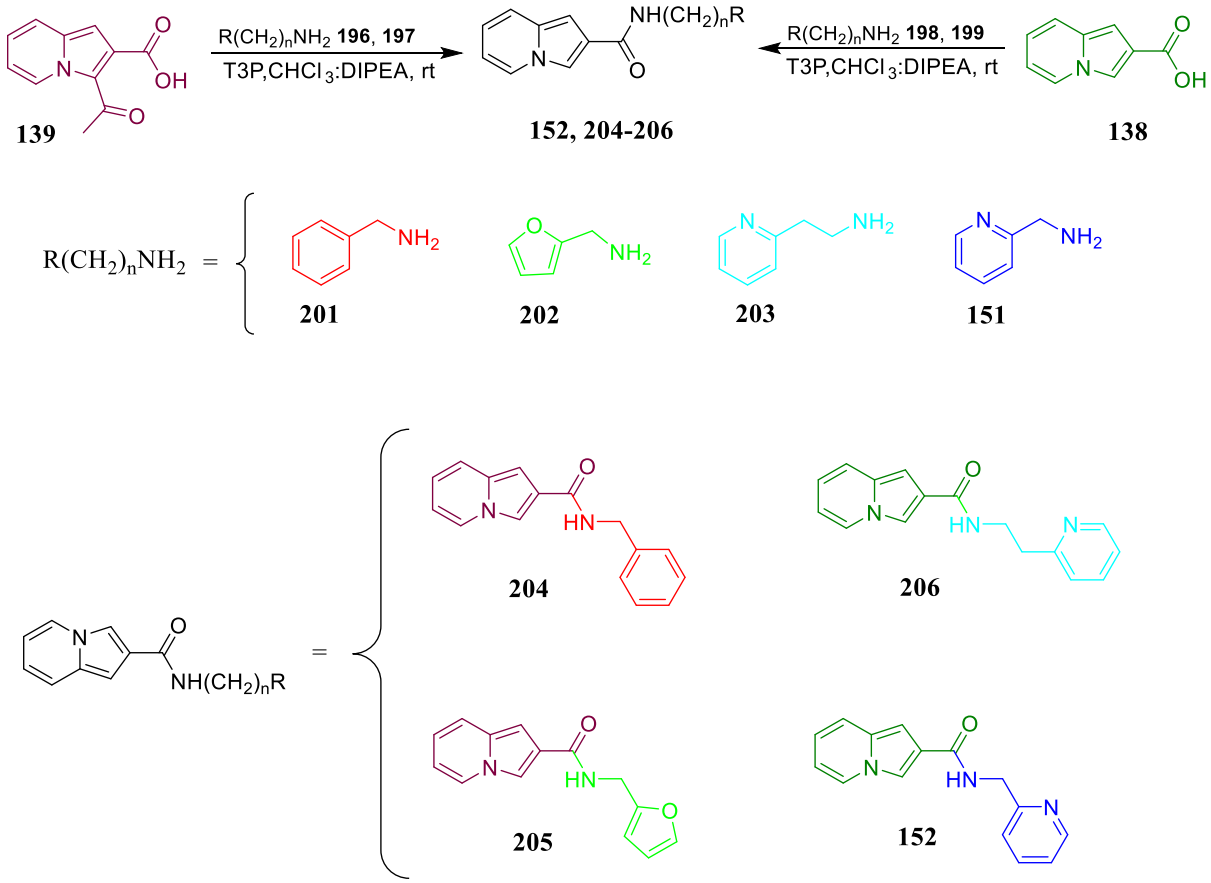

Scheme 56 Schematic representation of the synthesis of *N*-(heteroarylalkyl)indolizine-2-carboxamides, with structures coloured to reflect the originating synthons (n is an integer).

The simultaneous de-acetylation of the 3-acetylated acid **139** during the reaction is attributed to the high nucleophilicity indices[274] of the heteroarylalkylamines used. As illustrated below, amidation involving these nucleophilic heteroarylalkylamines and acid **139** resulted in the same carboxamides expected to be obtained when the parent acid **138** was used. For instance, the reaction of benzylamine **201** and the 3-acetylated acid **139** afforded the de-acetylated product *N*-benzylindolizine-2-carboxamide **204**. Similarly, the reaction involving the use of furfurylamine **202** with the acid **139** yielded the deacetylated product, *N*-furfurylindolizine-2-carboxamide **205**. The indolizine acid **138** was coupled with 2-(2-aminoethyl)pyridine **203** and, with 2-(aminomethyl)pyridine **151** to afford *N*-[2-(2-(pyridinyl)ethyl)]indolizine-2-

carboxamide **206** and *N*-(2-picolyl)indolizine-2-carboxamide **152**, respectively. These reactions again reflect the effectiveness of T3P-catalysed reactions compared to boron-catalysed reaction (**Section 2.2.4.1**).

Table 7 summarises yields of the *N*-(heteroarylalkyl)indolizine-2-carboxamides **152, 204-206** from their respective acid substrates. The first reaction involved the 3-acetylated acid **139** and benzylamine **201**. The reaction progress was monitored by TLC; after 6 hours the formation of some product, anticipated to be the 3-acetylated indolizine-2-carboxamide, was evident. The reaction was allowed to run for further 12 hours and the isolated product was extensively characterised by NMR, IR and mass spectroscopy which revealed that the product was, in fact, the deacetylated amide, *N*-benzylindolizine-2-carboxamide **204**. The subsequent amidation reactions involving selected amines (entries 2-4) were each run for a period of 24 hours.

Table 7. Yields of the *N*-(heteroarylalkyl)indolizine-2-carboxamides **152, 204-206**.

Entry	**Acid substrate**	**$R(CH_2)_nNH_2$**	**Product**	**Yield (%)**
1	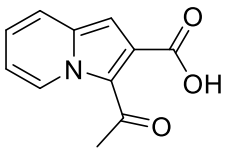	benzylamine **201**	**204**	37
2		furfurylamine **202**	**205**	36
3	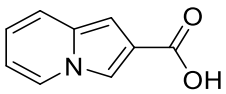	2-(2-aminoethyl)pyridine **203**	**206**	25
4		2-(aminomethyl)pyridine **151**	**152**	36

Figure 96 illustrates the ^{1}H NMR spectrum of *N*-furfurylindolizine-2-carboxamide **205** – a hybrid of indolizine and furan functionalities connected by an amide linker. The doublet at 4.01 ppm (clearly evident in the zoomed spectrum in **Figure 97**) corresponds to the methylene protons which couple with the NH proton, as shown in the corresponding COSY spectrum (**Figure 98**), and is indicative of successful amide synthesis. Further analysis of the COSY spectrum reveals that furan protons 12-H resonates at 5.81 ppm as a doublet (J = 1.8 Hz), 13-H at 5.93 ppm as a doublet (J = 3.0 Hz) and the 14-H proton at 7.10 ppm appears as a broad singlet. Signals corresponding to the protons of the indolizine moiety are clearly indicated in the COSY spectrum. As expected, the ^{13}C NMR spectrum (**Figure 99**) exhibits the expected fourteen carbon signals, whilst the accompanying DEPT 135 spectrum (**Figure 100**) exhibits ten signals – corresponding to nine aromatic proton-bearing carbons between 95 and 145 ppm and a methylene carbon (CH_2N) at 35.6 ppm. The HSQC spectrum (**Figure 101**) reveals that

the carbon signals at 106.8, 110.5 and 142.0 correlate to the C-12, C-13 and C-14, respectively. All of the four amides synthesised in this series were isolated as green crystals. The high-resolution mass spectrum of compound **204** revealed the presence of the pseudo-molecular ion peak at *m/z* 251.0914, whilst that of compound **205** revealed the pseudo-molecular ion at *m*/*z* 241.0737. For compounds **206** and **152**, the corresponding pseudo-molecular ion peaks were observed at *m*/*z* 253.0688 and *m*/*z* 240.0899, respectively.

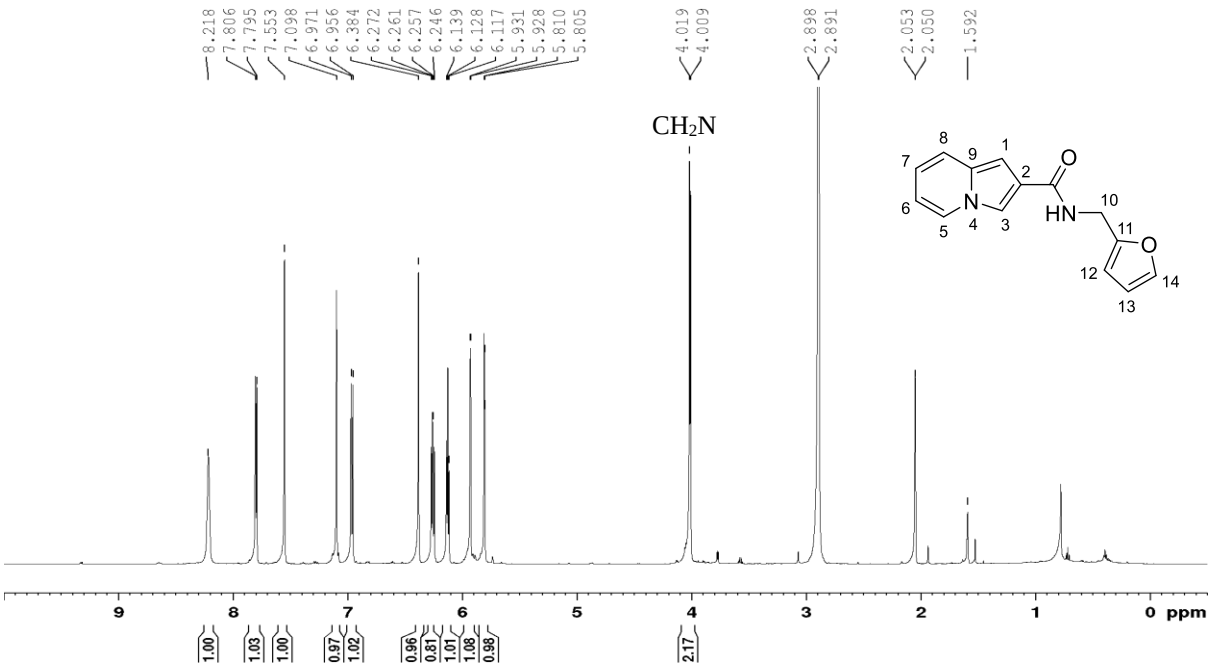

Figure 96. 600 MHz ^{1}H NMR spectrum of compound **205** in acetone-d_6.

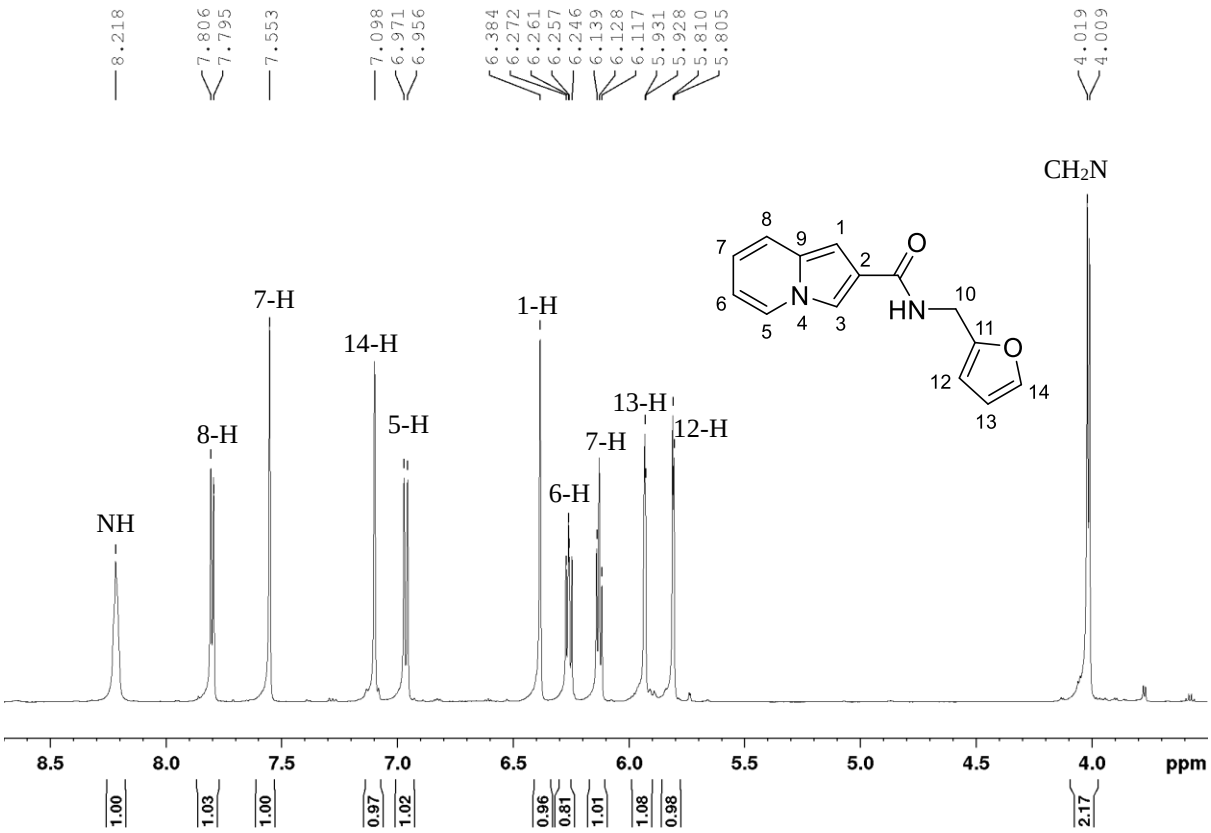

Figure 97. Zoomed, partial 600 MHz ^{1}H NMR spectrum of compound **205** in acetone-d_6.

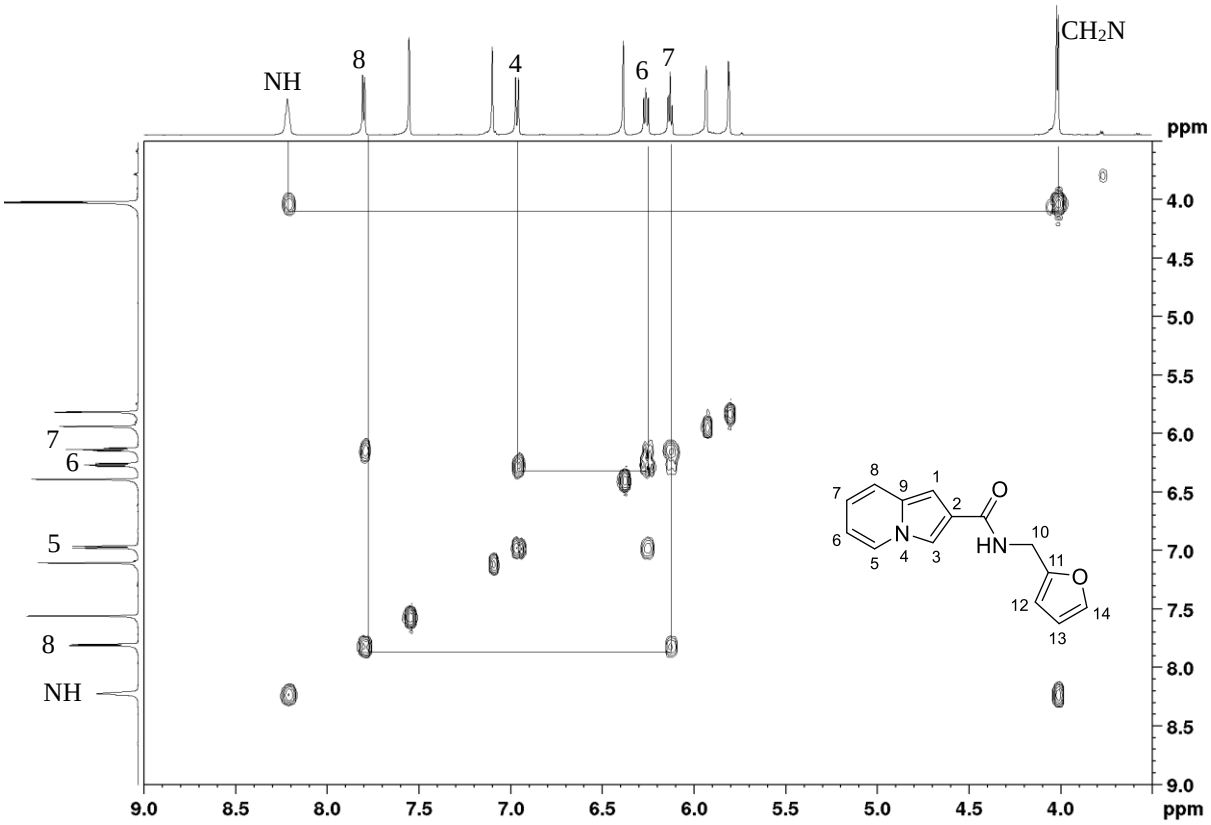

Figure 98. COSY spectrum of compound **205** in acetone-d_6.

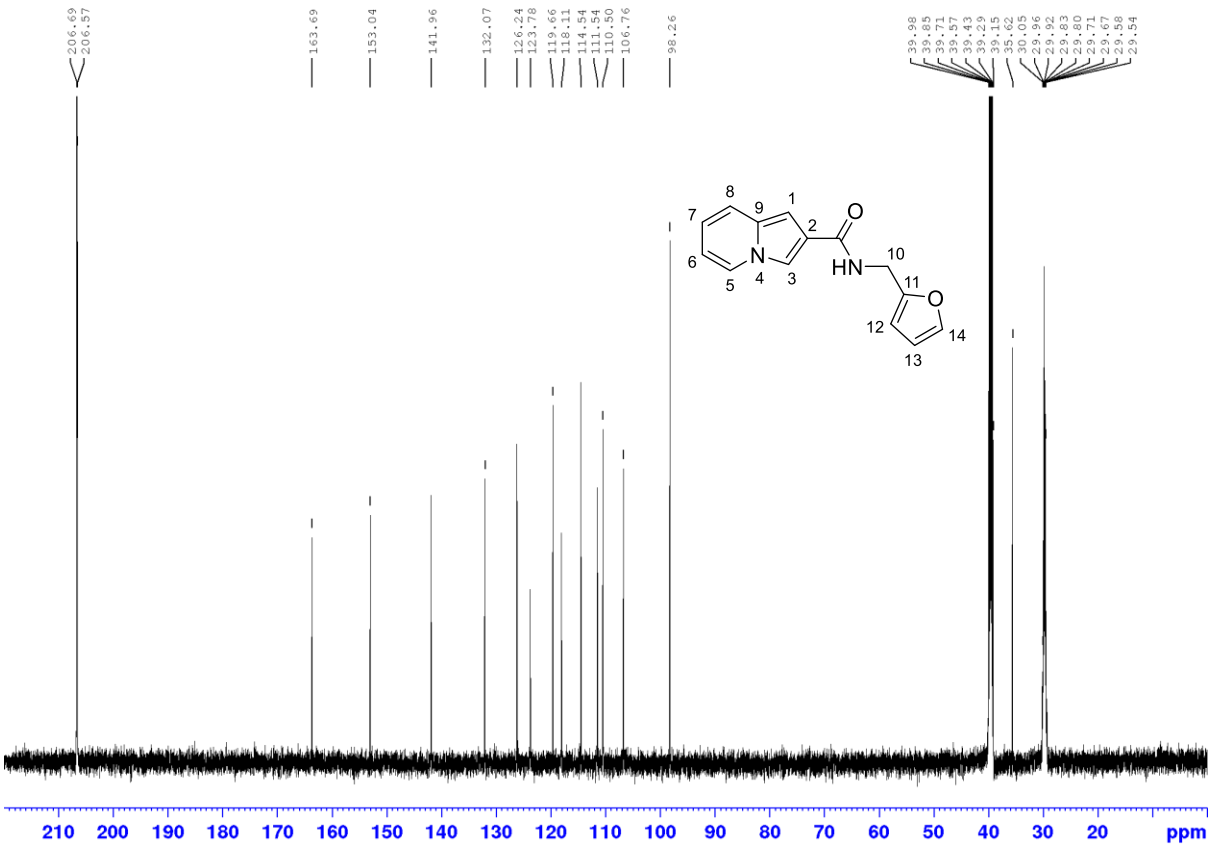

Figure 99. 150 MHz ^{13}C NMR spectrum of compound **205** in acetone-d_6.

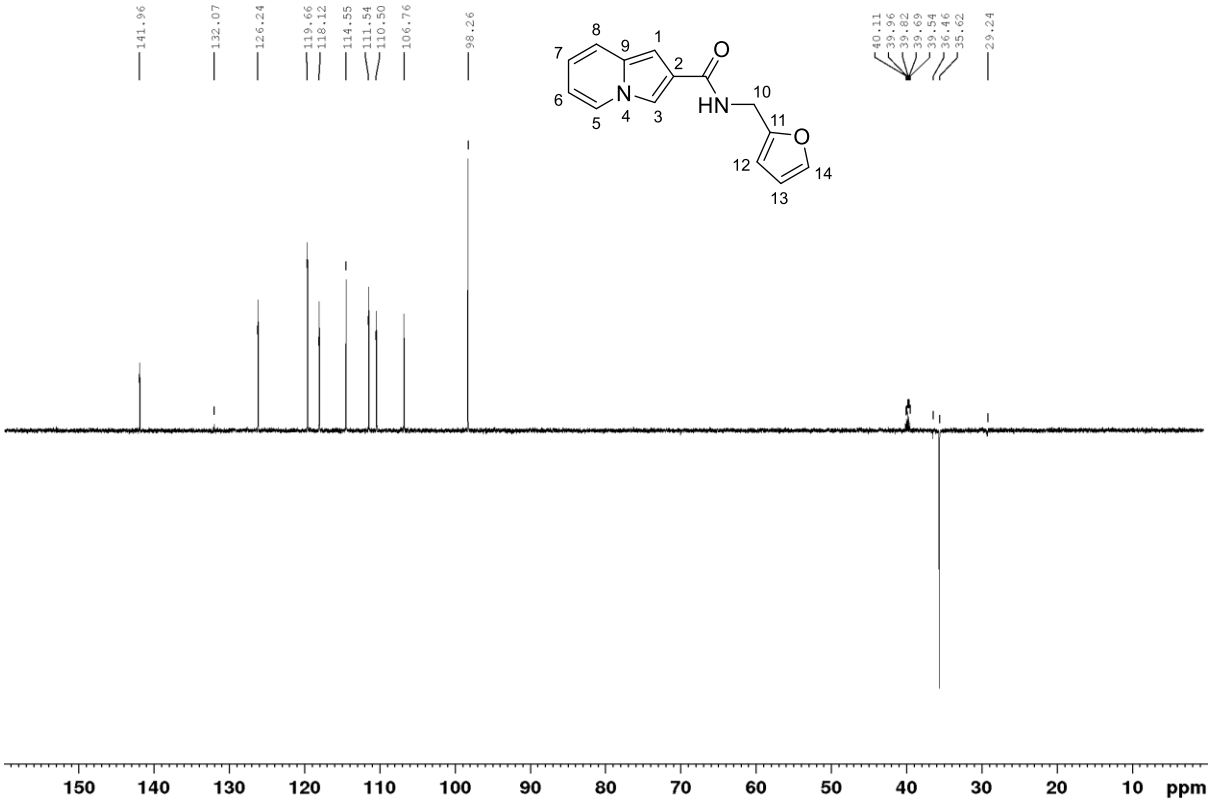

Figure 100. DEPT-135 NMR spectrum of compound **205** in acetone-d_6.

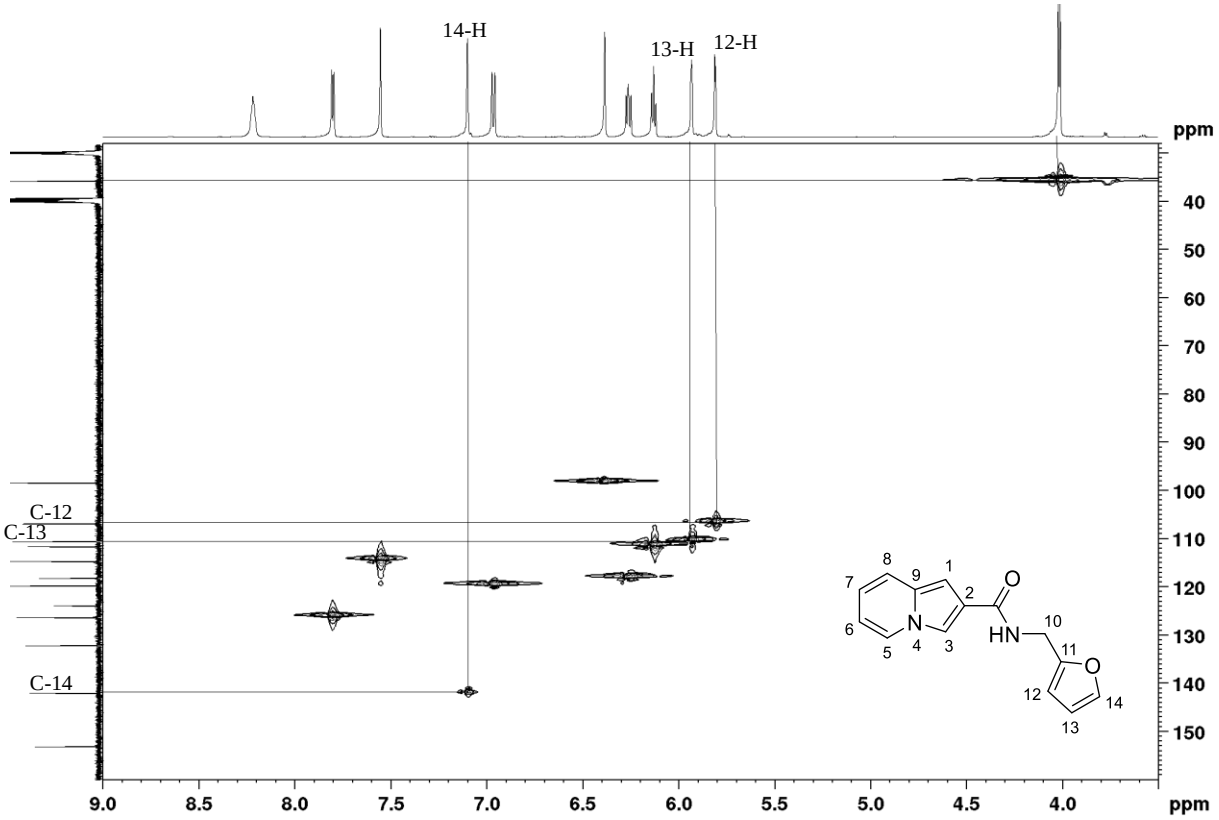

Figure 101. HSQC spectrum of compound **205** in acetone-d_6.

In addition to the amides listed in **Table 7** above, amidation of indolizine-2-carboxylic acid **138** with 1-(3-aminopropyl)imidazole **207** afforded *N*-[3-(1*H*-imidazol-1-yl)propyl)]indolizine-2-carboxamide **208**. However, the compound presented challenges of instability. After several attempts, an aqueous-free work-up afforded, as a light yellow gel, the desired *N*-[3-(1*H*-imidazol-1-yl)propyl)]indolizine-2-carboxamide **208** in miniscule yield (3%).

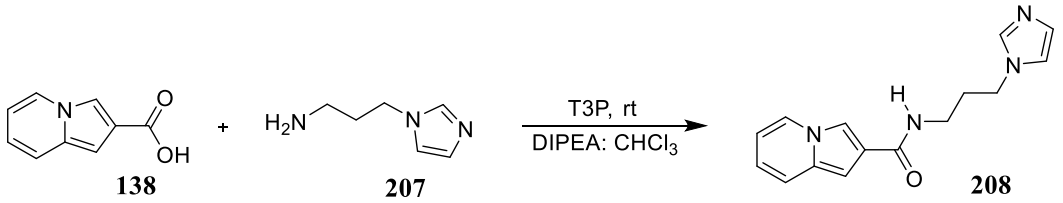

Scheme 57. T3P-catalysed amide synthesis with 1-(3-aminopropyl)imidazole **207** and indolizine-2-carboxylic acid **138**.

The product, which was contaminated with traces of 1-(3-aminopropyl)imidazole **207**, was characterised using NMR spectroscopy. The three methylene signals of *N*-[3-(1*H*-imidazol-yl)propyl)]indolizine-2-carboxamide **208** are clearly apparent in the ^{1}H NMR spectrum (**Figure 102**) and confirmed by the corresponding DEPT-135 NMR spectrum (**Figure 103**). It

is crucial to note that, in the corresponding ^{13}C NMR (**Figure 104**) the signal at *ca*. 168.0 corresponds to the C=O carbon of the amide moiety. In addition, the IR spectrum of compound **208** showed the NH band at 3337 cm^{-1} and the amide carbonyl band at 1672cm^{-1}

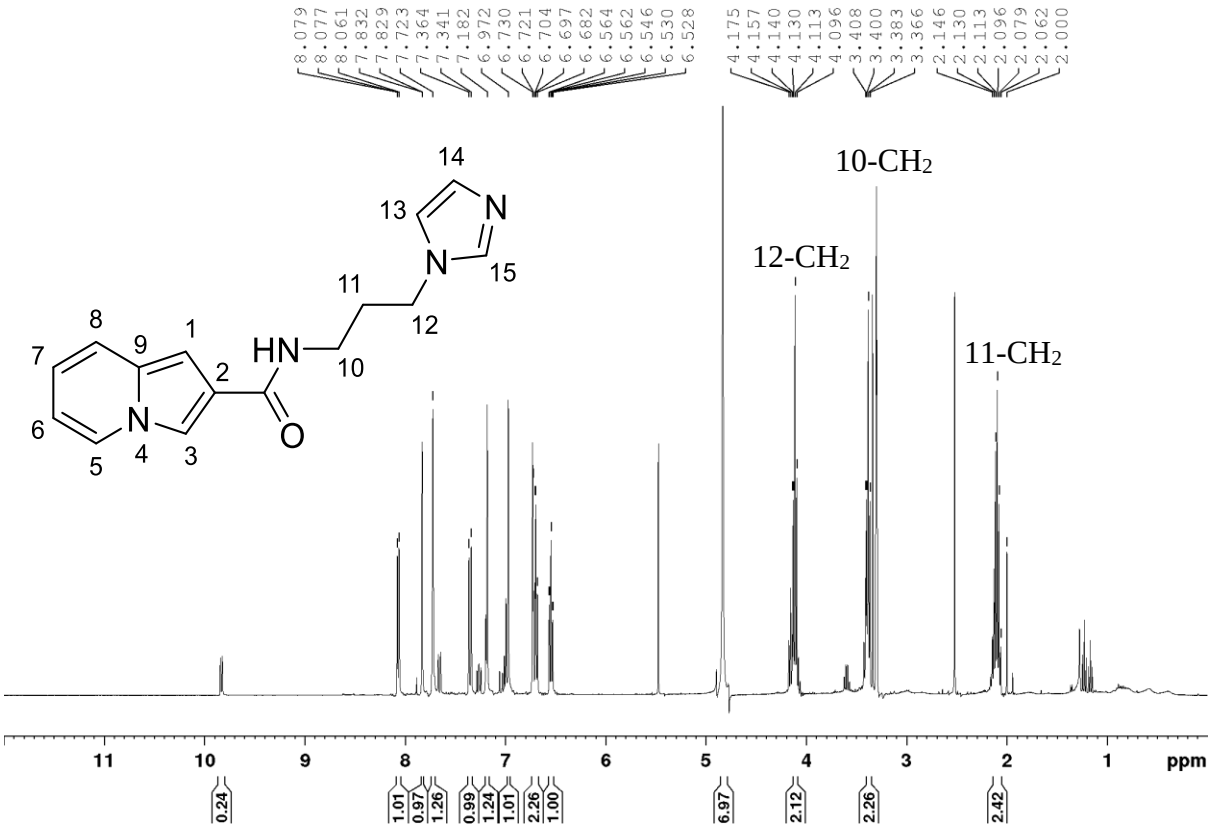

Figure 102. 600 MHz ^{1}H NMR spectrum of compound **208** in methanol-d_4.

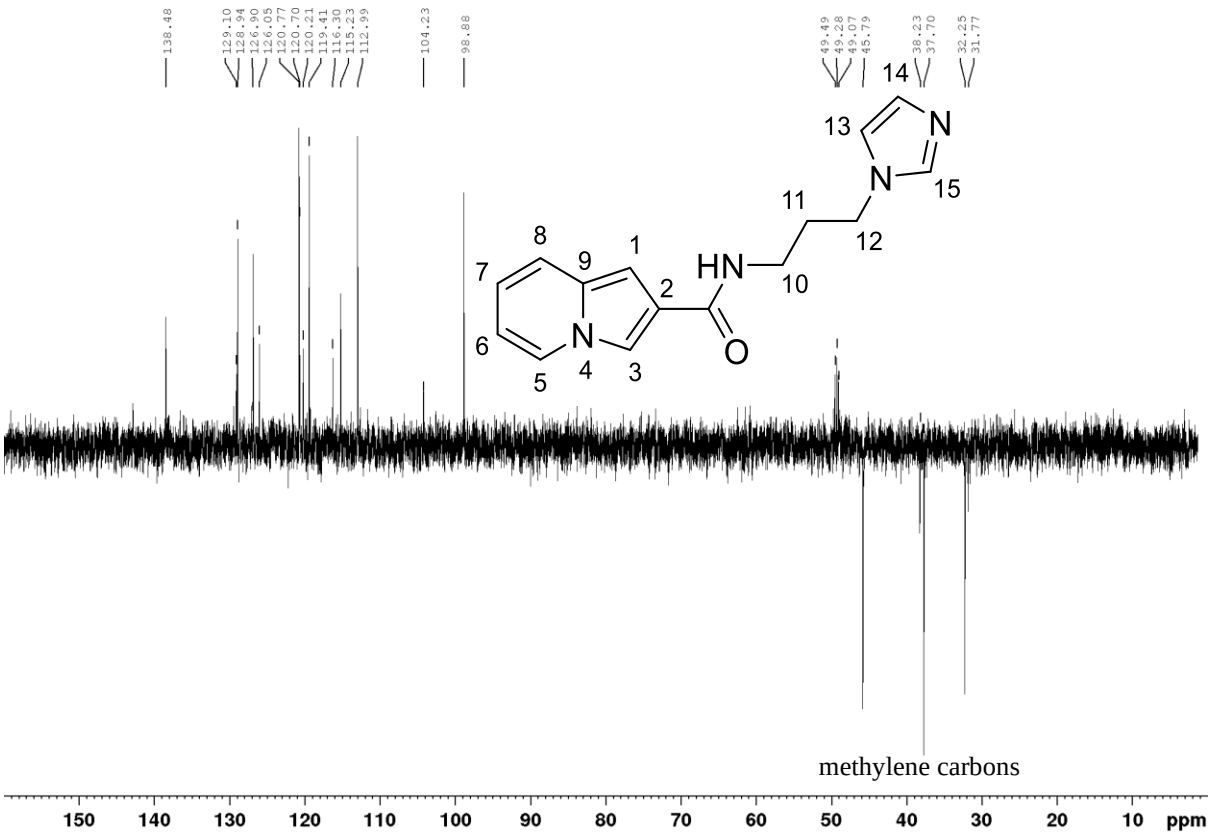

Figure 103. DEPT-135 NMR spectrum of compound **208** in methanol-d_4.

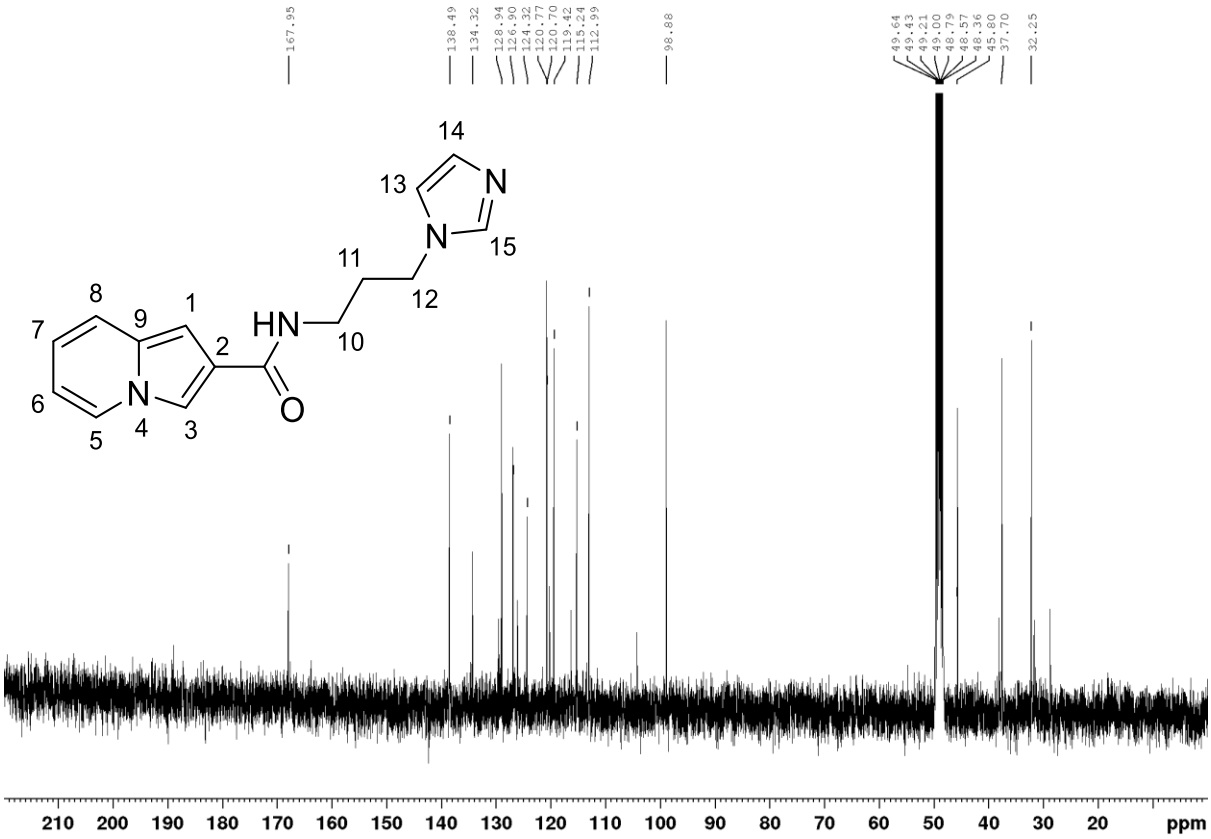

Figure 104. 150 MHz ^{13}C NMR spectrum of compound **208** in methanol-d_4.

2.3. Biological evaluation of 2-quinolone derivatives

Biological assays (bioassays) may be defined as experiments used to determine the potency or toxicity of a potential pharmaceutical agent on living cells or isolated enzymes and tissues and comparing the effects of these agents of unknown potency to the effect of reference standards.[275] Bioassays are essential for the development of new drugs. A typical bioassay involves introduction of a substance followed by measurement of its effect on a characteristic of the cells or tissues under study, with the magnitude of change dependent upon the dose.[276]

The 2-quinolones [quinoline-2(1*H*)-ones] have in recent years of medicinal chemistry research emerged as an important class of medicinally active compounds with a wide range of therapeutic activity and minimal adverse effects [116, 117, 118, 277] Of particular relevance to our own research are publications that reported that 2-quinolone derivatives, including 3-(amidomethyl)-2-quinolones, exhibit anti-HIV properties.[278, 279] Thus far, there are only three quinolone-based HIV-1 integrase (IN) inhibitors to have been approved for clinical use, *viz.*, Raltegravir (2007),[280] the 4-quinolone derivative, Elvitagravir (2012),[281] and a once-daily unsupplemented IN inhibitor, Dolutegravir (2013); the use of Dolutegravir as a monotherapy has recently been discouraged due to the emergence of resistance.[282, 283] The persisting failure to achieve viral suppression with standard treatments is due to the development of resistance, arising from viral mutations and the lack of patient compliance.[16, 284]

Inspired by *in silico* modelling results which indicated the capacity of 3-[(*N*-cycloalkylbenzamido)methyl]-2-quinolones to bind to the HIV-1 IN receptor,[285] we have evaluated the therapeutic potential of the 2-quinolones prepared in this study against HIV-1. A series of selected amines [3-cycloalkylaminomethyl-2(1*H*)-quinolone derivatives **114-116**] and their benzoylated derivatives, the amide amides, 3-[(*N*-cycloalkylbenzamido)methyl]-2(1*H*)-quinolones **117-119**, were evaluated *in vitro* against the HIV-1 enzymes – integrase (IN), protease (PR) and reverse transcriptase (RT). These bioassays were conducted for the author in the Bioassay facility of the Rhodes Centre for Chemico- and Biomedical research.

With the exception of 3-[(*N*-cyclopentylbenzamido)methyl]-8-methoxy-2(1*H*)-quinolone **118f** and 3-[(*N*-cyclopropylbenzamido)methyl]-8-methoxy-2(1*H*)-quinolone **119f**, all of the compounds exhibited a measure of HIV-1 inhibition at 20 µM with eight of them resulting in residual enzyme activity values in the range, 54-61% (**Table 8**). The most active IN inhibitor, producing residual enzyme activity of 40%, was the 3-[(cyclopentylamino)methyl-6-methoxy-2(1*H*)-quinolone **115e**. None of the compounds showed significant inhibition of either HIV-1 PR or RT and, in some cases, enzyme activity was enhanced. The opportunity was taken to

explore the anti-parasitic activity of the 2-quinolones but, apart from 3-[(*N*-cyclhexylamino)methyl]-6-methoxy-2(1*H*)-quinolone **114e** (55% *pf*LDH activity) which also shows similar activity against HIV-1 IN, most of the compounds exhibited minimal antiplasmodial activity (> 76% residual *pf*LDH activity), while none of them inhibited trypanosome (*T. brucei*) growth at 20 µM.

Cell toxicity data, as determined by % viability of HEK 293 (human embryonic kidney) cells, revealed that many of the compounds exhibit no significant effect on HEK 293 cells at a concentration of 20 µM.

Table 8. Bioassay data for 3-[(cycloalkylamino)methyl]-2-quinolones (**114**, **115** and **116**) and 3-[(*N*-cycloalkylbenzamido)methyl]-2-quinolones (**117-119**) showing: the % activity at 20 µM of HIV-1 IN, PR and RT enzymes; the antimalarial activity (as % viability of parasites using a *Pf*LDH assay at 20 µM); and the toxicity (as % viability of HEK 293 cells at 20 µM).

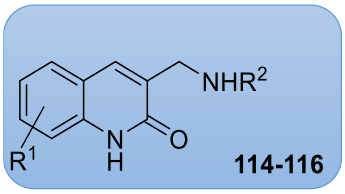

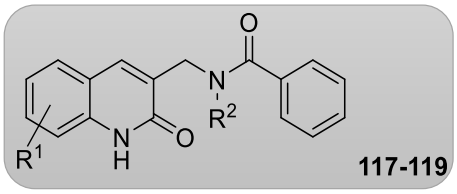

ntry	R^1	R^2	HIV-1 IN[a] % Activity	HIV-1 PR[b] % Activity	HIV-1 RT[c] % Activity	*Pf*LDH[d] % Viability	HEK 293[e] % Viability
114a	H	cyclohexyl	75.6	137.8	120.8	101.0	88.3
115a	H	cyclopentyl	54.5	163.0	116.7	86.1	131.4
116a	H	cyclopropyl	61.4	104.5	112.4	76.3	138.1
114e	6-OMe	cyclohexyl	55.7	144.7	111.4	54.6	105.1
115e	6-OMe	cyclopentyl	39.9	110.2	114.1	79.4	107.4
116e	6-OMe	cyclopropyl	76.7	99.5	130.0	84.9	122.6
114f	8-OMe	cyclohexyl	63.9	107.7	132.8	83.6	114.3
115f	8-OMe	cyclopentyl	88.9	118.3	140.1	90.6	87.2
116f	8-OMe	cyclopropyl	68.8	112.8	96.9	99.7	91.1
117a	H	cyclohexyl	67.2	117.9	85.8	90.2	122.3
118a	H	cyclopentyl	53.8	103.2	88.7	81.5	111.3
119a	H	cyclopropyl	60.5	121.1	88.0	85.2	113.6
117e	6-OMe	cyclohexyl	61.6	133.1	94.1	84.3	99.3
118e	6-OMe	cyclopentyl	60.1	120.0	94.9	91.1	93.6
119e	6-OMe	cyclopropyl	59.8	107.4	109.9	91.4	128.9
117f	8-OMe	cyclohexyl	70.0	115.6	119.4	92.3	74.6
118f	8-OMe	cyclopentyl	111.8	93.7	131.4	85.3	86.6
119f	8-OMe	cyclopropyl	117.0	103.5	104.0	89.4	85.6

[a]At 20 mM: Chicoric acid, 0.7% IN activity. [b]Ritonavir, 0% PR activity. [c]Nevirapine, 0.6% RT activity. [d]Chloroquine: IC50 7–12 nM. [e]Emetine IC50 0.04–0.1 mM.
Green shading: <40% enzyme activity; orange shading: <62% enzyme activity or cell viability.

2.4. Biological assay of indolizine derivatives

2.4.1. HIV-1 IN and PR assays

Indolizines are typically fluorescent molecules that exhibit a wide range of pharmacological properties including anti-microbial and anti-mycobacterial, [286] and have consequently been the focus of various synthetic studies.[287] Because of these interesting and promising biological properties, synthetic indolizines have claimed a preferred status in small molecules drug discovery, biological and pharmaceutical research.[133, 169, 288]

A number of researchers have recently identified indolizines with excellent potency towards the wild-type HIV-1, low toxicity and aqueous solubility.[289, 290] In addition, indolizines are particularly attractive due to their well-defined substitution patterns in synthesis which can offer advantages in quantitative structure-activity relationship studies.[134, 286] In this study, we have sought to assess the biological activity of twenty-five novel indolizine-2-carboxamides against HIV, malaria, trypanosomiasis and tuberculosis. The cytotoxicity of selected compounds was evaluated.

However, due to the limited availability of HIV bioassay toolkits, eleven selected indolizine-2-carboxamides were assayed for HIV-1 IN and HIV-1 PR activity. The selected amides included *N*-[*N*-(indolizin-2-ylcarbonyl)isoxazolin-3-on-4-yl]indolizine-2-carboxamide **180** (**Section 2.2.6.2**); two of four carboxamides constructed from the heterocyclic amines: 3-(indolizine-2-carbonyl)-2,4-imidazolidinedione **148** and 3-(indolizine-2-carbonyl)-1-methylimidazolidine-2,4-dione **150** (**Section** T3P-mediated reactions of acid (138 and 139) with 4-imidazolidinedione 146 and -methylimidazolidine-2,4-dione 147.); three of five 3-acetylindolizine-2-carboxamides: 3-acetyl-*N*-(5-aminotriazol-3-yl)indolizine-2-carboxamide **192**, 3-(3-acetylindolizine-2-carboxamido)-5-(indolizine-2-carboxamido)-1,2,4-triazole **193** and 3-acetyl-*N*-(thiazol-2-yl)indolizine-2-carboxamide **194** (**Section 2.2.7.2**); one of three isoniazid analogues: indolizine-2-carbonhydrazide **197**; and the four *N*-heteroarylalkylindolizine-2-carboxamides: *N*-benzylindolizine-2-carboxamide **204**, *N*-furfurylindolizine-2-carboxamide **205**, *N*-[2-(2-pyridinzyl)ethyl)]indolizine-2-carboxamide **206** and *N*-picolylindolizine-2-carboxamide **152** (**Section 2.2.7.4**).

The results summarised in **Figure 105** reveal that none of these carboxamides exhibited activity against HIV-1 PR – in fact the compounds appeared to increase activity. However, with the exception of the cycloserine-based amide **180**, and *N*-[2-(2-pyridinyl)ethyl)]indolizine-2-carboxamide **206**, all of the indolizine-2-carboxamides tested showed inhibition of HIV-1 IN. The isoniazid analogue **197** was the least active with 96% residual IN; residual IN activity for

the remaining analogues ranged from 52 to 64%, with the heterocyclic amine-based amides **148** and **150**, and the 3-acetylated indolizine-2-carboxamide **194** presenting the best enzyme inhibition with residual IN enzyme activity of 52%.

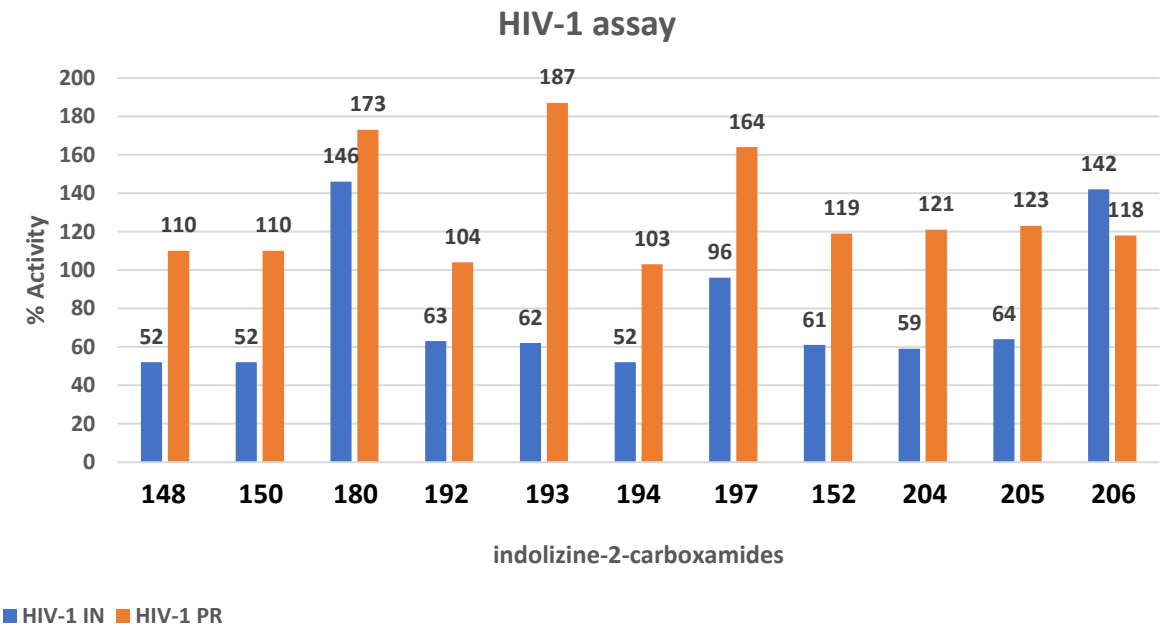

Figure 105. Bioassay of indolizine-2-carboxamides against HIV-1 integrase and protease at 20 µM concentration.

2.4.2. TB assays

Rifampicin was used as a reference for the antimicrobial TB assays and presented the lowest concentration required to inhibit 90% of the bacteria (MIC90) in the range of 0.016 to 0.021 µM after 7 days, 0.002 to 0.009 µM after 14 days in the 7H9 CAS GLU Tx medium, and 0.001 to 0.002 µM after both seven and fourteen days in the 7H9 ADC GLU Tw medium. The MIC values were determined by quantitative fluorescence and are presented as the compound concentration which inhibits the fluorescence by 90% (MIC_{90}) relative to the standard at days seven and fourteen post inoculation.

In this study, conducted for the author by the Institute for Infectious Disease and Molecular Medicine at the University of Cape Town, the assay started with an initial concentration of 10 µM of each compound. The minimum inhibitory concentration (MIC) values of a series of selected indolizine-2-carboxamides as potential anti-mycobacterials was explored and the corresponding dose response plots reflect the expression of the green fluorescent protein (GFP) on the engineered mycobacteria tuberculosis strain. Although, in the 7H9 GLU Tx medium, N^2-phenylindolizine-2- carbohydrazide **199** exhibited an MIC_{90} value of 31.25 µg/mL after 14

days (**Figure 106**), after seven days the desired MIC_{90} was not achieved but an MIC_{50} as shown in **Figure 107** was obtained. This class of compounds generally did not exhibit significant inhibition of mycobacterial TB.

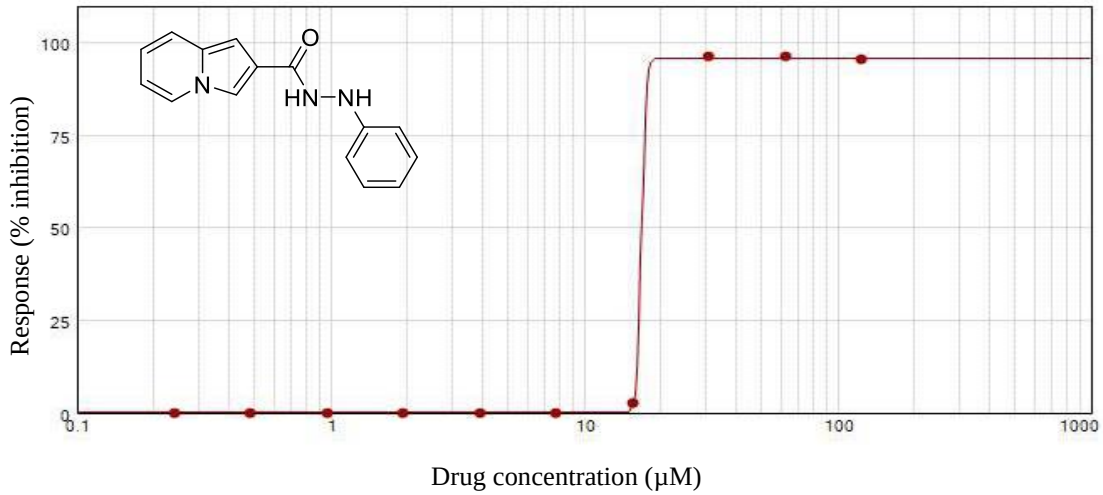

Figure 106. Concentration-response curve of the potential *mtb* drug drug **199** after fourteen days.

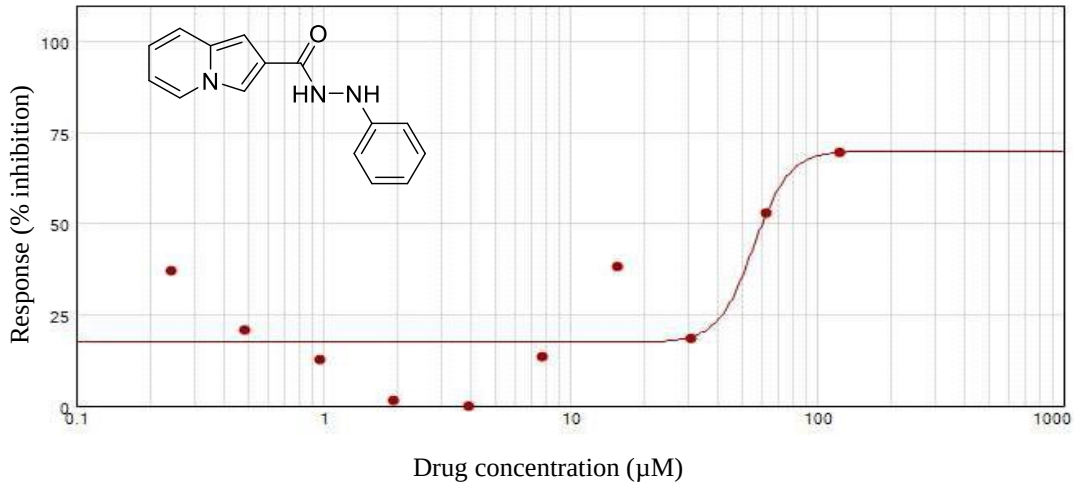

Figure 107. Concentration-response curve of the potential *mtb* drug **199** after seven days.

N-(5-aminotriazol-3-yl)indolizine-2-carboxamide **187** exhibited the same activity to compound **199** after fourteen days (MIC_{90} of 31.25 µg/mL; **Figure 108**). However, the dosage plot after seven days (**Figure 109**) showed significant scatter and could not be fitted to a conclusive pattern; this is attributed to apparent solubility issues presented by this molecule. It is worth noting that both of the above-mentioned compounds presented solubility challenges and addressing this could enhance their inhibition potential.

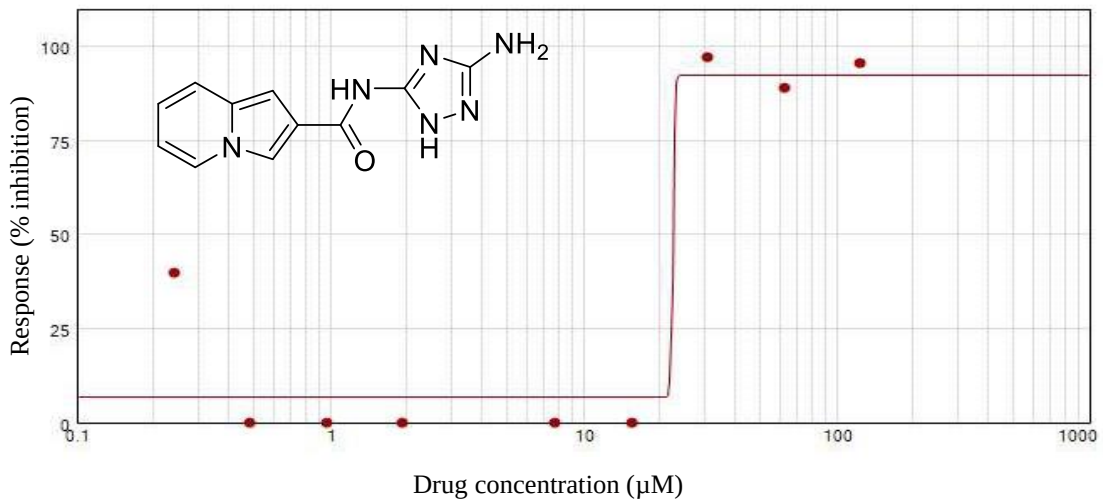

Figure 108. Concentration-response curve of the potential *mtb* drug **187** after fourteen days.

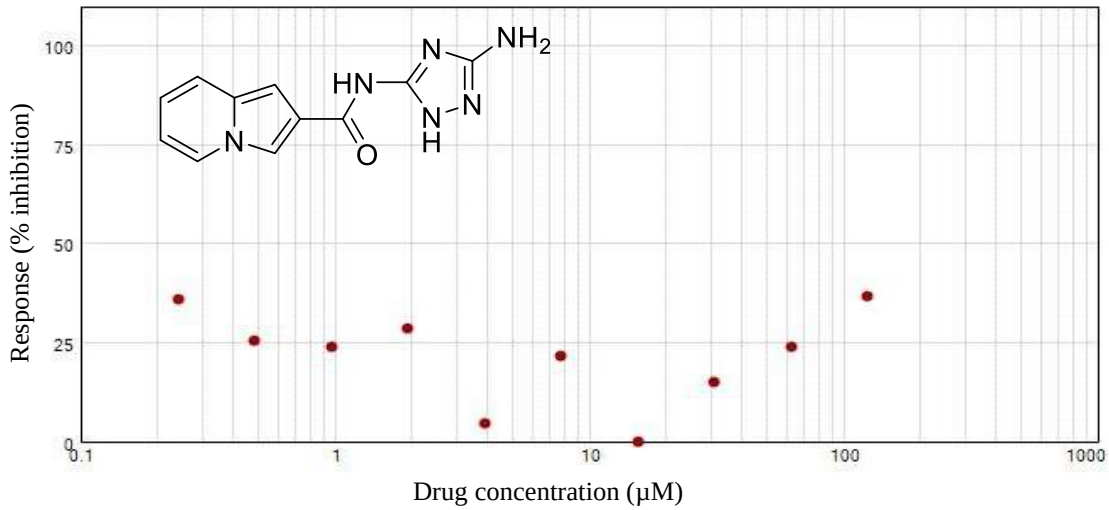

Figure 109. Concentration-response curve of the potential *mtb* drug **187** after seven days.

The anti-mycobacterial screening revealed that only three compounds, the amides **187**, **194** and **199** exhibited significant growth inhibition. As shown in **Figure 110** overleaf, the 3-acetyl-*N*-(thiazol-2-yl)-indolizine-2-carboxamide **194** showed that inhibition begins to be observed at a concentration of *ca.* 10 µg/mL after seven days, and, after 14 days, greatest inhibition with MIC_{90} of 15.63 µg/mL was achieved.

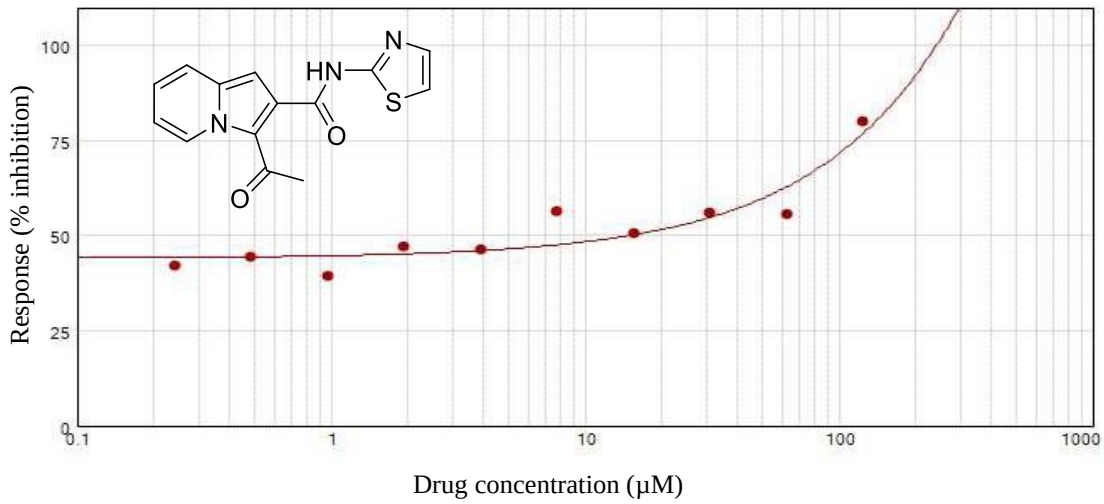

Figure 110. Concentration-response curve of the potential *mtb* drug **194** after seven days.

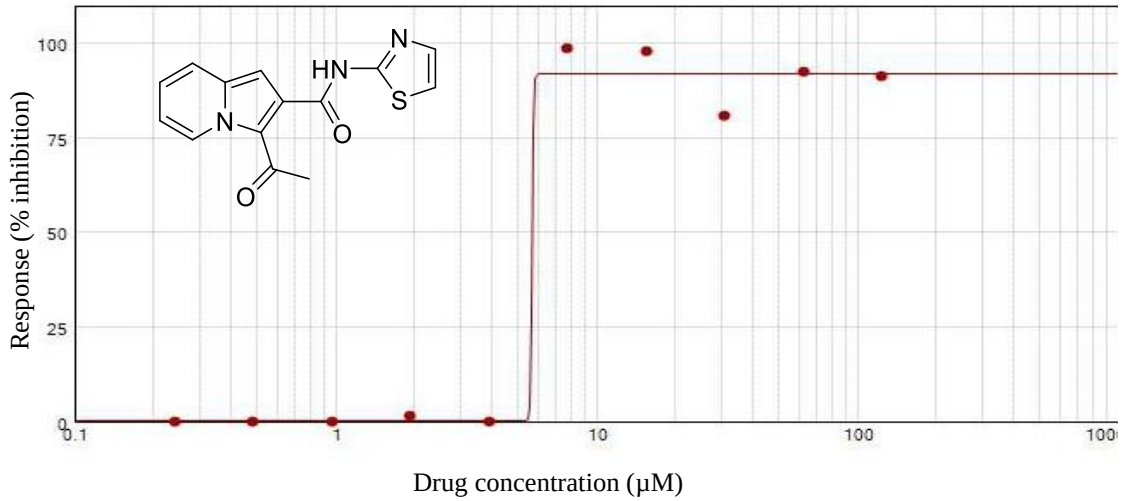

Figure 111. Concentration-response curve of the the potential *mtb* drug **194** after fourteen days.

2.4.3. Preliminary Malaria, trypanosome and cytotoxicity assays.

In these preliminary assays, a selected group of indolizine-2-carboxamides (**Figure 112**) were screened, at a concentration of 20 µM, against chloroquine sensitive *Plasmodium falciparum* using malaria parasite lactase dehydrogenase (*pf*LDH) and *Trypanosoma brucei*. Their cytotoxicity was also assessed against HEK 293 cells in a single-concentration screen. The activity of the compounds against *Plasmodium falciparum* was quantified on a Spectramax M3 microplate reader (Abs_{620}) using Malstat and a solution of nitroblue tetrazolium and 3-acetylpyridine ethosulfate (NBT/PES) solutions as fluorophores, whilst *T. brucei* viability was measured using resazurin which is reduced in the assay to resofurin as a fluorophore.

For each compound, the residual activities of the enzymes were measured as percentage viability and the results are summarised in **Table 9**. It is evident that these compounds exhibit some measure of activity against the *Plasmodium falciparum*, *N*-(2-thiazolyl)indolizine-2-carboxamide **154** and 3-(indolizine-2-carbonyl)-1-methylimidazolidine-2,4-dione **150** being the most active with *pf*LDH % viability values of 64.5 and 67.4%, respectively. The non-methylated analogue **148** of the amide **150** exhibited reduced activity resulting in percentage viability of *ca.* 83%. The cycloserine-derived *N*-[*N*-(indolizin-2-ylcarbonyl)isoxazolin-3-on-4-yl]indolizine-2-carboxamide **180** gave a percentage viability of *ca.* 78%. Indolizine-2-carbohydrazide **192** and *N*,*N*´-bis-(indolizine-2-carbonyl)hydrazine **198** presented *ca.* 87 and 89% viability, respectively, and N^2-phenylindolizine-2-carbonylhydrazide **199** was the least active compound with negligible antimalarial activity (97% PLDH viability). Results of the *Trypanosoma brucei* and cytotoxicity assays are also reported in **Table 9**. The percentage *T. brucei* viability ranged from 76 to 100% with the lipophilic *N*-[3-(1*H*-imidazol-yl)propyl)]indolizine-2-carboxamide **208** being the most active. None of these compounds showed toxicity against the HeLa (human cervix adenocarcinoma) cells.

Table 9. Bioassay data for indolizine-2-carboxamides showing the antimalarial activity (as % viability of parasites using a *Pf*LDH assay); anti-trypanocidal activity (as % parasite viability) and the toxicity (as % viability of HEK 293 cells) at 20 µM.

Compound	*Pf*LDH[a] (% Viability)	T. brucei[b] (% Viability)	HEK 293[c] (% Viability)
148	82.7	100.5	100.5
150	67.4	87.5	101.0
154	64.5	91.8	101.0
180	78.4	85.5	100.9
197	87.2	98.6	100.3
198	89.4	95.6	100.7
199	97.9	102.0	101.0
208	84.2	76.1	100.7

[a]Chloroquine: IC50 7–12 nM. [b]Pentamidine: IC_{50} 0.014 µM.[c]Emetine: IC50 0.014 µM.
Green shading: <70% cell viability; orange shading: <80% cell viability.

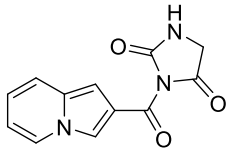

148

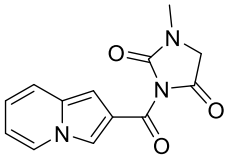

150

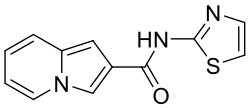

154

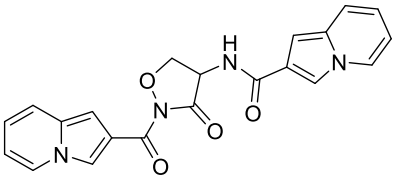

180

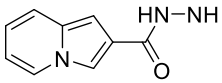

197

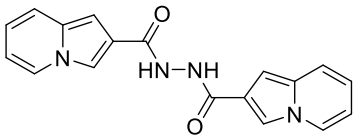

198

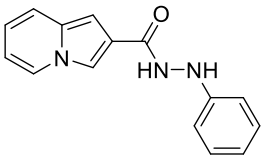

199

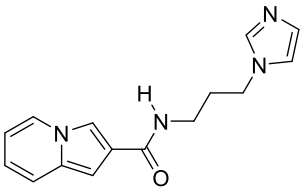

208

Figure 112. Indolizine-2-carboxamides used in malaria, trypanosome and toxicity assays.

2.5. Photophysical properties of indolizine-2-carboxamides

In view of the inherent fluorescence properties of indolizines and their subsequent use in a wide range of applications including as biomarkers in biology and medicine,[291, 292] the photophysical properties of the synthesised indolizine-2-carboxamides were explored. The fluorescent properties and biological activities of indolizines renders them an important class of small molecules with dual potential as bioimaging and therapeutic agents. It has been shown that conjugated indolizine derivatives, including polyindolizine systems, exhibit absorption and emission at wavelengths in the visible region with high quantum yield.[165, 293] Their Stokes shift ($\Delta\lambda$) which is the difference between the maxima of the absorption (λ_{abs}) and emission (λ_{em}) wavelengths for the same electronic transition is generally large.[293] The large Stokes shift and enhanced emission intensity make indolizine derivatives suitable for use in organic light-emitting devices (OLEDS) and as fluorescent molecular probes.[294]

Having successfully established the synthesis of a range of indolizine-2-carboxamides (**Section 2.2.1-2.2.5**) and evaluated their biological activities (**Section 2.4**), we have also explored the photophysical properties of selected indolizine-2-carboxamides (**Figure 113**). Their major absorption and corresponding emission bands, and the associated molar absorption coefficients (ε) expressed in the form of log ε are summarised in **Table 10**. The absorption and emission spectra for all of these compounds were obtained in MeOH except for compound **180** which was soluble only in DMSO. The observed extinction coefficients were substantial with *N*-picolylindolizine-2-carboxamide **152** exhibiting the lowest log ε value (3.29) and *N*-benzylindolizine-2-carboxamide **204** exhibiting the highest extinction coefficient with a log ε value of 4.40; both compounds belong to the same class of indolizine-2-carboxamides. Each log ε value was determined as the gradient of a serial dilution plot of absorbance versus concentration of the analyte. Emission spectra of all the compounds (**Figure 114**) exhibit bathochromic (red) shifts in the blue region of the visible spectrum (400-500 nm). Emission for amide **199** was not detected but Stokes shift ($\Delta\lambda$) values for the other compounds ranged from 55 to 97 nm. **Figure 115** and **Figure 116** show the UV visible spectra at different concentrations with insets demonstrating calculation of the molar absorption coefficient for 3-acetyl-*N*-(5-aminotriazol-3-yl)indolizine-2-carboxamide **192** and 3-acetyl-*N*-(thiazol-2-yl)indolizine-2-carboxamide **194**, respectively. Their absorption and emission wavelengths appearing within the visible colour range and their significantly high extinction coefficients (with log ε values averaging *ca.* 3.72) indicate that such indolizine-2-carboxamides are ideal for use as fluorophores. Their large extinction coefficients infer that they exhibit high quantum

yields, and few families of compounds have optimal photophysical properties that include high emission coefficient and quantum yield, large Stokes shift and red shift emission. A Stokes shift of greater than 80 nm is desirable to prevent re-absorption of emitted photons.[295]

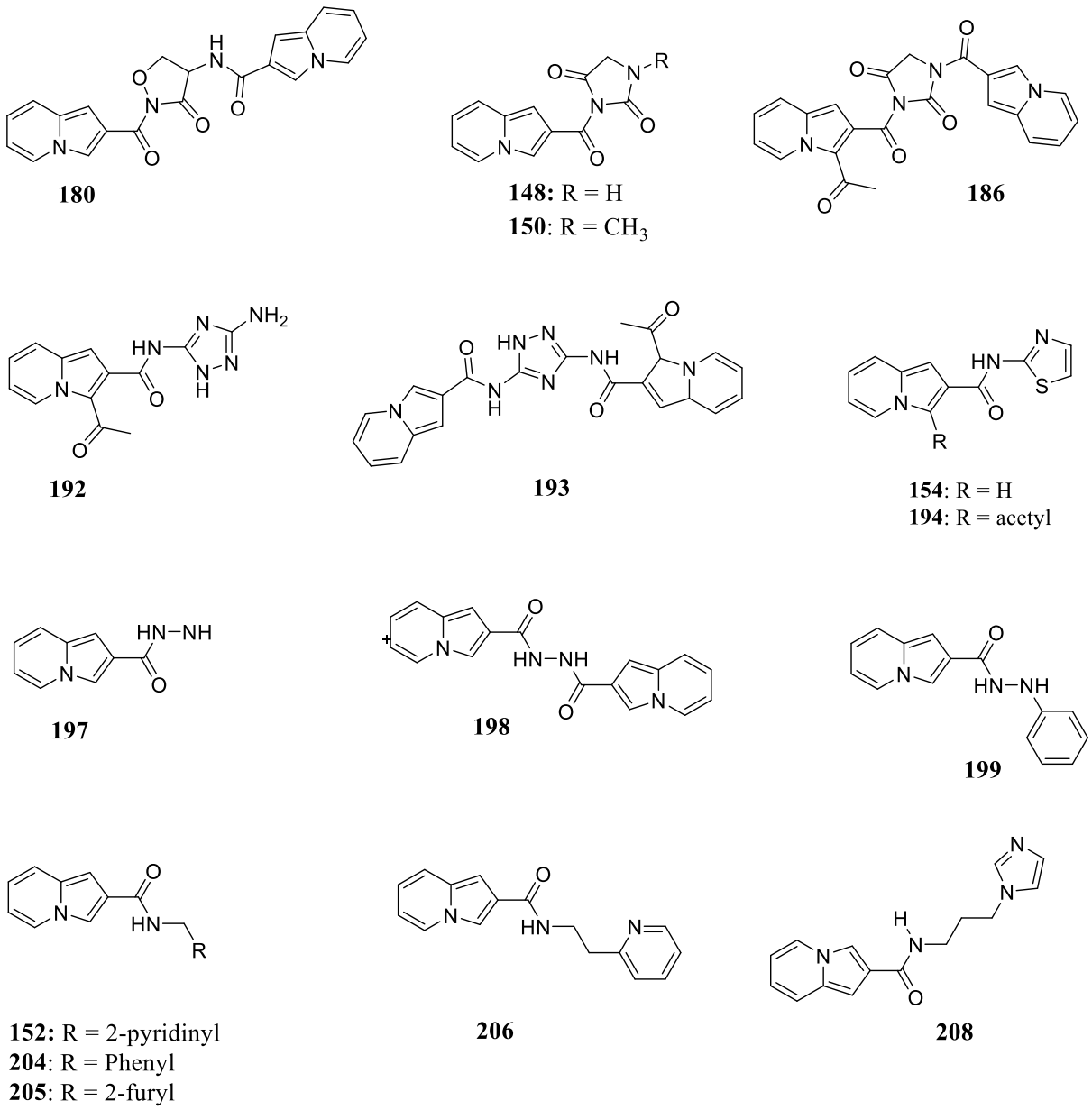

Figure 113. List of selected indolizine-2-carboxamides used in the photophysical study.

The disubstituted indolizine-2-carboxamides **180**, **193**, **198** and the hydrazide **192**, which of these had the greatest log Ɛ value of 3.98, exhibited desirable Stokes shifts (> 80 nm). Compound **192** exhibited the most red-shifted absorption and emission maxima at 420 and 517 nm, whilst its disubstituted analogue **193** had both absorption and emission wavelengths blue-shifted to 366 and 460 nm, respectively. Although 3-acetyl-*N*-(thiazol-2-yl)indolizine-2-carboxamide **194**, which contains the same 3-acetylated indolizine group as compound **192**,

exhibited the highest molar absorption coefficient (log Ɛ = 4.03), its Stokes shift (Δλ = 59 nm) fell below the desired value. The corresponding non-acetylated derivative **154** had an improved Stokes shift (Δλ = 76 nm) from almost the same absorption maximum but exhibited a red-shifted emission maximum. Thus, deacetylation has minimal influence on absorption wavelength but results in red-shifted emission. The acetylated amides **192** and **193** exhibit low emission intensity, and compound **194** had very low emission intensity (not shown). In the carbohydrazide group (**197-199**), the dimeric *N,N´*-bis-(indolizine-2-carbonyl)hydrazine **198** and N^2-phenylindolizine-2-carbohydrazide **199** exhibit absorption maxima that are blue-shifted relative to the unsubstituted indolizine-2-carbohydrazide **197**. Had any of the synthetic compounds exhibited any significant anti-TB activity, we had intended to use fluorescent microscopy techniques to follow their entry into the myocobacteria. Unfortunately, this opportunity did not arise.

Table 10. Photophysical properties of indolizine-2-carboxamides.

Sample	**Solvent**	**λ_{abs} (nm)**	**$^{*}\lambda_{em}$ (nm)**	**Δλ (nm)**	**log ε**
180	DMSO	363	457	94	3.90
148	MeOH	369	428	59	3.99
150	MeOH	359	435	76	3.61
186	MeOH	363	422	59	3.90
154	MeOH	365	441	76	3.82
192	MeOH	420	517	97	3.98
193	MeOH	366	460	94	3.75
194	MeOH	367	426	59	4.03
197	MeOH	365	420	55	3.87
198	MeOH	341	438	97	3.55
199	MeOH	357	ND	-	3.33
152	MeOH	356	426	70	3.29
204	MeOH	367	426	59	4.40
206	MeOH	356	433	77	3.47
205	MeOH	356	426	70	3.34
208	MeOH	358	436	78	3.42

Excitation wavelength 600nm and IR-820 was used as a standard in methanol (or DMSO); Excitation wavelength = 350 nm. ND = Not Detected

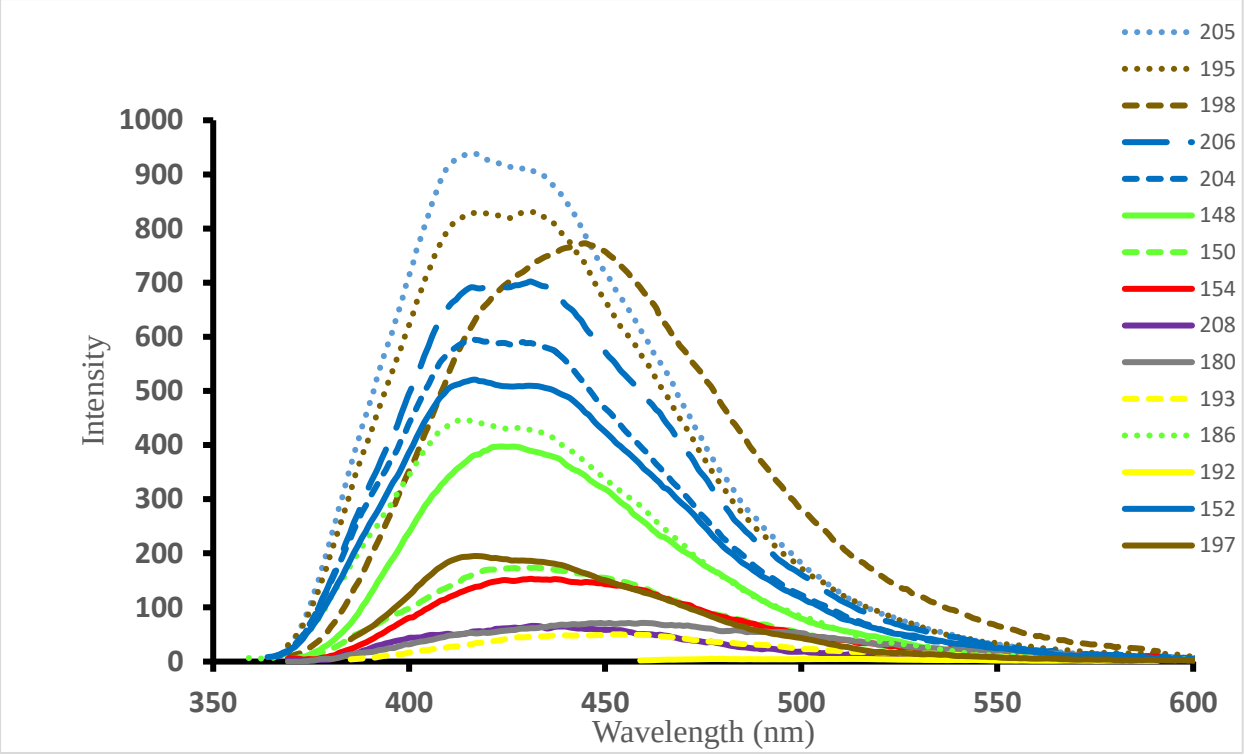

Figure 114. Emission spectra of indolizine-2-carboxamides at ambient temperature.

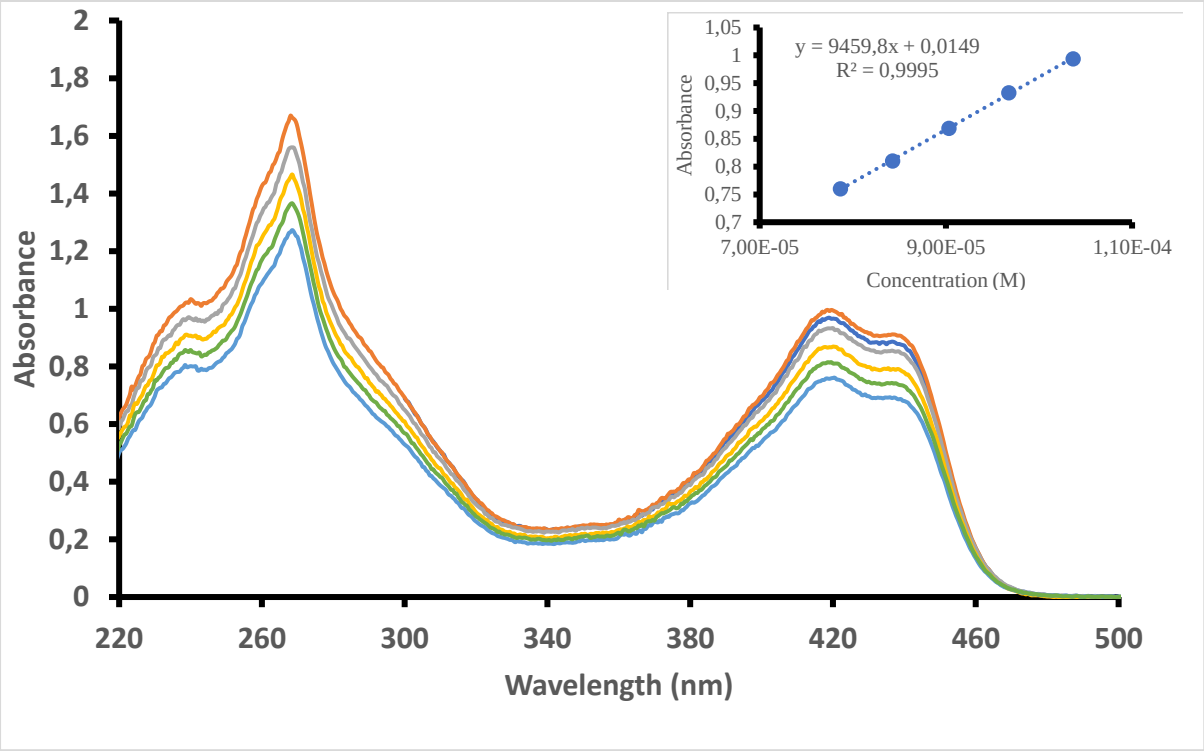

Figure 115. Absorption spectra at different concentrations of 3-acetyl-*N*-(5-amino-1,2,4-triazol-3-yl)indolizine-2-carboxamide **192** measured in MeOH at ambient temperature.

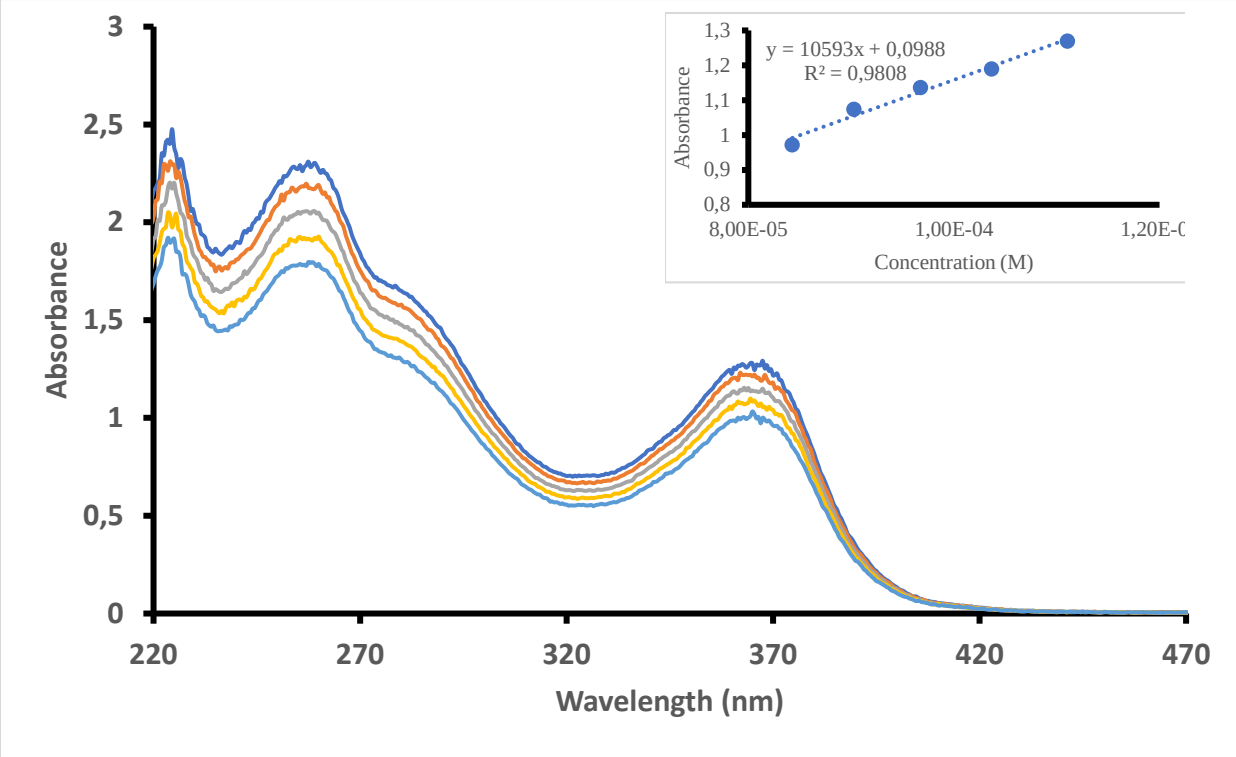

Figure 116. Absorption spectrum of 3-acetyl-*N*-(thiazol-2-yl)indolizine-2-carboxamide **194** measured in MeOH at ambient temperature.

2.6. Further chemical kinetic and mechanistic studies of the Baylis-Hillman reaction

The study of chemical kinetics covers the effects of concentration, temperature, ionic strength, solvents and hydrostatic pressure on various types of reactions.[296] Chemical kinetics can be fundamental or phenomenological.[297] The latter is widely used for application purposes, the former in seeking a fundamental understanding of underlying chemical processes which may also inform the optimisation of reaction conditions.[298, 299]

Following our earlier mechanistic contribution[218] and in the light of ongoing interest in the mechanism of the Baylis-Hillman reaction, high-field (600 MHz) ^{1}H- and DEPT 135 NMR spectroscopy were used to explore the kinetics of the reaction of pyridine-4-carboxaldehyde **209** (the symmetrical analogue of the pyridine-2-carboxaldehyde used in our synthetic studies) and methyl acrylate **46b** in the presence of 3-hydroxyquinuclidine (3-HQ) **123** in deuterated chloroform (**Scheme 58**). The reaction progress was followed by running automated ^{1}H- and DEPT 135 NMR spectra at 10-minute intervals, each ^{1}H NMR spectrum being followed by a DEPT 135 NMR spectrum. The reaction mixture was initially cooled in a dry-ice bath to inhibit reaction prior to inserting the NMR tube into the NMR probe, the temperature of which was fixed at 298 K. The reaction was followed until almost complete consumption (*ca.* 94%) of the starting materials (**Figure 117**). Illustrative spectra in **Figure 118-123** reveal the following.

i. Assigned ^{1}H-NMR signals for the product **210**, the reactants pyridine-4-carboxaldehyde **209** and methyl acrylate **46b**, the catalyst **123** and an unknown intermediate **X**, the presence of which was indicated by calculating the mass balance as a function of time (see **Figure 117**). The signals for the various species are marked with an asterisk in **Figure 118** and in the expanded and amplified partial spectrum (**Figure 121**).

ii. Assigned signals in a DEPT 135 spectrum for the product **210**, the reactants **209** and **46b**, the catalyst 3-hydroxyquinuclidine **123** and the unknown intermediate **X**, which are marked with coloured asterisks in the amplified spectrum (**Figure 123**).

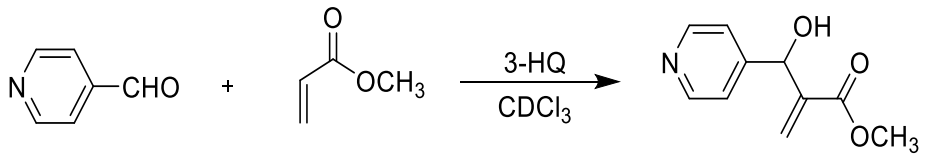

209 **46b** **210**

Scheme 58. The 3-HQ-catalysed, Baylis-Hillman reaction of pyridine-4-carboxaldehyde **209** and methyl acrylate **46b** in $CDCl_3$.

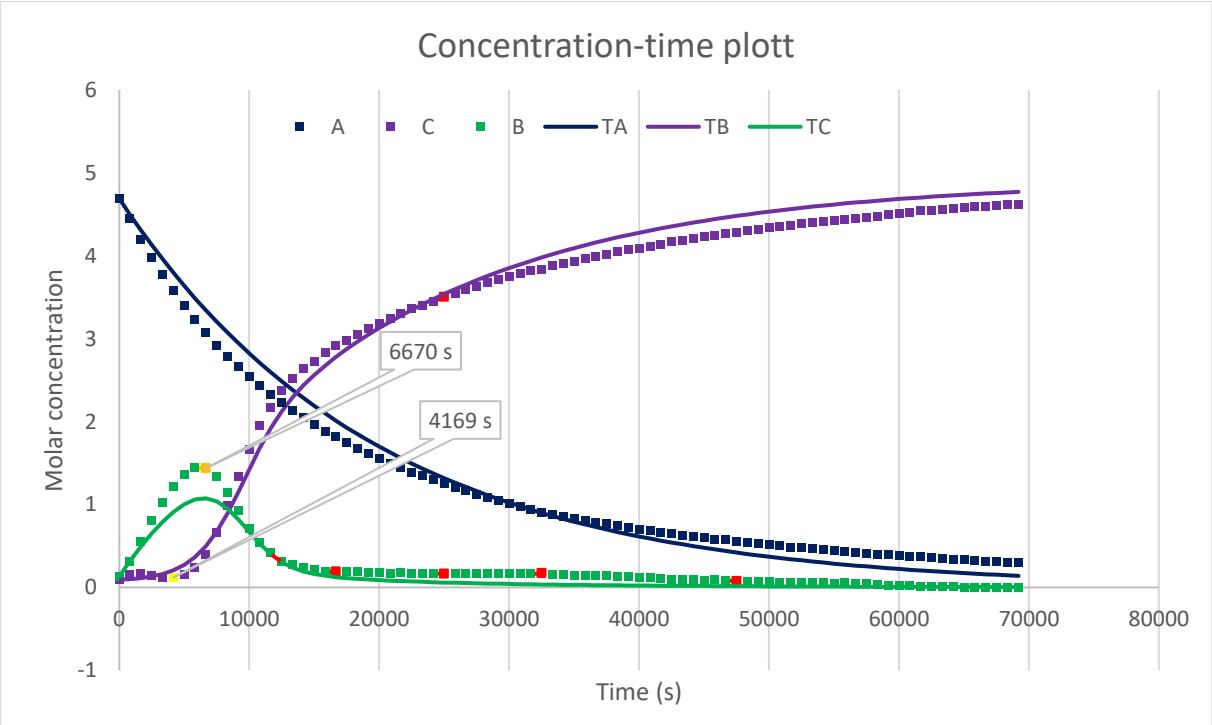

Figure 117. Progress of the 3-HQ catalysed Baylis-Hillman reaction of pyridine-4-carboxaldehyde **209** and methyl acrylate **46b** monitored by ^{1}H NMR analysis at 298 K. The points represent the experimentally determined concentrations, while the solid lines represent a theoretical fitting. A = consumption of the aldehyde, B = formation of the intermediate **X** and C= formation of the product; TA = theoretical consumption of the aldehyde, TB = theoretical formation of the intermediate **X** and TC = theoretical formation of the product (See discussion for the construction of the theoretical plots).

The ^{1}H NMR integral data were used to determine the concentrations of the various species at time intervals. The plot of the millimolar concentration against time (**Figure 117**) shows that, from t = 0 seconds (s) to the intersection point at *ca.* t = 12505 s, the concentration of the aldehyde **204** steadily declines whilst the rate of formation of the product **210** appears to follow an s-shaped curve suggesting the possibility of autocatalysis. The mass balance plot indicates the initial formation of an intermediate (designated **X**) which reaches a maximum concentration of 1.44 mM at *ca.* 6670 s, at which point the rate of formation of the product also appears to accelerate. The theoretical plots were constructed on the following assumptions.

i) During the first *ca.* 6670 s, formation of the intermediate **X** is associated with 1st order consumption of the aldehyde **209** at a common rate of 5.08×10^{-5} s^{-1}.

ii) Subsequent 1st order decomposition of intermediate **X** to form the product **210** is so slow that its contribution to the overall reaction rate can be approximated to zero. constant ($rate_2 = 0$ s^{-1}) and,

iii) 2nd Order autocatalysis involves the above-mentioned product **210** catalysing consumption of the intermediate **X** to generate more product **210** at a rate of 3.42×10^{-4} $mol^{-1}s^{-1}$.

Exploration of the apparent autocatalytic nature of the reaction provides important information about the mechanism. In autocatalysis, two mechanisms are involved, one of which is very slow and is responsible for the initial formation of the product, and a subsequent autocatalytic variation which uses the product to accelerate the reaction.[300] In the present study, it is apparent from **Figure 117** that an intermediate **X** is formed during the initial phase of the reaction and, at the time when this intermediate reaches a maximum concentration, rapid formation of the product **210** commences. The rapid initial consumption of the aldehyde (from t = 0 s) coupled with the very slow initial formation of the product suggests that the rate-determining step involves consumption of the intermediate **X**, formation of which accounts for the continued 1st order consumption of the aldehyde **209** throughout the reaction.

In summary, the autocatalytic nature of the reaction is clearly indicated by the S-shaped profile of the concentration-time plot of the product (**Figure 117**). It appears that formation of a maximum concentration of intermediate **X** at 6670 s, corresponds with the initiation of a rapid, but rate-limiting, autocatalytic phase during which product-catalysed consumption of the intermediate **X** occurs almost as rapidly as it is formed; a very low and slowly decreasing concentration of **X** is evident throughout the course of the reaction. The autocatalyzed process thus follows pseudo 2nd-order kinetics (assuming the concentration of the BH catalyst, 3-HQ, remains constant) and step III (**Scheme 59**) is rate-limiting.

The generally accepted molecular features of the Baylis-Hillman reaction are outlined in **Scheme 59**. Analysis of the ^{1}H NMR spectrum (**Figure 121**, p163) and the corresponding DEPT 135 spectrum (**Figure 123**, p165) at 6670 s indicate the presence of signals consistent with the structure of the zwitterionic intermediate **212** and, hence, its identification with intermediate **X**. This conclusion was reached by identifying characteristic ^{1}H and ^{13}C NMR signals that would correspond to the α-proton, the allylic (β′) proton and the diastereotopic β-

protons and the carbon to which they are attached in the proposed zwitterionic intermediate **212** (**Table 11**).

Various proposals for the mechanism of the Baylis-Hillman reaction based on experimental and theoretical analyses have been reported. Earlier experimental studies were undertaken by:- (i) Hill and Isaacs,[301, 302] based on pressure dependence; ii) our own group using a 60 MHz NMR instrument;[218] (iii) Singh and Kumar[303] using a gas-liquid chromatography-based approach and (iv) McQuade and co-workers[304] using kinetic isotope effect (KIE) data. Three of these groups (i, ii and iii) suggest that the rate determining step (RDS) involves reaction of the BH zwitterion **211** with the aldehyde **209** (step II, **Scheme 59**), while Singh and Kumar[303] propose that the RDS involves loss of the catalyst **118** and proton transfer *via* an intermediate complex between the zwitterion **212** and the aldehyde **209**, resulting in pseudo 3rd order kinetics (*i.e.* 2nd order in the aldehyde **209**).

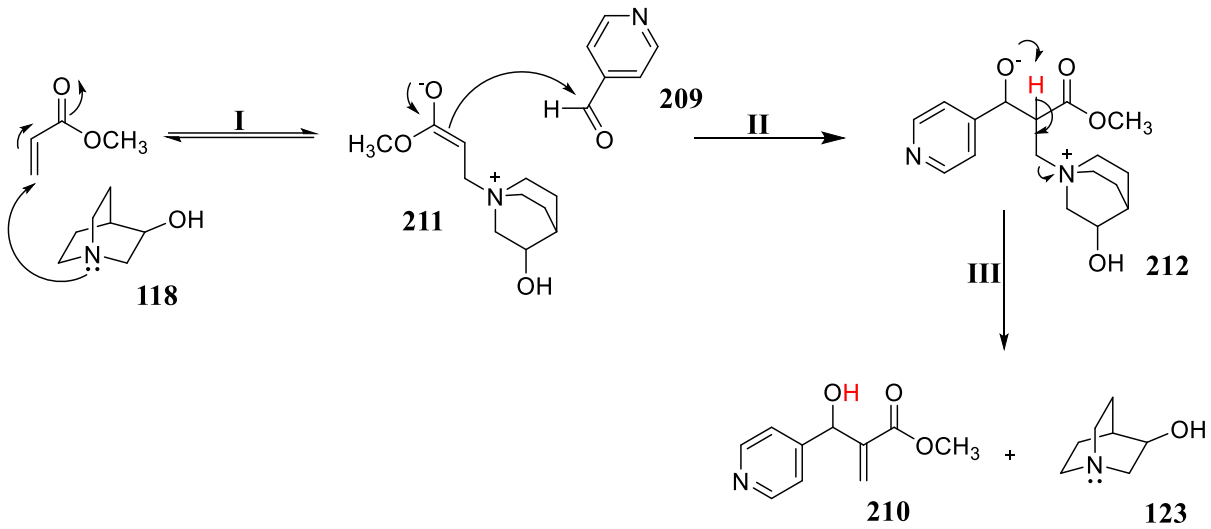

Scheme 59. Mechanism of the Baylis-Hillman reaction.

In addition to the effect of the catalyst on the rate of the BH reaction, protic additives or protic solvents, such as methanol and water, have also been shown to accelerate the reaction. [2, 250] This acceleration has been attributed to H-bonding activation of the aldehyde **209** in step II and an increase in the polarity of the medium (**Scheme 59**).[305, 306] McQuade and co-workers [304] using rate and isotope data, proposed that the BH reaction of various aldehydes and methyl acrylate in a protic medium was second-order in aldehyde but first-order in acrylate and the tertiary amine catalyst (DABCO) and, that the α-proton of intermediate **212** breaks in the step III. But, Plata and Singleton,[307] suggested that the mechanism exhibits competitive rate-

determining steps with the proton-transfer in step III being primary and the aldol step (step II) being a partial rate-determining step.

Interestingly, in the absence of protic solvents, the reaction has been reported to rely on autocatalysis where the alcohol group of the product acts as a hydrogen-bond donor promoting the reaction or acting as a shuttle for transferring a proton from the α-position to the alkoxide in step III.[307, 308] This observation emphasised the role of protic solvents in stabilising intermediates and transition-state complexes and, in turn, final liberation of the catalyst.[305] Our results clearly provide a new perspective on the mechanism of this important reaction.

In this study, the spectroscopic data obtained during the course of the reaction, which have facilitated the identification of the reactants, the product and, most importantly, the critical intermediate **X** may be summarised as follows:

i) **Figure 118** and the expanded partial spectrum thereof (**Figure 119**) which indicate the ^{1}H NMR signals for the reactants and the product.

ii) **Figure 121** – an amplified ^{1}H NMR spectrum at 6670 s which indicates the presence of reactants, the product and, most importantly, signals for the intermediate **X** which are detailed in **Table 11**.

iii) **Figure 120**, a DEPT 135 spectrum, indicates the ^{13}C signals of the catalyst (3-HQ) and, **Figure 123** illustrates the amplified DEPT 135 NMR spectrum of the reaction mixture at 6670 s and reveals ^{13}C signals corresponding to the proton-bearing α, β and β′ (allylic) carbons in intermediate **X**.

iv) **Figure 124** shows ^{1}H NMR signals for intermediate **X** in a stack plot of partial spectra from t = 0 to t = 6670 s.

v) **Figure 125** – a stack plot of partial ^{1}H NMR spectra which show the consumption of intermediate **X** over time.

Table 11. NMR characterisation of the critical intermediate **X** identified as species **212** (see **Figures 121-123**).

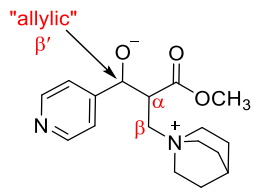		δ_H	δ_C (DEPT 135)
	α–CH	4.57 (dd)	-
	allylic β′–CH	4.03 (m)	-
	β–CH_2	4.03 (m) and 3.93 (m)	88.7

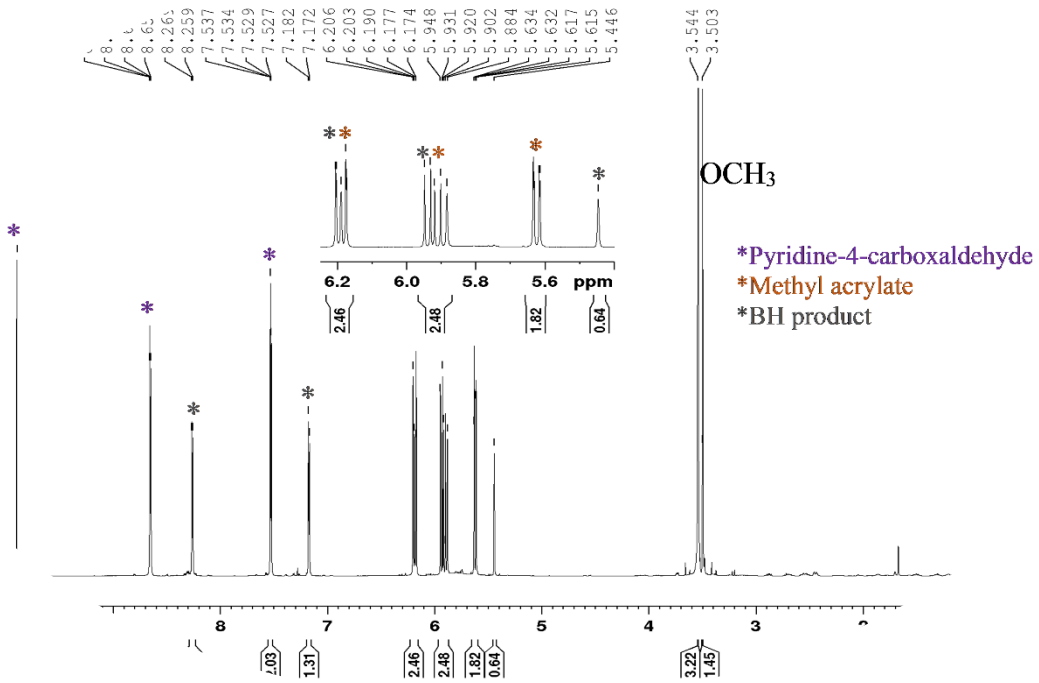

Figure 118.600 MHz ^{1}H NMR spectrum of the reaction mixture at 6670 seconds in $CDCl_3$ at 298 K. The NMR siganals for the intermediate and 3-HQ are visualised in **Figures 121** and **122**.

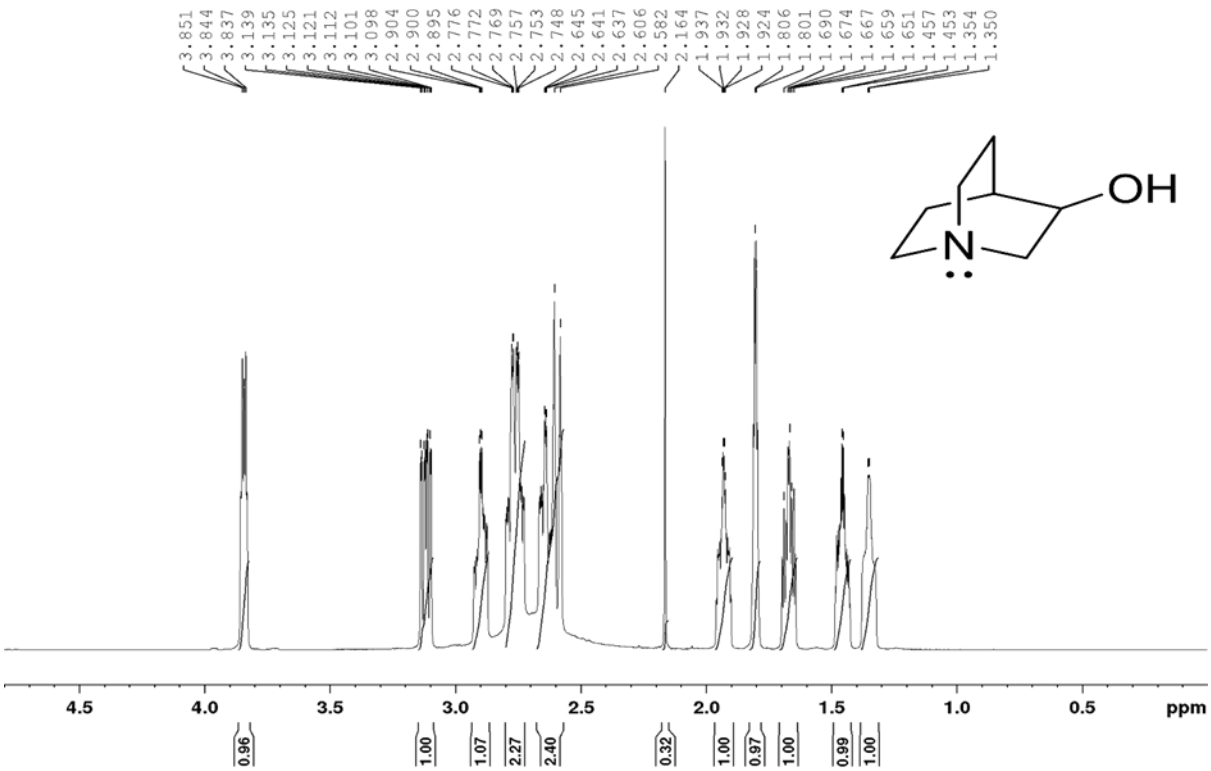

Figure 119. Expanded ^{1}H NMR spectrum of 3-hydroxyquinuclidine **123** in $CDCl_3$ at 298 K.

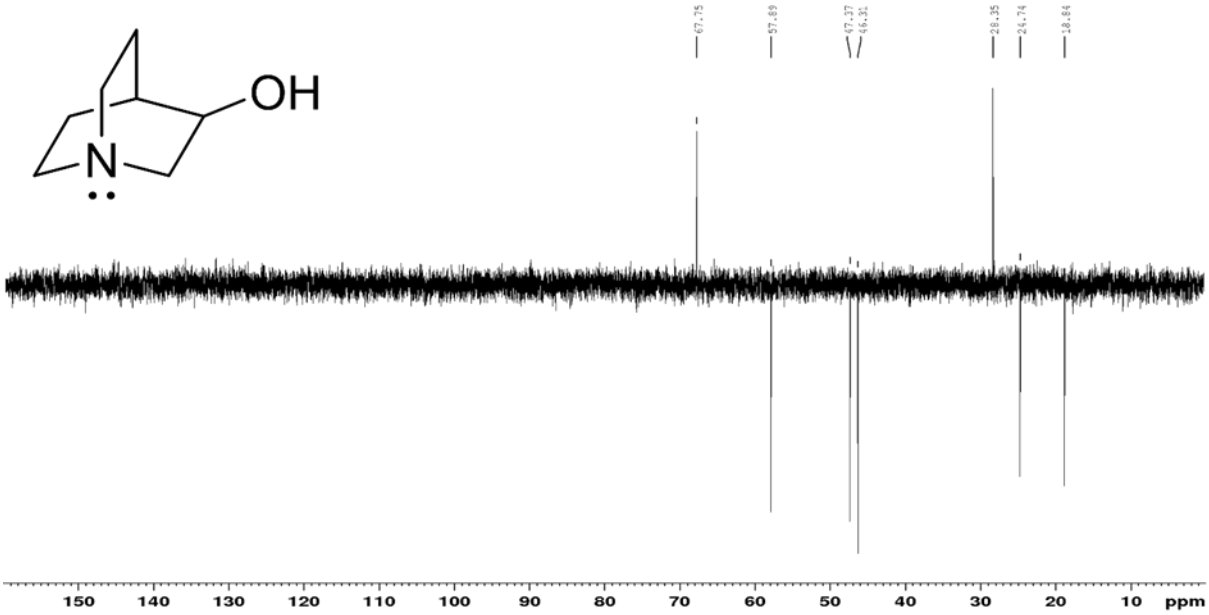

Figure 120. 150 MHz DEPT 135 NMR spectrum of 3-hydroxyquinuclidine **123** in $CDCl_3$ at 298 K.

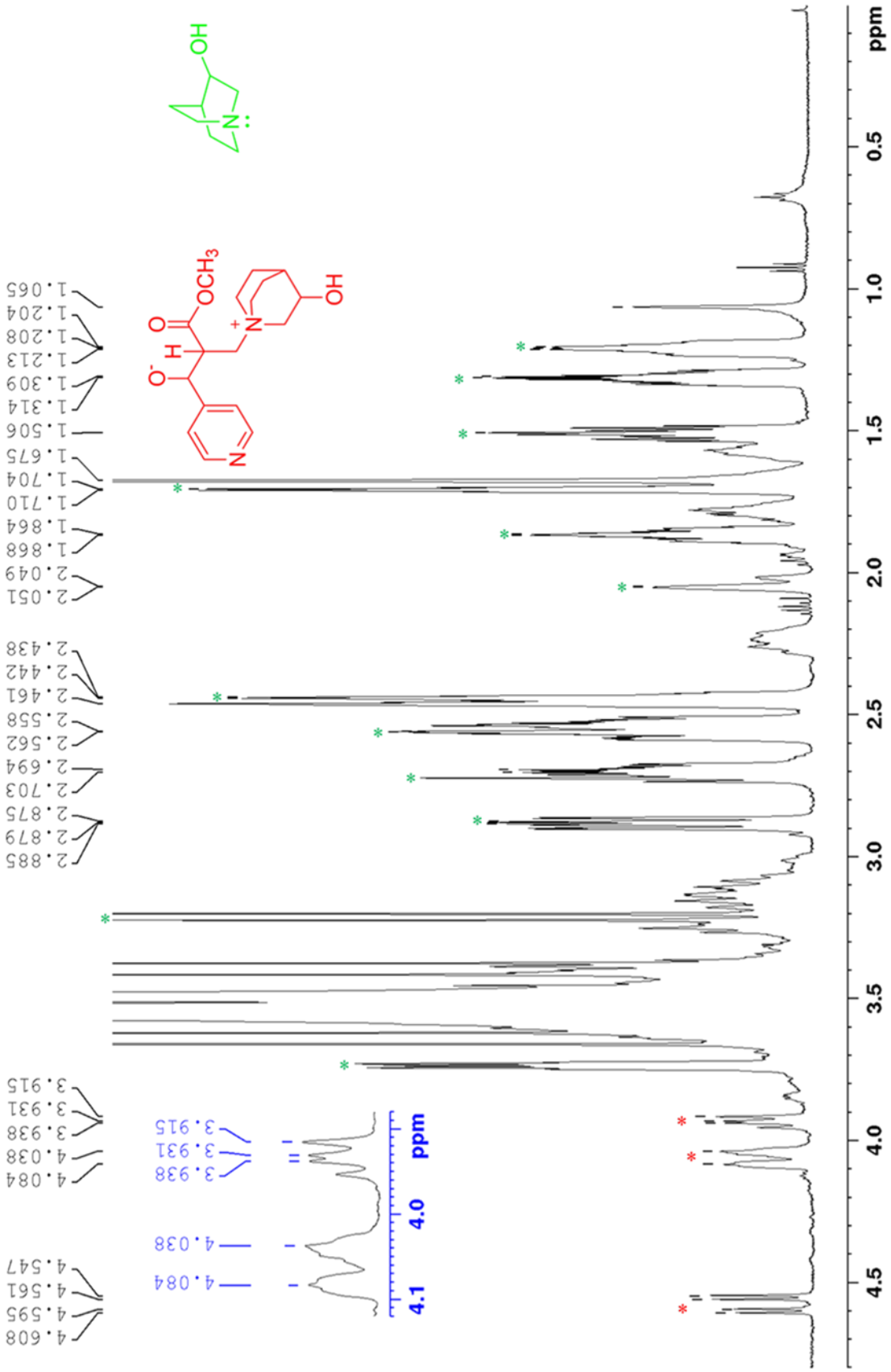

Figure 121. Expanded and amplified 600 MHz ^{1}H NMR spectrum of reaction mixture at 6670 seconds in $CDCl_3$ at 298 K.

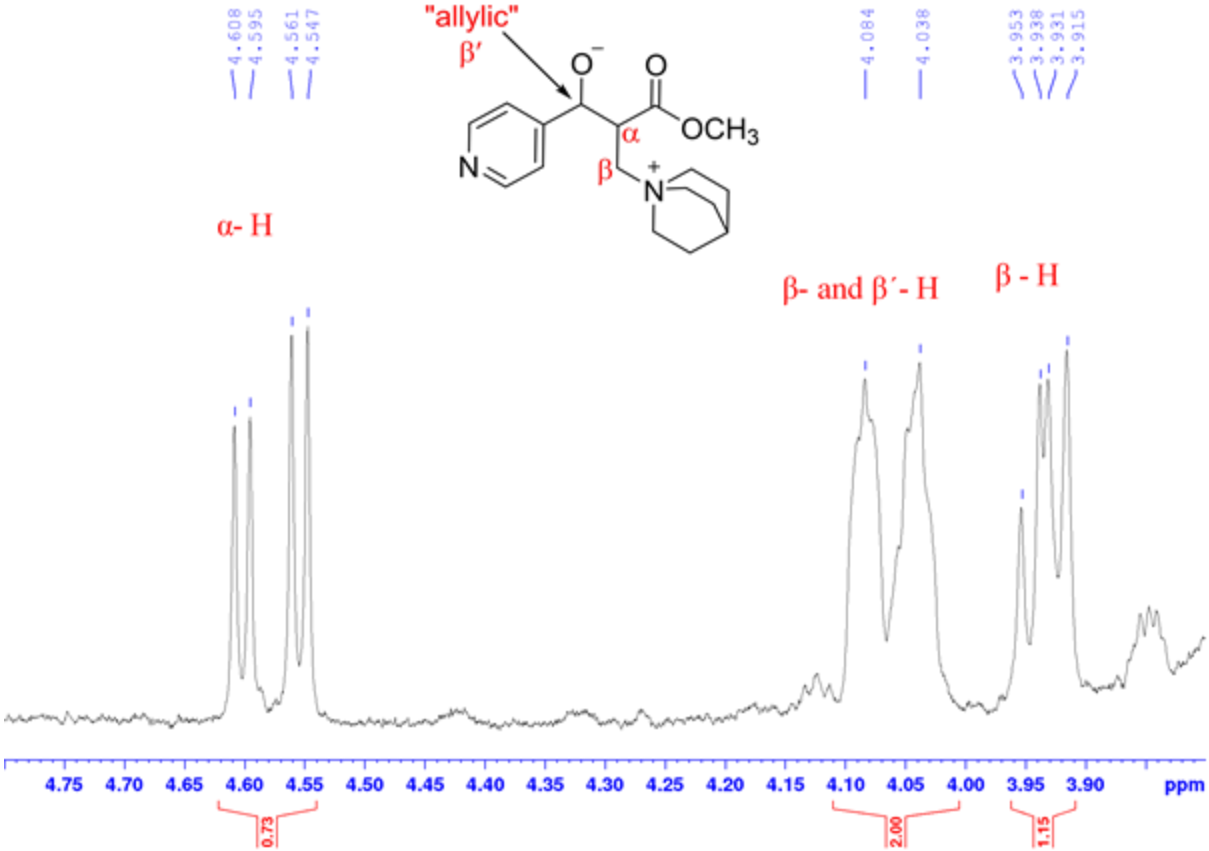

Figure 122. Expanded and amplified ^{1}H NMR spectrum illustrating integration of the α-proton, β-protons and the CH-oxide proton of the intermediate **212**.

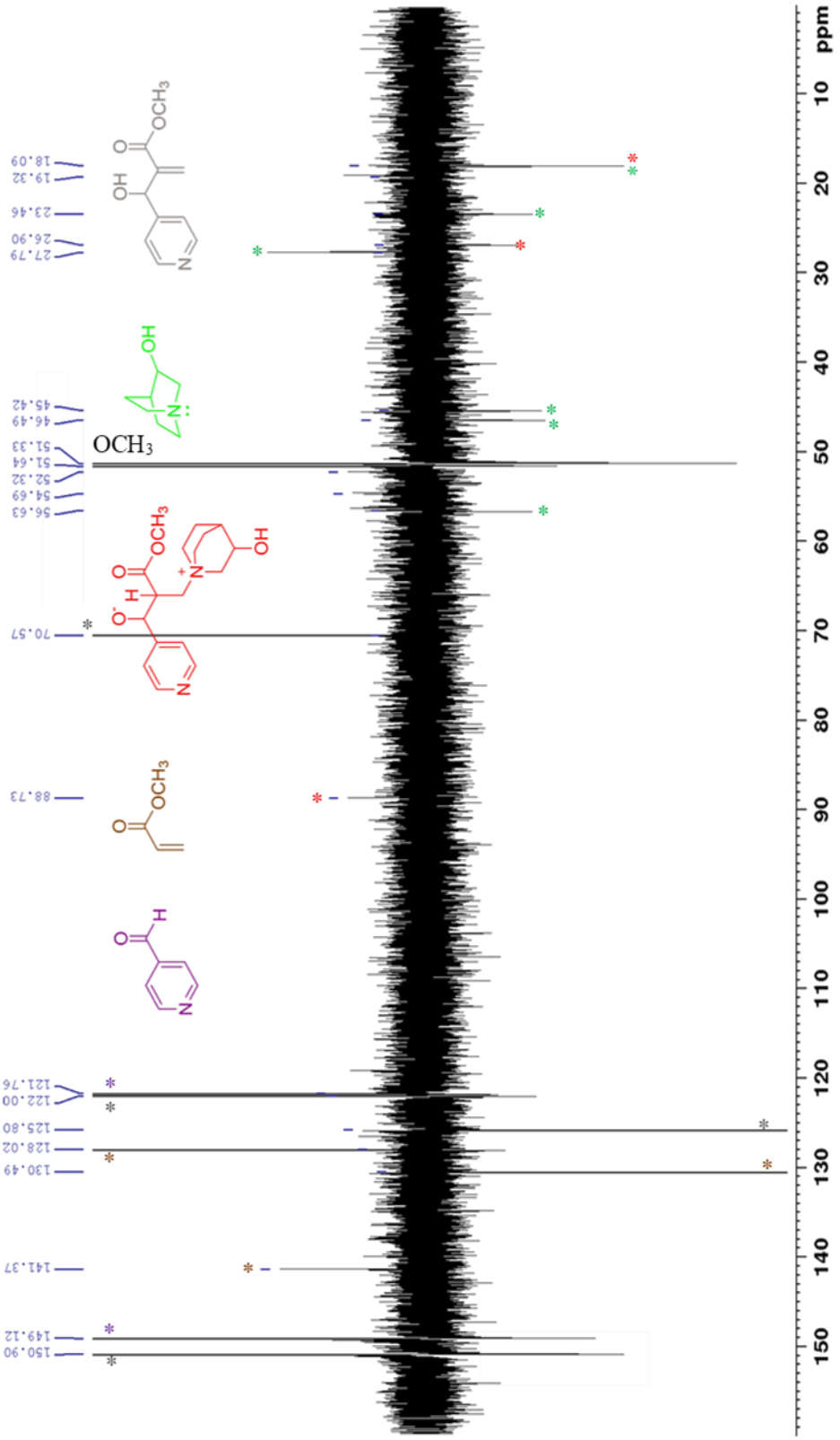

Figure 123. DEPT 135 NMR spectrum of the reaction mixture at 6670 seconds in $CDCl_3$ at 298 K.

The ^{1}H NMR stack-plots in **Figure 124** and **Figure 125** successively confirms the progressive formation of the intermediate **X** in the initial phase from t = 0 to 6670 s at which point maximum concentration was reached and, subsequent consumption of the intermediate **X** by showing potential ^{1}H NMR spectra at several indicative points that are marked in red at the concentration-time plot (**Figure 117)**. The consumption of the intermediate **X** is apparent in **Figure 125** which shows a progressive upfield shift and disappearance of a diastereotopic proton signal that resonated at 3.94 ppm, a slight downfield shift and convergence to a broad singlet with an increase in intensity of the other which resonated at 4.08 ppm and α-proton signal at *ca.* 4.57 ppm slightly shifted downfield with decrease in intensity.

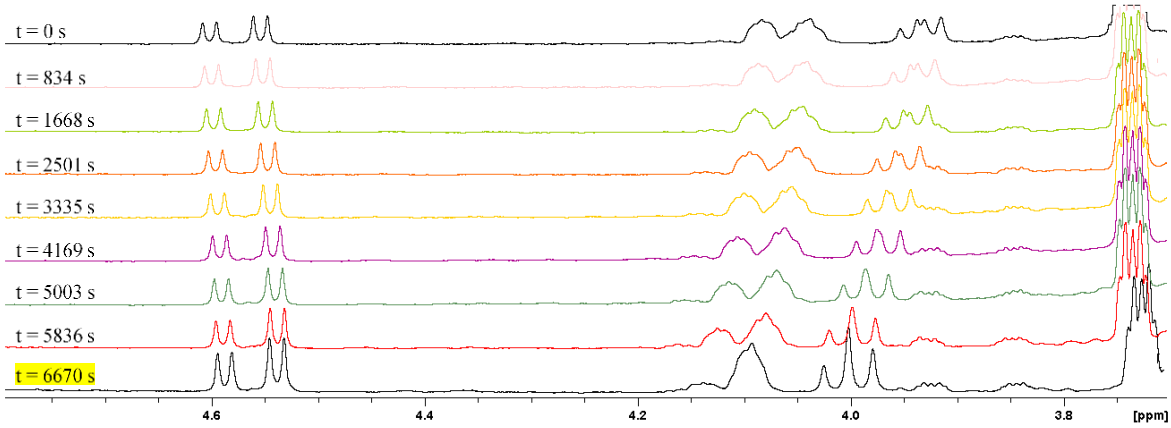

Figure 124. Partial 600 MHz ^{1}H NMR spectra which shows formation of intermediate X which reaches a maximum concentration at t = 6670 s.

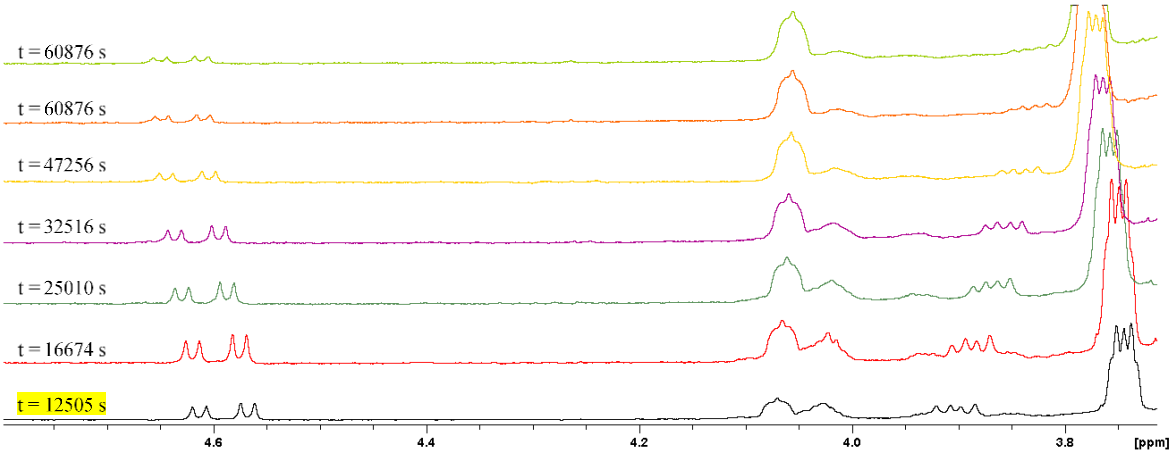

Figure 125. Partial 600 MHz ^{1}H NMR spectra which shows which shows consumption of intermediate **X** during the transition of the BH reaction of pyridine-4-carboxaldehyde **209** and methyl acrylate **46b** from "normal" 3-HQ-based catalysis to autocatalysis.

Analysis of the consumption of benzaldehyde as a function of time (**Figure 117**) showed constant duration for each succeeding half-life. Consequently, as shown in **Figure 126**, the plot of the natural logarithm of concentration of pyridine-4-carboxaldehyde **209** versus time shows an almost straight line with a negative slope denoting first order with respect to the aldehyde.

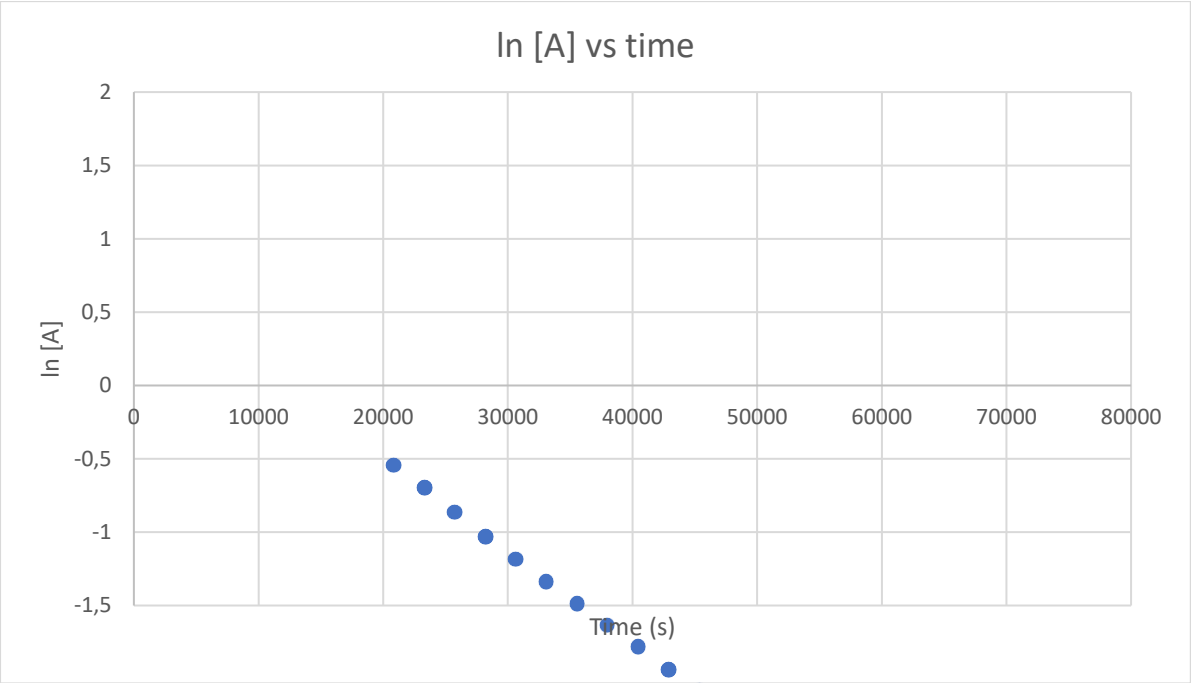

Figure 126. Plot of ln[aldehyde] versus time.

The order of the reaction with respect to methyl acrylate could not be readily determined from the ^{1}H NMR spectra due to overlapping of its proton signals with that of the product. Guided by significant points in the concentration time plots, we sought to identify possible species. The stack-plot of ^{1}H NMR spectra in **Figure 127** shows the progress of the reaction. At t = 0 s, signals corresponding to the pyridine ring of the product had already begun appearing and, at 1668 s (*ca.* 28 min) analysis of the concentration-time plot revealed that the product yield had reached 3%. The overlapping of the three characteristic BH signals (536 – 6.3 ppm) with signals of the three signals corresponding to vinylic protons of the acrylate is clearly shown (**Figure 128**). The corresponding stacked DEPT 135 NMR spectra (**Figure 129**) also shows formation of the product as the reaction progresses. Upon formation of the Baylis-Hillman adduct **210**, emergence of the signal at *ca.* 70 ppm corresponding to the alcoholic methine carbon is a key observation. Many of the spectra showed tiny signals especially in the aliphatic region representing the catalyst 3-HQ.

These preliminary results provide unambiguous insight into several critical aspects of the mechanism, *viz.*, (i) the autocatalytic character; (ii) experimental evidence of the structure of the intermediate **212**; (iii) identification of the rate-determining step with consumption of the intermediate **212**; and (iv) first-order consumption of the aldehyde **209**; and (v) pseudo 2nd order kinetics for the the rate-limiting autocatalytic step.

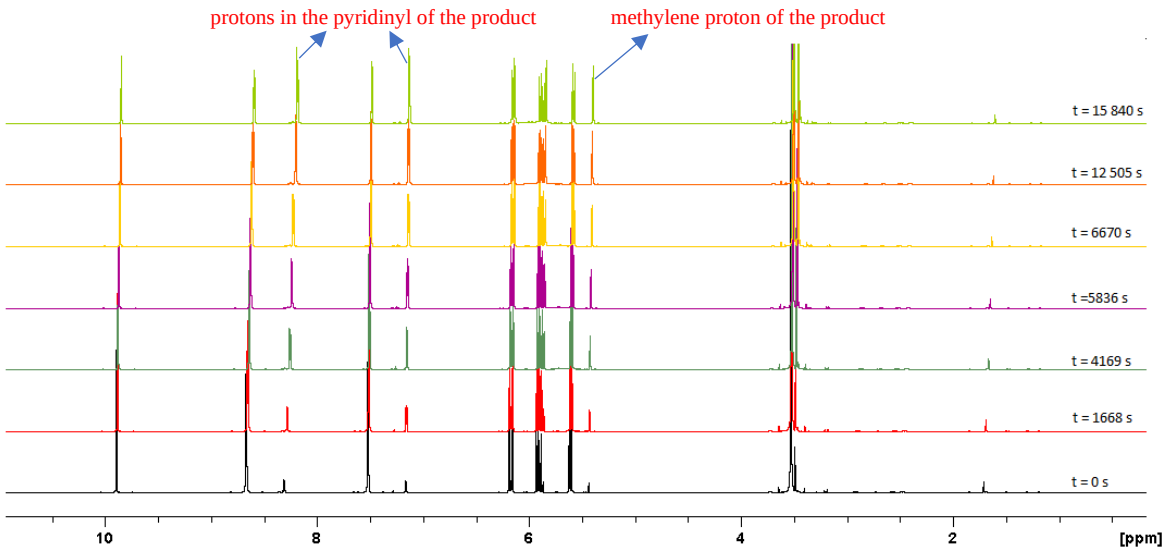

Figure 127. 600 MHz ^{1}H NMR spectra of the reaction mixture at different times at 298 K.

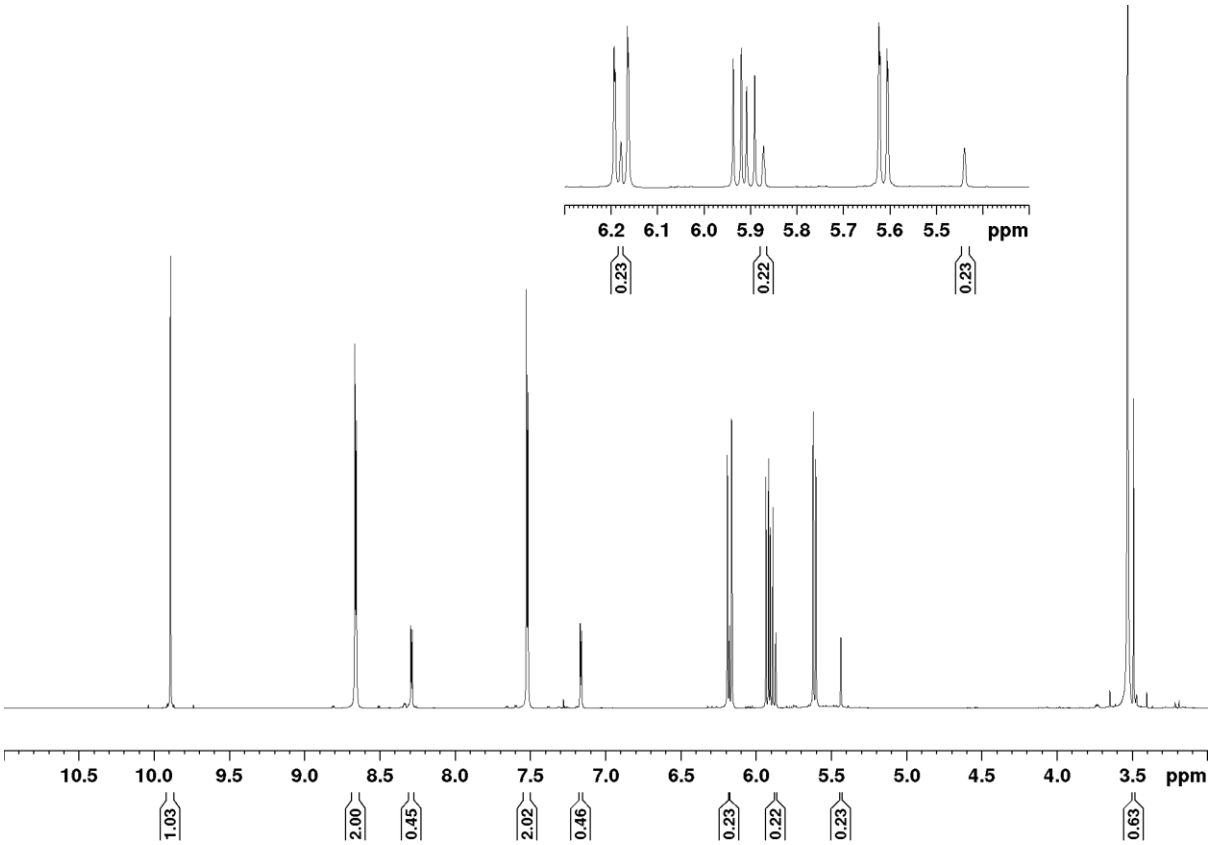

Figure 128. Kinetic ^{1}H NMR spectrum of the reaction mixture at 1668 s at 298 K.

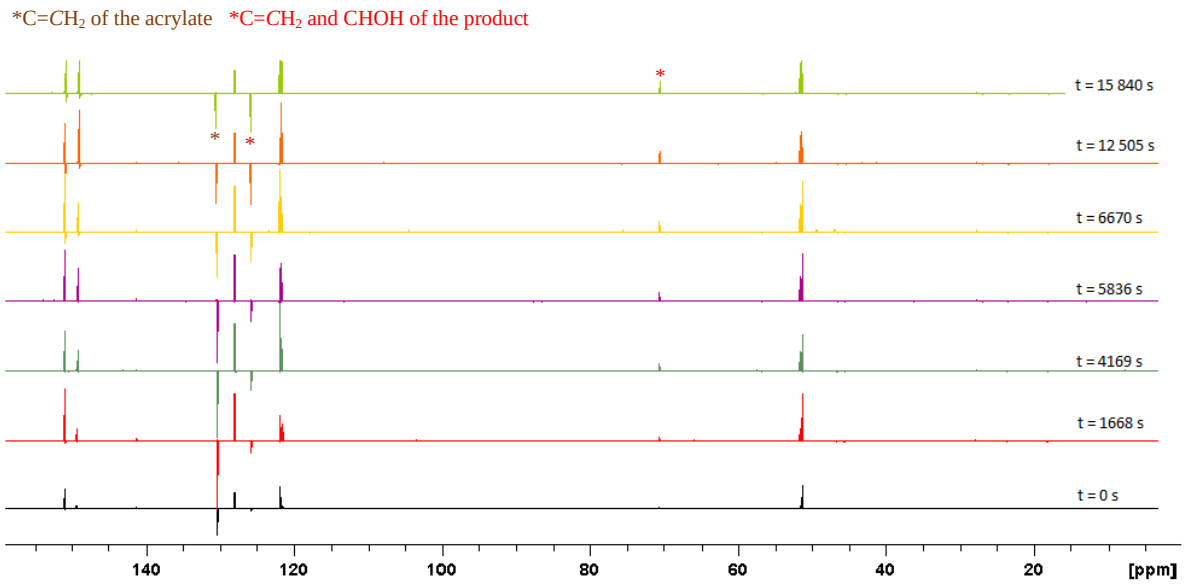

Figure 129. 150 MHz DEPT 135 NMR spectra of the reaction mixture at different times at 298 K.

2.7. Conclusions

The stated objectives of exploiting Baylis-Hillman methodology in developing efficient synthetic routes to series of 3-[(N-cycloalkylbenzamido)methyl]-2(1*H*)-quinolones and indolizine-2-carboxamide derivatives have been achieved. Access to former species was effected by optimising the generation of 3-chloromethyl-2(1*H*)-quinolones from the corresponding 3-hydroxymethyl-2(1*H*)-quinolones which were obtained through sequential reductive cyclisation of Baylis-Hillman adducts to 3-acetoxymethyl-2(1*H*)-quinolones and subsequent hydrolysis of the acetates. Reaction of the resulting alcohols with thionyl chloride afforded allylic halides, amination of which was effected by stirring each of them with primary cycloalkylamines (cyclopropropylamine, cyclopentylamine and cyclohexylamine). Finally, selected 3-[(cycloalkylamino)methyl]-2(1*H*)-quinolones were reacted with benzoyl chloride to afford a series of novel 3-[(cycloalkylbenzamidoamido)methyl]-2(1*H*)-quinolones. NMR characterisation of these compounds at ambient temperature was complicated due to broadening and signal multiplicity due to cycloalkyl ring flipping and the rotameric equilibria regularly encountered with carboxamides; variable temperature 1D- and 2D-NMR studies facilitated unambiguous characterisation of these compounds.

The key reactions in the preparation of the indolizine-2-carboxamides involved: (i) Baylis-Hillman reaction of pyridine-2-carboxaldehyde and methyl acrylate to afford methyl 3-hydroxy-2-methylene-3-(2-pyridinyl)propanoate; (ii) thermal cyclisation of the Baylis-Hillman adduct to afford indolizine esters; (iii) hydrolysis of the esters to esters to acids; (iv) and finally, amidation. Various approaches, *viz.*, boronic acid-, trimethyl borate- and phenylboronic acid-mediated coupling of the indolizine-2-carboxylic acid with amines proved unsuccessful. Exploration of a number of established coupling methodologies also proved unsatisfactory, but the relatively expensive tris(2,2,2-trifluoroethyl)borate, which is known to exhibit good functional group tolerance, facilitated preparation of *N*-(2-thiazolyl)indoliz-ine-2-carboxamide in low yield. The two-step procedure to access the desired amides *via* distillation of amido-Baylis-Hillman adducts prepared from the reaction of pyridine-2-carboxaldehyde and acrylamide derivatives proved to be particularly laborious especially when a series of indolizine-2-carboxamides was required. Moreover, the commercial availability of substituted acrylamides is limited and prior preparation would have been required. Ultimately, propylphosphonic anhydride (T3P) proved to be an effective coupling agent and permitted coupling of both acetylated and non-acetylated indolizine-2-carboxylic acids with a wide range

of amines under ambient to reflux conditions. Therefore, the synthesis of indolizine-2-carboxamide derivatives was achieved using propylphosphonic anhydride (T3P)-mediated coupling of indolizine-2-carboxulic acid derivatives with a range of amines of varying nucleophilic index.

Given the importance of the Baylis-Hillman reaction and ongoing international interest in the mechanism of this reaction, the opportunity was taken to use available high-field NMR facilities to search for possible reaction intermediates. Using a solution of pyridine-4-carboxaldehyde (the symmetrical analogue of pyridine-2-carboxaldehyde used in the foregoing studies), methyl acrylate and the tertiary amine catalyst, 3-hydroxyquinuclidine, in deuterated chloroform, high-field (600 MHz) ^{1}H and DEPT 135 NMR spectra were obtained. The results permitted clarification of the mechanistic sequence for this Baylis-Hillman reaction and, significantly, confirmation of autocatalysis and identification of a critical intermediate.

Bioassay of the 2-quinolone derivatives revealed a measure of HIV-1 IN inhibition, the most active inhibitor 3-[(*N*-cyclopentylamino)methyl-6-methoxy-2(1*H*)-quinolone **118e** producing residual HIV-1 activity of 40%. None of the compounds showed significant inhibition of either HIV-1 PR or RT and, apart from 3-[(*N*-cyclhexylamino)methyl]-6-methoxy-2(1*H*)-quinolone **117e** which resulted in 55% *pf*LDH residual activity, most of the compounds exhibited minimal anti-plasmodial activity, while none of them inhibited trypanosome growth. Many of these compounds presented no cytotoxic effect on HEK 293 cells at a concentration of 20 µM.

Selected indolizine-2-carboxamides were also subjected to bioassay and showed considerable inhibition of HIV-IN but no inhibition of RT at a concentration of 20 µM. Two of the acetylated derivatives [3-acetyl-*N*-(5-aminotriazol-3-yl)indolizine-2-carboxamide **187** (MIC_{90} of 31.25 µg/mL) and 3-acetyl-*N*-(thiazol-2-yl)-indolizine-2-carboxamide **194** (MIC_{90} of 15.63 µg/mL)] and, the isoniazid analolgue [N^2-phenylindolizine-2- carbohydrazide **199** (MIC_{90} of 31.25 µg/mL)] exhibited significant growth inhibition of mycobacteria after fourteen days. Screened at a single concentration of 20 µM, these amides also exhibited no cytotoxicity on HEK 293 cells but showed some activity against the malaria parasite. The lipophilic amide, *N*-[3-(1*H*-imidazol-yl)propyl)]indolizine-2-carboxamide **208**, exhibited the greatest activity against trypanosome with 76% residual activity of the parasite.

Inspired by the inherent fluorescent nature of indolizines and the possibility of using fluorescence microscopy to study their possible interaction with *mtb* cells, photophysical studies of the indolizine-2-carboxamides were undertaken. The results showed that these compounds generally exhibit absorption and red-shifted emission at wavelengths in the visible region with high molar absorption. The large, observed Stokes shifts of at least 55 nm indicate their suitability for use as fluorophores, particularly those with Stokes shifts greater that 80 nm, such as compounds **180, 192**, **193** and **198**. The non-acetylated amides appeared to exhibit enhanced emission compared to their acetylated analogues.

It is evident that various objectives of this study have been largely achieved and future research in this area is expected to include the following: -

i) Optimisation of the synthesis of indolizine-2-carboxamides and the envisaged synthesis of stable imides from coupling of the indolizine-2-carboxylic acid with amides bearing electron-donating substituents, for example, *p*-methoxybenzamide.

ii) Execution of structure activity relationship (SAR) studies on compounds that exhibited significant biological activity

iii) Consideration of employing varying reaction conditions to gain further insight into the kinetic and thermodynamic aspects of the Baylis-Hillman reaction.

3. Experimental

3.1. General details

The reagents used in this project were supplied by Merck® and were used without further purification. Thin layer chromatography (TLC) was carried out using Merck Silica gel 60 PF_{254} plates and were viewed under ultraviolet (UV) light, while column and preparatory plate chromatography was carried out using Merck silica gel 60 and Kieselgel 60 PF_{254}, respectively. Where required, solvents were purified according to methods prescribed by Vogel *et al.*[309] were used to purify solvents.

Melting points were measured using a Reichter 281313 hot-stage apparatus and are uncorrected. The IR data was obtained using Perkin-Elmer FT-IR spectrometer 100. NMR spectra were recorded on Bruker Fourier 300 MHz, Bruker Avance III 400 MHz or Bruker Avance II 600 MHz spectrometers in $CDCl_3$, methanol-d_4 or DMSO-d_6 and calibrated using solvent signals [[δ_H: 7.26 ppm for $CDCl_3$, 2.50 ppm for DMSO-d_6 and 3.31 ppm (quintuplet) for methanol-d_4; δ_C: 77.0 ppm for $CDCl_3$, 39.4 ppm for DMSO-d_6 and 49.05 for methanol-d_4]. The spectra were processed using Bruker Topspin 3.5 software®. High-resolution electrospray ionisation mass spectra (ESI-HRMS) were recorded on a Waters Synapt G2 instrument (University of Stellenbosch, Stellenbosch, South Africa); results marked with an asterisk reflect a calibration issue (using a Bruker Compact QTOF instrument at Rhodes) which will be addressed prior to publication.

Photophysical properties of selected indolizine-2-carboxamides were investigated by measuring ultraviolet-visible (UV–vis) spectra with a Shimadzu UV-2550 spectrophotometer and the corresponding emission spectra were with a Varian Eclipse spectrofluorometer at ambient temperature. All measurements have been performed using a 1 cm path length quartz cuvette for solution studies.

3.2. Part I

3.2.1. Synthesis of Baylis-Hillman adducts

General procedure: To a solution of the 2-nitrobenzaldehyde (**108**) derivative and methyl acrylate, ethyl acrylate or methyl vinyl ketone in $CHCl_3$, was added DABCO and the reaction mixture was stirred in a stoppered flask at room temperature. The reaction progress was monitored by TLC. The solvent and excess methyl acrylate, ethyl acrylate or methyl vinyl ketone were removed *in vacuo* and the crude product was purified by column chromatography.

Methyl 3-hydroxy-2-methylene-3-(2-nitrophenyl)propanoate 109a

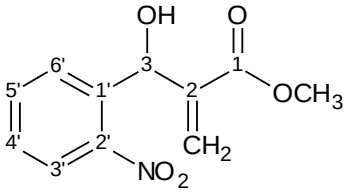

The general procedure was followed using 2-nitrobenzaldehyde **108a** (2.50 g, 16.5 mmol), methyl acrylate **46b** (2.24 g, 24.8 mmol) and DABCO (92.8 mg, 0.80 mmol) in $CHCl_3$ (5 mL), and the reaction mixture was stirred in a stoppered flask at room temperature for 7 days. The crude product was purified by column chromatography on silica gel [elution with hexane:EtOAc (3:1)] to afford, as a brown gel, methyl 3-hydroxy-2-methylene-3-(2-nitrophenyl)propanoate **109a** (1.28 g, 76%); ν_{max} (ATR)/cm^{-1} 3450 (OH) and 1729 (C=O); δ_H (400 MHz; $CDCl_3$) 3.39 (1H, s, OH), 3.73 (3H, s, OCH_3), 5.73 and 6.20 (2H, 2×s, C=CH_2), 6.36 (1H, s, 3-H), 7.46 (1H, t, *J* = 7.74 Hz, 4´-H), 7.65 (1H, t, *J* = 7.58 Hz, 5´-H), 7.75 (1H, d, J = 7.80, 6´-H), 7.94 (1H, d, J = 8.12, 3´-H); δ_c (100 MHz; $CDCl_3$) 52.0 (OCH_3), 67.5 (C-3), 124.4 (C-6´), 126.3 (C=CH_2), 128.7 (C-4´),128.9 C-5´), 129.0 (C-3´), 133.3(C-1´), 135.8 (C-2), 148.1 (C-2´) and 166.2 (C=O).

Methyl 3-hydroxy-2-methylene-3-(4,5-methylenedioxy-2-nitrophenyl)propanoate 109b

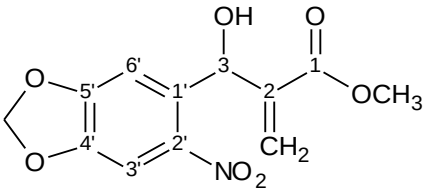

The general procedure was followed using 4,5-methylenedioxy-2-nitrobenzaldehyde **108b** (1.50 g, 7.70 mmol), methyl acrylate (0.73 g, 8.5 mmol) **46b** and DABCO (0.1 g, 0.9 mmol) in $CHCl_3$ (10 mL) and the reaction mixture was stirred in a stoppered flask at room temperature

for a month. The crude product was purified by column chromatography on silica gel [elution with hexane:EtOAc (3:1)] to afford, as white crystals, methyl 3-hydroxy-2-methylene-3-(4,5-methylenedioxy-2-nitrophenyl)propanoate **109b** (0.82 g, 38%), mp 121–124 ˚C (Lit.[37] 120-122 ˚C); (Found M-H: 280.0812. Calc. for $C_{12}H_{10}NO_7$: 280.0457); ν_{max} (ATR)/cm^{-1} 3487 (OH) and 1717 (C=O); δ_H (400 MHz; $CDCl_3$) 3.38 (1H, s, OH), 3.75 (3H, s, OCH_3), 5.69 and 6.18 (2H, 2 × s, C=CH_2), 6.11 (2H, s, OCH_2O),6.19 (1H,s 3-H), 7.16 (1H, s, 6´-H), 7.49 (1H, s, 3´-H); δ_c (100 MHz; $CDCl_3$) 52.2 (OCH_3), 67.6 (C-3), 103.0 (OCH_2O), 105.4 (C-6´), 107.7 (C-3´), 126.1 (C=*C*H_2), 133.7 (C-1´), 140.9 (C-2´), 142.1 (C-2), 147.3 (C-5´), 152.1 (C-4´) and 166.5 (C=O).

Methyl 3-(5-chloro-2-nitrophenyl)-3-hydroxy-2-methylenepropanoate 109c

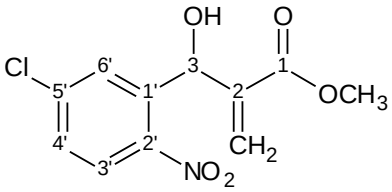

The general procedure was followed using 5-chloro-2-nitrobenzaldehyde **108c** (1.52 g, 8.3 mmol), methyl acrylate **46b** (1.07 g, 12.4 mmol) and DABCO (0.11 g, 0.91 mmol) in $CHCl_3$, and the reaction mixture was stirred in a stoppered flask at room temperature for several weeks. The crude product was purified by column chromatography on silica gel [elution with hexane:EtOAc (3:1)] to afford, as a brown solid, methyl 3-(5-chloro-2-nitrophenyl)-3-hydroxy-2-methylene-propanoate **109c** (1.87 g, 83%), mp 63–65 ˚C (Lit.[37] 64-66 ˚C); ν_{max} (ATR)/cm^{-1} 3471 (OH) and 1717 (C=O); δ_H (400 MHz; $CDCl_3$) 3.73 (1H, s, OH), 3.77 (3H, s, OCH_3), 5.69 and 6.37 (2H, 2×s, C=CH_2), 6.23 (1H, s, 3-H), 7.44 (1H, d, *J* = 8.56 Hz, 4´-H), 7.77 (1H, s, 6´-H) and 7.94 (1H, d, *J* = 8.68 Hz, 3´-H); δ_c (100 MHz; $CDCl_3$) 52.3 (OCH_3), 67.5 (C-3), 126.2 (C-4´), 126.8 (C=*C*H_2), 128.8 (C-6´), 129.1 (C-3´), 138.5 (C-1´), 139.6 (C-5´), 140.3 (C–2) 145.8 (C-2´) and 163.3 (C=O).

Methyl 3-(4-chloro-2-nitrophenyl)-3-hydroxy-2-methylenepropanoate 109d

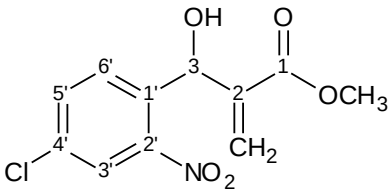

The general procedure was followed using 3-chloro-2-nitrobenzaldehyde **108d** (1.52 g, 8.30 mmol), methyl acrylate **44b** (1.07 g, 12.4 mmol) and DABCO (0.11 g, 0.91 mmol) in $CHCl_3$,

and the reaction mixture was stirred in a stoppered flask at room temperature for six weeks. The crude product was purified by column chromatography on silica gel [elution with hexane:EtOAc (3:1)] to afford, as a yellow-brown solid, methyl 3-(4-chloro-2-nitrophenyl)-3-hydroxy-2-methylene-propanoate **109d** (1.78 g, 79%), mp 68-71 ˚C (Lit.[37] 78-80 ˚C); ν_{max} (ATR)/cm^{-1} 3477 (OH) and 1710 (C=O); δ_H (400 MHz; $CDCl_3$) 3.42 (1H, br s, OH), 3.74 (3H, s, OCH_3), 5.73 and 6.37 (2H, 2×s, C=CH_2), 6.16 (1H, s, 3-H), 7.61 (1H, d, *J* = 8.22 Hz, 5´-H), 7.72 (1H, d, *J* = 8.48 Hz, 6´-H) and 7.95 (1H, s, 3´-H); δ_c (100 MHz; $CDCl_3$) 52.3 (OCH_3), 67.4 (C-3), 124.6 (C-6´), 126.7 (C=*C*H_2), 130.3 (C-5´), 133.5 (C-8´), 134.5 (C-1´), 134.6 (C-2), 140.3 (C-2´) and 166.3 (C=O).

Methyl 3-hydroxy-3-(5-methoxy-2-nitrophenyl)-2-methylenepropanoate 109e

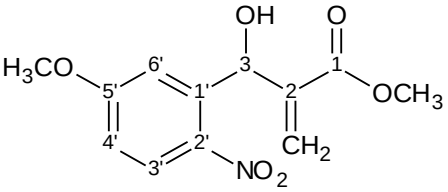

The general procedure was followed, using 3-methoxy-2-nitrobenzaldehyde **108e** (0.50 g, 2.8 mmol), methyl acrylate **46b** (0.26 g, 3.1 mmol) and DABCO (72.5 mg, 0.65 mmol) in $CHCl_3$ (5 mL) and the reaction mixture was stirred in a stoppered flask at room temperature for 4 weeks. The crude product was purified by column chromatography on silica gel [elution with hexane:EtOAc (3:1)] to afford, as a light yellow crystals, methyl 3-hydroxy-(5-methoxy-2-nitrophenyl)-2-methylene propanoate **109e** (0.63 g, 85%), mp 68-72 ˚C (Lit.[37] 69-71 ˚C); ν_{max} (ATR)/cm^{-1} 3380 (OH) and 1721 (C=O); δ_H (400 MHz; $CDCl_3$) 3.53 (1H, br s, OH), 3.76 (3H, s, OCH_3), 3.90 (H, s, 5´-OCH_3), 5.58 and 6.31 (1H, 2×s, C=C*H*$_2$), 6.30 (1H, s, 3-H), 6.90 (1H, d, *J* = 9.00 Hz, 3´-H), 7.39 (1H, s, 6´-H), and 8.08 (1H, d, *J* = 9.08 Hz, 4´-H); δ_c (100 MHz; $CDCl_3$) 52.2 (OCH_3), 59.9 (5´-OCH_3), 67.9 (C-3), 113.3 (C-4´), 113.6 (C-6´), 126.2 (C=*C*H_2), 127.8 (C-3´), 139.4 (C-5´), 140.8 (C-1´), 141.0 (C-2), 163.7, (C-2´) and 166.7 (C=O).

Methyl 3-hydroxy-3-(3-methoxy-2-nitrophenyl)-2-methylenepropanoate 109f

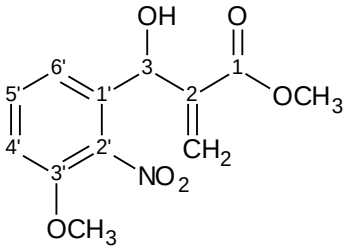

The general procedure was followed, using 3-methoxy-2-nitrobenzaldehyde **108f** (0.50 g, 2.8 mmol), methyl acrylate **46b** (0.26 g, 3.1 mmol) and DABCO (72.5 mg, 0.65 mmol) in $CHCl_3$ (5 mL) and the reaction mixture was stirred in a stoppered flask at room temperature for 2 weeks. The crude product was purified by column chromatography on silica gel [elution with hexane:EtOAc (3:1)] to afford, as a light yellow crystals, methyl 3-hydroxy-(3-methoxy-2-nitrophenyl)-2-methylene-propanoate **109f** (0.59 g, 79%), mp 109–112 ˚C (Lit.[37] 114-116 ˚C); ν_{max} (ATR)/cm^{-1} 3445 (OH) and 1708 (C=O); δ_H (400 MHz; $CDCl_3$) 3.70 (3H, s, OCH_3), 3.88 (3H, s, Ar-OCH_3), 3.94 (1H, s, OH), 5.64 and 5.86 (2H, 2×s, C=CH_2), 6.40 (1H, s, 3-H), 6.99 (1H, d, *J* = 8.24, 4´-H), 7.10 (1H, d, *J* = 9.00 Hz,6´-H) and 7.41 (1H, t, *J* = 8.10 Hz, 5´-H); δ_c (100 MHz; $CDCl_3$) 52.1 (OCH_3), 56.5 (Ar-OCH_3), 68.3 (C-3), 112.3 (C-4´), 119.4 (C-6´), 127.3 (C=*C*H_2), 131.3 (C-5´), 134.4 (C-1´), 139.7 (C-2 and C-3´), 150.9 (C-2´) and 166.1 (C=O).

3.2.2. Cyclisation of Baylis-Hillman adducts.

General procedure: Iron powder was added to a stirred solution of the Baylis-Hillman adduct in acetic acid at 110 °C. After stirring for 30 minutes, TLC showed the commencement of formation of a product and the reaction was allowed to run for 12 hours. The reaction mixture was then cooled to room temperature and the acetic acid removed *in vacuo*. Ethyl acetate was then added to the residue and the resulting mixture was stirred and filtered to remove the insoluble iron powder. The solid was washed with ethyl acetate and the washings were combined with the filtrate. The solvent was removed *in vacuo* and the crude product purified by column chromatography [on silica; elution with hexane:EtOAc (1:1)].

3-(Acetoxymethyl)-2(1*H*)-quinolone 111a

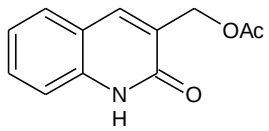

The general procedure was followed, using methyl 3-hydroxy-2-methylene-3-(2-nitrophenyl)propanoate **109a** (0.29 g, 1.2 mmol) and iron powder (0.31 g, 5.5 mmol) in acetic acid (10 mL) to afford, as white crystals, 3-(acetoxymethyl)-2(1*H*)-quinolone **111a** (0.19 g, 91%), mp 181-183 °C (Lit.[40] 167-169); (Found M+H: 218.0861. Calc. for $C_{12}H_{12}NO_3$: 218.0817); ν_{max} (ATR)/cm^{-1} 1735 and 1723 (double band) and 1659 (C=O); δ_H (400 MHz; $CDCl_3$) 2.19 (3H, s, OAc), 5.23 (2H, s, CH_2OAc), 7.23 (1H, t, *J* = 8.54 Hz, 6-H), 7.43 (1H, d, *J* = 8.16 Hz, 5-H), 7.53 (1H, t, *J* = 8.34 Hz, 7-H), 7.59 (1H, d, *J* = 7.88 Hz, 8-H), 7.88 (1H, s, 4-H) and 12.22 (1H, s, NH); δ_c (100 MHz; $CDCl_3$) 21.1 (CH_3), 61.4 (CH_2OAc), 115.9 (C-5), 119.6 (C-9), 122.8 (C-6), 127.5 (C-7), 127.9 (C-3), 130.6 (C-8), 138.0 (C-10), 138.5 (C-4), 163.1 (C -2) and 170.9 (C=O).

3-(Acetoxymethyl)-6,7-methylenedioxy-2(1*H*)-quinolone 111b

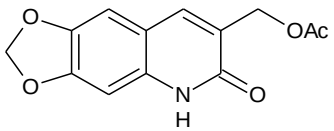

The general procedure was followed, using methyl 3-hydroxy-2-methylene-3-(4,5-methylenedioxy-2-nitrophenyl)propanoate **109b** (0.51 g, 1.8 mmol) and iron powder (0.41 g, 7.3 mmol) in acetic acid (15 mL) to afford, as white crystals, 3-(acetoxymethyl)-6,7-methylenedioxy-2(1*H*)-quinolone **111b** (0.24 g, 62%), mp 191-193 °C (Lit.[49] 227-228 °C); ν_{max}

(ATR)/cm^{-1} 1727 and 1659 (C=O); δ_H (400 MHz; $CDCl_3$) 2.15 (3H, s, CH_3), 5.17 (2H, s, CH_2OAc), 6.05 (2H, s, OCH_2O), 6.79 (1H, s, 5-H), 6..93 (1H, s, 8-H), 7.74 (1H, s 4-H) and 11.12 (NH); δ_c (100 MHz; $CDCl_3$) 20.7 (CH_3), 61.2 (CH_2OAc), 95.9 (C-8), 101.9 (OCH_2O), 105.1 (C-5), 114.5 (C-9), 128.9 (C-10), 134.9 (C-3), 139.5 (C-4), 144.8 (C-6), 151.2 (C-7), 163.3 C-2) and 170.8 (C=O).

3-(Acetoxymethyl)-6-chloro-2(1*H*)-quinolone 111c

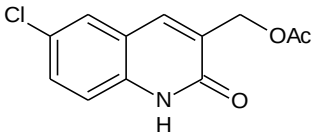

The general procedure was followed, using methyl 3-hydroxy-2-methylene-3-(5-chloro-2-nitrophenyl)propanoate **109c** (0.50 g, 1.9 mmol) and iron powder (0.49 g, 8.9 mmol) in acetic acid (10mL) to afford, as light yellow crystals, 3-(acetoxymethyl)-6-chloro-2(1*H*)-quinolone **111c** (0.42 g, 81%), mp 218-222 ˚C (Lit.[49] 229-230 ˚C); (Found M+H: 252.0417. Calc. for $C_{12}H_{11}ClNO_3$: 252.0428); ν_{max} (ATR)/cm^{-1} 1739 and 1663 (C=O); δ_H (400 MHz; $CDCl_3$) 2.18 (3H, s, OAc), 5.21 (2H, s, CH_2OAc), 7.36 (1H, d, *J* = 8.72 Hz, 7-H), 7.47 (1H, d, *J* = 9.42 Hz, 8-H), 7.57 (1H, s, 5-H), 7.77 (1H, s, 4-H) and 12.35 (1H, br s, NH); δ_c (100 MHz; $CDCl_3$) 20.9 (CH_3), 61.2 (CH_2OAc), 117.3 (C-8) , 120.5 (C-10), 127.0 (C-9), 128.2 (C-5), 129.0 (C-7), 130.8 (C-3), 136.4 (C-6), 136.9 (C-4), 162.8 (C-2) and 170.6 (C=O).

3-(Acetoxymethyl)-7-chloro-2(1*H*)-quinolone 111d

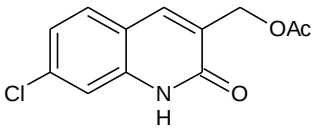

The general procedure was followed, using methyl 3-hydroxy-2-methylene-3-(4-chloro-2-nitrophenyl)propanoate **109d** (0.50 g, 1.9 mmol) and iron powder (0.49 g, 8.9 mmol) in acetic acid (10 mL) to afford, as white crystals, 3-(acetoxymethyl)-7-chloro-2(1*H*)-quinolone **111d** (0.44 g, 86%); mp 161-163 ˚C, ν_{max} (ATR)/cm^{-1} 1736 and 1665 (C=O); δ_H (400 MHz; $CDCl_3$) 2.18 (3H, s, CH_3), 5.19 (2H, s, CH_2OAC), 7.20 (1H, d, *J* = 9.00 Hz, 5-H), 7.30 (1H, s, 8-H), 7.51 (1H, d, *J* = 8.44 Hz, 6-H), 7.80 (1H, s, 4-H) and 10.80 (1H, br s, NH); δ_c (100 MHz; $CDCl_3$) 21.0 (CH_3), 61.2 (CH_2OAc), 115.2 (C-5), 118.1 (C–9 and 10), 123.6 (C-6), 128.1 (C–3), 129.2 (C-8), 136.8 (C-7), 137.8 (C-4), 162.5 (C-2) and 170.7 (C=O).

3-(Acetoxymethyl)-6-methoxy-2(1*H*)-quinolone 111e

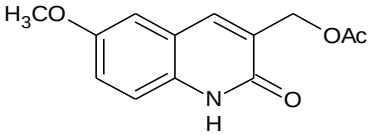

The general procedure was followed, using methyl 3-hydroxy-3-(5-methoxy-2-nitrophenyl)-2-methylenepropanoate **109e** (0.20 g, 0.7 mmol) and iron powder (0.19g, 3.5mmol) in acetic acid (5mL) to afford, as brown crystals, 3-(acetoxymethyl)-6-methoxy-2(1*H*)-quinolone **111e** (0.18 g, 99%), mp 183-185 ˚C; ν_{max} (ATR)/cm^{-1} 1728 and 1654 (C=O); δ_H (400 MHz; $CDCl_3$) 2.18 (3H, s, CH_3), 3.86 (3H, s, 6-OCH_3), 5.22 (2H, s, CH_2OAc), 7.00 (1H, s, 5-H), 7.16 (1H, d, *J* = 8.72 Hz, 7-H), 7.34 (1H, d, *J* = 8.84 Hz, 8-H), 7.82 (1H, s, 4-H), and 12.02 (1H, br s, NH); δ_c (100 MHz; $CDCl_3$) 21.1 (CH_3), 55.6 (6-OCH_3), 61.5 (CH_2OAc), 108.8 (C-8), 117.2 (C-5), 120.1 (C-7), 120.3 (C-9), 125.6 (C-10), 127.8 (C-3), 138.1 (C-4), 155.2 (C-6), 162.6 (C-2) and 170.9 (C=O).

3-(Acetoxymethyl)-8-methoxy-2(1*H*)-quinolone 111f

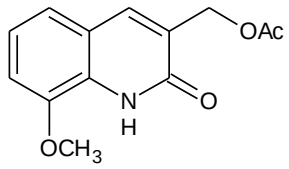

The general procedure was followed, using methyl 3-hydroxy-3-(3-methoxy-2-nitrophenyl)-2-methylenepropanoate **109f** (0.20 g, 0.8 mmol) and iron powder (0.26 g, 4.6 mmol) in acetic acid (10mL) to afford, as green crystals, 3-(acetoxymethyl)-8-methoxy-2(1*H*)-quinolone **111f** (0.12 g, 63%), mp 191-193 (Lit.[49] 170-172 ˚C); ν_{max} (ATR)/cm^{-1} 1740 and 1647 (C=O); δ_H (400 MHz; DMSO-d_6) 2.12 (CH_3), 3.90 (3H, s, 8-OCH_3), 4.98 (2H, s, CH_2OAc), 7.14 (2H, d, J = 5.00 Hz, 5- and 7-H), 7.28 (1H, t, *J* = 9.00 Hz, 6-H), 7.88 (1H, s, 4-H) and 10.97 (1H, br s, NH); δ_c (100 MHz; DMSO-d_6) 20.6 (CH_3), 56.0 (8-OCH_3), 60.9 (CH_2OAc), 110.9 (C-5), 119.1 (C-6), 119.6 (C-9), 121.9 (C-7), 128.2 (C-10), 128.3 (C-3), 136.8 (C-4), 145.6 (C-8), 160.4 (C-2) and 170.1 (C=O).

3.2.3. Hydrolysis of 3-(Acetoxymethyl)-2(1H)-quinolone derivatives.

General procedure: A mixture of 3-(acetoxymethyl)-2(1*H*)-quinolone derivative (1 eq) and potassium carbonate (3 eq) in methanol-water (1:1) was stirred at room temperature for 24 hours after which TLC showed complete conversion of the substrate. The reaction mixture was concentrated *in vacuo*, and the precipitate washed with dichloromethane. The filtrate and washings were dried with anhydrous $MgSO_4$, filtered, and then concentrated to give the 3-(hydroxymethyl)-2(1*H*)-quinolone derivative.

3-(Hydroxymethyl)-2(1*H*)-quinolone 112a

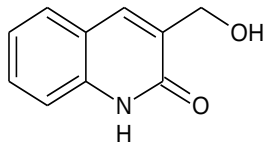

Method A: A mixture of 3-(acetoxymethyl)-2(1*H*)-quinolone **111a** (0.13 g, 0.59 mmol) and potassium carbonate (0.25g, 1.8 mmol) in methanol containing few drops of water was stirred at room temperature for one hour. The reaction mixture was filtered and the precipitate washed with methanol (5 mL). The combined methanolic filtrate and washings were concentrated and the crude product was purified by column chromatography [on silica gel; elution with hexane:EtOAc (1:1)] to provide, as yellow crystals, 3-(hydroxymethyl)-2(1*H*)-quinolone **112a** (65.0 mg, 63%), mp 208-210 °C (Lit.[40] 199-200 °C); (Found MH^+: 176.0714. Calc. for $C_{10}H_{10}NO_2$: 176.0712); ν_{max} (ATR)/cm^{-1} 3368 (OH) and 1643 (C=O); δ_H (400 MHz; DMSO-d_6) 4.40 (2H, s, CH_2OH), 5.24 (1H, s, OH), 7.16 (1H, t, *J*=7.16 Hz, 6-H), 7.30 (1H, d, *J* = 8.05 Hz, 5-H), 7.45 (1H, t, *J* = 7.58 Hz, 7-H), 7.68 (1H, d, *J* = 7.48 Hz, 8-H), 7.85 (1H, s, 4-H) and 11.81 (1H, br s, 1-H); δ_c (100 MHz; DMSO-d_6) 58.9 (CH_2OH), 115.3 (C-5), 119.8 (C-9), 122.3 (C-6), 128.0 (C-7), 129.9 (C-3), 134.0 (C-8), 134.5 (C-10), 138.1(C-4) and 161.6 (C-2).

Method B: The general procedure was followed, using 3-acetoxymethyl-2(1*H*)-quinolone **111a** (0.64 g, 2.94 mmol) and potassium carbonate (1.23 g, 8.9 mmol) in methanol:water (1:1). Work-up afforded, as yellow crystals, 3-(hydroxymethyl)-(1*H*)-2-quinolone **112a** (0.45 g, 87%).

3-(Hydroxymethyl)-6,7-methylenedioxy-2(1*H*)-quinolone 112b

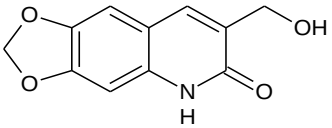

The general procedure was followed, using 3-(acetoxymethyl)-6,7-methylenedioxy-2(1*H*)-quinolone **111b** (0.10 g, 0.40 mmol) and potassium carbonate (0.17 g, 1.2 mmol). Work-up afforded, as yellow crystals, 3-(hydroxymethyl)-6,7-methylenedioxy-2(1*H*)-quinolone **112b** (69.6 mg, 79%), mp 188-190 ˚C; ν_{max} (ATR)/cm^{-1} 3149 (OH) and 1639 (C=O); δ_H (400 MHz; DMSO-d_6) 4.40 (2H, s, CH_2OH), 6.06 (2H, s, OCH_2O), 6.84 (1H, s, 5-H), 7.21 (1H, s, 8-H) and 7.72 (1H, s, 4-H).

3-(Hydroxymethyl)-6-chloro-2(1*H*)-quinolone 112c

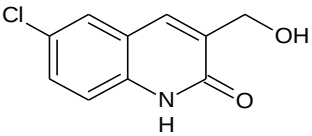

The general procedure was followed, using 3-(acetoxymethyl)-6-chloro-2(1*H*)-quinolone **111c** (0.30 g, 1.1 mmol) and potassium carbonate (0.47 g, 3.4 mmol). Work-up afforded, as yellow crystals, 3-(hydroxymethyl)-6-chloro-2(1*H*)-quinolone **112c** (0.20 g, 83%), mp 213-218 ^{0}C; ν_{max} (ATR)/cm^{-1} 3330 (OH) and 1644 (C=O); δ_H (400 MHz; $CDCl_3$) 4.66 (2H, s, CH_2OH), 7.14 (1H, d, *J* = 8.76 Hz, 7-H), 7.41 (1H, d, *J* = 8.68 Hz, 8-H), 7.51 (1H, s, 5-H), 7.64 (1H, s, 4-H) and 8.02 (1H, br s, 1-H); δ_C (100 MHz; $CDCl_3$) 58.8 (CH_2OH), 117.3 (C-8) , 120.5 (C-10), 127.0 (C-9), 128.2 (C-5), 129.0 (C-7), 130.8 (C-3), 136.4 (C-6), 136.9 (C-4) and 162.8 (C=O).

7-Chloro-3-(Hydroxymethyl)-2(1*H*)-quinolone 112d

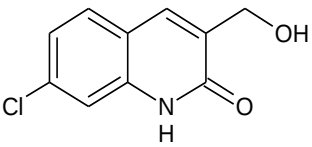

The general procedure was followed, using 3-(acetoxymethyl)-7-chloro-2(1*H*)-quinolone **111d** (0.11 g, 0.39 mmol) and potassium carbonate (0.16 g, 1.2 mmol). Work-up afforded, as yellow crystals, 7-chloro-3-(hydroxymethyl)-2(1*H*)-quinolone **112d** (68.6 mg, 85%), mp 209-212 ˚C; (Found MH$^+$: 210.0314. Calc. for $C_{10}H_9ClNO_2$: 210.0322); ν_{max} (ATR)/cm^{-1} 3081 (OH) and 1622 (C=O); δ_H (400 Hz; DMSO-d$_6$) 4.38 (2H, s, CH_2OH), 7.03 (1H, d, *J* = 58.34 Hz, 5-H),

7.26 (1H, s, 8-H), 7.58 (1H, d, J = 8.36 Hz, 6-H) and 7.67 (1H, s, 4-H); δ_c (100 MHz; DMSO-d_6) 58.8 (CH_2OH), 114.6 (C-5), 118.9 (C-9), 122.5 (C-10), 127.4 (C-6), 29.9 (C-3), 133.5 (C-8), 134.1 (C-7), 135.8 (C-4) and 161.4 (C-2).

3-(Hydroxymethyl)-6-methoxy-2(1*H*)-quinolone 112e

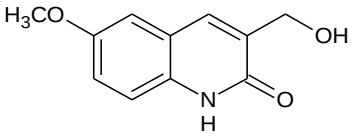

The general procedure was followed, using crude 3-(acetoxymethyl)-6-methoxy-2(1*H*)-quinolone **111e** (0.49 g, 2.0 mmol) and potassium carbonate (0.83 g, 6.0 mmol). Work up afforded, as yellow crystals, 3-(hydroxymethyl)-6-methoxy-2(1*H*)-quinolone **112e** (0.23 g, 56%), mp 101-103 °C; (Found MH^+: 206.0813. Calc. for $C_{11}H_{12}NO_3$: 206.0817), ν_{max} (ATR)/cm^{-1} 3345 (OH) and 1656 (C=O); δ_H (100 MHz; methanol-d_4) 3.79 (3H, br s, Ar-OCH_3), 4.54 (2H, s, CH_2OH), 7.12 (2H, br s, 7-and 8-H), 7.22 (1H, br s, 5-H) and 7.89 (1H, br s, 4-H); δ_c (100 MHz; methanol-d_4) 56.1 (Ar–OCH_3) , 60.4 (CH_2OH), 109.9 (C-8), 117.7 (C-5), 120.8 (C-9), 122.2 (C-7), 133.2 (C-10), 134.2 (C-3), 136.6 (C-4), 156.9 (C-6) and 163.4 (C-2).

3-(Hydroxymethyl)-8-methoxy-2(1*H*)-quinolone 112f

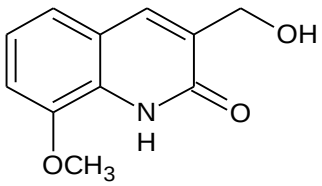

The general procedure was followed, using crude 3-acetoxymethyl-7-methoxy-2(1*H*)-quinolone **111f** (0. 53g, 2.15 mmol) and potassium carbonate (0.89 g, 6.5 mmol). Work-up afforded, as yellow crystals, 3-(hydroxymethyl)-7-methoxy-2(1*H*)-quinolone **112f** (0.15 g, 34%), mp 92-95 °C; (Found MH^+: 206.0807. Calc. for $C_{11}H_{12}NO_3$: 206.0817); ν_{max} (ATR)/cm^{-1} 3340 (OH) and 1640 (C=O); δ_H (100 MHz; methanol-d_4) 3.25 (1H, OH), 4.54 (2H, br s, CH_2OH), 7.05 (1H, br s, 5-H), 7.14 (2H, br s, 6 and 7-H) and 7.89 (1H, br s, 4-H); δ_c (100 MHz; methanol-d_4) 56.6 (8-OCH_3), 60.3 (CH_2OH), 111.1 (C-5), 120.6 (C-6), 121.8 (C-9), 123.9 (C-7), 128.7 (C-10), 134.5 (C-3), 136.8 (C-4), 147.5 (C-8) and 163.5 (C-2).

3.2.4. Chlorination of 3-(hydroxymethyl)-2(1*H*)-quinolones.

General procedure: An excess of thionyl chloride ($SOCl_2$) was added to the 3-(hydroxymethyl)-(1*H*)-2-quinolone derivative and the reaction mixture was stirred in a stoppered flask at room temperature. (*Caution: Thionyl chloride is very volatile and corrosive*.) After completion, the mixture was diluted with dichloromethane, and then excess thionyl chloride quenched with water. The organic layer was then dried and concentrated *in vacuo* to afford the 3-(chloromethyl)-(1*H*)-2-quinolone derivative **113**.

3-(Chloromethyl)-2(1*H*)-quinolone 113a

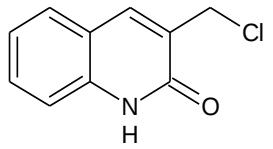

The general method was followed, using 3-(hydroxymethyl)-2(1*H*)-quinolone **112a** (0.25 g, 1.4 mmol) to obtain, as white crystals, 3-(chloromethyl)-2(1*H*)-quinolone **113a** (0.20 g, 91%), mp. 171-173 °C; (Found MH^+: 194.0376. Calc. for $C_{10}H_9ClNO$: 194.0379); ν_{max} (ATR)/cm^{-1} 1656 (C=O); δ_H (400 MHz; $CDCl_3$) 4.71 (2H, s, CH_2Cl), 7.25 (1H, t, *J* = 7.76 Hz, 6-H) 7.41 (1H, d, *J* = 8.20 Hz, 5-H), 7.54 (1H, t, *J* = 7.60 Hz, 7-H), 7.60 (1H, d, *J* = 7.88 Hz, 8-H), 7.80 (1H, s, 4-H) and 11.80 (1H, br s, 1-H); δ_c (100 MHz; $CDCl_3$) 41.4 (CH_2Cl), 115.8 (C-5), 119.6 (C-9), 123.0 (C-6), 128.6 (C-7), 128.9 (C-3), 130.9 (C-8), 138.1(C-10), 139.4 (C-4) and 162.6 (C-2).

3-(Chloromethyl)-6,7-methylenedioxy-2(1*H*)-quinolone 113b

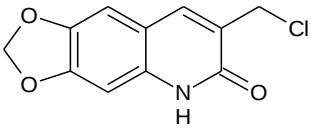

The general method was followed, using 3-(hydroxymethyl)-6,7-methylenedioxy-2(1*H*)-quinolone **112b** (0.16 g, 0.72 mmol) to obtain, as brick red crystals, 3-(chloromethyl)-6,7-methylenedioxy-2(1*H*)-quinolone **113b** (96.2 mg, 57%); mp 188-190 °C; ν_{max} (ATR)/cm^{-1} 1640 (C=O); δ_H (400 MHz; DMSO-d_6) 4.27 (2H, s, CH_2Cl), 6.07 (2H, s, OCH_2O), 6.81 (1H, s, 5-H), 7.21 (1H, s, 8-H), 7.72 (1H, s, 4-H), and 11.75 (1H, s, NH); δ_c (100 MHz; DMSO-d_6) 68.7 (CH_2Cl), 94.8 (C-8), 101.6 (OCH_2O), 105.2 (C-5), 113.2 (C-9), 126.8 (C-10), 134.7(C-3), 135.3 (C-4), 143.1(C-6), 149.5 (C-7) and 160.7 (C-2).

6-Chloro-3-(chloromethyl)-2(1*H*)-quinolone 113c

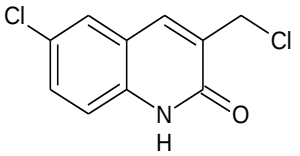

The general method was followed, using 6-chloro-3-(hydroxymethyl)-2(1*H*)-quinolone **112c** (0.44 g, 2.1 mmol) to obtain, as light yellow crystals, an tautomeric mixture of 3-(chloromethyl)-6-chloro-(*1H*)-quinol-2-one **113c** (0.30 g, 74%); mp 182-185°C; (Found M-H: 227.9973. Calc. for $C_{10}H_7Cl_2NO$: 228.0747); υ_{max} (ATR)/cm^{-1} 1654 (C=O).

Tautomer 1 (63%)

δ_H (400 MHz; DMSO-d_6) 4.64 (2H, s, CH_2Cl), 7.32 (1H, d, *J* = 8.60 Hz, 8-H), 7.56 (1H, d, *J* = 8.68 Hz, 7-H), 7.83 (1H, s, 5-H), 8.09 (1H, s, 4-H) and 12.14 (1H, s, NH); δ_c (100 MHz; DMSO-d_6) 41.6 (CH_2Cl), 116.9 (C-8), 119.8 (C-10), 125.8 (C-9), 127.0 (C-5), 134.4, 130.6 (C-7), 130.8 (C-3), 137.4 (C–6), 138.0 (C-4) and 160.3 (C=O).

Tautomer 2 (37%)

δ_H (400 MHz; DMSO-d_6) 4.67 (2H, s, CH_2Cl), 7.23 (1H, t, *J* = 7.68 Hz, 8-H), 7.69 (2H, m, *J* = 6.82 Hz, 7-H and 5-H), 8.18 (1H, s, 4-H), and 11.34 (1H, s, NH); δ_c (100 MHz; DMSO-d_6) 41.5 (CH_2Cl), 119.8 (C-10), 122.8 (C-8), 125.8 (C-9), 127.5 (C-10), 130.6 (C-7), 130.8 (C-3), 137.4 (C-6), 139.1 (C-4) and 160.3 (C=O).

7-Chloro-3-(chloromethyl)-2(1*H*)-quinolone 113d

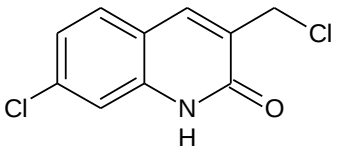

The general method was followed, using 7-chloro-3-(hydroxymethyl)-2(1*H*)-quinolone **112d** (0.20 g, 0.96 mmol) to obtain, as a white powder, 7-chloro-3-(chloromethyl)-2(1*H*)-quinolone **113d** (0.14 g, 79%), mp 208-210 °C; (Found M-H: 227.9976. Calc. for $C_{10}H_7Cl_2NO_3$: 228.0746); ν_{max} (ATR)/cm^{-1} ; δ_H (400 MHz; DMSO-d_6) 4.63 (2H, s, CH_2Cl), 7.25 (1H,d, *J* = 8.44 Hz, 5-H), 7.34 (1H, s, 8-H), 7.74 (1H, d, *J* = 8.48 Hz, 6-H) and 8.14 (1H, s, 4-H); δ_c (100 MHz; DMSO-d_6) 41.4 (CH_2Cl), 116.9 (C-5), 119.8 (C-9), 125.8 (C-10), 127.0 (C-6), 130.4 (C-3), 130.6 (C-8), 137.3 (C-7), 138.0 (C-4) and 160.3 (C-2).

Alternative method: To a stirred solution of 7-chloro-3-hydroxymethyl-2(1*H*)-quinolone **112d** (0.20g) in dry benzene was added $SOCl_2$ (0.6ml), the reaction mixture was stirred under

reflux for 2 days. The reaction mixture was diluted with CH_2Cl_2, sodium bicarbonate added, and the mixture filtered. The residue was washed with chloroform and filtrate concentrated *in vacuo* to obtain, as yellow crystals, 7-chloro-3-chloromethyl-2(1*H*)-quinolone **113d**. Crude NMR confirmed the formation of a product and prolonged time was require to enhance yield and removal of benzene presented challenges because of its high boiling point.

3-(Chloromethyl)-6-methoxy-2(1*H*)-quinolone 113e

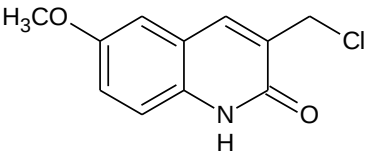

The general procedure was followed, using 3-(hydroxymethyl)-6-methoxy-2(1*H*)-quinolone **112e** (0.23 g, 1.1 mmol) to obtain, as light yellow crystals, 3-(chloromethyl)-6-methoxy-2(1*H*)-quinolone **113e** (0.10 g, 49%), mp 182-186 °C; (Found MH^+: 224.0474. Calc. for $C_{11}H_{11}ClNO_2$: 224.0479); ν_{max} (ATR)/cm^{-1} 1662 (C=O); δ_H (400 MHz, DMSO-d_6) 3.78 (3H, s, Ar-OCH_3), 4.64 (2H, s, CH_2Cl), 7.20 (1H, br s, Ar-H), 7.25 (2H, br s, 2×Ar-H), 8.06 (1H, br s, Ar-H), and 11.90 (1H, br s, NH); δ_c (100 MHz; DMSO-d_6) 41.4 (CH_2Cl), 55.03 (Ar–OCH_3), 108.9 (C-8), 115.9 (C-5), 118.9 (C-9), 119.7 (C-7), 129.0 (C-10), 132.8 (C-3), 138.5 (C-4), 153.8 (C-6) and 159.7 (C=O).

3-(chloromethyl)-8-methoxy-2(1*H*)-quinolone 113f

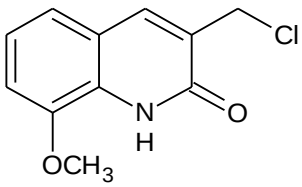

The general method was followed, using 3-(hydroxymethyl)-8-methoxy-2(1*H*)-quinolone **112f** (0.14 g, 0.70 mmol) to obtain, as light yellow crystals, 3-(chloromethyl)-8-methoxy-2(1*H*)-quinolone **113f** (0.12 g, 89%), mp 164-166 °C; (Found MH^+: 224.0468. Calc. for $C_{11}H_{11}ClNO_2$: 224.0479); ν_{max} (ATR)/cm^{-1} 1645 (C=O); δ_H (400 MHz; $CDCl_3$) 4.01 (3H, s, 8-OCH_3), 4.70 (2H, br s, CH_2Cl), 7.15 (1H, br s, Ar-H), 7.36 (1H, br s, Ar-H), 8.31 (1H, br s, Ar-H), 8.58 (1H, br s, Ar-H) and 12.25 (1H, br s, NH); δ_c (100 MHz; $CDCl_3$) 39.9 (CH_2Cl), 56.8 (8-OCH_3), 111.5 (C-5), 119.6 (C-6), 121.5 (C-9), 122.8 (C-10), 125.6 (C-7), 126.7 (C-3), 142.5, 147.2 (C-8) and 160.8 (C=O).

3.2.5. Synthesis of 3-[(cycloalkylamino)methyl]-2(1H)-quinolone.

General procedure: A solution 3-chloromethyl-2(*1H*)-quinolone derivative and cycloalkylamine in minimum solvent (CH_2Cl_2) was stirred in a stoppered flask at room temperature and the reaction monitored with TLC until completion. The reaction mixture was concentrated *in vacuo* and then purified by preparatory plate on silica gel (elution with EtOAc) to afford the desired product.

***3-[(Cyclohexylamino)methyl]-2(*1H*)-quinolone* 114a**

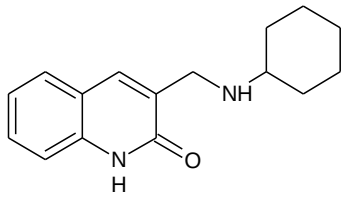

The general procedure was followed, using 3-(chloromethyl)-2(1*H*)-quinolone **113a** (94.4 mg, 0.49 mmol) and cyclohexylamine to afford as brown crystals, *3-[(cyclohexylamino)methyl]-2(1*H*)-quinolone* **114a** (83.5 mg, 74%), mp 114–117 °C (Found MH^+: 257.1644. Calc. for $C_{16}H_{21}N_2O$: 257.1654); m_{max} (ATR)/cm^1 3290 (NH) and 1648 (C=O); δ_H (600 MHz; $CDCl_3$) 1.46, 1.56, 1.73 and 1.91 (10H, m, cyclohexyl CH_2), 3.17 (1H, dd, J = 8.8 and 4.4 Hz, CH), 3.82 (2H, s, CH_2N), 7.21 (1H, t, J = 7.5 Hz, Ar-H), 7.29 (1H, d, J = 8.4 Hz, Ar-H), 7.46 (1H, t, J = 7.5 Hz, Ar-H), 7.55 (1H, d, J = 7.8 Hz, Ar-H), and 7.79 (1H, s, 4-H); δ_c (150 MHz; $CDCl_3$) 25.0, 26.1 and 33.5 (cyclohexyl CH_2), 46.4 (CH_2N), 56.0 (CHN). 115.5, 120.0, 122.6, 127.5, 129.8, 130.8, 137.2 and 137.5 (Ar-C) and 164.0 (C=O).

***3-[(Cyclopentylamino)methyl]-(*1H*)-2-quinolone* 115a**

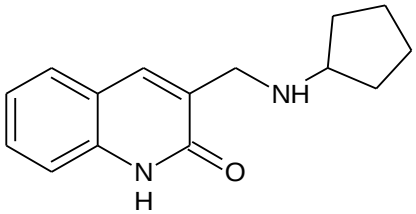

The general procedure was followed, using 3-(chloromethyl)-2(1*H*)-quinolone **113a** (0.10 g, 0.52 mmol) and cyclopentylamine to afford as light yellow crystals, *3-[(cyclopentylamino)methyl]-2(1*H*)-quinolone* **115a** (76.6 mg, 60%), mp 109-112 °C; (Found MH^+: 243.1483. Calc. for $C_{15}H_{19}N_2O_2$: 243.1498), ν_{max} (ATR)/cm^{-1} 3295 (NH) and 1652 (C=O); δ_H (600 MHz, DMSO-d_6) 1.35, 1.47, 1.63 and 1.73 (8H, 4 × m, cyclopentyl CH_2), 2.08 (1H, br s, 12-H), 3.03 (1H, br s, NH), 3.55 (2H, s, 11-H), 7.16 (1H, t, *J* = 6.6 Hz, 7-H), 7.30

(1H, d, J = 7.8 Hz, 8-H), 7.44 (1H, t, J = 8.1 Hz, 6-H), 7.64 (1H, d, J = 7.1 Hz, 5-H), 7.84 (1H, s, 4-H) and 11.79 (1H, s, NH); δ_C (150 MHz, DMSO-d_6) 23.7 and 32.6 (Cyclopentyl CH_2), 46.9 (CH_2N), 58.7 (CH), 114.8 (C-8), 119.3 (C-10), 121.8 (C-7), 127.5 (C-5), 129.4 (C-6), 132.4 (C-4), 135.4 (C-9), 137.7 (C-3) and 161.9 (C=O).

***3-[(Cyclopropylamino)methyl]-2(*1H*)-quinolone* 116a**

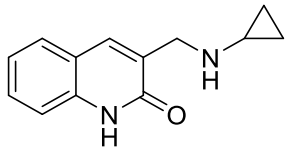

The general procedure was followed, using 3-(chloromethyl)-2(1*H*)-quinolone and cyclopropylamine to afford, as cream white crystals, *3-[(cyclopropylamino)methyl]-2(1*H*)-quinolone* **116a**; mp 140-143 ºC; (Found MH^+: 215.1086. Calc. for $C_{13}H_{15}N_2O$: 214.1185); ν_{max} (ATR)/cm^{-1} 3294 (NH) and 1643 (C=O); δ_H (600 MHz, DMSO-d_6) 0.27 and 0.37 (4H, 2 × m, cyclopropyl CH_2), 2.09 (1H, br s, NCH), 3.62 (2H, s, CH_2N), 7.15 (1H, t, J = 7.26 Hz, 7-H), 7.30 (1H, d, J = 7.26 Hz, 8-H), 7.44 (1H, t, J = 6.60 Hz, 6-H), 7.63 (1H, d, J = 6.30 Hz, 5-H), 7.81 (1H, s, 4-H) and 11.81 (1H, s, NH); δ_C (150 MHz, DMSO-d_6) 6.2 (13 and 14-C), 30.0 (C-12), 48.1 (11-C), 114.8 (C-8), 119.3 (C-10), 121.8 (C-7), 127.5 (C-5), 129.4 (C-6), 132.2 (C-9), 135.4 (C-4), 137.8 (C-3) and 161.9 (C=O).

***3-[(Cyclohexylamino)methyl]-6-methoxy-2(*1H*)-quinolone* 116e**

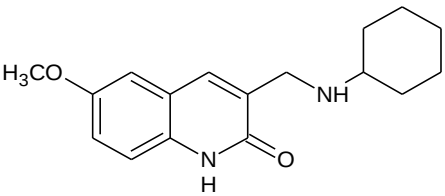

The general procedure was followed, using 3-(chloromethyl)-6-methoxy-2(1*H*)-quinolone **113e** (0.10 g, 0.45 mmol) and cyclohexylamine to afford, as cream white crystals, *3-[(cyclohexylamino)methyl]-6-methoxy-2(1*H*)-quinolone* **114e** (84.6 mg, 65%); mp 127-131°C; (Found MH^+: 287.1752. Calc. for $C_{17}H_{23}N_2O_2$: 287.1760); ν_{max} (ATR)/cm^{-1} 3289 (NH) and 1655 (C=O); δ_H (400 MHz; $CDCl_3$) 1.24-2.02 (series of unresolved m, cyclohexyl CH_2), 2.60 (1H, NCH), 3.81 (3H, s, OCH_3), 3.89 (2H, s, CH_2N), 6.92 (1H, s, Ar-H), 7.04 (1H, m, Ar-H), 7.29 (1H, m, Ar-H) and 7.80 (1H, s, Ar-H); δ_c (100 MHz; $CDCl_3$) 24.9, 26.0 and 33.0

(cyclohexyl CH_2), 46.1 (CH_2N), 55.6 (OCH_3), 56.2 (CHN), 108.8, 117.0, 119.0, 119.4, 120.5, 132.3, 155.0 (Ar-C) and 163.3 (C=O).

***6-Methoxy-3-[(cyclopentylamino)methyl]-2(*1H*)-quinolone* 115e**

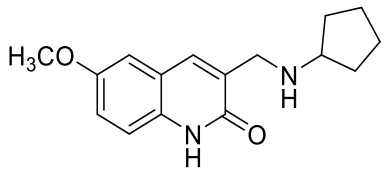

The general procedure was followed, using 3-(chloromethyl)-6-methoxy-2(1*H*)-quinolone **113e** and cyclopentylamine to afford, as light yellow crystals, *3-[(cyclopentylamino)methyl]-2(1*H*)-quinolone* **115e**; mp 121-124 °C; (Found MH^+: 273.1612. Calc. for $C_{16}H_{21}N_2O_2$: 273.1612); ν_{max} (ATR)/cm^{-1} 3158 (NH) and 1611 (C=O); δ_H (600 MHz, DMSO-d_6) 1.24 - 1.78 Hz (8H, series of unresolved m, cyclopentyl CH_2), 2.40 (1H, br s, CHN), 3.10 (1H, br s, NH), 3.63 (2H, s, CH_2N), 3.90 (3H, s, OCH_3), 7.13 (2H, d, *J* = 7.08 Hz, 7 and 8-H), 7.25 (1H,s 5-H) and 7.88 (1H,s 4-H); δ_C (150 MHz, DMSO-d_6) 23.6 (C-14/15), 32.5 (C-13/16), 46.9 (C-11), 55.4 (OCH_3), 58.6 (C-12), 109.0 (C-8), 116.1 (C-5), 118.5 (C-7)), 119.9 (C-10), 132.2 (C-4), 132.6 (C-3), 135.2 (C-9), 154.1 (C-6) and 161.5 (C=O).

***6-Methoxy-3-[(Cyclopropylamino)methyl]-2(*1H*)-quinolone* 116e**

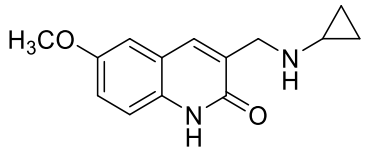

The general procedure was followed, using 3-(chloromethyl)-6-methoxy-2(1*H*)-quinolone **113e** (13.0 mg, 58.3 µmol) and cyclopropylamine to afford, as cream white crystals, an isomeric mixture of *3-[(cyclopentylamino)methyl]-6-methoxy-2(1*H*)-quinolone* **116e** (10.4 mg, 73%); mp 87-83 °C; [Found $(M-H)^-$: 243.1108. Calc. for $C_{14}H_{15}N_2O_2$: 243.1134); ν_{max} (ATR)/cm^{-1} 3307 (NH) and 1649 (C=O); δ_H (600 MHz, DMSO-d_6) 1.26 and 2.16/2.18 (4H, 2 × m, cyclopropyl CH_2), 3.86/3.98 (3H, 2 × s, OCH_3), 5.17/5.22 (2H, 2 × s), 6.97 - 7.34 (4H, series of signals, Ar-H), 7.81 (1H, d, *J* = 9.0 Hz, Ar-H), 9.43 and 11.93 (2H, 2 × br s, NH); δ_C (150 MHz, DMSO-d_6) 21.05/21.09 (cyclopropyl CH_2), 55.6/56.0 (CHN), 61.5 (CH_2N), 108.8/110.0, 117.1, 119.6/119.7, 120.3/122.4, 127.8/128.5, 138.0/138.2, 145.4/155.2 and 160.9/162.4 (Ar-C) and 170.8/170.9 (C=O).

***3-[(Cyclohexylamino)methyl]- 8-methoxy-2(*1H*)-quinolone* 114f**

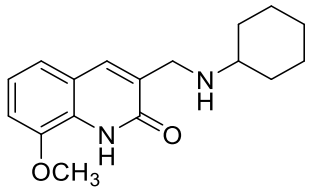

The general procedure was followed, using 3-(chloromethyl)-8-methoxy-2(1*H*)-quinolone **113f** and cyclohexylamine to affor, as cream white crystals, *3-[(cyclohexylamino)methyl]-8-methoxy-2(1*H*)-quinolone* **114f** (85.9 mg, 76%); mp 119-121 °C; (Found MH^+: 287.1635. Calc. for $C_{17}H_{23}N_2O_2$: 287.1760); ν_{max} (ATR)/cm^{-1} 3280 (NH) and 1646 (C=O); δ_H (600 MHz, DMSO-d_6) 1.15-1.29 (10-H, series of m, cyclohexyl CH_2), 2.60 (1H, br s, CHN), 3.71 (2H, s, CH_2N), 3.87 (3H, s, OCH_3), 7.19 (1H, d, *J* = 7.8 Hz, 5-H), 7.30 (1H, t, *J* = 6.57 Hz, 6-H), 7.33 (1H, d, *J* = 8.28, 7-H) and 7.93 (1H, s, 4-H); δ_C (150 MHz, DMSO-d_6) 24.5, 25.9 and 32.9 (cyclohexyl CH_2), 42.3 (CH_2N), 55.4 (OCH_3), 55.5 (CHN) 109.0 (C-5), 116.1 (C-6), 118.6 (C-9), 119.9 (C-7), 132.2 (C-10), 132.7 (C-3), 132.2 (C-4), 154.2 (C-8) and 161.5 (C=O)

***8-Methoxy-3-[(cyclopentylamino)methyl]-2(*1H*)-quinolone* 115f**

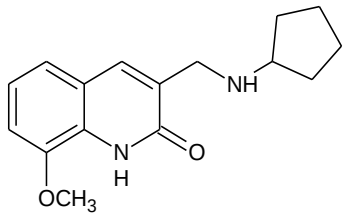

The general procedure was followed, using 3-(chloromethyl)-8-methoxy-2(1*H*)-quinolone **113f** (0.10 g, 0.38 mmol) and cyclopentylamine to afford, as pale yellow crystals, *8-methoxy-3-cyclopentylaminomethyl-2(1*H*)-quinolone* **115f** (74.5 mg, 88%); mp 96-99 °C; (Found MH^+: 273.1611. Calc. for $C_{16}H_{21}N_2O_2$: 273.1603); ν_{max} (ATR)/cm^{-1} 3287 (NH) and 1645 (C=O); δ_H (400 MHz; DMSO-d_6) 1.33, 1.45, 1.62 and 1.73 (8H, 4 ×m, cyclopentyl CH_2), 2.08 (1H, m, 12-H), 3.02 (1H, s, NH), 3.54 (2H, s, CH_2N), 3.76 (3H, s, OCH_3), 7.08 (1H, m, Ar-H). 7.20-7.22 (2H, m, Ar-H), 7.80 (1H, m, Ar-H) and 11.70 (br s, NH); δ_C (100 MHz; DMSO-d_6) 23.7 and 32.5 (cyclopentyl CH_2), 46.9 (CH_2N), 55.4 (CHN), 58.6 (OCH_3), 109.0, 116.1, 118.5, 119.9, 132.2, 132.6, 135.2 and 154.2 (Ar-C) and 161.5 (C=O).

***8-Methoxy-3-[(cyclopropylamino)methyl]-2(*1H*)-quinolone* 116f**

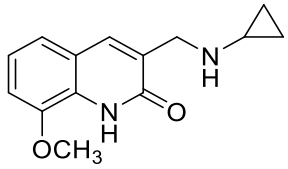

The general procedure was followed, using 3-(chloromethyl)-8-methoxy-2(1*H*)-quinolone **113f** and cyclopropylamine to afford, as cream white crystals, *3-[(cyclohexylamino)methyl]-8-methoxy-2(1*H*)-quinolone* **116f** (24 mg, 81%); mp 118-122 ^{o}C; (Found MH^{+}: 245.1301. Calc. for $C_{14}H_{17}N_2O_2$: 245.1290); ν_{max} (ATR)/cm^{-1} 3282 (NH) and 1652 (C=O); δ_H (600 MHz, $CDCl_3$) 1.68 and 2.16 (4H, cyclopropyl CH_2), 3.98 (3H, s, OCH_3), 5.16 (2H, s, CH_2N), 6.97 (1H, d, *J* =7.8 Hz, Ar-H), 7.13-7.18 (2H, m, Ar-H), 7.80 (1H, s, 4-H) and 9.25 (1H, sm NH)'; δ_C (150 MHz, $CDCl_3$)23.7 and 32.5 (cyclopentyl CH_2), 46.9 (CH_2N), 55.4 (CHN), 58.6 (OCH_3). 109.0, 116.1, 118.5, 119.9, 132.2, 132.6, 135.2 and 154.2 (Ar-C) and 161.5 (C=O).

***6-Chloro-3-[(cyclohexylamino)methyl]-2(*1H*)-quinolone* 114e**

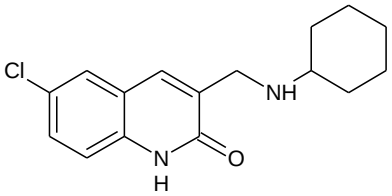

The general procedure was followed, using 6-chloro-3-(chloromethyl)-2(1*H*)-quinolone **113e** (85.9 mg, 0.38 mmol) and cyclohexylamine to afford, as light brown crystals, *6-chloro-3-[(cyclohexylamino)methyl]-2(1*H*)-quinolone* **114e** (60.2 mg, 89%), mp 151-155°C; (Found MH^{+}: 291.1258. Calc. for $C_{16}H_{20}ClN_2O$, M+H: 291.1266); ν_{max} (ATR)/cm^{-1} 3298 (NH) and 1651 (C=O); δ_H (400 MHz; $CDCl_3$) 1.04-1.97 (10H, series of unresolved m, cyclopropyl CH_2), 2.64 (1H, m, CHN), 3.86 (2H, s, *J* = 8.8 Hz, CH_2N), 7.29/7.33 (1H, 2 × m, Ar-H), 7.39/7.41 (1H, 2 × m, Ar-H), 7.48/7.51(1H, 2 × m, Ar-H) and 7.75/7.78 (1H, 2 × s, 4-H); δ_c (100 MHz; $CDCl_3$) 24.1/24.6 and 32.9/33.3 (cyclohexyl CH_2), 47.8 (CH_2N), 59.2/59.3 (CHN), 117.0, 120.9, 122.8, 126.4/126.6, 127.8, 129.4/130.0, 133.7, 136.1/136.4 and 162.2/163.5 (C=O).

***6-Chloro-3-[(cyclopentylamino)methyl]-2(*1H*)-quinolone* 115e**

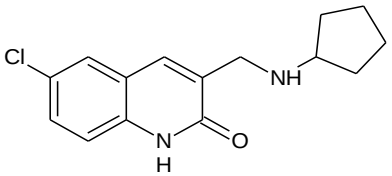

The general procedure was followed, using 6-chloro-3-(chloromethyl)-2(1*H*)-quinolone **113e** (0.10 g, 0.45 mmol) and cyclopentylamine to afford, as grey crystals, *6-chloro-3-[(cyclopentylamino)-methyl]-2(1*H*)-quinolone* **114e** (78.3 mg, 93%); mp 178-181 ˚C; (Found MH^+: 277.1096. Calc. for $C_{15}H_{18}ClN_2O$: 277.1109); ν_{max} (ATR)/cm^{-1} 1650 (C=O); δ_H (400 MHz; $CDCl_3$) 1.44-1.92 (8H, series of unresolved m, cyclopropyl CH_2), 3.17 (1H. m, CHN), 3.82 (2H, 2 × s, CH_2N), 7.18 (1H, m, Ar-H), 7.28 (1H, m, Ar-H), 7.48 (1H, m, Ar-H) and 7.78 (1H, br s, Ar-H); δ_c (100 MHz; $CDCl_3$) 24.8, 26.0 and 33.1(cyclopentyl CH_2), 46.2 (CH_2N), 56.1 (CHN), 115.6, 119.9, 122.5, 127.4, 129.8, 130.8 and 137.6, 137.7 (Ar-C) and 163.9 (C=O)

3.2.6. Synthesis of 3-(benzamidomethyl)-(1*H*)-2-quinolones

General procedure: To a solution of the 3-[(cycloalylamino)methyl]-2(1*H*)-quinolone (1 eq.) in DCM (3 mL) was added benzoyl chloride (1 eq.) and the reaction was stirred in a stoppered flask at room temperature. The reaction progress was monitored by TLC and, after completion, triethylamine (TEA, 1eq.) was added. The reaction mixture was stirred for an hour, then filtered and concentrated *in vacuo*.The crude residue was purified by column chromatography on silica gel (elution with EtOAC) to afford the desired 3-(benzamidomethyl)-2(1*H*)-quinolone.

***3-[(N-Cyclohexylbenzamido)methyl)]-2(1*H*)-quinolone* 117a**

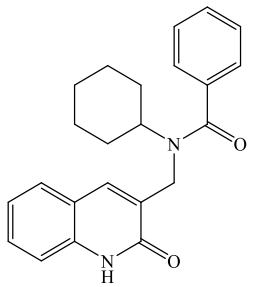

The general procedure was followed, using 3-[(cyclohexylamino)methyl]-2(1*H*)-quinolone **114a** (0.20 g, 0.82 mmol), benzoyl chloride (85.7 mg, 0.82 mmol) and TEA (82.9 mg, 0.82 mmol) to afford as a light brown gel, *3-[(N-cyclohexylbenzamido)methyl)]-2(1*H*)-quinolone* **117a** (0.18 mg, 60%), (Found MH^+: 361.1916. Calc. for $C_{23}H_{25}N_2O_2$: 361.1916); ν_{max} (ATR)/ cm^{-1} 1610 and 1601 (C=O); δ_H (600 MHz; DMSO-d_6) 0.9-1.7 (11H, series of m, cyclohexyl CH_2), 3.54 (1H, br s, CHN), 4.42 (2H, s, CH_2N), 7.18 (1H, t, *J* = 7.2 Hz, Ar-H), 7.3-7.9 (9H, series of signals, Ar-H) and 11.95 (1H, s, NH); δ_C (150 MHz; DMSO-d_6) 24.8, 25.7 and 31.1 (cyclohexyl CH_2), *ca*, 46.2(NCH from HSQC at 300 K), 58.9 (NCH_2), 115.2, 119.6, 122.3, 126.5, 128.3, 129.0, 129.7, 130.1, 130.3, 134.2, 137.6 and 137.9 (Ar-C), 161.8 and 171.5 (C=O).

***3-[(N-Cyclopentylbenzamido)methyl)]-2(1*H*)-quinolone* 118a**

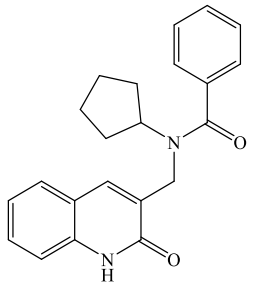

The general procedure was followed, using 3-[(cyclopentylamino)methyl]-2(1*H*)-quinolone **115a** (53.8 g, 0.21 mmol), benzoyl chloride (22.0 mg, 0.21 mmol) and TEA (21.2 mg, 0.21 mmol) to afford as a cream white crystals, *3-[(N-cyclopentylbenzamido)methyl)]-2(1*H*)-quinolone* **118a** (62.6 mg, 86%), mp 102-105 °C; (Found MH^+: 347.1764. Calc. for $C_{22}H_{23}N_2O_2$: 347.1760); ν_{max} (ATR)/ cm^{-1} 1656 and 1621 (C=O); δ_H (600 MHz; DMSO-d_6) 1.42, 1.63 and 1.79 (8H, 3 × m, cyclopentyl CH_2), 4.28 (1H, m, 12-H), 4.41 (2H, s, 11-H), 7.17 (1H, t, *J* = 7.2 Hz, Ar-H), 7.34 (1H, d, *J* = 8.4 Hz, Ar-H), 7.4-7.5 (6H, m, Ar-H), 7.67 (1H, s, 4-H), 7.71 (1H, d, *J* = 7.2 Hz, Ar-H) and 11.51 (1H, br s, NH); δ_C (150 MHz; DMSO-d_6) ; 22.9 and 28.8 (cyclopentyl CH_2), 58.8 (NCH), 114.4, 117.9, 118.6, 121.2, 125.6, 127.1, 127.7, 128.5, 129.0, 129.8, 133.9 and 137.1/137.3 (Ar-C), 160.6 and 170.9 (C=O)

***3-[(N-Cyclopropylbenzamido)methyl)]-2(1*H*)-quinolone* 119a**

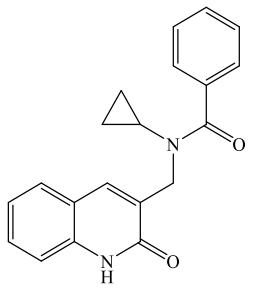

The general procedure was followed, using 3-[(cyclopropylamino)methyl]-2(1*H*)-quinolone **116a** (53.7 g, 0.25 mmol), benzoyl chloride (26.2 mg, 0.25 mmol) and TEA (25.4 mg, 0.25 mmol) to afford as a pale yellow crystals, *3-[(N-cyclopropylbenzamido)methyl)]-2(1*H*)-quinolone* **119a** (25.5 mg, 32%), mp 88-90 C; Found MH^+: 319.1461. Calc. for $C_{20}H_{19}N_2O_2$: 319.1447); ν_{max} (ATR)/ cm^{-1} 1619 (br, C=O); δ_H (600 MHz; DMSO-d_6; at 333 K) 1.18-1.21 (4H, m, cyclopropyl CH_2), 5.27 (2H, s, CH_2N), 7.19 (1H, t, *J* = 7.2 Hz, Ar-H), 7.55 (1H, d, *J*

= 7.8 Hz, Ar-H), 7.50 (1H, d, *J* = 7.2 Hz, Ar-H), 7.55 (1H, t, *J* = 7.8 Hz, Ar-H), 7.67 (1H, d, *J* = 7.2 Hz, Ar-H), 7.72 (1H, *J* =7.8 Hz, Ar-H), 8.03-8.06 (3H, m, Ar-H) and 11.85 (1H, s, NH); δ_C (150 MHz, DMSO-d_6) 24.2 (cyclopropyl CH_2), 61.6 (CH_2N), 114.6, 118.6, 121.7, 127.5, 127.8, 128.9, 129.1, 129.5, 132.2, 137.2 and 133.3 (Ar-C), 160.7 and 165.4 (C=O).

***3-[(N-Cyclopropylbenzamido)methyl)]-6-methoxy-2(1*H*)-quinolone* 117e**

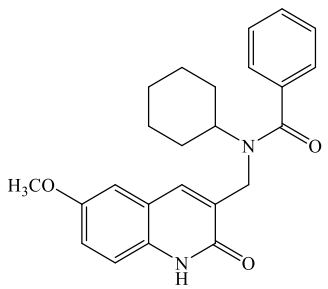

The general procedure was followed, using 3-[(cyclohexylamino)methyl]-6-methoxy-(1*H*)-2-quinolone **114e** (81.0 mg, 0.28 mmol), benzoyl chloride (29.6 mg, 0.28 mmol) and TEA (28.6 mg, 0.28 mmol) to afford as a light-yellow gel, *3-[(N-cyclohexylbenzamido)methyl)]-6-methoxy-2(1*H*)-quinolone* **117e** (19.0 mg, 17%); Found MH^+: 391.2033. Calc. for $C_{24}H_{27}N_2O_3$: 391.2022); ν_{max} (ATR)/ cm^{-1} 1640 and 1600; δ_H (600 MHz; DMSO-d_6) 1.06 – 1.77 (10H, series of m, cyclohexyl CH_2), 3.94 (3H, s, OCH_3), 4.45 (2H, s, CH_2N) and 7.13 – 7.96 (9H, series of signals, Ar-H); δ_c (150 MHz; DMSO-d_6) 24.1 and 24.9 (cyclohexyl CH_2), 30.1 (NCH), 55.9 (OCH_3), 110.4, 119.05/119.14, 121.3, 125.5, 127.3/127.7, 127.8, 128.4/128.6, 130.6, 132.0, 134.2, 137.1 and 145.1 (Ar-C), 160.0 and 170.8

***6-Methoxy-3-[(N-cyclopentylbenzamido)methyl)]-2(1*H*)-quinolone* 118e**

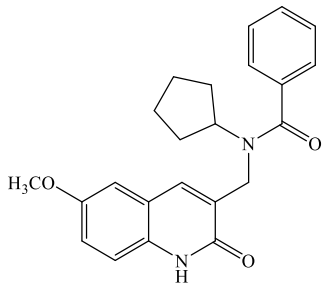

The general procedure was followed, using 6-methoxy-3-[(cyclopentylamino)methyl]-2(1*H*)-quinolone **115e** (71.8 mg, 0.26 mmol), benzoyl chloride (27.6 mg, 0.26 mmol) and TEA (23.6

mg, 0.26 mmol) to afford as pale yellow crystals, *6-methoxy-3-[(N-cyclopentylbenzamido)methyl)]-2(1*H*)-quinolone* **118e** (50.1 mg, 60%), mp 183-186 °C; Found MH^+: 377.1870. Calc. for $C_{23}H_{25}N_2O_3$: 377.1865); ν_{max} (ATR)/ cm^{-1} 1648 and 1617 (C=O); δ_H (600 MHz; DMSO-d_6) 1.06, 1.51, 1.69 and 1.78 (8H, 4 × m, cyclopentyl CH_2), 3.81/3.83 (3H, s, OCH_3), 3.94 (1H, s, CHN), 4.43/4.45 (2H, s; CH_2N), 7.11, m, Ar-H), 7.26 – 7.33 (2H, m, Ar-H), 7.43 – 7.47 (5H, m, Ar-H) and 7.69/7.71 (1H, s, 4-H); δ_c (150 MHz; DMSO-d_6) 24.1, 24.9 and 30.1 (cyclopentyl CH_2), 53.6 (CH_2N), 55.2 (OCH_3), 55.9 (CHN), 109.5/110.4, 112.0, 115.5, 118.2/118.9, 119.1/119.2, 121.2, 125.5, 127.7/127.8, 128.4/128.6, 130.3/131.8, 133.7/134.2 and 154.0 (Ar-C), 160.1 and 170.7 (C=O).

***6-Methoxy-3-[(N-cyclopropylbenzamido)methyl)]-2(1*H*)-quinolone* 119e**

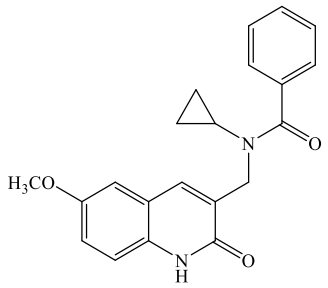

The general procedure was followed, using 6-methoxy-3-[(cyclopropylamino)methyl]-2(1*H*)-quinolone **116e** (13.1 mg, 53.6 µmol), benzoyl chloride (5.60 mg, 53.6 µmmol) and TEA (5.43 mg, 53.6 µmol) to afford as cream white crystals, *6-methoxy-3-[(N-cyclopropylbenzamido)methyl)]-2(1*H*)-quinolone* **119e** (10.4 mg, 57%), mp 59-62 °C; Found MH^+: 349.1563. calc. for $C_{21}H_{21}N_2O_3$: 349.1552); ν_{max} (ATR)/ cm^{-1} 1682 and 1652 (C=O); δ_H (600 MHz; DMSO-d_6 at 373 K) 0.50 – 0.54 (4H, 2 × m, cyclopropyl CH_2), 2.85 (1H, br s, NCH), 3.95/3.99 (3H, 2 × s, OCH_3), 4.53/4.81 (2H, 2 × s, CH_2N) and 7.1-8.4 (9H, series of signals, Ar-H); δ_H (150 MHz; DMSO-d_6 at 333 K) 5.43 (cyclopropyl CH_2), 55.3 (OCH_3), 61.7 (CH_2N), 109.4, 111.2, 116.1, 119.4, 126.9, 127.9, 128.5, 129.1/129.4, 130.9, 133.4, 136.4 and 137.1 (Ar-C), 154.1 and 160.2/165.4 (C=O).

***3-[(N-Cyclopropylbenzamido)methyl)]- 8-methoxy-2(1*H*)-quinolone* 117f**

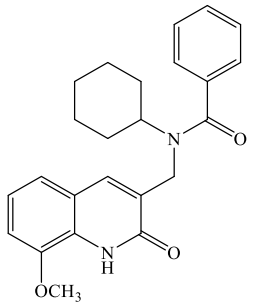

The general procedure was followed, using 3-[(cyclohexylamino)methyl]-8-methoxy-2(1*H*)-quinolone **114f** (3.7 mg, 0.22 mmol), benzoyl chloride (23.3 mg, 0.22 mmol) and TEA (22.5 mg, 0.22 mmol) to afford as pale-yellow gel, *3-[(N-cyclohexylbenzamido)methyl)]-8-methoxy-2(1*H*)-quinolone* **117f** (31.1 mg, 36%); Found MH^+: 391.2018. Calc. for $C_{24}H_{27}N_2O_3$: 391.2022); ν_{max} (ATR)/ cm^{-1} 1640 and 1600 (C=O); δ_H (600 MHz; DMSO-d_6) 1.05, 1.53, 1.70 and 1.77 (10H, 4 × m, cyclohexyl CH_2), 3.79 (1H, br s, CHN), 3.94 (3H, s, OCH_3), 4.45 (2H, s, CH_2N) and 7.13-7.95 (9H, series of signals, Ar-H); δ_C (150 MHz; DMSO-d_6) 25.2, 25.9 and 31.1 (cyclohexyl CH_2), 56.9 (OCH_3), 111.5, 120.1, 120.2, 122.3, 126.5, 128.3, 128.8, 129.0, 129.4, 131.6, 135.2 and 146.1 (Ar-C), 161.1 and 171.8 (C=O).

***8-Methoxy-3-[(N-cyclopentylbenzamido)methyl)]-2(1*H*)-quinolone* 118f**

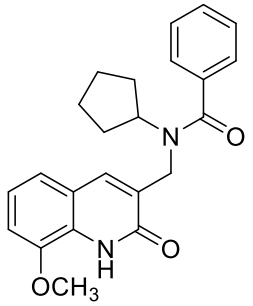

The general procedure was followed, using 8-methoxy-3-[(cyclopentylamino)methyl]-2(1*H*)-quinolone **114f** (33.5 g, 93.3 mmol), benzoyl chloride (12.5 mg, 0.12 mmol) and TEA (12.1 mg, 0.12 mmol) to afford as off-white crystals, *8-methoxy-3-[(N-cyclopentylbenzamido)methyl)]-2(1*H*)-quinolone* **118f** (24.6 mg, 53%), mp 192-195 C; Found MH^+: 377.1860. Calc. for $C_{23}H_{25}N_2O_3$: 377.1865); ν_{max} (ATR)/ cm^{-1} 1637 and 1602 (C=O); δ_H (600 MHz; DMSO-d_6) 1.41, 1.63 and 1.78 (8H, series of m, cyclopentyl CH_2), 3.94 (3H, s, OCH_3), 4.28 (1H, m, NCH), 4.44 (2H, s, NCH_2N), 7.13-7.96 (9H, series of signals, Ar-H); δ_H

(150 MHz; DMSO-d_6) 22.9 and 28.8 (cyclopentyl CH_2), 55.9 (OCH_3), 110.5, 119.1, 121.3, 125.6, 127.7/127.8, 128.5/128.6, 130.4/130.6, 132.0, 134.0, 137.1, 145.1 and 160.0 (Ar-C), 166.6 and 170.9 (C=O).

***8-Methoxy-3-[(N-cyclopropylbenzamido)methyl)]-2(1*H*)-quinolone* 119f**

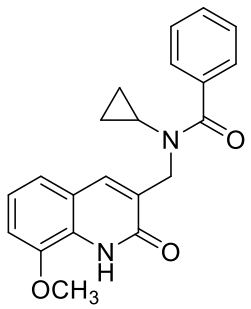

The general procedure was followed, using 8-methoxy-3-[(cyclopropylamino)methyl]-2(1*H*)-quinolone **114f** (43.9 mg, 0.18 mmol), benzoyl chloride (18.8 mg, 0.18 mmol) and TEA (18.2 mg, 0.18 mmol) to afford as cream white crystals, *8-methoxy-3-[(N-cyclopropylbenzamido)methyl)]-2(1*H*)-quinolone* **119f** (24.0 mg, 39%), mp 68-70 °C; Found MH^+: 349.1570. Calc. for $C_{21}H_{21}N_2O_3$: 349.1552); ν_{max} (ATR)/ cm^{-1} 1637 and 1603 (C=O); δ_H (600 MHz; DMSO-d_6) 0.54 (4H, s, cyclopropyl CH_2), 3.82/3.95 (3H, 2 × s, OCH_3), 4.51/4.53 (2H, 2 × m , CH_2N), 7.1-7.96 (9H, series of signals, Ar-H); δ_C (150 MHz; DMSO-d_6) 8.4/8.5 (cyclopropyl CH_2), 31.2 (NCH), 46.2 (CH_2N), 55.3/55.9 (OCH_3), 109.6/110.6, 115.7, 118.2/118.4, 119.1/119.4, 121.4/126.6, 127.4/128.1, 128.6/128.7, 129.4/129.6, 132.0/132.2, 134.8/135.5, 137.3/145.2 and 154.1 (Ar-C), 160.4/160.5, and 171.5 (C=O).

3.3. Part II

3.3.1. Synthesis of aza-Baylis-Hillman adducts

Methyl 3-hydroxy-2-methylene-3-(quinoline-2-yl)prpanoate 132

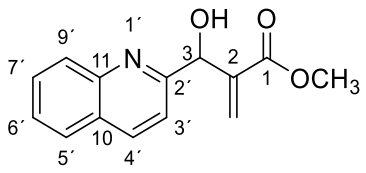

To a solution of quinoline-2-carboxaldehyde **127** (4.07 g, 25.9 mmol) and methyl acrylate **46b** (3.35 g, 38.9 mmol) in a mixture of MeOH:H_2O (2:1; 15 mL) was added 3-HQ (1.0 g, 7.86 mmol). The reaction mixture was stirred in a stoppered flask at room temperature for 2 days, after which it was concentrated *in vacuo*. The crude product was purified by column chromatography on silica gel [elution with hexane:EtOAC (2:1)] to afford, as a brick red gel, methyl 3-hydroxy-2-methylene-3-(2-quinolinyl)propanoate **132** (4.09 g, 45%); (Found MH^+: 244.0971. Calc. for $C_{14}H_{14}NO_3$: 244.0974); ν_{max} (ATR)/cm^{-1} 3258 (OH) and 1743 (C=O); δ_H (300 MHz; $CDCl_3$) 3.67 (3H, s, OCH3), 5.68 (1H, br s, OH), 5.87 and 5.97 (2H, 2 x s, CH2), 6.36 (1H, s, C*H*OH), 7.42 (1H, d, *J* = 8.4 Hz, 3´-H), 7.46 (1H, d, *J* = 7.6 Hz, 4´-H), 7.66 (1H, t, *J* = 7.6 Hz, 6´-H), 7.82 (1H, d, *J* = 8.0 Hz, 9´-H) and 8.04 (2H, m, 7´- and 8´-H); δ_C (75 MHz; $CDCl_3$) 51.6 (OCH3), 71.7 (C-3), 118.6 (Ar-C), 126.3 (Ar-C), 127.1 (Ar-C), 127.3 (Ar-C), 128.5 (Ar-C), 128.6 (Ar-C), 129.5 (Ar-C), 136.8 (Ar-C), 141.5 (Ar-C), 146.1 (Ar-C), 159.3 (Ar-C) and 166.3 (C=O).

Methyl 3-hydroxy-2-methylene-3-(2-pyridinyl)propanoate[126] 88

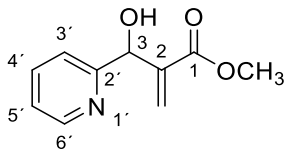

To a solution of 2-pyridinecarboxaldehyde **124** (5.00 g, 46.7 mmol) and methyl acrylate **46b** (4.82 g, 56.0 mmol) in $CHCl_3$ (10 mL) was added 3-HQ (0.59 g, 4.66 mmol). The reaction mixture was stirred in a stoppered flask at room temperature for 2 days, after which it was concentrated *in vacuo*. The crude product was purified by column chromatography on silica gel [elution with hexane:EtOAC (2:1)] to afford, as a light yellow gel, methyl 3-hydroxy-2-methylene-3-(2-pyridinyl)propanoate **88** (8.59 g, 95%); ν_{max} (ATR)/cm^{-1} 3227 (OH) and 1710 (C=O); δ_H (300 MHz; $CDCl_3$) 3.67 (3H, S, OCH_3), 5.59 and 5.94 (2H, 2 × s, C=CH_2), 6.32 (1H, s, C*H*OH), 7.16 (1H, t. *J* = 6.1 Hz, 4´-H), 7.38 (1H, d, *J* = 7.9 Hz, 6´-H), 7.63 (1H, t, *J* =

7.68 Hz, 5´-H) and 8.47 (1H, d, J = 4.5 Hz, 3´-H); δ_C (75 MHz; $CDCl_3$) 51.8 (OCH_3), 72.0 (*C*HOH), 121.2 (C-3´), 122.6 (C-5´), 126.8 (C=*C*H_2), 136.8 (C-4´), 141.5 (*C*=CH_2), 148.1 (C-6´), 159.4 (C-2´) and 166.4 (C=O).

Methyl 3-(6-formylpyridin-2-yl)-3-hydroxy-2-methylenepropanoate 130a and **2,6-bis(2-carbomethoxy-1-hydroxy-2-propenyl)pyridine 130b**

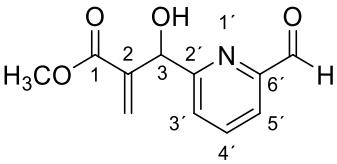

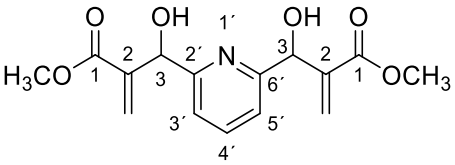

Using the procedure described for the synthesis of methyl 3-hydroxy-2-methylene-3-(2-pyridinyl)propanoate **88**, methyl acrylate **46b** (280 mg, 3.26 mmol) and 3-HQ (50.0 mg, 0.39 mmol) were added to a solution of 2,6-pyridinedicarboxaldehyde **120** (200 mg, 1.48 mmol) in methanol:water (1 ml; 1:1). The reaction progress was monitored by TLC. After a day, TLC showed completion of the reaction, and the crude mixture was concentrated *in vacuo* and purified by column chromatography on silica gel [elution with hexane:EtOAc (3:2)] to afford two fractions.

Fraction (i): as a light brown gel, methyl 3-(6-formylpyridin-2-yl)-3-hydroxy-2-methylenepropanoate **130a** (0.10 g, 35%); (Found MH^+: 222.0762. Calc. for $C_{11}H_{12}NO_4$: 222.0766); ν_{max} (ATR)/cm^{-1} 3277 (OH), 1727 and 1674 (C=O); δ_H (600 MHz; $CDCl_3$) 3.74 (3H, s OCH_3), 5.70 (1H, s, C*H*OH), 6.01 and 6.40 (2H, 2 × s, C=*CH*$_2$), 7.69 (1H, dd, J = 2.3 and 6.6 Hz, 4´-H), 7.87 (1H, d, J = 4.7 Hz, 5´-H), 7.89 (1H, d, J = 4.6 Hz, 3´-H) and 10.06 (1H, s, CHO); δ_C (150 MHz; $CDCl_3$) 52.0 (OCH_3), 72.4 (CHOH), 120.6 (C-5´), 125.6 (C-3´), 127.5 (C=*C*H_2), 137.9(C-4´), 141.0 (*C*=CH_2), 151.3 (C-6´), 160.5 (C-2´), 166.4 (OC=O) and 192.9 (C=O).

Fraction (ii): as a reddish-brown gel, 2,6-bis(2-carbomethoxy-1-hydroxy-2-propenyl)pyridine **130b** (0.11 g, 22%); (Found MH^+: 308.1136. Calc. for $C_{15}H_{18}NO_6$: 308.1134); ν_{max} (ATR)/cm^{-1} 3404 (OH) and 1706 (C=O); δ_H (600 MHz; $CDCl_3$) 3.72 (3H, s, OCH_3), 3.73 (3H, s, OCH_3), 4.40 (2H, br s, OH), 5.60 (2H, s, 2×C*H*OH), 5.89 (2H, d, J = 2.3 Hz, C=C*H*$_2$), 6.34 (2H, d, J = 2.4 Hz, C=*CH*$_2$), 7.36 (2H, d, J = 7.74 Hz, 3 and 5´-H) and 7.69 (1H, td, J = 1.0 and 7.7 Hz, 4´-H); δ_C (150 MHz; $CDCl_3$) 51.9 (OCH_3), 72.6 (CHOH), 120.1(C-3´ and C-5´), 127.0 (C=*C*H_2), 137.8 (C-4´), 141.4 (*C*=CH_2), 158.5 (C-2´ and C-5´) and 166.6 (C=O).

Methyl 3-hydroxy-2-methylene-3-(2-indolyl)propanoate 131a

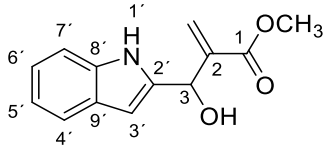

Using the procedure described for the synthesis of methyl 3-hydroxy-2-methylene-3-(2-pyridinyl)propanoate **88**, 3-HQ (1.00 g, 7.86 mmol) was added to a solution of indole-2-carboxaldehyde **121** (0.96 g, 6.62 mmol) and methyl acrylate **46b** (0.85 g, 9.93 mmol) in $CHCl_3$ (10 mL). The crude product was purified by column chromatography on silica gel [elution with hexane:EtOAC (2:1)] to afford, as a light brown gel, methyl 3-hydroxy-2-methylene-3-(2-indolyl)propanoate **131** (0.34 g, 22%); [Found (MH^+-H_2O-H·)]: 213.0875. Calc. for $C_{13}H_{11}NO_2$: 213.0790); ν_{max} (ATR)/cm^{-1} 3266 (OH), 1729; δ_H (600 MHz; $CDCl_3$) 3.48 (1H, br s, OH), 3.79 (3H, s, OCH_3), 5.72 (1H, s, C*H*OH), 5.93 and 6.37 (2H, 2 × s, C=C*H₂*), 6.34 (1H, s, 3´-H), 7.09 (1H, t, *J*=7.40 Hz, 5´-H), 7.17 (1H, t, *J*=7.59 Hz, 6´-H), 7.35 (1H, d, *J*=8.10 Hz, 7´-H), 7.56 (1H, d, *J*=7.86 Hz, 4´-H) and 8.58 (1H, br s, NH); δ_C (150 MHz; $CDCl_3$) 52.2 (OCH_3), 68.8 (CHOH), 99.9 (C-3´), 111.0 (C-7´), 119.9 (C-5´), 120.6 (C-4´), 122.0 (C-6´), 127.0 (C=*C*H_2), 128.1 (C-8´), 134.0 (C-9´), 138.3 (C-2´), 139.9 (*C*=CH_2) and 167.1 (C=O).

***Methyl 3-acetoxy-3-(1*H*-indol-2-yl)-2-methylenepropanoate* 131b**

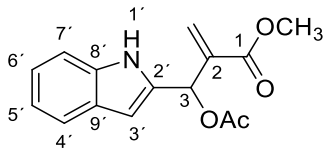

A mixture of methyl 3-hydroxy-3-(1*H*-indol-2-yl)-2-methylenepropanoate **131a** (0.33 g, 1.42 mmol), Ac_2O (0.72 g, 7.08 mmol) and $NaHCO_3$ (0.24 g, 2.83 mmol) in CH_2Cl_2 (5 mL) was stirred in a stoppered flask at room temperature and the reaction progress monitored by TLC. After 48 hours, TLC showed total completion of the reaction and the reaction mixture was concentrated, diluted with CH_2Cl_2 (25 mL), added H_2O (5 mL) and the product extracted. The organic layer was dried over $MgSO_4$ and the filtrate concentrated *in vacuo* to afford, as a light yellowish-brown gel, *methyl 3-acetoxy-3-(1*H*-indol-2-yl)-2-methylenepropanoate* **131b** (0.24 g, 61%); (Found MH^+-AcOH: 214.0885. Calc. for $C_{13}H_{12}NO_2$: 214.0868); ν_{max} (ATR)/cm^{-1} 3322 (NH), 1698 and 1608 (C=O); δ_H (600 MHz; CDCl3) 2.13 (3H, s, $COCH_3$), 3.74 (3H, s, OCH_3), 6.13 and 6.51 (2H, 2 × s, C=*CH₂*), 6.44 (1H, d, *J*=1.98 Hz, C*H*OH), 6.87 (1H, s, 3´-H), 7.09 (1H, t, *J*=7.89 Hz, 5´-H), 7.19 (1H, m, 6´-H), 7.35 (1H, dd, *J*=0.60, 8.22 Hz, 7´-H),

7.56 (1H, d, *J*=7.92 Hz, 4´-H) and 8.76 (1H, br s, NH); ^{13}C NMR. (150 MHz, $CDCl_3$) 21.0 ($COCH_3$), 52.2 (OCH_3), 67.7 (CHOH), 102.3 (C-3´), 111.4(C-7´), 119.9 (C-5´), 120.9 (C-4´), 122.6 (C-6´), 126.7 (C=*C*H_2), 127.4 (C-8´), 134.9 (C-9´), 136.3 (C-2´), 137.4 (*C*=CH_2), and 165.5 and 166.4 (C=O).

Attempted synthesis of 3-hydroxy-3-(imidazol-4-yl)-2-methylenepropanoate 133

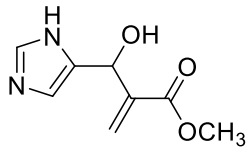

Using the procedure described for the synthesis of methyl 3-hydroxy-2-methylene-3-(2-pyridinyl)propanoate **88**, 3-HQ (1.00 g, 7.86 mmol) was added to a solution of imidazole-2-carboxaldehyde **128** (4.04 g, 42.0 mmol) and methyl acrylate (5.43 g, 63.0 mmol) **46b** in $CHCl_3$ (10 mL). The reaction progress was monitored by TLC and NMR analysis of the amide reaction mixture. The reaction was not successful due to inactivity of the aldehyde.

Methyl 3-hydroxy-2-methylene-3-(4-methyl-1-phenylpyrazol-3-yl)propanoate 134

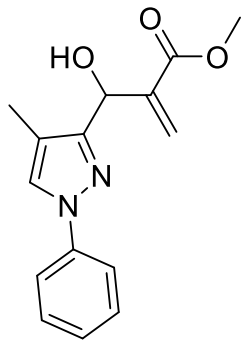

Using the procedure described for the synthesis of methyl 3-hydroxy-2-methylene-3-(2-pyridinyl)propanoate **88**, a solution of 4-methyl-1-phenylpyrazol-3-carboxaldehyde **129** (3.00 g, 16.1 mmol), methyl acrylate (2.08 g, 24.2 mmol) **46b** and 3-HQ (0.22 g, 1.61 mmol) in $CHCl_3$ (10 mL) was stirred for 21 days. The crude product was purified by column chromatography on silica gel [elution with hexane:EtOAC (2:1)] to afford, as a light brown gel, methyl 3-hydroxy-2-methylene-3-(4-methyl-1-phenylpyrazol-3-yl)propanoate **134** (0.84

g, 19%), (Found MH^+: 273.1242. Calc. for $C_{15}H_{17}N_2O_3$: 273.1239); ν_{max} (ATR)/cm^{-1} 3214 (OH) and 1668 (C=O)

3-Hydroxy-2-methylene -3-(2-pyridinyl)propanamide 164

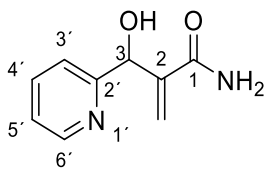

The procedure described for the synthesis of methyl 3-hydroxy-2-methylene-3-(2-pyridinyl)propanoate **88** was followed, using 2-pyridinecarboxaldehyde **124** (2.0 g, 18.7 mmol) and acrylamide (1.59 g, 22.4 mmol) and 3-HQ (0.47 g, 3.73 mmol) in $CHCl_3$ (10 mL). After 2 days, the crude product was purified by column chromatography on silica gel [elution with hexane:EtOAC (2:1)] to afford, as off-white gel, 3-hydroxy-2-methylene-3-(2-pyridinyl)propanamide **164** (1.05 g, 73%), (Found MH^+: 179.0818. Calc. for $C_9H_{11}N_2O_2$: 179.0821); ν_{max} (ATR)/cm^{-1} 3375 (OH), 3146 (NH_2), 1676 (C=O); δ_H (600 MHz; DMSO) 5.53 (2H, m, overlapping C=*CH_2*), 5.86 (2H, s, $CONH_2$), 7.01 (1H, s, C*H*OH),7.25 (1H, td, J=0.94 and 8.20 Hz, 4´-H), 7.44 (1H, d, *J* =7.88 Hz, 6´-H), 7.51 (1H, s, $CONH_2$) 7.76 (1H, td, *J* =1.77 and 7.68 Hz, 5´-H) and 8.46 (1H, d, *J* =4.78 Hz, 3´-H); δ_C (150 MHz; DMSO) 72.7, 119.0 (CH=*C*H_2), 120.9 (Ar-C), 122.3 (Ar-C), 136.6 (Ar-C), 146.4 (Ar-C), 148.3 (Ar-C), 162.0 (*C*=CH_2) and 168.6 ($CONH_2$).

***N*-picolylacrylamide 161a**

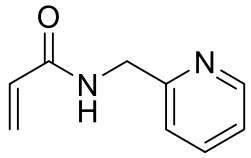

Picolylamine **160a** (2.63 g, 24.3 mmol) and TEA (2.46 g, 24.3 mmol) were added sequentially to a solution of acryloyl chloride (2.0 g, 22.1 mmol) in DCM (5 mL) at 0 °C. After 2 hours TLC showed completion of the reaction. The reaction mixture was diluted with H_2O (50 mL) and extracted with CH_2Cl_2 (2 × 100 mL). The combined organic extracts were dried over anhydrous $MgSO_4$ and filtered. The filtrate was concentrated *in vacuo* to afford, as a light yellow gel, *N*-picolylacrylamide **161a** (1.63 g, 45%); ν_{max} (ATR)/cm^{-1} 3269 (OH) and 1658 (C=O); δ_H (400 MHz; CDCl3) 4.53 (2H, d, *J* = 5.40 Hz, CH_2N), 5.54 (1H, dd, *J* = 2.80 and

9.0 Hz, C*H*=CH_2), 6.18 and 6.21 (2H, m, CH=CH_2), 7.11 (1H, td, J=2.04 Hz, J=6.06 Hz, Ar-H), 7.23 (2H,d, *J* = 7.8 Hz, Ar-H), 7.58 (2H, m, 2 × Ar-H) and 8.42 (1H, d, J=4.84 Hz, N-H); δ_C (100 MHz, $CDCl_3$) 44.4 (CH_2N), 122.2 (Ar-C), 122.4 (Ar-C), 126.5 (CH=*C*H_2) , 130.7 (Ar-C), 136.8 (Ar-C), 148.9 (Ar-C), 156.2 (Ar-C) and 165.6 (C=O).

N-Picolyl-[3-hydroxy-2-methylene-3-(2-pyridinyl)]propenamide **162a**

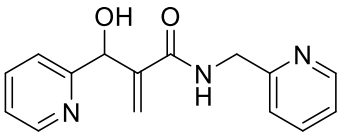

Using the procedure described for the synthesis of methyl 3-hydroxy-2-methylene-3-(2-pyridinyl)propanoate **88**, a solution of 2-pyridinecarboxaldehyde **124** (1.33 g, 12.4 mmol) and *N*-picolylacrylamide **161a** (1.65 g, 10.3 mmol) and 3-HQ (0.26 g, 2.06 mmol) in $CHCl_3$ (10 mL) was stirred for 3 days. The crude product was purified by column chromatography on silica gel [elution with hexane:EtOAC (3:2) and then EtOAc:Acetone (1:1)] to afford, as a reddish-brown gel, *N-picolyl-[3-hydroxy-2-methylene-3-(2-pyridinyl)]propanamide* **162a** (1.24 g, 45%), ν_{max} (ATR)/cm^{-1} 33335 (NH), 3126 (OH), 1709 (C=O); ; δ_H (400 MHz; CDCl3) 5.22 (2H, s, CH_2N), 7.38 (2H, td, J=0.72 Hz, *J* = 6.18 Hz, Ar-H), 7.48 (1H, td, *J* = 0.96 and 6.20 Hz, Ar-H), 7.66 (1H, br s, Ar-H), 7.68 (1H, br s, Ar-H), 7.77 (2H, td, *J* =1.65 and 8.0 Hz, Ar-H), 7.93 (1H, td, *J* =1.54 and 7.73 Hz, Ar-H), 8.22 (1H, d, *J* =7.84 Hz, Ar-H), 8.59 (1H, d, *J* = 4.72 Hz, Ar-H) and 8.63 (2H, d, *J* = 4.80 Hz, Ar-H); δ_C (100 MHz; CDCl3) 29.7 (CH_2N), 82.0 (CHOH), 122.3 (Ar-C), 124.4 (Ar-C), 125.0 (Ar-C), 127.9 (Ar-C), 136.4 (Ar-C), 137.2 (Ar-C), 147.9 (Ar-C), 149.5 (Ar-C), 151.7 (Ar-C) and 152.6 (C=O).

3.3.2. Preparation of indolizine esters and acids

Methyl indolizine-2-carboxylate 90

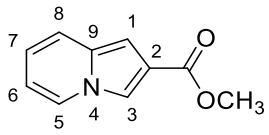

A stirred solution of methyl 3-hydroxy-2-methylene-3-(2-pyridinyl)propanoate **88** (2.00 g, 10.4 mmol) in acetic anhydride (15 mL) was refluxed for 2 days. The reaction mixture was cooled to room temperature, concentrated *in vacuo* and the crude mixture poured with saturated aqueous $NaHCO_3$. The phases were separated and the organic phase was washed with 10% aqueous $NaHCO_3$ and dried over anhydrous $MgSO_4$. The resultant crude product was purified by column chromatography on silica gel [elution with hexane:EtOAc (3:2)] to afford, as light green crystals, methyl indolizine-2-carboxylate **90** (1.69 g, 93%), mp. 99-101°C (Lit.[310] 98-100); ν_{max} (ATR)/cm^{-1} 1730 (C=O); δ_H (300 MHz; $CDCl_3$) 3.88 (3H, s, OCH_3), 6.53 (1H, td, *J* = 2.26 and 6.90 Hz, 7-H), 6.68 (1H. m, 6-H), 6.82 (1H, s, 1-H), 7.35 (1H, d, *J* = 8.90 Hz, 5-H), 7.79 (1H, dd, *J* = 0.60 and 1.59 Hz, 3-H) and 7.85 (1H, dd, *J* = 1.05 and 7.17 Hz, 8-H); δ_C (75 MHz; $CDCl_3$) 51.5 ($COCH_3$), 100.4 (C-1), 112.3 (C-7), 115.8 (C-3), 118.1 (C-6), 119.6 (C-5), 120.3 (C-8), 125.3 (C-9), 132.7 (C-2) and 165.6 (C=O).

Methyl 3-acetylindolizine-2-carboxylate 136

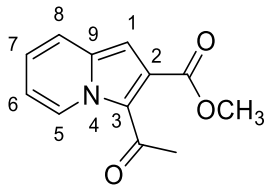

Using the procedure described for the synthesis of methyl indolizine-2-carboxylate **90**, a solution of methyl 3-hydroxy-2-methylene-3-(2-pyridinyl)propanoate **88** (2.00 g, 10.4 mmol) in acetic anhydride (15 mL) was refluxed for 14 days. Purification of the resultant crude product using column chromatography on silica gel [elution with hexane:EtOAc (1:1)] afforded, as light brown crystals, methyl 3-acetylindolizine-2-carboxylate **136** (1.87 g, 83%), mp 89-90 °C; (Found MH^+: 218.0814. Calc. for $C_{12}H_{12}NO_3$: 218.0817); ν_{max} (ATR)/cm^{-1} 1724 and 1619 (C=O); δ_H (400 MHz; $CDCl_3$) 2.623 (3H, s, $COCH_3$), 3.96 (3H, s, OCH_3), 6.83 (1H, s, 1-H), 6.91 (1H, td, *J* = 0.81 and 7.0 Hz, 7-H), 7.14 (1H, m, 6-H), 7.53 (1H, d, *J* = 8.80 Hz, 5-H) and 9.80 (1H, d, *J* = 7.26 Hz, 8-H); δ_C (100 MHz; $CDCl_3$) 30.1 ($COCH_3$), 52.5 (OCH_3), 104.9 (C-

1), 115.3 (C-7), 119.2 (C-5), 121.1 (C-9), 124.0 (C-6), 126.8 (C-3), 128.3 (C-8), 135.8 (C-2), 166.2 (CO_2CH_3) and 189.8 ($COCH_3$).

Indolizine-2-carboxylic acid 138

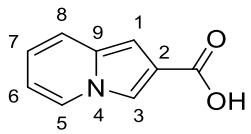

To a solution of methyl indolizine-2-carboxylate **90** (1.18 g, 6.70 mmol) in a mixture of methanol:water (1:1; 10 mL) was added NaOH (1.61 g, 40.2 mmol) and the reaction mixture was stirred at room temperature for 2 days. Sufficient water was added to solubilize the solid material present in the reaction mixture and the pH was adjusted with dilute HCl to *ca.* pH 2-3. The aqueous layer was extracted with EtOAc (2 × 100 mL) and the combined organic extracts were dried over $MgSO_4$ and concentrated *in vacuo* to afford, as yellow crystals, indolizine-2-carboxylic acid **138** (0.93 g, 86%); mp 216-218 (Lit.[310] 219-222); ν_{max} (ATR)/cm^{-1} 3500-2500 (OH) and 1710 (C=O); δ_H (600 MHz; $CDCl_3$) 7.72 (1H, m, Ar-H), 7.86 (1H, t, *J* = 7.7 Hz, Ar-H), 7.96 (1H, d, *J* = 8.2 Hz, Ar-H), 8.18 (1H, d, *J* = 8.5 Hz, Ar-H), 8.29 (1H, d, *J* = 8.4 Hz, Ar-H) and 8.43 (1H, d, *J* = 8.4 Hz, Ar-H); δ_C (150 MHz; $CDCl_3$) 119.1 (Ar-C), 127.9 (Ar-C), 129.2 (Ar-C), 129.4 (Ar-C), 130.0 (Ar-C), 131.0 (Ar-C), 138.9 (Ar-C), 145.9 (Ar-C) and 164.2 (C=O).

3-Acetylindolizine-2-carboxylic acid 139

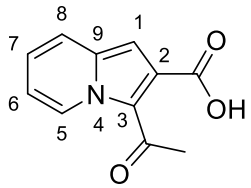

The procedure described for the synthesis of indolizine-2-carboxylic acid **134** was followed, using methyl 3-acetylindolizine-2-carboxylate **134** (1.50 g, 6.91 mmol), methanol:water (1:1; 10 mL) and NaOH (1.66 g, 41.5 mmol). The dried organic extract was concentrated *in vacuo* to afford, as light green crystals, 3-acetylindolizine-2-carboxylic acid **139** (1.30 g, 93%), mp 207-209 °C; (Found MH^+: 204.0657. Calc. for $C_{11}H_{10}NO_3$: 204.0661); ν_{max} (ATR)/cm^{-1} 3500 - 3000 (OH), 1724 and 1619 (C=O); δ_H (600 MHz; DMSO-d_6) 2.56 (3H, s, $COCH_3$), 6.90 (1H, s, 1-H), 7.07 (1H, dt, J=1.29, 6.95 Hz, 7-H), 7.26 (1H, m, 6-H), 7.74 (1H, d, J=8.82 Hz, 5-H)

and 9.62 (1H, d, J=7.20 Hz, 8-H); δ_C (150 MHz; DMSO-d_6) 29.6 ($COCH_3$), 104.2 (Ar-C), 115.5 (Ar-C), 119.6 (Ar-C), 120.0 (Ar-C), 124.2 (Ar-C), 127.3 (Ar-C), 128.6 (Ar-C), 135.5 (Ar-C), 167.1 (CO_2H) and 188.1 ($COCH_3$).

3.3.3. Synthesis of *N*-(heteroarylalkyl)indolizine-2-carboxamides

***N-Benzylindolizine-2-carboxamide* 204**

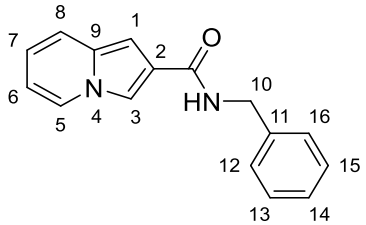

A stirred solution of 3-acetylindolizine-2-carboxylic acid **139** (0.21 g, 1.1 mmol), benzylamine **196** (0.17g, 1.6 mmol) in a mixture of DIPEA:CH_2Cl_2 (2:1; 12 mL) in a stoppered flask was cooled to between -20°C and -10°C. Propylphosphonic anhydride solution (0.16g, 3.2 mmol) was slowly added to maintain an internal temperature below 0°C. After 6 hours TLC showed the formation of the product and the reaction was allowed to run for a further 12 hours. The reaction mixture was diluted with H_2O (10 mL), and the pH was adjusted to *ca* 2-3 using concentrated HCl and then extracted with $CHCl_3$ (2 × 100mL). The combined organic solutions were washed with aqueous 1M $NaHCO_3$ (2 × 50 mL), dried over anhydrous $MgSO_4$ and then concentrated *in vacuo*. The resulting crude mixture was purified by column chromatography on silica gel [elution with hexane:EtOAc (1:2)] to afford, as green crystals, *N-benzylindolizine-2-carboxamide* **204** (92.4 mg, 37%), mp. 123-125 °C; (Found MH^+: 251.1181. Calc. for $C_{16}H_{15}N_2O$: 251.1184); ν_{max} (ATR)/cm^{-1} 3249 (NH) and 1630 (C=O); δ_H (600 MHz; DMSO-d_6) 4.46 (2H, d, J = 6.1 Hz, CH_2N), 6.59 (1H, t, J = 6.4 Hz, 7-H), 6.71 (1H, d, J = 7.7 Hz, 6-H), 6.83 (1H, s, 1-H), 7.23 (2H, m, 13- and 15-H), 7.31 (2H, br s, 12 and 16-H), 7.32 (1H, br signal, 14-H), 7.42 (1H, d, J = 9.1 Hz, 5-H), 8.00 (1H, s, 3-H), 8.26 (1H, d, J = 6.83 Hz, 8-H) and 8.80 (1H, t, J = 6.0 Hz, NH); δ_C (150 MHz; DMSO-d_6) 42.1 (CH_2N) 98.1 (C-1), 111.4 (C-7), 114.4 (C-3), 118.1 (C-6), 119.6 (C-5), 123.8 (C-9), 126.2 (C-8), 126.7 (C-13/15), 127.2 (C-112/116), 128.3 (C-115), 131.9 (C-12), 140.1 (C-2) and 163.7 (C=O).

***N-[2-(2-Pyridinyl)ethyl]indolizine-2-carboxamide* 206**

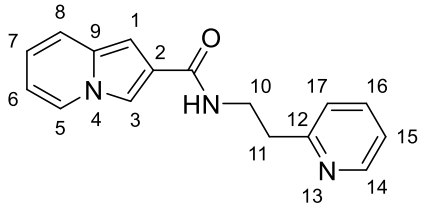

The procedure described for the synthesis of *N*-benzylindolizine-2-carboxamide **199** was followed, using indolizine-2-carboxylic acid **138** (0.21 g, 1.03 mmol), 2-(2-aminoethyl)pyridine (0.19 g, 1.02 mmol) **203** and propylphosphonic anhydride solution (0.98 g, 3.08 mmol) in a mixture of DIPEA:CH_2Cl_2 (2:1; 12 mL) in a stoppered flask. Work-up and subsequent purification of the resultant crude mixture using column chromatography on silica gel [elution with hexane:EtOAc (1:2)] afforded, as green crystals, *N-[2-(2-pyridinyl)ethyl]indolizine-2-carboxamide* **206** (67.4 mg, 25%), mp. 150-152 °C; (Found MNa^+ -$H^{\cdot}$: 287.1006. Calc. for $C_{16}H_{14}N_3ONa$: 287.1035); ν_{max} (ATR)/cm^{-1} 3238 (NH) and 1622 (C=O); δ_H (600 MHz; Acetone-d_6) 3.10 (2H, t, *J* = 7.17 Hz, 11-H), 3.77 (2H, *J* = 6.7 Hz, 10-H), 6.55 (1H, td, *J* = 0.81 and 6.80 Hz, 7-H), 6.69 (1H, td, *J*= 0.81 and 6.50 Hz, 6-H), 6.79 (1H, s, 1-H), 7.23 (1H, t, *J* = 6.2 Hz, 15-H), 7.32 (1H, d, *J* = 7.74 Hz, 17-H), 7.37 (1H, d, *J* = 9.06 Hz, 8-H), 7.71 (1H, dt, *J* = 1.83, 7.67 Hz, 16-H), 7.90 (1H, br s, NH) 7.95 (1H, d, *J* = 1.1 Hz, 3-H), 8.17 (1H, dd, *J* = 0.96 and 7.1 Hz, 5-H) and 8.53 (1H, d, *J* = 4.32 Hz, 14-H); δ_C (150 MHz; Acetone-d_6) 38.0 (C-11), 39.7 (C-10), 98.6 (C-1), 112.2 (C-7), 114.9 (C-3), 118.7 (C-6), 120.3 (C-8), 122.4 (C-15), 124.3 (C-17), 125.3 (C-9), 126.7 (C-5), 133.3 (C-12), 137.8 (C-15), 149.3 (C-14), 160.3 (C-2) and 164.8 (C=O).

***N-Furfurylindolizine-2-carboxamide* 205**

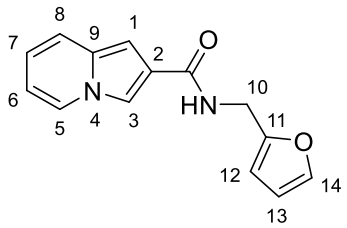

The procedure described for the synthesis of *N*-benzylindolizine-2-carboxamide **199** was followed, using 3-acetylindolizine-2-carboxylic acid **139** (0.14 g, 0.67 mmol), <u>furfurylamine</u> **202** (0.11 g, 0.10 mmol) and propylphosphonic anhydride solution (0.64 g, 2.0 mmol) in a mixture of DIPEA:CH_2Cl_2 (2:1; 12 mL) in a stoppered flask. The resulting crude mixture was purified by column chromatography on silica gel [elution with hexane:EtOAc (1:2)] to afford, as green crystals, *N-furfurylindolizine-2-carboxamide* **205** (86.6 mg, 36%), mp. 65-68 °C; (Found M+H: 241.0974. Calc. for $C_{14}H_{13}N_2O_2$: 241.0977); ν_{max} (ATR)/cm^{-1} 3238 (NH) and 1622 (C=O); δ_H (600 MHz; Acetone-d_6) 4.01 (1H, d, *J* = 5.77 Hz, 10-H), 5.81 (1H, d, *J* = 3.0 Hz, 12-H), 5.93 (1H, t, *J* = 1.8 Hz, 13-H), 6.13 (1H, t, *J* = 6.70 Hz, 7-H), 6.26 (1H, t, *J* = 7.7 Hz, 6-H), 6.38 (1H, s, 1-H), 6.96 (1H, d, *J* = 9.06 Hz, 5-H), 7.10 (1H, br s, 14-H), 7.55 (1H, s,

3-H). 7.80 (1H, d, J = 6.99 Hz, 8-H) and 8.22 (1H, s, NH); δ_C (150 MHz; Acetone-d_6) 35.6 (C-10), 98.3 (C-1), 106.8 (C-12), 110.5 (C-13), 111.5 (C-7), 114.5 (C-3), 118.1 (C-6), 119.7 (C-5), 123.8 (C-9), 126.2 (C-8), 132.1 (C-11), 142.0 (C-14), 153.0 (C-2) and 163.7 (C=O).

***N-Picolylindolizine-2-carboxamide* 152**

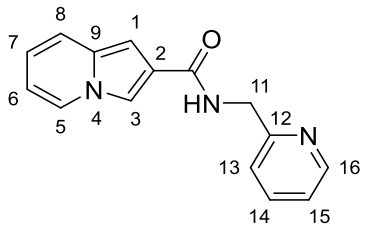

The procedure described for the synthesis of *N*-benzylindolizine-2-carboxamide **204** was followed, using indolizine-2-carboxylic acid **138** (0.21 g, 1.0 mmol), 2-(2-aminomethyl)pyridine **151** (0.19 g, 1.5 mmol) and propylphosphonic anhydride solution (0.98 g, 3.1 mmol) in a mixture of DIPEA:CH_2Cl_2 (2:1; 12 mL) in a stoppered flask. The resulting crude mixture was purified by column chromatography on silica gel [elution with hexane:EtOAc (1:2)] to afford as green crystals, *N-picolylindolizine-2-carboxamide* **152** (89.4 mg, 36%), mp. 105-107 °C; ν_{max} (ATR)/cm^{-1} 3265 (NH) and 1625 (C=O); δ_H (600 MHz; Methanol-d_4) 2.62 (2H. s, CH_2N) 6.54 (1H, t, J = 6.8 Hz, 7-H), 6.68 (1H, t, J = 7.8 Hz, 6-H), 6.74 (1H, br s, NH), 6.88 (1H, s, 1-H), 6.99 (1H, t, J = 7.4 Hz, 15-H), 7.22 (1H, t, J = 7.7 Hz, 14-H), 7.35 (1H, d, J = 9.1 Hz, 5-H), 7.64 (1H, d, J = 8.8 Hz, 13-H), 7.89 (1H, s, 3-H), 8.06 (1H, d, J = 7.0 Hz, 8-H), 9.70 (1H, d, J = 7.3 Hz,16-H); ^{13}C-NMR (150 MHz; Methanol-d_4) 29.9 (CH_2N), 101.3, 106.2, 113.2, 116.6, 119.4, 120.6, 121.0, 125.6, 126.9, 129.1, 130.3, 134.3, 137.9 (Ar-C) and 169.1 (C=O).

3.3.4. Synthesis of tertiary indolizine-2-carboxamides

***3-(Indolizine-2-carbonyl)-1-methylimidazolidine-2,4-dione* 150**

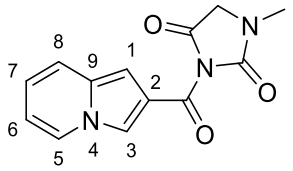

A stirred solution of indolizine-2-carboxylic acid **138** (0.20 g, 1.3 mmol), 1-methylimidazolidine-2,4-dione **147** (0.17 g, 1.5 mmol) in a mixture of DIPEA:$CHCl_3$ (2:1; 12 mL) was cooled to between -20 °C and -10 °C and propylphosphonic anhydride solution (0.94 g, 3.0 mmol) was slowly added to maintain the internal temperature below 0 °C. The resulting mixture was stirred at room temperature for 2 days, diluted with $CHCl_3$ (10 mL) and filtered. The filtrate was concentrated *in vacuo*, and the crude residue was purified by column chromatography on silica gel [elution with hexane:EtOAC (2:3)] to afford as a light green gel, 3-(indolizine-2-carbonyl)-1-methylimidazolidine-2,4-dione **150** (40.0 mg, 16%); (Found MH^+: 258.2348*. Calc. for $C_{13}H_{12}N_3O_3$: 258.0879); ν_{max} 1713, 1572 and 1582 (C=O); δ_H (600 MHz; Methanol-d_4) 2.90 (3H, s, NCH_3), 3.95 (2H, s, CH_2N), 6.56 (1H, br s, 7-H), 6.69 (1H, br s, 6-H), 6.70 (1H, s, 1-H), 7.37 (1H, d, J = 9.0 Hz, 5-H), 7.90 (1H, s, 3-H) and 8.09 (1H, d, J = 9.0 Hz, 8-H); δ_C (150 MHz; Methanol-d_4) 43.7 (CH_2N) , 55.8 (NCH_3), 101.3 (C-1), 113.3 (C-7), 117.6 (C-3), 119.4 (C-6), 121.0 (C-5), 126.9 (C-8), 134.2 (C-9). 159.3 (C-2) and, 168.9 and 173.8 (C=O).

***3-(Indolizine-2-carbonyl)-1-(3´-acetylindolizine-2´-carbonyl)imidazolidine-2,4-dione* 185** and ***3-(indolizine-2-carbonyl)imidazolidine-2,4-dione* 148**

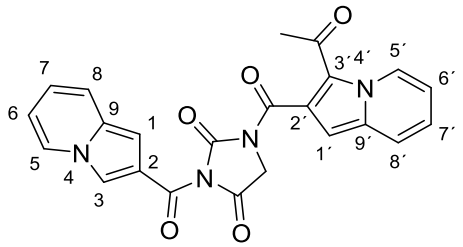

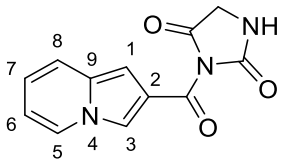

A stirred solution of 3-acetylindolizine-2-carboxylic acid **139** (0.20 g, 0.98 mmol), 2,4-imidazolidinedione **146** (0.12 g, 1.2 mmol) in a mixture of DIPEA:CH_2Cl_2 (2:1; 12 mL) was cooled to between -20°C and -10°C and propylphosphonic anhydride solution (0.94g, 3.0

mmol) was slowly added to maintain an internal temperature below 0°C. The resulting mixture was stirred for 2 days at which time TLC showed the formation of two products. The reaction mixture was diluted with $CHCl_3$ (10 mL), filtered and the residue washed with cooled $CHCl_3$ to afford product 1. The filtrate was concentrated *in vacuo* and the crude mixture purified by column chromatography on silica gel [elution with hexane:EtOAc (1:2) to afford product 2.

Product 1: as yellowish-brown crystals, *3-(indolizine-2-carbonyl)-1-(3´-acetylindolizine-2´-carbonyl)imidazolidine-2,4-dione* **185** (40.0 mg, 10%); mp. 128-132 °C; (Found MH^+: 429.3096*. Calc. for $C_{23}H_{17}N_4O_5$: 429.1199); ν_{max} (ATR)/cm^{-1} 1713, 1666 and 1582 (C=O); δ_H (600 MHz; Methanol-d_6) 2.62 (2H, s, CH_2N), 3.34 (3H, s, $COCH_3$), 6.56 (1H, td, *J* = 1.1 and 7.32 Hz, 7-H), 6.70 (1H, d, m, 6-H), 6.75 (1H, s, 1-H), 6.89 (1H, s, 1´-H), 7.01 (1H, td, *J* =1.38 and 6.99 Hz, 7´-H), 7.24 (1H, m, 6´-H), 7.37 (1H, d, *J* = 9.12 Hz, 5-H), 7.67 (1H, dt, *J* = 1.30 and 8.80 Hz,7´-H), 7.90 (1H, s, 3-H), 8.09 (1H, dd, *J* = 1.0 and 7.3 Hz, 8-H) and 9.74 (1H, dd, *J* = 0.82 and 7.30 Hz, 8´-H); δ_C (150 MHz; Methanol-d_6) 29.9 (CH_2N) , 49.9 ($COCH_3$) ,101.3 (C-1), 106.0 (C-1´), 113.3(C-7), 116.6 (C-7´), 117.6 (C-3), 119.4(C-6), 120.6 (C-5´), 120.9 (C-9/9´), 121.0 (C-5), 121.7 (C-9/9´), 125.6 (C-6´), 127.0 (C-8), 129.2 (C-8´), 131.1 (C-3´), 134.3 (C-2´), 138.0 (C-2) and,169.0, 169.6 and 190.5 (C=O).

Product 2: as green amorphous solid, *3-(indolizine-2-carbonyl)imidazolidine-2,4-dione* **148** (54.3 mg, 23%), mp.144-145 °C; ν_{max} (ATR)/cm^{-1} 3212 (NH), 1722 (C=O); δ_H (600 MHz; $CDCl_3$) 4.09 (2H, s, CH_2N), 7.66 (1H, t, *J* = 7.15 Hz, Ar-H), 7.80 (1H, m, Ar-H), 7.89 (1H, d, *J* = 8.15 Hz, Ar-H), 8.21 (1H, d, *J* = 8.48 Hz, Ar-H) and 8.32 (2H, d, *J* = 8.37 Hz, Ar-H); δ_C (150 MHz; $CDCl_3$) 53.2 (CH_2N), 121.0, 127.5, 128.5, 128.6, 129.4, 130.3, 130.7, 137.3 (Ar-C), 147.5, 147.9 and 166.0 (C=O).

***3-(Indolizine-2-carbonyl)imidazolidine-2,4-dione* 148** and ***1,3-bis(indolizine-2-carbonyl)imidazolidine-2,4-dione* 149**

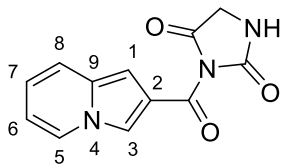

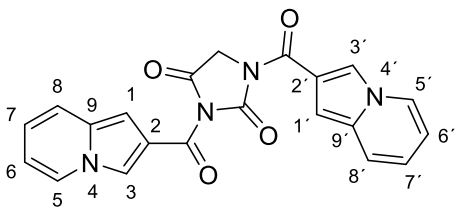

A solution of indolizine-2-carboxylic acid **138** (0.10 g, 0.63 mmol) and 2,4-imidazolidinedione **146** (85.7 mg, 0.75 mmol) in a mixture of pyridine:$CHCl_3$ (2:1; 12 mL) in a stoppered flask was cooled to between -20°C and -10°C and phosphonic anhydride solution (0.20 g, 0.63 mmol) was slowly added to maintain the internal temperature below 0°C. The reaction was

stirred in a stoppered flask for 3 days at which time the reaction mixture was diluted with $CHCl_3$ and filtered. The filtrate was concentrated *in vacuo* and the crude product purified by column chromatography on silica gel [elution with hexane:EtOAc (1:2)] to afford fraction 1 and a trace amount of fraction 2.

Fraction 1: as blue gel, *3-(indolizine-2-carbonyl)imidazolidine-2,4-dione* **148** (73.2 mg, 48%).

Fraction 2: as reddish-brown gel, *1,3-bis(indolizine-2-carbonyl)imidazolidine-2,4-dione* **149** (21.9 mg, 9%); ν_{max} (ATR)/cm^{-1} 1723 and 1689 (C=O); δ_H (600 MHz; $CDCl_3$) 5.54 (2H, s, CH_2N), 7.36 (1H, t, *J* = 7.3 Hz, Ar-H), 7.40 (2H, t, *J* = 7.4 Hz, Ar-H), 7.53 (2H, d, *J* = 7.4 Hz, Ar-H), 7.65 (1H, t, *J* = 7.5 Hz, Ar-H), 7.79 (1H, t, *J* = 7.1 Hz, Ar-H), 7.88 (1H, d, *J* = 8.2 Hz, Ar-H), 8.18 (1H, d, *J* = 8.5 Hz, Ar-H), 8.29 (1H, d, J = 8.5 Hz, Ar-H) and 8.32 (1H, d, J= 8.6 Hz, Ar-H).

***N-[3-(imidazol-1-yl)propyl]indolizine-2-carboxamide* 208**

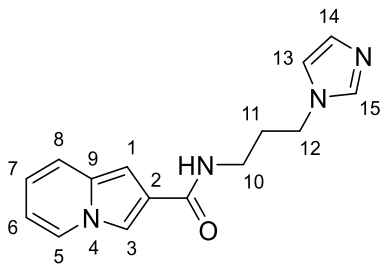

The procedure for the synthesis of 3-(indolizine-2-carbonyl)-1-methylimidazolidine-2,4-dione **150** was followed, using indolizine-2-carboxylic acid **138** (0.10 g, 0.62 mmol), 1-(3-aminopropyl)imidazole **207** (85.2 mg, 0.68 mmol), propylphosphonic anhydride solution (0.47 g, 1.5 mmol) and a mixture of DIPEA:CH_2Cl_2 (12 mL; 2:1) to afford, as a blue gel, an isomeric mixture of *N-[3-(midazol-1-yl)propyl]indolizine-2-carboxamide* **208** (5.6 mg; 3%); ν_{max} (ATR)/cm^{-1}3337 (NH) and 1672 (C=O); δ_H (600 MHz; Methanol-d_4) 2.10 (2H, m, 11-H), 3.38 (2H, m, 10-H), 4.11 (1H, t, *J* = 6.92 Hz, 12-H), 6.55 (1H, t, *J* =6.32 Hz, Ar-H), 6.70 (2H, m, Ar-H), 6.97 (1H, s, Ar-H),7.18 (1H, s, Ar-H), 7.35 (1H, d, *J* = 9.08 Hz, (1H, s, Ar-H)), 7.72 (1H, s, Ar-H), 7.83 (1H, d, *J* = 1.08 Hz, Ar-H) and 8.08 (1H, d, *J* = 0.68 Hz, Ar-H); δ_C (150 MHz; Methanol-d_4) 32.2, 37.7 and 45.8 (3 × CH_2), 98.9, 113.0, 115.2, 119.4, 120.7, 124.3, 126.9, 128.9, 134.3, 138.5 (Ar-C) and 167.9 (C=O).

3.3.5. Further synthesis of acetylated and non-acetylated *N*-heteroarylindolizine-2-carboxamides

3-Acetyl-N-(5-amino-1,2,4-triazol-3-yl)indolizine-2-carboxamide **192** and ***3-(3-acetylindolizine-2-carboxamido)-5-(indolizine-2-carboxamido)-1,2,4-triazole*** **193**

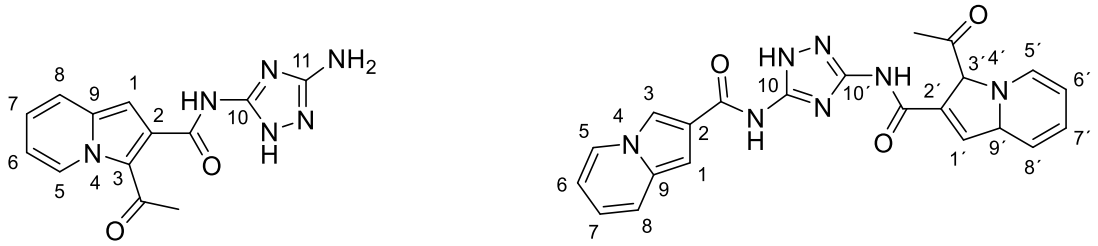

To a round-bottomed flask equipped with a stirrer bar was added 3-acetylindolizine-2-carboxylic acid **139** (0.36 g, 1.8 mmol.), 3,5-diamino-1,2,4-triazole **186** (0.26 g, 2.7 mmol) and a mixture of DIPEA:CH_2Cl_2 (2:1; 12 mL), and the resulting mixture was cooled to between -20 °C and -10 °C, and propylphosphonic anhydride solution (3.37 g, 5.30 mmol) was slowly added to maintain an internal temperature below 0°C. The resulting mixture was stirred for 2 days after which time TLC showed the formation of two products. The reaction mixture was diluted with $CHCl_3$ (10 mL), filtered and the solid residue washed with cool $CHCl_3$ (10 mL) to afford product 1. The filtrate was concentrated *in vacuo* and the crude mixture purified by column chromatography on silica gel [elution with hexane:EtOAc (1:2)] to afford product 2.

Product 1: as yellow crystals, *3-acetyl-N-(5-amino-1,2,4-triazol-3-yl)indolizine-2-carboxamide* **192** (16.1g, 3%). mp. 187-188 °C; (Found MH^+: 285.0819*. Calc. for $C_{13}H_{13}N_6O_2$: 285.1100); ν_{max} (ATR)/cm^{-1} 3427 (NH), 3317, 3125 (NH_2), 1692 and 1624 (C=O); δ_H (600 MHz; DMSO-d_6) 3.03 (3H, s, $COCH_3$), 6.21 (2H, s, NH_2), 7.25 (1H, t, J = 6.42 Hz, 7-H), 7.46 (1H, d, , J = 7.4 Hz, 6-H), 7.60 (1H, s, 1-H), 7.98 (1H, d, , J = 8.59 Hz, 5-H) and 9.11 (1H, d, , J = 6.94 Hz, 8-H); δ_C (150 MHz; DMSO-d_6) 29.5 ($COCH_3$), 106.7 (C-1), 115.8 (C-7), 120.6 (C-5) , 122.0 (C-9), 125.8 (C-6) , 126.3 (C-11), 129.9 (C-4), 137.8 (C-10), 152.7 (C-3), 154.9 (C-2) and, 155.9 and 164.0 (C=O).

Product 2: as yellow crystals, *3-(3-acetylindolizine-2-carboxamido)-5-(indolizine-2-carboxamido)-1,2,4-triazole* **193** (0.10 g, 14%); mp. 150-153 °C; (Found MH^+: 430.9071*. Calc. for $C_{22}H_{18}N_7O_3$: 430.1628); ν_{max} (ATR)/cm^{-1} 3439 (NH), 1661, 1612 and 1567 (C=O); δ_H (600 MHz; DMSO-d_6) 2.26 (3H, s, OCH_3), 6.64 (1H, t, , J = 6.72 Hz, 7-H), 6.75 (1H, t, , J =7.7 Hz, 6-H), 6.86 (1H, s, 1´-H), 7.12 (2H, m, 7´- and 1-H), 7.32 (1H, t, , J = 7.8 Hz, 6´-H), 7.47 (1H, d, , J = 9.13 Hz, 5-H), 7.62 (2H, br s, NH), 7.71 (1H, br s, NH), 7.77 (1H, d, , J = 8.79 Hz, 5´-H), 8.28 (1H, d, , J = 7.04 Hz, 8-H), 8.57 (1H, s, 3-H) and 9.72 (1H, d, , J =7.16

Hz, 8´-H); δ_C (150 MHz; DMSO-d_6) 28.1 ($COCH_3$), 102.3 (C-7´), 103.0 (C-1´), 112.6 (C-7), 115.6 (C-1), 118.8 (C-6), 119.0 (C-9), 119.4 (C-3), 119.5 (C-5´), 119.9 (C-3´), 120.0 (C-5), 124.9 (C-6´), 126.4 (C-8), 127.5 (C-8´), 130.4 (C-2´), 131.6 (C-2), 136.3 (C-9´), 162.2 (C-10), 162.4 (C=10´), and 162.7, 165.3 and 186.0 (C=O).

***N-(5-Amino-1,3,4-triazol-3-yl)indolizine-2-carboxamide* 187 and *3,5-bis(indolizine-2-carboxamido)-1,2,4-triazole* 188**

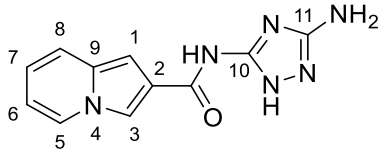

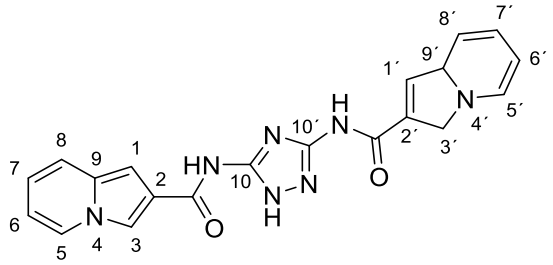

Indolizine-2-carboxylic acid **138** (0.10 g, 0.63 mmol), 3,5-diamino-1,2,4-triazole **186** (73.8 mg, 0.75 mmol) and a mixture of DIPEA:$CHCl_3$ (2:1; 12 mL) were placed in a round-bottomed flask and cooled to between -20°C and -10°C. Propylphosphonic anhydride solution (0.59 g, 1.86 mmol) was slowly added to the stirred mixture to maintain the internal temperature below 0°C. After stirring for 2 days the reaction mixture was filtered and the solid residue washed with cool $CHCl_3$ (10 mL) to afford product 1. The filtrate was concentrated *in vacuo* and the crude residue purified by column chromatography on silica gel [elution with hexane:EtOAc (1:2)] to afford product 2.

Product 1: as yellow crystals, *N-(5-amino-1,2,4-triazol-3-yl)indolizine-2-carboxamide* **187** (76.0 mg, 32%), mp. 184-187 °C; (Found MH^+: 243.1502*. Calc. for $C_{11}H_{11}N_6O$: 243.0994); ν_{max} (ATR)/cm^{-1} 3133 and 3102 (NH_2) and 1668 (C=O); δ_H (600 MHz; DMSO-d_6) 6.64 (1H, td, J =1.2 and 6.6 Hz, 7-H), 6.77 (1H, m, 6-H), 7.10 (1H, s, 1-H), 7.24 (1H, d, J = 3.5 Hz, NH), 7.48 (1H, d, J = 9.0 Hz, 5-H), 7.53 (1H, d, J = 3.5 Hz, NH), 8.29 (2H, m, 3- and 8-H).and 12.4 (1H, br s, NH); δ_C (150 MHz; DMSO-d_6) 99.0, 112.2, 113.6, 115.7, 118.7, 119.9, 121.2, 126.4, 137.7, 158.6 (Ar-C) and 162.1 (C=O).

Product 2: as yellow crystals, *3,5-bis(indolizine-2-carboxamido)-1,2,4-triazole* **188** (52.8 mg, 14%)**,** mp. 192-194 °C; (Found MH^+: 388.1464*. Calc. for $C_{20}H_{16}N_7O_2$: 388.1522); ν_{max} (ATR)/cm^{-1} 3113 and 1656 (C=O); δ_H (600 MHz; DMSO-d_6); 6.54 (1H, d, J =3.66 Hz, Ar-H), 6.65 (1H, t, J =6.45 Hz, Ar-H), 6.77 (1H, m, Ar-H), 6.88 (2H, s, Ar-H), 6.92 (1H, d, J =3.66 Hz, Ar-H), 7.10 (1H, s, Ar-H), 7.23 (1H, d, J =3.48 Hz, Ar-H), 7.48 (1H, d, J =9.12 Hz, Ar-H), 7.53 (1H, d, J =3.54 Hz, Ar-H), 8.30 (2H, m, Ar-H) and 12.40 (1H, br s NH); δ_C (150 MHz;

DMSO-d_6) 99.0, 106.6. 112.2, 113.6, 115.7, 118.7, 119.9, 121.2, 126.4, 132.2, 137.7, 138.7, 158.6 (Ar-C), and 162.1 and 168.9 (C=O).

***N-(2-Thiazolyl)indolizine-2-carboxamide* 154**

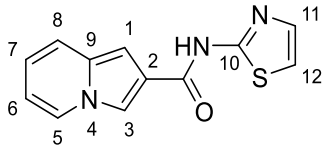

Method A: The procedure used for the synthesis of 3-(indolizine-2-carbonyl)-1-methylimidazolidine-2,4-dione **150** was followed, using indolizine-2-carboxylic acid **138** (50 mg, 0.31 mmol.), 2-aminothiazole **153** (37.3 mg, 0.37 mmol) and propylphosphonic anhydride solution (0.30 g, 0.93 mmol) in a mixture of DIPEA:$CHCl_3$ (2:1; 12 mL). The crude product was purified by preparatory plate chromatography on silica gel [elution with hexane:EtOAc (1:5)] to afford, as yellow crystals, *N-(2-thiazolyl)indolizine-2-carboxamide* **154** (19.7 mg, 26%), mp. 166-168 °C; ν_{max} (ATR)/cm^{-1} 3113 (NH) and 1657 (C=O); δ_H (600 MHz; DMSO-d_6) 6.65 (1H, td, J=1.20 and 6.7 Hz,7-H), 6.77 (1H, m, 6-H), 7.10 (1H,s, 1-H), 7.24 (1H, d, J=3.54 Hz, 11-H), 7.48 (1H, d, J=9.00 Hz, 5-H), 7.53 (1H, d, J=3.54 Hz,12-H), 8.30 (2H, m, 3- and 8-H) and 12.4 (1H, br s, NH);. δ_C (150 MHz; DMSO-d_6) 99.0, 112.2, 113.6, 115.7, 118.7, 119.9, 121.2, 126.4, 132.2, 137.7, 158.6 and 162.1 (=O).

Method B: 2,2,2-Trifluoroethyl borate (0.91g, 2.94 mmol) was added to a solution of indolizine-2-carboxylic acid **138** (0.16g, 0.98 mmol) and 2-aminothiazole **153** (0.12 g, 1.18 mmol) in acetonitrile (10 mL), and the mixture was refluxed at 80 °C. After 24 hours, TLC analysis showed the formation of a product. The solvent was removed *in vacuo* and the crude product purified by column chromatography on silica gel [elution with hexane:EtOAc (1:5)] to afford, as yellow crystals, *N-(2-thiazolyl)indolizine-2-carboxamide* **154** (4.76 mg , 2%).

***3-Acetyl-N-(thiazol-2-yl)indolizine-2-carboxamide* 194**

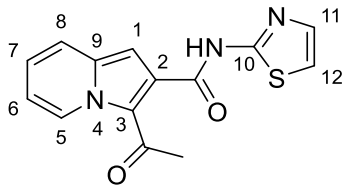

The procedure used for the synthesis of 3-(indolizine-2-carbonyl)-1-methylimidazolidine-2,4-dione **150** was followed, using 3-acetylindolizine-2-carboxylic acid **139** (0.21 g, 1.03 mmol),

2-aminothiazole **153** (0.15 g, 1.54 mmol) and propylphosphonic anhydride solution (0.98 g, 3.1 mmol) in a mixture of DIPEA:$CHCl_3$ (2:1; 12 mL). The crude mixture was purified by column chromatography on silica gel [elution with hexane:EtOAc (1:2)] to afford, as yellow crystals, *3-acetyl-N-(thiazol-2-yl)indolizine-2-carboxamide* **194** (67.2 mg, 23%), mp. 144-146 °C; (Found MH^+: 286.0648. Calc. for $C_{14}H_{12}N_3O_2S$: 286.0650); ν_{max} (ATR)/cm^{-1} 3115 (NH), 1669 and 1615 (C=O); δ_H (600 MHz; DMSO-d_6) 2.40 (3H, s, $COCH_3$), 6.95 (1H, s, 1-H), 7.14 (1H, t, *J* = 6.91 Hz, 7-H), , 7.34 (2H, m, 6 and 6- and 11-H), 7.56 (1H, d, *J* =3.54 Hz, 12-H), 7.81 (1H, d, *J* = 8.79 Hz, 5-H), 9.76 (1H, d, *J* = 7.17 Hz, 8-H) and 12.90 (1H, br s, NH).; δ_C (150 MHz; DMSO-d_6) 28.7 ($COCH_3$) 103.6 (C-1), 114.2 (C-6), 115.7 (C-7), 119.4 (C-9) 119.6 (C-5), 124.8 (C-11), 127.6 (C-8), 130.5 (C-10), 135.9 (C-3), 138.0 (C-12), 157.8 (C-2),and 164.4 and 186.8 (C=O)

***3-Acetyl-N-(triazol-3-yl)indolizine-2-carboxamide* 195**

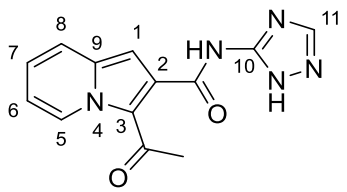

The procedure used for the synthesis of 3-(indolizine-2-carbonyl)-1-methylimidazolidine-2,4-dione **150** was followed, using 3-acetylindolizine-2-carboxylic acid **138** (0.21 g, 1.0 mmol.), 3-amino-1,2,4-triazole **191** (0.13 g, 1.6 mmol.) and propylphosphonic anhydride solution (0.98g 3.1 mmol) in a mixture of DIPEA:$CHCl_3$ (2:1; 12 mL). The crude product was purified by preparatory plate chromatography on silica gel [elution with hexane:EtOAc (1:3)] to afford as yellow crystals, 3-acetyl-*N*-(triazol-3-yl)indolizine-2-carboxamide **195** (25.0 mg, 9%), mp. 99-101 °C; (Found MH^+: 270.0984. Calc. for $C_{13}H_{12}N_5O_2$: 270.0991); ν_{max} (ATR)/cm^{-1} 3115 (OH) and 1737 (C=O); δ_H (600 MHz; DMSO-d_6) 2.07 (3H, s, $COCH_3$), 6.91 (1H, s, 1-H) 7.12 (1H, t, *J* =6.9 Hz, 7-H), 7.32 (1H, d, *J* = 7.40 Hz, 6-H), 7.80 (2H, d, *J* =8.46 Hz, 5- and 11-H) and 9.75 (1H, d, *J* = 6.96 Hz, 8-H); δ_C (150 MHz; DMSO-d_6) 28.9 ($COCH_3$), 103.4 (Ar-C), 115.6 (Ar-C), 119.3 (Ar-C), 119.5 (Ar-C), 124.7 (Ar-C), 127.6 (overlapping 2× Ar-c), 136.0 (Ar-C), 150.3 (Ar-C), 164.9 (Ar-C) and, 169.2 and 186.9 (C=O).

Attempted synthesis of ***N-(2-pyridinyl)indolizine-2-carboxamide*** **190**

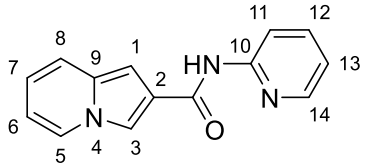

A stirred solution of indolizine-2-carboxylic acid **138** (50.0 mg, 0.31 mmol), 2-aminopyridine **189** (35.1 mg, 0.37 mmol) in a mixture of DIPEA:$CHCl_3$ (12 mL; 2:1) in a stoppered flask was cooled to between -20°C and -10°C. Propylphosphonic anhydride solution (0.30 g, 0.93 mmol) was slowly added to maintain the internal temperature below 0°C and the stirred mixture was allowed to warm to room temperature. After 2 days, the reaction mixture was diluted with $CHCl_3$ (10 mL), filtered and the filtrate concentrated *in* vacuo. Attempted purification of the desired product involved use of preparatory plate chromatography on silica gel [elution with hexane:EtOAc (4:7)]. The product was difficult to isolate and decomposed rapidly, precluding NMR analysis. Crude mixture of *N-(2-pyridinyl)indolizine-2-carboxamide* **190**, (Found MH^+: 238.0916*. Calc. for $C_{14}H_{12}N_3O$: 238.0980); ν_{max} (ATR)/cm^{-1} 3337 (NH) and 1672 (C=O).

3-Acetyl-N-(2-pyridinyl)indolizine-2-carboxamide **196**

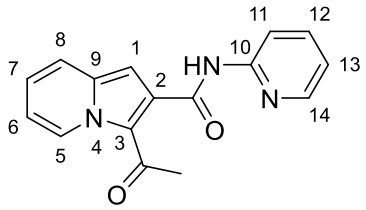

The procedure for the synthesis of 3-(indolizine-2-carbonyl)-1-methylimidazolidine-2,4-dione **150** was followed, using 3-acetylindolizine-2-carboxylic acid **139** (0.20 g, 0.90 mmol), 2-aminopyridine **189** (0.14 g, 1.5 mmol) and propylphosphonic anhydride solution (0.86 g, 2.7 mmol) in a mixture of DIPEA:$CHCl_3$ (2:1; 12 mL). The crude product was purified by column chromatography on silica gel [elution with hexane:EtOAc (1:2) to afford, as orange crystals, *3-acetyl-N-(2-pyridinyl)indolizine-2-carboxamide* **196** (6.50 mg, 3%), mp. 126-129 °C; (Found MH^+: 280.1082. Calc. for $C_{16}H_{14}N_3O_2$: 280.1086); ν_{max} 3241 (NH), 1682 and 1603 (C=O); δ_H (600 MHz; Acetone-d_6) 2.54 (3H, s, $COCH_3$), 6.90 (1H, br s, Ar-H), 7.07 (1H, br s, Ar-H), 7.14 (1H, br s, Ar-H), 7.30 (1H, br s, Ar-H), 7.74 (1H, d, J = 8.3 Hz, Ar-H), 7.86 (1H, br s, Ar-H), 8.28 (1H, s, Ar-H), 8.37 (1H, d, J = 7.0 Hz, Ar-H), 9.85 (1H, d, J = 6.2 Hz, Ar-H) and 10.0 (1H, s, NH); δ_C (150 MHz; Acetone-d_6) 29.2 ($COCH_3$), 103.5, 114.7, 115.8, 120.0, 120.8, 125.0, 128.7, 133.6, 137.1, 139.0, 149.0, 152.9 (Ar-C) and, 166.2 and 187.8 (C=O).

***N-(2-Pyrazinecarbonyl)indolizine-2-carboxamide* 179**

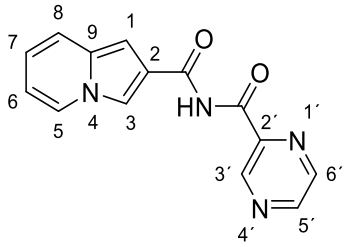

A stirred solution of indolizine-2-carboxylic acid **138** (0.20 g, 1.2 mmol), pyrazinecarboxamide **171** (0.18 g, 1.5 mmol) in a mixture of DIPEA:$CHCl_3$ (2:1; 12 mL) in a stoppered flask was cooled to between -20°C and -10°C. Propylphosphonic anhydride solution (0.98 g, 3.08 mmol) was slowly added to maintain the internal temperature below 0°C. The stirred mixture was allowed to warm to room temperature and then refluxed. After 2 days, the reaction mixture was cooled to room temperature, diluted with $CHCl_3$ (10 mL) and filtered. The filtrate was concentrated *in vacuo* and the crude product purified by preparatory plate chromatography on silica gel [elution with EtOAc:MeOH (9:1)] to afford, as a light yellow gel, a trace amount of *N-(2-pyrazinecarbonyl)indolizine-2-carboxamide* **179**; (Found MH^+: 267.2486*:. Calc. for $C_{14}H_{11}N_4O_2$: 267.0882); δ_H (600 MHz; Methanol-d_4) 6.56 (1H, td, *J* = 1.10 and 7.32 Hz, 7-H), 6.69 (1H, m, 6-H), 6.75 (1H, s, 1-H), 7.37 (1H, d, *J* =9.14 Hz, 5-H), 7.90 (1H, d, *J* =1.00 Hz, 3-H), 8.08 (1H, dd, *J* = 0.94 and 7.09 Hz, 8-H), 8.68 (1H, t, *J* = 1.53 Hz, 15-H), 8.77 (1H, d, *J* = 2.47 Hz, 14-H) and 9.24 (1H, d, J=1.40 Hz, 16-H).

***N-[N-(Indolizin-2-carbonyl)isoxazolin-3-on-4-yl]indolizine-2-carboxamide* 180**

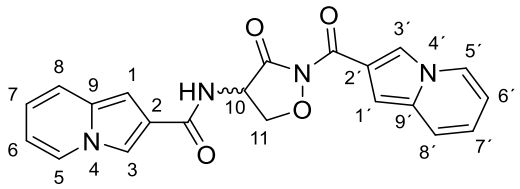

The procedure for the synthesis of *N*-(2-pyrazinecarboxanoyl)indolizine-2-carboxamide **179** was followed, using indolizine-2-carboxylic acid **138** (0.20 g, 1.2 mmol), (R)-4-amino-3-isoxazolidone **170** (0.18 g, 1.5 mmol) and propylphosphonic anhydride solution (0.98 g, 3.1 mmol) in a mixture of DIPEA:$CHCl_3$ (12 mL; 2:1). After 2 days, the reaction mixture was cooled to room temperature, diluted with $CHCl_3$ (10 mL) and filtered. The residue was washed with chilled methanol to afford, as brick-red crystals, *N-[N-(indolizin-2-carbonyl)isoxazolin-3-on-4-yl]indolizine-2-carboxamide* **180** (10.4 mg, 2%), mp. 171-173 °C; (Found MH^+: 389.2417*. Calc. for $C_{21}H_{17}N_4O_4$: 389.1250); ν_{max} (ATR)/cm^{-1} 3320 (NH), 1644 and 1599

(C=O); δ_H (600 MHz; DMSO-d_6 at 353 K) 1.27 (1H, m, 10-H), 6.61 (1H, t, J = 6.6 Hz, Ar-H), 6.72 (2H, m, Ar-H), 6.79 (2H, d, J = 7.7 Hz, Ar-H), 6.87 (1H,s, Ar-H), 7.14 (2H, t, J = 7.8 Hz, Ar-H), 7.44 (1H, d, J = 9.1 Hz, Ar-H), 8.03 (1H, s, Ar-H), 8.25 (1H, d, J = 7.0 Hz, Ar-H) and 9.98 (1H, s, Ar-H); δ_C (150 MHz; DMSO-d_6) 30.3, 53.6, 97.9, 111.4, 112.2, 114.2, 118.0, 118.4, 119.3, 121.7, 125.9, 128.7, 131.9, 149.6 and 163.7 (C=O).

δ_H (600 MHz; DMSO-d_6 at 298 K) 1.26 (1H. br s, 10-H), 3.81 (2H, s, CHCH_2O), 6.58 (1H, t, J = 6.7 Hz, Ar-H), 6.64 (1H, t, J= 6.7 Hz, Ar-H), 6.72 (1H, m, Ar-H), 6.76 (2H, m, Ar-H), 7.41 (1H, d, J = 9.1 Hz, Ar-H), 7.45 (1H, d, J = 9.1 Hz, Ar-H), 7.94 (1H, s, Ar-H), 8.07 (1H, s, Ar-H), 8.23 (1H, d, J = 7.0 Hz, Ar-H), 8.28 (1H, t, J = 6.4 Hz, Ar-H) and 9.34 (1H, s, Ar-H).

3.3.6. Synthesis of indolizine-2-carbohydrazides 197-199

***Indolizine-2-carbohydrazide* 197** and ***N,N´-bis(indolizine-2-carbonyl)hydrazine* 198**

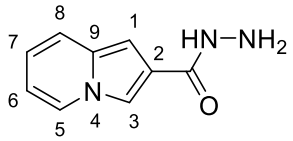

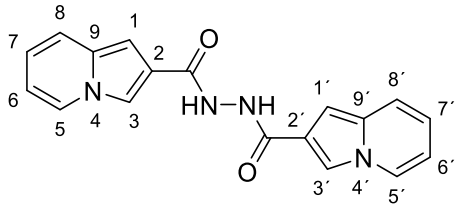

The procedure for the synthesis of *N*-(2-pyrazinecarbonyl)indolizine-2-carboxamide **179** was followed, using indolizine-2-carboxylic acid **138** (0.20 g, 1.2 mmol), hydrazinemonohydrate (74.7 mg, 1.49 mmol) and propylphosphonic anhydride solution (0.98 g, 3.1 mmol) in a mixture of DIPEA:$CHCl_3$ (12 mL; 2:1). The reaction mixture was cooled to room temperature, diluted with $CHCl_3$ (10 mL) and filtered to obtain product 1. The filtrate was concentrated *in vacuo* and the crude residue purified by preparatory plate chromatography on silica gel [elution with EtOAc:MeOH (9:1)] to afford product 2.

Product 1: as a light brown amorphous solid, *indolizine-2-carbohydrazide* **197** (0.15 g, 7%), mp. 120-123 °C; (Found MH^+: 176.0275*. Calc. for $C_9H_{10}N_3O$: 176.0824); ν_{max} 3325 (NH), 3182 and 3127 (NH_2), 1666 (C=O); δ_H (600 MHz; DMSO-d_6) 4.48 (2H, br s, NH_2), 6.58 (1H, t, J =7.17 Hz, 7-H), 6.71 (1H, t, J = 7.74, 6-H), 6.76 (1H, s, 1-H), 7.40 (1H, d, J = 9.06 Hz, 5-H), 7.94 (1H, s, 3-H), 8.24 (1H, d, J = 6.96 Hz, 8-H) and 9.50 (1H, s, NH); δ_C (150 MHz; DMSO-d_6) 97.6, 111.4, 114.0, 118.1, 119.5, 122.3, 126.1, 131.8 (Ar-C) and 163.7 (C=O).

Product 2: as yellow gel, *N,N´-bis-(indolizine-2-carbonyl)hydrazine* **198** (14.1 mg, 4%); (Found MH^+: 319.2048*. Calc. for $C_{18}H_{15}N_4O_2$: 319.1195); ν_{max} 3229, 3323 (NH), 1643 and 1582 (C=O); δ_H (600 MHz; $CDCl_3$) 6.54 (1H, td, J = 1.11 and 6.69 Hz, 7-H), 6.69 (1H, m, 6-H), 6.72 (1H, s, 1-H), 7.05 (1H, s, NH), 7.35 (1H, d, J = 9.2 Hz, 5-H), 7.82 (1H, d, J = 1.3 Hz, 3-H), 7.92 (1H, s, NH) and 8.06 (1H, dd, J = 0.90 and 6.6 Hz, 8-H).

***N²-Phenylindolizine-2-carbobydrazide* 199**

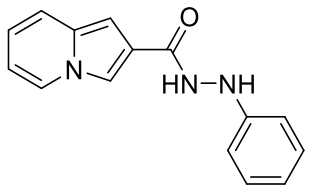

A stirred solution of indolizine-2-carboxylic acid **138** (0.10 g, 0.62 mmol), phenyl hydrazine (73.6 mg, 0.68 mmol) in a mixture of DIPEA:$CHCl_3$ (12 mL; 2:1) in a stoppered flask was cooled to between -20°C and -10°C. Propylphosphonic anhydride solution (0.59 g, 1.9 mmol

was slowly added to maintain the internal temperature below 0°C. The resulting homogeneous brick-red solution was allowed to warm to room temperature and stirred for 2 days. The reaction mixture was diluted with $CHCl_3$ (10 mL), and filtered, and the filtrate was concentrated *in vacuo.* The crude product was purified by preparatory plate chromatography on silica gel [elution with hexane:EtOAc (5:2) to afford, as red crystals, N^2-phenylindolizine-2-carbohydrazide **199** (25.8 mg, 17%), mp. 199-201 °C; (Found MH^+: 252.1135. Calc. for $C_{15}H_{14}N_3O$: 252.1137); ν_{max} (ATR)/cm^{-1} 3339, 3223 (NH) and 1643 (C=O); δ_H (600 MHz; DMSO) 6.62 (1H, t, *J* = 7.29 Hz, Ar-H), 6.70 (1H, t, *J* = 7.27 Hz, Ar-H), 6.75 (3H, m, Ar-H), 6.78 (1H, s, Ar-H), 6.88 (1H, s, 3-H), 7.14 (2H, t, *J* = 7.89 Hz, Ar-H), 7.45 (1H, d, *J* = 9.07 Hz, Ar-H), 7.85 (1H, d, *J* = 2.67 Hz, NH), 8.05 (1H, s, Ar-H), 8.28 (1H, d, *J* = 7.02 Hz, Ar-H) and 10.10 (1H, d, *J* = 2.65 Hz, NH); δ_C (150 MHz; DMSO) 98.0, 111.6, 112.2, 114.4, 118.3, 118.4, 119.6, 121.8, 126.2, 128.7, 132.0, 149.8 (Ar-C) and 163.8 (C=O).

3.4. Bioassay protocols

The HIV-1 (3.4.1), PR (3.4.2) and RT (3.4.3), *Pf* (pLDH; 3.4.4), *T. brucei* (3.4.5) enzyme bioassays and cytotoxicity studies (3.4.6) were performed for the author by the Bioassay Facility of the Rhodes Centre for Chemico- and Biomedicinal Research (CCBR).

3.4.1. HIV-1 Integrase Assay

The HIV-1 IN strand transfer inhibition assay was performed using the following protocol. Briefly, the 20 nM double-stranded biotinylated donor DNA (5´-5BiotinTEG/ACCCTTTTAGTCAGTGTGGAAAATCTCTAGCA-3´ annealed to 5´-ACTGCTAGAGATTTTCCACACTGACTAAAAG-3´) was immobilized in wells of streptavidin-coated 96-well microtiter plates (R&D Systems, USA). Following incubation at room temperature for 40 minutes and a stringent wash step, 5 µg/ml purified recombinant HIV-1 subtype C IN in integrase buffer 1 (50 mm NaCl, 25 mM Hepes, 25 mM $MnCl_2$, 5 mM β-mercaptoethanol, 50 µg/ml BSA, pH 7.5) was added to individual wells. Test compounds and chicoric acid were added to individual wells to a final concentration of 20 µM. Recombinant HIV-1 subtype C IN was assembled onto the pre-processed donor DNA through incubation for 45 minutes at room temperature. Strand transfer reaction was initiated through the addition of 10 nM (final concentration) double-stranded FITC-labelled target DNA (5´-TGACCAAGGGCTAATTCACT/36-FAM/-3´ annealed to 5´-AGTGAATTAGCCCTTGGTCA-/36-FAM/-3´) in integrase buffer 2 (same as buffer 1, except 25 mM $MnCl_2$ replaced with 2.5 mM $MgCl_2$). After an incubation period of 60 minutes at 37 °C, the plates were washed using PBS containing 0.05% Tween 20 and 0.01% BSA, followed by the addition of peroxidase-conjugated sheep anti-FITC antibody (Thermo Scientific, USA) diluted 1:1000 in the same PBS buffer. Finally, the plates were washed and peroxidase substrate (SureBlue Reserve™, Seracare) was added to allow for detection at 620 nm using a Synergy MX (BioTek®) plate reader. Absorbance values were converted to % enzyme activity relative to the readings obtained from control wells (enzyme without inhibitor).[311]

3.4.2. HIV-1 Protease assay

The HIV protease assay was performed using the flourogenic substrate Arg-Glu(EDANS)-Ser-Gln-Asn-Tyr-Pro-Ile-Val-Gln-Lys(DABCYL)-Arg (Sigma Aldrich) as previously described by Lam *et al*. (2000). The substrate was dissolved in DMSO to make a 500 µM stock. Test compounds were diluted to desired concentrations in the reaction buffer (0.1 M sodium acetate, 1 M NaCl, 1

mM EDTA, 1 mM DTT, 0.1% BSA, 5% DMSO, pH 4.7) in a separate plate before being added to a fluorescence assay plate at 50 µl per well. Substrate (25 µl) to the final concentration of 8 µM and HIV subtype C protease (25 µl) to the final concentration of 50 ng/µl were added. The mixture was incubated at 37 °C for 40 minutes after which fluorescence was read at an excitation wavelength 340 nm and emission wavelength 485 nm using a Synergy MX (BioTek®) plate reader. Ritonavir was used as the standard inhibitor. Fluorescence values were converted to % enzyme activity relative to the readings obtained from control wells (enzyme without inhibitor).[312]

3.4.3. HIV-1 RT assay

Quantification of the inhibitory effect of the synthesised ligands was performed using a commercial HIV-RT kit (Roche Applied Science, USA) as per manufacturer's instruction. The inhibitory activity of the reverse transcriptase inhibitors was calculated as the percentage of the enzyme activity compared to a sample that does not contain any inhibitor. Nevirapine was used as the standard inhibitor.

3.4.4. Plasmodium falciparum (pLDH) assay

Routine culturing of *P. falciparum* blood-stage parasites (3D7 strain) was carried out at 37 degrees in RPMI1640 medium supplemented with 25 mM HEPES, 0.5% (w/v) Albumax II, 22 mM glucose, 0.65 mM hypoxanthine, 0.05 mg/mL gentamicin and 2-4% (v/v) human erythrocytes in sealed culture vessels filled with a 5% CO_2, 5% O_2, 90% N_2 gas mixture. For compound assays, cultures were adjusted to 2% parasitaemia and 1% (v/v) red blood cells and incubated with test compounds at a final concentration of 20 µM for 48 h in 96-well plates. A parasite lactate dehydrogenase (pLDH) was subsequently carried out to determine the level of parasites remaining in each well. Twenty µL of culture was removed from the individual wells and transferred to a second 96-well plate containing 125 µL per well pLDH assay reagent (44 mM Tris buffer, pH 9, containing 0.18 M L-lactic acid, 0.13 mM acetylpyridine adenine dinucleotide, 0.39 mM nitrotetrazolium blue chloride, 0.048 mM phenazineethosulphate and 0.16% (v/v) Triton X-100) and incubated at ambient temperature for 10 – 30 minutes. Colour development was measured as absorbance at 620 nm and the absorbance values were used to calculate percentage parasite viability relative to control wells containing untreated parasite cultures. Chloroquine was used as a standard compound.

3.4.5. Trypanosome assay

To assess trypanocidal activity, compounds were added to cultures of *T. brucei* in 96-well plates at a fixed concentration of 20 µM/50 µg/mL for pure compounds and 25 µg/mL for natural extracts (unless otherwise stated). After a 48-hour incubation, parasites surviving drug treatment were enumerated by adding a resazurin based reagent. Resazurin is reduced to resorufin (a fluorophore (Exc_{560}/Em_{590})) in viable cells and was thus quantified in a Spectramax M3 microplate reader.

Results were expressed as % parasite viability – the resorufin fluorescence in compound-treated wells relative to untreated controls. Compounds were tested in duplicate and standard deviations (SD) derived. Compounds/extracts that reduced parasite viability to <20% are considered for further testing (dose-response and cytotoxicity assays). Pentamidine (an existing drug treatment for trypanosomiasis) was used as a control drug standard.

3.4.6. Cytotoxicity assay

HEK 293 human embryonic kidney cells (Cellonex) were cultured in DMEM medium supplemented with 10% foetal bovine serum and antibiotics (penicillin /streptomycin/amphotericin B) in a 5% CO_2 incubator. The cells were plated in 96-well plates at a density of $2x10^4$ cells per well on the day prior to compound addition. After a 24 hour incubation in the presence of 20 µM of the compounds, 20 µL of resazurin toxicology reagent (Sigma-Aldrich) was added to each well and after an additional 2 hour incubation fluorescence was measured at 560 nm and 590 nm (excitation and emission wavelengths, respectively) in a Spectramax M3 plate reader (Molecular Devices). Fluorescence readings were converted to % cell viability relative to the average readings obtained in untreated control wells (cells without compound). Emetine was included as a cytotoxic standard compound.

3.5. Mechanistic studies

Kinetic studies were conducted using Bruker Avance II 600 MHz spectrometer. Reactants were mixed in a small vial in the order: pyridine-4-carboxaldehyde, methyl acrylate and the tertiary amine catalyst in $CDCl_3$. The liquid pyridine-4-carboxaldehyde and methyl acrylate were measured using a micro syringe. The resulting reaction mixture was immediately transferred to an NMR tube and cooled in a dry-ice bath to inhibit reaction prior to inserting the NMR tube into the NMR probe, the temperature of which was fixed at 298 K. A ^1H NMR and corresponding DEPT-135 NMR spectra were promptly run, and the pair of spectra were automatically run at regular intervals over the duration of the reaction.

The reaction mixture contained a mixture of 0.107g pyridine-4-carboxaldehyde, 0.086g methyl acrylate and 0.007g 3-hydroxyquinuclidine in 0.5 ml $CDCl_3$, with the duration of the reaction being 70 873 seconds. The data obtained enabled the following:

(i) identification of the crucial intermediate

(ii) determining that the reaction is second order with respect to the aldehyde and,

(iii) reveal the s-shaped profile on the concentration-time plot of the reaction which denotes autocatalysis.

Table 12. Data for consumption of the aldehyde and formation of the product.

Expt #	Time (s)	[Pyridine-4-CHO]	[Product]
100	0	4.689179551	0.094026278
101	834	4.445254035	0.158162191
102	1668	4.19925494	0.163254641
103	2501	3.972271223	0.138789684
104	3335	3.771546103	0.120522523
105	4169	3.577252193	0.120395341
106	5003	3.400122885	0.151308322
107	5836	3.235582367	0.233528388
108	6670	3.076641041	0.398697491
109	7503	2.921561835	0.658844104
110	8337	2.783869101	0.985541559
111	9171	2.659117068	1.333875489
112	10004	2.540538016	1.661772441
113	10836	2.428085263	1.946975454
114	11669	2.325062699	2.173540385
115	12505	2.228249325	2.374829124
116	13339	2.133622779	2.512030661
117	14174	2.046859911	2.634145953
118	15006	1.965292708	2.730039175
119	15840	1.884744118	2.83655669
120	16674	1.814773441	2.910756654
121	17507	1.743329165	2.974647256
122	18341	1.678213025	3.049452125
123	19174	1.617677474	3.120151746
124	20007	1.556562894	3.17773532
125	20841	1.498948507	3.24659987
126	21673	1.444451423	3.29536833
127	22507	1.389008452	3.363731198
128	23342	1.342338841	3.404610559
129	24176	1.296005276	3.451967671
130	25010	1.247190125	3.501703123
131	25843	1.207453484	3.539847295
132	26680	1.162107404	3.588667527
133	27513	1.122474226	3.628440296
134	28347	1.083016775	3.669738442
135	29180	1.042685626	3.708627115
136	30014	1.007865614	3.744274296
137	30848	0.971256911	3.780345494
138	31682	0.935620054	3.816674934
139	32516	0.908043326	3.836491524
140	33351	0.881593601	3.873767307

141	34184	0.855014605	3.907977248
142	35018	0.832582001	3.934075289
143	35853	0.80757984	3.962184662
144	36687	0.783415249	3.988494714
145	37521	0.76340221	4.013450423
146	38355	0.740819614	4.044749521
147	39189	0.721271891	4.06660826
148	40023	0.703393989	4.092706301
149	40857	0.68481303	4.112099173
150	41690	0.664898216	4.139101959
151	42524	0.647408049	4.165748211
152	43357	0.628765076	4.187813719
153	44191	0.613430845	4.205360741
154	45025	0.601121054	4.22732302
155	45859	0.581697364	4.243727399
156	46693	0.568736206	4.262256513
157	47526	0.55545445	4.284058548
158	48360	0.539748005	4.303063452
159	49193	0.525690775	4.319261057
160	50027	0.512259105	4.337050908
161	50860	0.499410616	4.352571181
162	51694	0.487440029	4.3659356
163	52530	0.476261434	4.384863161
164	53364	0.463238726	4.395632287
165	54198	0.452006901	4.408789932
166	55031	0.44091933	4.422893619
167	55865	0.426909131	4.435487646
168	56699	0.420050619	4.449901642
169	57533	0.409464496	4.464046928
170	58367	0.400358063	4.479427611
171	59200	0.392334761	4.497015925
172	60034	0.37994847	4.508627859
173	60867	0.373217146	4.521464715
174	61701	0.36578889	4.538856735
175	62535	0.353780515	4.546844442
176	63368	0.345847651	4.558358078
177	64202	0.338706868	4.56729676
178	65036	0.332466172	4.586762048
179	65869	0.323430537	4.590344672
180	66703	0.316335244	4.597680943
181	67536	0.310135897	4.610771409
182	68370	0.30178323	4.611081723
183	69207	0.29732412	4.618273162
184	70039	0.290761317	4.627842635

185	70873	0.285053632	4.62918712

4. References

1. J. Drews, *Science*, 2000, **287**, 1960-1964.
2. G. N. Ling, *Life at the cell and below-cell level: The hidden history of a fundamental revolution in biology*, Pacific Press, New York, NY, USA:, 2001.
3. E. Farber, *The evolution of chemistry: a history of its ideas, methods, and materials*, Ronald Press, New York, 1969.
4. Y.-W. Chin, M. J. Balunas, H. B. Chai and A. D. Kinghorn, *AAPSJ*, 2006, **8**, 239-253.
5. D. J. Newman and G. M. Cragg, *J. Nat. Prod.*, 2007, **70**, 461-477.
6. D. J. Newman, G. M. Cragg and K. M. Snader, *Nat. Prod. Rep.*, 2000, **17**, 215-234.
7. D. J. Newman and G. M. Cragg, *J. Nat. Prod*, 2016, **79**, 629-661.
8. D. J. Newman, G. M. Cragg and K. M. Snader, *J. Nat. Prod.*, 2003, **66**, 1022-1037.
9. G. M. Cragg, D. J. Newman and K. M. Snader, *J. Nat. Prod.*, 1997, **60**, 52-60.
10. A. Nostro, M. Germano, V. D'angelo, A. Marino and M. Cannatelli, *Lett. Appl. Microbiol.*, 2000, **30**, 379-384.
11. M. J. Balunas and A. D. Kinghorn, *Life Sci.*, 2005, **78**, 431-441.
12. S. M. K. Rates, *Toxicon*, 2001, **39**, 603-613.
13. R. Hare, *Med. Hist.*, 1982, **26**, 1.
14. R. Bentley, *Perspect. Biol. Med.*, 2005, **48**, 444-452.
15. B. L. Ligon, *Semin. Pediatr. Infect. Dis.*, 2004, **15**, 52-57.
16. B. Grinsztejn, B.-Y. Nguyen, C. Katlama, J. M. Gatell, A. Lazzarin, D. Vittecoq, C. J. Gonzalez, J. Chen, C. M. Harvey and R. D. Isaacs, *Lancet*, 2007, **369**, 1261-1269.
17. R. Gaynes, *Emerg. Infect. Dis.s*, 2017, **23**, 849.-853
18. A. Crump and S. Omura, *Proc. Jpn. Acad., Series B*, 2011, **87**, 13-28.
19. L. J. Sharpe and A. J. Brown, *J. Biol. Chem.*, 2013, **288**, 18707-18715.
20. A. K. Ghose, V. N. Viswanadhan and J. J. Wendoloski, *J. Comb. Chem.*, 1999, **1**, 55-68.
21. B. C. Doak, J. Zheng, D. Dobritzsch and J. Kihlberg, *J. Med. Chem*, 2015, **59**, 2312-2327.
22. P. Matsson, B. C. Doak, B. Over and J. Kihlberg, *Adv. Drug Deliv. Rev.*, 2016, **101**, 42-61.
23. B. C. Doak, B. Over, F. Giordanetto and J. Kihlberg, *Chem. Biol*, 2014, **21**, 1115-1142.

24. C. A. Lipinski, *Adv. Drug Deliv. Rev.*, 2016, **101**, 34-41.
25. E. Van Cutsem, C. Twelves, J. Cassidy, D. Allman, E. Bajetta, M. Boyer, R. Bugat, M. Findlay, S. Frings and M. Jahn, *J. Clin. Oncol*, 2001, **19**, 4097-4106.
26. M. Wilhelm, J. Schlegl, H. Hahne, A. M. Gholami, M. Lieberenz, M. M. Savitski, E. Ziegler, L. Butzmann, S. Gessulat and H. Marx, *Nature*, 2014, **509**, 582-587.
27. F. E. Koehn and G. T. Carter, *Nat. Rev. Drug Disc.*, 2005, **4**, 206-220.
28. M. Kansy, F. Senner and K. Gubernator, *J. Med. Chem*, 1998, **41**, 1007-1010.
29. P. Artursson and J. Karlsson, *Biochem. Biophys. Res. Commun.*, 1991, **175**, 880-885.
30. L. Barthe, J. Woodley and G. Houin, *Fundam. Clin. Pharmacol.*, 1999, **13**, 154-168.
31. V. Pade and S. Stavchansky, *Pharm. Res.*, 1997, **14**, 1210-1215.
32. R. B. Van Breemen and Y. Li, *Expert Opin. Drug Metab. Toxicol.*, 2005, **1**, 175-185.
33. P. D. Dobson and D. B. Kell, *Nat. Rev. Drug Disc.*, 2008, **7**, 205.
34. F. E. Koehn, *Med. Chem. Comm.*, 2012, **3**, 854-865.
35. R. Mullin, *Chem. Eng. News*, 2014, **92**, 6.
36. J. A. DiMasi, H. G. Grabowski and R. W. Hansen, *J. Health Econ.*, 2016, **47**, 20-33.
37. J. A. DiMasi, *Clin. Pharmacol. Ther.*, 2001, **69**, 297-307.
38. J. W. Scannell, A. Blanckley, H. Boldon and B. Warrington, *Nat. Rev. Drug. Disc.*, 2012, **11**, 191-200.
39. K. H. Bleicher, H.-J. Böhm, K. Müller and A. I. Alanine, *Nat. Rev. Drug. Disc.*, 2003, **2**, 369-378.
40. J. A. DiMasi, L. Feldman, A. Seckler and A. Wilson, *Clin. Pharmacol. Ther.*, 2010, **87**, 272-277.
41. A. Ganesan, *Curr. Opin. Biotechnol.*, 2004, **15**, 584-590.
42. N. Tayar, A. Mark, P. Vallat, R. Brunne, B. Testa and W. van Gunsterent, *J. Mol. Graphics*, 1993, **11**, 260-261.
43. A. Alex, D. S. Millan, M. Perez, F. Wakenhut and G. A. Whitlock, *Med. Chem. Comm.*, 2011, **2**, 669-674.
44. D. F. Veber, S. R. Johnson, H.-Y. Cheng, B. R. Smith, K. W. Ward and K. D. Kopple, *J. Med. Chem*, 2002, **45**, 2615-2623.
45. R. Langer, *Science*, 1990, 1527-1533.
46. A. Sosnik, D. A. Chiappetta and Á. M. Carcaboso, *J. Controlled Release*, 2009, **138**, 2-15.
47. U. Gupta and N. K. Jain, *Adv. Drug Deliv. Rev.*, 2010, **62**, 478-490.
48. A. S. Fauci,*Nat. Med.*, 2003, **9**, 839-843.

49. P. J. Kanki, D. J. Hamel, J.-L. Sankalé, C.-c. Hsieh, I. Thior, F. Barin, S. A. Woodcock, A. Guèye-Ndiaye, E. Zhang and M. Montano, *J. Infect. Dis.*, 1999, **179**, 68-73.
50. K. C. Idahosa, PhD *Thesis*, Rhodes University, 2012.
51. Y. C. Lee, *M.Sc. thesis*, Rhodes University, 2009, 1-5.
52. T. O. Olomola, *PhD thesis*, Rhodes University, 2011, 1-4.
53. T. W. Chun, S. Moir and A. S. Fauci, *Nat. Immunol.*, 2015, **16**, 584-589.
54. WHO, *Vaccines*, *https*://www.who.int/topics/vaccines/en/. Accessed October 06, 2017.
55. M. I. Johnston and A. S. Fauci, *New Eng. J. Med.*, 2007, **356**, 2073-2081.
56. I. M. Belyakov, M. A. Derby, J. D. Ahlers, B. L. Kelsall, P. Earl, B. Moss, W. Strober and J. A. Berzofsky,*Proc. Natl. Acad. Sci.*, 1998, **95**, 1709-1714.
57. D. R. Burton, R. C. Desrosiers, R. W. Doms, W. C. Koff, P. D. Kwong, J. P. Moore, G. J. Nabel, J. Sodroski, I. A. Wilson and R. T. Wyatt, *Nat. Immunol.*, 2004, **5**, 233-236.
58. S. Rerks-Ngarm, P. Pitisuttithum, S. Nitayaphan, J. Kaewkungwal, J. Chiu, R. Paris, N. Premsri, C. Namwat, M. de Souza and E. Adams, *New Eng. J. Med.*, 2009, **361**, 2209-2220.
59. R. Cross, *Chem. Eng. News*, 2016, **94**, 18-21.
60. J. Johnson, *HIV* Vaccine, https://www.jnj.com/tag/hiv. Accessed October 06, 2017.
61. E. De Clercq, *Int. J. Antimicrob. Agents*, 2009, **33**, 307-320.
62. WHO, *Global Statistics*, *https*://www.hiv.gov/hiv-basics/overview/data-and-trends/global-statistics. Accessed October 07, 2017.
63. Avert, *Global HIV and AIDS statistics*, *https*://www.avert.org/hlobal-hiv-and-aids-statistics. Accessed October 07, 2017..
64. M. Barnhart and J. D. Shelton, Global Health: Science and Practice, 2015, **3**, 1-11.
65. UNAIDS, *UNAIDS*, *https*://www.unaids.org/en. Accessed October 07, 2017.
66. F. Clavel and A. J. Hance, *New Eng. J. Med.*, 2004, **350**, 1023-1035.
67. Y. Mehellou and E. De Clercq, *J. Med. Chem*, 2010, **53**, 521-538.
68. J. D. Auerbach and T. A. Hoppe, *J. Int. AIDS Soc.*, 2015, **18**, 1-5.
69. G. A. Millett, J. S. Crowley, H. Koh, R. O. Valdiserri, T. Frieden, C. W. Dieffenbach, K. A. Fenton, R. Benjamin, J. Whitescarver and J. Mermin, *JAIDS*, 2010, **55**, 144-147.
70. H.-J. Stellbrink, *Antivir. Chem. Chemother.*, 2009, **19**, 189-200.
71. R. L. Hamers, A. M. Wensing, N. K. Back, M. S. Arcilla and J. P. Frissen, *Antivir. Ther.*, 2011, **16**, 115-118.
72. S. Sungkanuparph, W. Manosuth, S. Kiertiburanakul, B. Piyavong, N. Chumpathat and W. Chantratita, *Clin. Infect. Dis.*, 2007, **44**, 447-452.

73. R. A. Murphy, R. Court, G. Maartens and H. Sunpath, *AIDS Res. Hum. Retroviruses*, 2017, **33**, 1181-1184.
74. B. Jayashree, S. Thomas and Y. Nayak, *Med. Chem. Res.*, 2010, **19**, 193-209.
75. F. O'Donnell, T. Smyth, V. Ramachandran and W. Smyth, *Int. J. Antimicrob. Agents*, 2010, **35**, 30-38.
76. W. A. Chow, C. Jiang and M. Guan, *Lancet oncol.*, 2009, **10**, 61-71.
77. D. V. Kadnikov and R. C. Larock, *J. Org. Chem.*, 2004, **69**, 6772-6780.
78. J. J. Kulagowski, R. Baker, N. R. Curtis, I. M. Mawer, A. M. Moseley, M. P. Ridgill, M. Rowley, I. Stansfield and P. D. Leeson, *J. Med. Chem*, 1994, **37**, 1402-1405.
79. F. Curreli, H. Zhang, X. Zhang, I. Pyatkin, Z. Victor, A. Altieri and A. K. Debnath, *Bioorg. Med. Chem.*, 2011, **19**, 77-90.
80. U. Songsiang, T. Thongthoom, C. Boonyarat and C. Yenjai, *J. Nat. Prod.*, 2011, **74**, 208-212.
81. S. Heeb, M. P. Fletcher, S. R. Chhabra, S. P. Diggle, P. Williams and M. Cámara, *FEMS Microbiol. Rev.*, 2011, **35**, 247-274.
82. A. A. Al-Amiery, R. I. Al-Bayati, K. Y. Saour and M. F. Radi, *Res. Chem. Intermed.*, 2012, **38**, 559-569.
83. P. Saha, C. Debnath and G. Bérubé, *J. Steroid Biochem. Mol. Biol.*, 2013, **137**, 271-300.
84. M. Binaschi, G. Capranico, P. De Isabella, M. Mariani, R. Supino, S. Tinelli and F. Zunino, *Int. J. Cancer*, 1990, **45**, 347-352.
85. B. Joseph, F. Darro, A. Béhard, B. Lesur, F. Collignon, C. Decaestecker, A. Frydman, G. Guillaumet and R. Kiss, *J. Med. Chem*, 2002, **45**, 2543-2555.
86. D. A. Sabbah, N. A. Simms, W. Wang, Y. Dong, E. L. Ezell, M. G. Brattain, J. L. Vennerstrom and H. A. Zhong, *Bioorg. Med. Chem.*, 2012, **20**, 7175-7183.
87. A. Doléans-Jordheim, J. B. Veron, O. Fendrich, E. Bergeron, A. Montagut-Romans, Y. S. Wong, B. Furdui, J. Freney, C. Dumontet and A. Boumendjel, *Chem. Med. Chem*, 2013, **8**, 652-657.
88. A. V. Aksenov, A. N. Smirnov, N. A. Aksenov, I. V. Aksenova, L. V. Frolova, A. Kornienko, I. V. Magedov and M. Rubin, *Chem. Commun.*, 2013, **49**, 9305-9307.
89. J. R. Woodgett and M. Takahashi, *eLS*, 2001, **276**, 10025-10031, .
90. J. F. Glickman, A. Schmid and S. Ferrand, *Assay Drug Dev. Technol.*, 2008, **6**, 433-455.

91. H. Bazin, M. Preaudat, E. Trinquet and G. Mathis, *Spectrochim. Acta Part A, Mol. Biomol. Spectrosc.*, 2001, **57**, 2197-2211.

92. M. Kawaguchi, T. Terai, R. Utata, M. Kato, K. Tsuganezawa, A. Tanaka, H. Kojima, T. Okabe and T. Nagano, *Bioorg. Med. Chem. Lett.*, 2008, **18**, 3752-3755.

93. L. Ma, T. Leng, K. Wang, C. Wang, Y. Shen and W. Zhu, *Tetrahedron*, 2017, **73**, 1306-1310.

94. X. Liu, Z. Xu and J. M. Cole, *J. Phys. Chem. C*, 2013, **117**, 16584-16595.

95. Y. Hoshina, Y. Yamada, H. Tanaka, T. Doi and T. Takahashi, *Bioorg. Med. Chem. Lett.*, 2007, **17**, 2904-2907.

96. A. Knierzinger, and O.S. Wolfbeis, *J. Heterocycl. Chem.*, 1980, **17**, 225-229.

97. M. J. Wall, J. Chen, S. Meegalla, S. K. Ballentine, K. J. Wilson, R. L. DesJarlais, C. Schubert, M. A. Chaikin, C. Crysler and I. P. Petrounia, *Bioorg. Med. Chem. Lett.*, 2008, **18**, 2097-2102.

98. V. B. Kovalska, K. D. Volkova, A. V. Manaev, M. Y. Losytskyy, I. N. Okhrimenko, V. F. Traven and S. M. Yarmoluk, *Dyes Pigm.*, 2010, **84**, 159-164.

99. T. Ishida, S. Kikuchi and T. Yamada, *Org. Lett.*, 2013, **15**, 3710-3713.

100. J. Zhang, X. Han and X. Lu, *Synlett*, 2015, **26**, 1744-1748.

101. N. A. Cortese, C. B. Ziegler Jr, B. J. Hrnjez and R. F. Heck, *J. Org. Chem.*, 1978, **43**, 2952-2958.

102. W.-P. Mai, G.-C. Sun, J.-T. Wang, G. Song, P. Mao, L.-R. Yang, J.-W. Yuan, Y.-M. Xiao and L.-B. Qu, *J. Org. Chem.*, 2014, **79**, 8094-8102.

103. Y. Tagawa, T. Kawaoka and Y. Goto, *J. Heterocycl. Chem.*, 1997, **34**, 1677-1683.

104. F. Ameer, S. E. Drewes, S. Freese and P. T. Kaye, *Synth. Commun.* , 1988, **18**, 495-500.

105. O. Familoni, P. Kaye and P. Klaas, *Chem. Commun.*, 1998, 2563-2564.

106. O. B. Familoni, P. J. Klaas, K. A. Lobb, V. E. Pakade and P. T. Kaye, *Org. Biomol. Chem.*, 2006, **4**, 3960-3965.

107. P. T. Kaye, *S. Afr. J. Sci.*, 2004, **100**, 545-548.

108. P. T. Kaye, M. A. Musa, X. W. Nocanda and R. S. Robinson, *Org. Biomol. Chem.*, 2003, **1**, 1133-1138.

109. V. Singh and S. Batra, *Tetrahedron*, 2008, **64**, 4511-4574.

110. L.P. Mciteka, *PhD Thesis*, Rhodes University, 2012..

111. P. J. Klaas, *PhD* Thesis, Rhodes University, 2001.

112. J. Cai, Z. Zhou, G. Zhao and C. Tang, *Org. Lett.*, 2002, **4**, 4723-4725.
113. L. Moira, *J. Chem. Soc., Perkin Trans. 1*, 1993, 1809-1813.
114. M. L. Bode, P. T. Kaye and R. George, *J. Chem. Soc., Perkin Trans. 1*, 1994, 3023-3027.
115. K. C. Sekgota, *MSc Thesis*, Rhodes University, 2015.
116. P. Cheng, Q. Zhang, Y. B. Ma, Z.-Y. Jiang, X. M. Zhang, F. X. Zhang and J. J. Chen, *Bioorg. Med. Chem. Lett.*, 2008, **18**, 3787-3789.
117. J. T. Kuethe, A. Wong, C. Qu, J. Smitrovich, I. W. Davies and D. L. Hughes, *J. Org. Chem.*, 2005, **70**, 2555-2567.
118. N. J. O'Brien, M. Brzozowski, D. J. Wilson, L. W. Deady and B. M. Abbott, *Bioorg. Med. Chem.*, 2014, **22**, 3781-3790.
119. C. Mugnaini, A. Brizzi, A. Ligresti, M. Allarà, S. Lamponi, F. Vacondio, C. Silva, M. Mor, V. Di Marzo and F. Corelli, *J. Med. Chem*, 2016, **59**, 1052-1067.
120. S. Madapa, V. Singh and S. Batra, *Tetrahedron*, 2006, **62**, 8740-8747.
121. D. Basavaiah, R. M. Reddy, N. Kumaragurubaran and D. S. Sharada, *Tetrahedron*, 2002, **58**, 3693-3697.
122. N. Nishiwaki, *Molecules*, 2010, **15**, 5174-5195.
123. J. N. Kim, K. Y. Lee, H. S. Kim and T. Y. Kim, *Org. Lett.*, 2000, **2**, 343-345.
124. K. Y. Lee, J. M. Kim and J. N. Kim, *Tetrahedron*, 2003, **59**, 385-390.
125. K.-Y. Lee, S. Gowrisankar and J.-N. Kim, *Bull. Korean Chem. Soc.*, 2005, **26**, 1481-1490.
126. M. L. Bode and P. T. Kaye, *J. Chem. Soc., Perkin Trans. 1*, 1990, 2612-2613.
127. F. Borges, F. Roleira, N. Milhazes, L. Santana and E. Uriarte, *Curr. Med. Chem.*, 2005, **12**, 887-916.
128. V. Sharma and V. Kumar, *Med. Chem. Res.*, 2014, **23**, 3593-3606.
129. V. R. Vemula, S. Vurukonda and C. K. Bairi, *Int. J. Pharm. Sci. Rev. Res.*, 2011, **11**, 159-163.
130. D. Lerner, P. Horowitz and E. Evleth, *J. Phys. Chem.*, 1977, **81**, 12-17.
131. M. E. Wall, M. Wani, C. Cook, K. H. Palmer, A. A. McPhail and G. Sim, *J. Am. Chem. Soc.*, 1966, **88**, 3888-3890.
132. G. M. Cragg and D. J. Newman, *J. Ethnopharmacol.*, 2005, **100**, 72-79.
133. V. R. Vemula, S. Vurukonda and C. K. Bairi, *Int. J. Pharm. Sci. Rev. Res*, 2011, **11**, 159-163.
134. G. S. Singh and E. E. Mmatli, *European J. Med. Chem*, 2011, **46**, 5237-5257.

135. K. N. Venugopala, M. A. Khedr, M. Attimarad, B. Padmashali, R. S. Kulkarni, R. Venugopala and B. Odhav, *Journal of Basic and Clinical Pharmacy*, 2017, **8**, 49-60.
136. A. R. Katritzky and C. W. Rees, *Comprehensive Heterocyclic Chemistry: Five-membered rings with two or more oxygen, sulfur or nitrogen atoms*, Pergamon Press, New York, 1984.
137. K. N. Venugopala, M. A. Khedr, M. Attimarad, B. Padmashali, R. S. Kulkarni, R. Venugopala and B. Odhav, *J. Basic and Clin. Pharm.*, 2017, **8**, 49-61.
138. D. A. James, K. Koya, H. Li, G. Liang, Z. Xia, W. Ying, Y. Wu and L. Sun, *Bioorg. Med. Chem. Lett.*, 2008, **18**, 1784-1787.
139. B. Sadowski, J. Klajn and D. T. Gryko, *Org. Biomol. Chem.*, 2016, **14**, 7804-7828.
140. C. Zhang, H. Zhang, L. Zhang, T. B. Wen, X. He and H. Xia, *Organometallics*, 2013, **32**, 3738-3743.
141. S. Chuprakov and V. Gevorgyan, *Org. Lett.*, 2007, **9**, 4463-4466.
142. V. Helan, A. Gulevich and V. Gevorgyan, *Chem. Sci.*, 2015, **6**, 1928-1931.
143. T. Xu and H. Alper, *Org. Lett.*, 2015, **17**, 4526-4529.
144. E. I. Kostik, A. Abiko and A. Oku, *J. Org. Chem.*, 2001, **66**, 2618-2623.
145. M. Tukulula, *MSc Thesis*, Rhodes University, 2009.
146. P. O. Deane, R. George and P. T. Kaye, *Tetrahedron*, 1998, **54**, 3871-3876.
147. M. Tukulula, R. Klein and P. T. Kaye, *Synth. Commun.*, 2010, **40**, 2018-2028.
148. I. O. Ghinea and R. M. Dinica, in *Scope of Selective Heterocycles from Organic and Pharmaceutical Perspective*, InTech, London, 2016.
149. C. Sandeep, K. N. Venugopala, M. A. Khedr, B. Padmashali, R. S. Kulkarni, R. Venugopala and B. Odhav, *Indian J. Pharm. Educ. Res.*, 2017, **51**, 452-460.
150. C. L. Lins, J. H. Block, R. F. Doerge and G. J. Barnes, *J. Pharm. Sci.*, 1982, **71**, 614-617.
151. M. Fraser, S. McKenzie and D. Reid, *J. Chem. Soc. B, Phys. Org.*, 1966, 44-48.
152. V. K. Outlaw, J. Zhou, A. E. Bragg and C. A. Townsend, *RSC adv.*, 2016, **6**, 61249-61253.
153. S. Bobrovskii, D. Lushnikov and Y. G. Bundel, *Khim. Geterosikl. Soedin II*, 1989, 1634-1638.
154. W. Armarego, *J. Chem. Soc.*, 1964, 4226-4233.
155. C. L. K. Lins, *PhD Thesis*, Oregon State University, 1980.
156. J. Wiench, L. Stefaniak and G. Webb, *J. Mol. Struct.*, 2002, **605**, 33-39.

157. M. F. Amaral, L. A. Deliberto, C. R. de Souza, R. M. Naal, Z. Naal and G. C. Clososki, *Tetrahedron*, 2014, **70**, 3249-3258.

158. C.-H. Park, V. Ryabova, I. V. Seregin, A. W. Sromek and V. Gevorgyan, *Org. Lett.*, 2004, **6**, 1159-1162.

159. A. G. Kuznetsov, A. A. Bush, V. B. Rybakov and E. V. Babaev, *Molecules*, 2005, **10**, 1074-1083.

160. B. Koszarna, R. Matczak, M. Krzeszewski, O. Vakuliuk, J. Klajn, M. Tasior, J. T. Nowicki and D. T. Gryko, *Tetrahedron*, 2014, **70**, 225-231.

161. P. Olejníková, L. Birošová, L. U. Švorc, Z. Vihonská, M. Fiedlerová, Š. Marchalín and P. Šafář, *Chem. Pap.*, 2015, **69**, 983-992.

162. Y. R. Song, C. W. Lim and T. W. Kim, *Luminescence*, 2016, **31**, 364-371.

163. D. A. Lerner and E. Evleth, *Chem. Phys. Lett.*, 1972, **15**, 260-262.

164. Y. Zhang, J. Garcia-Amorós, B. Captain and F. M. Raymo, *J. Mater. Chem. C*, 2016, **4**, 2744-2747.

165. A. Rotaru, I. Druta, E. Avram and R. Danac, *Arkivoc*, 2009, **13**, 287-299.

166. E. Kim, Y. Lee, S. Lee and S. B. Park, *Acc. Chem. Res.*, 2015, **48**, 538-547.

167. E. Kim, M. Koh, J. Ryu and S. B. Park, *J. Am. Chem. Soc.*, 2008, **130**, 12206-12207.

168. E. J. Choi and S. B. Park, *Org. Biomol. Chem.*, 2015, **13**, 5202-5208.

169. S. Park, D. I. Kwon, J. Lee and I. Kim, *ACS Comb. Sci.*, 2015, **17**, 459-469.

170. Y. Lee, A. Jo and S. B. Park, *Angew. Chem.*, 2015, **127**, 15915-15919.

171. A. Kakehi, H. Suga, Y. Kaneko, T. Fujii and N. Tanaka, *Chem. Pharm. Bull.*, 2005, **53**, 1430-1438.

172. R. B. Mujumdar, L. A. Ernst, S. R. Mujumdar, C. J. Lewis and A. S. Waggoner, *Bioconjugate Chem.*, 1993, **4**, 105-111.

173. G. Kubheka, I. Uddin, E. Amuhaya, J. Mack and T. Nyokong, *JJ. Porphyrins Pthalocyanines*, 2016, **20**, 1016-1024.

174. H. Zhang, Y. Wu, M. Fan, X. Xiao, J. Mack, G. Kubheka, T. Nyokong and H. Lu, *New J. Chem.*, 2017, **41**, 5802-5807.

175. R. Sjöback, J. Nygren and M. Kubista, *Spectrochim. Acta Part A, Mol. Biomol. Spectrosc.*, 1995, **51**, L7-L21.

176. A. Farag and I. Yahia, *Opt. Commun.*, 2010, **283**, 4310-4317.

177. A. R. H. Narayan, *New Reactions and Synthetic Strategies Toward Indolizidine Alkaloids and Pallavicinia Diterpenes*, University of California, Berkeley, 2011.

178. Y. Liu, H. Hu, J. Zhou, W. Wang, Y. He and C. Wang, *Org. Biomol. Chem.*, 2017, **15**, 5016-5024.
179. M. Vasilescu, R. Bandula, F. Dumitrascu and H. Lemmetyinen, *J. Fluoresc.*, 2006, **16**, 631-639.
180. B. Furdui, R. Dinică, M. Demeunynck, I. Drută and A. Vlahovici, *Rev. Roum. Chim.*, 2007, **52**, 633-637.
181. F. Delattre, P. Woisel, G. Surpateanu, M. Bria, F. Cazier and P. Decock, *Tetrahedron*, 2004, **60**, 1557-1562.
182. W. O. Foye, *Foye's principles of medicinal chemistry*, Lippincott Williams and Wilkins, Baltimore, USA, 2008.
183. S. L. Schreiber, *Science*, 2000, **287**, 1964-1969.
184. W. O. Foye, *Principles of medicinal chemistry*, Lea and Febiger, Philadelphia, 1974.
185. N. K. Terrett, M. Gardner, D. W. Gordon, R. J. Kobylecki and J. Steele, *Tetrahedron*, 1995, **51**, 8135-8173.
186. M. E. Welsch, S. A. Snyder and B. R. Stockwell, *Curr. Opin. Chem. Biol.*, 2010, **14**, 347-361.
187. S. Mandal, M. N. Moudgil and S. K. Mandal, *Eur. J. Pharmacol.*, 2009, **625**, 90-100.
188. W. G. Kaelin Jr, *Nat. Rev. Cancer*, 2005, **5**, 689.
189. P. D. Leeson and B. Springthorpe, *Nat. Rev. Drug. Disc.*, 2007, **6**, 881.
190. J. G. Lombardino and J. A. Lowe III, *Nat. Rev. Drug. Disc.*, 2004, **3**, 853.
191. V. M. Cornel, *J. Org. Chem.*, 2001, **66**, 352-362.
192. K. C. Idahosa, *PhD Thesis*, Rhodes University, 2012.
193. V. Dragojlovic, *Chem. Texts*, 2015, **1**, 1-30.
194. M. M. Joullié and K. M. Lassen, *Arkivoc*, 2010, **81**, 189-250.
195. S. D. Roughley and A. M. Jordan, *J. Med. Chem*, 2011, **54**, 3451-3479.
196. C. A. Montalbetti and V. Falque, *Tetrahedron*, 2005, **61**, 10827-10852.
197. K. Scheidt, *Nature*, 2010, **465**, 1020.
198. K. Sasaki and D. Crich, *Org. Lett.*, 2011, **13**, 2256-2259.
199. J. R. Dunetz, J. Magano and G. A. Weisenburger, *Org. Process Res. Dev.*, 2016, **20**, 140-177.
200. T. Vishwanatha, N. R. Panguluri and V. V. Sureshbabu, *Synthesis*, 2013, **45**, 1569-1601.
201. G. M. Raghavendra, A. B. Ramesha, C. N. Revanna, K. N. Nandeesh, K. Mantelingu and K. S. Rangappa, *Tetrahedron letters*, 2011, **52**, 5571-5574.

202. J. R. Dunetz, Y. Xiang, A. Baldwin and J. Ringling, *Org. Lett.*, 2011, **13**, 5048-5051.
203. P. Starkov and T. D. Sheppard, *Org. Biomol. Chem.*, 2011, **9**, 1320-1323.
204. R. M. Lanigan, V. Karaluka, M. T. Sabatini, P. Starkov, M. Badland, L. Boulton and T. D. Sheppard, *Chem. Commun.*, 2016, **52**, 8846-8849.
205. F. P. Gasparro and N. H. Kolodny, *J. Chem. Educ.*, 1977, **54**, 258.
206. T. Drakenberg, K. I. Dahlqvist and S. Forsen, *J. Phys. Chem.*, 1972, **76**, 2178-2183.
207. R. E. Carter and J. Sandstrom, *J. Phys. Chem.*, 1972, **76**, 642-647.
208. B. E. Mann, *Prog. Nucl. Mag. Reson. Spectrosc.*, 1977, **11**, 95-114.
209. K. S. Pitzer and W. E. Donath, in *Molecular Structure And Statistical Thermodynamics: Selected Papers of Kenneth S Pitzer*, World Scientific, Singapore, 1993, 98-103.
210. S. E. Drewes and G. H. Roos, *Tetrahedron*, 1988, **44**, 4653-4670.
211. D. Basavaiah, P. D. Rao and R. S. Hyma, *Tetrahedron*, 1996, **52**, 8001-8062.
212. E. Ciganek, *Org. React.*, 1997, **62**, 8251-8254.
213. D. Basavaiah, A. J. Rao and T. Satyanarayana, *Chem. Rev.*, 2003, **103**, 811-892.
214. J. Kim and K. Lee, *Curr. Org. Chem.*, 2002, **6**, 627-645.
215. L. P. Mciteka, *PhD* Thesis, Rhodes University, 2012.
216. S. Bobrovskii, E. Babaev and Y. G. Bundel, *Chem. Heterocycl. Compnd.*, 1987, **23**, 169-174.
217. V. Theodorou, K. Skobridis, A. G. Tzakos and V. Ragoussis, *Tetrahedron Letters*, 2007, **48**, 8230-8233.
218. M. L. Bode, *PhD* Thesis, Rhodes University, 1994.
219. A. De and B. Saha, *J. Pharm. Sci.*, 1975, **64**, 249-252.
220. R. J. Hodgkiss, R. W. Middleton, J. Parrick, H. K. Rami, P. Wardman and G. D. Wilson, *J. Med. Chem*, 1992, **35**, 1920-1926.
221. M. Kimura, T. Nakato and T. Okuhara, *Appl. catal. A, General*, 1997, **165**, 227-240.
222. K. Nicolaou, A. A. Estrada, M. Zak, S. H. Lee and B. S. Safina, *Angew. Chem.*, 2005, **117**, 1402-1406.
223. H. Gutmann, U. Seal and C. Irving, *Cancer Res.*, 1960, **20**, 1072-1078.
224. P. R. Sultane, T. B. Mete and R. G. Bhat, *Org. Biomol. Chem.*, 2014, **12**, 261-264.
225. H. K. No, Y. I. Cho, H. R. Kim and S. P. Meyers, *J. Agric. Food Chem.*, 2000, **48**, 2625-2627.
226. W.-C. Gao, J.-J. Zhao, F. Hu, H.-H. Chang, X. Li and W.-L. Wei, *RSC adv.*, 2015, **5**, 25222-25228.
227. C. He, S. Guo, L. Huang and A. Lei, *J. Am. Chem. Soc.*, 2010, **132**, 8273-8275.

228. A. J. Grenning, C. K. Van Allen, T. Maji, S. B. Lang and J. A. Tunge, *J. Org. Chem.*, 2013, **78**, 7281-7287.
229. L. H. Zou, D. L. Priebbenow, L. Wang, J. Mottweiler and C. Bolm, *Adv. Synth. Catal.*, 2013, **355**, 2558-2563.
230. Q. Xing, P. Li, H. Lv, R. Lang, C. Xia and F. Li, *Chem. Commun.*, 2014, **50**, 12181-12184.
231. S. L. Prabu, T. S. Prakash and R. Thirumurugan, in *Developments in Surface Contamination and Cleaning*, Elsevier, Boca Raton, 2015, 129-186.
232. R. L. Furlán, E. G. Mata and O. A. Mascaretti, *J. Chem. Soc., Perkin Trans. 1*, 1998, 355-358.
233. R. M. Lanigan and T. D. Sheppard, *Eur. J. Org. Chem.*, 2013, **2013**, 7453-7465.
234. R. M. de Figueiredo, J.-S. Suppo and J.-M. Campagne, *Chem. Rev.*, 2016, **116**, 12029-12122.
235. H. Lundberg, F. Tinnis, N. Selander and H. Adolfsson, *Chem. Soc. Rev.*, 2014, **43**, 2714-2742.
236. I. S. Blagbrough, N. E. Mackenzie, C. Ortiz and A. I. Scott, *Tetrahedron Lett.*, 1986, **27**, 1251-1254.
237. P. Nelson and A. Pelter, *J. Chem. Soc.*, 1965, 5142-5144.
238. P. Tang, *Org. Synth.*, 2003, **81**, 262-272.
239. B. M. Trost, H.-C. Tsui and F. D. Toste, *J. Am. Chem. Soc.*, 2000, **122**, 3534-3535.
240. V. Singh and S. Batra, *Tetrahedron*, 2008, **64**, 4511-4574.
241. H. Charville, D. Jackson, G. Hodges and A. Whiting, *Chem. Commun.*, 2010, **46**, 1813-1823.
242. C. L. Allen and J. M. Williams, *Chem. Soc. Rev.*, 2011, **40**, 3405-3415.
243. A. Ojeda-Porras and D. Gamba-Sánchez, *J. Org. Chem.*, 2016, **81**, 11548-11555.
244. M. Hosseini-Sarvari and H. Sharghi, *J. Org. Chem.*, 2006, **71**, 6652-6654.
245. A. C. Shekhar, A. R. Kumar, G. Sathaiah, V. L. Paul, M. Sridhar and P. S. Rao, *Tetrahedron Lett.*, 2009, **50**, 7099-7101.
246. R. Arora, S. Paul and R. Gupta, *Can. J. Chem.*, 2005, **83**, 1137-1140.
247. C. Han, J. P. Lee, E. Lobkovsky and J. A. Porco, *J. Am. Chem. Soc.*, 2005, **127**, 10039-10044.
248. M. H. S. Hamid, C. L. Allen, G. W. Lamb, A. C. Maxwell, H. C. Maytum, A. J. Watson and J. M. Williams, *J. Am. Chem. Soc.*, 2009, **131**, 1766-1774.
249. L. Ortona and A. Antinori, *Rays*, 1998, **23**, 181-192.

250. C. V. Smith, V. Sharma and J. C. Sacchettini, *Tuberculosis*, 2004, **84**, 45-55.
251. J. A. Caminero, G. Sotgiu, A. Zumla and G. B. Migliori, *Lancet infect. Dis.*, 2010, **10**, 621-629.
252. D. J. Sloan and J. M. Lewis, *Trans. R. Soc. Trop. Med. Hyg.*, 2016, **110**, 163-172.
253. E. Pietersen, E. Ignatius, E. M. Streicher, B. Mastrapa, X. Padanilam, A. Pooran, M. Badri, M. Lesosky, P. van Helden and F. A. Sirgel, *Lancet*, 2014, **383**, 1230-1239.
254. C. D. Wells, J. P. Cegielski, L. J. Nelson, K. F. Laserson, T. H. Holtz, A. Finlay, K. G. Castro and K. Weyer, *J. Infect. Dis.*, 2007, **196**, S86-S107.
255. J. W. Pape, S. S. Jean, J. L. Ho, A. Hafner and W. D. Johnson Jr, *Lancet*, 1993, **342**, 268-272.
256. M. Black, J. Mitchell, H. Zimmerman, K. Ishak and G. Epler, *Gastroenterology*, 1975, **69**, 289-302.
257. Y. Zhang, B. Heym, B. Allen, D. Young and S. Cole, *Nature*, 1992, **358**, 591-593.
258. M. Goble, M. D. Iseman, L. A. Madsen, D. Waite, L. Ackerson and C. R. Horsburgh Jr, *New Eng. J. Med.*, 1993, **328**, 527-532.
259. B. Bax, C.-w. Chung and C. Edge, *Acta Crystallogr. Sect. D*, 2017, **73**, 131-140.
260. B. Bandyopadhyay and P. Biswas, *RSC adv.*, 2015, **5**, 34588-34593.
261. R. M. Beteck, R. Seldon, D. Coertzen, M. E. van der Watt, J. Reader, J. S. Mackenzie, D. A. Lamprecht, M. Abraham, K. Eribez, J. Müller, F. Rui, G. Zhu, R. V. de Grano, I. D. Williams, F. J. Smit, A. J. C. Steyn, E. A. Winzeler, A. Hemphill, L.-M. Birkholtz, D. F. Warner, D. D. N'Da and R. K. Haynes, *Commun. Chem.*, 2018, **1**, 62-69.
262. D. Coertzen, J. Reader, M. van der Watt, S. H. Nondaba, L. Gibhard, L. Wiesner, P. Smith, S. D'Alessandro, D. Taramelli and H. N. Wong, *Antimicrob. Agents Chemother.*, 2018, AAC. 02214-02217.
263. M. Mbaba, A. N. Mabhula, N. Boel, A. L. Edkins, M. Isaacs, H. C. Hoppe and S. D. Khanye, *J. Inorg. Biochem.*, 2017, **172**, 88-93.
264. G. F. D. S. Fernandes, C. Man Chin and J. L. dos Santos, *Pharmaceuticals*, 2017, **10**, 1-17.
265. S. K. Bhal, K. Kassam, I. G. Peirson and G. M. Pearl, *Mol. Pharm.*, 2007, **4**, 556-560.
266. A. H. Diacon, R. Dawson, F. von Groote-Bidlingmaier, G. Symons, A. Venter, P. R. Donald, C. van Niekerk, D. Everitt, H. Winter and P. Becker, *Lancet*, 2012, **380**, 986-993.

267. A. H. Diacon, A. Pym, M. P. Grobusch, J. M. de Los Rios, E. Gotuzzo, I. Vasilyeva, V. Leimane, K. Andries, N. Bakare and T. De Marez, *New Eng. J. Med.*, 2014, **371**, 723-732.
268. L. Blake and M. ES Soliman, *Lett. Drug Des. Discov.*, 2013, **10**, 706-712.
269. A. Alemu, Y. Shiferaw, Z. Addis, B. Mathewos and W. Birhan, *Parasit. Vectors*, 2013, **6**, 1-8.
270. F. W. Muregi and A. Ishih, *Drug Dev. Res.*, 2010, **71**, 20-32.
271. M. Berriman, E. Ghedin, C. Hertz-Fowler, G. Blandin, H. Renauld, D. C. Bartholomeu, N. J. Lennard, E. Caler, N. E. Hamlin and B. Haas, *Science*, 2005, **309**, 416-422.
272. A. H. Fairlamb, *Trends Parasitol.*, 2003, **19**, 488-494.
273. R. J. Burchmore, P. O. Ogbunude, B. Enanga and M. P. Barrett, *Curr. Pharm. Des.*, 2002, **8**, 257-267.
274. L. R. Domingo and P. Pérez, *Org. Biomol. Chem.*, 2011, **9**, 7168-7175.
275. C. Bliss, *Am. Sci.*, 1957, **45**, 449-466.
276. A. Rosso, *MSc Thesis*, Lund University, 2010.
277. C. Mugnaini, A. Brizzi, A. Ligresti, M. Allarà, S. Lamponi, F. Vacondio, C. Silva, M. Mor, V. Di Marzo and F. Corelli, *J. Med. Chem*, 2016, **59**, 1052-1067.
278. G. A. Freeman, C. W. Andrews, A. L. Hopkins, G. S. Lowell, L. T. Schaller, J. R. Cowan, S. S. Gonzales, G. W. Koszalka, R. J. Hazen and L. R. Boone, *J. Med. Chem*, 2004, **47**, 5923-5936.
279. P. Cheng, Q. Gu, W. Liu, J.-F. Zou, Y.-Y. Ou, Z.-Y. Luo and J.-G. Zeng, *Molecules*, 2011, **16**, 7649-7661.
280. V. Summa, A. Petrocchi, F. Bonelli, B. Crescenzi, M. Donghi, M. Ferrara, F. Fiore, C. Gardelli, O. Gonzalez Paz and D. J. Hazuda, *J. Med. Chem*, 2008, **51**, 5843-5855.
281. P. E. Sax, E. DeJesus, A. Mills, A. Zolopa, C. Cohen, D. Wohl, J. E. Gallant, H. C. Liu, L. Zhong and K. Yale, *Lancet*, 2012, **379**, 2439-2448.
282. S. L. Walmsley, A. Antela, N. Clumeck, D. Duiculescu, A. Eberhard, F. Gutiérrez, L. Hocqueloux, F. Maggiolo, U. Sandkovsky and C. Granier, *New Eng. J. Med.*, 2013, **369**, 1807-1818.
283. I. E. Wijting, C. Lungu, B. J. Rijnders, M. E. van der Ende, H. T. Pham, T. Mesplede, S. D. Pas, J. J. Voermans, R. Schuurman and D. A. Van De Vijver, *J. Infect. Dis.*, 2018, **218**, 688-697.

284. R. T. Steigbigel, D. A. Cooper, P. N. Kumar, J. E. Eron, M. Schechter, M. Markowitz, M. R. Loutfy, J. L. Lennox, J. M. Gatell and J. K. Rockstroh, *New Eng. J. Med.*, 2008, **359**, 339-354.
285. D. T. Traut, *Advanced Materials Division*, Mintek, South Africa, 2016.
286. S. Gupta, A. N. Mathur, A. Nagappa, D. Kumar and S. Kumaran, *European J. Med. Chem*, 2003, **38**, 867-873.
287. T. Okano, T. Sakaida and S. Eguchi, *Heterocycles*, 1997, **1**, 227-236.
288. A. Ghinet, C.-M. Abuhaie, P. Gautret, B. Rigo, J. Dubois, A. Farce, D. Belei and E. Bîcu, *European J. Med. Chem*, 2015, **89**, 115-127.
289. W.-G. Lee, K. M. Frey, R. Gallardo-Macias, K. A. Spasov, A. H. Chan, K. S. Anderson and W. L. Jorgensen, *Bioorg. Med. Chem. Lett.*, 2015, **25**, 4824-4827.
290. W. Huang, T. Zuo, X. Luo, H. Jin, Z. Liu, Z. Yang, X. Yu, L. Zhang and L. Zhang, *Chem. Biol. Drug Des.*, 2013, **81**, 730-741.
291. H. Sonnenschein, G. Hennrich, U. Resch-Genger and B. Schulz, *Dyes Pigm.*, 2000, **46**, 23-27.
292. F. Dumitraşcu, M. Vasilescu, C. Drăghici and M. T. Căproiu, *Arkivoc*, 2011, **10**, 338-350.
293. R. Sarkar, T. Chaudhuri, A. Karmakar and C. Mukhopadhyay, *Org. Biomol. Chem.*, 2015, **13**, 11674-11686.
294. J. L. Jin, H. B. Li, Y. Geng, Y. Wu, Y. A. Duan and Z. M. Su, *Chem. Phys. Chem.*, 2012, **13**, 3714-3722.
295. J. F. Araneda, W. E. Piers, B. Heyne, M. Parvez and R. McDonald, *Angew. Chem. Int. Ed.*, 2011, **50**, 12214-12217.
296. K. J. Laidler, *Chemical kinetics*, Harper and Row, New York, 1987.
297. J. L. Ramsey, *Philos. Sci.*, 1997, **64**, 627-653.
298. K. A. Connors, *Chemical kinetics: the study of reaction rates in solution*, John Wiley and Sons, New York, 1990.
299. A. K. Burnham, *Global chemical kinetics of fossil fuels*, Springer, Livermore, 2017.
300. F. Mata-Perez and J. F. Perez-Benito, *J. Chem. Educ.*, 1987, **64**, 925.
301. J. S. Hill and N. S. Isaacs, *Tetrahedron Lett.*, 1986, **27**, 5007-5010.
302. J. S. Hill and N. S. Isaacs, *J. Phys. Org. Chem.*, 1990, **3**, 285-288.
303. A. Singh and A. Kumar, *RSC adv.*, 2015, **5**, 2994-3004.
304. K. E. Price, S. J. Broadwater, H. M. Jung and D. T. McQuade, *Org. Lett.*, 2005, **7**, 147-150.

305. V. K. Aggarwal, D. K. Dean, A. Mereu and R. Williams, *J. Org. Chem.*, 2002, **67**, 510-514.

306. C. Yu, B. Liu and L. Hu, *J. Org. Chem.*, 2001, **66**, 5413-5418.

307. R. E. Plata and D. A. Singleton, *J. Am. Chem. Soc.*, 2015, **137**, 3811-3826.

308. R. Robiette, V. K. Aggarwal and J. N. Harvey, *J. Am. Chem. Soc.*, 2007, **129**, 15513-15525.

309. A. I. Vogel, A. R. Tatchell, B. S. Furnis, A. J. Hannaford, P. W. G. Smith, *Vogel's textbook of practical organic chemistry*, John Wiley and Sons, New York, 1989.

310. M. Tukulula, *MSc Thesis*, Rhodes University, 2009.

311. J. A. Grobler, K. Stillmock, B. Hu, M. Witmer, P. Felock, A. S. Espeseth, A. Wolfe, M. Egbertson, M. Bourgeois and J. Melamed,*Proc. Natl. Acad. Sci.*, 2002, **99**, 6661-6666.

312. T. Lam, M. Lam, T. Au, D. Ip, T. Ng, W. Fong and D. Wan, *Life Sci.*, 2000, **67**, 2889-2896.